

P-146

AERONAUTICAL ENGINEERING

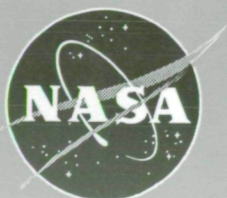
(NASA-SP-7037(316)) AERONAUTICAL
ENGINEERING: A CONTINUING
BIBLIOGRAPHY WITH INDEXES
(SUPPLEMENT 316) (NASA) 146 p

N95-24465

Unclas

00/01 0045753

A CONTINUING BIBLIOGRAPHY WITH INDEXES



National Aeronautics and
Space Administration

Scientific and Technical
Information Office

The NASA STI Office ... in Profile

Since its founding, NASA has been dedicated to the advancement of aeronautics and space science. The NASA Scientific and Technical Information (STI) Office plays a key part in helping NASA maintain this important role.

The NASA STI Office provides access to the NASA STI Database, the largest collection of aeronautical and space science STI in the world. The Office is also NASA's institutional mechanism for disseminating the results of its research and development activities.

Specialized services that help round out the Office's diverse offerings include creating custom thesauri, translating material to or from 34 foreign languages, building customized databases, organizing and publishing research results ... even providing videos.

For more information about the NASA STI Office, you can:

- **Phone** the NASA Access Help Desk at (301) 621-0390
- **Fax** your question to the NASA Access Help Desk at (301) 621-0134
- **E-mail** your question via the **Internet** to help@sti.nasa.gov
- **Write** to:

NASA Access Help Desk
NASA Center for AeroSpace Information
800 Elkridge Landing Road
Linthicum Heights, MD 21090-2934

NASA SP-7037 (316)
April 1995

AERONAUTICAL ENGINEERING

A CONTINUING BIBLIOGRAPHY WITH INDEXES



National Aeronautics and Space Administration
Scientific and Technical Information Office
Washington, DC 1995

This publication was prepared by the NASA Center for AeroSpace Information,
800 Elkridge Landing Road, Linthicum Heights, MD 21090-2934, (301) 621-0390.

INTRODUCTION

This issue of *Aeronautical Engineering — A Continuing Bibliography with Indexes* (NASA SP-7037) lists 413 reports, journal articles, and other documents recently announced in the NASA STI Database.

Accession numbers cited in this issue include:

<i>Scientific and Technical Aerospace Reports (STAR)</i> (N-10000 Series)	N95-15919 — N95-19505
Open Literature (A-60000 Series)	A95-62971 — A95-65815

The coverage includes documents on the engineering and theoretical aspects of design, construction, evaluation, testing, operation, and performance of aircraft (including aircraft engines) and associated components, equipment, and systems. It also includes research and development in aerodynamics, aeronautics, and ground support equipment for aeronautical vehicles.

Each entry in the publication consists of a standard bibliographic citation accompanied, in most cases, by an abstract. The listing of the entries is arranged by the first nine *STAR* specific categories and the remaining *STAR* major categories. This arrangement offers the user the most advantageous breakdown for individual objectives. The citations include the original accession numbers from the respective announcement journals.

Seven indexes—subject, personal author, corporate source, foreign technology, contract number, report number, and accession number—are included.

A cumulative index for 1995 will be published in early 1996.

The NASA CASI price code table, addresses of organizations, and document availability information are located at the back of this issue.



SCAN Goes Electronic!

If you have NASA Mail or if you can access the Internet, you can get biweekly issues of *SCAN* delivered to your desk—top absolutely free!

Electronic SCAN takes advantage of computer technology to alert you to the latest aerospace-related, worldwide scientific and technical information that has been published.

No more waiting while the paper copy is printed and mailed to you. You can review *Electronic SCAN* the same day it is released! And you get all 191—or any combination of—subject areas of announcements with abstracts to browse at your leisure. When you locate a publication of interest, you can print the announcement or electronically add it to your publication order list.

Electronic SCAN
Timely
Flexible
Complete
Free!

For instant access via Internet:

<ftp.sti.nasa.gov>
<gopher.sti.nasa.gov>
listserv@sti.nasa.gov

For additional information:

e-mail: help@sti.nasa.gov
scan@sti.nasa.gov

(Enter this address on the "To" line. Leave the subject line blank and send. You will receive an automatic reply with instructions in minutes.)

Phone: (301) 621-0390 Fax: (301) 621-0134

Write: NASA Access Help Desk
NASA STI Office
NASA Center for AeroSpace Information
800 Elkridge Landing Road
Linthicum Heights, MD 21090-2934



National Aeronautics and
Space Administration
Scientific and Technical
Information Office

TABLE OF CONTENTS

Category 01	Aeronautics	103
Category 02	Aerodynamics Includes aerodynamics of bodies, combinations, wings, rotors, and control surfaces; and internal flow in ducts and turbomachinery.	105
Category 03	Air Transportation and Safety Includes passenger and cargo air transport operations; and aircraft accidents.	123
Category 04	Aircraft Communications and Navigation Includes digital and voice communication with aircraft; air navigation systems (satellite and ground based); and air traffic control.	125
Category 05	Aircraft Design, Testing and Performance Includes aircraft simulation technology.	126
Category 06	Aircraft Instrumentation Includes cockpit and cabin display devices; and flight instruments.	137
Category 07	Aircraft Propulsion and Power Includes prime propulsion systems and systems components, e.g., gas turbine engines and compressors; and onboard auxiliary power plants for aircraft.	138
Category 08	Aircraft Stability and Control Includes aircraft handling qualities; piloting; flight controls; and autopilots.	141
Category 09	Research and Support Facilities (Air) Includes airports, hangars and runways; aircraft repair and overhaul facilities; wind tunnels; shock tubes; and aircraft engine test stands.	144
Category 10	Astronautics Includes astronautics (general); astrodynamics; ground support systems and facilities (space); launch vehicles and space vehicles; space transportation; space communications, spacecraft communications, command and tracking; spacecraft design, testing and performance; spacecraft instrumentation; and spacecraft propulsion and power.	148
Category 11	Chemistry and Materials Includes chemistry and materials (general); composite materials; inorganic and physical chemistry; metallic materials; nonmetallic materials; propellants and fuels; and materials processing.	151
Category 12	Engineering Includes engineering (general); communications and radar; electronics and electri- cal engineering; fluid mechanics and heat transfer; instrumentation and photogra- phy; lasers and masers; mechanical engineering; quality assurance and reliability; and structural mechanics.	153

Category 13	Geosciences	168
	Includes geosciences (general); earth resources and remote sensing; energy production and conversion; environment pollution; geophysics; meteorology and climatology; and oceanography.	
Category 14	Life Sciences	N.A.
	Includes life sciences (general); aerospace medicine; behavioral sciences; man/system technology and life support; and space biology.	
Category 15	Mathematical and Computer Sciences	168
	Includes mathematical and computer sciences (general); computer operations and hardware; computer programming and software; computer systems; cybernetics; numerical analysis; statistics and probability; systems analysis; and theoretical mathematics.	
Category 16	Physics	171
	Includes physics (general); acoustics; atomic and molecular physics; nuclear and high-energy; optics; plasma physics; solid-state physics; and thermodynamics and statistical physics.	
Category 17	Social Sciences	175
	Includes social sciences (general); administration and management; documentation and information science; economics and cost analysis; law, political science, and space policy; and urban technology and transportation.	
Category 18	Space Sciences	N.A.
	Includes space sciences (general); astronomy; astrophysics; lunar and planetary exploration; solar physics; and space radiation.	
Category 19	General	176
Subject Index		A-1
Personal Author Index		B-1
Corporate Source Index		C-1
Foreign Technology Index		D-1
Contract Number Index		E-1
Report Number Index		F-1
Accession Number Index		G-1
Appendix		APP-1

TYPICAL REPORT CITATION AND ABSTRACT

NASA SPONSORED

↓
ON MICROFICHE

ACCESSION NUMBER → N95-10318*# Dow Chemical Co., Midland, MI. ← CORPORATE SOURCE
 TITLE → NOVEL MATRIX RESINS FOR COMPOSITES FOR AIRCRAFT
 PRIMARY STRUCTURES, PHASE 1 Final Report, Apr. 1989 -
 Mar. 1992
 AUTHORS → EDMUND P. WOO, P. M. PUCKETT, S. MAYNARD, M. T. BISHOP,
 K. J. BRUZA, J. P. GODSCHALX, AND M. J. MULLINS Aug. 1992 ← PUBLICATION DATE
 164 p
 CONTRACT NUMBERS → (Contracts NAS1-18841; RTOP 510-02-11-02)
 REPORT NUMBERS → (NASA-CR-189657; NAS 1.26:189657) Avail: CASI HCA08/MFA02 ← AVAILABILITY AND
 PRICE CODE

The objective of the contract is the development of matrix resins with improved processability and properties for composites for primarily aircraft structures. To this end, several resins/systems were identified for subsonic and supersonic applications. For subsonic aircraft, a series of epoxy resins suitable for RTM and powder prepreg was shown to give composites with about 40 ksi compressive strength after impact (CAI) and 200 F/wet mechanical performance. For supersonic applications, a thermoplastic toughened cyanate prepreg system has demonstrated excellent resistance to heat aging at 360 F for 4000 hours, 40 ksi CAI and useful mechanical properties at greater than or equal to 310 F. An AB-BCB-maleimide resin was identified as a leading candidate for the HSCT. Composite panels fabricated by RTM show CAI of approximately 50 ksi, 350 F/wet performance and excellent retention of mechanical properties after aging at 400 F for 4000 hours. Author

TYPICAL JOURNAL ARTICLE CITATION AND ABSTRACT

NASA SPONSORED

↓

ACCESSION NUMBER → A95-60192* National Aeronautics and Space Administration. Ames. ← CORPORATE SOURCE
 Research Center, Moffett Field, CA.
 TITLE → AERODYNAMIC INTERACTIONS BETWEEN A ROTOR AND
 WING IN HOVER
 AUTHORS → FORT F. FELKER NASA. Ames Research Center, Moffett Field, ← AUTHOR'S AFFILIATION
 CA, US and JEFFREY S. LIGHT NASA. Ames Research Center,
 Moffett Field, CA, US Journal of the American Helicopter Society ← JOURNAL TITLE
 PUBLICATION DATE → 2 Jun. 1986 p. 53-61
 REPORT NUMBER → (HTN-94-00714) Copyright

An experimental investigation of rotor/wing aerodynamic interactions in hover is described. The investigation consisted of both a large-scale and a small-scale test. A 0.658-scale V-22 rotor and wing was used in the large-scale test. Wing download, wing surface pressure, rotor performance, and rotor downwash data from the large-scale test are presented. A small-scale experiment was conducted to determine how changes in the rotor/wing geometry affected the aerodynamic interactions. These geometry variations included the distance between the rotor and wing, wing incidence angle, wing flap angle, rotor rotation direction, and configurations both with the rotor axis at the tip of the wing (tilt rotor configuration) and with the rotor axis at the center of the wing (compound helicopter configuration). Author (Hermer)

AERONAUTICAL ENGINEERING

A Continuing Bibliography (Suppl. 316)

April 1995

01

AERONAUTICS (GENERAL)

A95-63520

LINEAR INSTABILITY WAVES IN SUPERSONIC JETS CONFINED IN CIRCULAR AND NON-CIRCULAR DUCTS

K. VISWANATHAN Pennsylvania State Univ., University Park, PA, P. J. MORRIS, and G. CHEN *Journal of Sound and Vibration* (ISSN 0022-460X) vol. 171, no. 2 March 24, 1994 p. 231-253 refs (BTN-94-EIX94341340068) Copyright

The linear instability of supersonic jets confined in circular and non-circular ducts is investigated both analytically and numerically. In the case of the non-circular duct, the numerical solution is based on the boundary element method. It is shown that the presence of an outer wall introduces additional instability modes. A highly supersonic unconfined jet possesses many modes of instability. These include the Kelvin-Helmholtz instability and supersonic instabilities. The modifications to these instabilities by a coflowing stream and an outer wall are examined. For the case of a circular jet in a circular duct, both a vortex sheet model and a model that includes the effect of a finite thickness shear layer are considered. The results of these calculations are compared with those for unconfined supersonic jets with an external flow. Finally, the effects of changes in the duct geometry on the instability modes are examined. Author (EI)

A95-63646

MATHEMATICAL MODELLING CONCERNING THE DEVELOPMENT OF A SYSTEM OF SIMILAR INSTALLATIONS, TAKING INTO ACCOUNT THEIR OPERATIONAL INTENSITY (AN AIRCRAFT-HELICOPTER FLEET TAKEN AS AN EXAMPLE)

R. T. SIRAZETDINOV KGTU, Kazan (Russia) *Izvestiya VUZ: Aviatcionnaya Tekhnika* (ISSN 0579-2975) no. 1 January-March 1994 p. 63-68 In RUSSIAN (BTN-94-EIX94461408763) Copyright

A problem concerning the development of a system of similar installations is considered. It is assumed that these installations have resources given. It means that each installation can be operated within the permissible number of hours. The decommissioning of installations due to their wear and ageing is taken into account. A system of equations, describing the development of such systems, has been obtained. An example of the development of an aircraft-helicopter fleet has been given. EI

A95-63655

CALCULATION OF GEOMETRY OF STAMPS WITH SMALL ALLOWANCES FOR PIECES OF THE AERODYNAMIC PROFILE

A. N. LUNEV KGTU, Kazan (Russia) and L. T. MOISEEVA *Izvestiya VUZ: Aviatcionnaya Tekhnika* (ISSN 0579-2975) no. 1 January-March 1994 p. 99-102 In RUSSIAN refs (BTN-94-EIX94461408772) Copyright

A method has been developed to calculate geometry of stamps for pieces of the aerodynamic profile. The method takes into account the

distortion of stamps, caused by the mechanical treatment of pieces. A system of equations has been used to implement the method. The introduction of the method developed to calculate allowances gives the opportunity to increase the utilization coefficient of the material twice as much, to eliminate the milling of the profile part and to make the mechanical treatment of pieces of the aerodynamic profile less labor-intensive. EI

A95-64608

AIRCRAFT SAFETY EVALUATION

ANON *Aerospace Engineering* (Warrendale, Pennsylvania) (ISSN 0736-2536) vol. 13, no. 7 July 1993 p. 7-9 (BTN-94-EIX94511309382) Copyright

The article presents a way to evaluate the airworthiness of aging aircraft. Data in this article came from various aircraft, including single-engine trainers and private aircraft, twin-engine turboprop executive and training aircraft, and twin turbofan business jets, military trainers, and commuters. The results were considered in customer support of ongoing and past evaluations of these aircraft. EI

A95-64610

FIBER-OPTIC TECHNOLOGY FOR TRANSPORT AIRCRAFT

ANON *Aerospace Engineering* (Warrendale, Pennsylvania) (ISSN 0736-2536) vol. 13, no. 7 July 1993 p. 35-40 (BTN-94-EIX94511309384) Copyright

Researchers at McDonnell Douglas Aerospace have been developing fiber-optic technology since the late 1970s. Fiber-optic systems have been installed successfully in both military and commercial aircraft. Application of fiber-optic technology for transport aircraft has reduced system weight, complexity, cable routing paths, and maintenance and manufacturing costs. EI

A95-65339

IMPROVED ANALYTICAL SOLUTION FOR VARYING SPECIFIC HEAT PARALLEL STREAM MIXING

JIYA CUI Beijing Univ of Aeronautics & Astronautics, Beijing (China) *Tuijin Jishu/Journal of Propulsion Technology* (ISSN 1001-4055) no. 3 June 1994 p. 1-5 In CHINESE refs (BTN-94-EIX94481415349) Copyright

In view of the fact that the original varying specific heat parallel mixing accurate solution by the author utilizes the critical temperature that is not actually experienced by the physical process and may introduce unnecessary errors, an improved set of formulae relying mainly on the static parameters was hereby derived. Some illustrative examples show that the original accurate solution only gives very small errors, yet the improved solution, being not only more rational but also much simpler and quicker, is therefore more advanced. Author (revised by EI)

A95-65346

DIRECT SPLITTING OF COEFFICIENT MATRIX FOR NUMERICAL CALCULATION OF TRANSONIC NOZZLE FLOW

XINGHONG JIANG Northwestern Polytechnical Univ., Xi'an (China), FULIAN CHEN, and XINGPING WU *Tuijin Jishu/Journal of Propulsion Technology* (ISSN 1001-4055) no. 3 June 1994 p. 44-48 In CHINESE refs

A
B
S
T
R
A
C
T
S

01 AERONAUTICS (GENERAL)

(BTN-94-EIX94481415356) Copyright

Some concise expressions for the direct splitting of coefficient matrix were derived and presented in this paper, hence the computational work for matrix splitting can be greatly reduced and simplified. By referring to Beam-Warming's explicit finite difference scheme, a second-order accurate scheme in consistency with the SCM method was constructed and analyzed, followed by a detail analysis on its numerical characteristics. Our calculations show that this algorithm is still robust even when there is an oblique shock in the nozzle supersonic flow region, and even without introducing any artificial parameters to control the numerical instability. The calculation results are in good agreement with the experimental ones in a wide range of Mach number.

Author (revised by EI)

A95-65347

AERODYNAMIC DESIGN AND CALCULATION OF FLOW AROUND THE PLANE CASCADE OF TURBINE

JUNYOU SUI The 31st Research Inst., Beijing (China) Tuijin Jishu/ Journal of Propulsion Technology (ISSN 1001-4055) no. 3 June 1994 p. 49-55 In CHINESE refs

(BTN-94-EIX94481415357) Copyright

A convenient and speedy method used for the aerodynamic design and calculation of turbine cascade profiles, based on the numerical integral of velocity potential equation and approximate factorization procedure, was presented which is applicable to the steady flows from subsonic, transonic to supersonic flow. Compared with the widely used schemes which introduce the artificial compressibility for the supersonic zone to control the numerical instability, this method has its obvious superiority in predicting the performance concerning with the presence of shock wave.

Author (revised by EI)

N95-16249# Nanjing Univ. of Aeronautics and Astronautics, Nanjing, Jiangsu (China).

JOINT PROCEEDINGS ON AERONAUTICS AND ASTRONAUTICS (JPAA)

JIANYING ZHU, ed. and G. L. DEGTAREV, ed. May 1993 271 p Prepared in cooperation with Kazan Inst. of Aviation, USSR (ISBN-7-80-046602-7) Avail: CASI HC A12/MF A03

These proceedings contain the papers presented at a joint Chinese - Russian symposium dealing with: aerodynamic characteristics of airfoils, aircraft design, liquid fuels for aircraft, wind tunnel equipment and testing, mathematical modeling of dynamic systems, signal processing, aircraft engine testing and maintainability, radar imaging, radioelectronic equipment design, aircraft landing systems, computational mathematics, computer aided design and manufacturing, and robotics. For individual titles, see N95-16250 through N95-16281.

N95-16560*# National Aeronautics and Space Administration, Langley Research Center, Hampton, VA.

MEASUREMENTS OF UNSTEADY PRESSURE AND STRUCTURAL RESPONSE FOR AN ELASTIC SUPERCRITICAL WING

CLINTON V. ECKSTROM, DAVID A. SEIDEL, and MAYNARD C. SANDFORD Nov. 1994 140 p (Contract(s)/Grant(s): RTOP 505-63-50-13) (NASA-TP-3443; L-17073; NAS 1.60:3443) Avail: CASI HC A07/MF A02

Results are presented which define unsteady flow conditions associated with the high-dynamic structural response of a high-aspect-ratio, elastic, supercritical wing at transonic speeds. The wing was tested in the Langley Transonic Dynamics Tunnel with a heavy gas test medium. The supercritical wing, designed for a cruise lift coefficient of 0.53 at a Mach number of 0.80, experienced the high-dynamic structural response from Mach 0.90 to 0.94 with the maximum response occurring at about Mach 0.92. At the maximum response conditions of the wing, the forcing function appears to be the oscillatory chordwise movement of strong shocks located on the upper and lower surfaces of the wing in conjunction with the flow separation on the lower surface of the wing in the trailing-edge cove region. Author

N95-17451 National Defence Research Establishment, Stockholm (Sweden). Huvudavdelning foer Foersvarsanalys.

MILITARY AVIATION MAINTENANCE INDUSTRY IN WESTERN EUROPE: CONCENTRATION AND INTERNATIONALIZATION [MILITAERA FLYGUNDERHALLSINDUSTRI I VAESTEUEUROPA: DESS KONCENTRATION OCH INTERNATIONALISERING]

K. BAECKLUND and K. NYBLOM Jan. 1994 129 p In SWEDISH (PB94-189180; FOA-C-10358-1.3) Avail: Issuing Activity (National Technical Information Service (NTIS))

The study presents the market structure and its development in the military aviation maintenance industry in Western Europe. Chapter 1-3 gives the purpose, method, and theoretical frame of the report as well as some definitions. The situations and the companies on the military aviation maintenance market in Germany, Great Britain, France, Belgium, the Netherlands, Spain, Portugal, and Italy are described in chapter 4. The most important maintenance companies are compared according to the variables the authors pointed out as the most important ones. They close the discussion in chapter 6 with conclusions and reflections. The result of the study shows that although the market for the military aviation maintenance is overestablished it is rare that companies totally withdraw from the market. However, there is a clear tendency among the companies to diversify away from the military sector. NTIS

N95-17466 Battelle Columbus Labs., OH.

BICARBONATE OF SODA BLASTING TECHNOLOGY FOR AIRCRAFT WHEEL DEPAINTING Report, Jun. 1991 - May 1992

A. S. C. CHEN, L. A. SMITH, and R. F. OLFENBUTTEL Jul. 1994 82 p Prepared for Environmental Protection Agency, Cincinnati, OH Limited Reproducibility: More than 20% of this document may be affected by microfiche quality

(Contract(s)/Grant(s): EPA-68-CO-0003)

(PB94-193323; EPA/600/R-94/127) Avail: CASI HC A05

This evaluation addressed product quality, waste reduction/pollution prevention and economics in replacing chemical solvent strippers with a bicarbonate of soda blasting technology for removal of paint from aircraft wheels. Because the paint being removed contained hazardous metal constituents, the liquid and solid wastes as well as the cloud of spray generated were evaluated for metal concentrations present and their leachability. Analyses for Cd, Cr, Cu, Pb, Mn, Ni, and Zn were made as well as total metals concentrations, pH, total suspended solids, and oil and grease. The blasting technology is effective for removing paint from aircraft wheels without significant damage to the anodized surface under the paint. In comparison to solvent depainting this technology reduced the amount of hazardous waste generated as well as cost savings due to operating and disposal costs, resulting in a 15% return on investment in about 4 years. NTIS

N95-17657*# National Aeronautics and Space Administration, Lewis Research Center, Cleveland, OH.

MICROGRAVITY ISOLATION SYSTEM DESIGN: A CASE STUDY

R. D. HAMPTON (McNeese State Univ., Lake Charles, LA.), C. R. KNOSPE (Virginia Univ., Charlottesville, VA.), P. E. ALLAIRE (Virginia Univ., Charlottesville, VA.), and C. M. GRODSINSKY Dec. 1994 21 p Sponsored by Commonwealth of Virginia's Center for Innovative Technology

(Contract(s)/Grant(s): NCC3-365; RTOP 963-70-OH)

(NASA-TM-106804; E-9282; NAS 1.15:106804) Avail: CASI HC A03/MF A01

Many acceleration-sensitive, microgravity science experiments will require active vibration isolation from manned orbiters on which they will be mounted. The isolation problem, especially in the case of a tethered payload, is a complex three-dimensional one that is best suited to modern-control design methods. In this paper, extended H(sub 2) synthesis is used to design an active isolator (i.e., controller) for a realistic single-input-multiple-output (SIMO) microgravity vibration isolation problem. Complex mu-analysis methods are used to analyze the

isolation system with respect to sensor, actuator, and umbilical uncertainties. The paper fully discusses the design process employed and the insights gained. This design case study provides a practical approach for isolation problems of greater complexity. Issues addressed include a physically intuitive state-space description of the system, disturbance and noise filters, filters for frequency weighting, and uncertainty models. The controlled system satisfies all the performance specifications and is robust with respect to model uncertainties.

Author

N95-18044*# Rocket Research Corp., Redmond, WA.
ARCJET THRUSTER RESEARCH AND TECHNOLOGY, PHASE 2 Final Report, Mar. 1987 - Feb. 1990

STEVE E. YANO Cleveland, OH NASA Mar. 1991 254 p
(Contract(s)/Grant(s): NAS3-24631; RTOP 506-42-31)
(NASA-CR-182276; E-9332; NAS 1.26:182276; REPT-91-R-1475)
Avail: CASI HC A12/MF A03

The principle objective of Phase 2 was to produce an engineering model N2H4 arcjet system which met typical performance, lifetime, environmental, and interface specifications required to support a 10-year N-S stationkeeping mission for a communications spacecraft. The system includes an N2H4 arcjet thruster, power conditioning unit (PCU), and the interconnecting power cable assembly. This objective was met with the successful conclusion of an extensive system test series.

Derived from text

N95-18197*# National Aeronautics and Space Administration. Lewis Research Center, Cleveland, OH.

MICROGRAVITY ISOLATION SYSTEM DESIGN: A MODERN CONTROL SYNTHESIS FRAMEWORK

R. D. HAMPTON (McNeese State Univ., Lake Charles, LA.), C. R. KNOSPE (Virginia Univ., Charlottesville, VA.), P. E. ALLAIRE (Virginia Univ., Charlottesville, VA.), and C. M. GRODSINSKY Dec. 1994 34 p Sponsored by Commonwealth of Virginia's Center for Innovative Technology
(Contract(s)/Grant(s): NCC3-365; RTOP 963-70-OH)
(NASA-TM-106805; E-9283; NAS 1.15:106805) Avail: CASI HC A03/MF A01

Manned orbiters will require active vibration isolation for acceleration-sensitive microgravity science experiments. Since umbilicals are highly desirable or even indispensable for many experiments, and since their presence greatly affects the complexity of the isolation problem, they should be considered in control synthesis. A general framework is presented for applying extended H2 synthesis methods to the three-dimensional microgravity isolation problem. The methodology integrates control and state frequency weighting and input and output disturbance accommodation techniques into the basic H2 synthesis approach. The various system models needed for design and analysis are also presented. The paper concludes with a discussion of a general design philosophy for the microgravity vibration isolation problem.

Author

N95-18486*# National Aeronautics and Space Administration. Lewis Research Center, Cleveland, OH.

MICROGRAVITY ISOLATION SYSTEM DESIGN: A MODERN CONTROL ANALYSIS FRAMEWORK

R. D. HAMPTON (McNeese State Univ., Lake Charles, LA.), C. R. KNOSPE (Virginia Univ., Charlottesville, VA.), P. E. ALLAIRE (Virginia Univ., Charlottesville, VA.), and C. M. GRODSINSKY Dec. 1994 36 p Sponsored by Commonwealth of Virginia's Center for Innovative Technology
(Contract(s)/Grant(s): NCC3-365; RTOP 963-70-OH)
(NASA-TM-106803; E-9281; NAS 1.15:106803) Avail: CASI HC A03/MF A01

Many acceleration-sensitive, microgravity science experiments will require active vibration isolation from the manned orbiters on which they will be mounted. The isolation problem, especially in the case of a tethered payload, is a complex three-dimensional one that is best suited to modern-control design methods. These methods, although more powerful than their classical counterparts, can nonetheless go

only so far in meeting the design requirements for practical systems. Once a tentative controller design is available, it must still be evaluated to determine whether or not it is fully acceptable, and to compare it with other possible design candidates. Realistically, such evaluation will be an inherent part of a necessary iterative design process. In this paper, an approach is presented for applying complex mu-analysis methods to a closed-loop vibration isolation system (experiment plus controller). An analysis framework is presented for evaluating nominal stability, nominal performance, robust stability, and robust performance of active microgravity isolation systems, with emphasis on the effective use of mu-analysis methods.

Author

N95-18606# National Aerospace Lab., Bangalore (India). Structural Integrity Div.

AGEING NUCLEAR POWER PLANT MANAGEMENT: AN AERONAUTICAL VIEWPOINT

R. SUNDER Oct. 1993 15 p Presented at the 77th Meeting of the AGARD Structures and Materials Panel, Bordeaux, France, Sep. 1993 (NAL-PD-SN-9306) Avail: CASI HC A03/MF A01

Aircraft like nuclear power plants are extremely safety critical. Aircraft development programs have evolved over many decades and the standards governing their evolution are reasonably well established. This paper attempts to describe ASIP (Aircraft Structural Integrity Program) and ENSIP (Engine Structural Integrity Program) standards for airframes and aeroengines and how their background may interest specialists in the design, development and operation of nuclear power plant facilities including the management of ageing plants. The accent of ASIP ENSIP is on inspectability and fail-safety to enable maintenance on condition.

Author

02

AERODYNAMICS

Includes aerodynamics of bodies, combinations, wings, rotors, and control surfaces; and internal flow in ducts and turbomachinery.

N95-15994# Naval Postgraduate School, Monterey, CA.
AN INVESTIGATION OF THE TRANSONIC PRESSURE DRAG COEFFICIENT FOR AXI-SYMMETRIC BODIES M.S. Thesis

EDDY PRIYONO Mar. 1994 94 p
(AD-A280990) Avail: CASI HC A05/MF A01

This thesis investigates the pressure drag coefficient in the transonic regime over an axi-symmetric body, with a set of unique contour surfaces developed in a previous thesis. The contour surfaces were obtained by an exact solution of the small perturbation transonic equation, using the guidelines and tools developed at NPS. In this work, computational fluid dynamics (CFD) was not only used to compute the afterbody contour surface, but also to investigate a conical afterbody and complete bodies, which are composed of an arbitrary forebody (ellipsoid) and a variable afterbody (contour and conical). Euler as well as Navier-Stokes flow-solvers were applied to the geometries of interest, giving Mach-number contours for viscous and inviscid flow, pressure drag coefficient magnitude, and depicting shock wave location. On the basis of these results, it can be verified that our contour surface afterbodies will decrease by 15 percent the peak of the pressure drag coefficient (C sub d) versus Mach number curves in the transonic regime. These results can be used to design low pressure drag surfaces for missiles, projectiles, and aircraft engine nacelles.

DTIC

N95-16038*# National Aeronautics and Space Administration. Lewis Research Center, Cleveland, OH.

NUMERICAL SIMULATION OF SUPERSONIC COMPRESSION CORNERS AND HYPERSONIC INLET FLOWS USING THE RPLUS2D CODE

KAMLESH KAPOOR, BERNHARD H. ANDERSON, and ROBERT J. SHAW Nov. 1994 14 p Original contains color illustrations

02 AERODYNAMICS

(Contract(s)/Grant(s): RTOP 537-02-23)
(NASA-TM-106580; E-8840; NAS 1.15:106580) Avail: CASI HC A03/MF A01; 1 functional color page

A two-dimensional computational code, PRLUS2D, which was developed for the reactive propulsive flows of ramjets and scramjets, was validated for two-dimensional shock-wave/turbulent-boundary-layer interactions. The problem of compression corners at supersonic speeds was solved using the RPLUS2D code. To validate the RPLUS2D code for hypersonic speeds, it was applied to a realistic hypersonic inlet geometry. Both the Baldwin-Lomax and the Chien two-equation turbulence models were used. Computational results showed that the RPLUS2D code compared very well with experimentally obtained data for supersonic compression corner flows, except in the case of large separated flows resulting from the interactions between the shock wave and turbulent boundary layer. The computational results compared well with the experiment results in a hypersonic NASA P8 inlet case, with the Chien two-equation turbulence model performing better than the Baldwin-Lomax model. Author

N95-16069* National Aeronautics and Space Administration. Langley Research Center, Hampton, VA.

EXPERIMENTAL STUDY AT LOW SUPERSONIC SPEEDS OF A MISSILE CONCEPT HAVING OPPOSING WRAPAROUND TAILS

JERRY M. ALLEN and CAROLYN B. WATSON Nov. 1994 57 p
(Contract(s)/Grant(s): RTOP 505-59-30-01)
(NASA-TM-4582; L-17337; NAS 1.15:4582) Avail: CASI HC A04/MF A01

A wind-tunnel investigation has been performed at low supersonic speeds (at Mach numbers of 1.60, and 2.16) to evaluate the aerodynamic characteristics of a missile concept capable of being tube launched and controlled with a simple one-axis canard controller. This concept, which features an axisymmetric body with two planar canards and four wraparound tail fins arranged in opposing pairs, must be in rolling motion to be controllable in any radial plane with the planar canards. Thus, producing a constant rolling moment that is invariant with speed and attitude to provide the motion is desirable. Two tail-fin shaping designs, one shaved and one beveled, were evaluated for their efficiency in producing the needed rolling moments, and the results showed that the shaved fins were much more desirable for this task than the beveled fins. Author

N95-16076 Physical Sciences, Inc., Andover, MA.
**ULTRAVIOLET EMISSIONS OCCURRING ABOUT
HYPERSONIC VEHICLES IN RAREFIED FLOWS** Final Report,
4 Jun. 1993 - 4 Feb. 1994

GEORGE E. CALEDONIA and ROBERT H. KRECH Apr. 1994
60 p Limited Reproducibility: More than 20% of this document may be affected by microfiche quality
(Contract(s)/Grant(s): DAAH04-93-C-0015)
(AD-A281452; PSI-1177/TR-1305; ARO-31210.2-EG-SDI) Avail:
CASI HC A04

This report includes: (1) an investigation of the kinetic mechanisms for the visible shuttle glow; (2) an overview of flight and laboratory investigations of VUV to IR surface glows observed at hypersonic velocities in low earth orbit conditions; (3) a summary of the flight-measured absolute intensities observed for rarefied ram flow at VUV, UV and visible wavelengths as a function of altitude; and (4) a brief look at seeker sensor survivability/ viability issues associated with a High Velocity Missile (HVM) intended for boost phase interception. DTIC

N95-16099 Ohio State Univ., Columbus.
WING-BODY JUNCTURE FLOWS Final Report

RICHARD J. BODONYL Jan. 1994 44 p Limited Reproducibility: More than 20% of this document may be affected by microfiche quality
(Contract(s)/Grant(s): DAAL03-90-G-0186)
(AD-A281526; ARO-28249.2-EG) Avail: Issuing Activity (Defense Technical Information Center (DTIC))

Researchers have considered the flow structure near a small-

scale wing-body combination within the framework of triple-deck theory. Thin airfoil theory was used to obtain the pressure distribution around a wing which in turn triggers a viscous-inviscid interaction near the wing-body juncture. As part of the formulation of the problem they have followed the lead of Smith and Gajjar, utilizing the concept of an 'effective hump shape' in the formulation of the nonlinear problem. This technique not only simplifies the pressure expression but also enhances the convergence of the numerical scheme even though the concept itself is just a transformation to convert the wing-body problem into a more conventional problem for computational efficiency. DTIC

N95-16160# Stanford Univ., CA. Dept. of Aeronautics and Astronautics.

HIGH ALTITUDE HYPERSONIC FLOWFIELD RADIATION Final Report, 1 Jan. 1990 - 31 Mar. 1994

ROBERT W. MACCORMACK and DEAN R. CHAPMAN Apr. 1994
9 p

(Contract(s)/Grant(s): DAAL03-90-G-0031)
(AD-A281386; ARO-27480.6-EG-SDI) Avail: CASI HC A02/MF A01

Methods for computing radiation spectra and intensity are compared with available experimental data from three flight tests and five laboratory experiments. These involve both nonequilibrium and equilibrium flow. The comparison was facilitated by development of an improved radiation code, termed NEQAIR 2, incorporating vectorized programming to enable fine-structure spectra to be computed in a practical amount of time. The main sources of computational inaccuracy are found to stem from imperfect understanding of (1) what temperature or combination thereof in a multitemperature flowfield governs electronic excitation; (2) the physics of rotational relaxation at very high temperatures; and (3) the reaction rates for NO production at very high temperatures. Computed radiation is most accurate at low altitudes and hypersonic velocities, and least accurate at high altitudes and velocities. DTIC

N95-16251# Nanjing Univ. of Aeronautics and Astronautics, Nanjing, Jiangsu (China). Research Inst. of Pilotless Aircraft.

AN APPROACH TO AERODYNAMIC CHARACTERISTICS OF LOW RADAR CROSS-SECTION FUSELAGES

JIAZHENG PAN, YIFEI WANG, and CAIWEN ZHANG *In its* Joint Proceedings on Aeronautics and Astronautics (JPAA) p 11-18 May 1993

Avail: CASI HC A02/MF A03

This paper proves that polygonal section fuselages are better than circular section fuselage not only in stealthy characteristics (low radar cross section (RCS)), but also in aerodynamic characteristics, especially in lift force and maximum lift-drag ratio, by investigating low speed aerodynamic characteristics for three 'panel' polygonal section fuselage models with low RCS and one regular circular section fuselage model, through low speed tunnel testing of measuring forces, water tunnel field visualization and comparison between the results of the engineering evaluation and experiments at an angle of attack up to 50 degrees. Moreover, they can produce steady side forces larger than those of the circular section fuselage at high angles of attack and zero sideslip, and the produced angle of attack is lower than that of a circular one. The calculation method of polygonal section fuselages has not yet been perfected. In this paper a correction evaluation method is proposed that is given according to the contour characteristics of the corresponding section on the basis of the calculation method of a low aspect ratio wing and the calculated results are in good agreement with those of the experiments. Author (revised)

N95-16252# Nanjing Univ. of Aeronautics and Astronautics, Nanjing, Jiangsu (China). Research Inst. of Pilotless Aircraft.

AN IMPROVED METHOD OF AIRFOIL DESIGN

CAIWEN ZHANG *In its* Joint Proceedings on Aeronautics and Astronautics (JPAA) p 19-22 May 1993 See also A91-44768
Avail: CASI HC A01/MF A03

An improved method of airfoil design is proposed in this paper,

which transforms the design problem into the solution of a minimization problem of a multivariable function. It can be applied to the subcritical airfoil design, taking viscosity into consideration. Author

N95-16257# Nanjing Univ. of Aeronautics and Astronautics, Nanjing, Jiangsu (China). Dept. of Aerodynamics.

WALL-SIGNATURE METHODS FOR HIGH SPEED WIND TUNNEL WALL INTERFERENCE CORRECTIONS

QIWEI ZHANG *In its* Joint Proceedings on Aeronautics and Astronautics (JPAA) p53-62 May 1993 See also A93-20803 Avail: CASI HC A02/MF A03

Wall-signature methods for wall interference correction in NH-1 high speed wind tunnel model tests are presented. The methods correct tunnel wall interference effects using the measured pressure distribution near tunnel walls and the model force data. They do not require the knowledge of wall cross-flow properties, so can be used for various ventilated wall or solid wall wind tunnels. Hundreds of test cases of several models in various tunnels including solid wall, adaptive wall, perforated wall, slotted wall test sections are corrected by these methods. The test Mach number range is 0.5 to 0.9. The test Reynolds number range is 2×10^6 to 1×10^7 . The corrected results are compared with other correcting methods and Navier-Stokes free-air solutions. The correctness and practicality of these methods are proved. Author

N95-16563# National Technical Univ., Athens (Greece). Lab. of Thermal Turbomachines.

SINGLE-PASS METHOD FOR THE SOLUTION OF INVERSE POTENTIAL AND ROTATIONAL PROBLEMS. PART 1: 2-D AND QUASI 3-D THEORY AND APPLICATION

P. CHAVIAROPOULOS, V. DEDOUSSIS, and K. D. PAPAILIOU *In* AGARD, Optimum Design Methods for Aerodynamics 19 p Nov. 1994

Copyright Avail: CASI HC A03/MF A03

A methodology for the solution of the 2-D and 3-D inverse inviscid subsonic flow problem is introduced. The proposed methodology handles the 2-D and axisymmetric rotational and the 3-D potential target pressure problem in a single-pass manner. The method is based on a potential function/stream function formulation where the physical space is mapped onto a natural one using the potential and stream function(s) as body-fitted coordinates. A novel procedure based on differential geometry and generalized tensor analysis arguments is employed to formulate the method in a modular way. The governing equations for the inverse problem are derived through the metrics compatibility condition on the natural space. Geometry is determined by integrating generalized Frenet equations along the natural coordinate lines. Rotationality, when present, is due to incoming (stagnation) thermodynamic quantities and/or preswirl gradients. The Clebsch formulation is, then, adopted to decompose the velocity field into a potential and a rotational part. To validate the method inverse calculation results are compared to results of direct 'reproduction' calculations. The design procedure of some optimized shapes is also presented. Part 1 of this lecture focuses on 2-D and axisymmetric inverse potential or rotational flow problems, while the fully 3-D inverse potential problem is considered in Part 2. Author

N95-16564# National Technical Univ., Athens (Greece). Lab. of Thermal Turbomachines.

SINGLE-PASS METHOD FOR THE SOLUTION OF INVERSE POTENTIAL AND ROTATIONAL PROBLEMS. PART 2: FULLY 3-D POTENTIAL THEORY AND APPLICATIONS

P. CHAVIAROPOULOS, V. DEDOUSSIS, and K. D. PAPAILIOU *In* AGARD, Optimum Design Methods for Aerodynamics 14 p Nov. 1994

Copyright Avail: CASI HC A03/MF A03

A potential function/stream function formulation is introduced for the solution of the fully 3-D inverse potential 'target pressure' problem. Potential function and two stream vectors are used as the independent natural coordinates, whilst the velocity magnitude, as

well as, the aspect ratio and the cross-section angle of the elementary stream tubes are assumed to be the dependent ones. A novel procedure based on differential geometry is employed to formulate the method. The governing differential equations are derived by requiring the curvature tensor of the flat 3-D physical Euclidean space, expressed in terms of the curvilinear natural coordinates, to be zero. The resulting equations are discussed and investigated with particular emphasis to the existence and uniqueness of their solution. It is shown that the general 3-D inverse potential problem with target pressure boundary conditions only, is ill-posed accepting multiple solutions. This multiplicity is alleviated by considering elementary stream tubes with orthogonal cross-sections. The assumption of orthogonal stream surfaces reduces the number of dependent variables by one, simplifying the governing equations to an elliptic PDE, for the velocity magnitude and to a second order ODE for the stream tube aspect ratio. The solution of these two equations provides the flow field. Geometry is determined independently by integrating Frenet equations along the natural coordinate lines, after the flow field has been calculated. The numerical implementation as well as validation test cases for the proposed inverse methodology are presented in the last part of the lecture. Author

N95-16589*# California Univ., Davis, CA. Dept. of Mechanical and Aeronautical Engineering.

NUMERICAL SIMULATION OF HELICOPTER ENGINE PLUME IN FORWARD FLIGHT Final Report

ARSENIO C. B. DIMANLIG, CORNELIS P. VANDAM, and EARL P. N. DUQUE 1994 12 p Original contains color illustrations (Contract(s)/Grant(s): NCC2-5061) (NASA-CR-197488; NAS 1.26:197488) Avail: CASI HC A03/MF A01; 5 functional color pages

Flowfields around helicopters contain complex flow features such as large separated flow regions, vortices, shear layers, blown and suction surfaces and an inherently unsteady flow imposed by the rotor system. Another complicated feature of helicopters is their infrared signature. Typically, the aircraft's exhaust plume interacts with the rotor downwash, the fuselage's complicated flowfield, and the fuselage itself giving each aircraft a unique IR signature at given flight conditions. The goal of this project was to compute the flow about a realistic helicopter fuselage including the interaction of the engine air intakes and exhaust plume. The computations solve the Thin-Layer Navier Stokes equations using overset type grids and in particular use the OVERFLOW code by Buning of NASA Ames. During this three month effort, an existing grid system of the Comanche Helicopter was to be modified to include the engine inlet and the hot engine exhaust. The engine exhaust was to be modeled as hot air exhaust. However, considerable changes in the fuselage geometry required a complete regriding of the surface and volume grids. The engine plume computations have been delayed to future efforts. The results of the current work consists of a complete regeneration of the surface and volume grids of the most recent Comanche fuselage along with a flowfield computation. Author

N95-16808# Wright Lab., Wright-Patterson AFB, OH.

NUMERICAL SIMULATION OF TRANSIENT VORTEX BREAKDOWN ABOVE A PITCHING DELTA WING Final Report, 1 Jan. - 31 Dec. 1992

MIGUEL R. VISBAL 4 May 1994 43 p (Contract(s)/Grant(s): AF PROJ. 2307) (AD-A281075; WL-TR-93-3048) Avail: CASI HC A03/MF A01

Computational results are presented for transient vortex breakdown above a delta wing subject to a pitch-and-hold maneuver to high angle of attack. The flows are simulated by solving the full three-dimensional Navier-Stokes equations on a moving grid using the implicit Beam-Warming algorithm. An assessment of the effects of numerical resolution and favorable comparison with experimental data suggest the computational approach captures the basic dynamics of this transient breakdown. The pressure gradient along the vortex axis is found to play a dominant role in the initiation of breakdown. A description of the three-dimensional instantaneous structure of the flow field is provided using critical-point theory. The reversed-flow region in

02 AERODYNAMICS

the vortex core is associated with pairs of opposite spiral/saddle critical points. At its onset, the vortex breakdown is fairly axisymmetric; however, as it proceeds upstream and a stronger transition takes place along the axis, asymmetric effects become important and result in the formation of a bubble-type breakdown. This bubble structure is open and contains within itself a pair of stagnation points which are diametrically opposed and which rotate in the same sense as the base flow.

DTIC

N95-16824# Naval Postgraduate School, Monterey, CA.
MACH NUMBER, FLOW ANGLE, AND LOSS MEASUREMENTS DOWNSTREAM OF A TRANSONIC FAN-BLADE CASCADE M.S. Thesis

JEFFREY G. AUSTIN Mar. 1994 85 p
(AD-A280907) Avail: CASI HC A05/MF A01

Two dimensional flow measurements of Mach number and flow angle were conducted downstream of a transonic fan-blade cascade at a Mach number of 1.4 to provide baseline data for assessing the effect of vortex generating devices on the suction surface shock-boundary layer interaction. The experimental program consisted of the design and calibration of a traversing three-port pneumatic probe to measure Mach number and flow angle and initial cascade measurements to provide baseline data for the fully-mixed-out total pressure loss coefficient and flow turning angle. Similar tests are planned with the vortex generating devices installed. Comparisons with and without the vortex generating devices are needed to quantify the overall effect on the shock-boundary interaction in a transonic fan-blade passage, and to assess the potential for using vortex generating devices in military engine fans.

DTIC

N95-16858*# National Aeronautics and Space Administration. Hugh L. Dryden Flight Research Center, Edwards, CA.
DEVELOPMENT OF A LOW-ASPECT RATIO FIN FOR FLIGHT RESEARCH EXPERIMENTS

DAVID M. RICHWINE (Planning Research Corp., Edwards, CA.) and JOHN H. DELFRATE Washington Aug. 1994 16 p Presented at the 6th Biennial Flight Test Conference, Colorado Springs, CO, 20-23 Jun. 1993 Original contains color illustrations
(Contract(s)/Grant(s): RTOP 505-68-00)
(NASA-TM-4596; H-1993; NAS 1.15:4596; AIAA PAPER 94-2133)
Avail: CASI HC A03/MF A01; 3 functional color pages

A second-generation flight test fixture, developed at NASA Dryden Flight Research Center, offers a generic testbed for aerodynamic and fluid mechanics research. The new fixture, a low-aspect ratio vertical fin shape mounted on the centerline of an F-15B aircraft lower fuselage, is designed for flight research at Mach numbers up to 2.0. The new fixture is a composite structure with a modular configuration and removable components for functional flexibility. This report describes the multidisciplinary design and analysis approach used to develop the fixture. The approach integrates conservative assumptions with simple analysis techniques to minimize the time and cost associated with its development. Presented are the principal disciplines required for this effort, which include aerodynamics, structures, stability, and operational considerations. In addition, preliminary results from the first phase of flight testing are presented. Acceptable directional stability and flow quality are documented and show agreement with predictions. Future envelope expansion activities will minimize current limitations so that the fixture can be used for a wide variety of high-speed aerodynamic and fluid mechanics research experiments.

Author

N95-16887*# Sverdrup Technology, Inc., Brook Park, OH.
AN ANALYSIS CODE FOR THE RAPID ENGINEERING ESTIMATION OF MOMENTUM AND ENERGY LOSSES (REMEL) Final Report

LAWRENCE J. DECHANT Cleveland, OH NASA Nov. 1994 86 p
(Contract(s)/Grant(s): NAS3-25266; RTOP 505-69-50)
(NASA-CR-191178; E-8079; NAS 1.26:191178) Avail: CASI HC A05/MF A01

Nonideal behavior has traditionally been modeled by defining efficiency (a comparison between actual and isentropic processes), and subsequent specification by empirical or heuristic methods. With the increasing complexity of aeropropulsion system designs, the reliability of these more traditional methods is uncertain. Computational fluid dynamics (CFD) and experimental methods can provide this information but are expensive in terms of human resources, cost, and time. This report discusses an alternative to empirical and CFD methods by applying classical analytical techniques and a simplified flow model to provide rapid engineering estimates of these losses based on steady, quasi-one-dimensional governing equations including viscous and heat transfer terms (estimated by Reynold's analogy). A preliminary verification of REMEL has been compared with full Navier-Stokes (FNS) and CFD boundary layer computations for several high-speed inlet and forebody designs. Current methods compare quite well with more complex method results and solutions compare very well with simple degenerate and asymptotic results such as Fanno flow, isentropic variable area flow, and a newly developed, combined variable area duct with friction flow solution. These solution comparisons may offer an alternative to transitional and CFD-intense methods for the rapid estimation of viscous and heat transfer losses in aeropropulsion systems.

Author

N95-16908*# National Aeronautics and Space Administration. Langley Research Center, Hampton, VA.
COMPARISON OF COMPUTATIONAL AND EXPERIMENTAL RESULTS FOR A SUPERCRITICAL AIRFOIL

MELISSA B. RIVERS and RICHARD A. WAHLS Nov. 1994 30 p
(Contract(s)/Grant(s): RTOP 505-59-10-31)
(NASA-TM-4601; L-17330; NAS 1.15:4601) Avail: CASI HC A03/MF A01

A computational investigation was performed to study the flow over a supercritical airfoil model. Solutions were obtained for steady-state transonic flow conditions using a thin-layer Navier-Stokes flow solver. The results from this computational study were compared with time-averaged experimental data obtained over a wide Reynolds number range at transonic speeds in the Langley 0.3-Meter Transonic Cryogenic Tunnel. Comparisons were made at a nominal Mach number of 0.72 and at Reynolds numbers ranging from 6 x 10⁶ (exp 6) to 35 x 10⁶ (exp 6).

Author

N95-17178# Defence Science and Technology Organization, Melbourne (Australia).
DATA ACQUISITION AND PROCESSING SOFTWARE FOR THE LOW SPEED WIND TUNNEL TESTS OF THE JINDIVIK AUXILIARY AIR INTAKE

S. S. LAM Aug. 1994 46 p
(AD-A285455; DSTO-TR-0043; DODA-AR-007-100) Avail: CASI HC A03/MF A01

Data acquisition software has been developed for the wind tunnel tests of the auxiliary air intake of the Jindivik pilotless target aircraft in the AMRL Low Speed Wind Tunnel (LSWT) using the new Pressure Systems Incorporated (PSI) 8400 Measurement System under the control of an IBM PS/2 computer. The recent upgrade of the data acquisition system for the LSWT and the replacement of the mechanical Scanivalve pressure measuring system with PSI electronic pressure scanners has required major modifications to be made to existing software. To minimize the changes needed and to provide compatibility with data processing for previous tests, the data acquired by the PSI electronic pressure equipment are transferred to the dedicated LSWT DEC PDP-11/44 mini-computer for storage and processing. This report describes the development and operation of new software for the LSWT tests of the Jindivik auxiliary air intake.

DTIC

N95-17273*# Vigyan Research Associates, Inc., Hampton, VA.
TRANSONIC NAVIER-STOKES CALCULATIONS ABOUT A 65 DEG DELTA WING Final Report

W. KELLY LONDENBERG NASA Nov. 1994 71 p

(Contract(s)/Grant(s): NAS1-18585; RTOP 505-59-54-01)
(NASA-CR-4635; NAS 1.26:4635) Avail: CASI HC A04/MF A01

A computational study has been conducted in which the CFL3D Navier-Stokes solver coupled with an algebraic and a one-equation nonequilibrium turbulence model has been used to predict the flow over a 65 degree delta wing at transonic conditions for Reynolds numbers ranging from 6×10^6 to 120×10^6 based on mean aerodynamic chord. Solutions obtained indicated that the computational method when used with the one-equation turbulence model predicts results that compare well with experiment for attached flow conditions. Comparisons with experimental pressure at separated conditions show that the computational method, even though primary flow-field features are predicted well, does not predict secondary flow features. Author

N95-17291* Jet Propulsion Lab., California Inst. of Tech., Pasadena, CA.

FIELD VERIFICATION OF THE WIND TUNNEL COEFFICIENTS
W. K. GAWRONSKI and J. A. MELLSTROM *In its* The Telecommunications and Data Acquisition Report p 210-220 15 Nov. 1994
(Contract(s)/Grant(s): RTOP 314-40-52-01-02)
Avail: CASI HC A03/MF A03

Accurate information about wind action on antennas is required for reliable prediction of antenna pointing errors in windy weather and for the design of an antenna controller with wind disturbance rejection properties. The wind tunnel data obtained 3 years ago using a scaled antenna model serves as an antenna industry standard, frequently used for the first purpose. The accuracy of the wind tunnel data has often been challenged, since they have not yet been tested in a field environment (full-sized antenna, real wind, actual terrain, etc.). The purpose of this investigation was to obtain selected field measurements and compare them with the available wind tunnel data. For this purpose, wind steady-state torques of the DSS-13 antenna were measured, and dimensionless wind torque coefficients were obtained for a variety of yaw and elevation angles. The results showed that the differences between the wind tunnel torque coefficients and the field torque coefficients were less than 10 percent of their values. The wind-gusting action on the antenna was characterized by the power spectra of the antenna encoder and the antenna torques. The spectra showed that wind gusting primarily affects the antenna principal modes. Author

N95-17435 Naval Postgraduate School, Monterey, CA.
NUMERICAL OPTIMIZATION OF SYNERGETIC MANEUVERS
M.S. Thesis

JOHN C. NICHOLSON Jun. 1994 181 p Limited Reproducibility: More than 20% of this document may be affected by microfiche quality (AD-A283398) Avail: Issuing Activity (Defense Technical Information Center (DTIC))

The use of atmospheric forces to produce an orbital plane change requires less energy than a pure exoatmospheric propulsion maneuver. The combination of aerodynamic and propulsive forces to cause a change in orbital inclination is termed a synergetic maneuver. Several methods have been proposed to control the critical heating rate while performing the procedure. This thesis examines these control methods by numerically optimizing the trajectory for several fuel weights and heat rate constraints. The Program to Optimize Simulated Trajectories (POST) is used to simulate the maneuvers and control schemes and to perform the optimization. For no active heat constraints, it is shown that a gliding atmospheric entry followed by a maximum throttle bang produces significantly more inclination change than other proposed maneuvers. If the heat constraints are active, the recently proposed aerobang maneuvers produces a substantial inclination change while providing significant heating rate control and shows definite advantages over the long-studied aerocruise maneuver. DTIC

N95-17846# Advisory Group for Aerospace Research and Development, Neuilly-Sur-Seine (France). Fluid Dynamics Panel.
A SELECTION OF EXPERIMENTAL TEST CASES FOR THE

VALIDATION OF CFD CODES, VOLUME 2 [RECUEIL DE CAS D'ESSAI EXPERIMENTAUX POUR LA VALIDATION DES CODES DE L'AERODYNAMIQUE, VOLUME 2]
Aug. 1994 577 p See also 95N-14201 and diskette supplement AGARD-AR-303-Suppl (AGARD-AR-303-VOL-2; ISBN-92-836-1003-2) Copyright Avail: CASI HC A25/MF A06

This report presents the results of a study by Working Group 14 of the AGARD Fluid Dynamics Panel. The thirty nine test cases that are documented cover the subsonic, transonic, and supersonic flow regimes and five classes of geometries. Included in the five classes of geometries are: Two Dimensional Airfoils; Three Dimensional Wings, designed for predominantly attached flow conditions; Slender Bodies, typical of missile type configurations; Delta Wings, characterized by a conical type of vortex flow; and Complex Configurations, either in a geometrical sense or because of complicated flow interactions. The report is presented in two volumes. Volume 1 provides a review of the theoretical and experimental requirements, a general introduction, summary of the test cases and recommendations for the future. Volume 2 contains detailed information on the test cases. Relevant data has been compiled on floppy disks. For individual titles, see N95-17847 through N95-17885.

N95-17848# Defence Research Agency, Farnborough, Hampshire (England).
MEASUREMENTS ON A TWO-DIMENSIONAL AEROFOIL WITH HIGH-LIFT DEVICES

I. R. M. MOIR *In* AGARD, A Selection of Experimental Test Cases for the Validation of CFD Codes, Volume 2 12 p Aug. 1994
Copyright Avail: CASI HC A03/MF A06

The tests detailed in this submission were carried out by the former British Aircraft Corporation in support of the National High Lift Programme. This Programme was a collaborative project between the Royal Aerospace Establishment Farnborough (now part of the the DRA) and the aircraft industry with the aim of increasing the understanding and knowledge of all aspects of high-lift systems, and to provide a fund of data which would benefit the design of future transport aircraft. Wind-Tunnel tests were carried out on four models: (1) A 3-D half model (RAE); (2) a swept panel wing (HSA Hatfield); (3) a quasi-2D (end-plate) model (BAC Weybridge); and (4) a 2D model (BAC Weybridge). BAC Warton also carried out structural analyses on various leading-edge and trailing-edge devices. The present cases are results from the 2D tests which covered investigations into two leading-edge and two trailing-edge devices. The model had a supercritical aerofoil section, a chord of 0.7635m, and was mounted between turnables in the floor and roof of the BAC 3.96m x 2.74m low-speed wind-tunnel. Two-dimensional conditions were maintained by local suction around the wing/wall junctions. Surface pressures were measured on all the components of the wing, at two spanwise stations, one near the tunnel centerline, and one near the roof. These pressures were integrated to give overall lift, drag and pitching moment coefficients. A pilot/static traverse through the wake provided the total momentum deficit. Traverses perpendicular to the wing surface at various chordwise locations provided information on wake and boundary layer development and interaction. Flow visualization was provided by tufting of the wing surfaces. Author

N95-17849# Defence Research Agency, Bedford (England).
INVESTIGATION OF THE FLOW OVER A SERIES OF 14 PERCENT-THICK SUPERCritical AEROFOILS WITH SIGNIFICANT REAR CAMBER

P. R. ASHILL *In* AGARD, A Selection of Experimental Test Cases for the Validation of CFD Codes, Volume 2 13 p Aug. 1994
Copyright Avail: CASI HC A03/MF A06

The experiments described in this submission were performed

02 AERODYNAMICS

on various airfoil sections, all of 14 percent thickness/chord ratio and with significant rear camber. The main aim was to obtain an improved understanding of viscous effects on flows over airfoils with severe adverse pressure gradients. Such gradients can be found at the rear airfoils with significant rear camber and at the foot of shock waves. The tests were performed in the 8ft x 8ft Pressurized, Subsonic/Supersonic Wind Tunnel at the Defense Research Agency (DRA, formerly the Royal Aerospace Establishment) Bedford between November 1976 and February 1982. This wind tunnel has solid walls and, since the airfoil chord to tunnel height is relatively large (0.26), the data are strictly not correctable. This was recognized from the outset, the main concern of the investigation being studying flows rather than performing tests on a prescribed shape. However, the wall boundary conditions are well defined and so the data may be useful for validating CFD codes which include allowance for the wind-tunnel walls. In addition, measurements were made of the static pressures on the roof and floor of the working section, providing an independent check on the accuracy of the representation of the walls in any CFD method. Despite the caveat above about correctability, it is believed that the cases presented having weak shock waves may be used to assess free-air calculation methods provided that allowance is made in the calculation for wall-induced camber. Cases suitable for such work are highlighted in Section 6.2 where details are also given of the camber correction.

Author

N95-17850# National Research Council of Canada, Ottawa (Ontario). Inst. for Aerospace Research.

SURFACE PRESSURE AND WAKE DRAG MEASUREMENTS ON THE BOEING A4 AIRFOIL IN THE IAR 1.5X1.5M WIND TUNNEL FACILITY

D. J. JONES and Y. NISHIMURA *In* AGARD, A Selection of Experimental Test Cases for the Validation of CFD Codes, Volume 2 10 p Aug. 1994

Copyright Avail: CASI HC A02/MF A06

This 10.2 percent maximum thickness to chord airfoil has become a standard airfoil for Boeing wind tunnel tests in the IAR 1.5 X 1.5m facility. In order to study wall constraint effects, several different chord lengths have been used in the narrow span (38.1 cm) IAR facility and a 30.5 cm chord model was tested in the 1.5 wide facility. The latter data from the wide span facility are presented here. This data has a small sidewall correction while the upper and lower walls are accounted for using Mokry's wall correction procedures. Transition was fixed at 10 percent and all runs were made at a chord Reynolds number of 14 million. The tests were carried out in June-July, 1991.

Author

N95-17851# McDonnell-Douglas Corp., Long Beach, CA.

2-D AILERON EFFECTIVENESS STUDY

V. D. CHIN, C. J. DOMINIK, F. T. LYNCH, and D. L. RODRIGUEZ *In* AGARD, A Selection of Experimental Test Cases for the Validation of CFD Codes, Volume 2 20 p Aug. 1994

Copyright Avail: CASI HC A03/MF A06

The experimental data described in this contribution were obtained in the IAR High Reynolds Number 60 x 15 (1.5m x 0.38m) Two-Dimensional Test Facility. The purpose of the experiment was to investigate the effects of Reynolds number and Mach number on aileron effectiveness and to evaluate effectiveness of viscous scaling techniques that attempt to simulate flow at higher Reynolds numbers. The advent of the modern transport wing has prompted a renewed interest in the transonic characteristics of ailerons. In addition to their traditional role of lateral (roll) control, aileron are used for wing load alleviation and to improve cruise performance through the 'drooped aileron' concept. An understanding of the prevailing flow physics which limit the transonic performance of ailerons is necessary for the successful design of a control system that satisfies the multi-role requirements of the aileron. Results showed a linear variation of lift for upward trailing edge deflections but a highly nonlinear variation for downward deflections. This nonlinear behavior, equivalent to a loss in aileron effectiveness, became worse at higher angles of attack and higher Mach numbers. In addition, the viscous scaling technique that was used at lower

Reynolds numbers was found to be inadequate for modeling flow at higher Reynolds numbers. The data acquired from this test were for a series of aileron deflections varying from -5 to +5 deg at Mach numbers of 0.717 and 0.746 and chord Reynolds numbers of 5, 15, and 25 million. The following types of data were obtained: airfoil surface pressure distributions; wake drag, which was determined by wake transversing probes; lift and drag forces and pitching moment, which were determined by force balance readings and surface pressure integrations; and floor and ceiling pressure distributions, which were used to compute wall interference effects. One of the difficulties in wind tunnel testing is accounting for the effects of wall interference to reinterpret the data for 'free air' conditions. Corrections for interference effects of the floor and ceiling and for the wall sidewall boundary layer effects were applied to the data. The data are available corrected for floor and ceiling effects, and corrected for both floor and ceiling interference and sidewall boundary layer effects.

Author

N95-17852# Technische Hochschule, Aachen (Germany). Aerodynamisches Inst.

INVESTIGATION OF AN NLF(1)-0416 AIRFOIL IN COMPRESSIBLE SUBSONIC FLOW

P. GUNTERMANN and G. DIETZ *In* AGARD, A Selection of Experimental Test Cases for the Validation of CFD Codes, Volume 2 10 p Aug. 1994

Copyright Avail: CASI HC A02/MF A06

The data presented in this contribution were obtained in the 40 x 40 sq cm Transonic Wind Tunnel at the Aerodynamisches Institut of the RWTH Aachen within the research program 'Entwicklung von Berechnungsverfahren für Probleme der Strömungsmechanik' sponsored by the Stiftung Volkswagenwerk. The aim of the experimental part of the research program was to investigate the influence of compressibility on the location of transition. For this purpose a natural-laminar-flow airfoil NLF (1)-0416, designed for incompressible flow, was investigated. Starting with incompressible free stream conditions the Mach number was increased until transonic flow was obtained. The experiments on the NLF(1)-0416 should provide aerodynamical forces such as lift and drag and data concerning the location and the underlying physical mechanism of transition. Therefore different measuring techniques, e.g. liquid crystal coating and multi-sensor hot-film technique, were tested. To verify the existence of a laminar separation bubble the topology of the boundary layer was visualized. Regarding the different turbulence levels there is a good agreement of the experimental results with those obtained at NASA-Langley, which are available up to Mach numbers of 0.4. Numerical results correspond to the experiments at higher Mach numbers too. Experiments were carried out to get information about the influence of small disturbances of the profile surface on the pressure distribution, the drag, and the location of transition. In continuation of this research a wind tunnel model with adjustable geometry of its upper surface was developed and manufactured. The influence of small surface variations on the location of transition or separation will be investigated experimentally, but these tests are not part of the presented data set.

Author

N95-17853# Technische Hogeschool, Delft (Netherlands). Low Speed Aerodynamics Lab.

EXPERIMENTS IN THE TRAILING EDGE FLOW OF AN NLR 7702 AIRFOIL

L. H. J. ABSIL and D. M. PASSCHIER *In* AGARD, A Selection of Experimental Test Cases for the Validation of CFD Codes, Volume 2 16 p Aug. 1994

Copyright Avail: CASI HC A03/MF A06

Detailed mean flow and turbulence properties are presented of the flow in the vicinity of an airfoil trailing edge, to provide data for the development of turbulence models and the validation of computational methods.

Author

N95-17854# National Aerospace Lab., Amsterdam (Netherlands). **TWO-DIMENSIONAL 16.5 PERCENT THICK SUPERCRITICAL AIRFOIL NLR 7301**

S. O. T. H. HAN *In* AGARD, A Selection of Experimental Test Cases for the Validation of CFD Codes, Volume 2 11 p Aug. 1994
Copyright Avail: CASI HC A03/MF A06

This thick supercritical airfoil designed for a lift-coefficient of 0.595 at a Mach number of 0.721 (potential flow conditions) was an early NLR design of a supercritical airfoil made in 1973. The airfoil was designed with the hodograph method and has a rather blunt nose with a roof-top type pressure distribution. A typical other feature of this airfoil is that it is highly rear loaded, both on the upper surface and on the lower surface. Because of this rear loading, the airfoil is close to trailing edge separation on the upper surface and separation in the cove region around 70% chord at the lower surface. Tests have been made originally in the NLR (Transonic) Pilot Tunnel at a Reynolds number of 2.2 million (the design condition). The results of these tests have been included in AGARDograph AR-138. At about the same time test were made in the Compressible Flow Facility (CFD) of Lockheed (Georgia, USA) for the Reynolds number of 10, 20 and 30 million. In the eighties, when more advanced computer codes became available that could cope with airfoils that experienced a limited extent of separation, there was an urgent need for reliable data to validate the computer codes for these conditions. Also, the problem of scaling (low Reynolds number) wind tunnel tests to (the much higher) flight Reynolds numbers raised (again) considerably interest. For both reasons it was decided to repeat the original NLR 7301 experiments on a larger two-dimensional model in the large transonic wind tunnel HST of NLR. The tests covered the low speed and transonic speed regimes whereas part of the measurements was performed at constant lift for range of Reynolds numbers of study the indirect Reynolds number effects in more detail.
Author

**N95-17855# National Aerospace Lab., Amsterdam (Netherlands).
LOW-SPEED SURFACE PRESSURE AND BOUNDARY LAYER
MEASUREMENT DATA FOR THE NLR 7301 AIRFOIL
SECTION WITH TRAILING EDGE FLAP**

B. VANDENBERG and J. H. M. GOODEN *In* AGARD, A Selection of Experimental Test Cases for the Validation of CFD Codes, Volume 2 12 p Aug. 1994
Copyright Avail: CASI HC A03/MF A06

Test data are given for a two-dimensional wing flap configuration, which has been so designed that nowhere flow separations occur, apart from a small laminar separation bubble on the wing nose. The 32% chord trailing edge flap is deflected 20 deg. Two widths of the gap between wing and flap have been applied, with mixing of the wing wake and flap boundary layer occurring with the smaller gap. The experiment has been carried out at a Reynolds number $Re_c = 2.51 \cdot E6$ and a Mach number of about $Ma = 0.185$. The measurements comprise surface pressure data, from which lift and pitching moment coefficients were calculated, at various angles of attack from zero up to beyond stall. At three angles of attack the drag has been determined from wake traverses. At these angles mean flow measurements in the boundary layer and wake have been executed at 16 stations. In addition turbulence data were obtained at 5 stations in the wing wake above the flap. Surface flow visualization data are also available.
Author

**N95-17856# Office National d'Etudes et de Recherches Aeronautiques,
Toulouse (France).**

**DATA FROM THE GARTEUR (AD) ACTION GROUP 02
AIRFOIL CAST 7/DOA1 EXPERIMENTS**

A. MIGNOSI, J. P. ARCHAMBAUD, and E. STANEWSKY (Deutsche Forschungs- und Versuchsanstalt fuer Luft- und Raumfahrt, Goettingen, Germany.) *In* AGARD, A Selection of Experimental Test Cases for the Validation of CFD Codes, Volume 2 12 p Aug. 1994
Copyright Avail: CASI HC A03/MF A06

In order to gain a better understanding of the various forms and the magnitude of wind tunnel interferences that may arise in two-dimensional testing and to find improved methods of correction, a

GARTEur Action Group was formed in 1979 with the primary objectives of (1) comparing test results obtained with one airfoil (CAST 7) in a number of facilities in order to assess wall interference in the individual tunnels and to assess the accuracy of correction methods currently used and (2) evaluating three-dimensional interference effects associated with the side wall boundary layer. The wind tunnels considered consisted of five conventional tunnels with either slotted or perforated test section walls and two adaptive wall wind tunnels. Based on a comparison of the results from these tunnels, it was concluded that for these two-dimensional airfoil tests the freestream conditions, Mach number and angle of attack, were generally predicted with an accuracy of $\Delta M_\infty = \text{plus or minus } 0.002$ and $\Delta \alpha = \text{plus or minus } 0.1 \text{ deg}$ to plus or minus 0.05 deg , respectively, and the lift and drag coefficients with an accuracy of $\Delta C_{(sub L)} = \text{plus or minus } 0.015$ and $\Delta C_{(sub D)} = \text{plus or minus } 0.0003 \text{ deg}$, respectively. For the adaptive wall wind tunnel T2 of ONERA/CERT the accuracy in freestream conditions was determined to be $\Delta M_\infty = \text{plus or minus } 0.001$ and $\Delta \alpha = \text{plus or minus } 0.03 \text{ deg}$. Due to their relatively high accuracy, only the ONERA T2 adaptive wall tests are considered hereafter. The data, obtained with well defined boundary conditions, are believed to be the most suitable for CFD - assessment. Author

**N95-17857# Office National d'Etudes et de Recherches Aeronautiques,
Toulouse (France).**

OAT15A AIRFOIL DATA

A. M. RODDE and J. P. ARCHAMBAUD *In* AGARD, A Selection of Experimental Test Cases for the Validation of CFD Codes, Volume 2 13 p Aug. 1994
Copyright Avail: CASI HC A03/MF A06

The OAT15A airfoil is a supercritical airfoil for transport aircraft designed a few years ago within the framework of an ONERA/ Aeronautique joint programme devoted to the study of various designs. The design point is $M = 0.73$, $C_{(sub L)} = 0.65$ and the thickness to chord ratio of the airfoil is 12.3 percent. The tests which were performed in the ONERA/CERT T2 wind tunnel were devoted to the Reynolds number effects on the airfoil performance. These effects were investigated within the range 3-20 10^6 (exp 6) taking advantage of the cryogenic capability of the tunnel. The adaptive top and bottom walls of the tunnel give quasi free air conditions. However some sidewall effects are present and are taken into account in the correction procedure. Tests performed on another model in the S3MA wind tunnel with perforated top and bottom walls show good agreement with the T2 tests which give more confidence concerning the quality of the data. The proposed test cases concern mainly pressure distributions for various Reynolds numbers with fixed transition. However for a selected number of test cases boundary layer measurements with an external probe and LDV flow field data are also given. The set of data can be used for different purposes: (1) computer code capability for the prediction of Reynolds number effect; and (2) detailed 2D computer code assessment.

Author (revised)

**N95-17858*# National Aeronautics and Space Administration. Ames
Research Center, Moffett Field, CA.**

A SUPERCRITICAL AIRFOIL EXPERIMENT

GEORGE G. MATEER, H. LEE SEEGMILLER, LAWRENCE A. HAND, and JOACHIM SZODRUCH (Messerschmitt-Boelkow-Blohm G.m.b.H., Bremen, Germany.) *In* AGARD, A Selection of Experimental Test Cases for the Validation of CFD Codes, Volume 2 12 p Aug. 1994

Copyright Avail: CASI HC A03/MF A06

The purpose of this investigation is to provide a comprehensive data base for the validation of numerical simulations. The initial results of the study (single angle of attack) were presented in ref. 1, where the effects of various parameters and the adequacies of selected turbulence models were discussed. The objective of the present paper is to provide a tabulation of the experimental data. The

02 AERODYNAMICS

data were obtained in the two-dimensional, transonic flowfield surrounding a supercritical airfoil. A variety of flows were studied in which the boundary layer at the trailing edge of the model was either attached or separated. Unsteady flows were avoided by controlling the Mach number and angle of attack. Surface pressures were measured on both the model and wind tunnel walls, and the flowfield surrounding the model was documented using a laser Doppler velocimeter (LDV). Although wall interference could not be completely eliminated, its effect was minimized by employing the following techniques. Sidewall boundary layers were reduced by aspiration, and upper and lower walls were contoured to accommodate the flow around the model and the boundary-layer growth on the tunnel walls. A data base with minimal interference from a tunnel with solid walls provides an ideal basis for evaluating the development of codes for the transonic speed range because the codes can include the wall boundary conditions more precisely than interference corrections can be made to the data sets. Author

**N95-17859# Boeing Commercial Airplane Co., Seattle, WA.
TWO-DIMENSIONAL HIGH-LIFT AIRFOIL DATA FOR CFD
CODE VALIDATION**

G. W. BRUNE *In* AGARD, A Selection of Experimental Test Cases for the Validation of CFD Codes, Volume 2 13 p Aug. 1994
Copyright Avail: CASI HC A03/MF A06

The purpose of the experimental investigation summarized below was to provide a complete data set for the validation of two-dimensional multi-element airfoil computer codes. The airfoil model used for this investigation features four elements including a double slotted trailing edge flap and a slotted leading edge device representing a section of a transport wing in high-lift configuration with take-off flap setting. The leading edge flap was tested in a nonoptimum setting in order to produce a thick confluent boundary layer on the upper airfoil surface. In this wind tunnel experiment, all data were measured on a single high-lift airfoil configuration with a fixed flap setting at one tunnel freestream condition. Emphasis was placed on the acquisition of a few high quality airfoil data with many repeat runs and redundant measurements. Measured data comprise airfoil lift, drag, pitching moment, surface pressures, mean velocity profiles and Reynolds stresses of the confluent boundary layer. The data was obtained in the Boeing Research Wind Tunnel located in Seattle at 0.11 Mach number and 1.55 million Reynolds number based on tunnel freestream velocity and a flaps-up airfoil chord of 0.6096 m (2 ft). Care was taken to achieve a close approximation to two-dimensional flow by means of turntable and tunnel side wall blowing. Two-dimensional flow was verified by comparing boundary layer mean velocity and turbulence profiles at several spanwise stations, and by various surface flow visualizations methods. In addition, lift curves from balance measurements and an integration of surface pressures were compared. Confluent boundary layer measurements were conducted employing a Pitot probe and hot wires. Probes were mounted on a mechanical traverser designed to minimize disturbances of overall airfoil circulation and of the local flow at the measuring station. Author

**N95-17860# Defence Research Agency, Farnborough, Hampshire (England). Aerodynamics and Propulsion Dept.
MEASUREMENTS OF THE FLOW OVER A LOW ASPECT-RATIO WING IN THE MACH NUMBER RANGE 0.6 TO 0.87 FOR THE PURPOSE OF VALIDATION OF COMPUTATIONAL METHODS. PART 1: WING DESIGN, MODEL CONSTRUCTION, SURFACE FLOW. PART 2: MEAN FLOW IN THE BOUNDARY LAYER AND WAKE, 4 TEST CASES**

M. C. P. FIRMIN and M. A. MCDONALD *In* AGARD, A Selection of Experimental Test Cases for the Validation of CFD Codes, Volume 2 18 p Aug. 1994
Copyright Avail: CASI HC A03/MF A06

The experiments presented should improve the understanding of the flow over a wing as the speed is increased towards the buffet and separation boundaries. These boundaries limit the flight envelopes of both military and civil aircraft, and the measurements

reported will allow Computational Fluid Dynamic (CFD) methods for viscous flow to be validated. The measurements are reported in two documents (Parts 1 & 2) giving detailed measurements of the subsonic free stream flow over a low aspect-ratio wing (RAE Model 2155) at conditions where the boundary layers are subjected to severe adverse pressure gradients. Part 1 provides measurements of pressure distributions on both the wing and on the tunnel walls for a wide range of Mach numbers and lift coefficients, as well as of wing surface skin friction and surface flow direction measurements for four test cases, while Part 2 contains detailed mean flow measurements within the shear layers. For this detailed study, the same four test cases have been used, as presented in Part 1. They were chosen to provide examples of flows with severe adverse pressure gradients, including those with shock waves, and leading in some cases to separation. Author

**N95-17861# Defence Research Agency, Bedford (England).
DETAILED STUDY AT SUPERSONIC SPEEDS OF THE FLOW
AROUND DELTA WINGS**

M. J. SIMMONS *In* AGARD, A Selection of Experimental Test Cases for the Validation of CFD Codes, Volume 2 17 p Aug. 1994
Copyright Avail: CASI HC A03/MF A06

The tests described in this submission were made on two half-models of delta-wing/body configuration suitable for supersonic combat aircraft. The aim of the program of work was to improve the understanding of supersonic flows over wing with rounded leading edges. The reason for choosing the large half-model design were: (1) the attainment of high chordal Reynolds numbers; (2) the facility to make detailed flow measurements; and (3) the ability to manufacture the large wing to the desired model accuracy with conventional machine tolerances. The last requirement is particularly important in the highly-curved region of the leading edge which controls the development of transonic flows on the upper surface. Both wings are of the same quasi-delta planform of 60 leading edge sweep and thickness form of 4% thickness/chord ratio but with differing camber distributions. Wing A has a complex camber surface with camber in both spanwise and streamwise planes. Wing C has an uncambered symmetrical section and was used as a datum case for the study. The only design constraint on model size was the need to ensure that the flow over the wing was not disturbed by shock-wave reflections from the solid walls of the tunnel. The tests were performed in the 8ft x 8ft Pressurized, Subsonic/Supersonic Wind Tunnel at the Defense Research Agency (DRA Aerospace Division, formerly the Royal Aerospace Establishment) Bedford in July 1985. Author (revised)

**N95-17862# Defence Research Agency, Bedford (England).
PRESSURE DISTRIBUTIONS ON RESEARCH WING W4
MOUNTED ON AN AXISYMMETRIC BODY**

J. L. FULKER *In* AGARD, A Selection of Experimental Test Cases for the Validation of CFD Codes, Volume 2 12 p Aug. 1994
Copyright Avail: CASI HC A03/MF A06

The experiments described in this submission were performed on a wing-body configuration suitable for a civil transport aircraft. When the wing was designed (1972) it was recognized that, in order to achieve an advance in technology, a significant increase in rear loading would be required compared to that of earlier designs. As a consequence, the boundary layer conditions close to the trailing edge on the upper surface were expected to be more adverse than in previous designs. This requirement led to the need for a high test Reynolds number, which was achieved by testing a large half model in the Defense Research Agency (DRA) 8ft x 8ft Wind Tunnel at Reynolds numbers, based on geometric mean chord, of up to 15 x 10⁶ (exp 6). Complementary tests were also performed on a smaller complete model in order to provide an accurate assessment of the drag characteristics of the wing. The wing was designed to have a weak shock wave near mid chord on the upper surface at the cruise condition ($C_{sub L} = 0.32$, $M = 0.78$). The overall aims of the investigation were to obtain an improved understanding of the behavior of the flow over wings of this type over a wide range of subsonic Mach numbers and Reynolds numbers. The tests were

performed during 1977 on the complete model and 1978 on the half model. The wind tunnel has solid walls, and since the models are relatively large, the data are strictly not correctable. However, the wall boundary conditions are well defined and so the data may be useful for validating CFD codes which include allowance for the wind-tunnel walls. In addition measurements were made on the static pressures on the roof and floor of the working section, providing an independent check on the accuracy of the representation of the walls in any CFD method. Derived from text

N95-17864# Deutsche Forschungsanstalt fuer Luft- und Raumfahrt, Goettingen (Germany).

DLR-F5: TEST WING FOR CFD AND APPLIED AERODYNAMICS

H. SOBIECZKY *In* AGARD, A Selection of Experimental Test Cases for the Validation of CFD Codes, Volume 2 11 p Aug. 1994
Copyright Avail: CASI HC A03/MF A06

A swept wing with symmetrical sections was originally created to serve two purposes. First, the surface generator used for data definition was under development for aerodynamic design and optimization. The wing created was intended therefore to be a selected case of a whole family of configurations obtained by variation of the input parameters. Aerodynamic design and optimization strategies call for such variations. Second, CFD code development needs both accurate test case geometries as well as experimental results from wind tunnels. The latter usually suffer from corrections which still might suit practical purposes of measuring aerodynamic coefficients but fall short of the requirement to define the flow conditions to the same accuracy as geometrical boundaries are known. Using the generator software, a compromise was chosen by including the closed wind tunnel wall geometry as a channel boundary surrounding an aerodynamic component. In order to also avoid model support problems, a wing half model mounted on and including a splitter plate was used as 'configuration.' Geometry of the flow boundaries was completely defined through the simple rectangular channel geometry completed by chosen inlet and exit planes. Flow data were required at these planes to formulate a boundary value problem for CFD. In a workshop to compare CFD results with the first test case experiment (1986), partners had obtained and used a computer code to generate the wing and the wind tunnel boundary conditions, along with the absolutely necessary parameters to formulate fluid dynamic boundary conditions for the Navier-Stokes equations. This software is a simplified version of the geometry generator for aerospace configurations and CFD grid generation which has since been further developed as an industrial tool for design aerodynamics. The experiment and the refined half-model technique was published and the results of the workshop, comparing numerical results, have been summarized. Based on these results we may conclude that for CFD this test case turns out to be a complicated one basically because of the observed viscous flow phenomena on the wing. On the other hand, the definition of the complete boundary value problem makes the case rather unique and, with the help of generator software and experimental data, easy to implement for CFD validation. The workshop software and experimental results for surface pressure distributions is made available in one package. Derived from text

N95-17865*# National Aeronautics and Space Administration. Ames Research Center, Moffett Field, CA.

LOW ASPECT RATIO WING EXPERIMENT

MIKE OLSEN and H. LEE SEEGMILLER *In* AGARD, A Selection of Experimental Test Cases for the Validation of CFD Codes, Volume 2 11 p Aug. 1994

Copyright Avail: CASI HC A03/MF A06

This test was initiated to provide validation data on low aspect ratio wings at transonic speeds. The test was conducted so that the data obtained would be useful in the validation of codes, and all boundary condition data required would be measured as part of the test. During the conduct of the test, the measured quantities were checked for repeatability, and when the data would not repeat, the

cause was tracked down and either eliminated or included in the measurement uncertainty. The accuracy of the data was in the end limited by wall imperfections of the wind tunnel in which the test was run. Derived from text

N95-17866# Deutsche Forschungsanstalt fuer Luft- und Raumfahrt, Cologne (Germany). Hauptabteilung Windkanale.

WIND TUNNEL INVESTIGATIONS OF THE APPEARANCE OF SHOCKS IN THE WINDWARD REGION OF BODIES WITH CIRCULAR CROSS SECTION AT ANGLE OF ATTACK

H. ESCH *In* AGARD, A Selection of Experimental Test Cases for the Validation of CFD Codes, Volume 2 16 p Aug. 1994

Copyright Avail: CASI HC A03/MF A06

Originally the model was designed to investigate differences in the interference of fuselage and control surfaces attached to bodies of circular and rectangular cross sections. During the test it was found difficult to define the interference since the reference configuration, the isolated body without controls, showed some disturbances in the pressure distribution at certain combinations of Mach number and angle of attack. These disturbances are connected with the appearance of shock waves on the windward side of isolated circular bodies. By checking schlieren pictures made during earlier test series of missiles the range could be defined in which this type of shock occurs. Pressure distribution measurements were made in order to find an explanation for the formation of the shocks and their bending into the windward region. It is believed that three conditions must be fulfilled: (1) Crossflow Mach number must be high enough that a shock forms in front of the wedge-like primary separation. (2) The primary separation line must move towards the windward side of the body. As a result the local Mach number normal to the separation line decreases, and eventually the shock detaches - if the crossflow Mach number is not too high. (3) When the local surface Mach number normal to the body axis is less than one, the disturbances propagate towards the windward region of the body. In some cases this type of disturbance may lead to confusion especially when there are not enough pressure taps: in the pressure distribution one finds only one or two peaks and from this, one cannot identify the shock trace. The model is extremely simple and thus the generation of a grid should not be too expensive. The data are considered valuable for CFD validation but on the other hand CFD should be useful to get more information of the outer flow field and further insight into this more fundamental flow phenomenon. Derived from text

N95-17868# Deutsche Forschungsanstalt fuer Luft- und Raumfahrt, Goettingen (Germany).

FORCE AND PRESSURE DATA OF AN OGIVE-NOSED SLENDER BODY AT HIGH ANGLES OF ATTACK AND DIFFERENT REYNOLDS NUMBERS

K. HARTMANN *In* AGARD, A Selection of Experimental Test Cases for the Validation of CFD Codes, Volume 2 13 p Aug. 1994

Copyright Avail: CASI HC A03/MF A06

Force, moment, flow field, and pressure measurements (steady and unsteady) were carried out on an ogive-nosed circular cylinder body with a smooth surface. The tests were performed in the two open jet low speed wind tunnels of the DLR in Gottingen (NWG, test section size 3 m x 3 m) and in Braunschweig (NWB, test section size 2.8 m x 3.25 m). A body diameter of $D = 200$ mm was chosen to achieve Reynolds numbers as high as possible at the maximum speed in these tunnels. The tests comprise angles of attack from 0 to 90 deg and Reynolds numbers of 2.5×10^5 (exp 5), 3.7×10^5 (exp 5), and 7.7×10^5 (exp 5) (based on body diameter and freestream conditions). For six angles of attack between 20 and 70 deg the dependence on different roll positions of the body was systematically investigated with a complete coverage of 360 deg. In some cases the turbulence level of the freestream was varied. The body vortices were visualized in a water towing tank using hydrogen bubbles and in the wind tunnel with the aid of smoke and a laser lightsheet. Derived from text

02 AERODYNAMICS

N95-17870# Office National d'Etudes et de Recherches Aeronautiques, Paris (France).

SUPERSONIC VORTEX FLOW AROUND A MISSILE BODY

D. BARBERIS *In* AGARD, A Selection of Experimental Test Cases for the Validation of CFD Codes, Volume 2 11 p Aug. 1994
Copyright Avail: CASI HC A03/MF A06

Boundary-layer separation occurring on a missile body at moderate or high angle of incidence leads to the formation of well organized vortical structures, especially at supersonic flight Mach numbers. Even though a certain number of experimental results are available for this type of flow, none of the published data provide complete information for a supersonic flow. A experimental study of the flowfield around a 3 caliber tangent ogive-cylinder body in a supersonic flow has been carried out to provide a consistent description of the flow. This experiment includes oil flow visualizations, primary separation line determination, surface pressure measurements and five hole pressure probe surveys for a Mach number of 2 and an angle of incidence varying from 0 to 20 deg. Results are obtained for a natural and fixed transition. Author

N95-17872# National Aerospace Lab., Amsterdam (Netherlands).

WIND TUNNEL TEST ON A 65 DEG DELTA WING WITH A SHARP OR ROUNDED LEADING EDGE: THE INTERNATIONAL VORTEX FLOW EXPERIMENT

A. ELSENAAR *In* AGARD, A Selection of Experimental Test Cases for the Validation of CFD Codes, Volume 2 18 p Aug. 1994
Copyright Avail: CASI HC A03/MF A06

The windtunnel tests carried out on this model resulted from an international co-operation that involved the aeronautical laboratories AFWAL (US), DLR (Germany), FFA (Sweden), NLR (The Netherlands) and the Universities of Braunschweig (Germany) and Delft (The Netherlands). It was the basic aim of these measurements to provide detailed pressure and flow field data on a 65 deg delta wing configuration of a generic shape for the validation of CFD methods, notably Euler methods. For this reason one of the basic configurations had a sharp leading edge. However, there was also considerable interest for configurations with more realistic features and therefore other configurations were added. These featured a wing with a smaller sweep angle (55 instead of 65 deg), a rounded instead of a sharp leading edge shape, a drooped leading edge and the addition of a canard wing. The windtunnel tests were made in different wind tunnels with different models. They covered a large range of flow conditions and measuring techniques (including force, pressure and flow field measurements). The test case to be described here covers only the force and pressure measurements as carried out at NLR in the transonic windtunnel HST and the supersonic windtunnel SST. The measurements executed at DLR, including flow field measurements, can be found in case D-4. Author

N95-17873# Office National d'Etudes et de Recherches Aeronautiques, Paris (France).

DELTA-WING MODEL

D. BARBERIS *In* AGARD, A Selection of Experimental Test Cases for the Validation of CFD Codes, Volume 2 11 p Aug. 1994
Copyright Avail: CASI HC A03/MF A06

A detailed study has been made on the flow around a 75 sweep angle delta wing to provide reference material or numerical codes. Experiments were carried out in the F2 wind tunnel of the ONERA Le Fauga - Mauzac Centre. Firstly an examination of the surface flow properties was carried out using surface pressure measurements and surface flow visualizations with a viscous coating. The angle of incidence was varied between 5 and 30 deg and the upstream velocity between 10 and 75 m/s. Secondly, the aerodynamic field was characterized by means of laser tomography visualizations and surveys with a two component laser Doppler velocimeter system. Mean and fluctuating velocity fields were determined in several vertical planes normal to the wind tunnel longitudinal axis. These measurements were carried out for an angle of incidence of 20 deg and for two values of the upstream velocity (24 m/s and 40 m/s). Author

N95-17874# Technische Hogeschool, Delft (Netherlands). Faculty of Aerospace Engineering.

EXPERIMENTAL INVESTIGATION OF THE VORTEX FLOW OVER A 76/60-DEG DOUBLE DELTA WING

N. G. VERHAAGEN and J. E. J. MASELAND *In* AGARD, A Selection of Experimental Test Cases for the Validation of CFD Codes, Volume 2 15 p Aug. 1994
Copyright Avail: CASI HC A03/MF A06

Data was obtained from a low-speed wind-tunnel experiment carried out on a sharp-edged 76/60-deg double-delta wing. The objective of the investigation was to generate data on the vortex interaction downstream of the strake-wing leading-edge kink of a double-delta wing. An oil-flow and laserlight-sheet technique was used to visualize the flow on and off the surface of the wing. Balance measurements were performed to determine the forces and moments acting on the wing. In addition, the pressure on the upper surface of the wing was measured at several wing chordwise stations. Using a thin five-hole probe, the flowfield over the wing panel was surveyed in detail for an incidence of 20 deg. The data provide information on the interaction process of the wing and strake vortex as well as the development of the secondary separation downstream of the leading-edge kink. Author

N95-17875# Deutsche Forschungsanstalt fuer Luft- und Raumfahrt, Goettingen (Germany).

WIND TUNNEL TEST ON A 65 DEG DELTA WING WITH ROUNDED LEADING EDGES: THE INTERNATIONAL VORTEX FLOW EXPERIMENT

K. HARTMANN, K. A. BUETEFISCH, and H. PSZOLLA *In* AGARD, A Selection of Experimental Test Cases for the Validation of CFD Codes, Volume 2 12 p Aug. 1994
Copyright Avail: CASI HC A03/MF A06

The wind tunnel tests carried out on this model resulted from an international cooperation that involved the aeronautical laboratories AFWAL (US), DLR (Germany), FFA (Sweden), NLR (The Netherlands) and the Universities of Braunschweig (Germany) and Delft (The Netherlands). It was the basic aim of these measurements to provide detailed pressure and flow field data on a 65 deg delta wing configuration of a generic shape for the validation of CFD methods, notably Euler methods. For this reason one of the basic configurations had a sharp leading edge. However, there was also considerable interest for configurations with more realistic features and therefore other configurations were added. These featured a wing with a smaller sweep angle (55 instead of 65 deg), a rounded instead of a sharp leading edge shape, a drooped leading edge and the addition of a canard wing. The wind tunnel tests were made in different wind tunnels with different models. They covered a large range of flow conditions and measuring techniques including force, pressure and flow field measurements. The test case to be described here covers the force, pressure and flow field measurements and flow visualization as carried out at DLR in the transonic wind tunnel TWG on the smaller scale model with round leading edges. This configuration was designed and manufactured by the MBB company in Germany. Author

N95-17876# Aircraft Research Association Ltd., Bedford (England). **INVESTIGATION OF THE FLOW DEVELOPMENT ON A HIGHLY SWEEPED CANARD/WING RESEARCH MODEL WITH SEGMENTED LEADING- AND TRAILING-EDGE FLAPS**

D. STANNILAND *In* AGARD, A Selection of Experimental Test Cases for the Validation of CFD Codes, Volume 2 18 p Aug. 1994
Copyright Avail: CASI HC A03/MF A06

The results included in this submission are drawn from the extensive testing which has been carried out on a simple canard/wing research model with a low aspect ratio (2.3), highly swept (58 deg) wing with leading- and trailing-edge flaps. The purpose of these tests was to improve the understanding of the flow development of

this class of configuration, to validate the CFD method and philosophy used for the wing design and to provide an extensive data base of pressure data on a precisely specified model geometry for the validation of CFD methods which are capable of handling more complex geometries. The wing was designed using an FP wing/body code, aiming for attached flow at a high subsonic maneuver design point. This results in a highly cambered and twisted wing with a complex flow breakdown on the upper surface. The use of a segmented leading-edge flap means that the vortical flow develops as a series of part-span vortices, even at a constant flap setting with the gaps between the flap segments sealed. The model has been tested in the ARA 9ft by 8ft Transonic Wind Tunnel over the period 1985 - 1992 to investigate: (1) the effect of a canard, including variation in its position and setting angle; (2) the effect of alternative leading- and trailing-edge flap angles, including both positive and negative settings, although the model is capable of being tested with graded settings across the span (this option has not been investigated to date); (3) a three surface configuration (canard/wing/tailplane); and (4) a blended wing/body derivative of the model, using the existing outer wing and canard designs. Obviously these tests provide an extensive data base and the results included here comprise the datum wing without flap deflection, both with and without a canard. Author

N95-17877# Deutsche Forschungsanstalt fuer Luft- und Raumfahrt, Brunswick (Germany). Inst. fuer Entwurfsaerodynamik.
SUBSONIC FLOW AROUND US-ORBITER MODEL FALKE IN THE DNW

R. RADESPIEL and A. QUAST *In* AGARD, A Selection of Experimental Test Cases for the Validation of CFD Codes, Volume 2 13 p Aug. 1994

Copyright Avail: CASI HC A03/MF A06

The contribution describes wind tunnel measurements of aerodynamic forces, pressure distributions and surface visualization for the FALKE model. FALKE is a model of the US-Orbiter in the scale 1:5.427. The test results taken in the subsonic wind tunnel DNW enable validation of computational methods for reentry vehicles in landing conditions at high Reynolds numbers, where strong vortical flow occurs on the upper side of the configuration. Author

N95-17878# Deutsche Forschungsanstalt fuer Luft- und Raumfahrt, Brunswick (Germany). Inst. fuer Entwurfsaerodynamik.
PRESSURE DISTRIBUTION MEASUREMENTS ON AN ISOLATED TPS 441 NACELLE

R. KIOCK and W. BAUMERT (Deutsche Forschungsanstalt fuer Luft- und Raumfahrt, Goettingen, Germany.) *In* AGARD, A Selection of Experimental Test Cases for the Validation of CFD Codes, Volume 2 9 p Aug. 1994

Copyright Avail: CASI HC A02/MF A06

The demand for even more economic jet engines requires extensive experimental investigations of the complete flow field around wing-body-engine-pylon (WBEP) configurations. The engine can be simulated best by pressure-driven devices, so-called Turbine-Powered Simulators (TPS). Though they have been applied for about 20 years, very few nacelle surface pressure measurements were carried out up to now. The reason is seen in the small size of the engine and in the poor theoretical capabilities in the past. Nowadays, WBEP configurations are handled by the Euler code, but experimental validation is required. One pre-step is the experimental investigation of the isolated nacelle which is presented here. Author

N95-17879# National Aeronautics and Space Administration, Langley Research Center, Hampton, VA.

SINGLE-ENGINE TAIL INTERFERENCE MODEL

BOBBY L. BERRIER *In* AGARD, A Selection of Experimental Test Cases for the Validation of CFD Codes, Volume 2 23 p Aug. 1994

Copyright Avail: CASI HC A03/MF A06

The data presented in this contribution were obtained in the NASA Langley 16-Foot Transonic Tunnel. Multiple test entries were completed and the results have been completely reported in five NASA reports. The objective of the initial investigation was to determine the effect of empennage (tail) interference on the drag characteristics of an axisymmetric model with a single engine fighter aft-end with convergent divergent nozzles. Two nozzle power settings, dry and maximum afterburning, were investigated. Several empennage arrangements and afterbody modifications were investigated during the initial investigation. Subsequent investigations were used to determine the effects of other model variables including tail incidence, tail span, and nozzle shape. For the final investigation, extensive surface pressure instrumentation was added to the model in order to develop an understanding of the flow interactions associated with afterbody/empennage integration and also to provide data for code validation. Extensive computational analysis has been conducted on the staggered empennage configuration at a Mach number of 0.6 utilizing a three-dimensional Navier Stokes code. Most of the investigations were conducted at Mach numbers from 0.60 to 1.20 and at ratios of jet total pressure to free stream static pressure (nozzle pressure ratio) from 0.1 (jet off) to 8.0. Some angle of attack variation was obtained at jet off conditions. Author

N95-17880# National Aeronautics and Space Administration, Langley Research Center, Hampton, VA.

TWIN ENGINE AFTERBODY MODEL

DAVID J. WING *In* AGARD, A Selection of Experimental Test Cases for the Validation of CFD Codes, Volume 2 17 p Aug. 1994

Copyright Avail: CASI HC A03/MF A06

This test was originally conducted to determine the effects of several empennage and afterbody parameters on the aft-end aerodynamic characteristics of a twin-engine fighter-type configuration. Model variables were as follows: horizontal tail axial location and incidence, vertical tail axial location and configuration (twin-vs single-tail arrangements), tail booms, and nozzle power setting. Jet propulsion was simulated by exhausting high-pressure, cold-flow air from the nozzles. Following a successful test conducted on a single engine nacelle model to validate a CFD code, this model was chosen to be instrumented with pressure taps on the afterbody and nozzles and used as a follow-on test, providing a more complex geometry for the CFD code validation. A more limited test matrix was run to collect the pressure data, employing only the twin-tail configuration and varying only the horizontal and vertical tail locations. Mach number was varied from 0.6 to 1.2. Nozzle pressure ratio was varied from jet-off to 8. Angle-of-attack varied from 0 to 8 deg. Author

N95-17881# National Aeronautics and Space Administration, Ames Research Center, Moffett Field, CA.

STOVL CFD MODEL TEST CASE

KARLIN R. ROTH *In* AGARD, A Selection of Experimental Test Cases for the Validation of CFD Codes, Volume 2 16 p Aug. 1994

Copyright Avail: CASI HC A03/MF A06

The transitional flight characteristics of a geometrically simplified Short Take-Off Vertical Landing (STOVL) aircraft configuration have been measured in the NASA Ames 7- by 10-Foot Wind Tunnel. The experiment is the first in a sequence of tests designed to provide detailed data for evaluating the capability of computational fluid dynamics methods to predict the important flow parameters for powered lift. The model consists of a 60 deg cropped delta wing platform, blended fuselage and two circular in-line jets that exit perpendicularly from the flat lower surface. The measured flows have a maximum freestream Mach number of 0.2. Model angle of attack is varied between -10 and +20 deg. The flow is ambient temperature in both jet exits and the nozzle pressure ratios are varied between 1 and 3. The data presented includes forces and moments, pressures measured at 281 surface pressure ports and

02 AERODYNAMICS

the pressures of the jets. Measurements of the flow are also made in the tunnel test section upstream and downstream of the model and at the jet exits to guide boundary condition selection for the planned computations. Flow visualization and total pressure measurements in the jet plumes provide a description of the three-dimensional jet efflux flowfield. Author

N95-17882# Aeronautical Research Inst. of Sweden, Bromma. Flygtekniska Foersoeksanstalten.

LOW SPEED PROPELLER SLIPSTREAM AERODYNAMIC EFFECTS

I. SAMUELSSON In AGARD, A Selection of Experimental Test Cases for the Validation of CFD Codes, Volume 2 21 p Aug. 1994 Copyright Avail: CASI HC A03/MF A06

The data presented in this contribution to AGARD WG-14: 'EXPERIMENTAL TEST CASES FOR CFD VALIDATION' were obtained at tests in the FFA Low Speed Wind Tunnel LT1 (diameter 3.6 m) as part of an aeronautical research programme sponsored by the Swedish Board for Technical Development (STU). The intent of the experiment was two-fold: (1) to gain some physical insight to the complex aerodynamic interference phenomena occurring when the slip-stream from a highly loaded propeller washes downstream located surfaces (nacelle and wing); (2) to provide surface pressures and flow field data for evaluation of three-dimensional flow computation methods. The performed wind tunnel tests show that in high power conditions at low speeds large asymmetrical loads can develop on the nacelle and on the wing. For e.g. an aircraft with two propellers having the same sense of rotation these loads do not cancel out but combine to a net increase in asymmetrical loads (in particular side force and yawing moment). These effects, if not known or accounted for in advance, could lead to a resizing of the aircraft control surfaces and/or necessary trim changes with subsequent increased trim drag. Author

N95-17883# Maryland Univ., College Park, MD. Center for Rotorcraft Education and Research.

EXPERIMENTAL DATA ON THE AERODYNAMIC INTERACTIONS BETWEEN A HELICOPTER ROTOR AND AN AIRFRAME

J. G. LEISHMAN and NAI-PEI BI In AGARD, A Selection of Experimental Test Cases for the Validation of CFD Codes, Volume 2 17 p Aug. 1994 Copyright Avail: CASI HC A03/MF A06

The data presented in this contribution were obtained at the Center for Rotorcraft Education and Research at the University of Maryland under part of a research program sponsored by the United States Army Research Office. The experiments were performed in several wind-tunnel entries during the period from June 1988 through June 1990. The purpose of the experiments was to provide a better understanding into the origin of rotor/airframe interaction aerodynamic effects that are present on helicopters and other rotary wing aircraft. The measured results provide several unique and challenging engineering test cases for computational fluid dynamic methods used to model helicopter rotor wakes and rotor/airframe interaction phenomena. Author

N95-17884# Aircraft Research Association Ltd., Bedford (England). INVESTIGATION INTO THE AERODYNAMIC CHARACTERISTICS OF A COMBAT AIRCRAFT RESEARCH MODEL FITTED WITH A FORWARD SWEEP WING

D. STANNILAND In AGARD, A Selection of Experimental Test Cases for the Validation of CFD Codes, Volume 2 26 p Aug. 1994 Copyright Avail: CASI HC A03/MF A06

The submission covers a series of tests on a combat aircraft research model fitted with a forward swept wing. The purpose of the tests was to investigate the flow development of the upper surface of the wing and to establish a level of confidence in the CFD methods

used for the wing design. The fuselage was specified algebraically in order to permit a precise definition of the geometry both for CFD calculations and model manufacture, and the model was fitted with pressure tapings on the wing, fuselage and canard. The tests were performed in the ARA 9ft x 8ft Transonic Wind Tunnel in February 1985. Author

N95-17885# Aircraft Research Association Ltd., Bedford (England). INVESTIGATION OF THE INFLUENCE OF PYLONS AND STORES ON THE WING LOWER SURFACE FLOW

D. STANNILAND In AGARD, A Selection of Experimental Test Cases for the Validation of CFD Codes, Volume 2 16 p Aug. 1994 Copyright Avail: CASI HC A03/MF A06

The submission describes a series of tests on a large half model with a constant chord, untwisted, constant section wing with 25 sweep. The aim of these tests was to investigate the influence of pylons and stores on the wing surface flow, particularly the development of shocks and separations around the pylons with an associated increase in drag. To this end a large number of surface pressure tapings were provided on the wing lower surface (17 stations), on the inboard and outboard sides of each of the pylons and around the mid-pylon store. Since these data were to be used primarily for the validation of CFD codes, for this class of configuration, the fuselage and store are precisely defined bodies of revolution which can be modelled easily by the CFD geometry packages. The tests were performed in the ARA 9ft x 8 ft Transonic Wind Tunnel in February 1986. Author

N95-18101*# National Aeronautics and Space Administration. Ames Research Center, Moffett Field, CA.

PARAMETRIC STUDY ON LAMINAR FLOW FOR FINITE WINGS AT SUPERSONIC SPEEDS

JOSEPH AVILA GARCIA Dec. 1994 101 p (Contract(s)/Grant(s): RTOP 537-07-00) (NASA-TM-108852; A-94146; NAS 1.15:108852) Avail: CASI HC A06/MF A02

Laminar flow control has been identified as a key element in the development of the next generation of High Speed Transports. Extending the amount of laminar flow over an aircraft will increase range, payload, and altitude capabilities as well as lower fuel requirements, skin temperature, and therefore the overall cost. A parametric study to predict the extent of laminar flow for finite wings at supersonic speeds was conducted using a computational fluid dynamics (CFD) code coupled with a boundary layer stability code. The parameters investigated in this study were Reynolds number, angle of attack, and sweep. The results showed that an increase in angle of attack for specific Reynolds numbers can actually delay transition. Therefore, higher lift capability, caused by the increased angle of attack, as well as a reduction in viscous drag, due to the delay in transition, can be expected simultaneously. This results in larger payload and range. Author

N95-18337 Department of the Navy, Washington, DC.

CORNER VORTEX SUPPRESSOR Patent

PROMODE R. BANDYOPADHYAY, inventor (to Navy) 19 Apr. 1994 6 p Filed 22 Feb. 1993 Supersedes AD-D015772 (AD-D016423; US-PATENT-5,303,882; US-PATENT-APPL-SN-020940; US-PATENT-CLASS-244-130) Avail: US Patent and Trademark Office

A corner vortex forms at the corners of a square or rectangular wind tunnel or water tunnel and disrupts the flow and creates excessive drag, turbulence, noise and wake. The corners defined by a wing/fuselage interface creates the same type of situation. The suppressor provides many small corners to prevent forming of the single large vortex. A honeycomb or mesh provides parallel passageways, each having a size that is a fraction (1/5th to 1/10th) of the depth of the boundary layer (defined as that point in the fluid flow where the velocity is 99% of free stream velocity. DTIC

N95-18340# Army Natick Research and Development Command, MA. Engineering Center.

PARACHUTE INFLATION: A PROBLEM IN AEROELASTICITY Final Report

KEITH R. STEIN and RICHARD J. BENNEY Aug. 1994 86 p
(Contract(s)/Grant(s): DA PROJ. 1L1-62786-D-283; DA PROJ. 1L1-61102-AH-52)

(AD-A284375) Avail: CASI HC A05/MF A01

In parachute research, canopy inflation is the least understood and most complex process to model. Unfortunately, it is during the opening process that the canopy experiences the largest deformations and loadings. The complexity of modeling the opening process stems from the coupling between the structural dynamics of the canopy, lines plus payload and the aerodynamics of the surrounding fluid medium. The addition of a computational capability to model the coupled opening behavior would greatly assist in understanding the canopy inflation process. Ongoing research at the U.S. Army Natick Research, Development and Engineering Center (Natick) focuses on this coupled problem. The solution to this problem will assist in the development of future U.S. Army airdrop systems, which include the capability of deploying at low altitudes and high speeds. This report describes research at Natick that currently involves coupling a computational fluid dynamics (CFD) code to a mass spring damper (MSD) parachute structural code. The model is described and results are presented. DTIC

N95-18380 Lockheed Corp., Fort Worth, TX.
OVERVIEW OF UNSTEADY TRANSONIC WIND TUNNEL TEST ON A SEMISPAN STRAKED DELTA WING OSCILLATING IN PITCH Final Report, Mar. 1989 - Dec. 1993

ATLEE M. CUNNINGHAM, JR. and RUUD G. DEN BOER Aug. 1994 57 p Limited Reproducibility: More than 20% of this document may be affected by microfiche quality

(Contract(s)/Grant(s): AF PROJ. 2401)

(AD-A284097; WL-TR-94-3017) Avail: Issuing Activity (Defense Technical Information Center (DTIC))

A wind tunnel investigation was conducted in 1992 to investigate the unsteady aerodynamic aspects of transonic high incidence flows over a simple straked wing model. This test was designed to show how low speed vortex type flows evolve into complicated shock vortex interacting flows at transonic speeds. Requirements for this test were based on a low speed test conducted in 1986 on a full span model in the NLR Low Speed Tunnel. The transonic model was a semispan version of the low speed model with some modifications. It was equipped with a three-component semispan balance to measure total wing loads, seven rows of high response pressure transducers to measure unsteady pressures and 15 vertical accelerometers to measure model motion and vibrations. The model was oscillated sinusoidally in pitch at various amplitudes and frequencies for mean model incidences varying from 4 deg to 48 deg. In addition, maneuver type transient motions of the model were tested with amplitudes of 16 deg and 30 deg total rotation at various starting angles. The test was conducted in the NLR HST in the Mach range of 0.225 to 0.90 with some preliminary vapor screen flow visualization data taken at $M=0.6$ and 0.9 . DTIC

N95-18457*# National Aeronautics and Space Administration. Lewis Research Center, Cleveland, OH.

MEASUREMENT OF GUST RESPONSE ON A TURBINE CASCADE

A. P. KURKOV and B. L. LUCCI Jan. 1995 12 p Presented at the Turbo Expo 1995, Houston, TX, 5-8 Jun. 1995; sponsored by the ASME (Contract(s)/Grant(s): RTOP 505-63-5B) (NASA-TM-106776; E-9227; NAS 1.15:106776) Avail: CASI HC A03/MF A01

The paper presents benchmark experimental data on a gust response of an annular turbine cascade. The experiment was particularly designed to provide data for comparison with the results of a typical linearized gust-response analysis. Reduced frequency, Mach number, and incidence were varied independently. Except for

the lowest reduced frequency, the gust velocity distribution was nearly sinusoidal. For the high inlet-velocity series of tests, the cascade was near choking. The mean flow was documented by measuring blade surface pressures and the cascade exit flow. High-response pressure transducers were used to measure the unsteady pressure distribution. Inlet-velocity components and turbulence parameters were measured using hot wire. In addition to the synchronous time-average pressure spectra, typical power spectra are included for several representative conditions. Author

N95-18503 National Aerospace Lab., Amsterdam (Netherlands).
SECTIONAL PREDICTION OF 3D EFFECTS FOR SEPARATED FLOW ON ROTATING BLADES

H. SNEL, R. HOUWINK, and W. J. PIERS 1992 31 p Limited Reproducibility: More than 20% of this document may be affected by microfiche quality

(PB94-201696; NLR-TP-92409-U) Avail: Issuing Activity (National Technical Information Service (NTIS))

A method is presented which allows the computation of air load coefficients for rotor blade sections at attached and separated flow conditions, including leading effects of blade rotation. The method consists of an existing computer code for 2D unsteady flow with strong viscous-inviscid interaction, in which the turbulent boundary layer integral method has been modified by including leading terms for steady 3D effects on a high aspect ratio rotating blade. A summary is presented of the approach made, and a first set of results are compared with wind-tunnel data for a wind-turbine model. Computed 2D polars and corresponding pressure distributions for a nonrotating and rotating blade section appear to be qualitatively similar to experimental data, including high values of the lift coefficient measured at 30% of the tip radius. For sufficient accuracy in practice, however, various aspects of the method need further analysis and improvement. NTIS

N95-18539 Advisory Group for Aerospace Research and Development, Neuilly-Sur-Seine (France). Fluid Dynamics Panel.

A SELECTION OF EXPERIMENTAL TEST CASES FOR THE VALIDATION OF CFD CODES. SUPPLEMENT: DATASETS A-E (Diskette Supplement)

Aug. 1994 See also N95-14201 and N95-17846 Diskette supplement: nine 3.5-inch DSHD diskettes

(AGARD-AR-303-SUPPL; NONP-AGARD-SUPPL-VT-95-38380) Copyright Avail: CASI DK A18

Relevant data of all 39 test cases for the validation of Computational Fluid Dynamics (CFD) codes by Working Group 14 of the AGARD Fluid Dynamics Panel is compiled on these 9 diskettes to accompany Volumes 1 and 2 of the report. The test cases cover the subsonic, transonic, and supersonic flow regimes. CASI

N95-18565*# National Aeronautics and Space Administration. Hugh L. Dryden Flight Research Facility, Edwards, CA.

IN-FLIGHT LIFT-DRAG CHARACTERISTICS FOR A FORWARD-SWEPT WING AIRCRAFT AND COMPARISONS WITH CONTEMPORARY AIRCRAFT)

EDWIN J. SALTZMAN (PRC Kentron, Inc., Edwards, CA.), JOHN W. HICKS, and SUE LUKE, ed. Washington Dec. 1994 61 p (Contract(s)/Grant(s): RTOP 505-68-50)

(NASA-TP-3414; H-1913; NAS 1.60:3414) Avail: CASI HC A04/MF A01

Lift (L) and drag (D) characteristics have been obtained in flight for the X-29A airplane (a forward swept-wing demonstrator) for Mach numbers (M) from 0.4 to 1.3. Most of the data were obtained near an altitude of 30,000 ft. A representative Reynolds number for $M = 0.9$, and a pressure altitude of 30,000 ft, is $18.6 \times 10^{(exp 6)}$ based on the mean aerodynamic chord. The X-29A data (forward-swept wing) are compared with three high-performance fighter aircraft: the F-15C, F-16C, and F/A18. The lifting efficiency of the X-29A, as defined by the Oswald lifting efficiency factor, e , is about average for a cantilevered monoplane for $M = 0.6$ and angles of attack up to those required for maximum L/D. At $M = 0.6$ the level of

02 AERODYNAMICS

L/D and e , as a function of load factor, for the X-29A was about the same as for the contemporary aircraft. The X-29A and its contemporaries have high transonic wave drag and equivalent parasite area compared with aircraft of the 1940's through 1960's. Author

N95-18604# De Havilland Aircraft Co. of Canada Ltd., Downsview (Ontario).

A REVIEW OF GUST LOAD CALCULATION METHODS AT DE HAVILLAND

JOHN GLASER In AGARD, Aircraft Loads due to Turbulence and their Impact on Design and Certification 9 p Dec. 1994

Copyright Avail: CASI HC A02/MF A01

The development of an analysis system for the routine calculation of gust response loads is reviewed in some detail in this report. While the system provides adequate design strength margins, a more robust and effective system would reduce user workload, computer costs and analysis time. It is suggested that other analysis systems could benefit similarly, particularly when considering the demands imposed by highly nonlinear aircraft systems, the trend toward full finite element structural dynamic models and the relentless quest for structural efficiency. It is proposed that improvements in analysis systems could evolve from the collective experience in gust loads methodologies acquired within the aeronautical community. To capitalize on that collective experience, it is recommended that a working group of gust load specialists be formed to assemble and evaluate current and promising methods for calculating gust loads and to recommend standardized airplane test cases, both rigid and elastic, for validating analysis methods and results. Author

N95-18611# Army Research Lab., Aberdeen Proving Ground, MD. **STATIC AERODYNAMICS CFD ANALYSIS FOR 120-MM HYPERSONIC KE PROJECTILE DESIGN Final Report, Sep. 1992 - Apr. 1994**

BERNARD J. GUIDOS Sep. 1994 37 p
(Contract(s)/Grant(s): DA PROJ. 1L1-62618-AH-80)
(ARL-MR-184) Avail: CASI HC A03/MF A01

Computational fluid dynamics (CFD) predictions of static aerodynamic coefficients for large caliber (120 mm) M829-like come-cylinder-flare kinetic energy (KE) projectile shapes are presented. Zero-yaw drag and static pitch-plane aerodynamic coefficients are presented for velocities in the range 1.5 to 3.0 km/sec for several flare angles. The aerodynamic coefficients are required to assess the velocity retardation and static stability of candidate configurations that use the M829 projectile as a basis for design. Comparisons of the aerodynamic coefficients are made with those of the fielded M829 projectile, and a preliminary evaluation is made of the performance of these shapes in hypersonic flight. Author

N95-18624# Federal Aviation Administration, Cambridge, MA. National Transportation Systems Center.

AIRCRAFT WAKE VORTEX TAKEOFF TESTS AT O'HARA INTERNATIONAL AIRPORT Final Report, Feb. - May 1992

J. YARMUS, D. BURNHAM, A. WRIGHT, and T. TALBOT Aug. 1994 88 p

(AD-A283828; DOT-VNTSC-FAA-94-12; DOT/FAA/RD-94-25) Avail: CASI HC A05/MF A01

Three wake vortex measurement systems (anemometer, acoustic doppler, and laser doppler) were used to collect wake vortex data from aircraft departing Runway 22L at Chicago's O'Hare Airport for nine months in 1980. The data were analyzed to determine vortex decay and vortex transport probabilities. The results support the classification of all B-707 and DC-8 aircraft in the large wake vortex class. The acoustic doppler system was found to be significantly more sensitive than the ground anemometer system to vortices transported long distances laterally by a crosswind. The most efficient lateral transport was noted for crosswinds greater than seven knots. The horizontal and vertical ground wind signatures of a wake vortex are compared. DTIC

N95-18645# National Renewable Energy Lab., Golden, CO. **WIND TURBINE BLADE AERODYNAMICS: THE COMBINED EXPERIMENT**

M. C. ROBINSON (Colorado Univ., Boulder, CO.), M. W. LUTTGES (Colorado Univ., Boulder, CO.), M. S. MILLER (Colorado Univ., Boulder, CO.), D. E. SHIPLEY (Colorado Univ., Boulder, CO.), and T. S. YOUNG (Colorado Univ., Boulder, CO.) Aug. 1994 10 p
Presented at the Windpower 1993, San Francisco, CA, 12-16 Jul. 1993
(Contract(s)/Grant(s): DE-AC36-83CH-10093)
(DE94-011866; NREL/TP-441-7107; CONF-930726-8) Avail: CASI HC A02/MF A01

Data obtained from the National Renewable Energy Laboratory site test of a wind turbine (The Combined Experiment) was analyzed specifically to capture information regarding the aerodynamic loading experienced by such machines. The analysis showed that inflow conditions were extremely variable and that these inflows yielded three different operational regimes. Each regime produces very different aerodynamic loading conditions that must be tolerated by the turbine. The two conditions not predicted from wind tunnel data are being subjected to further analyses to provide new guidelines for both designers and operators. Author

N95-18646# National Renewable Energy Lab., Golden, CO. **WIND TURBINE BLADE AERODYNAMICS: THE ANALYSIS OF FIELD TEST DATA**

M. W. LUTTGES (Colorado Univ., Boulder, CO.), M. S. MILLER (Colorado Univ., Boulder, CO.), M. C. ROBINSON (Colorado Univ., Boulder, CO.), D. E. SHIPLEY (Colorado Univ., Boulder, CO.), and T. S. YOUNG (Colorado Univ., Boulder, CO.) Aug. 1994 8 p
Presented at the 13th Energy-Sources Technology Conference and Exhibition (ETCE) on Wind Energy, New Orleans, LA, 23-26 Jan. 1994
(Contract(s)/Grant(s): DE-AC36-83CH-10093)
(DE94-011867; NREL/TP-441-7108; CONF-940113-11) Avail: CASI HC A02/MF A01

Data obtained from the National Renewable Energy Laboratory site test of a wind turbine (The Combined Experiment) was analyzed specifically to capture information regarding the aerodynamic loading experienced by the machine rotor blades. The inflow conditions were shown to be extremely variable. These inflows yielded three different operational regimes about the blades. Each regime produced very different aerodynamic loading conditions. Two of these regimes could not have been readily predicted from wind tunnel data. These conditions are being subjected to further analyses to provide new guidelines for both designers and operators. The roles of unsteady aerodynamics effects are highlighted since periods of dynamic stall were shown to be associated with brief episodes of high aerodynamic forces. Author

N95-18663 Arnold Engineering Development Center, Arnold AFS, TN.

HYPERSONIC WIND TUNNEL TEST TECHNIQUES Final Report, Jul. 1992 - May 1993

R. K. MATTHEWS and R. W. RHUDY Aug. 1994 57 p Limited
Reproducibility: More than 20% of this document may be affected by microfiche quality

(AD-A284057; AEDC-TR-94-6) Avail: CASI HC A04

This report describes the procedures used in the continuous flow hypersonic tunnels of the AEDC for static stability, pressure, heat transfer, materials/structures, boundary-layer transition, and electromagnetic wave testing. Particular emphasis is placed on heat-transfer techniques because of the importance of defining the thermal environment of hypersonic vehicles. An overview of the materials/structures test methodology used in the development of hypersonic vehicle components is presented. Unfortunately the methodology to predict transition has eluded the aerodynamicist for over three decades, and there are still many unanswered questions. This report briefly touches on the many parameters that affect transition and provides numerous references for those who are interested in specializing in this topic. The methodology of using trip spheres is discussed, and illustrative data are

presented. Electromagnetic wave testing represents a relatively new test technique that involves the union of several disciplines: aerothermodynamics, electromagnetics, materials/structures, and advanced diagnostics. The essence of this new technique deals with the transmission and possible distortion of electromagnetic waves (RF or IR) as they pass through the bow shock, flow field, and electromagnetic (EM) window of a missile flying at hypersonic speeds. DTIC

N95-18669 Naval Postgraduate School, Monterey, CA.
INTERACTION, BURSTING AND CONTROL OF VORTICES OF A CROPPED DOUBLE-DELTA WING AT HIGH ANGLE OF ATTACK M.S. Thesis

ABDULLAH M. ALKHOZAM Mar. 1994 224 p Limited
Reproducibility: More than 20% of this document may be affected by microfiche quality

(AD-A283656) Avail: CASI HC A10

A flow visualization study of the vortical flow over a cropped double-delta wing model with sharp leading edges and its three derivatives with small geometric modifications (fillets) at the strake wing junction was conducted in the Naval Postgraduate School water tunnel using the dye-injection technique. The fillets increased the wing area of the baseline model by 1%. The main focus of this study was to evaluate the effect of fillets on vortex core trajectories, interactions and breakdown on the leeward surface at high angle of attack (AOA) with zero sideslip angle. Comparison of test results for different fillet shapes indicates delay in both vortex interaction and breakdown at high AOA, particularly for the diamond fillet shapes. The vortex breakdown data implies lift augmentation for both static and dynamic case, with the static data correlating well with recently published numerical data. DTIC

N95-18670 Army Research Lab., Aberdeen Proving Ground, MD.
NUMERICAL COMPUTATIONS OF SUPERSONIC BASE FLOW WITH SPECIAL EMPHASIS ON TURBULENCE MODELING
Final Report, Dec. 1991 - Dec. 1992

JUBARAJ SAHU Jun. 1994 39 p Supersedes BRL-IMR-971
Limited Reproducibility: More than 20% of this document may be affected by microfiche quality

(Contract(s)/Grant(s): DA PROJ. 1L1-61102-AH-43)

(AD-A283688; ARL-TR-438; BRL-IMR-971) Avail: CASI HC A03

A zonal, implicit, time-marching Navier-Stokes computational technique has been used to compute the turbulent supersonic base flow over cylindrical afterbodies. A critical element of calculating such flows is the turbulence model. Various eddy viscosity turbulence models have been used in the base region flow computations. These models include two algebraic turbulence models and a two-equation k-epsilon model. The k-epsilon equations are developed in a general coordinate system and solved using an implicit algorithm. Calculations with the k-epsilon model are extended up to the wall. Flow field computations have been performed for a cylindrical afterbody at $M = 2.46$ and at angle of attack $\alpha = 0$. The results are compared to the experimental data for the same conditions and the same configuration. Details of the mean flow field as well as the turbulence quantities have been presented. In addition, the computed base pressure distribution has been compared with the experiment. In general, the k-epsilon turbulence model performs better in the near wake than the algebraic models and predicts the base pressure much better. DTIC

N95-18674 Arnold Engineering Development Center, Arnold AFS, TN.

HYPERSONIC FLOW-FIELD MEASUREMENTS: INTRUSIVE AND NONINTRUSIVE Final Report, Jul. 1992 - Jul. 1993

R. K. MATTHEWS and W. D. WILLIAMS Aug. 1994 54 p Limited
Reproducibility: More than 20% of this document may be affected by microfiche quality

(AD-A283867; AEDC-TR-94-5) Avail: CASI HC A04

Flow-field measurement techniques that require a probe or other device to be inserted into the flow are classified as intrusive. In general,

these intrusive techniques are currently viewed as inferior to the more popular nonintrusive techniques. However, it should be remembered that in general these intrusive techniques have evolved over several decades while the flow-field experience of nonintrusive techniques is relatively limited. Included in the intrusive classification are pitot tubes, total temperature probes, Mach/angularity probes, static pressure devices, and others. For many years nonintrusive diagnostics have also been under development to meet the demands of hypersonic testing. Today, a large number of nonintrusive techniques at various levels of maturity and complexity are available for application. These techniques provide measurement of species number density, rotational and vibrational temperatures, static pressure, flow velocity, and visualization of flow structure. DTIC

N95-18904# National Aerospace Lab., Bangalore (India). Computer Supports and Services.

SOLUTION OF FULL POTENTIAL EQUATION ON AN AIRFOIL BY MULTIGRID TECHNIQUE

C. SRINIVASA Apr. 1993 17 p

(NAL-TM-CSS-9303) Avail: CASI HC A03/MF A01

Multigrid technique is a method which accelerates the convergence and hence reduces the CPU time for a given flow problem. This technique has been used to solve the full potential equation for an airfoil in cartesian grid. This report describes the multigrid technique solutions obtained for two to three grid levels and for an angle of attack of zero degree and one degree. This report also gives the grid size details for various levels. Author

N95-18910# Deutsche Forschungsanstalt fuer Luft- und Raumfahrt, Brunswick (Germany). Inst. fuer Entwurfsaerodynamik.

THEORETICAL INVESTIGATIONS OF SHOCK/BOUNDARY LAYER INTERACTIONS ON A MA(INFINITY) = 8 WAVERIDER [THEORETISCHE UNTERSUCHUNGEN UEBER STOSS-GRENZSCHICHT-WECHSELWIRKUNGEN AN EINEM MA(INFINITY) = 8 WELLENRITER]

MICHAEL WAIBEL 1994 149 p In GERMAN

(ISSN 0939-2963)

(DLR-FB-94-12) Avail: CASI HC A07/MF A02

Shock/boundary layer interactions are investigated on a $Ma(\text{sub}) = 8$ waverider, which has a sharp leading edge. This is done by comparing Euler and Navier-Stokes calculations at the design point and at higher angles of attack. The original waverider configuration was modified with a blunt leading edge to investigate the influence of leading edge bluntness. This comparison is made at the design point and higher angles of attack using Euler calculations. Author

N95-18933*# National Aeronautics and Space Administration. Lewis Research Center, Cleveland, OH.

ENHANCED CAPABILITIES AND MODIFIED USERS MANUAL FOR AXIAL-FLOW COMPRESSOR CONCEPTUAL DESIGN CODE CSPAN

ARTHUR J. GLASSMAN (Toledo Univ., OH.) and THOMAS M. LAVELLE Jan. 1995 24 p

(Contract(s)/Grant(s): RTOP 505-69-50)

(NASA-TM-106833; E-9394; NAS 1.15:106833) Avail: CASI HC A03/MF A01

Modifications made to the axial-flow compressor conceptual design code CSPAN are documented in this report. Endwall blockage and stall margin predictions were added. The loss-coefficient model was upgraded. Default correlations for rotor and stator solidity and aspect-ratio inputs and for stator-exit tangential velocity inputs were included in the code along with defaults for aerodynamic design limits. A complete description of input and output along with sample cases are included. Author

N95-19041*# National Aeronautics and Space Administration. Ames Research Center, Moffett Field, CA.

AN ASSESSMENT OF THE ADAPTIVE UNSTRUCTURED TETRAHEDRAL GRID, EULER FLOW SOLVER CODE FELISA
M. JAHED DJOMEHRI (Calspan Corp., Moffett Field, CA.) and

02 AERODYNAMICS

LARRY L. ERICKSON Dec. 1994 37 p
(Contract(s)/Grant(s): RTOP 505-59-20)
(NASA-TP-3526; A-94147; NAS 1.60:3526) Avail: CASI HC A03/MF A01

A three-dimensional solution-adaptive Euler flow solver for unstructured tetrahedral meshes is assessed, and the accuracy and efficiency of the method for predicting sonic boom pressure signatures about simple generic models are demonstrated. Comparison of computational and wind tunnel data and enhancement of numerical solutions by means of grid adaptivity are discussed. The mesh generation is based on the advancing front technique. The FELISA code consists of two solvers, the Taylor-Galerkin and the Runge-Kutta-Galerkin schemes, both of which are spatially discretized by the usual Galerkin weighted residual finite-element methods but with different explicit time-marching schemes to steady state. The solution-adaptive grid procedure is based on either remeshing or mesh refinement techniques. An alternative geometry adaptive procedure is also incorporated. Author

N95-19042*# National Aeronautics and Space Administration. Langley Research Center, Hampton, VA.
STATIC INVESTIGATION OF TWO FLUIDIC THRUST-VECTORING CONCEPTS ON A TWO-DIMENSIONAL CONVERGENT-DIVERGENT NOZZLE
DAVID J. WING Dec. 1994 203 p
(Contract(s)/Grant(s): RTOP 505-62-30-01)
(NASA-TM-4574; L-17350; NAS 1.15:4574) Avail: CASI HC A10/MF A03

A static investigation was conducted in the static test facility of the Langley 16-Foot Transonic Tunnel of two thrust-vectoring concepts which utilize fluidic mechanisms for deflecting the jet of a two-dimensional convergent-divergent nozzle. One concept involved using the Coanda effect to turn a sheet of injected secondary air along a curved sidewall flap and, through entrainment, draw the primary jet in the same direction to produce yaw thrust vectoring. The other concept involved deflecting the primary jet to produce pitch thrust vectoring by injecting secondary air through a transverse slot in the divergent flap, creating an oblique shock in the divergent channel. Utilizing the Coanda effect to produce yaw thrust vectoring was largely unsuccessful. Small vector angles were produced at low primary nozzle pressure ratios, probably because the momentum of the primary jet was low. Significant pitch thrust vector angles were produced by injecting secondary flow through a slot in the divergent flap. Thrust vector angle decreased with increasing nozzle pressure ratio but moderate levels were maintained at the highest nozzle pressure ratio tested. Thrust performance generally increased at low nozzle pressure ratios and decreased near the design pressure ratio with the addition of secondary flow. Author

N95-19110 Air Force Inst. of Tech., Wright-Patterson AFB, OH.
NUMERICAL SIMULATION OF DYNAMIC-STALL SUPPRESSION BY TANGENTIAL BLOWING Ph.D. Thesis
MATTHEW C. TOWNE Jul. 1994 164 p Limited Reproducibility. More than 20% of this document may be affected by microfiche quality (AD-A284887; AFIT/DS/AA/94-4) Avail: CASI HC A08

The use of tangential blowing to suppress the dynamic stall of a pitching airfoil is investigated numerically. The laminar two-dimensional, compressible Navier-Stokes equations are solved time-accurately using a Beam-Warming algorithm. A slot is located at four different positions along the surface of a NACA 0015 airfoil and air is injected in a nearly tangential sense along the upper surface. Suction control is also employed at one of these slot locations to directly compare with tangential-blowing control. Solution sensitivity to grid refinement, time-step size, numerical smoothing, and initial conditions is investigated at a Reynolds number of 2.4×10^4 (exp 4). Initial-condition and initial-airfoil-acceleration effects are analyzed for various pitch rates. Compressibility of M infinity = 0.2 solutions is investigated. Numerical simulation uncertainties of jet-orientation angle and jet velocity profile are investigated. Studies are conducted to establish the effects of slot position, slot width,

blowing-initiation angle, blowing velocity, pulsed blowing, and blowing at different pitch rates. DTIC

N95-19114*# National Aeronautics and Space Administration. Langley Research Center, Hampton, VA.
NAVIER-STOKES, FLIGHT, AND WIND TUNNEL FLOW ANALYSIS FOR THE F/A-18 AIRCRAFT
FARHAD GHAFARI Dec. 1994 67 p Original contains color illustrations
(Contract(s)/Grant(s): RTOP 505-68-30-03)
(NASA-TP-3478; L-17336; NAS 1.60:3478) Avail: CASI HC A04/MF A01; 5 functional color pages

Computational analysis of flow over the F/A-18 aircraft is presented along with complementary data from both flight and wind tunnel experiments. The computational results are based on the three-dimensional thin-layer Navier-Stokes formulation and are obtained from an accurate surface representation of the fuselage, leading-edge extension (LEX), and the wing geometry. However, the constraints imposed by either the flow solver and/or the complexity associated with the flow-field grid generation required certain geometrical approximations to be implemented in the present numerical model. In particular, such constraints inspired the removal of the empennage and the blocking (fairing) of the inlet face. The results are computed for three different free-stream flow conditions and compared with flight test data of surface pressure coefficients, surface tuft flow, and off-surface vortical flow characteristics that included breakdown phenomena. Excellent surface pressure coefficient correlations, both in terms of magnitude and overall trend, are obtained on the forebody throughout the range of flow conditions. Reasonable pressure agreement was obtained over the LEX; the general correlation tends to improve at higher angles of attack. The surface tuft flow and the off-surface vortex flow structures compared qualitatively well with the flight test results. To evaluate the computational results, a wind tunnel investigation was conducted to determine the effects of existing configurational differences between the flight vehicle and the numerical model on aerodynamic characteristics. In most cases, the geometrical approximations made to the numerical model had very little effect on overall aerodynamic characteristics. Author

N95-19119*# National Aeronautics and Space Administration. Ames Research Center, Moffett Field, CA.
2-D AND 3-D OSCILLATING WING AERODYNAMICS FOR A RANGE OF ANGLES OF ATTACK INCLUDING STALL
R. A. PIZIALI (Army Aviation Systems Command, Moffett Field, CA.)
Sep. 1994 570 p Prepared in cooperation with Army Aviation Systems Command, Moffett Field, CA
(Contract(s)/Grant(s): RTOP 505-59-52)
(NASA-TM-4632; A-94053; NAS 1.15:4632; USAATCOM-TR-94-A-011) Avail: CASI HC A24/MF A04

A comprehensive experimental investigation of the pressure distribution over a semispan wing undergoing pitching motions representative of a helicopter rotor blade was conducted. Testing the wing in the nonrotating condition isolates the three-dimensional (3-D) blade aerodynamic and dynamic stall characteristics from the complications of the rotor blade environment. The test has generated a very complete, detailed, and accurate body of data. These data include static and dynamic pressure distributions, surface flow visualizations, two-dimensional (2-D) airfoil data from the same model and installation, and important supporting blockage and wall pressure distributions. This body of data is sufficiently comprehensive and accurate that it can be used for the validation of rotor blade aerodynamic models over a broad range of the important parameters including 3-D dynamic stall. This data report presents all the cycle-averaged lift, drag, and pitching moment coefficient data versus angle of attack obtained from the instantaneous pressure data for the 3-D wing and the 2-D airfoil. Also presented are examples of the following: cycle-to-cycle variations occurring for incipient or lightly stalled conditions; 3-D surface flow visualizations; supporting blockage and wall pressure distributions; and underlying detailed pressure results. Author

N95-19259# Technische Univ., Delft (Netherlands). High Speed Aerodynamics Lab.

THE UTILIZATION OF A HIGH SPEED REFLECTIVE VISUALIZATION SYSTEM IN THE STUDY OF TRANSONIC FLOW OVER A DELTA WING

S. R. DONOHOE and W. J. BANNINK *In* AGARD, Wall Interference, Support Interference and Flow Field Measurements 13 p Jul. 1994 Copyright Avail: CASI HC A03/MF A04

An experimental study was conducted to examine the flow over a non-cambered 65 deg swept delta wing with a sharp leading edge in high subsonic compressible flow at various angles of attack. This flow is known to be highly three dimensional. At certain combinations of Mach number and high angle of attack, an unsteady and often non axial symmetric phenomenon known as vortex breakdown is found to occur above the wing. The present experimental study includes both visualizations of the flow over the model surface and of the flow field itself. The surface flow visualization study is done using a conventional oil-flow visualization technique. Flow field visualizations are done using both a traditional transmission visualization system as well as a newly developed Surface Reflective Visualization (SRV) technique. The development and application of this SRV system will be the main topic addressed in the current report. The SRV technique provides a new perspective on the compressible flow over wings. This technique incorporates a specially designed model with a reflective surface to enable visualization of the flow over the wing in plan view. The technique has been developed and applied to the transonic flow over a delta wing presently under investigation in a vortex breakdown research program. The plan view perspective makes it possible to visualize the span-wise distribution of the shock system present in the flow field and provides confirmation of the existence of cross flow shocks for certain combinations of Mach number and angle of attack. Combining this technique with the use of a high-speed camera enables the high speed shock fluctuations associated with this flow to be assessed for the first time. The SRV system, thus, allows insight to be gained into the time scales associated with these shock fluctuations and the vortex breakdown phenomenon in general. Author

N95-19260# British Aerospace Aircraft Group, Preston (England). Aerodynamics Dept.

TRANSONIC AND SUPERSONIC FLOWFIELD MEASUREMENTS ABOUT AXISYMMETRIC AFTERBODIES FOR VALIDATION OF ADVANCED CFD CODES

MARTIN BURT, PHILIP MILLER (Miller and Wilson Aerodynamics Research, Bath, England.), and JOHAN AGRELL (Aeronautical Research Inst. of Sweden, Bromma.) *In* AGARD, Wall Interference, Support Interference and Flow Field Measurements 28 p Jul. 1994 Sponsored by Swedish Ministry of Defence Copyright Avail: CASI HC A03/MF A04

Two axisymmetric afterbody experimental programs, aimed at providing necessary and sufficient data for CFD code validation, were conducted in the FFA S5 suckdown wind-tunnel. Flow conditions covered the range of transonic to supersonic. Mean and fluctuating flowfield velocities in a single longitudinal plane were measured using LDA along many traverses, both over the afterbody and in the jet and mixing regions. Flow separated on the boattail of the AGARD 10 and 15 degree geometries at all conditions tested. Separation also occurred on a conical afterbody at supersonic Mach number. Comprehensive sets of boundary condition data were also recorded, through a wide variety of techniques. Extensive error analyses have been undertaken to evaluate the accuracy of all data. Transonic Navier-Stokes computations on the configurations were performed and showed the benefit of having static pressure information along the slotted tunnel roof. An algebraic stress model of turbulence returned predictions of afterbody surface pressures superior to two more simple models, in both attached and separated flow. Author

N95-19261# Technische Univ., Munich (Germany). Lehrstuhl fuer Fluidmechanik.

VELOCITY MEASUREMENTS WITH HOT-WIRES IN A

VORTEX-DOMINATED FLOWFIELD

CHRISTIAN BREITSAMTER and BORIS LASCHKA *In* AGARD, Wall Interference, Support Interference and Flow Field Measurements 13 p Jul. 1994 Sponsored by MBB Original contains color illustrations

Copyright Avail: CASI HC A03/MF A04

Selected results from a quantitative experimental investigation documenting the low-speed flow environment over a 75 deg swept delta wing and over a delta-canard-configuration are presented. The hot-wire measurement techniques using cross-wire and triple-wire probes are described. Results obtained include detailed flowfields of the time-dependent velocity components for angles of attack from 12.5 deg to 31.5 deg at a test Reynolds number of 1.0×10^6 (exp 6). The structure of the highly turbulent vortex dominated flow is clearly shown by time-averaged, root-mean-square and spectral distributions. Thus the delta wing vortex substructure organized by discrete vortices and vortex breakdown characteristics are analyzed. With increasing incidence both the wing and the canard leading-edge vortices move inboard resulting in increase of the velocity fluctuations due to the bursting of these vortices. At the delta-canard configuration strong interference effects between the canard and the wing vortex systems are found. Peaked velocity spectra are detected in the vorticity sheets at burst flow conditions related to a narrow-band concentration of kinetic turbulent energy in the flow of the wing/canard vortex sheets. Author

N95-19268# Georgia Inst. of Tech., Atlanta, GA. Aerospace Lab. **DEVELOPMENT OF PNEUMATIC TEST TECHNIQUES FOR SUBSONIC HIGH-LIFT AND IN-GROUND-EFFECT WIND TUNNEL INVESTIGATIONS**

ROBERT J. ENGLAR *In* AGARD, Wall Interference, Support Interference and Flow Field Measurements 11 p Jul. 1994 Sponsored by NASA. Langley Research Center Copyright Avail: CASI HC A03/MF A04

Wind tunnel evaluations of two-dimensional high-lift airfoils and of vehicles operating in ground effect near the tunnel floor require special test facilities and procedures. These are needed to avoid errors caused by proximity to the walls and interference from the wall boundary layers. Pneumatic test techniques and facilities were developed for GTRI aerodynamic research tunnels and calibrated to verify that these wall effects had been removed. The modified facilities were then employed to evaluate the aerodynamic characteristics of blown very-high-lift airfoils and of racing hydroplanes operating in ground effect at various levels above the floor. The pneumatic facilities, techniques and calibrations are discussed and typical aerodynamic data recorded both with and without the test-section blowing systems are presented. Author

N95-19270# National Aeronautics and Space Administration. Ames Research Center, Moffett Field, CA.

WALL INTERACTION EFFECTS FOR A FULL-SCALE HELICOPTER ROTOR IN THE NASA AMES 80- BY 120-FOOT WIND TUNNEL

PATRICK M. SHINODA *In* AGARD, Wall Interference, Support Interference and Flow Field Measurements 14 p Jul. 1994 Prepared in cooperation with Army Aviation Research and Development Command, Moffett Field, CA Copyright Avail: CASI HC A03/MF A04

A full-scale helicopter rotor test was conducted in the NASA Ames 80- by 120-Foot Wind Tunnel with a four-bladed S-76 rotor system. This wind tunnel test generated a unique and extensive data base covering a wide range of rotor shaft angles-of-attack and rotor thrust conditions from 0 to 100 knots. Three configurations were tested: (1) empty tunnel; (2) test stand body (fuselage) and support system; and (3) fuselage and support system with rotor installed. Empty tunnel wall pressure data are evaluated as a function of tunnel speed to understand the baseline characteristics. Aerodynamic interaction effects between the fuselage and the walls of the tunnel are investigated by comparing wall, ceiling, and floor pressures for various tunnel velocities and fuselage angles-of-attack. Aerodynamic interaction effects between the rotor and the walls of

02 AERODYNAMICS

the tunnel are also investigated by comparing wall, ceiling, and floor pressures for various rotor shaft angles, rotor thrust conditions, and tunnel velocities. Empty tunnel wall pressure data show good repeatability and are not affected by tunnel speed. In addition, the tunnel wall pressure profiles are not affected by the presence of the fuselage apart from a pressure shift. Results do not indicate that the tunnel wall pressure profiles are affected by the presence of the rotor. Significant changes in the wall, ceiling, and floor pressure profiles occur with changing tunnel speeds for constant rotor thrust and shaft angle conditions. Significant changes were also observed when varying rotor thrust or rotor shaft angle-of-attack. Other results indicate that dynamic rotor loads and blade motion are influenced by the presence of the tunnel walls at very low tunnel velocity and, together with the wall pressure data, provide a good indication of flow breakdown. Author

N95-19278# Institute for Aerospace Research, Ottawa (Ontario). High Speed Aerodynamics Lab.

EVALUATION OF COMBINED WALL- AND SUPPORT- INTERFERENCE ON WIND TUNNEL MODELS

M. MOKRY *In* AGARD, Wall Interference, Support Interference and Flow Field Measurements 11 p Jul. 1994
Copyright Avail: CASI HC A03/MF A04

Coupled interference effects of model support systems and ventilated test section walls on stream parameters at the model are calculated using a subsonic source panel method. The configurations discussed are the movable sting support system and the model plate mount in the IAR 1.5 m x 1.5 m perforated-wall wind tunnel, and an automobile model in the DSMA slotted-wall wind tunnel. Author

N95-19279# Aerospatiale, Toulouse (France).

INTERACTION OF A THREE STRUT SUPPORT ON THE AERODYNAMIC CHARACTERISTICS OF A CIVIL AVIATION MODEL [INTERACTION D'UN SUPPORT DE TYPE 3 MATS SUR LES CARACTERISTIQUES AERODYNAMIQUES D'UNE MAQUETTE D'AVION CIVIL]

J. WILLAUME, C. QUEMARD (Office National d'Etudes et de Recherches Aeronautiques, Toulouse, France.), and A. BONNET (Ecole Nationale Supérieure de l'Aéronautique et de l'Espace, Toulouse, France.) *In* AGARD, Wall Interference, Support Interference and Flow Field Measurements 25 p Jul. 1994 *In* FRENCH
Copyright Avail: CASI HC A03/MF A04

The interference effects of a three strut support system on the longitudinal aerodynamic characteristics of a model is mainly due to the guards. Our purpose is to describe two theoretical methods allowing to gain access to the level of correction to apply to the wind tunnel gross measurements. The first one is a well known panel method which provides a global correction of the forces; the second one is a simplified method which calculates separately both the displacement effect (thickness) of the guards and the mutual lift effect between them and the wing. The validity of these theoretical results has been checked by specific tests in wind tunnel F1 (ONERA) on a model of the AIRBUS A310. The experimental interference due to the struts and the influence of the model on the strut tares are also discussed. Author

N95-19280# De Havilland Aircraft Co. of Canada Ltd., Downsview (Ontario). Aerodynamic Research and Development.

INTERFERENCE CORRECTIONS FOR A CENTRE-LINE PLATE MOUNT IN A POROUS-WALLED TRANSONIC WIND TUNNEL

RICHARD J. D. POOLE and ROBIN D. GALWAY (Institute for Aerospace Research, Ottawa, Ontario.) *In* AGARD, Wall Interference, Support Interference and Flow Field Measurements 10 p Jul. 1994 Sponsored by Industry, Science and Technology Canada and Inst. for Aerospace Research Copyright
Avail: CASI HC A02/MF A04

A program of collaborative research between the National Research Council of Canada, Institute for Aerospace Research

(IAR), and de Havilland Inc. included the design and manufacture of a slim center-line plate mount model support for installation in the IAR 1.5 m Trisonic Wind Tunnel. The primary objective of the collaborative research program was to provide a mounting method suitable for accurate measurement of the drag increments resulting from configuration changes on typical transport aircraft models. The secondary objective was to derive the tare effect of the model mounting plate so that datum aerodynamic parameters could be measured. To obtain the tare effect of the mounting plate on a model, an alternative mount from the tunnel ceiling was designed and built. The 'Y-Mount' allowed the model to be held in close proximity to a dummy plate and also to be tested without the plate in the tunnel. Comparative plate in and plate out measurements were made for a range of Mach numbers and model incidences to obtain the plate tares. Author

N95-19281# German-Dutch Wind Tunnel, North East Polder (Netherlands).

CORRECTION OF SUPPORT INFLUENCES ON MEASUREMENTS WITH STING MOUNTED WIND TUNNEL MODELS

D. ECKERT *In* AGARD, Wall Interference, Support Interference and Flow Field Measurements 11 p Jul. 1994
Copyright Avail: CASI HC A03/MF A04

The structures of wind tunnel model supports always penetrate the so-called near field of the flow around the model. Therefore, support corrections of aerodynamic coefficients, evaluated either by measurement or by calculation, depend on the specific configuration of the model and of the model/support intersection. As a consequence support influences known for the correction of a wind tunnel measurement with one model are, in general, not transferrable to another configuration. Nevertheless, such a generalization, at least between models of the same aircraft family, would in principle be very helpful in avoiding the time consuming measurements or the viscous flow calculations necessary for the evaluation of support corrections. To this end, at DNW a comprehensive data-base of measured influences of three sting support types on different low-speed aircraft models was analyzed. The aim was to split up the total support effects in terms representing the effect of support volumes located in the far field of the model and in terms representing the effect of support elements located in the near field of the model. The data-base has been analyzed with the aid of a physical model which interprets support influences as flow perturbations relevant for the wing, the fuselage, and the tail of the model. This analysis showed that for some fuselage/sting arrangements the near field effects may be considered small compared with the far field effects and independent of the wing's slat/flap configuration. These findings offered the important possibility of using near field dependent correction terms known for one model configuration for measurements with new configurations (e.g. new wing slat/flap combination). In order to determine the far field influence on new configurations, the physical model mentioned before is used in DNW's on-line data processing system to calculate the support corrections by combining previously determined flow perturbations with the actual measurements during routine tests. Examples show the successful application of the method to measurements with different models. Author

N95-19282# Analytical Methods, Inc., Redmond, WA.

CALCULATION OF SUPPORT INTERFERENCE IN DYNAMIC WIND-TUNNEL TESTS

D. ALMOSNINO *In* AGARD, Wall Interference, Support Interference and Flow Field Measurements 6 p Jul. 1994
Copyright Avail: CASI HC A02/MF A04

An unsteady, subsonic flow panel method is applied to predict the support interference effects in dynamic wind tunnel test simulation. Interference effects are calculated by simulating the unsteady flow around the aircraft model, both in the presence and absence of the support system, unlike common experimental techniques that try to measure these effects. The present study uses the standard

dynamics model (SDM) in pitch oscillations as a test case. Calculated results for free flight conditions are compared with results obtained when simulating the presence of an existing side-wall-mounted support system in a dynamic wind-tunnel test facility. The calculated results are also compared with experimental data available from different dynamic wind tunnel test facilities. Author

N95-19457# National Aerospace Lab., Bangalore (India). Computational and Theoretical Fluid Dynamics Div.
VISCOUS FLOW PAST AEROFOILS AXISYMMETRIC BODIES AND WINGS
 S. S. DESAI *In its* CFD: Advances and Applications, 1994 p 43-76 Oct. 1994
 Avail: CASI HC A03/MF A04

A brief outline is given here of computing viscous flow past aerospace components such as aerofoils, bodies of revolution and wings, based on a coupling of potential flow computations and integral boundary layer calculations. Direct and semi-inverse procedures for viscous-inviscid coupling are described. Keeping in mind transonic and high Reynolds number flows, only turbulent flow computations are considered; laminar and transitional flows are not covered here. Author

N95-19464# National Aerospace Lab., Bangalore (India). Computational and Theoretical Fluid Dynamics Div.
PARABOLIZED NAVIER-STOKES SOLUTION OF SUPERSONIC/HYPERSONIC FLOWS
 DINESH K. PRABHU *In its* CFD: Advances and Applications, 1994 p 321-371 Oct. 1994
 Avail: CASI HC A04/MF A04

In this lecture we will (1) develop the governing PNS (Parabolized Navier-Stokes) equations for ideal gas, equilibrium air and nonequilibrium air, (2) develop the numerical algorithm to solve these equations, (3) apply the algorithm to compute the hypersonic flow past a simple geometrical shape such as a sharp cone at zero incidence, and (4) discuss the results in terms of the various gas models. Some of the expressions in this lecture have been derived in detail for the ideal/equilibrium model only. Author

03

AIR TRANSPORTATION AND SAFETY

Includes passenger and cargo air transport operations; and aircraft accidents.

N95-16404# Army Aeromedical Research Lab., Fort Rucker, AL.
A CORRELATIVE INVESTIGATION OF SIMULATED OCCUPANT MOTION AND ACCIDENT REPORT IN A HELICOPTER CRASH
 DAVID G. BEALE, NABIH M. ALEM, and BARCLAY P. BUTLER Aug. 1994 31 p
 (AD-A285190; USAARL-94-42) Avail: CASI HC A03/MF A01

In 1987, an Army Apache helicopter crashed during a training mission at Fort Rucker, Alabama, resulting in fatal injuries to the rear seat pilot and survivable injuries to the front seat copilot. U.S. Army Safety Center (USASC) investigators at Fort Rucker, Alabama, reported the aircraft damage assessment and aircrew member injuries. U.S. Army Aeromedical Research Laboratory (USAARL) researchers at Fort Rucker, Alabama, concurrently examined the helmets, restraint systems, and crashworthy seats. Crash kinematics were derived from the investigation; including estimates of the motion of the harnessed occupants during the crash. DTIC

N95-17476# Federal Aviation Administration, Washington, DC.
FEDERAL AVIATION REGULATIONS, PART 91. GENERAL OPERATING AND FLIGHT RULES. CHANGE 5
 15 May 1994 24 p See also PB94-159944
 (PB94-194883) Avail: CASI HC A03/MF A01

This change incorporates three amendments on Special Visual Flight Rules (SVFR)—Amendments 91-236, 91-237, and 91-128—which affect Appendix D. This change also incorporates Amendment 91-239, Airspace Reclassification, issued March 7, which affects Sections 91.126, 91.127, and 91-130. NTIS

N95-17646# National Transportation Safety Board, Washington, DC.
AIRCRAFT ACCIDENT REPORT: STALL AND LOSS OF CONTROL ON FINAL APPROACH, ATLANTIC COAST AIRLINES, INC./UNITED EXPRESS FLIGHT 6291 JETSTREAM 4101, N304UE COLUMBUS, OH, 7 JANUARY 1994
 6 Oct. 1994 124 p
 (PB94-910409; NTSB/AAR-94/07) Avail: CASI HC A06/MF A02

This report explains the crash of United Express flight 6291, a Jetstream 4101 airplane, while on approach to runway 28L at Port Columbus International Airport, Columbus, Ohio, on January 7, 1994. The safety issues in the report focused on aircraft safety belts and training programs for Part 135 pilots that emphasize stall warning recognition and recovery techniques, and that lead to proficiency in both high speed and coupled approaches. Safety recommendations concerning these issues were made to the Federal Aviation Administration. Author

N95-17748# National Transportation Safety Board, Washington, DC.
ANNUAL REVIEW OF AIRCRAFT ACCIDENT DATA: US AIR CARRIER OPERATIONS, CALENDAR YEAR 1992
 15 Sep. 1994 73 p
 (PB95-100319; NTSB/ARC-94/02) Avail: CASI HC A04/MF A01

This publication presents the record of aviation accidents involving revenue operations of U.S. Air Carriers including Commuter Air Carriers and On Demand Air Taxis for calendar year 1992. The report is divided into three major sections according to the federal regulations under which the flight was conducted - 14 CFR 121, Scheduled 14 CFR 135, or Nonscheduled 14 CFR 135. In each section of the report tables are presented to describe the losses and characteristics of 1992 accidents to enable comparison with prior years. NTIS

N95-18582*# National Aeronautics and Space Administration. Lewis Research Center, Cleveland, OH.
COLLECTION EFFICIENCY AND ICE ACCRETION CALCULATIONS FOR A SPHERE, A SWEEP MS(1)-317 WING, A SWEEP NACA-0012 WING TIP, AN AXISYMMETRIC INLET, AND A BOEING 737-300
 COLIN S. BIDWELL and STANLEY R. MOHLER, JR. (NYMA, Inc., Brook Park, OH.) Jan. 1995 45 p Presented at the 33rd Aerospace Sciences Meeting and Exhibit, Reno, NV, 9-12 Jan. 1995; sponsored by AIAA
 (Contract(s)/Grant(s): NAS3-27186; RTOP 505-68-10)
 (NASA-TM-106831; E-9381; NAS 1.15:106831; AIAA PAPER 95-0755) Avail: CASI HC A03/MF A01

Collection efficiency and ice accretion calculations have been made for a sphere, a swept MS(1)-317 wing, a swept NACA-0012 wing tip, an axisymmetric inlet, and a Boeing 737-300 inlet using the NPARC flow solver and the NASA Lewis LEWICE3D grid based ice accretion code. Euler flow solutions for the geometries were generated using the NPARC flow solver. The LEWICE3D grid based ice accretion program was used to calculate the impingement efficiencies and ice shapes. Ice shapes specifying rime and mixed icing conditions were generated for a 30 minute hold condition. All calculations were performed on an SGI Model Power Challenge Computer. The results have been compared to experimental flow and impingement data. In general, the calculated flow and collection efficiencies compared well with experiment, and the ice shapes looked reasonable and appeared representative of the rime and mixed icing conditions for which they were calculated. Author

03 AIR TRANSPORTATION AND SAFETY

N95-19132# National Transportation Safety Board, Washington, DC. SAFETY STUDY: COMMUTER AIRLINE SAFETY

Nov. 1994 134 p

(PB94-917004; NTSB/SS-94/02) Avail: CASI HC A07/MF A02

The commuter airline industry has grown dramatically and has experienced significant changes in operating characteristics in the past 15 years. In response to safety recommendations issued by the National Transportation Safety Board and through other initiatives taken by government and industry, regulatory revisions and other actions have resulted in an improved safety record for commuter airlines and conducting operations under title 14 Code of Federal Regulations Part 135. However, despite efforts to bring about safety improvements, accident rates for commuter airlines continue to be higher than the rates for domestic Part 121 airlines. The higher accident rate, the difference in regulatory standards between Parts 135 and 121, and findings of the Safety Board's investigations of recent accidents prompted the Board to initiate this study of commuter airline safety. The safety issues discussed in the study are: (1) the need for sweeping regulatory action; (2) the adequacy of Part 135 regulations concerning flight time limits and rest requirements; (3) the need for licensed dispatch personnel; (4) the adequacy of Part 135 pilot training; (5) the adequacy of flight attendant training practices; (6) the need for mandated safety programs at commuter airlines and for operational oversight by major air carrier code-sharing partners; (7) the training of Federal Aviation Administration inspectors; and (8) the certification of airports served by scheduled passenger operations. As a result of the safety study, recommendations concerning these issues were made to the Federal Aviation Administration, the U.S. Department of Transportation, major U.S. domestic air carriers, and the Regional Airline Association. Author

N95-19167# National Research Council of Canada, Ottawa (Ontario). Structures and Materials Lab.

SPECTROGRAM DIAGNOSIS OF AIRCRAFT DISASTERS

F. W. SLINGERLAND *In* AGARD, Impact of Acoustic Loads on Aircraft Structures 6 p Sep. 1994 Original contains color illustrations

Copyright Avail: CASI HC A02/MF A03

Impulsive forces applied to an aircraft fuselage generate radial vibration waves in the structure analogous to those in a classical thin shell. It has been found that these waves are detected by the cockpit area microphone, and that spectrogram analysis of the microphone recording can provide information on the nature, origin and strength of the source, whether an explosion or a sudden decompression.

Author

N95-19284*# National Aeronautics and Space Administration. Lewis Research Center, Cleveland, OH.

METHODS FOR SCALING ICING TEST CONDITIONS

DAVID N. ANDERSON Jan. 1995 11 p Presented at the 33rd Aerospace Sciences Meeting and Exhibit, Reno, NV, 9-12 Jan. 1995; sponsored by AIAA

(Contract(s)/Grant(s): RTOP 505-68-10)

(NASA-TM-106827; E-9376; NAS 1.15:106827; AIAA PAPER 95-0540) Avail: CASI HC A03/MF A01

This report presents the results of tests at NASA Lewis to evaluate several methods to establish suitable alternative test conditions when the test facility limits the model size or operating conditions. The first method was proposed by Olsen. It can be applied when full-size models are tested and all the desired test conditions except liquid-water content can be obtained in the facility. The other two methods discussed are: a modification of the French scaling law and the AEDC scaling method. Icing tests were made

with cylinders at both reference and scaled conditions representing mixed and glaze ice in the NASA Lewis Icing Research Tunnel. Reference and scale ice shapes were compared to evaluate each method. The Olsen method was tested with liquid-water content varying from 1.3 to .8 g/m(exp3). Over this range, ice shapes produced using the Olsen method were unchanged. The modified French and AEDC methods produced scaled ice shapes which approximated the reference shapes when model size was reduced to half the reference size for the glaze-ice cases tested. Author

N95-19285*# National Aeronautics and Space Administration. Lewis Research Center, Cleveland, OH.

ICE ACCRETION WITH VARYING SURFACE TENSION

ALAN J. BILANIN (Continuum Dynamics, Inc., Princeton, NJ.) and DAVID N. ANDERSON Jan. 1995 13 p Presented at the 33rd Aerospace Sciences Meeting and Exhibit, Reno, NV, 9-12 Jan. 1995; sponsored by AIAA

(Contract(s)/Grant(s): RTOP 505-68-10)

(NASA-TM-106826; E-9375; NAS 1.15:106826; AIAA PAPER 95-0538) Avail: CASI HC A03/MF A01

During an icing encounter of an aircraft in flight, super-cooled water droplets impinging on an airfoil may splash before freezing. This paper reports tests performed to determine if this effect is significant and uses the results to develop an improved scaling method for use in icing test facilities. Simple laboratory tests showed that drops splash on impact at the Reynolds and Weber numbers typical of icing encounters. Further confirmation of droplet splash came from icing tests performed in the NaSA Lewis Icing Research Tunnel (IRT) with a surfactant added to the spray water to reduce the surface tension. The resulting ice shapes were significantly different from those formed when no surfactant was added to the water. These results suggested that the droplet Weber number must be kept constant to properly scale icing test conditions. Finally, the paper presents a Weber-number-based scaling method and reports results from scaling tests in the IRT in which model size was reduced up to a factor of 3. Scale and reference ice shapes are shown which confirm the effectiveness of this new scaling method. Author

N95-19468*# National Aeronautics and Space Administration. Langley Research Center, Hampton, VA.

FAA/NASA INTERNATIONAL SYMPOSIUM ON ADVANCED STRUCTURAL INTEGRITY METHODS FOR AIRFRAME DURABILITY AND DAMAGE TOLERANCE, PART 2

CHARLES E. HARRIS, ed. Sep. 1994 572 p Symposium held at Hampton, VA, 4-6 May 1994; sponsored by NASA and FAA

(Contract(s)/Grant(s): RTOP 538-02-10-01)

(NASA-CP-3274-PT-2; L-17432-PT-2; NAS 1.55:3274-PT-2) Avail: CASI HC A24/MF A04

The international technical experts in the areas of durability and damage tolerance of metallic airframe structures were assembled to present and discuss recent research findings and the development of advanced design and analysis methods, structural concepts, and advanced materials. The principal focus of the symposium was on the dissemination of new knowledge and the peer-review of progress on the development of advanced methodologies. Papers were presented on the following topics: structural concepts for enhanced durability, damage tolerance, and maintainability; new metallic alloys and processing technology; fatigue crack initiation and small crack effects; fatigue crack growth models; fracture mechanics failure criteria for ductile materials; structural mechanics methodology for residual strength and life prediction; development of flight load spectra for design and testing; and corrosion resistance. For individual titles, see N95-19469 through N95-19500.

AIRCRAFT COMMUNICATIONS AND NAVIGATION

Includes digital and voice communication with aircraft; air navigation systems (satellite and ground based); and air traffic control.

A95-64288

COMMENTARY ON WALTON CORRESPONDENCE RELATING TO THE ILS GLIDE SLOPE

RICHARD H. MCFARLAND Ohio Univ, Athens, OH IEEE Transactions on Aerospace and Electronic Systems (ISSN 0018-9251) vol. 30, no. 3 July 1994 p. 933-935 refs (BTN-94-EIX94441380856) Copyright

The conclusions reached by Dr. Walton regarding the reliability of the instrument landing system (ILS) glide slope is highly erroneous and can be attributed to the author's close ties with the plaintiff in the Alpena plane crash case. Dr. Walton's contention lacks credence and is contrary to proven scientific principles that define the effects of snow on an aircraft's landing system. The null-reference glide slope is a highly reliable navigation tool and there is not a single recorded case wherein an accident was traced to a defective glide slope signal. EI

A95-64294

CONVERSION OF EARTH-CENTERED EARTH-FIXED COORDINATES TO GEODETIC COORDINATES

IEEE Transactions on Aerospace and Electronic Systems (ISSN 0018-9251) vol. 30, no. 3 July 1994 p. 957-962 refs (BTN-94-EIX94441380862) Copyright

The transformations between Earth-centered Earth-fixed (ECEF) coordinates and geodetic coordinates are required in many applications, for example, in NAVSTAR/GPS navigation and geodesy. The transformation from ECEF coordinates to geodetic coordinates is usually carried out by approximation methods in practice, and the exact transformation methods are not used frequently. In this paper, several exact transformation formulas from ECEF coordinates to geodetic coordinates are reviewed, and compared with the approximation methods in complexity and in sensitivity to computer round-off error. The relationship among some exact transformation solutions and the approaches are pointed out. Author (EI)

N95-16277# Nanjing Univ. of Aeronautics and Astronautics, Nanjing, Jiangsu (China). Dept. of Automatic Control.

APPLICATION OF GPS/SINS/RA INTEGRATED SYSTEM TO AIRCRAFT APPROACH LANDING

XIN YUAN, JIANYE LIU, and YONGXI NI *In its* Joint Proceedings on Aeronautics and Astronautics (JPAA) p 184-190 May 1993 See also A92-21466

Avail: CASI HC A02/MF A03

A design scheme for integrating a global positioning system (GPS), strap down inertial navigation system (SINS) and a radio altimeter (RA) for precise aircraft landing is presented and the dynamic model is established with the application of a Kalman filter technique. The simulation for the GPS/SINS/RA performance is carried out, using a SPS simulator, considering a glide slope inclination of 3 degrees for aircraft landings. Simulation results indicate that the integrated system, on condition that the GPS receiver uses either P code, or C/A code with the aid of pseudolite technology, and works in the differential mode, is able to meet the ICAO positioning requirements for aircraft precision landing.

Author (revised)

N95-17196*# Centre National d'Etudes Spatiales, Toulouse (France). A PROCESSING CENTRE FOR THE CNES CE-GPS EXPERIMENTATION

NORBERT SUARD and JEAN-CLAUDE DURAND *In* NASA.

Goddard Space Flight Center, Third International Symposium on Space Mission Operations and Ground Data Systems, Part 1 p 149-154 Nov. 1994

Avail: CASI HC A02/MF A06

CNES is involved in a GPS (Global Positioning System) geostationary overlay experimentation. The purpose of this experimentation is to test various new techniques in order to select the optimal station synchronization method, as well as the geostationary spacecraft orbitography method. These new techniques are needed to develop the Ranging GPS Integrity Channel services. The CNES experimentation includes three transmitting/receiving ground stations (manufactured by IN-SNEC), one INMARSAT 2 C/L band transponder and a processing center named STE (Station de Traitements de l'Experimentation). Not all the techniques to be tested are implemented, but the experimental system has to include several functions; part of the future system simulation functions, such as a servo-loop function, and in particular a data collection function providing for rapid monitoring of system operation, analysis of existing ground station processes, and several weeks of data coverage for other scientific studies. This paper discusses system architecture and some criteria used in its design, as well as the monitoring function, the approach used to develop a low-cost and short-life processing center in collaboration with a CNES subcontractor (ATTDATAID), and some results. Author (revised)

N95-17373 CCG Associates, Inc., Silver Spring, MD.

IDENTIFICATION OF ARTIFICIAL INTELLIGENCE (AI) APPLICATIONS FOR MAINTENANCE, MONITORING, AND CONTROL OF AIRWAY FACILITIES Final Report, Jul. 1991 - Mar. 1992

LORI ADKISSON, KAMAL KARNA, DONALD KATZ, ANITA KARNA, and KEJITAN DONTAS May 1994 172 p Limited Reproducibility: More than 20% of this document may be affected by microfiche quality (AD-A282479; DOT/FAA/CT-TN92/41-1) Avail: Issuing Activity (Defense Technical Information Center (DTIC))

This document provides information acquired from a study conducted on artificial intelligence (AI). The study had four goals, as follows: (1) to identify airway facilities (AF) maintenance, monitoring, and control of activities suitable for AI application development; (2) to determine the AI technologies, tools, architectures, and algorithms that would be most suitable for the identified applications; (3) to develop a set of criteria for AI applications development, and evaluate each of the identified applications in terms of this criteria; and (4) to make short- and long-term recommendations for AI applications development within AF. DTIC

N95-17384*# National Aeronautics and Space Administration, Langley Research Center, Hampton, VA.

MODELING OF INSTRUMENT LANDING SYSTEM (ILS) LOCALIZER SIGNAL ON RUNWAY 25L AT LOS ANGELES INTERNATIONAL AIRPORT

RICHARD M. HUESCHEN and CHARLES E. KNOX Nov. 1994 30 p (Contract(s)/Grant(s): RTOP 505-64-13-04) (NASA-TM-4588; L-17334; NAS 1.15:4588) Avail: CASI HC A03/MF A01

A joint NASA/FAA flight test has been made to record instrument landing system (ILS) localizer receiver signals for use in mathematically modeling the ILS localizer for future simulation studies and airplane flight tracking tasks. The flight test was conducted on a portion of the ILS localizer installed on runway 25L at the Los Angeles International Airport. The tests covered the range from 10 to 32 n.mi. from the localizer antenna. Precision radar tracking information was compared with the recorded localizer deviation data. Data analysis showed that the ILS signal centerline was offset to the left of runway centerline by 0.071 degrees and that no significant bends existed on the localizer beam. Suggested simulation models for the ILS localizer are formed from a statistical analysis. Author

04 AIRCRAFT COMMUNICATIONS AND NAVIGATION

N95-17706 Carnegie-Mellon Univ., Pittsburgh, PA. Robotics Inst. **A FEEDFORWARD CONTROL APPROACH TO THE LOCAL NAVIGATION PROBLEM FOR AUTONOMOUS VEHICLES** ALONZO KELLY 2 May 1994 71 p Limited Reproducibility: More than 20% of this document may be affected by microfiche quality (Contract(s)/Grant(s): DACA76-89-C-0014; DAAE07-90-C-R059) (AD-A282787; CMU-RI-TR-94-17) Avail: CASI HC A04

RANGER is an acronym for Real-time Autonomous Navigator with a Geometric Engine. This report describes the 'geometric engine' part of RANGER - the state space model and the associated control algorithms. A new approach to the high speed autonomy problem is presented which is based fundamentally on the state space representation of a multi-input multi-output linear system. The system closes the overall perceive-think-act loop for a robot vehicle at relatively high update bandwidth and incorporates both somatic and environmental feedback. A high fidelity feedforward actuator dynamics and terrain following model is introduced which formulates the local navigation problem as an optimal control problem. The system is concerned with the high level coordinated control problem. It is a state space controller because it explicitly forms an expression of the vehicle dynamic state vector in order to predict the hazard signals upon which decisions are based. Derived from text

N95-18059# Systems Control Technology, Inc., Arlington, VA. **HELIPORT/VERTIPORT MLS PRECISION APPROACHES Final Report** DEBORAH PEISEN and BRIAN SAWYER Jul. 1994 68 p (AD-A283505; REPT-92RR-28; DOT/FAA/RD-94/23) Avail: CASI HC A04/MF A01

In the early 1990's, the Federal Aviation Administration initiated an effort to answer certain questions on precision approaches to heliports and vertiports. Of particular interest were issues of economic justification and available airspace. Among the tasks included in this effort were the following: (1) Develop a criteria of what is required to establish an instrument approach at a heliport or vertiport. (2) Develop a selection process to qualify potential IFR heliport and vertiport candidates. This effort was focused on MLS. The implementation of GPS instrument approaches has required us to re-focus our thinking. This re-focusing is now well underway as evidenced with the commissioning of the Chattanooga hospital heliport GPS nonprecision approach. The publication of this report is not likely to have broad implications regarding the implementation of GPS instrument approaches. However, some portions of the work may have application to GPS instrument approaches and this document is published with this in mind. DTIC

N95-18088# Federal Aviation Administration, Atlanta, GA. **OPERATIONAL AND SUPPORTABILITY IMPLEMENTATION SYSTEM (OASIS) TEST AND EVALUATION MASTER PLAN** WILLIAM E. BENNER and JAMES A. MCCULLOUGH Sep. 1994 83 p (AD-A284765; DOT/FAA/CT-TN94/6) Avail: CASI HC A05/MF A01

This Test and Evaluation Master Plan (TEMP) is for the Operational And Supportability Implementation System (OASIS) and describes the Test and Evaluation (T&E) processes that ensure the system meets the requirements allocated to the project in the NAS-SS-1000, volumes 1 and 2, and the NAS-SR-1000. The document defines test strategy, test requirements, and organizational roles and responsibilities. The purpose of the plan is to define the overall T&E phases necessary to ensure the integration of the OASIS within the environment of the National Airspace System (NAS). The OASIS will replace the Model 1 Full Capacity (M1FC) work station position equipment, located at the 61 Automated Flight Service Stations (AFSS) and provide a planned capability for new Flight Service Automation System (FSAS) AFSS state-of-the-art work station equipment which can be logistically supported. The hardware and software will mainly be comprised of commercial-off-the-shelf (COTS) and/or nondevelopmental item (NDI) acquisitions.

The capability will include functionality to store, retrieve, display, highlight, zoom, and transfer information applying to any set of weather conditions, route of flight, or aircraft type. Weather and flight route information will be displayed simultaneously. The specialist will review visual notification of flight route problems including severe weather, and other safety concerns. DTIC

N95-18347* National Aeronautics and Space Administration. Ames Research Center, Moffett Field, CA.

VSTOL SYSTEMS RESEARCH AIRCRAFT (VSRA) HARRIER (Videotape)

Dec. 1994 Videotape: 9 min. 30 sec. playing time, in color, with sound (NASA-TM-110117; NONP-NASA-VT-95-37002) Avail: CASI VHS A02/BETA A22

NASA's Ames Research Center has developed and is testing a new integrated flight and propulsion control system that will help pilots land aircraft in adverse weather conditions and in small confined areas (such as, on a small ship or flight deck). The system is being tested in the VSTOL (Vertical/Short Takeoff and Landing) Systems research Aircraft (VSRA), which is a modified version of the U.S. Marine Corps's AV-8B Harrier jet fighter, which can take off and land vertically. The new automated flight control system features both head-up and panel-mounted computer displays and also automatically integrates control of the aircraft's thrust and thrust vector control, thereby reducing the pilot's workload and help stabilize the aircraft for landing. Visiting pilots will be encouraged to test the new system and provide formal evaluation flights data and feedback. An actual flight test and the display panel of control system are shown in this video. CASI

N95-18927# Advisory Group for Aerospace Research and Development, Neuilly-Sur-Seine (France). Guidance and Control Panel. **ON-LINE HANDLING OF AIR TRAFFIC: MANAGEMENT, GUIDANCE AND CONTROL [CONDUITE EN LIGNE DU TRAFIC AERIEN: GESTION, GUIDAGE, AND PILOTAGE]** ANDRE BENOIT, ed., C. GARCIA-AVELLO, J. LEMAITRE, M. PELEGRIN, E. PETRE, and S. SWIERTRA Nov. 1994 220 p Original contains color illustrations (AGARD-AG-321; ISBN-92-835-0758-4) Copyright Avail: CASI HC A10/MF A03

Following a summary of the activities of the Guidance and Control Panel of AGARD in the field of Air Traffic Handling, this volume constitutes essentially an introduction for those new to the Air Traffic Control Research and Development community, offering, on the one hand, a broad view of the present situation and actual limitations, on the other hand, some precise idea of a long term system objective. It is composed of a preface, a general introduction and ten chapters, each constituting an introduction to the corresponding topics, successively entitled: the air transport system, air traffic complexity, traffic evolution, electronic aids to controllers, arrivals management systems, decision making aids, a look further into the future, towards global optimization, systems evaluation facilities, and the airport of the future. Author

05

AIRCRAFT DESIGN, TESTING AND PERFORMANCE

Includes aircraft simulation technology.

A95-63634
ANALYTICAL DESCRIPTION OF AND FORECAST FOR STRESS RELAXATION OF AVIATION MATERIALS UNDER THE VIBRATION CONDITIONS

G. V. VASIL'EV KGTU, Kazan (Russia) and YU. P. KATAEV

Izvestiya VUZ: Aviatsionnaya Tekhnika (ISSN 0579-2975) no. 1 January-March 1994 p. 8-13 In RUSSIAN refs (BTN-94-EIX94461408751) Copyright

The problem of forecasting for dynamic stress relaxation by the static stress characteristics is rather vital. That's why a method to calculate the growth of creep flow and of stress relaxation has been developed. It is assumed that the load is vibrationally applied, according to the parameter of relaxation internal friction. Creeping curves and stress relaxations are described by equations of the hardening theory in the power version. Calculated and experimental values have been compared. EI

A95-64609

X-29 HIGH-ANGLE-OF-ATTACK

ANON Aerospace Engineering (Warrendale, Pennsylvania) (ISSN 0736-2536) vol. 13, no. 7 July 1993 p. 11-17 (BTN-94-EIX94511309383) Copyright

A program to test the X-29-2 at high angle of attack is described. The program cleared the aircraft to fly in a broad flight regime, provided insight to its critical forebody flow field, and supplied data regarding the operation of various subsystems. EI

N95-15971*# Rockwell International Corp., Downey, CA. Space Systems Div.

PROGRAM TEST OBJECTIVES MILESTONE 3

T. L. GAYNOR 15 Nov. 1994 78 p

(Contract(s)/Grant(s): NCC8-47)

(NASA-CR-197030; NAS 1.26:197030; SSD94D0335) Avail: CASI HC A05/MF A01

The following conclusions have been developed relative to propulsion system technology adequacy for efficient development and operation of recoverable and expendable launch vehicles (RLV and ELV) and the benefits which the integrated propulsion technology demonstrator will provide for enhancing technology: (1) Technology improvements relative to propulsion system design and operation can reduce program cost. Many features or improvement needs to enhance operability, reduce cost, and improve payload are identified. (2) The Integrated Propulsion Technology Demonstrator (IPTD) Program provides a means of resolving the majority of issues associated with improvement needs. (3) The IPTD will evaluate complex integration of vehicle and facility functions in fluid management and propulsion control systems, and provides an environment for validating improved mechanical and electrical components. (4) The IPTD provides a mechanism for investigating operational issues focusing on reducing manpower and time to perform various functions at the launch site. These efforts include model development, collection of data to validate subject models, and ultimate development of complex time line models. (5) The IPTD provides an engine test bed for tri/bi-propellant engine development firings which is representative of the actual vehicle environment. (6) The IPTD provides for only a limited multiengine configuration integration environment for RLV. Multiengine efforts may be simulated for a number of subsystems and a number of subsystems are relatively independent of the multiengine influences. Derived from text

N95-16171# Loral Systems, Inc., Orlando, FL. Adst Program Office.

ADST SYSTEM TEST REPORT FOR THE ROTARY WING AIRCRAFT AIRNET AEROMODEL AND WEAPON MODEL MERGE WITH THE ATAC 2 BASELINE

JOE ALMANZA, LYNN THOMPSON, and MARY KRUCK 20 Jan. 1994 290 p

(Contract(s)/Grant(s): N61339-91-D-0001)

(AD-A281580; ADST/WDL/TR-93-003274) Avail: CASI HC A13/MF A03

The results and corrective actions of the AIRNET/ATAC 2 test activities which were conducted at the Ft Rucker, AL, Aviation Training Facility during the periods of 8-12 February 1993 and 9-18 August 1993 are documented. DTIC

N95-16264# Kazan Aviation Inst. (USSR). Scientific School of Aircraft Strength.

DEVELOPMENT OF STRENGTH ANALYSIS METHODS AND DESIGN MODEL FOR AIRCRAFT CONSTRUCTIONS IN KAZAN AVIATION INSTITUTE

M. V. VAKHITOV In Nanjing Univ. of Aeronautics and Astronautics, Joint Proceedings on Aeronautics and Astronautics (JPAA) p 103-106 May 1993

Avail: CASI HC A01/MF A03

Research on problems of aircraft structural strength have been carried out at Kazan Aviation Institute since the day of foundation of the chair 'Aircraft strength analysis' in 1938. The well known school of aircraft strength was developed under Yu G. Odinov's supervision. Eight doctoral dissertations and more than 70 master's theses give witness to its fruitfulness and success. Its followers work as the leading engineers in the field of strength analysis in two large national centers - Central Aerohydrodynamic Institute and the Siberian Aircraft Research Institute and at a number of higher education institutions. Author (revised)

N95-16356# Naval Postgraduate School, Monterey, CA.

LOW RATE INITIAL PRODUCTION IN ARMY AVIATION SYSTEMS DEVELOPMENT M.S. Thesis

LAWRENCE P. MEDLER Mar. 1994 123 p

(AD-A281871) Avail: CASI HC A06/MF A02

The purpose of this thesis is to analyze DOD's use of Low Rate Initial Production (LRIP) on selected Army Aviation programs within the acquisition life cycle of weapon systems development. A comparative analysis is conducted on the selected programs concentrating on significant issues which affect the use of LRIP. The thesis focuses on the preproduction phases of the acquisition process, the organizations that influence LRIP policies and future trends in procurement policy. The research includes an examination of the AH-64 Longbow Apache, the OH-58D Kiowa Warrior, the MH-47 and the EH-60 Special Operations Aircraft and the RAH-66 Comanche. This thesis concludes that premature entry into LRIP is a systemic deficiency in acquisition oversight which leads to a proliferation in the required number of LRIP systems. A recommendation to overcome this deficiency and obtain a more accurate number is to identify the three LRIP quantity determination elements separately. This would provide the Milestone II Decision Authority more accurate data with which to render a decision. DTIC

N95-16562# Advisory Group for Aerospace Research and Development, Neuilly-Sur-Seine (France). Fluid Dynamics Panel.

OPTIMUM DESIGN METHODS FOR AERODYNAMICS [LES METHODES DE CONCEPTION OPTIMALE POUR L'AERODYNAMIQUE]

Nov. 1994 270 p Special course held in Rhode-Saint-Genese, Belgium, 25-29 Apr. 1994; sponsored by AGARD and VKI

(AGARD-R-803; ISBN-92-836-1007-5) Copyright Avail: CASI HC A12/MF A03

The course addresses the ingredients of new algorithms for accurate and cost effective numerical solutions of design problems. A special emphasis is given to the following topics: fundamental mathematical properties of methodologies for solving optimization problems using control theory and variational formulations; numerical aspects of fast algorithms coupling constrained optimizers and flow analysis solvers and their implementation; geometric representations and choice of design variables; and real life 3-D applications encountered in Aerospace Engineering in order to demonstrate the usefulness of these design methodologies to practical design problems. For individual titles, see N95-16563 through N95-16573.

N95-16565# Princeton Univ., NJ. Dept. of Mechanical and Aerospace Engineering.

OPTIMUM AERODYNAMIC DESIGN VIA BOUNDARY CONTROL

ANTONY JAMESON In AGARD, Optimum Design Methods for Aerodynamics 33 p Nov. 1994 Sponsored in cooperation with

USRA

(Contract(s)/Grant(s): AF-AFOSR-0391-91; N00014-92-J-1976)

Copyright Avail: CASI HC A03/MF A03

These lectures describe the implementation of optimization techniques based on control theory for airfoil and wing design. In previous studies it was shown that control theory could be used to devise an effective optimization procedure for two-dimensional profiles in which the shape is determined by a conformal transformation from a unit circle, and the control is the mapping function. Recently the method has been implemented in an alternative formulation which does not depend on conformal mapping, so that it can more easily be extended to treat general configurations. The method has also been extended to treat the Euler equations, and results are presented for both two and three dimensional cases, including the optimization of a swept wing.

Author

N95-16566# National Aerospace Lab., Amsterdam (Netherlands). Theoretical Aerodynamics Dept.

RESIDUAL-CORRECTION TYPE AND RELATED COMPUTATIONAL METHODS FOR AERODYNAMIC DESIGN. PART 1: AIRFOIL AND WING DESIGN

TH. E. LABRUJERE *In* AGARD, *Optimum Design Methods for Aerodynamics* 24 p Nov. 1994

Copyright Avail: CASI HC A03/MF A03

The present paper discusses the problem of inverse shape design, where the geometry of a wing should be determined such that it will have a prescribed surface pressure distribution at the design condition considered. A survey is given of so-called decoupled-solution methods for this problem. With this type of methods the flow field around a current estimate of the wing and a subsequent new estimate of the wing are determined by two separate computational steps in an iterative process. A global description is given of the main features of the underlying theories and some examples of application are given. A detailed description is given of the NLR method for inverse shape design based on the residual-correction approach.

Author

N95-16567# National Aerospace Lab., Amsterdam (Netherlands). Theoretical Aerodynamics Dept.

RESIDUAL-CORRECTION TYPE AND RELATED COMPUTATIONAL METHODS FOR AERODYNAMIC DESIGN. PART 2: MULTI-POINT AIRFOIL DESIGN

TH. E. LABRUJERE *In* AGARD, *Optimum Design Methods for Aerodynamics* 31 p Nov. 1994

Copyright Avail: CASI HC A03/MF A03

The present paper considers the problem of multi-point airfoil design, where the geometry of an airfoil is to be determined such that it will approximate simultaneously, at different design points, a priori specified aerodynamic requirements. Some attention is paid to approaches published in the open literature. The main part of the paper concerns work in progress at NLR. Some preliminary results are shown.

Author

N95-16568# Paris VI Univ. (France). Lab. Analyse Numerique.

OPTIMAL SHAPE DESIGN FOR AERODYNAMICS

O. PIRONNEAU *In* AGARD, *Optimum Design Methods for Aerodynamics* 38 p Nov. 1994

Copyright Avail: CASI HC A03/MF A03

After a brief recall on the history of the field of optimal shape design, we shall present a few applications to aerodynamics, then recall the variational approach, the numerical methods and the recent developments both in applied mathematics and in computer sciences.

Author

N95-16569*# National Aeronautics and Space Administration. Lewis Research Center, Cleveland, OH.

AIRFOIL OPTIMIZATION BY THE ONE-SHOT METHOD

G. KURUVILA (Vigyan Research Associates, Inc., Hampton, VA.), SHLOMO TAASAN (Institute for Computer Applications in Science and Engineering, Hampton, VA.), and M. D. SALAS *In* AGARD, *Optimum Design Methods for Aerodynamics* 21 p Nov. 1994

Copyright Avail: CASI HC A03/MF A03

An efficient numerical approach for the design of optimal aerodynamic shapes is presented in this paper. The objective of any optimization problem is to find the optimum of a cost function subject to a certain state equation (Governing equation of the flow field) and certain side constraints. As in classical optimal control methods, the present approach introduces a costate variable (Lagrange multiplier) to evaluate the gradient of the cost function. High efficiency in reaching the optimum solution is achieved by using a multigrid technique and updating the shape in a hierarchical manner such that smooth (low-frequency) changes are done separately from high-frequency changes. Thus, the design variables are changed on a grid where their changes produce nonsmooth (high-frequency) perturbations that can be damped efficiently by the multigrid. The cost of solving the optimization problem is approximately two to three times the cost of the equivalent analysis problem.

Author

N95-16570# Deutsche Airbus G.m.b.H., Bremen (Germany). Aerodynamic Design Section.

TOOLS FOR APPLIED ENGINEERING OPTIMIZATION

A. VANDERVELDEN *In* AGARD, *Optimum Design Methods for Aerodynamics* 10 p Nov. 1994

Copyright Avail: CASI HC A02/MF A03

This paper is an introduction to applied optimization of engineering problems, with an emphasis on aircraft design. First, the optimization problem is described—namely, the objective function and the problems often involved in its optimization, the variables or parameters over which the objective function is optimized, and the constraints upon the objective function. Formulation of the optimization problem to ensure rapid and accurate convergence is discussed and illustrated with specific examples. Three classes of optimization methods: evolution, downhill simplex and gradient optimization, are discussed. The robustness and speed of these optimization methods are evaluated and compared. Finally, a number of practical implementation issues related to optimization are highlighted.

Author

N95-16571# Deutsche Airbus G.m.b.H., Bremen (Germany). Aerodynamic Design Section.

THE GLOBAL AIRCRAFT SHAPE

A. VANDERVELDEN *In* AGARD, *Optimum Design Methods for Aerodynamics* 11 p Nov. 1994

Copyright Avail: CASI HC A03/MF A03

This work describes the methodology used to compare supersonic design concepts and its use in industry. The design concepts are analyzed with a modular synthesis model and compared on the basis of operating economy with specified performance and environmental impact. The analysis routines of the synthesis model are mainly configuration independent and represent fixed levels of structural, aerodynamic and propulsion technology. The specialist departments are responsible for the content of the routines, and later verify the design with more refined methods. At present more than two hundred variables describe the aircraft geometry, engine characteristics and mission. More than twenty of those variables representing the aircraft and its flight-profile are optimized simultaneously as a function of Mach number, payload and range. Because the various designs are analyzed with the same routines and optimization procedures they can be easily compared. This aircraft pre-optimization results in a significant reduction of the number of follow-on detail-design cycles, especially for non-conventional designs.

Author

N95-16572# Deutsche Airbus G.m.b.H., Bremen (Germany). Aerodynamic Design Section.

AERODYNAMIC SHAPE OPTIMIZATION

A. VANDERVELDEN *In* AGARD, *Optimum Design Methods for Aerodynamics* 13 p Nov. 1994

Copyright Avail: CASI HC A03/MF A03

This paper will discuss examples of aerodynamic shape optimization at Deutsche Airbus in Bremen. First, we will introduce a general approach to aerodynamic shape design based on minimization of aircraft life energy costs. Realistic constraints are introduced on lift,

pitching moments and thickness. This method is applied to the quasi-3D design of multipoint transonic wings which are analyzed by a full potential code with a coupled boundary layer calculation. Finally, this method is applied to the wing-body design of a Supersonic Civil Transport that is analyzed with a linear potential code with real flow corrections and a decoupled boundary layer calculations. Author

N95-16573# Avions Marcel Dassault-Breguet Aviation, Saint-Cloud (France).

REVIEW OF THE EUROPT PROJECT AERO-0026
 B. MANTEL, J. PERIAUX, and B. STOUFFLET *In* AGARD, Optimum Design Methods for Aerodynamics 43 p Nov. 1994
 (Contract(s)/Grant(s): BRITE-EURAM-AERO-0026)
 Copyright Avail: CASI HC A03/MF A03

Despite progress toward automated shape design in Industry has been penalized until now by excessive computing costs, useful innovative design methodologies have been recently proposed for computing different academic and industrial designs of nozzles, airfoils and wing-body combinations operating in inviscid flows modelled by the potential and Euler equations. Since the designer has a precise idea of the pressure distribution that will produce the desired performance, not only optimization problems but also inverse problems have to be considered in current design. The goal of this lecture is to describe the major ingredients of new algorithms developed by european partners of the AERO 89-0026 project, which allow accurate and cost effective numerical solutions of optimization problems and also to illustrate the capabilities of design software on test cases proposed in a Workshop for validation purpose. Industrial applications illustrating these methodologies are also presented. Finally a new emergent search method for non linear optimization problems provided by simple Genetic Algorithms (GA's) is briefly described and illustrated by a few examples related to inverse problems and applied to reduction of viscous drag. Author

N95-16899*# Old Dominion Univ., Norfolk, VA. Dept. of Mathematics and Statistics.

AUTOMATION OF REVERSE ENGINEERING PROCESS IN AIRCRAFT MODELING AND RELATED OPTIMIZATION PROBLEMS Progress Report, period ending Dec. 1994

W. LI and J. SWETTITS Nov. 1994 87 p
 (Contract(s)/Grant(s): NCC1-68)
 (NASA-CR-197109; NAS 1.26:197109; ODURF-124303) Avail: CASI HC A05/MF A01

During the year of 1994, the engineering problems in aircraft modeling were studied. The initial concern was to obtain a surface model with desirable geometric characteristics. Much of the effort during the first half of the year was to find an efficient way of solving a computationally difficult optimization model. Since the smoothing technique in the proposal 'Surface Modeling and Optimization Studies of Aerodynamic Configurations' requires solutions of a sequence of large-scale quadratic programming problems, it is important to design algorithms that can solve each quadratic program in a few interactions. This research led to three papers by Dr. W. Li, which were submitted to SIAM Journal on Optimization and Mathematical Programming. Two of these papers have been accepted for publication. Even though significant progress has been made during this phase of research and computation times was reduced from 30 min. to 2 min. for a sample problem, it was not good enough for on-line processing of digitized data points. After discussion with Dr. Robert E. Smith Jr., it was decided not to enforce shape constraints in order to simplify the model. As a consequence, P. Dierckx's nonparametric spline fitting approach was adopted, where one has only one control parameter for the fitting process - the error tolerance. At the same time the surface modeling software developed by Imageware was tested. Research indicated a substantially improved fitting of digitalized data points can be achieved if a proper parameterization of the spline surface is chosen. A winning strategy is to incorporate Dierckx's surface fitting with a natural parameterization for aircraft parts. The report consists of 4 chapters. Chapter 1 provides an overview of reverse engineer-

ing related to aircraft modeling and some preliminary findings of the effort in the second half of the year. Chapters 2-4 are the research results by Dr. W. Li on penalty functions and conjugate gradient methods for quadratic programming problems. Author (revised)

N95-16969# Electronics Research Lab., Salisbury (Australia).
A PC-BASED INTERACTIVE SIMULATION OF THE F-111C PAVE TACK SYSTEM AND RELATED SENSOR, AVIONICS AND AIRCRAFT ASPECTS

DAVID A. FOGG, MIKE DAVIES, FRED D. BOWDEN, and RAY JANUS Mar. 1994 217 p
 (AD-A285500; ERL-0656-RR; DODA-AR-007-005) Avail: CASI HC A10/MF A03

Pave Tack is an all weather, day and night, navigation and weapon delivery system fitted to the F-111C aircraft. A PC-based, interactive digital computer simulation has been written which can be used to assess the performance of the Pave Tack system and also as a computer-aided training device. In forming the simulation, it was necessary to model a number of avionics and sensor aspects and an F-111C flight path generator was used to produce accurate data off-line. This report details the history, structure and general capabilities of the F-111C Pave Tack Simulation (FPTS). DTIC

N95-16982* National Aeronautics and Space Administration, Washington, DC.

REVITALIZING GENERAL AVIATION (Videotape)

20 Jul. 1994 Videotape: 6 min. 30 sec. playing time, in color, with sound
 (NASA-TM-110113; NASA-ASR-268; NONP-NASA-VT-95-35013)
 Avail: CASI VHS A02/BETA A22

This video contains a short feature of NASA and the FAA joint effort to incorporate new technology into the design of general aviation aircraft. CASI

N95-17397*# National Aeronautics and Space Administration, Langley Research Center, Hampton, VA.

ACTIVE LOAD CONTROL DURING ROLLING MANEUVERS

JESSICA A. WOODS-VEDELER, ANTHONY S. POTOTZKY (Lockheed Engineering and Sciences Co., Hampton, VA.), and SHERWOOD T. HOADLEY Oct. 1994 61 p

(Contract(s)/Grant(s): RTOP 505-63-36-01)
 (NASA-TP-3455; L-17053; NAS 1.60:3455) Avail: CASI HC A04/MF A01

A rolling maneuver load alleviation (RMLA) system has been demonstrated on the active flexible wing (AFW) wind tunnel model in the Langley Transonic Dynamics Tunnel (TDT). The objective was to develop a systematic approach for designing active control laws to alleviate wing loads during rolling maneuvers. Two RMLA control laws were developed that utilized outboard control-surface pairs (leading and trailing edge) to counteract the loads and that used inboard trailing-edge control-surface pairs to maintain roll performance. Rolling maneuver load tests were performed in the TDT at several dynamic pressures that included two below and one 11 percent above open-loop flutter dynamic pressure. The RMLA system was operated simultaneously with an active flutter suppression system above open-loop flutter dynamic pressure. At all dynamic pressures for which baseline results were obtained, torsion-moment loads were reduced for both RMLA control laws. Results for bending-moment load reductions were mixed; however, design equations developed in this study provided conservative estimates of load reduction in all cases. Author

N95-17631# Naval Air Warfare Center, Warminster, PA. Air Vehicle and Crew Systems Technology Dept.

EVALUATION OF ALTERNATE F-14 WING LUG COATING

Final Report, 1 Jan. 1991 - 30 Sep. 1993
 JANET L. MCGOVERN and ALAN E. ANKENY 1 Dec. 1993 28 p
 (AD-A283207; NAWCADWAR-93082-60) Avail: CASI HC A03/MF A01

The F-14 wing lug is coated with specific formulation polyurethane coating which prevents scoring of the wing lug by providing a wear

05 AIRCRAFT DESIGN, TESTING AND PERFORMANCE

surface for the outside diameter of the wing pivot bearing. The manufacture of this coating material was discontinued in 1991 because the original formulation used talcs which contained asbestos as impurities. The new formulation, containing asbestos free talcs, was inadequate in providing the abrasion resistance required to protect the F-14 wing lug. A new coating or coating process was required. A centrifugation processing procedure for the new formulation was developed which appeared to provide a coating that exhibited similar wear characteristics as the original coating. Oscillation wear tests were required to determine bearing wear performance of the alternate coating under normal and high stress in both the dry and fluid contaminated states. DTIC

N95-17661# Veda, Inc., Dayton, Ohio,
**INDUSTRY REVIEW OF A CREW-CENTERED COCKPIT
DESIGN PROCESS AND TOOLSET** Interim Report, Aug. -
Sep. 1993

EDWARD LEHMAN, MICHAEL ROUNTREE, KATHERINE JACKSON, BRETT STOREY, and PHILIP KULWICKI Apr. 1994 81 p
(Contract(s)/Grant(s): F33615-92-C-5936)
(AD-A282966; REPT-63193-94U/P60099; AL/CF-TR-1994-0063) Avail:
CASI HC A05/MF A01

This report contains the results of an industry review done for the Crew-Centered Cockpit Design (CCCD) Field Demonstration Program, USAF Contract F33615-92-C-5936. The objectives of the program are to upgrade and validate a new system for cockpit design. The system consists of a crew-centered system design process (CSDP) and a cockpit design system (CDS). The CSDP is intended to improve design practice, allowing designers to base decisions on mission requirements and crew capabilities while meeting installation constraints. The CDS offers improved design efficiency and includes traceability functions that preserve the rationale for design decisions. The CCCD Program Office recognizes that the acceptance and long-term utility of the CCCD products depend on the interest and support of the cockpit development community, which includes aircraft prime contractors and government aircraft acquisition organizations. For this reason, a survey of four aircraft prime contracts was made during August and September of 1993. The objective of the survey was to elicit end-user requirements for CCCD products. Information was obtained from engineers, scientists, and managers who are involved in different crew station activities including pilot-vehicle interface (PVI) design, crew station design, human factors analysis, systems engineering, and operational analysis. The report documents the results of the survey. DTIC

N95-17863# Deutsche Forschungsanstalt fuer Luft- und Raumfahrt, Brunswick (Germany). Inst. fuer Entwurfsaerodynamik.

DLR-F4 WING BODY CONFIGURATION

G. REDEKER *In* AGARD, A Selection of Experimental Test Cases for the Validation of CFD Codes, Volume 2 21 p Aug. 1994
Copyright Avail: CASI HC A03/MF A06

These tests have been carried out under the auspices of GARTEUR in order to provide an experimental data base for a modern commercial transport type aircraft against which results of various computational methods may be checked. The tests were carried out in three major European wind tunnels (NLR-HST, ONERA-S2MA, and DRA-8ft x 8ft DRA Bedford) in order to compare the results of the same model in different wind tunnels. For the purpose of these tests the available geometry of the DLR-F4 model of a wing body configuration, which was developed as a research configuration of a modern transport type aircraft, was selected by the GARTEUR Action Group AD (AG01) 'Wing body aerodynamics at transonic speeds.' Derived from text

N95-17953 Naval Air Warfare Center, Patuxent River, MD. Aircraft Div.

FLIGHT TESTING HIGH LATERAL ASYMMETRIES ON HIGHLY AUGMENTED FIGHTER/ATTACK AIRCRAFT

G. D. DUNGAN and C. M. CLARK 23 Jun. 1994 13 p Presented

at the Seventh Biennial AIAA Flight Test Conference, Colorado Springs, CO, 20-23 Jun. 1994 Limited Reproducibility: More than 20% of this document may be affected by microfiche quality
(AD-A284206) Avail: CASI HC A03

The F/A-18's flight control system (FCS) is highly augmented to tailor flying qualities, increase departure resistance, and help protect the airframe structure throughout the flight envelope. Since the F/A-18 flight control laws were designed primarily for the symmetrically loaded airplane, the effects of the high lateral asymmetries represent a significant off-design condition where control margins may be substantially reduced. Adequately defining the flight envelope limits requires a flight test program that addresses the stability and control, structural, and mission suitability issues associated with these large lateral weight asymmetries. This paper will address the risk reduction techniques, test methodologies, and real-time analysis tools that have been used in the past or are planned to be used in an ongoing flight test program to expand the lateral asymmetry limit of the F/A-18. DTIC

N95-18008# Naval Postgraduate School, Monterey, CA.
**WIND TUNNEL PERFORMANCE COMPARATIVE TEST
RESULTS OF A CIRCULAR CYLINDER AND 50 PERCENT
ELLIPSE TAILBOOM FOR CIRCULATION CONTROL
ANTITORQUE APPLICATIONS M.S. Thesis**

DAVID T. FISHER Mar. 1994 115 p
(AD-A283335) Avail: CASI HC A06/MF A01

A low speed wind tunnel study to quantitatively evaluate the performance (lift and drag) of a circular cylinder and comparable 50% ellipse was conducted. Circular cylinder performance was evaluated at slot positions of 80 deg to 135 deg, measured relative to freestream; 50% ellipse performance was measured for angles of attack between -5 deg and 30 deg. Tests were conducted at three blowing coefficients, 0.3, 0.4 (optimal historically) and 0.5, to evaluate tailboom performance sensitivity. Circulation control test results revealed optimal c_1 values at an approximate 116 deg slot position, corresponding to c_d values no greater than that of a smooth cylinder. The 50% ellipse results revealed optimal c_1 values at approximately 18 deg AOA, though associated with considerable drag. For all three blowing coefficients, the circular cylinder L/D values were consistently three to four times greater than their 50% ellipse counterparts. Recommendations for future NOTAR(TM) tailboom design modifications and later research are made. DTIC

N95-18090*# Mississippi State Univ., Mississippi State, MS. Dept. of Aerospace Engineering.

WING DESIGN FOR A CIVIL TILTROTOR TRANSPORT AIRCRAFT Performance Report, 25 Jan. - 24 Nov. 1994

MASOUD RAIS-ROHANI 24 Nov. 1994 6 p

(Contract(s)/Grant(s): NAG1-1571)

(NASA-CR-197523; NAS 1.26:197523) Avail: CASI HC A02/MF A01

The goal of this research is the proper tailoring of the civil tiltrotor's composite wing-box structure leading to a minimum-weight wing design. With focus on the structural design, the wing's aerodynamic shape and the rotor-pylon system are held fixed. The initial design requirement on drag reduction set the airfoil maximum thickness-to-chord ratio to 18 percent. The airfoil section is the scaled down version of the 23 percent-thick airfoil used in V-22's wing. With the project goal in mind, the research activities began with an investigation of the structural dynamic and aeroelastic characteristics of the tiltrotor configuration, and the identification of proper procedures to analyze and account for these characteristics in the wing design. This investigation led to a collection of more than thirty technical papers on the subject, some of which have been referenced here. The review of literature on the tiltrotor revealed the complexity of the system in terms of wing-rotor-pylon interactions. The aeroelastic instability or whirl flutter stemming from wing-rotor-pylon interactions is found to be the most critical mode of instability demanding careful consideration in the preliminary wing design. The placement of wing fundamental natural frequencies in bending and torsion relative to each other and relative to the rotor 1/rev frequen-

cies is found to have a strong influence on the whirl flutter. The frequency placement guide based on a Bell Helicopter Textron study is used in the formulation of frequency constraints. The analysis and design studies are based on two different finite-element computer codes: (1) MSC/NASATRAN and (2) WIDOWAC. These programs are used in parallel with the motivation to eventually, upon necessary modifications and validation, use the simpler WIDOWAC code in the structural tailoring of the tiltrotor wing. Several test cases were studied for the preliminary comparison of the two codes. The results obtained so far indicate a good overall agreement between the two codes. Derived from text

N95-18097# Sydney Univ. (Australia). Dept. of Aeronautical Engineering.

SIX DEGREE OF FREEDOM FLIGHT DYNAMIC AND PERFORMANCE SIMULATION OF A REMOTELY-PILOTED VEHICLE

D. M. NEWMAN and K. C. WONG Jun. 1993 57 p
(AERO-TN-9301) Avail: CASI HC A04/MF A01

The purpose of this technical note is to describe the aerodynamic, propulsive and inertial data on which the remotely piloted vehicle (RPV) simulation is based, the limits of applicability of the data, and the analytic modelling techniques used in the simulation process. The note also acts as a user guide for other simulation programs and for post-processing of simulation histories. A full performance and flight dynamic simulation of the RPV was developed in Fortran 77, using the Lahey F77L-EM/32 Version 5.01 compiler to run on IBM-compatible 386/486 personal computers with numeric coprocessors. The main Fortran simulation called several locally-developed PC-specific assembly language interface routines for control input via mouse or other hardware device and graphics output to screen. The input/output routines were not considered part of the simulation proper. The simulation was designed to be applicable to all gross weights, center of gravity positions, power settings and flight conditions throughout the normal operating envelope of the RPV as shown in Appendix A. Computational model characteristics were derived from wind tunnel testing, engine manufacturer's data and computational aerodynamic and inertial data. Post-stall behavior was incompletely modelled. The model extended to flight conditions beyond the normal operating envelope in several areas. Atmospheric conditions used were those of the International Standard Atmosphere (ISA), and wind shear and turbulence models were derived from those of MIL-F-8785C. All work was performed in SI units, with inputs and outputs transformed where necessary to ICAO-approved forms. A series of test maneuvers and performance data points were run to examine the simulation validity. Results were compared to classical small-perturbation theory. As the RPV first prototype was under construction during the period when this simulation was developed, simulator validation against flight test data was not possible. The simulation was performed by repeated numerical integration of the non-linear equations of motion for a rigid aircraft with time-varying control inputs, using aircraft characteristic data based on experiment and analysis. The aircraft database consisted of an aerodynamic model, a propeller and engine model, an inertial model, and a control actuator model. Derived from text

N95-18162# Dayton Univ. Research Inst., OH.
CONFERENCE ON AEROSPACE TRANSPARENT MATERIALS AND ENCLOSURES. VOLUME 2: SESSIONS 5-9 Interim Report, 9 Aug. - 13 Aug. 1993

SAMUEL A. MAROLO Mar. 1994 563 p Conference held in San Diego, CA, 9-13 Aug. 1993 See also AD-A283925
(Contract(s)/Grant(s): F33615-92-C-3400)
(AD-A283926; WL-TR-94-4084-VOL-2) Avail: CASI HC A24/MF A04

The purpose of this report is to make available the technical papers presented at the Sixteenth Conference on Aerospace Transparent Materials and Enclosures. Sixty-seven technical papers are presented in nine sessions that address transparent material for enclosures, coatings for transparencies, transparency design; bird

impact resistance; human factors and optics; operational problems; design criteria on transparent plastics, glasses and elastomers; aircraft-structural integration of windshields and canopies; computed design; testing techniques; and cost of ownership reduction. The papers contained herein have been reproduced directly from the original manuscripts. DTIC

N95-18198# National Aeronautics and Space Administration. Langley Research Center, Hampton, VA.
MICROBURST VERTICAL WIND ESTIMATION FROM HORIZONTAL WIND MEASUREMENTS

DAN D. VICROY Dec. 1994 83 p Sponsored in part by FAA
Original contains color illustrations
(Contract(s)/Grant(s): RTOP 505-64-13-01)
(NASA-TP-3460; L-17376; NAS 1.60:3460; DOT/FAA/RD-94/7) Avail: CASI HC A05/MF A01; 32 functional color pages

The vertical wind or downdraft component of a microburst-generated wind shear can significantly degrade airplane performance. Doppler radar and lidar are two sensor technologies being tested to provide flight crews with early warning of the presence of hazardous wind shear. An inherent limitation of Doppler-based sensors is the inability to measure velocities perpendicular to the line of sight, which results in an underestimate of the total wind shear hazard. One solution to the line-of-sight limitation is to use a vertical wind model to estimate the vertical component from the horizontal wind measurement. The objective of this study was to assess the ability of simple vertical wind models to improve the hazard prediction capability of an airborne Doppler sensor in a realistic microburst environment. Both simulation and flight test measurements were used to test the vertical wind models. The results indicate that in the altitude region of interest (at or below 300 m), the simple vertical wind models improved the hazard estimate. The radar simulation study showed that the magnitude of the performance improvement was altitude dependent. The altitude of maximum performance improvement occurred at about 300 m. Author

N95-18381 Army Research Lab., Aberdeen Proving Ground, MD.
HELICOPTER PERFORMANCE EVALUATION (HELPE) COMPUTER MODEL Final Report, Sep. 1992 - Oct. 1993

ABDUL R. KIWAN Jul. 1994 54 p Limited Reproducibility: More than 20% of this document may be affected by microfiche quality
(Contract(s)/Grant(s): DA PROJ. 1L1-62618-AH-80)
(AD-A284319; ARL-TR-489) Avail: CASI HC A04

A HELicopter Performance Evaluation (HELPE) computer model has been developed. The model is empirically based on the energy balance method. For a helicopter at a given mission, the model computes for a helicopter at given weight and flight conditions, the maximum possible level speed, its maneuverability in a turn, and its hover and climb capabilities in the in-ground and out-of-ground effects modes. The code also computes the speeds of maximum endurance in the air and of maximum range for the helicopter. DTIC

N95-18398 Aeronautical Systems Div., Wright-Patterson AFB, OH.
KC-135 COCKPIT MODERNIZATION STUDY. PHASE 1:

EQUIPMENT EVALUATION Final Report, 1 Feb. - 31 May 1994
JOHN E. EHRHART, JR. and THOMAS C. HUGHES Jul. 1994 100 p Limited Reproducibility: More than 20% of this document may be affected by microfiche quality
(AD-A284099; ASC-TR-94-5026-PHASE-1) Avail: Issuing Activity (Defense Technical Information Center (DTIC))

Future KC-135 missions will require significant increases in aircraft flexibility to respond to the Air Force vision of 'Global Reach, Global Power.' Such flexibility typically translates into advanced avionics systems and system and capabilities; however, a large percentage of the avionics systems currently installed on the KC-135 are late 1950s and 1960s technology which has degraded the efficiency, reliability, maintainability and safety of the KC-135 mission. Strategic Air Command (SAC), now Air Mobility Command (AMC) issued a statement of need (SON, 1987) addressing the need

05 AIRCRAFT DESIGN, TESTING AND PERFORMANCE

to modernize the KC-135 cockpit avionics to attend to these problems. This report documents the evaluation of the Phase 1 modification plan as proposed by HQ/AMC. The evaluation of the reduced crew consisted of a comparison of crew workload and performance across three missions: Minot, Castle and McChord. Based on crew workload, safety of flight issues and crew interviews, study results did not support the two-person (No Nav) cockpit, given the Phase 1 modifications. Based on these results, the CSEF recommended that the feasibility of the Phase 1 modification plan be re-assessed prior to installation into the KC-135. Recommendations are based upon using the final design, identical in system capabilities, as evaluated at the Crew Station Evaluation Facility. DTIC

N95-18407 Naval Air Development Center, Warminster, PA. Systems Dept.

PRELIMINARY EVALUATION OF THE F/A-18 QUANTITY/ MULTIPLE ENVELOPE EXPANSION

WIN EVERETT and JOHN OSTER 1994 40 p Limited Reproducibility: More than 20% of this document may be affected by microfiche quality
(AD-A284119; NAWCAD-SA80) Avail: CASI HC A03

Currently the F/A-18 Hornet has restrictions on performing ripple salvo (quantity greater than multiple, multiple greater than 1) releases when Vertical Ejection Racks (VER) or Canted Vertical Ejection Racks (CVER) are loaded on (the inboard) wing stations 3 and 7 due to bomb to bomb collisions upon release. Hornet test pilots assigned to the Ordnance System Department of the Flight Test and Evaluation Group (NAWCAD) located at Patuxent River MD, sought to remedy this restriction. As Strike Leaders in the fleet, we recognized the need to eliminate these release restrictions. By testing a representative sample of weapons loadouts, we sought to increase the Hornet's weapon delivery options. DTIC

N95-18415 Naval Air Warfare Center, Patuxent River, MD. Aircraft Div.

TILT ROTOR UNMANNED AIR VEHICLE SYSTEM (TRUS) DEMONSTRATOR FLIGHT TEST PROGRAM

MICHAEL J. MEYERS 10 Mar. 1994 28 p Limited Reproducibility: More than 20% of this document may be affected by microfiche quality
(AD-A284151) Avail: Issuing Activity (Defense Technical Information Center (DTIC))

The Tilt Rotor UAV System flight demonstration program commenced in July 1993 and concluded with conversion to airplane mode and a level flight speed of 160 kts in February 1994. The purpose of the flight tests was to evaluate the utility of Tilt Rotor UAV technology in order to develop requirements for a Government maritime system. The TRUS program was divided into three test phases: Ground, Helicopter Mode, and Conversion to Airplane Mode. Helicopter Mode testing occurred at the contractor's facilities in Fort Worth, TX over two periods and consisted of fourteen flights totaling 3.0 flight-hours. During phase 2, the aircraft conducted IGE (In Ground Effect) and OGE (Out Ground Effect) hovers, longitudinal and lateral translations at up to 20 kts, as well as pitch, roll, and yaw control response testing. Handling qualities during the takeoff and landing flight regimes were also assessed. DTIC

N95-18417 Naval Air Warfare Center, Patuxent River, MD. Aircraft Div.

APPLICATION OF PHOTOGRAMMETRY OF F-14D STORE SEPARATION

CHRIS J. FERGUSON and E. S. GETSON 20 May 1994 32 p Limited Reproducibility: More than 20% of this document may be affected by microfiche quality
(AD-A284154) Avail: Issuing Activity (Defense Technical Information Center (DTIC))

Conceived in the 1960's as a replacement for the F-4 Phantom, the 'A' variant of the F-14 Tomcat was first deployed as an air

superiority fighter in the early 1970's. Designed as a follow-on to the F-14A, the F-14D was introduced to the U.S. Navy in 1990. Improvements were manifold and included addition of the A/N-AAS-429 Infrared Search and Track Set (IRSTS) to the 'chin' pod located beneath the radome forward of the nose landing gear. This chin pod, which was smaller and housed only the A/N AXX-1 Television Camera Set (TCS) in the F-14A variant, was postulated to adversely affect air-to-air and air-to-ground weapon separation from the aircraft fuselage stations. This warranted additional testing to validate the separation envelope previously tested and authorized on the F-14A. In an attempt to bring state-of-the-art separation prediction techniques to the F-14D weapon certification program, the Navy's flight clearance authority mandated the use of wind tunnel generated predictions to minimize program risk. Validation of the air-to-ground predictions, performed at the Naval Air Warfare Center - Aircraft Division, NAS Patuxent River, MD required a precise method by which store six-degree-of-freedom motion could be determined. Several methods of obtaining this quantitative data were evaluated with photogrammetric analysis selected as the most suitable. While tailored for the particular application detailed in this paper, photogrammetry may be used wherever precise position and orientation of objects in three-dimensional space is a requirement. DTIC

N95-18483# McDonnell-Douglas Corp., Saint Louis, MO.
**AEROMECHANICS TECHNOLOGY, VOLUME 1. TASK 1:
THREE-DIMENSIONAL EULER/NAVIER-STOKES
AERODYNAMIC METHOD (TEAM) ENHANCEMENTS Final
Report, Jul. 1991 - Feb. 1992**

R. K. AGARWAL and T. P. GIELDA 26 Jul. 1994 22 p
(Contract(s)/Grant(s): F33617-91-C-3004; AF PROJ. 2404)
(AD-A285713; WL-TR-93-3010-VOL-1) Avail: CASI HC A02/MF A01

McDonnell Douglas has implemented a Johnson-King turbulence model into the Wright Laboratory TEAM code. Solutions were obtained for several test cases using the standard Baldwin-Lomax model and the incorporated Johnson-King model. Comparisons with experimental data were made where possible. General agreement was seen between the two turbulence models; however, poor agreement with the experimental data was noted for the Onera M6 wing test case. Grid sensitivity studies and further calibration of the TEAM code are needed. DTIC

N95-18599# Aerospatiale, Toulouse (France). Dept. Etudes Generales-Structures.

GYROSCOPIC AND PROPELLER AERODYNAMIC EFFECTS ON ENGINE MOUNTS DYNAMIC LOADS IN TURBULENCE CONDITIONS [EFFETS GYROSCOPIQUES ET AERODYNAMIQUES DES PROPULSEURS SUR LES CHARGES DES MOTEURS D'AVIONS EN CONDITIONS TURBULENTES]

J. M. SAUCRAY In AGARD, Aircraft Loads due to Turbulence and their Impact on Design and Certification 12 p Dec. 1994 In FRENCH
Copyright Avail: CASI HC A03/MF A01

This paper deals with the problem of calculating loads on engines and their supporting structures when inertial characteristic, high engine speeds, large displacements, imposed by extreme atmospheric disturbances, give an important impact of gyroscopic effect. A direct method integrating the gyroscopic action in Lagrange's equations as a function of the polar moment of inertia, engine revolution speed and precession speed is presented and compared to the more common practice of superimposing gyroscopic effects on the basis of the angular speed calculated at the engine center of gravity. The results establish a good correlation between the two methods on pitch and yaw moments on engine. On the other hand, transfer function modifications due to gyroscopic effects generate an increase of other loads for the direct method calculations, for both the turboprop and the turbojet aircraft. Effects of the aerodynamic force of the propeller due to the engine response are also examined.

Author

N95-18601# Construcciones Aeronauticas S.A., Madrid (Spain). Structural Dynamics Dept.

A STUDY OF THE EFFECT OF STORE UNSTEADY AERODYNAMICS ON GUST AND TURBULENCE LOADS

M. OLIVER, J. CASALENGUA, C. MADERUELO, Y. CAMACHO, and H. CLIMENT *In* AGARD, Aircraft Loads due to Turbulence and their Impact on Design and Certification 12 p Dec. 1994

Copyright Avail: CASI HC A03/MF A01

Gust and turbulence loads are the most severe conditions for some parts of the aircraft, especially in the outboard wing region. The addition of external stores usually alleviates the gust/turbulence loads on the wing but becomes critical for other components as pylons and wing/pylon attachments. Safety implications and all-weather envelope of current fighters force an accurate study of the gust/turbulence response of the aircraft for each store configuration. Inertia is the most important contribution of the store to the gust/turbulence loads. Nevertheless, store unsteady aerodynamics should be included if significantly changes the results of the gust/turbulence response. This paper is devoted to the analytical study of the effect of store unsteady aerodynamics on gust/turbulence response. A large number of configurations have been included in the study. Several regulations to define the gust/turbulence excitation have been used. Author

N95-18602# McDonnell-Douglas Aerospace, Long Beach, CA. Transport Aircraft.

COMPARISON OF STOCHASTIC AND DETERMINISTIC NONLINEAR GUST ANALYSIS METHODS TO MEET CONTINUOUS TURBULENCE CRITERIA

PATRICK J. GOGGIN *In* AGARD, Aircraft Loads due to Turbulence and their Impact on Design and Certification 12 p Dec. 1994

Copyright Avail: CASI HC A03/MF A01

Current continuous turbulence Power Spectral Density (PSD) gust analysis methods are valid only for linear aircraft. In the past, many methods for the analysis of nonlinear aircraft to meet the current PSD gust criteria have been proposed. In this paper, three stochastic simulation based and one deterministic function based methods are compared and evaluated for the compliance of nonlinear aircraft to the current continuous turbulence gust criteria. The aircraft configurations analyzed in this paper include a symmetric aircraft model coupled to a nonlinear gust load alleviation (GLA) system and an anti-symmetric aircraft model coupled to a nonlinear yaw damper system. Results from these four nonlinear methods are compared to linear closed and open-loop results as well as currently used linear approximation methods. Computing performance issues are addressed to provide the reader with a complete picture of the trade-off between the analysis' accuracy and computing cost. Author

N95-18603# Cessna Aircraft Co., Wichita, KS. Aircraft Structural Integrity Dept.

DESIGN LIMIT LOADS BASED UPON STATISTICAL DISCRETE GUST METHODOLOGY

D. L. HULL *In* AGARD, Aircraft Loads due to Turbulence and their Impact on Design and Certification 8 p Dec. 1994

Copyright Avail: CASI HC A02/MF A01

Statistical Discrete Gust (SDG) methodology for extreme turbulence provides the basis of a design criterion that accounts for: (1) the statistical nature of design level turbulence; (2) the effects of lightly damped aircraft responses; (3) critical responses that may have significant frequency separation; and (4) the effects of nonlinear control systems. The criterion would eliminate the need for multiple design criteria and could increase the structural efficiency of new aircraft. The increased efficiency would be the result of having equally probable design limit loads for all gust critical components of the aircraft. Author

N95-18605*# National Aeronautics and Space Administration. Langley Research Center, Hampton, VA.

SPECIAL EFFECTS OF GUST LOADS ON MILITARY AIRCRAFT

JOHN C. HOUBOLT *In* AGARD, Aircraft Loads due to Turbulence and

their Impact on Design and Certification 7 p Dec. 1994

Copyright Avail: CASI HC A02/MF A01

In the operation of airplanes, atmospheric turbulence creates a broad spectrum of problems. The nature of these problems is presented in this paper. Those that are common to both the commercial carriers and to the military fleet are discussed first. Attention is then focused on the problems that are of special concern in military operations. An aim is to bring out the need for continued effort in the gust research area. Author

N95-18616# Naval Postgraduate School, Monterey, CA.

COURSE MODULE FOR AA201: WING STRUCTURAL DESIGN PROJECT M.S. Thesis

STEPHEN A. BURRIS Mar. 1994 132 p

(AD-A283618) Avail: CASI HC A07/MF A02

This thesis defined a fundamental approach for aircraft wingbox design appropriate for an introductory course in aircraft structures based upon material strength and stiffness requirements. The process developed sought to encompass major conceptual engineering design considerations that ranged from load estimation at various points in the subsonic flight envelope, to initial structural sizing and layout. The goal was to present a process that could be readily conducted via hand calculations and applied by any student entering basic aircraft structures design. The sequence of analysis began with application of a comprehensive panel code method developed by NASA Ames Research Center known as PMARC. Loads obtained from the code were then used to formulate a strength of materials study of the structure subjected to combined bending, shear and torsion. The static load approach allowed initial estimation of component sizing based upon material or buckling allowable stress selection. Finally, the study demonstrated a strength to weight ratio comparison. Several calculation examples and computer-based spreadsheets were prepared for rapid analysis of multiple option design scenarios. Since the study employed analysis methods that could be performed without the aid of a finite element routine or extensive computer programming knowledge, it serves as a good introduction for the entry and intermediate level structural engineer. DTIC

N95-18621# Naval Postgraduate School, Monterey, CA.

PLANT AND CONTROLLER OPTIMIZATION BY CONVEX METHODS Ph.D. Thesis

ROBERT J. NIEWOEHNER, JR. Jun. 1994 283 p

(AD-A283700) Avail: CASI HC A13/MF A03

This report presents results of a three phase effort to demonstrate the use of convex control design techniques in aeronautical applications. The first phase was the demonstration of a methodology by which classical aircraft controller design requirements could be translated into the weighting matrices for H infinity controller synthesis. The second phase extended that methodology to the design of mixed H2 / H infinity controllers. The third phase considered the problem of minimizing the size of aircraft control surfaces while meeting closed-loop dynamic performance requirements. Control sizing is a critical element in the design of Reduced Static Stability (RSS) aircraft. Inadequate control power places the vehicle in peril, while too much control power forfeits the benefits of RSS, resulting in poorer performance, increased weight, increased cost, increased drag, and increased observability. Non-heuristic methods have been required by which the physical configuration and the accompanying controller can be designed directly from the flying qualities specifications. The optimization of the surfaces should be done while searching over the set of all controllers which, together in closed-loop, satisfy the flying qualities requirements. This report presents a methodology which simultaneously optimizes both the physical configuration and the control system of a rigid body, using performance requirements which can be posed as Linear Matrix Inequalities. DTIC

N95-18677 Dayton Univ., OH.

CONFERENCE ON AEROSPACE TRANSPARENT MATERIALS AND ENCLOSURES, VOLUME 1 Interim Report, 9-13 Aug. 1993

05 AIRCRAFT DESIGN, TESTING AND PERFORMANCE

SAMUEL A. MAROLO Mar. 1994 647 p Conference held in San Diego, CA, 9-13 Aug. 1993 Limited Reproducibility: More than 20% of this document may be affected by microfiche quality (Contract(s)/Grant(s): F33615-92-C-3400; AF PROJ. 1926) (AD-A283925; WL-TR-94-4083-VOL-1) Avail: CASI HC A99

The purpose of this report is to make available the technical papers presented at the Sixteenth Conference on Aerospace Transparent Materials and Enclosures. Sixty-seven technical papers are presented in nine sessions that address transparent materials for enclosures, coatings for transparencies, transparency design; bird impact resistance; human factors and optics; operational problems; design criteria on transparent plastics, glasses and elastomers; aircraft-structural integration of windshields and canopies; computed design; testing techniques; and cost of ownership reduction. The papers contained herein have been reproduced directly from the original manuscripts.

DTIC

N95-18726 Naval Air Warfare Center, Patuxent River, MD. Aircraft Div.

ASSESSING AIRCRAFT SURVIVABILITY TO HIGH FREQUENCY TRANSIENT THREATS

SAMUEL J. FRAZIER, EDWARD M. PARIMUHA, WILLIAM PRATHER, MICHAEL ANTLEY, and DONALD MCLEMORE 1994 7 p Limited Reproducibility: More than 20% of this document may be affected by microfiche quality

(AD-A283999) Avail: CASI HC A02

Throughout the United States Department of Defense (DOD), the need exists to assess and characterize aircraft system survivability to High Frequency (HF) electromagnetic (EM) transient threats. These threats include the HF Electromagnetic Pulse (EMP) and other ultra wideband (UWB) transient environments. The Navy recognizes this need and is taking the initiative to investigate the feasibility of a realistic, low-cost test methodology to assess, characterize and validate aircraft survivability to threats that may range from a few hundred Kiloherztz to the low Gigahertz region. The proposed Navy technical approach is based on established system-level RDT&E technology using existing high frequency test laboratories and equipment. The approach will be validated using a combination of High Level Pulse (HLP) testing at the Naval Air Warfare Center Aircraft Division Patuxent Rivers Horizontally Polarized Dipole (HPD) and Vertically Polarized Dipole (VPD) free-field EMP simulators, electromagnetic effects generating equipment to simulate the carrier shipboard environment free-field low-level continuous wave (LLCW) testing to acquire the stress response data, and wideband direct-drive tests to characterize system strength. The Navy is developing a new wideband (up to 1 GHz) direct-drive technology and waveform combination techniques using stress response data to develop worst-case stress envelopes to be used during the direct-drive tests.

DTIC

N95-18891 Arnold Engineering Development Center, Arnold AFS, TN.

HYPERSONIC FLIGHT TESTING Final Report, Jul. 1992 - Jul. 1993

V. K. SMITH, R. K. MATTHEWS, and J. R. MAUS Aug. 1994 37 p Limited Reproducibility: More than 20% of this document may be affected by microfiche quality

(AD-A283981; AEDC-TR-94-7) Avail: CASI HC A03

The challenges of hypersonic system development require a combination of integrated ground testing, flight testing, and computational/simulation approaches. This report addresses the role of flight testing in the triad of development approach and is sub-divided into three parts: Propulsion, Aerothermal and Extrapolation of ground test data to flight. The reasons for propulsion flight test are illustrated by specific mini-case studies. The second part reviews some of the fundamental issues of flight testing and provides an overview of the aerothermal techniques. Specific examples include heat-transfer gage measurements and some of the common problems that have been encountered. The third part of this report discusses the initial flights of the Space Shuttle which uncovered a number of differences between preflight aerodynamic predictions and actual flight data. Most notable

among these discrepancies was for longitudinal trim during high-speed re-entry. To investigate these differences, several computer codes were applied to a modified Space Shuttle Orbiter to determine aerodynamic parameters over a wide range of conditions. Computations were carried out for wind tunnel conditions and flight conditions to assess Mach number, real gas, and viscous effects on the reentry aerodynamics of the orbiter.

DTIC

N95-19044*# National Aeronautics and Space Administration. Hugh L. Dryden Flight Research Facility, Edwards, CA.

DETERMINATION OF STORES POINTING ERROR DUE TO WING FLEXIBILITY UNDER FLIGHT LOAD

WILLIAM A. LOKOS, CATHERINE M. BAHM, and ROBERT A. HEINLE Washington Jan. 1995 25 p Presented at the 7th Biennial Flight Test Conference, Colorado Springs, CO, 20-23 Jun. 1994 (NASA-TM-4646; H-2022; NAS 1.15:4646; AIAA PAPER 94-2112) Avail: CASI HC A03/MF A01

The in-flight elastic wing twist of a fighter-type aircraft was studied to provide for an improved on-board real-time computed prediction of pointing variations of three wing store stations. This is an important capability to correct sensor pod alignment variation or to establish initial conditions of iron bombs or smart weapons prior to release. The original algorithm was based upon coarse measurements. The electro-optical Flight Deflection Measurement System measured the deformed wing shape in flight under maneuver loads to provide a higher resolution database from which an improved twist prediction algorithm could be developed. The FDMS produced excellent repeatable data. In addition, a NASTRAN finite-element analysis was performed to provide additional elastic deformation data. The FDMS data combined with the NASTRAN analysis indicated that an improved prediction algorithm could be derived by using a different set of aircraft parameters, namely normal acceleration, stores configuration, Mach number, and gross weight.

Author

N95-19067 Naval Air Warfare Center, Patuxent River, MD. Aircraft Div.

E-6A HARDNESS ASSURANCE, MAINTENANCE AND SURVEILLANCE PROGRAM

JOEL HAINES, MARK MALLORY, WILLIAM DEPASQUALE, and BERND LUBOSCH 1994 14 p Limited Reproducibility: More than 20% of this document may be affected by microfiche quality (AD-A283994) Avail: CASI HC A03

The challenge facing aircraft program managers and the Fleet is to ensure that the electromagnetic hardness of design is maintained throughout the aircraft life-cycle. The electromagnetic pulse (EMP) community must work closely with aircraft program managers and aircraft design contractors to properly integrate the logistics elements necessary to accomplish this effort. This process must begin early in the acquisition phase and be dynamic enough to evolve as changes in life-cycle mission requirements occur. This paper identifies the Hardness Assurance, Maintenance, and Surveillance Program for the U.S. Navy's E-6A aircraft. The program includes various test techniques that are used to monitor aircraft hardness integrity and maintenance procedures to direct the hardness critical process. A database was also developed which integrates all test and maintenance data to aid aircraft hardness surveillance.

DTIC

N95-19130*# California Univ., Los Angeles, CA.

THE ACCURACY OF PARAMETER ESTIMATION IN SYSTEM IDENTIFICATION OF NOISY AIRCRAFT LOAD MEASUREMENT Ph.D. Thesis

JEFFREY KONG 1994 138 p

(Contract(s)/Grant(s): NCC2-374)

(NASA-CR-197516; NAS 1.26:197516) Copyright Avail: CASI HC A07/MF A02

This thesis focuses on the subject of the accuracy of parameter estimation and system identification techniques. Motivated by a complicated load measurement from NASA Dryden Flight Research Center, advanced system identification techniques are needed. The objective of this problem is to accurately predict the load experienced by the

aircraft wing structure during flight determined from a set of calibrated load and gage response relationship. We can then model the problem as a black box input-output system identification from which the system parameter has to be estimated. Traditional LS (Least Square) techniques and the issues of noisy data and model accuracy are addressed. A statistical bound reflecting the change in residual is derived in order to understand the effects of the perturbations on the data. Due to the intrinsic nature of the LS problem, LS solution faces the dilemma of the trade off between model accuracy and noise sensitivity. A method of conflicting performance indices is presented, thus allowing us to improve the noise sensitivity while at the same time configuring the degradation of the model accuracy. SVD techniques for data reduction are studied and the equivalence of the Correspondence Analysis (CA) and Total Least Squares Criteria are proved. We also looked at nonlinear LS problems with NASA F-111 data set as an example. Conventional methods are neither easily applicable nor suitable for the specific load problem since the exact model of the system is unknown. Neural Network (NN) does not require prior information on the model of the system. This robustness motivated us to apply the NN techniques on our load problem. Simulation results for the NN methods used in both the single load and the 'warning signal' problems are both useful and encouraging. The performance of the NN (for single load estimate) is better than the LS approach, whereas no conventional approach was tried for the 'warning signals' problems. The NN design methodology is also presented. The use of SVD, CA and Collinearity Index methods are used to reduce the number of neurons in a layer. Author

**N95-19151# Wright Lab., Wright-Patterson AFB, OH.
NONLINEAR DYNAMIC RESPONSE OF AIRCRAFT
STRUCTURES TO ACOUSTIC EXCITATION**

H. F. WOLFE and R. G. WHITE (Southampton Univ., England.) In AGARD, Impact of Acoustic Loads on Aircraft Structures 10 p Sep. 1994

Copyright Avail: CASI HC A02/MF A03

Acoustic fatigue failure in aerospace structures has been a concern for many years. New prediction techniques are needed for the new materials and structural concepts of interest and higher sound pressure levels encountered. The objective of this program of work is to improve the fundamental understanding of the nonlinear behavior of beams and plates excited from low to high levels of excitation. Experiments have been conducted utilizing a clamped-clamped (C-C) beam statically tested and shaker driven at increasing levels of excitation. Similarly, C-C-C-C plates were excited by a vibration shaker and in a progressive wave tube. The total strains and the components, bending and axial, and the displacements were measured with increasing levels of excitation. Bistable behavior was observed with sinusoidal excitation for both the beams and plates. The measured axial or membrane strains were very low compared to the bending strains for high levels of excitation. The beams randomly excited exhibited a slight frequency shift and peak broadening, which can be attributed to an increased stiffening or hard spring nonlinearity. The plates randomly excited exhibited a greater frequency shift and peak broadening than the beams. The dynamic tests resulted in a nonlinear relationship between the response strains and displacements and the excitation levels. A multimodal model is discussed to estimate the mean square stress response due to high levels of excitation. Author

**N95-19154# Wright Lab., Wright-Patterson AFB, OH.
MODELLING STRUCTURALLY DAMAGING TWIN-JET
SCREECH**

MARY KAE LOCKWOOD, STEVEN H. WALKER, and ALAN B. CAIN (McDonnell-Douglas Corp., Saint Louis, MO.) In AGARD, Impact of Acoustic Loads on Aircraft Structures 8 p Sep. 1994

Copyright Avail: CASI HC A02/MF A03

Closely spaced twin jet aircraft have been known to be susceptible to aft-end structural damage due to the high sound pressure levels resulting from twin jet screech. An initial engineering workstation tool to predict the occurrence of screech, ultimately allowing the design of configurations which will not result in screech, is presented here. The model has been developed in a modular fashion to facilitate upgrades.

The implementation takes advantage of a graphical interface, yielding predictions of screech amplitude versus frequency within a few seconds once the initial flowfield is defined. The four physically based modules in the code, for the instability waves, shock-vortex interaction, acoustic feedback and receptivity, are based on analytical, computational and experimental research. Preliminary results for 2-D jets illustrate the effects freestream Mach number and shear layer growth rate have on the screech amplitude and frequency.

Author

**N95-19469# Systems and Electronics, Inc., Elk Grove Village, IL.
FLIGHT PARAMETERS MONITORING SYSTEM FOR
TRACKING STRUCTURAL INTEGRITY OF ROTARY-WING
AIRCRAFT**

JAMSHID MOHAMMADI and CRAIG OLKIEWICZ In NASA. Langley Research Center, FAA/NASA International Symposium on Advanced Structural Integrity Methods for Airframe Durability and Damage Tolerance, Part 2 p 505-516 Sep. 1994

Avail: CASI HC A03/MF A04

Recent developments in advanced monitoring systems used in conjunction with tracking structural integrity of rotary-wing aircraft are explained. The paper describes: (1) an overview of rotary-wing aircraft flight parameters that are critical to the aircraft loading conditions and each parameter's specific requirements in terms of data collection and processing; (2) description of the monitoring system and its functions used in a survey of rotary-wing aircraft; and (3) description of the method of analysis used for the data. The paper presents a newly-developed method in compiling flight data. The method utilizes the maneuver sequence of events in several pre-identified flight conditions to describe various flight parameters at three specific weight ranges. Author

N95-19478# Technische Hogeschool, Delft (Netherlands). Dept. of Aerospace Engineering.

**FATIGUE LIFE UNTIL SMALL CRACKS IN AIRCRAFT
STRUCTURES: DURABILITY AND DAMAGE TOLERANCE**

J. SCHIJVE In NASA. Langley Research Center, FAA/NASA International Symposium on Advanced Structural Integrity Methods for Airframe Durability and Damage Tolerance, Part 2 p 665-681 Sep. 1994

Avail: CASI HC A03/MF A04

Crack initiation in notched elements occurs very early in the fatigue life. This is also true for riveted lap joints, an important fatigue critical element of a pressurized fuselage structure. Crack nucleation in a riveted lap joint can occur at different locations, depending on the riveting operation. It can occur at the edge of the rivet hole, at a small distance away from the hole, but still with subsequent crack growth through the hole, and ahead of the hole with a crack no longer passing through the hole. Moreover, crack nucleation can occur in the top row at the countersunk holes (outer sheet) or in the bottom row at the non-countersunk holes. Fractographic evidence is shown. The initial growth of the small cracks occurs as an (invisible) part through crack. As a consequence, predictions on the crack initiation life are problematic. After a though crack is present, the major part of the fatigue life has been consumed. There is still an apparent lack of empirical data on crack growth and residual strength of riveted lap joints, five years after the Aloha accident. Such data are very much necessary for further developments of prediction models. Some test results are presented. Author

N95-19479# Deutsche Airbus G.m.b.H., Hamburg (Germany). Dept. of Fatigue and Fracture Mechanics.

**DEVELOPMENT OF LOAD SPECTRA FOR AIRBUS A330/A340
FULL SCALE FATIGUE TESTS**

H.-J. SCHMIDT and THOMAS NIELSEN In NASA. Langley Research Center, FAA/NASA International Symposium on Advanced Structural Integrity Methods for Airframe Durability and Damage Tolerance, Part 2 p 683-697 Sep. 1994

Avail: CASI HC A03/MF A04

For substantiation of the recently certified medium range Airbus A330 and long range A340 the full scale fatigue tests are in progress.

05 AIRCRAFT DESIGN, TESTING AND PERFORMANCE

The airframe structures of both aircraft types are tested by one set of A340 specimens. The development of the fatigue test spectra for the two major test specimens which are the center fuselage and wing test and the rear fuselage test is described. The applied test load spectra allow a realistic simulation of flight, ground and pressurization loads and the finalization of the tests within the pre-defined test period. The paper contains details about the 1 g and incremental flight and ground loads and the establishment of the flight-by-flight test program, i.e., the definition of flight types, distribution of loads within the flights and randomization of flight types in repeated blocks. Special attention is given to procedures applied for acceleration of the tests, e.g. omission of lower spectrum loads and a general increase of all loads by ten percent. Author

N95-19480* Southwest Research Inst., San Antonio, TX. Structural Engineering Dept.

AIRCRAFT STRESS SEQUENCE DEVELOPMENT: A COMPLEX ENGINEERING PROCESS MADE SIMPLE

K. H. SCHRADER, D. G. BUTTS, and W. A. SPARKS *In* NASA. Langley Research Center, FAA/NASA International Symposium on Advanced Structural Integrity Methods for Airframe Durability and Damage Tolerance, Part 2 p 699-701 Sep. 1994
Avail: CASI HC A01/MF A04

Development of stress sequences for critical aircraft structure requires flight measured usage data, known aircraft loads, and established relationships between aircraft flight loads and structural stresses. Resulting cycle-by-cycle stress sequences can be directly usable for crack growth analysis and coupon spectra tests. Often, an expert in loads and spectra development manipulates the usage data into a typical sequence of representative flight conditions for which loads and stresses are calculated. For a fighter/trainer type aircraft, this effort is repeated many times for each of the fatigue critical locations (FCL) resulting in expenditure of numerous engineering hours. The Aircraft Stress Sequence Computer Program (ACSTRSEQ), developed by Southwest Research Institute under contract to San Antonio Air Logistics Center, presents a unique approach for making complex technical computations in a simple, easy to use method. The program is written in Microsoft Visual Basic for the Microsoft Windows environment. Derived from text

N95-19485* Georgia Inst. of Tech., Atlanta, GA. FAA Center of Excellence for Computational Modeling of Aircraft Structures.

RESIDUAL LIFE AND STRENGTH ESTIMATES OF AIRCRAFT STRUCTURAL COMPONENTS WITH MSD/MED

RIPUDAMAN SINGH (Indian Inst. of Science, Bangalore.), JAI H. PARK (Chungbuk National Univ., Republic of Korea.), and SATYA N. ATLURI *In* NASA. Langley Research Center, FAA/NASA International Symposium on Advanced Structural Integrity Methods for Airframe Durability and Damage Tolerance, Part 2 p 771-783 Sep. 1994
Sponsored by FAA

Avail: CASI HC A03/MF A04

Economic and safe operation of the flight vehicles flying beyond their initial design life calls for an in-depth structural integrity evaluation of all components with potential for catastrophic damages. Fuselage panels with cracked skin and/or stiffening elements is one such example. A three level analytical approach is developed to analyze the pressurized fuselage stiffened shell panels with damaged skin or stiffening elements. A global finite element analysis is first carried out to obtain the load flow pattern through the damaged panel. As an intermediate step, the damaged zone is treated as a spatially three-dimensional structure modeled by plate and shell finite elements, with all the neighboring elements that can alter the stress state at the crack tip. This is followed by the Schwartz-Neumann alternating method for local analysis to obtain the relevant crack tip parameters that govern the onset of fracture and the crack growth. The methodology developed is generic in nature and aims at handling a large fraction of problem areas identified by the Industry Committee on Wide-Spread Fatigue Damage. Author

N95-19486* Battelle Columbus Labs., OH.

ULTRASONIC TECHNIQUES FOR REPAIR OF AIRCRAFT STRUCTURES WITH BONDED COMPOSITE PATCHES

S. H. SMITH, N. SENAPATI, and R. B. FRANCINI *In* NASA. Langley Research Center, FAA/NASA International Symposium on Advanced Structural Integrity Methods for Airframe Durability and Damage Tolerance, Part 2 p 785-800 Sep. 1994
Avail: CASI HC A03/MF A04

This is a paper on a research and development project to demonstrate a novel ultrasonic process for the field application of boron/epoxy (B/Ep) patches for repair of aircraft structures. The first phase of the project was on process optimization and testing to develop the most practical ultrasonic processing techniques. Accelerated testing and aging behavior of precured B/Ep patches, which were ultrasonically bonded to simulated B-52 wing panel assemblies, were performed by conducting flight-by-flight spectrum loading fatigue tests. The spectrum represented 2340 missions/flights or 30 years of service. The effects of steady-state applied temperature and prior exposure of the B/Ep composite patches were evaluated. Representative experimental results of this phase of the project are presented. Author

N95-19488* Federal Aviation Administration, Long Beach, CA.

WIDESPREAD FATIGUE DAMAGE MONITORING: ISSUES AND CONCERNS

T. SWIFT *In* NASA. Langley Research Center, FAA/NASA International Symposium on Advanced Structural Integrity Methods for Airframe Durability and Damage Tolerance, Part 2 p 829-870 Sep. 1994
Presented at 5th International Conference on Structural Airworthiness of New and Aging Aircraft, Hamburg, Germany, 16-18 Jun. 1993
Avail: CASI HC A03/MF A04

This paper is intended to illustrate the considerable effect that small in-service undetectable multi-site-damage (MSD) can have on the residual strength capability of aging aircraft structures. In general, very few people in the industry believe that tiny cracks of undetectable size are a problem because they know that many aircraft have been able to survive much larger damage. In fact they have been certified for this large damage capability. However, this is not the issue. The real issue is the effect the tiny cracks, at multiple sites, have on the large damage capability which the industry has become accustomed to expect and which the aircraft have been certified to sustain. The concern is that this message does not appear to be fully understood by many people outside the fracture community. The prime purpose of this paper, therefore, has been to convey this message by describing in simple terms the net section yielding phenomenon in ductile materials which causes loss in lead crack residual strength in the presence of MSD. The explanation continues with a number of examples on complex stiffened structures, using the results of previous finite element analyses, which illustrate that the effect of MSD is extremely sensitive to structural configuration. It is hoped that those members of the aviation community who believe that tiny cracks are not a problem will read this paper very carefully. Author

N95-19491* National Aerospace Lab., Amsterdam (Netherlands). **RESULTS OF UNIAXIAL AND BIAXIAL TESTS ON RIVETED FUSELAGE LAP JOINT SPECIMENS**

H. VIEGER *In* NASA. Langley Research Center, FAA/NASA International Symposium on Advanced Structural Integrity Methods for Airframe Durability and Damage Tolerance, Part 2 p 911-931 Sep. 1994

Avail: CASI HC A03/MF A04

As part of an FAA-NLR collaborative program on structural integrity of aging aircraft, NLR carried out uniaxial and biaxial fatigue tests on riveted lap joint specimens being representative for application in a fuselage. All tests were constant amplitude tests with maximum stresses being representative for fuselage pressurization cycles and R-values of 0.1. The parameters selected in the testing program were the stress level ($\sigma_{sub\ max}$) = 14 and 16 ksi and the rivet spacing (0.75 and 1.0 inch). All specimens contained 3 rows

of countersunk rivets, the rivet row spacing was 1 inch and the rivet orientation continuous. Author

**N95-19495*# Tennessee Technological Univ., Cookeville, TN.
FATIGUE AND RESIDUAL STRENGTH INVESTIGATION OF
ARALL(R) -3 AND GLARE(R) -2 PANELS WITH BONDED
STRINGERS**

MING WU, DALE A. WILSON, and S. V. REDDY (Textron Aerostructures, Nashville, TN.) *In* NASA Langley Research Center, FAA/NASA International Symposium on Advanced Structural Integrity Methods for Airframe Durability and Damage Tolerance, Part 2 p 985-998 Sep. 1994

Avail: CASI HC A03/MF A04

Stiffened panels were fabricated from ARALL-3 and GLARE-3 laminates for the purpose of providing improved structural performance of lower wing panels for aircraft. To verify the designs fatigue crack growth and residual strength tests were conducted and compared to those for conventional monolithic aluminum panels.

Author

**N95-19497*# Textron Bell Helicopter, Fort Worth, TX.
AIRCRAFT FATIGUE AND CRACK GROWTH CONSIDERING
LOADS BY STRUCTURAL COMPONENT**

J. D. YOST *In* NASA Langley Research Center, FAA/NASA International Symposium on Advanced Structural Integrity Methods for Airframe Durability and Damage Tolerance, Part 2 p 1015-1028 Sep. 1994

Avail: CASI HC A03/MF A04

The indisputable 1968 C-130 fatigue/crack growth data is reviewed to obtain additional useful information on fatigue and crack growth. The proven Load Environment Model concept derived empirically from F-105D multichannel recorder data is refined to a simpler method by going from 8 to 5 variables in the spectra without a decrease in accuracy. This approach provides the true fatigue/crack growth and load environment by structural component for both fatigue and strength design. Methods are presented for defining fatigue scatter and damage at crack initiation. These design tools and criteria may be used for both metal and composite aircraft structure. Author

**N95-19499*# National Aeronautics and Space Administration.
Langley Research Center, Hampton, VA.**

**NONLINEAR ANALYSIS OF DAMAGED STIFFENED
FUSELAGE SHELLS SUBJECTED TO COMBINED LOADS**

JAMES H. STARNES, JR., VICKI O. BRITT, RICHARD D. YOUNG (Lockheed Engineering and Sciences Co., Hampton, VA.), CHARLES C. RANKIN (Lockheed Missiles and Space Co., Palo Alto, CA.), CHARLES P. SHORE, and JANE C. BAINS *In its* FAA/NASA International Symposium on Advanced Structural Integrity Methods for Airframe Durability and Damage Tolerance, Part 2 p 1045-1075 Sep. 1994

Avail: CASI HC A03/MF A04

The results of an analytical study of the nonlinear response of stiffened fuselage shells with long cracks are presented. The shells are modeled with a hierarchical modeling strategy that accounts for global and local response phenomena accurately. Results are presented for internal pressure and mechanical bending loads. The effects of crack location and orientation on shell response are described. The effects of mechanical fasteners on the response of a lap joint and the effects of elastic and elastic-plastic material properties on the buckling response of tension-loaded flat panels with cracks are also addressed. Author

06

AIRCRAFT INSTRUMENTATION

Includes cockpit and cabin display devices; and flight instruments.

**N95-15970*# National Aeronautics and Space Administration. Lewis
Research Center, Cleveland, OH.**

**SENSOR FAULT DETECTION AND DIAGNOSIS SIMULATION
OF A HELICOPTER ENGINE IN AN INTELLIGENT CONTROL
FRAMEWORK**

JONATHAN LITT (Army Research Lab., Cleveland, OH.), MEHMET KURTKAYA (Florida Atlantic Univ., Boca Raton, FL.), and AHMET DUYAR (Florida Atlantic Univ., Boca Raton, FL.) Nov. 1994 15 p Presented at the 1994 Conference of Military, Government and Aerospace Simulation, San Diego, CA, 11-13 Apr. 1994; sponsored by Society for Computer Simulation Prepared in cooperation with Army Research Lab., Cleveland, OH (Contract(s)/Grant(s): NAG3-1198; RTOP 505-62-0X; DA PROJ. 1L1-61102-AH-45)

(NASA-TM-106784; E-9237; NAS 1.15:106784; ARL-TR-637) Avail: CASI HC A03/MF A01

This paper presents an application of a fault detection and diagnosis scheme for the sensor faults of a helicopter engine. The scheme utilizes a model-based approach with real time identification and hypothesis testing which can provide early detection, isolation, and diagnosis of failures. It is an integral part of a proposed intelligent control system with health monitoring capabilities. The intelligent control system will allow for accommodation of faults, reduce maintenance cost, and increase system availability. The scheme compares the measured outputs of the engine with the expected outputs of an engine whose sensor suite is functioning normally. If the differences between the real and expected outputs exceed threshold values, a fault is detected. The isolation of sensor failures is accomplished through a fault parameter isolation technique where parameters which model the faulty process are calculated on-line with a real-time multivariable parameter estimation algorithm. The fault parameters and their patterns can then be analyzed for diagnostic and accommodation purposes. The scheme is applied to the detection and diagnosis of sensor faults of a T700 turboshaft engine. Sensor failures are induced in a T700 nonlinear performance simulation and data obtained are used with the scheme to detect, isolate, and estimate the magnitude of the faults. Author

Author

**N95-16456*# National Aeronautics and Space Administration. Langley
Research Center, Hampton, VA.**

**A STUDY OF SOFTWARE STANDARDS USED IN THE
AVIONICS INDUSTRY**

KELLY J. HAYHURST *In its* The Role of Computers in Research and Development at Langley Research Center p 85-105 Oct. 1994

Avail: CASI HC A03/MF A06

Within the past decade, software has become an increasingly common element in computing systems. In particular, the role of software used in the aerospace industry, especially in life- or safety-critical applications, is rapidly expanding. This intensifies the need to use effective techniques for achieving and verifying the reliability of avionics software. Although certain software development processes and techniques are mandated by government regulating agencies, no one methodology has been shown to consistently produce reliable software. The knowledge base for designing reliable software simply has not reached the maturity of its hardware counterpart. In an effort to increase our understanding of software, the Langley Research Center conducted a series of experiments over 15 years with the goal of understanding why and how software fails. As part of this program, the effectiveness of current industry standards for the development of avionics is being investigated. This study involves the generation of a controlled environment to conduct scientific experiments on software processes. Derived from text

06 AIRCRAFT INSTRUMENTATION

N95-18164# Burnette Engineering, Fairborn, OH.
AN EVALUATION OF AIRCRAFT CRT AND DOT-MATRIX DISPLAY LEGIBILITY REQUIREMENTS Interim Report, 17 Apr. 1985 - 25 Jun. 1991

KEITH T. BURNETTE Jun. 1994 73 p
(Contract(s)/Grant(s): F33615-84-C-3627)
(AD-A283933; WL-TR-91-7020) Avail: CASI HC A04/MF A01

Pilot satisfaction with the legibility performance of the absorption bandpass filtered green P-43 phosphor cathode ray tube (CRT) electronic displays employed in the F-15, F-16 and F-18 aircraft, prior to 1980 has been used in this report as a basis for establishing minimum luminance and contrast requirements for both CRT and dot-matrix electronic aircraft displays. The data drawn on and the methods used to derive the alphanumeric, graphic and video information legibility requirements that should as a minimum be met by aircraft electronic display portrayals under direct sunlight, glare source and other high ambient viewing conditions are described. The sunlight readability/legibility requirements and tests of the night vision imaging system (NVIS) compatibility specification MIL-L-85762 were in part founded on the data contained in this report.

DTIC

07

AIRCRAFT PROPULSION AND POWER

Includes prime propulsion systems and systems components, e.g., gas turbine engines and compressors; and on-board auxiliary power plants for aircraft.

A95-63643
INVESTIGATION OF HEAT TRANSFER BETWEEN ROTATING SHAFTS OF TRANSMISSIONS OF TURBOJET ENGINES
N. N. SALOV SPI, Sevastopol (Ukraine) *Izvestiya VUZ: Aviatzionnaya Tekhnika* (ISSN 0579-2975) no. 1 January-March 1994 p. 49-53 In RUSSIAN
(BTN-94-EIX94461408760) Copyright

Heat transfer of a cylindrical surface between shafts has been experimentally investigated. The shafts are coaxially located in the channel. The channel has geometry characteristic of transmissions of turbojet engines, with shafts rotating in different directions. The test results have been generalized on the basis of the similarity theory. EI

A95-63657
MODELLING FOR OPTIMAL OPERATIONS OF LINE MILLING OF AERODYNAMIC SURFACES
E. M. KOROVIN KGTU, Kazan (Russia) and A. V. BASHKIRTSEV *Izvestiya VUZ: Aviatzionnaya Tekhnika* (ISSN 0579-2975) no. 1 January-March 1994 p. 106-109 In RUSSIAN refs
(BTN-94-EIX94461408774) Copyright

An advanced method is offered to select regimes for the line milling of the fin surface of large-sized blades for gas-turbine engines (GTE). The principles of the optimal control of regimes during the cutting process are outlined. Ways to increase productivity of the line milling of GTE blades are discussed. The optimization problem of the line milling includes the search for such regimes that would provide an extremum of an optimization criterion and meet the requirements for treatment quality. EI

N95-16265# Kazan Aviation Inst. (USSR).
THEORETICAL FUNDAMENTALS OF THE AIRCRAFT GTE TESTS
YU. V. KOZHEVNIKOV *In Nanjing Univ. of Aeronautics and Astronautics, Joint Proceedings on Aeronautics and Astronautics (JPAA)* p 107-111 May 1993
Avail: CASI HC A01/MF A03

We discuss the methodology of a new scientific theory taking as an example the aircraft gas turbine engine (GTE) tests. We

formulate a theory of construction principles and practical approaches to the problem. Author (revised)

N95-16317# General Electric Co., Cincinnati, OH. Aircraft Engine Div.
SCRAMJET TESTING GUIDELINES Status Report
P. KUTSCHENREUTER *In JHU, The 1993 JANNAF Propulsion Meeting, Volume 1* p 247-259 Nov. 1993
Avail: CPIA, 10630 Little Patuxent Pkwy., Suite 202, Columbia, MD 21044-3200 HC

This is the first status report on the JANNAF Airbreathing Engine Testing Panel's project of developing scramjet testing guidelines. The motivation for such an effort is driven by the perceived need to get more meaningful results from the shrinking U.S. resources available for high Mach number airbreathing propulsion development considering recent significant changes in the political and economic environment. It is the panel's vision that formulation and use of these guidelines would make such a contribution. A quick, first rough cut at their preparation was completed in less than 12 months, including an evaluation designed to identify required areas of refinement. These interim results are the subject of this paper. Author

N95-16323# Sundstrand Power Systems, San Diego, CA.
SMALL TURBOJETS: DESIGNS AND INSTALLATIONS
C. RODGERS *In JHU, The 1993 JANNAF Propulsion Meeting, Volume 1* p 335-352 Nov. 1993
Avail: CPIA, 10630 Little Patuxent Pkwy., Suite 202, Columbia, MD 21044-3200 HC

Smaller, smarter airbreathing propelled tactical missiles are being proposed and developed. They will function for various operational duties currently performed by larger, limited range missiles or manned interdiction aircraft. The extreme compactness of these advanced missiles require relatively high power density small turbojets. Several design configuration options are possible for these turbojets, including centrifugal and axial turbomachinery compressor and turbines, straight annular and reverse flow annular combustors, and various types of fuel injection systems. The attributes of candidate configurations are discussed with respect to maximum thrust per frontal area, range, and endurance optimization, and low manufacturing costs. Installation constraints upon engine design, in particular, the inlet and exhaust nozzle and start system are reviewed. Early recognition of these constraints is paramount in minimizing overall propulsion system cost, and volume; thereby producing maximum weapon system effectiveness. Author

N95-17371# Pacific Northwest Lab., Richland, WA.
AN ARTIFICIAL NEURAL NETWORK SYSTEM FOR DIAGNOSING GAS TURBINE ENGINE FUEL FAULTS
O. J. ILLI, JR. (Army Ordnance Center and School, Aberdeen Proving Ground, MD.), F. L. GREITZER, L. J. KANGAS, and T. REEVE (Expert Solutions, Stratford, CT.) Apr. 1994 10 p Presented at the Mechanical Failures Prevention Group Conference, Wakefield, MA, 19-21 Apr. 1994
(Contract(s)/Grant(s): DE-AC06-76RL-01830)
(DE94-013960; PNL-SA-22914; CONF-9404179-1) Avail: CASI HC A02/MF A01

The US Army Ordnance Center and School and Pacific Northwest Laboratories are developing a turbine engine diagnostic system for the M1A1 Abrams tank. This system employs artificial neural network (ANN) technology to perform diagnosis and prognosis of the tank's AGT-1500 gas turbine engine. This paper describes the design and prototype development of the ANN component of the diagnostic system, which we refer to as 'TEDANN' for turbine engine diagnostic artificial neural networks. DOE

N95-17402*# Case Western Reserve Univ., Cleveland, OH. Dept. of Mechanical and Aerospace Engineering.
THREE DIMENSIONAL COMPRESSIBLE TURBULENT FLOW

COMPUTATIONS FOR A DIFFUSING S-DUCT WITH/WITHOUT VORTEX GENERATORS Final Report

SOO-YONG CHO and ISAAC GREBER NASA Dec. 1994 216 p
(Contract(s)/Grant(s): NCC3-181; RTOP 505-62-52)
(NASA-CR-195390; E-9160; NAS 1.26:195390) Avail: CASI HC A10/MF A03

Numerical investigations on a diffusing S-duct with/without vortex generators and a straight duct with vortex generators are presented. The investigation consists of solving the full three-dimensional unsteady compressible mass averaged Navier-Stokes equations. An implicit finite volume lower-upper time marching code (RPLUS3D) has been employed and modified. A three-dimensional Baldwin-Lomax turbulence model has been modified in conjunction with the flow physics. A model for the analysis of vortex generators in a fully viscous subsonic internal flow is evaluated. A vortical structure for modeling the shed vortex is used as a source term in the computation domain. The injected vortex paths in the straight duct are compared with the analysis by two kinds of prediction models. The flow structure by the vortex generators are investigated along the duct. Computed results of the flow in a circular diffusing S-duct provide an understanding of the flow structure within a typical engine inlet system. These are compared with the experimental wall static-pressure, static- and total-pressure field, and secondary velocity profiles. Additionally, boundary layer thickness, skin friction values, and velocity profiles in wall coordinates are presented. In order to investigate the effect of vortex generators, various vortex strengths are examined in this study. The total-pressure recovery and distortion coefficients are obtained at the exit of the S-duct. The numerical results clearly depict the interaction between the low velocity flow by the flow separation and the injected vortices. Author

N95-17749 Jiaotong Univ., Shanghai (China). SIMULATION INVESTIGATION ON SYSTEM IDENTIFICATION OF GAS TURBINE

M. SU 1993 8p Sponsored by Institute of Scientific and Technical Information of China, Beijing (PB95-104238; ISTIC-TR-93123) Avail: Issuing Activity (National Technical Information Service (NTIS))

To this paper the hybrid simulation system for identification is introduced. The analysis and the comparison between the results in open loop and closed loop are made. Three different speed regulators are tested in closed loop identification simulation experiments. The effect of external input signal on identification results is examined. A piecewise linear model of a marine gas turbine is developed. NTIS

N95-18133*# National Aeronautics and Space Administration. Lewis Research Center, Cleveland, OH.

NUMERICAL MIXING CALCULATIONS OF CONFINED REACTING JET FLOWS IN A CYLINDRICAL DUCT
VICTOR L. OECHSLE (Allison Engine Co., Indianapolis, IN.) and J. D. HOLDEMAN Jan. 1995 46 p Presented at the 33rd Aerospace Sciences Meeting and Exhibit, Reno, NV, 9-12 Jan. 1995; sponsored by AIAA Original contains color illustrations
(Contract(s)/Grant(s): NAS3-25950; RTOP 537-02-21)
(NASA-TM-106736; E-9349; NAS 1.15:106736; AIAA PAPER 95-0733) Copyright Avail: CASI HC A03/MF A01; 22 functional color pages

The results reported in this paper describe some of the main flow characteristics and NOx production results which develop in the mixing process in a constant cross-sectional cylindrical duct. A 3-dimensional numerical model has been used to predict the mixing flow field and NOx characteristics in a mixing section of an RQL combustor. Eighteen configurations have been analyzed in a circular geometry in a fully reacting environment simulating the operating condition of an actual RQL gas turbine combustion liner. The evaluation matrix was constructed by varying three parameter: (1) jet-to-mainstream momentum-flux ration (J), (2) orifice shape or orifice aspect ratio, and (3) slot slant angle. The results indicate that

the mixing flow field and NOx production significantly vary with the value of the jet penetration and subsequently, slanting elongated slots generally improve the NOx production at high J conditions. Round orifices produce low NOx at low J due to the strong jet penetration. The NOx production trends do not correlate with the mixing non-uniformity parameters described herein. Author

N95-18383 Naval Air Warfare Center, Trenton, NJ. Aircraft Div. UNMANNED AERIAL VEHICLE HEAVY FUEL ENGINE TEST Final Report, Apr. 1992 - Jan. 1993

ROBERT BRUCATO, JOSEPH LAWTON, and ANTHONY MAGGIO Oct. 1993 129 p Limited Reproducibility: More than 20% of this document may be affected by microfiche quality (AD-A284332; NAWCADTRN-PE-261) Avail: Issuing Activity (Defense Technical Information Center (DTIC))

This report documents the test results of three heavy fuel engines designed to demonstrate that Unmanned Aerial Vehicle operational requirements can feasibly be met utilizing heavy fuels (JP-5, JP-8 and Diesel) versus gasoline. The three engines included rotary engines delivered by AA-1 Corporation and Defense Group Industries Incorporated and a two cylinder, two stroke engine delivered by Southwest Research Institute. The testing was conducted at the Naval Air Warfare Center Aircraft Division Trenton during the period of 17 April 1992 through 22 January 1993. DTIC

N95-18911# Deutsche Forschungsanstalt fuer Luft- und Raumfahrt, Cologne (Germany). Inst. fuer Antriebstechnik.

ONE-DIMENSIONAL FLOW DESCRIPTION FOR THE COMBUSTION CHAMBER OF A SCRAMJET Ph.D. Thesis [EINDIMENSIONALE BRENNKAMMERBETRACHTUNGEN FUER EIN STAUSTRAHLTRIEBWERK MIT UEBERSCHALLVERBRENNUNG]
FRANS G. J. KREMER 1994 171 p In GERMAN (ISSN 0939-2963)
(DLR-FB-94-06) Avail: CASI HC A08/MF A02

A theoretical calculation model for the determination of the one-dimensional flow data in the combustion chamber of a scramjet is established. This model serves to improve the physical understanding of such flows in order to enable a more profound design of a scramjet combustor. It is shown, that the analytic notation of the continuity, momentum and energy equation of the non-constant area combustor is not useful to describe the physical relations. This is due to the unknown wall pressure integral, for which usually the formulation of the pressure-area power family, introduced by Crocco, is assumed. Therefore a model is established, which bases on the differential notation of the laws of conservation. This is solved using distribution functions and verified with experimental data. The model is used to quantify the influence of several parameters on the flow data. Finally design considerations for flight Mach number 15 and off-design considerations for flight Mach numbers 5, 10 and 15 are performed. Author

N95-19017# Advisory Group for Aerospace Research and Development, Neuilly-Sur-Seine (France). Propulsion and Energetics Panel. MATHEMATICAL MODELS OF GAS TURBINE ENGINES AND THEIR COMPONENTS [LES MODELES MATHEMATQUES DES TURBOMOTEURS ET DE LEURS ORGANES]

Dec. 1994 183 p Lecture series held in Cleveland, OH, 7-8 Dec. 1994, in Wessling, Germany, 12-13 Dec. 1994 and in Paris, France, 15-16 Dec. 1994
(AGARD-LS-198; ISBN-92-836-1008-3) Copyright Avail: CASI HC A09/MF A02

This Lecture Series will present and discuss the scientific problems of modern mathematical simulation of gas turbine engines and their components. Some peculiarities of complex multicomponent and multidisciplinary models for whole flow passage of bypass gas turbine engine, core, multistage compressors and turbines, and other engine components will be studied. Solutions of steady and unsteady problems are given using high efficiency monotone nu-

07 AIRCRAFT PROPULSION AND POWER

merical methods and the theoretical bases of these methods are presented. Many practical results of aerodynamic and thermostress simulations for engine components are shown. These results are compared widely with experimental data for accurate verification of developing computational codes. This Lecture Series, endorsed by the Propulsion and Energetics Panel of AGARD, has been implemented by the Technology Cooperation Program. For individual titles, see N95-19018 through N95-19026.

N95-19020# Central Inst. of Aviation Motors, Moscow (Russia).
THE MATHEMATICAL MODELS OF FLOW PASSAGE FOR GAS TURBINE ENGINES AND THEIR COMPONENTS
RAVIL Z. NIGMATULLIN and MIKHAIL J. IVANOV *In* AGARD, *Mathematical Models of Gas Turbine Engines and their Components* 28 p Dec. 1994
Copyright Avail: CASI HC A03/MF A02

Mathematical models for gas turbine engines and installation component flow passages based on real 3D geometry of flow passages, in particular spatial shape of blades, are considered. The models are based on numerical solving of unsteady Euler equations and so it allows simulation of some unsteady transitional functioning regimes of engines and installations together with steady ones. The models take into consideration the viscous losses, leakage in axial gaps and tip clearances, cooling air injection and selection. The first level mathematical models are based on 2D steady and unsteady methods on $S(\text{sub } 1)$ and $S(\text{sub } 2)$ surfaces. Some features of numerical algorithms based on these methods are considered. The second level models are based on 3D approaches anywhere in computational domains excluding the middles of axial gaps between neighboring blade rows where for the simplification of the problem the averaging in angular direction is fulfilled. Author (revised)

N95-19021# Central Inst. of Aviation Motors, Moscow (Russia).
SIMULATION OF MULTIDISCIPLINARY PROBLEMS FOR THE THERMOSTRESS STATE OF COOLED HIGH TEMPERATURE TURBINES
VALEREY K. KOSTEGE, V. A. HALTURIN, and V. G. SUNDURIN *In* AGARD, *Mathematical Models of Gas Turbine Engines and their Components* 15 p Dec. 1994
Copyright Avail: CASI HC A03/MF A02

Numerical models for the thermostress state analysis of turbine rotor elements are discussed. Steady and unsteady temperature fields are calculated and result in solution of conjugate heat and hydraulic problems for blades (quasi three-dimensional model) for disk (two-dimensional model) and for the whole cooled rotor (three-dimensional model). A lot of attention is given to mass flow calculation in blade passages and turbine circumferential disk cavities. They are determined by using experimental data for pressure loss and generalized dependencies for friction and heat transfer coefficients on stators and rotors surfaces. On external blade surfaces the boundary conditions are defined from the solution of two-dimensional and three-dimensional gas dynamics problems and corrected from experimental data base for film cooling. The thermostress state is calculated by a finite element method for realistic geometry using common equations of elasticity theory. Author

N95-19022# Central Inst. of Aviation Motors, Moscow (Russia).
APPLICATION OF MULTICOMPONENT MODELS TO FLOW PASSAGE SIMULATION IN MULTISTAGE TURBOMACHINES AND WHOLE GAS TURBINE ENGINES
RAVIL Z. NIGMATULLIN *In* AGARD, *Mathematical Models of Gas Turbine Engines and their Components* 17 p Dec. 1994
Copyright Avail: CASI HC A03/MF A02

Some features of used numerical algorithms for gas turbine engines components flow simulation are considered. Among them are topology of computational grids in 2D and 3D cases for flow passages of complex geometry, details of realization of conservative scheme at joints of different grids. In $S(\text{sub } 2)$ -calculations it is necessary to consider the problem of inlet and outlet angles; in Euler calculation the ways of accounting for viscous loss effects are briefly

described. Examples of calculations of flow through by-pass engine components are presented. Author

N95-19023# Central Inst. of Aviation Motors, Moscow (Russia).
SIMULATION OF STEADY AND UNSTEADY VISCOUS FLOWS IN TURBOMACHINERY
VLADISLAV G. KRUPA *In* AGARD, *Mathematical Models of Gas Turbine Engines and their Components* 39 p Dec. 1994
Copyright Avail: CASI HC A03/MF A02

A Navier-Stokes code has been used to compute the viscous turbulent cascade flows. The numerical method employs implicit high-order accurate Godunov scheme and a two equation ($q - \omega$) turbulence model based on the integration to the wall. The generation of the O-H grid system for viscous cascade flow simulations is discussed. Numerical solutions were obtained for 2D and 3D turbine cascade flows and 2D unsteady rotor-stator interactions. Available experimental data are used for verification of the computed results. Author

N95-19024# Central Inst. of Aviation Motors, Moscow (Russia).
APPLICATION OF MULTIDISCIPLINARY MODELS TO THE COOLED TURBINE ROTOR DESIGN
VALERY K. KOSTEGE, V. D. VENEDIKTOV, and A. V. GRANOVSKII *In* AGARD, *Mathematical Models of Gas Turbine Engines and their Components* 10 p Dec. 1994
Copyright Avail: CASI HC A02/MF A02

A computer program for designing turbine vane and blade cooling systems is discussed. This program is based on the complex use of 2D and 3D gas dynamic, heat-transfer and thermostress models. FEM Thermostress models are formatted based on geometry data from the computer design system. One-dimensional mass flow and conjugate thermal models are quickly created by using graphic dialogue regimes for different cooling systems. Quasi-3D and 3D thermostress models are used to carry out cooling system optimization or comparison of alternative cooling systems. Author

N95-19025# Central Inst. of Aviation Motors, Moscow (Russia).
VERIFICATION OF MULTIDISCIPLINARY MODELS FOR TURBOMACHINES
VALEREY K. KOSTEGE *In* AGARD, *Mathematical Models of Gas Turbine Engines and their Components* 7 p Dec. 1994
Copyright Avail: CASI HC A02/MF A02

Accurate prediction of the temperature distribution in rotating blades is an important and difficult task. An approach for the verification of hydraulic and thermal models in real blades is discussed in the lecture. For static conditions, predicted local internal convective heat transfer coefficients on blades are corrected using a quasi-3D thermal-hydraulic model with the blade unsteady surface temperatures measured by the Thermovision system. External boundary conditions are corrected using the blade base surface temperatures measured by thermocouples on a hot static rig. The final identification of the models is carried out using measurements of the gas temperature distribution within the rotating blade passage, and the measured blade external surface temperature in the engine. Author

N95-19026# Central Inst. of Aviation Motors, Moscow (Russia).
PERSPECTIVE PROBLEMS OF GAS TURBINE ENGINES SIMULATION
MIKHAIL J. IVANOV *In* AGARD, *Mathematical Models of Gas Turbine Engines and their Components* 19 p Dec. 1994
Copyright Avail: CASI HC A03/MF A02

The purpose of the last lecture is to present the activity of CIAM in the field of the development of Computer Turbojet Test Technology based on aero-engine models of high 3D level. Using this technology the aero-engine design may be transformed into new quality. It's the predictions of steady and transient working processes, performance and efficiency on the first stage of engine design (without the real metal engine testing). These aero-engine models must accompany the whole engine life - from design to production and use on aircraft. Author

N95-19380* National Aeronautics and Space Administration. Lewis Research Center, Cleveland, OH.

NASA LEWIS RESEARCH CENTER WORKSHOP ON FORCED RESPONSE IN TURBOMACHINERY
 GEORGE L. STEFKO, comp., DURBHAV. MURTHY, comp. (Toledo Univ., OH.), MICHAEL MOREL, comp. (NYMA, Inc., Brook Park, OH.), DAN HOYNIK, comp., and JIM W. GAUNTNER, comp. Dec. 1994 135 p Workshop held in Cleveland, OH, 11 Aug. 1993 (Contract(s)/Grant(s): RTOP 505-63-5B) (NASA-CP-10147; E-9111; NAS 1.55:10147) Avail: CASI HC A07/MF A02

A summary of the NASA Lewis Research Center (LeRC) Workshop on Forced Response in Turbomachinery in August, 1993 is presented. It was sponsored by the following NASA organizations: Structures, Space Propulsion Technology, and Propulsion Systems Divisions of NASA LeRC and the Aeronautics and Advanced Concepts & Technology Offices of NASA Headquarters. In addition, the workshop was held in conjunction with the GUIDe (Government/Industry/Universities) Consortium on Forced Response. The workshop was specifically designed to receive suggestions and comments from industry on current research at NASA LeRC in the area of forced vibratory response of turbomachinery blades which includes both computational and experimental approaches. There were eight presentations and a code demonstration. Major areas of research included aeroelastic response, steady and unsteady fluid dynamics, mistuning, and corresponding experimental work. For individual titles, see N95-19381 through N95-19383.

N95-19381* United Technologies Research Center, East Hartford, CT.

UNSTEADY AERODYNAMIC ANALYSES FOR TURBOMACHINERY AEROELASTIC PREDICTIONS
 JOSEPH M. VERDON, M. BARNETT, and T. C. AYER In NASA. Lewis Research Center, NASA Lewis Research Center Workshop on Forced Response in Turbomachinery p 13-36 Dec. 1994 Avail: CASI HC A03/MF A02

Applications for unsteady aerodynamics analysis in this report are: (1) aeroelastic: blade flutter and forced vibration; (2) aeroacoustic: noise generation; (3) vibration and noise control; and (4) effects of unsteadiness on performance. This requires that the numerical simulations and analytical modeling be accurate and efficient and contain realistic operating conditions and arbitrary modes of unsteady excitation. The assumptions of this application contend that: (1) turbulence and transition can be modeled with the Reynolds averaged and using Navier-Stokes equations; (2) 'attached' flow with high Reynolds number will require thin-layer Navier-Stokes equations, or inviscid/viscid interaction analyses; (3) small-amplitude unsteady excitations will need nonlinear steady and linearized unsteady analyses; and (4) Re to infinity will concern inviscid flow. Several computer programs (LINFLO, CLT, UNSVIS, AND SFLOW-IV) are utilized for these analyses. Results and computerized grid examples are shown. This report was given during NASA LeRC Workshop on Forced Response in Turbomachinery in August of 1993. CASI

N95-19382* National Aeronautics and Space Administration. Lewis Research Center, Cleveland, OH.

STEADY POTENTIAL SOLVER FOR UNSTEADY AERODYNAMIC ANALYSES
 DAN HOYNIK In its NASA Lewis Research Center Workshop on Forced Response in Turbomachinery p 37-49 Dec. 1994 Avail: CASI HC A03/MF A02

Development of a steady flow solver for use with LINFLO was the objective of this report. The solver must be compatible with LINFLO, be composed of composite mesh, and have transonic capability. The approaches used were: (1) steady flow potential equations written in nonconservative form; (2) Newton's Method; (3) implicit, least-squares, interpolation method to obtain finite difference equations; and (4) matrix inversion routines from LINFLO. This report was given during the NASA LeRC Workshop on Forced Response in Turbomachinery in August of 1993. CASI

N95-19383* Michigan Univ., Ann Arbor, MI.

FORCED RESPONSE OF MISTUNED BLADED DISKS
 CHRISTOPHE PIERRE In NASA. Lewis Research Center, NASA Lewis Research Center Workshop on Forced Response in Turbomachinery p 95-120 Dec. 1994 Avail: CASI HC A03/MF A02

Small mistuning can cause large, catastrophic changes in blade vibrational response whereby the amplitudes of vibration of some blades may increase by several hundred percent. This can produce 'rogue' blades and HCF failure. The free and forced responses may be highly sensitive to mistuning, and the tuned system predictions may be qualitatively in error and grossly underestimate blade forced response and overestimate fatigue life. Manufacturing tolerances, material non-uniformities, nonidentical root fixtures, and in-service degradation result in blade-to-blade differences that destroy cyclic symmetry in bladed discs. Therefore, a credible forced response prediction system for turbomachinery vibration must take mistuning into account. This report addresses these problems, states several objectives, and introduces NASA research program thrusts concerning this problem. This report was given during the NASA LeRC Workshop on Forced Response in Turbomachinery in August of 1993. CASI

08

AIRCRAFT STABILITY AND CONTROL

Includes aircraft handling qualities; piloting; flight controls; and autopilots.

A95-63064
ENGINEERING METHODS FOR THE EVALUATION OF TRANSONIC FLUTTER CHARACTERISTICS FOR AERODYNAMIC CONTROL SURFACES

A. V. SAFRONOV Kievskoe Vyshee Voennoe Aviatsionnoe Inzhenernoe Uchilishche, Kiev (Ukraine) and V. A. SAFRONOV Problemy Prochnosti (ISSN 0556-171X) no. 6 June 1994 p. 78-85 In RUSSIAN refs (BTN-94-EIX94461408589) Copyright

Engineering methods for the evaluation of flutter characteristics of control surfaces with the account taken of their interaction with shock waves are proposed on the basis of the results of theoretical and experimental investigations into a transonic flow around the airfoils. A comparison of the rudder hinge moments, obtained both by calculation and in flight experiments, has revealed their satisfactory agreement. EI

A95-64584
H(SUP 2)/H(SUP INF) CONTROLLER DESIGN FOR A TWO-DIMENSIONAL THIN AIRFOIL FLUTTER SUPPRESSION
 HITAY OEZBAY Ohio State Univ., Columbus, OH and GLEN R. BACHMANN Journal of Guidance, Control, and Dynamics (ISSN 0731-5090) vol. 17, no. 4 July-August 1994 p. 722-728 refs (BTN-94-EIX94511433918) Copyright

In this paper we study the problem of active feedback controller design for a thin airfoil, whose mathematical model is derived from classical Theodorsen's formulation. A finite dimensional controller stabilizing the original infinite dimensional model is obtained using H(sup infinity) control techniques. We also consider the gust alleviation problem and show that it can be formulated as a disturbance attenuation problem in the mixed H(sup 2)/H(sup infinity) control framework. We use existing results on H(sup infinity) and mixed H(sup 2)/H(sup infinity) control to illustrate our approach with a numerical example. Author (EI)

A95-64586
DESIGN OF NONLINEAR CONTROL LAWS FOR HIGH-ANGLE-OF-ATTACK FLIGHT

08 AIRCRAFT STABILITY AND CONTROL

RICHARD J. ADAMS Wright-Patterson Air Force Base, OH,
JAMES M. BUFFINGTON, and SIVA S. BANDA Journal of
Guidance, Control, and Dynamics (ISSN 0731-5090) vol. 17,
no. 4 July-August 1994 p. 737-746 refs
(BTN-94-EIX94511433920) Copyright

High-angle-of-attack flight control laws are developed for a supermaneuverable fighter aircraft. The methods of dynamic inversion and structured singular value synthesis are combined into an approach which addresses both the nonlinearity and robustness problems of flight at extreme operating conditions. The primary purpose of the dynamic inversion control elements is to linearize the vehicle response across the flight envelope. Structured singular value synthesis is used to design a dynamic controller which provides robust tracking to pilot commands. The resulting control system achieves desired flying qualities and guarantees a large margin of robustness to uncertainties for high-angle-of-attack flight conditions. High-fidelity nonlinear simulation results show that the combined dynamic inversion/structured singular value synthesis control law achieves a high level of performance in a realistic environment. Author (EI)

A95-64587 AIRCRAFT MODEL FOR THE AIAA CONTROLS DESIGN CHALLENGE

RANDAL W. BRUMBAUGH PRC Inc., Edwards, CA Journal of
Guidance, Control, and Dynamics (ISSN 0731-5090) vol. 17, no. 4
July-August 1994 p. 747-752 refs
(BTN-94-EIX94511433921) Copyright

This paper describes a generic, state-of-the-art, high-performance aircraft model, including detailed, full-envelope, nonlinear aerodynamics, and full-envelope thrust and first-order engine response data. Although this model was developed primarily for the AIAA Controls Design Challenge, the availability of such a model provides a common focus for research in aeronautical control theory and methodology. Figures showing vehicle geometry, surfaces, and sign conventions are included. Author (EI)

A95-64606 TIME-OPTIMAL TURN TO A HEADING: AN ANALYTIC SOLUTION

RAINER WALDEN Univ. of Paderborn, Paderborn (Germany)
Journal of Guidance, Control, and Dynamics (ISSN 0731-5090) vol.
17, no. 4 July-August 1994 p. 873-875 refs
(BTN-94-EIX94511433940) Copyright

The paper deals with the problem of the time optimal turn of an aircraft to a given heading using a simplified model. The investigation is limited to a horizontal turn, neglecting the effects of the gravitational forces. The authors use a quadratic drag law and they aim to develop a feedback strategy with analytic tools that can be easily applied. The feedback control obtained gives insight into the structure of the turning problem and may be used as a basis for the construction of more realistic controls. EI

N95-16109 Naval Postgraduate School, Monterey, CA. A COMPUTATIONAL INVESTIGATION OF WAKE-INDUCED AIRFOIL FLUTTER IN INCOMPRESSIBLE FLOW AND ACTIVE FLUTTER CONTROL M.S. Thesis

MARK A. TURNER Mar. 1994 108p Limited Reproducibility: More
than 20% of this document may be affected by microfiche quality
(AD-A281534) Avail: Issuing Activity (Defense Technical Information
Center (DTIC))

Several incompressible oscillatory flow and flutter problems were investigated. A previously developed unsteady panel code for single airfoil bending torsion flutter analysis was compared to Theodorsen's classical theory. The panel code agrees with Theodorsen's bending-torsion flutter analysis for natural frequency ratios (ω sub h / ω sub alpha) less than 1.2. Also, a two airfoil unsteady panel code was modified for one degree of freedom flutter analysis. Code verification was completed by first comparing flat plate theory to the unsteady aerodynamic force and moment coefficients and then using the equation of motion to determine regions of instability. The possibility of active

flutter control was investigated by positioning a small control airfoil in front of a neutrally stable reference airfoil. Results show that the flutter boundary may be changed through the placement, oscillation, or scaling of a second airfoil upstream. A comparison with pitch damping curves published by Loewy confirms that the code is capable of predicting wake-induced airfoil flutter. DTIC

N95-16392# National Aeronautical Lab., Bangalore (India). Civil
Aviation Unit.

EVALUATION OF THE DYNAMIC STABILITY CHARACTERISTICS OF THE NAL LIGHT TRANSPORT AIRCRAFT

S. M. KANNAN Dec. 1992 33 p
(Contract(s)/Grant(s): NAL PROJ. ID-8-117L)
(NAL-PD-CA-9217) Avail: CASI HC A03/MF A01

A study of the dynamic stability characteristics of the NAL Light Transport Aircraft, LTA-7 is made in this report. The dynamic stability derivatives of the aircraft are evaluated at low angles of attack (unseparated flows) and incompressible flows. A comparison is made of the estimated derivatives with the range of experimental values available in the open literature for light aircraft for validation of the computer code used. The characteristic equations of the linear small disturbance equations of motion for both the longitudinal and the lateral dynamics are solved and the stability characteristics evaluated. A discussion of the flying qualities vis-a-vis the FAR regulations is also made. Author

N95-17404*# Maryland Univ., College Park, MD. Dept. of Aerospace
Engineering.

COOPERATIVE CONTROL THEORY AND INTEGRATED FLIGHT AND PROPULSION CONTROL Final Report, 1990- 1993

DAVID K. SCHMIDT and JOHN D. SCHIERMAN Nov. 1994
104 p

(Contract(s)/Grant(s): NAG3-998)
(NASA-CR-197493; NAS 1.26:197493) Avail: CASI HC A06/MF A02

This report documents the activities and research results obtained under a grant (NAG3-998) from the NASA Lewis Research Center. The focus of the research was the investigation of dynamic interactions between airframe and engines for advanced ASTOVL aircraft configurations, and the analysis of the implications of these interactions on the stability and performance of the airframe and engine control systems. In addition, the need for integrated flight and propulsion control for such aircraft was addressed. The major contribution of this research was the exposition of the fact that airframe and engine interactions could be present, and their effects could include loss of stability and performance of the control systems. Also, the significance of two directional, as opposed to one-directional, coupling was identified and explained. A multi variable stability and performance analysis methodology was developed, and applied to several candidate aircraft configurations. Also exposed was the fact that with interactions present along with some integrated control approaches, the engine command/limiting logic (which represents an important non-linear component of the engine control system) can impact closed-loop airframe/engine system stability. Finally, a brief investigation of control-law synthesis techniques appropriate for the class of systems was pursued, and it was determined that multi variable techniques, included model-following formulations of LQG and/or H (infinity) methods showed promise. However, for practical reasons, decentralized control architectures are preferred, which is an architecture incompatible with these synthesis methods. Author (revised)

N95-17454 National Defence Research Establishment, Stockholm
(Sweden). Dept. of Weapon Systems, Effects and Protection.
EVALUATION OF AN AUTOPILOT BASED MULTIMODELLING
[UTVAERDERING AV STYRAUTOMAT FOER MISSILER,
BASERAD PA MULTIMODELLERING]

S. L. WIRKANDER Jan. 1994 49 p In SWAHILI
(PB94-190725; FOA-C-20957-2.1) Avail: Issuing Activity (National
Technical Information Service (NTIS))

The report describes an investigation and development of the autopilot, which was described in an earlier report. This autopilot law was based on a library, consisting of missile models corresponding to different speeds and altitudes, which makes it possible to give the missile the same guidance properties independently of speed and altitude. In the present report an autopilot of a conventional type is constructed, with the intention to constitute an object of comparison for the multimodel autopilot. The report presents such a comparison, in which it is demonstrated that the multimodel autopilot works satisfactorily for all speeds and altitudes for which it has models, whereas the conventional one works only in the neighborhood of one special (nominal) speed-altitude combination. It is also shown that the multimodel autopilot can be improved by means of interpolation between the models in the library. This version of multimodel autopilot is always preferable, because of its superior controlling qualities. In this investigation the same library has been used as in the earlier report. NTIS

N95-18567*# Rockwell International Corp., Downey, CA. Space Systems Div.
STRATEGIC AVIONICS TECHNOLOGY DEFINITION STUDIES. SUBTASK 3-1A3: ELECTRICAL ACTUATION (ELA) SYSTEMS TEST FACILITY

J. P. ROGERS, K. L. CURETON, and J. R. OLSEN 30 Sep. 1994 53 p

(Contract(s)/Grant(s): NAS9-18880)

(NASA-CR-188360; NAS 1.26:188360; SSD94D0298) Avail: CASI HC A04/MF A01

Future aerospace vehicles will require use of the Electrical Actuator systems for flight control elements. This report presents a proposed ELA Test Facility for dynamic evaluation of high power linear Electrical Actuators with primary emphasis on Thrust Vector Control actuators. Details of the mechanical design, power and control systems, and data acquisition capability of the test facility are presented. A test procedure for evaluating the performance of the ELA Test Facility is also included.

Author

N95-18597# Advisory Group for Aerospace Research and Development, Neuilly-Sur-Seine (France). Structures and Materials Panel.
AIRCRAFT LOADS DUE TO TURBULENCE AND THEIR IMPACT ON DESIGN AND CERTIFICATION [EFFORTS AVION DUS A LA TURBULENCE ATMOSPHERIQUE ET LEURS IMPACTS SUR LA CONCEPTION ET LA CERTIFICATION]

Dec. 1994 93 p In ENGLISH and FRENCH Workshop held in Lillehammer, Norway, 5 May 1994

(AGARD-R-798; ISBN-92-836-0002-9) Copyright Avail: CASI HC A05/MF A01

The AGARD Structures and Materials Panel has always been heavily involved in the field of the effects of atmospheric disturbances on the behavior of aircraft. The Panel organized a Workshop on the theme 'Aircraft Loads due to Turbulence and their Impact on Design and Certification'. This Workshop was held on 5 May 1994. This document reproduces the papers presented. For individual titles, see N95-18598 through N95-18605.

N95-18598# British Aerospace Airbus Ltd., Bristol (England).
THE IMPACT OF NON-LINEAR FLIGHT CONTROL SYSTEMS ON THE PREDICTION OF AIRCRAFT LOADS DUE TO TURBULENCE

R. M. WARMAN In AGARD, Aircraft Loads due to Turbulence and their Impact on Design and Certification 8 p Dec. 1994

Copyright Avail: CASI HC A02/MF A01

During the past ten years the extensive use of electronic flight control systems has introduced a high level of non-linearity, to the behavior of civil transport aircraft, in response to both pilot inputs and external influences such as turbulence. These systems that control, protect, and, in some instances, alleviate the loads experienced by the aircraft have had a significant impact on the prediction of aircraft loads. There is an increasing need both to model control system non-linearity to avoid designing control systems that degrade structural performance, and to demonstrate the effectiveness of alleviation systems for

aircraft certification. The introduction of non-linear flight control systems presents little problem when using time-based simulations to predict aircraft loads due to discrete gusts. Frequency domain, Power-Spectral Density (PSD), analysis used to predict aircraft loads due to Continuous Turbulence (CT), however, is severely restrictive, requiring a linear mathematical model of both the aircraft and control systems. Over the past ten-to-fifteen years various analysis techniques have been developed that provide time-based interpretations of the CT atmosphere and, therefore, means by which loads due to CT can be predicted for aircraft with non-linear flight control systems. Recent involvement in the design of Airbus aircraft has led to British Aerospace Airbus Limited taking an active role in both developing and using these non-linear analysis techniques. By drawing on experience gained during the design of recent Airbus aircraft, the impact of non-linear flight control systems on the prediction of aircraft loads due to turbulence is discussed.

Author

N95-18600# Deutsche Airbus G.m.b.H., Hamburg (Germany). Structural Dynamics.

TREATMENT OF NON-LINEAR SYSTEMS BY TIMEPLANE-TRANSFORMED CT METHODS: THE SPECTRAL GUST METHOD

H. LUSEBRINK and J. BRINK-SPALINK In AGARD, Aircraft Loads due to Turbulence and their Impact on Design and Certification 8 p Dec. 1994

Copyright Avail: CASI HC A02/MF A01

The present paper discusses the problems which occur when PSD/Continuous Turbulence (C.T.) gust methods, originally developed for linear dynamic gust analysis in the frequency plane, are applied to modern transport A/C with flight control systems, containing a variety of nonlinearities for signal shaping. Power spectral density (PSD) gust velocity intensities are defined by the von Karman power spectrum in the frequency plane, scaled by the design gust intensity $U(\text{sub } \sigma)$ (RMS). This definition of gust in the frequency plane causes the basic problems for nonlinear dynamic analysis, in contrary to the timeplane defined Tuned Discrete Gusts. Discrete Gust calculations show that aircraft nonlinearities cannot be neglected. To treat nonlinearities for C.T. there are basically three approaches (apart from linearization methods): (1) (SSB) Stochastic Simulation Based Methods (timeplane stochastic simulation), usually in combination with exceedance rate based design load definition; (2) (MFB) Matched Filter Based Methods ('Worst Case Gusts'): for each load station, a search within a class of shape functions of prescribed 'spectral energy' is necessary to find that shape giving the highest load; and (3) (SG) Spectral Gust Method: uses discrete gusts having exactly the von Karman spectrum, and computes the energy norm of the loadtime history. A practical method for nonlinear C.T. method should have the following characteristics: give loads consistent to existing requirements (for linear aircraft); give correlated (balanced) loads; and be straight-forward and economical, when applied for a large number of design cases to be calculated. Since the SSB methods need long simulation times and give no balanced loads (together with exceedance rate counting), and the MFB methods are very expensive, the present paper proposes the SG method. It needs only one step to derive design loads, is consistent to Design Envelope Analysis and provides correlated loads.

Author

N95-18641# Wright Lab., Wright-Patterson AFB, OH.
PRESSURE MEASUREMENTS ON AN F/A-18 TWIN VERTICAL TAIL IN BUFFETING FLOW. VOLUME 4, PART 2: BUFFET CROSS SPECTRAL DENSITIES Final Report, 15 Apr. 1993 - 15 Aug. 1994

CHRIS PETTIT, MICHAEL BANFORD, DANSEN BROWN, and ED PENDLETON Aug. 1994 693 p See also AD-A279126, AD-A281581 and AD-A281444

(Contract(s)/Grant(s): AF PROJ. 2401)

(AD-A285555; WL-TM-94-3132-VOL-4-PT-2) Avail: CASI HC A99/MF A06

Buffeting pressure measurements were made on the vertical tail surface of a full scale F/A-18 aircraft model in the National Full Scale Aerodynamics Complex at NASA Ames Research Center. Test vari-

ables included angle-of-attack, aircraft sideslip angle, and dynamic pressure. Accelerometers were used to obtain vertical tail accelerations. Pressure transducers were mounted on the starboard vertical tail. Steady and unsteady pressures were obtained. Unsteady pressure data were reduced to PSD and CSD forms. Both steady and unsteady RMS pressure coefficients are also presented. Volume 1 contains the general description of the model, the test program, and highlights of the reduced data. Volume 2 contains steady and unsteady RMS data. Volume 3 contains unsteady PSD results. Volume 4 contains unsteady CSD results. DTIC

N95-18902 Stanford Univ., CA.
DESIGN AND FLIGHT TEST OF A SIMPLIFIED CONTROL SYSTEM FOR A TRANSPORT HELICOPTER Ph.D. Thesis
 CHRISTOPHER REECE PURVIS 1994 230 p
 Avail: Univ. Microfilms Order No. DA9414640

Helicopter transport pilots must give priority to aircraft control tasks when flying in a high-workload cockpit. To test a control system that would enhance safety and expedite pilot training in high-workload cockpits, the investigator test flew on the NASA CH-47 variable-stability helicopter a command-and-hold control system that required only constant inputs by the pilot to generate ramp responses in groundspeed, heading, and altitude. If undelayed, these ramp responses are ideal for simplified control, but in practice each controlled output, particularly groundspeed, experiences a distracting time lag. This distraction can be eliminated by presenting the integral of the pilot's output-rate commands on a cockpit display. Distractions caused by overshoots in pitch and roll following each command change are minimized by employing the dynamic feedforward of asymptotic model following (AMF), which generates in real time attitude commands correct to fly a constant velocity rate. Tailored to be well-damped, these feedforward attitude commands are particular solutions, or forced responses, that can be tracked asymptotically by a stabilized aircraft. In the baseline control logic these attitude commands were tightly tracked using the stabilization of the linear quadratic regulator. Because the attitude feedback is relatively noise free and not subject to drop-outs, tight tracking of attitude instead of velocity commands not only minimizes the control distraction of pitch and roll overshoots but also minimizes feedback noise on the aircraft controls. After the pilot releases his controls, the distraction of having to monitor and correct the groundspeed response during velocity-hold flight is removed through use of integral-error feedback on the controlled outputs. Turns were coordinated by gain-scheduling the lateral-directional compensation. Turn coordination was also evaluated using an alternative design that employed nonlinear cancellation compensation in translation. During flight the groundspeed, heading, and altitude for both the baseline and alternative designs tracked their particular solutions with small errors, and both designs achieved satisfactory handling qualities in pitch. Handling only one control at a time and using simple, pulse-like inputs, the pilot was able to change and hold groundspeed, heading, and altitude. The two designs were exercised using various maneuvers; among these were longitudinal dash/quickstops, lateral sidesteps, bobups, pedal turns, coordinated slalom turns, and a climbing/descending 180 degree course reversal. Dissert. Abstr.

N95-19029* National Aeronautics and Space Administration. Ames Research Center, Moffett Field, CA.
NASA DEVELOPS NEW DIGITAL FLIGHT CONTROL SYSTEM
 MICHAEL MEWHINNEY 12 Dec. 1994 2 p
 (NASA-NEWS-RELEASE-94-47) Avail: CASI HC A04

This news release reports on the development and testing of a new integrated flight and propulsion automated control system that aerospace engineers at NASA's Ames Research Center have been working on. The system is being tested in the V/STOL (Vertical/hort Takeoff and Landing) Systems Research Aircraft (VSRA). CASI

RESEARCH AND SUPPORT FACILITIES (AIR)

Includes airports, hangars and runways; aircraft repair and overhaul facilities; wind tunnels; shock tube facilities; and engine test blocks.

N95-16258# Nanjing Univ. of Aeronautics and Astronautics, Nanjing, Jiangsu (China). Dept. of Aerodynamics.
AN INVESTIGATION OF POLYNOMIAL CALIBRATIONS METHODS FOR WIND TUNNEL BALANCES
 BUZHANG HAN and INGMAR JOHNSON *In its* Joint Proceedings on Aeronautics and Astronautics (JPAA) p 63-66 May 1993
 Avail: CASI HC A01/MF A03

For wind tunnel balance calibration the factorial method is used in Sweden, whereas the orthogonal method is used in China. This report is a comparison between calibration results of these two methods, by using a certain six component wind tunnel balance in the MK6 calibrating rig at FFA Sweden. Author

N95-16318# Arnold Engineering Development Center, Arnold AFS, TN.

A MODEL FOR PRELIMINARY FACILITY DESIGN INCLUDING SIMULATION ISSUES

E. S. POWELL *In* JHU, The 1993 JANNAF Propulsion Meeting, Volume 1 p 261-274 Nov. 1993
 Avail: CPIA, 10630 Little Patuxent Pkwy., Suite 202, Columbia, MD 21044-3200 HC

A new procedure has been developed to aid in the preliminary design of aerodynamic simulation facilities using instream combustion as an energy source. The aerothermodynamic parameters necessary to address the issue of simulation are calculated for each simulation point considered. The new procedure uses the desired simulation conditions as input. Those conditions and the equations for the conservation of mass, momentum, energy, entropy, and the thermally perfect equation of state are used to determine facility flow rates, pressures, and nozzle expansion ratio. Accepted procedures are used to calculate the test medium thermodynamic and transport properties. Simplifying assumptions and engineering approximations have been made where they do not adversely affect accuracy of the predictions. The new procedure is easy to use and is accurate when compared to an accepted equilibrium expansion code. The new procedure requires minimal computational resources. A facility to test a hypersonic propulsion system will be used as an example. Author

N95-16319# Arnold Engineering Development Center, Arnold AFS, TN.

HYPersonic AIR-BREATHING AEROPROPULSION FACILITY TEST SUPPORT REQUIREMENTS

BRIAN WETTLAUFER *In* JHU, The 1993 JANNAF Propulsion Meeting, Volume 1 p 275-292 Nov. 1993
 Avail: CPIA, 10630 Little Patuxent Pkwy., Suite 202, Columbia, MD 21044-3200 HC

The ground testing of hypersonic propulsion systems presents some interesting issues and challenges for today's facilities. The current concepts of hypersonic propulsion systems for vehicles indicate that they will be highly integrated with the airframe and use vehicle forebody and afterbody surfaces for compression and expansion surfaces. The trade studies indicate that these propulsion systems will be large devices and will probably use cryogenic fuels for engine and airframe active cooling. This makes the operational characteristics and performance of the engine highly dependent on the thermal loads on the engine and the vehicle. Test articles used for development testing in a ground test facility will also be very large because they must include or simulate the complete thermal cycle of the propulsion device, and the kinetics of the combustion process are not scalable. The ground test facilities to support development

testing on hypersonic propulsion systems must be capable of providing the proper test conditions, be of adequate size, and provide ample testing durations to accommodate thermal stabilization of large test articles. Current propulsion ground test facilities with near-term enhancements are capable of supporting full-size propulsion test articles to Mach 3.8 and small propulsion test articles or component test rigs to about Mach 7 true temperature and pressure conditions. This paper will review the hypersonic ground test requirements for the development of hypersonic air-breathing propulsion systems. It will review the direct-connect and freejet testing approach using reference planes, the facility configurations, as well as their capabilities and shortfalls. Facility adequacy will be evaluated and future needs will be assessed. Author

N95-16320* General Applied Science Labs., Inc., Ronkonkoma, NY.

FREE-JET TESTING AT MACH 3.44 IN GASL'S AERO/THERMO TEST FACILITY

D. CRESCI, S. KOONTZ, and C. Y. TSAI *In* JHU, The 1993 JANNAF Propulsion Meeting, Volume 1 p 293-307 Nov. 1993 (Contract(s)/Grant(s): NAS1-18450) Avail: CPIA, 10630 Little Patuxent Pkwy., Suite 202, Columbia, MD 21044-3200 HC

A supersonic blow-down tunnel has been used to conduct tests of a hydrogen burning ramjet engine at simulated Mach 3.44 conditions. A pebble-bed type storage heater, a free standing test cabin, and a 48 foot diameter vacuum sphere are used to simulate the flight conditions at nearly matched enthalpy and dynamic pressure. A two dimensional nozzle with a nominal 13.26 inch square exit provides a free-jet test environment. The facility used for these tests is described as are the results of a flow calibration performed on the M = 3.44 nozzle. Some facility/model interactions are discussed as are the eventual hardware modifications and operational procedures required to alleviate the interactions. Some engine test results are discussed briefly to document the success of the test program. Author

N95-16509# Sandia National Labs., Albuquerque, NM. ERROR PROPAGATION EQUATIONS FOR ESTIMATING THE UNCERTAINTY IN HIGH-SPEED WIND TUNNEL TEST RESULTS

E. L. CLARK 1994 22 p Presented at the 18th American Institute of Aeronautics and Astronautics (AIAA) Aerospace Ground Test Conference, Colorado Springs, CO, 20-23 Jun. 1994 (Contract(s)/Grant(s): DE-AC04-94AL-85000) (DE94-014136; SAND-93-0208C; CONF-9406188-1) Avail: CASI HC A03/MF A01

Error propagation equations, based on the Taylor series model, are derived for the nondimensional ratios and coefficients most often encountered in high-speed wind tunnel testing. These include pressure ratio and coefficient, static force and moment coefficients, dynamic stability coefficients, and calibration Mach number. The error equations contain partial derivatives, denoted as sensitivity coefficients, which define the influence of free-stream Mach number, M sub infinity, on various aerodynamic ratios. To facilitate use of the error equations, sensitivity coefficients are derived and evaluated for five fundamental aerodynamic ratios which relate free-stream test conditions to a reference condition. DOE

N95-17388# Advisory Group for Aerospace Research and Development, Neuilly-Sur-Seine (France). Flight Mechanics Panel. AIRCRAFT AND SUB-SYSTEM CERTIFICATION BY PILOTED SIMULATION [HOMOLOGATION DES AERONEFS ET DE LEURS SOUS-SYSTEMES PAR LA SIMULATION PILOTEE] Sep. 1994 53 p (AGARD-AR-278; ISBN-92-835-0757-6) Copyright Avail: CASI HC A04/MF A01

There is a steadily increasing tendency to use piloted flight simulators for official clearance of selected areas of flight envelopes and of system behavior or malfunctions. This is a natural and desirable

evolution from the wide use of simulation during the development of new aircraft. However, there is a lack of guidance for certification authorities and aircraft manufacturers on simulation standards, validation procedures and general information on the advantages and disadvantages of using simulation as part of a clearance program. This could lead to either inappropriate use of simulators, or unnecessary (and costly) reluctance to use simulation when it is appropriate. In particular, there is concern by many involved with research and engineering development simulators that subjective pilot opinion is often the primary criterion for acceptance of simulators for certification activities. However, clearance demonstrations on a simulator will not usually be experienced in flight until an operational pilot encounters the conditions or configurations of the clearance. Thus validation of the simulator for clearance tasks must involve rigorous model and simulation system validation as well as pilot subjective tests. Subjective adjustments are unacceptable. Working Group 16 was formed by the Flight Mechanics Panel of AGARD to produce an Advisory Report on this subject. The aim was to provide advice and guidance to Certification and Acceptance Authorities, and Aircraft Manufacturers on the appropriate use of piloted simulation as the sole demonstration for aircraft and system flight clearances. The Group included members from Canada, Germany, Italy, Netherlands, United Kingdom and the United States. Government R&D Establishments, Armed Service R&D Establishments, and aircraft and simulator manufacturers were all represented. Author

N95-17444 Air Force Inst. of Tech., Wright-Patterson AFB, OH. School of Engineering.

DEVELOPMENT OF AN AUTOMATED AIRFIELD DYNAMIC CONE PENETROMETER (AADCP) PROTOTYPE AND THE EVALUATION OF UNSURFACED AIRFIELD SEISMIC SURVEYING USING SPECTRAL ANALYSIS OF SURFACE WAVES (SASW) TECHNOLOGY M.S. Thesis

DAVID WEINTRAUB Dec. 1993 327 p Limited Reproducibility: More than 20% of this document may be affected by microfiche quality (AD-A281985; AFIT/CI/CIA-94-013D) Avail: Issuing Activity (Defense Technical Information Center (DTIC))

The mission of U.S. Air Force Combat Controllers is to infiltrate unused airfields. A specially trained evaluation team, carrying limited portable testing equipment, evaluates the unsurfaced airfield for use as a landing zone. The equipment used to evaluate the bearing capacity of the airfield is the Dynamic Cone Penetrator (DCP). Empirically based relationships are used to predict the type and number of aircraft passes on the unsurfaced airfield based on inputs from the DCP. It was the goal of this research to improve on the field testing equipment used in the unsurfaced airfield evaluation process. DTIC

N95-18054*# National Aeronautics and Space Administration. Lewis Research Center, Cleveland, OH.

BACKGROUND NOISE LEVELS MEASURED IN THE NASA LEWIS 9- BY 15-FOOT LOW-SPEED WIND TUNNEL

RICHARD P. WOODWARD, JAMES H. DITTMAR, DAVID G. HALL (NYMA, Inc., Brook Park, OH.), and BONNIE KEE-BOWLING Dec. 1994 17 p Presented at the 33d Aerospace Sciences Meeting and Exhibit, Reno, NV, 9-12 Jan. 1995; sponsored by AIAA (Contract(s)/Grant(s): NAS3-27186; RTOP 538-03-11) (NASA-TM-106817; E-9356; NAS 1.15:106817; AIAA PAPER 95-0720) Copyright Avail: CASI HC A03/MF A01

The acoustic capability of the NASA Lewis 9 by 15 Foot Low Speed Wind Tunnel has been significantly improved by reducing the background noise levels measured by in-flow microphones. This was accomplished by incorporating streamlined microphone holders having a profile developed by researchers at the NASA Ames Research Center. These new holders were fabricated for fixed mounting on the tunnel wall and for an axially traversing microphone probe which was mounted to the tunnel floor. Measured in-flow noise levels in the tunnel test section were reduced by about 10 dB with the new microphone holders compared with those measured with the older, less refined

09 RESEARCH AND SUPPORT FACILITIES (AIR)

microphone holders. Wake interference patterns between fixed wall microphones were measured and resulted in preferred placement patterns for these microphones to minimize these effects. Acoustic data from a model turbofan operating in the tunnel test section showed that results for the fixed and translating microphones were equivalent for common azimuthal angles, suggesting that the translating microphone probe, with its significantly greater angular resolution, is preferred for sideline noise measurements. Fixed microphones can provide a local check on the traversing microphone data quality, and record acoustic performance at other azimuthal angles. Author

N95-18087# Federal Aviation Administration, Atlanta, GA.
EVALUATION OF AN UNLIGHTED SWINGING AIRPORT SIGN
ERIC S. KATZ Aug. 1994 13 p
(AD-A284763; DOT/FAA/CT-TN94/29) Avail: CASI HC A03/MF A01

An unlighted swinging airport sign was evaluated at the Federal Aviation Administration Technical Center. The purpose of the evaluation was to determine the readability of the sign under varying wind and jet blast conditions. Results indicate that the sign is readable under all of the test conditions except when subjected to wind speeds of approximately 35 to 40 knots with gusts produced by the additive effect of the ambient winds and the jet blast. Even under this condition, readability of the sign remained adequate except at the most extreme angular displacement. DTIC

N95-18405 Naval Air Warfare Center, Patuxent River, MD. Aircraft Div.

COMPARISON OF FREQUENCY RESPONSE AND PERTURBATION METHODS TO EXTRACT LINEAR MODELS FROM A NONLINEAR SIMULATION

KEITH A. BALDERSON and JEFFREY T. WEATHERS 1994 14 p
Limited Reproducibility: More than 20% of this document may be affected by microfiche quality
(AD-A284115) Avail: CASI HC A03

The purpose of this paper is to compare two distinct methods to extract a linear state-space model about a reference flight condition from a nonlinear simulation. The frequency response method uses a time history input which contains the frequencies of interest to drive the simulation. The frequency response method uses a time history input which contains the frequencies of interest to drive the simulation frequency input and the output of the simulation are transformed to the frequency domain, and the desired frequency responses of the simulation are calculated. A linear model is then fit to the frequency responses using system identification techniques. The perturbation method extracts a linear model by perturbing the model states and inputs from the reference flight condition and calculating the resulting model coefficients. Both methods were used to extract a fourth order longitudinal state-space model from the V-22 full nonlinear simulation. The time history responses and system matrices of the extracted model were compared. The comparison showed that both methods are effective means to reduce a nonlinear simulation to a linear state-space model. DTIC

N95-18586*# National Aeronautics and Space Administration. Lewis Research Center, Cleveland, OH.

USERS GUIDE FOR NASA LEWIS RESEARCH CENTER DC-9 REDUCED-GRAVITY AIRCRAFT PROGRAM

JOHN S. YANIEC Jan. 1995 78 p
(Contract(s)/Grant(s): RTOP 694-03-0C)
(NASA-TM-106755; E-9175; NAS 1.15:106755) Avail: CASI HC A05/MF A01

The document provides guidelines and information for users of the DC-9 Reduced-Gravity Aircraft Program. It describes the facilities, requirements for test personnel, equipment design and installation, mission preparation, and in-flight procedures. Those who have used the KC-135 reduced-gravity aircraft will recognize that many of the procedures and guidelines are the same, to ensure a commonality between the DC-9 and KC-135 programs. Author

N95-18724 Naval Air Warfare Center, Patuxent River, MD. Aircraft Div.

THE GENERIC SIMULATION EXECUTIVE AT MANNED FLIGHT SIMULATOR

JAMES NICHOLS 1994 9 p Limited Reproducibility: More than 20% of this document may be affected by microfiche quality
(AD-A283997) Avail: Issuing Activity (Defense Technical Information Center (DTIC))

The Manned Flight Simulator (MFS) at the Naval Air Warfare Center Aircraft Division (formerly the Naval Air Test Center) was created to provide rapid response to a wide range of US Navy simulation requirements. The necessity to simulate any aircraft in the US Navy inventory stimulated the idea of creating 'roll-in, roll-out' simulation bays that would accept any cockpit having standard geometric and electrical interfaces. The capability to use any cockpit at any simulation bay in turn led to the need for a flexible and generic software package for simulating any airframe. The Controls Analysis and Test Loop Environment (CASTLE) executive allows the user to easily generate and operate an aircraft simulation, while also providing a very powerful set of tools for simulation development and engineering analysis. Although the CASTLE package was originally designed to operate on Digital Equipment Corporation (DEC) machines using the VMS operating system and DEC screen management software, recent developments include a MOTIF-based window interface environment and compatibility with the UNIX operating system. The CASTLE package is being proposed as a starting point for a standard airframe simulation package to satisfy US Navy requirements. DTIC

N95-18725 Naval Air Warfare Center, Patuxent River, MD. Aircraft Div.

HELICOPTER IN-FLIGHT SIMULATION DEVELOPMENT AND USE IN TEST PILOT TRAINING

R. V. MILLER and L. A. KHINOO 1994 15 p Limited Reproducibility: More than 20% of this document may be affected by microfiche quality
(AD-A283998) Avail: CASI HC A03

The U.S. Naval Test Pilot School (USNTPS) trains pilots, flight officers and engineers in the technical and managerial skills necessary to conduct aircraft and airborne systems test and evaluation. An integral part of this training is the use of ground and in-flight simulators to demonstrate the effects of varying aircraft flying qualities parameters. The USNTPS has developed specialized simulation facilities to meet the unique training requirements. This paper describes the development of a Variable Stability and Control (VSC) system installed in an SH-60B helicopter as a specialized training aid for use at the USNTPS. The development of the VSC system is traced from requirements through syllabus introduction. DTIC

N95-18903 Georgia Inst. of Tech., Atlanta, GA.

A LINEAR SYSTEM IDENTIFICATION AND VALIDATION OF AN AH-64 APACHE AEROELASTIC SIMULATION MODEL Ph.D. Thesis

SELWYN HOWARD STURISKY 1993 269 p
Avail: Univ. Microfilms Order No. DA9415668

This study addresses a linear math model validation of a global, nonlinear real-time rotary wing flight simulator at hover and 130 knots. The simulation is the AH-64 attack helicopter with a rotor blade element model. The main rotor dynamics have been formulated to provide a consistent matching between structural and aerodynamic theory. The structural model is a representation of the flexible blade based on a priori mode shape data. The dynamic inflow model is an adaptation of the Peters/He theory. Frequency response testing of the simulation model permits an evaluation of the mid to high frequency range. The Comprehensive Identification from Frequency Responses (CIFER) program is used to (1) extract a complete set of nonparametric input-to-output frequency responses that fully characterize the coupled helicopter dynamics, and (2) conduct a nonlinear search for a state space model that matches the frequency response data set. CIFER is used to extract state space

stability derivative models from both flight test data and simulator generated responses. These linear models are compared with the vehicle response in both the frequency domain and in the time domain to confirm predictive capabilities to dissimilar input forms. The hover results obtained showed that a high fidelity identification of the state space linear models was achieved. Both linear models proved an excellent match with the frequency response set and demonstrated excellent predictive capabilities. The six-DOF model fit was significantly improved by inclusion of the higher order rotor terms. The effects of these higher order terms were most apparent on the pitch rate, roll rate, and collective response of the aircraft. The forward flight data set was not as high quality as the hover data set and low signal to noise ratios hindered the identification process. Nevertheless, it was possible to identify a six-DOF model that matched the aircraft frequency response set quite closely. Of extreme significance is confirmation that the FLIGHTLAB solution technique used to model the Apache correctly predicts the off-axis response of the aircraft. The methodology described herein explores a new approach to the rotorcraft system identification problem, simplifying the selection of model parameters to be changed and aiding in determining an adequate model form and structure.

Dissert. Abstr.

N95-19150# Industrieranlagen-Betriebsgesellschaft m.b.H., Ottobrunn (Germany).

DESIGN AND OPERATION OF A THERMOACOUSTIC TEST FACILITY

G. BAYERDOERFER and L. FREYBERG *In* AGARD, Impact of Acoustic Loads on Aircraft Structures 5 p Sep. 1994 Sponsored in cooperation with BMFT and the Deutsche Agentur fuer Raumfahrtangelegenheiten G.m.b.H., Bonn, Germany Copyright Avail: CASI HC A01/MF A03

Aerothermal environments as encountered during the missions of reusable spacecraft, hypersonic vehicles, advanced launchers, etc. are the major design driver for an advanced Thermal Protection System (TPS) technology. In developing such materials and structures ground testing under simulated operational conditions is of eminent importance. In order to meet these requirements IABG has designed a thermoacoustic facility which was recently put into operation. The facility is able to produce surface temperatures up to 1300 C and sound pressure levels up to 160 dB. The design approach and operational aspects from test work performed so far are described.

Author

N95-19267# Naples Univ. (Italy). Inst. di Aerodinamica.

ADAPTIVE WIND TUNNEL WALLS VERSUS WALL INTERFERENCE CORRECTION METHODS IN 2D FLOWS AT HIGH BLOCKAGE RATIOS

G. P. RUSSO, G. ZUPPARDI, and M. BASCIANI *In* AGARD, Wall Interference, Support Interference and Flow Field Measurements 12 p Jul. 1994 Sponsored by Ministry of University and Scientific and Technological Research Copyright Avail: CASI HC A03/MF A04

The aim of the present work is to compare the effectiveness of adaptive-wall approach with the capabilities of WIAC (wall interference assessment and correction) methods in reducing wall interference effects in wind tunnel testing. Tests have been made in the 20 cm x 20 cm subsonic Adaptive Walls Wind Tunnel in Naples. Three different models having a chord of 100 mm, 150 mm and 200 mm have been used. The corresponding blockage ratios at $\alpha = 0$ degrees are 6 percent, 9 percent and 12 percent, respectively. Results of the tests show that wall adaptation and measured boundary condition WIAC methods are equivalent in correcting wall interference at moderate angles of incidence and/or with medium size models (i.e. at moderate blockage ratios). Furthermore adaptive walls wind tunnels can give data correctable with a WIAC method also at very large blockage ratios as high as 4 times the blockage ratio used in conventional wind tunnels.

Author

N95-19269# City Univ., London (England). Center for Aeronautics. **INTERFERENCE DETERMINATION FOR WIND TUNNELS WITH SLOTTED WALLS**

M. M. FREESTONE and S. R. MOHAN *In* AGARD, Wall Interference, Support Interference and Flow Field Measurements 12 p Jul. 1994 Sponsored by Dept. of Trade and Industry Copyright Avail: CASI HC A03/MF A04

The effectiveness of a 'two-variable' scheme, for evaluating wall interference with slotted liners installed, is assessed. Test data from transonic wind tunnel tests with a two-dimensional model geometry are utilized. In these tests untypically high levels of wall interference are produced. In the first tests, solid wall liners were used, in order to establish a standard. Selected results from two further series of tests, in which slotted roof and floor liners were fitted, are then presented and analyzed. In the first of these, divergent liners were used, and it was found that the slot flows generated large disturbances in the wall shear region, causing the normal velocity of the equivalent inviscid flow to be amplified in relation to the normal velocity in the slot. An allowance therefore had to be made in the proposed interference scheme to account for this amplification. With convergent wall liners, large disturbances were avoided, and no such allowance was needed. Implications of the investigation for tests in large slotted liner wind tunnels are discussed.

Author

N95-19271# McDonnell-Douglas Aerospace, Saint Louis, MO.

TRANSONIC WIND TUNNEL BOUNDARY INTERFERENCE CORRECTION

M. L. RUEGER, R. C. CRITES, R. F. WEIRICH, F. CREASMAN, R. K. AGARWAL, and J. E. DEESE *In* AGARD, Wall Interference, Support Interference and Flow Field Measurements 14 p Jul. 1994 Copyright Avail: CASI HC A03/MF A04

A continuous effort in the area of transonic boundary interference correction has been underway at McDonnell Douglas Aerospace for over 6 years. A method of interference correction based on force and moment increments computed from CFD solutions was proposed in 1986. An extensive validation database has been acquired of transonic wind tunnel data for a set of geometrically similar models of different sizes. An empirical model of the flow at a porous transonic wind tunnel wall has been used in conjunction with panel codes and Euler solvers to yield corrections at a variety of conditions in both the MDA Polysonic Wind Tunnel (PSWT) and the MDA Trisonic Wind Tunnel (TWT).

Author

N95-19272# British Columbia Univ., Vancouver (British Columbia). Dept. of Mechanical Engineering.

UNSTEADY FLOW TESTING IN A PASSIVE LOW-CORRECTION WIND TUNNEL

L. KONG and G. V. PARKINSON *In* AGARD, Wall Interference, Support Interference and Flow Field Measurements 7 p Jul. 1994 Sponsored by Natural Sciences and Engineering Research Council Copyright Avail: CASI HC A02/MF A04

A passive low-correction wind tunnel designed for two-dimensional testing has a test section consisting of transverse airfoil-slatted side walls separating it from outer plenum chambers. The uniform spacing of the airfoil slats determines the open-area ratio (OAR). The tests described were on two sizes of NACA 0015 airfoil in plunging oscillation, and instantaneous pressure distributions were measured for different values of airfoil reduced amplitude and frequency, and over a full range of tunnel OAR. It was found that, despite the relatively large sizes of test airfoil, values of pressure, lift, and moment coefficient close to theoretical free-air values were obtained for 0.6 less than OAR less than 0.8, whereas values were much too high in the presence of solid walls and much too low in open-jet testing. Test Reynolds numbers were in the range $(2.5-8.0) \times 10^6$ (exp 5).

Author

09 RESEARCH AND SUPPORT FACILITIES (AIR)

N95-19286* National Aeronautics and Space Administration. Lewis Research Center, Cleveland, OH.

OPERATING CAPABILITY AND CURRENT STATUS OF THE REACTIVATED NASA LEWIS RESEARCH CENTER HYPERSONIC TUNNEL FACILITY

SCOTT R. THOMAS, CHARLES J. TREFNY, and WILLIAM D. PACK
Jan. 1995 13 p Presented at the 6th International Aerospace Planes and Hypersonics Technologies Conference, Chattanooga, TN, 3-7 Apr. 1995; sponsored by AIAA

(Contract(s)/Grant(s): RTOP 505-70-62)

(NASA-TM-106808; E-9294; NAS 1.15:106808; AIAA PAPER 95-6146) Copyright Avail: CASI HC A03/MF A01

The NASA Lewis Research Center's Hypersonic Tunnel Facility (HTF) is a free-jet, blowdown propulsion test facility that can simulate up to Mach-7 flight conditions with true air composition. Mach-5, -6, and -7 nozzles, each with a 42 inch exit diameter, are available. Previously obtained calibration data indicate that the test flow uniformity of the HTF is good. The facility, without modifications, can accommodate models approximately 10 feet long. The test gas is heated using a graphite core induction heater that generates a nonvitiated flow. The combination of clean-air, large-scale, and Mach-7 capabilities is unique to the HTF and enables an accurate propulsion performance determination. The reactivation of the HTF, in progress since 1990, includes refurbishing the graphite heater, the steam generation plant, the gaseous oxygen system, and all control systems. All systems were checked out and recertified, and environmental systems were upgraded to meet current standards. The data systems were also upgraded to current standards and a communication link with NASA-wide computers was added. In May 1994, the reactivation was complete, and an integrated systems test was conducted to verify facility operability. This paper describes the reactivation, the facility status, the operating capabilities, and specific applications of the HTF.

Author

10

ASTRONAUTICS

Includes astronautics (general); astrodynamics; ground support systems and facilities (space); launch vehicles and space vehicles; space transportation; spacecraft communications, command and tracking; spacecraft design, testing and performance; spacecraft instrumentation; and spacecraft propulsion and power.

A95-63640

ULTIMATE CHARACTERISTICS OF A ROCKET ENGINE WITH A TURBO-PUMP SUPPLY SYSTEM

S. V. KOMEL' NPO Energomash, Moscow (Russia) and A. A. SERGIENKO Izvestiya VUZ: Aviatsionnaya Tekhnika (ISSN 0579-2975) no. 1 January-March 1994 p. 34-38 In RUSSIAN (BTN-94-EIX94461408757) Copyright

A liquid-propellant rocket engine of the closed cycle is considered. In this case, one-stage combustion of all fuel ahead of the turbine is meant. It has been shown that the gas temperature in the blades of the turbine rotor can be reduced. The efficiency of this system is estimated by calculation methods. The parameters of the system are compared with the existing systems RD-0120, RD-170, and SSME and space shuttle. The numerical experiments have demonstrated that in the boundary layer the significant changes of the composition and temperature of combustion products take place.

EI

N95-16312# Johns Hopkins Univ., Columbia, MD. Chemical Propulsion Information Agency.

THE 1993 JANNAF PROPULSION MEETING, VOLUME 1

DEBRA S. EGGLESTON, ed. Nov. 1993 464 p Meeting held in Monterey, CA, 15-19 Nov. 1993; sponsored by the Joint NASA,

Army, Navy, Air Force Interagency Committee

(Contract(s)/Grant(s): N00014-91-C-0001)

(CPIA-PUBL-602-VOL-1) Avail: CPIA, 10630 Little Patuxent Pkwy., Suite 202, Columbia, MD 21044-3200 HC

This volume, the first of six volumes, is a collection of 34 unclassified/unlimited distribution papers which were presented at the 1993 Joint Army-Navy-NASA-Air Force (JANNAF) Propulsion Meeting, held 15-19 November 1993 at the Hyatt Regency Hotel and Conference Center and the Naval Postgraduate School in Monterey, California. Specific subjects discussed include the following: (1) propellant liners; (2) bondlines; (3) booster motors; (4) motor case manufacturing; (5) hazard and sensitivity assessment; (6) divert propulsion; (7) insensitive munitions; (8) scramjets; (9) tubojets; (10) free-jet testing; (11) large caliber guns; and (12) LOVA propellants. For individual titles, see N95-16313 through N95-16323.

N95-16316# Delavan, Inc., West Des Moines, IA.

THERMAL CHEMICAL ENERGY OF ABLATING SILICA SURFACES IN AIR BREATHING SOLID ROCKET ENGINES

M.S. Thesis - George Washington Univ.

MICHAEL D. CORNWELL In JHU, The 1993 JANNAF Propulsion Meeting, Volume 1 p 237-245 Nov. 1993

Avail: CPIA, 10630 Little Patuxent Pkwy., Suite 202, Columbia, MD 21044-3200 HC

This paper provides theoretical adaptation and extension of current industry methodologies for analytical predictions of insulation ablation in solid fuel ramjets. Solid fuel ramjets predominantly operate in a fuel-lean state and require thermal protection systems that are highly oxidation resistant, such as insulation materials that form silica-based char. However, local regions of fuel rich gases exist in ramjets where mixing and combustion of fuel and air is incomplete. Modeling corrosion of silica based char in fuel rich regions of the combustor requires new methods. Accurate ablation prediction of these fuel rich regions are in the design of ramjets. Current analytical methods used to model the ablation of insulation are most suitable for oxidative corrosion of carbonaceous insulation char. Silica-based insulation will ablate corrosively by reduction reactions with carbon and carbon based fuels. Silica ablation by carbon reduction reactions with silica is not correctly modeled by the current industry code, ACE. This paper describes the causes of the current limitations and provides extensions to the ACE methodology to allow for the modeling of silica ablation.

Author

N95-16321# Applied Thermal Sciences, Orono, ME.

COMBUSTOR KINETIC ENERGY EFFICIENCY ANALYSIS OF THE HYPERSONIC RESEARCH ENGINE DATA

K. V. HOOSE In JHU, The 1993 JANNAF Propulsion Meeting, Volume 1 p 309-317 Nov. 1993

Avail: CPIA, 10630 Little Patuxent Pkwy., Suite 202, Columbia, MD 21044-3200 HC

A one-dimensional method for measuring combustor performance is needed to facilitate design and development scramjet engines. A one-dimensional kinetic energy efficiency method is used for measuring inlet and nozzle performance. The objective of this investigation was to assess the use of kinetic energy efficiency as an indicator for scramjet combustor performance. A combustor kinetic energy efficiency analysis was performed on the Hypersonic Research Engine (HRE) data. The HRE data was chosen for this analysis due to its thorough documentation and availability. The combustor, inlet, and nozzle kinetic energy efficiency values were utilized to determine an overall engine kinetic energy efficiency. Finally, a kinetic energy effectiveness method was developed to eliminate thermochemical losses from the combustion of fuel and air. All calculated values exhibit consistency over the flight speed range. Effects from fuel injection, altitude, angle of attack, subsonic-supersonic combustion transition, and inlet spike position are shown and discussed. The results of analyzing the HRE data indicate that the kinetic energy efficiency method is effective as a measure of scramjet combustor performance.

Author

N95-16333# Hercules Aerospace Co., Magna, UT. Bacchus Works. **RECENT ADVANCES IN GRAPHITE/EPOXY MOTOR CASES** WILLIAM G. WILSON, PAUL E. CHRISTENSEN, and JAMES L. YORK *In* JHU, The 1993 JANNAF Propulsion Meeting, Volume 2 p 115-123 Nov. 1993
Avail: CASI HC A02/MF A04

Much has been published concerning improvements and enhancements in materials and technology used in the design and construction of solid rocket motors. However, there are important aspects of the improvement process that are seldom discussed, particularly process control and continuous improvement. This has been applied successfully to the resolution of challenges, which remained at the termination of the Filament Wound Case (FWC) Program. The FWC Program for the Space Shuttle boosters was terminated in 1986. At that time, although the FWC met all requirements, there were issues with composites that needed improvement. This paper discusses the success in resolving those challenges and describes how the continuous improvement methodologies were implemented at Hercules for design and fabrication of graphite/epoxy motor cases. Advancements in materials and engineering data are first evaluated. The implementation of an approach that includes concurrent engineering, process controls, statistical process controls, continuous improvement, and product acceptance are then discussed. The successes in recent years have been realized from application of these principles. Discrepancies have been reduced by an order of magnitude. Delaminations have been virtually eliminated. Voids have been reduced to 'hardly detectable.' Enhancements in manufacturing technology and cost reductions have also been realized. The application of process control and continuous improvement principles has resulted in 100 percent flight performance success while simultaneously achieving improved vehicle performance. Author

N95-16352# National Academy of Sciences - National Research Council, Washington, DC. Commission on Engineering and Technical Systems. **ASSESSMENT OF THE SPACE STATION PROGRAM** JACK L. KERREBROCK (Massachusetts Inst. of Tech., Cambridge.) 27 Jun. 1994 6 p
Avail: CASI HC A02/MF A01

This letter report by the National Research Council's (NRC's) Aeronautics and Space Engineering Board addresses comments on NASA's response to the Board's 1993 letter report, NASA's response to technical and management recommendations from previous NRC technical reports on the Space Station, and an assessment of the current International Space Station Alpha (ISSA) program. CASI

N95-16776# Krug Life Sciences, Inc., Houston, TX. **A SURGICAL SUPPORT SYSTEM FOR SPACE STATION FREEDOM Abstract Only** M. R. CAMPBELL, R. D. BILLICA, and S. L. JOHNSTON *In* Aerospace Medical Association, Aerospace Medical Association 63rd Annual Scientific Meeting Program 1 p 14 May 1992 Sponsored by NASA. Lyndon B. Johnson Space Center, Houston, TX
Avail: CASI HC A01/MF A02

Surgical techniques in microgravity are being developed for the Health Maintenance Facility (HMF) on Space Station Freedom (SSF). This will be a presentation of the proposed surgical capabilities and ongoing hardware and procedural investigations. Methods: Procedures and prototype hardware, which include a medical restraint system, a surgical overhead isolation canopy, a suction device, and a regional laminar flow device were evaluated. This was accomplished by realistic sterile surgical simulations involving both mannequins and animals during KC-135 parabolic flight and in a high fidelity ground based HMF mockup. Results: Animal surgery in the environment of microgravity allowed the observation of unique arterial and venous bleeding characteristics for the first time. The ability to control bleeding and to prevent cabin atmosphere contamination was also demonstrated. Conclusions: The procedures and

prototype hardware tested provided valuable information and should be investigated and developed further. The use of standard surgical techniques are possible in microgravity if the principles of personnel and supply restraint and operative field containment are adhered to. Author

N95-17248*# European Space Agency. European Space Operations Center, Darmstadt (Germany). **SAFETY ASPECTS OF SPACECRAFT COMMANDING** N. PECCIA *In* NASA. Goddard Space Flight Center, Third International Symposium on Space Mission Operations and Ground Data Systems, Part 1 p 599-605 Nov. 1994
Avail: CASI HC A02/MF A06

The commanding of spacecraft is a potentially hazardous activity for the safety of the spacecraft. Present day control systems contain safety features in their commanding subsystem and in addition, strict procedures are also followed by operations staff. However, problems have occurred on a number of missions as a result of erroneous commanding leading in some cases to spacecraft contingencies and even to near loss of the spacecraft. The problems of checking commands in advance are increased by the tendency in modern spacecraft to use blocked/time-tagged commands and the increased usage of on-board computers, for which commands changing on-board software tables can radically change spacecraft or subsystem behavior. This paper reports on an ongoing study. The study aims to improve the approach to safety of spacecraft commanding. It will show how ensuring 'safe' commanding can be carried out more efficiently, and with greater reliability, with the help of knowledge based systems and/or fast simulators. The whole concept will be developed based on the Object-Oriented approach. Author

N95-17252*# European Space Agency. European Space Operations Center, Darmstadt (Germany). **EURECA MISSION CONTROL EXPERIENCE AND MESSAGES FOR THE FUTURE** H. HUEBNER, P. FERRI, and W. WIMMER *In* NASA. Goddard Space Flight Center, Third International Symposium on Space Mission Operations and Ground Data Systems, Part 1 p 633-640 Nov. 1994
Avail: CASI HC A02/MF A06

EURECA is a retrievable space platform which can perform multi-disciplinary scientific and technological experiments in a Low Earth Orbit for a typical mission duration of six to twelve months. It is deployed and retrieved by the NASA Space Shuttle and is designed to support up to five flights. The first mission started at the end of July 1992 and was successfully completed with the retrieval in June 1993. The operations concept and the ground segment for the first EURECA mission are briefly introduced. The experiences in the preparation and the conduction of the mission from the flight control team point of view are described. Author

N95-17278# Advisory Group for Aerospace Research and Development, Neuilly-Sur-Seine (France). Propulsion and Energetics Panel. **EXPERIMENTAL AND ANALYTICAL METHODS FOR THE DETERMINATION OF CONNECTED-PIPE RAMJET AND DUCTED ROCKET INTERNAL PERFORMANCE [METHODES EXPERIMENTALES ET ANALYTIQUES POUR LA DETERMINATION EN CONDUITE FORCEE DES PERFORMANCES DES STATOREACTEURS ET DES STATOFUSEES]** Jul. 1994 103 p (AGARD-AR-323; ISBN-92-835-0755-X) Copyright Avail: CASI HC A06/MF A02

Connected-pipe, subsonic combustion ramjet and ducted rocket performance determination procedures used by the NATO countries have been reviewed and evaluated. A working document has been produced which provides recommended methods for reporting test results and delineates the parameters that are required to be measured. Explanations and detailed numerical examples are presented covering the determination of both theoretical and experi-

10 ASTRONAUTICS

mental performances, the use of air heaters and uncertainty and error analysis. Author

N95-17493* California Univ., Los Angeles, CA. Dept. of Mechanical, Aerospace and Nuclear Engineering.

DEMONSTRATION OF THE DYNAMIC FLOWGRAPH METHODOLOGY USING THE TITAN 2 SPACE LAUNCH VEHICLE DIGITAL FLIGHT CONTROL SYSTEM

M. YAU, S. GUARRO, and G. APOSTOLAKIS Jun. 1993 102 p (Contract(s)/Grant(s): NCC2-374; NAG5-1440) (NASA-CR-197517; NAS 1.26:197517; UCLA ENG-93-43) Avail: CASI HC A06/MF A02

Dynamic Flowgraph Methodology (DFM) is a new approach developed to integrate the modeling and analysis of the hardware and software components of an embedded system. The objective is to complement the traditional approaches which generally follow the philosophy of separating out the hardware and software portions of the assurance analysis. In this paper, the DFM approach is demonstrated using the Titan 2 Space Launch Vehicle Digital Flight Control System. The hardware and software portions of this embedded system are modeled in an integrated framework. In addition, the time dependent behavior and the switching logic can be captured by this DFM model. In the modeling process, it is found that constructing decision tables for software subroutines is very time consuming. A possible solution is suggested. This approach makes use of a well-known numerical method, the Newton-Raphson method, to solve the equations implemented in the subroutines in reverse. Conversion can be achieved in a few steps. Author

N95-17596* European Space Agency. European Space Operations Center, Darmstadt (Germany).

PACKET UTILISATION DEFINITIONS FOR THE ESA XMM MISSION

H. R. NYE In NASA. Goddard Space Flight Center, Third International Symposium on Space Mission Operations and Ground Data Systems, Part 2 p 1235-1242 Nov. 1994 Avail: CASI HC A02/MF A06

XMM, ESA's X-Ray Multi-Mirror satellite, due for launch at the end of 1999 will be the first ESA scientific spacecraft to implement the ESA packet telecommand and telemetry standards and will be the first ESOC-controlled science mission to take advantage of the new flight control system infrastructure development (based on object-oriented design and distributed-system architecture) due for deployment in 1995. The implementation of the packet standards is well defined at packet transport level. However, the standard relevant to the application level (the ESA Packet Utilization Standard) covers a wide range of on-board 'services' applicable in varying degrees to the needs of XMM. In defining which parts of the ESA PUS to implement, the XMM project first considered the mission objectives and the derived operations concept and went on to identify a minimum set of packet definitions compatible with these aspects. This paper sets the scene as above and then describes the services needed for XMM and the telecommand and telemetry packet types necessary to support each service. Author

N95-18196* Lockheed Sanders, Inc., Nashua, NH. Engineering Div.

NEW TECHNOLOGIES FOR SPACE AVIONICS Final Report, 1994

DAVID W. AIBEL, PETER DINGUS, MARK LANCAULT, DEBRA HURDLEBRINK, INNA GUREVICH, and LYDIA WENGLAR Dec. 1994 85 p

(Contract(s)/Grant(s): NAS9-18873) (NASA-CR-197574; NAS 1.26:197574) Avail: CASI HC A05/MF A01

This report reviews a 1994 effort that continued 1993 investigations into issues associated with the definition of requirements, with the practice concurrent engineering and rapid prototyping in the context of the development of a prototyping of a next-generation

reaction jet driver controller. This report discusses lessons learned, the testing of the current prototype, the details of the current design, and the nature and performance of a mathematical model of the life cycle of a pilot operated valve solenoid. Author

N95-18720# Instituto de Pesquisas Espaciais, Sao Paulo (Brazil). **REGENERATIVE COOLING FOR LIQUID PROPELLANT ROCKET THRUST CHAMBERS M.S. Thesis [REFRIGERACAO REGENERATIVA PARA CAMARAS DE EMPUXO DE MOTORES FOGUETE A PROPELENTES LIQUIDOS]** RAFAEL LEVY RUBIN Apr. 1994 121 p In PORTUGUESE (INPE-5565-TDI/540) Avail: CASI HC A06/MF A02

This work describes a calculation model for regeneratively cooled rocket thrust chambers. A computational program, based on a one-dimensional coolant pressure drop in the cooling channels. Radiation is included in the model. The channels have rectangular cross sections, the dimensions being determined during the calculations in order to maintain the wall temperature distributions at tolerable levels, with a minimum channel pressure drop. Several wall materials were investigated, as well as the employment of the hydrocarbon fuels JP-4 and JP-5 and Aerozine 50 as coolants. The influence of many design parameters on the cooling system performance is verified for the analysis of the system capabilities and limitations. Author

N95-18743* Praxair, Inc., Tonawanda, NY. **AIRBORNE ROTARY SEPARATOR STUDY Final Report** R. F. DRNEVICH and J. J. NOWOBILSKI Dec. 1992 141 p (Contract(s)/Grant(s): NAS3-25560) (NASA-CR-191045; E-9387; NAS 1.26:191045) Avail: CASI HC A07/MF A02

Several air breathing propulsion concepts for future earth-to-orbit transport vehicles utilize air collection and enrichment, and subsequent storage of liquid oxygen for later use in the vehicle mission. Work performed during the 1960's established the feasibility of substantially reducing weight and volume of a distillation type air separator system by operating the distillation elements in high 'g' fields obtained by rotating the separator assembly. The purpose of this study was to evaluate various fuels and fuel combinations with the objective of minimizing the weight and increase the ready alert capability of the plane. Fuels will be used to provide energy as well as act as heat sinks for the on-board heat rejection system. Fuel energy was used to provide power for air separation as well as to produce refrigeration for liquefaction of oxygen enriched air, besides its primary purpose of vehicle propulsion. The heat generated in the cycle was rejected to the fuel and water which is also carried on board the vehicle. The fuels that were evaluated include JP4, methane, and hydrogen. Hydrogen served as a comparison to the JP4 and methane cases. Author (revised)

N95-18993* State Univ. of New York, Oneonta, NY. Dept. of Physics and Astronomy.

A CMC DATABASE FOR USE IN THE NEXT GENERATION LAUNCH VEHICLES (ROCKETS)

KAMALA MAHANTA In Alabama Univ., Research Reports: 1994 NASA/ASEE Summer Faculty Fellowship Program 6 p Oct. 1994 Avail: CASI HC A02/MF A03

Ceramic matrix composites (CMC's) are being envisioned as the state-of-the-art material capable of handling the tough structural and thermal demands of advanced high temperature structures for programs such as the SSTO (Single Stage to Orbit), HSCT (High Speed Civil Transport), etc. as well as for evolution of the industrial heating systems. Particulate, whisker and continuous fiber ceramic matrix (CFCC) composites have been designed to provide fracture toughness to the advanced ceramic materials which have a high degree of wear resistance, hardness, stiffness, and heat and corrosion resistance but are notorious for their brittleness and sensitivity to microscopic flaws such as cracks, voids and impurity. Author

N95-19073 Department of the Navy, Washington, DC.
INTEGRATED AERODYNAMIC FIN AND STOWABLE TVC VANE SYSTEM Patent
 ARNOLD O. DANIELSON, inventor (to Navy) 16 Jun. 1994 11 p Filed 15 Mar. 1991
 (AD-D016457; US-PATENT-5,320,304; US-PATENT-APPL-SN-666104; US-PATENT-CLASS-244-3.22) Avail: US Patent and Trade-mark Office

An aerodynamic fin and stowable jet vane system preferably for rocket motor missile applications to control roll, pitch, and yaw, in either the aerodynamic or thrust flight control conditions, has a retractable and stowable aerodynamic vane integrated with a stowable aerodynamic vane integrated with a stowable thrust vector reaction steering system on a common support. The integrated aerodynamic fins and thrust vector control reduce the overall missile mainframe dimensions and are mounted on a single, space saving support.

DTIC

N95-19237* National Aeronautics and Space Administration. Lyndon B. Johnson Space Center, Houston, TX.
DOCUMENTATION AND ARCHIVING OF THE SPACE SHUTTLE WIND TUNNEL TEST DATA BASE. VOLUME 1: BACKGROUND AND DESCRIPTION
 PAUL O. ROMERE and STEVE WESLEY BROWN (Lockheed Engineering and Sciences Co., Houston, TX.) Jan. 1995 191 p (NASA-TM-104806-VOL-1; 9-786-VOL-1; NAS 1.15:104806-VOL-1) Avail: CASI HC A09/MF A02

Development of the space shuttle necessitated an extensive wind tunnel test program, with the cooperation of all the major wind tunnels in the United States. The result was approximately 100,000 hours of space shuttle wind tunnel testing conducted for aerodynamics, heat transfer, and structural dynamics. The test results were converted into Chrysler DATAMAN computer program format to facilitate use by analysts, a very cost effective method of collecting the wind tunnel test results from many test facilities into one centralized location. This report provides final documentation of the space shuttle wind tunnel program. The two-volume set covers evolution of space shuttle aerodynamic configurations and gives wind tunnel test data, titles of wind tunnel data reports, sample data sets, and instructions for accessing the digital data base. Author

11

CHEMISTRY AND MATERIALS

Includes chemistry and materials (general); composite materials; inorganic and physical chemistry; metallic materials; nonmetallic materials; and propellants and fuels.

N95-16256# Kazan Aviation Inst. (USSR).
SERVICE AND PHYSICAL PROPERTIES OF LIQUID-JET FUELS
 V. I. SKOMOROKHOV and A. F. DREGALIN In Nanjing Univ. of Aeronautics and Astronautics, Joint Proceedings on Aeronautics and Astronautics (JPAA) p 48-52 May 1993
 Avail: CASI HC A01/MF A03

In the present paper we discuss a relation between the service physical properties of liquid composite aircraft and rocket fuels. We give also calculation methods of physical fuel mixture properties, on the net-component basis. Author

N95-16371# DACCO SCI, Inc., Columbia, MD.
THE USE OF ELECTROCHEMISTRY AND ELLIPSOMETRY FOR IDENTIFYING AND EVALUATING CORROSION ON AIRCRAFT Annual Report
 CHESTER M. DACRES 14 Sep. 1994 2 p

(Contract(s)/Grant(s): F49620-94-C-0042)
 (AD-A285323; AFOSR-94-0640TR) Avail: CASI HC A01/MF A01
 Electrochemical corrosion testing using AC Impedance measurements, ellipsometry and X-Ray Photoelectron Spectroscopy (XPS) is progressing according to the Plan of Action and Milestones (POAM) submitted in July, 1994. The development of the corrosion sensor is on schedule and the feasibility study shows that the proposal to build the sensor is technically sound. A detailed report dated August 15, 1994 was presented to the Program Manager explaining the theory of the AC Impedance, ellipsometry and XPS. The report also explained what the physical concept of the corrosion monitor is, and how it will respond to the various stages of corrosion. The preliminary data presented in the report showed the 'signature' of the initial stages of corroding aircraft structures. DTIC

N95-16859* Analytical Services and Materials, Inc., Hampton, VA.
COMPOSITE CHRONICLES: A STUDY OF THE LESSONS LEARNED IN THE DEVELOPMENT, PRODUCTION, AND SERVICE OF COMPOSITE STRUCTURES Final Report
 LOUIS F. VOSTEEN and RICHARD N. HADCOCK (RNH Associates, Huntington, NY.) NASA Nov. 1994 59 p
 (Contract(s)/Grant(s): NAS1-19317; RTOP 510-02-13-01) (NASA-CR-4620; NAS 1.26:4620) Avail: CASI HC A04/MF A01

A study of past composite aircraft structures programs was conducted to determine the lessons learned during the programs. The study focused on finding major underlying principles and practices that experience showed have significant effects on the development process and should be recognized and understood by those responsible for using of composites. Published information on programs was reviewed and interviews were conducted with personnel associated with current and past major development programs. In all, interviews were conducted with about 56 people representing 32 organizations. Most of the people interviewed have been involved in the engineering and manufacturing development of composites for the past 20 to 25 years. Although composites technology has made great advances over the past 30 years, the effective application of composites to aircraft is still a complex problem that requires experienced personnel with special knowledge. All disciplines involved in the development process must work together in real time to minimize risk and assure total product quality and performance at acceptable costs. The most successful programs have made effective use of integrated, collocated, concurrent engineering teams, and most often used well-planned, systematic development efforts wherein the design and manufacturing processes are validated in a step-by-step or 'building block' approach. Such approaches reduce program risk and are cost effective. Author

N95-16860* Analytical Services and Materials, Inc., Hampton, VA.
MULTI-LAB COMPARISON ON R-CURVE METHODOLOGIES: ALLOY 2024-T3 Final Report
 ANTHONY P. REYNOLDS Oct. 1994 41 p
 (Contract(s)/Grant(s): NAS1-19708; RTOP 537-06-20-06) (NASA-CR-195004; NAS 1.26:195004) Avail: CASI HC A03/MF A01

In an effort to determine an optimum method for ranking the fracture toughness of developmental aluminum alloys for High Speed Civil Transport applications, five labs performed K and/or J based fracture tests on aluminum alloy 2024-T3. Two material thicknesses were examined: 0.063 in. and 0.125 in. Middle crack tension and compact tension specimens were excised from 60 in. wide middle crack tension panels which had been previously tested at Boeing. The crack resistance curves generated were compared to the R-curves from 60 in. wide specimens. The experimental program indicated that effective stress intensity from secant compliance based crack length and stress intensity calculated from J-integral testing were equivalent. In addition, comparison of different specimen sizes and configurations indicated that standard validity requirements for compact tension specimens may be overly restrictive. Author

11 CHEMISTRY AND MATERIALS

N95-16905*# National Aeronautics and Space Administration. Lewis Research Center, Cleveland, OH.

STATIC AND DYNAMIC FRICTION BEHAVIOR OF CANDIDATE HIGH TEMPERATURE AIRFRAME SEAL MATERIALS

C. DELLACORTE, V. LUKASZEWICZ (Calspan Corp., Fairview Park, OH.), D. E. MORRIS (Rockwell International Corp., Canoga Park, CA.), and B. M. STEINETZ Dec. 1994 20 p
(Contract(s)/Grant(s): NAS3-25685; RTOP 505-63-1A)
(NASA-TM-106571; E-8774; NAS 1.15:106571) Avail: CASI HC A03/MF A01

The following report describes a series of research tests to evaluate candidate high temperature materials for static to moderately dynamic hypersonic airframe seals. Pin-on-disk reciprocating sliding tests were conducted from 25 to 843 C in air and hydrogen containing inert atmospheres. Friction, both dynamic and static, was monitored and serves as the primary test measurement. In general, soft coatings lead to excessive static friction and temperature affected friction in air environments only. Author

N95-18068# Pratt and Whitney Aircraft, West Palm Beach, FL. Government Engines and Space Propulsion.

FATIGUE IN SINGLE CRYSTAL NICKEL SUPERALLOYS

Progress Report, 16 Oct. 1993 - 15 Oct. 1994
DANIEL P. DELUCA and CHARLES ANNIS 15 Oct. 1994 33 p
(Contract(s)/Grant(s): N00014-91-C-0124)
(AD-A285727) Avail: CASI HC A03/MF A01

This program investigates the seemingly unusual behavior of single crystal airfoil materials. The fatigue initiation processes in single crystal (SC) materials are significantly more complicated and involved than fatigue initiation and subsequent behavior of a (single) macrocrack in conventional, isotropic, materials. To understand these differences is the major goal of this project. DTIC

N95-18410 Princeton Univ., NJ. Dept. of Mechanical and Aerospace Engineering.

STUDIES ON HIGH PRESSURE AND UNSTEADY FLAME PHENOMENA Annual Report, 15 Apr. 1993 - 14 Apr. 1994

C. K. LAW 20 Jun. 1994 55 p Limited Reproducibility: More than 20% of this document may be affected by microfiche quality
(Contract(s)/Grant(s): F49620-92-J-0227)
(AD-A284126; AFOSR-94-0501TR) Avail: Issuing Activity (Defense Technical Information Center (DTIC))

The objective of the present program is to study the structure and response of steady and unsteady laminar premixed and nonpremixed flames in reduced and elevated pressure environments through: (1) non-intrusive experimentation; (2) computational simulation using detailed flame and kinetic codes; and (3) asymptotic analysis with reduced kinetic mechanisms. During the reporting period progress has been made in the following projects: (1) a theoretical and experimental study of unsteady diffusion flames; (2) a computational and experimental study of hydrogen/air diffusion flames at sub- and super-atmospheric pressures; (3) an asymptotic analysis of the structure of premixed flames with volumetric heat loss; (4) asymptotic analyses of ignition in the supersonic hydrogen/air mixing layer with reduced mechanisms; (5) a new numerical algorithm for generating the ignition-extinction S-curves. A total of three reprints are appended. DTIC

N95-19008*# State Univ. of New York, Farmingdale, NY. Mfg. and Mechanical Research Div.

QUALITY OPTIMIZATION OF THERMALLY SPRAYED COATINGS PRODUCED BY THE JP-5000 (HVOF) GUN USING MATHEMATICAL MODELING

HAZEM TAWFIK In Alabama Univ., Research Reports: 1994 NASA/ASEE Summer Faculty Fellowship Program 9 p Oct. 1994
Avail: CASI HC A02/MF A03

Currently, thermal barrier coatings (TBC) of gas-turbine blades and similar applications have centered around the use of zirconia as a protective coating for high thermal applications. The advantages of zirconia include low thermal conductivity and good thermal shock

resistance. Thermally sprayed tungsten carbide hardface coatings are used for a wide range of applications spanning both the aerospace and other industrial markets. Major aircraft engine manufacturers and repair facilities use hardface coatings for original engine manufacture (OEM), as well as in the overhaul of critical engine components. The principle function of these coatings is to resist severe wear environments for such wear mechanisms as abrasion, adhesion, fretting, and erosion. The (JP-5000) thermal spray gun is the most advanced in the High Velocity Oxygen Fuel (HVOF) systems. Recently, it has received considerable attention because of its relative low cost and its production of quality coatings that challenge the very successful but yet very expensive Vacuum Plasma Spraying (VPS) system. The quality of thermal spray coatings is enhanced as porosity, oxidation, residual stress, and surface roughness are reduced or minimized. Higher densification, interfacial bonding strength, hardness and wear resistance of coating are desirable features for quality improvement.

Derived from text

N95-19090 Department of the Navy, Washington, DC.

SOLID FUEL RAMJET COMPOSITION Patent

GEORGE W. BURDETTE, inventor (to Navy) and GARY W. MEYERS, inventor (to Navy) 14 Jun. 1994 3 p Filed 25 Nov. 1981
(AD-D016458; US-PATENT-5,320,692; US-PATENT-APPL-SN-329621; US-PATENT-CLASS-149-19.9) Avail: US Patent and Trademark Office

A ramjet solid fuel composed of Hydroxyl terminated polybutadiene aluminum, magnesium, and boron carbide is described. The high volumetric heating value fuel of the present invention significantly increases the distance range of missiles. DTIC

N95-19100# Sandia National Labs., Albuquerque, NM.

EVALUATION OF SCANNERS FOR C-SCAN IMAGING IN NONDESTRUCTIVE INSPECTION OF AIRCRAFT

J. H. GIESKE Apr. 1994 60 p
(Contract(s)/Grant(s): DE-AC04-94AL-85000)
(DE94-012473; SAND-94-0945) Avail: CASI HC A04/MF A01

The goal of this project was to produce a document that contains information on the usability and performance of commercially available, fieldable, and portable scanner systems as they apply to aircraft NDI inspections. In particular, the scanners are used to generate images of eddy current, ultrasonic, or bond tester inspection data. The scanner designs include manual scanners, semi-automated scanners, and fully automated scanners. A brief description of the functionality of each scanner type, a sketch, and a list of the companies that support the particular design are provided. Vendors of each scanner type provided hands-on demonstrations of their equipment on real aircraft samples in the FAA Aging Aircraft Nondestructive Inspection Validation Center (AANC) in Albuquerque, NM. From evaluations recorded during the demonstrations, a matrix of scanner features and factors and ranking of the capabilities and limitations of the design, portability, articulation, performance, usability, and computer hardware/software was constructed to provide a quick reference for comparing the different scanner types. Illustrations of C-scan images obtained during the demonstration are shown. DOE

N95-19482*# Alcoa Technical Center, Alcoa Center, PA.

AN ARTIFICIAL CORROSION PROTOCOL FOR LAP-SPLICES IN AIRCRAFT SKIN

BEVIL J. SHAW In NASA. Langley Research Center, FAA/NASA International Symposium on Advanced Structural Integrity Methods for Airframe Durability and Damage Tolerance, Part 2 p 725-739 Sep. 1994 Sponsored in part by Boeing Co.
(Contract(s)/Grant(s): F34601-90-C-1336)
Avail: CASI HC A03/MF A04

This paper reviews the progress to date to formulate an artificial corrosion protocol for the Tinker AFB C/KC-135 Corrosion Fatigue Round Robin Test Program. The project has provided new test methods to faithfully reproduce the corrosion damage within a lap-

splice by accelerated means, the rationale for a new laboratory test environment, and a means for corrosion damage quantification. The approach is pragmatic and the resulting artificial corrosion protocol lays the foundation for future research in the assessment of aerospace alloys. The general means for quantification of corrosion damage has been presented in a form which can be directly applied to structural integrity calculations. Author

N95-19490* Cornell Univ., Ithaca, NY. Dept. of Theoretical and Applied Mechanics.

FATIGUE CRACK GROWTH IN 2024-T3 ALUMINUM UNDER TENSILE AND TRANSVERSE SHEAR STRESSES

MARK J. VIZ and ALAN T. ZEHNDER *In* NASA. Langley Research Center, FAA/NASA International Symposium on Advanced Structural Integrity Methods for Airframe Durability and Damage Tolerance, Part 2 p 891-910 Sep. 1994

(Contract(s)/Grant(s): NAG1-1311)

Avail: CASI HC A03/MF A04

The influence of transverse shear stresses on the fatigue crack growth rate in thin 2024-T3 aluminum alloy sheets is investigated experimentally. The tests are performed on double-edge cracked sheets in cyclic tensile and torsional loading. This loading generates crack tip stress intensity factors in the same ratio as the values computed for a crack lying along a lap joint in a pressurized aircraft fuselage. The relevant fracture mechanics of cracks in thin plates along with the details of the geometrically nonlinear finite element analyses used for the test specimen calibration are developed and discussed. Preliminary fatigue crack growth data correlated using the fully coupled stress intensity factor calibration are presented and compared with fatigue crack growth data from pure delta K(sub I) fatigue tests. Author

12

ENGINEERING

Includes engineering (general); communications; electronics and electrical engineering; fluid mechanics and heat transfer; instrumentation and photography; lasers and masers; mechanical engineering; quality assurance and reliability; and structural mechanics.

A95-63201* National Aeronautics and Space Administration. Langley Research Center, Hampton, VA.

A GRID GENERATION AND FLOW SOLUTION METHOD FOR THE EULER EQUATIONS ON UNSTRUCTURED GRIDS

W. KYLE ANDERSON NASA. Langley Research Center, Hampton, VA, US *Journal of Computational Physics* (ISSN 0021-9991) vol. 110, no. 1 January 1994 p. 23-38

(HTN-95-20003) Copyright

A grid generation and flow solution algorithm for the Euler equations on unstructured grids is presented. The grid generation scheme utilizes Delaunay triangulation and self-generates the field points for the mesh based on cell aspect ratios and allows for clustering near solid surfaces. The flow solution method is an implicit algorithm in which the linear set of equations arising at each time step is solved using a Gauss Seidel procedure which is completely vectorizable. In addition, a study is conducted to examine the number of subiterations required for good convergence of the overall algorithm. Grid generation results are shown in two dimensions for a National Advisory Committee for Aeronautics (NACA) 0012 airfoil as well as a two-element configuration. Flow solution results are shown for two-dimensional flow over the NACA 0012 airfoil and for a two-element configuration in which the solution has been obtained through an adaptation procedure and compared to an exact solution. Preliminary three-dimensional results are also shown in which subsonic flow over a business jet is computed. Author (Hemer)

A95-63638

GAS-TURBINE ENGINES WITH INCREASED EFFICIENCY OF TWO CIRCUITS, DUE TO THE USE OF THE UTILIZING STEAM-TURBINE CIRCUIT

O. N. EMIN Moskovskij Aviatsionnyj Inst, Moscow, Russia and V. I. KUZNETSOV *Izvestiya VUZ: Aviatsionnaya Tekhnika* (ISSN 0579-2975) no. 1 January-March 1994 p. 27-29 In RUSSIAN (BTN-94-EIX94461408755) Copyright

The possibility of significantly increasing the efficiency of the two circuits of a turbojet engine is justified. It is assumed that for this purpose the power of an additional steam turbine will be used, when utilizing heat of exhaust gases in the internal circuit of the gas-turbine engine. The main equations describing the working process have been derived. The parameters of the steam-turbine circuit have been assessed. Calculations for an engine with a thrust of 45-50 t for an aircraft, accommodating 500-800 persons, have been made. EI

A95-63648

A STATIONARY FLOW OF A VISCOUS LIQUID IN RADIAL CLEARANCES OF ROTOR BEARINGS IN THE TURBOCOMPRESSOR OF AN INTERNAL COMBUSTION ENGINE

V. G. ZHARINOV KG TU, Kazan (Russia) *Izvestiya VUZ: Aviatsionnaya Tekhnika* (ISSN 0579-2975) no. 1 January-March 1994 p. 72-76 In RUSSIAN refs (BTN-94-EIX94461408765) Copyright

Both stationary and floating rotating bushes are used in bearings of turbo-compressors applied in systems for supercharging internal combustion engines. The paper investigates the effect of geometric parameters on the work of bearings with a floating bush. Also, the distribution of friction losses in lubricant layers of bearings with floating bushes is studied. The solution of the problem concerning the stationary flow of a viscous liquid in radial clearances of plain bearings with rotating bushes has been presented. EI

A95-63652

NEW APPROACH TO GEOMETRIC PROFILING OF THE DESIGN ELEMENTS OF THE PASSAGE PART IN TURBO-MACHINES

I. V. AFANAS'EV NPO Saturn, Moscow (Russia) and I. L. OSIPOV *Izvestiya VUZ: Aviatsionnaya Tekhnika* (ISSN 0579-2975) no. 1 January-March 1994 p. 87-91 In RUSSIAN refs (BTN-94-EIX94461408769) Copyright

In designing highly economical up-to-date aviation turbo-machines, specific requirements for structural elements, contacting a working medium, should be met. For this purpose, at the preliminary design stage, some support points of the contours of pieces are calculated. Further, a corresponding function discreetly specified is interpolated. The paper suggests to use multiplications of the well known functions to construct curves, forming passage parts of turbo-machines. In this case, curves are continuously twice differentiated. EI

A95-64524

ON THE DYNAMICS OF AEROELASTIC OSCILLATORS WITH ONE DEGREE OF FREEDOM

T. I. HAAKER Delft Univ. of Technology, Delft (Netherlands) and A. H. P. VANDERBURGH *SIAM Journal on Applied Mathematics* (ISSN 0036-1399) vol. 54, no. 4 August 1994 p. 1033-1047 refs (BTN-94-EIX94501431527) Copyright

In this paper two aeroelastic oscillators in crossflow with one degree of freedom are considered. The first oscillator is a special mass-spring system that is able to oscillate in crossflow, that is perpendicular to the direction of a one-dimensional uniform flowing medium. The second oscillator is a seesaw-type oscillator in crossflow. The geometry of the oscillators is such that for both oscillators an axis of symmetry can be defined. The interesting difference between the two oscillators is the

12 ENGINEERING

difference between the dynamical behaviour of this axis. For the first oscillator the slope of the axis of symmetry with the horizontal plane does not change with time, whereas for the seesaw-type oscillator this slope is time-dependent. By using a quasi-steady theory as model equations, a Lienard equation and a generalized Lienard equation are obtained. For the first equation a global analysis is presented, and for the second equation a local analysis is presented resulting in conditions for the existence and uniqueness of limit cycles. Author (EI)

A95-65345 DEVELOPMENT AND APPLICATION OF THE DOUBLE V TYPE FLAME STABILIZER

HONGBIN ZHANG Beijing Aeronautical Technology Research Centre, Beijing (China) and JIGEN WANG Tuijin Jishu/Journal of Propulsion Technology (ISSN 1001-4055) no. 3 June 1994 p. 38-43 In CHINESE refs (BTN-94-EIX94481415355) Copyright

The double V type flame stabilizer is an advanced stabilizer of low drag constructed with a big V type stabilizer overlapping to a small V type one. It has the advantages of good ignition performance, low drag loss, improved afterburning efficiency, low skin temperature, and leaner blowout boundary, hence the overall performance of turbojet engine will be improved and the flight reliability increased. More than 40 tests on stand rig, 10 tests in aircraft and 8 tests in flight were carried out for its birth, and thereafter, it started to be in service for the turbojet engine on a small batch scale in 1986-1987. Author (revised by EI)

N95-16048*# Naval Research Lab., Washington, DC.
PROBLEMS WITH AGING WIRING IN NAVAL AIRCRAFT
FRANK J. CAMPBELL NASA. Lewis Research Center, First NASA Workshop on Wiring for Space Applications p 61-71 Sep. 1994 Avail: CASI HC A03/MF A02

The Navy is experiencing a severe aircraft electrical wiring maintenance problem as a result of the extensive use of an aromatic polyimide insulation that is deteriorating at a rate that was unexpected when this wire was initially selected. This problem has significantly affected readiness, reliability, and safety and has greatly increased the cost of ownership of Naval aircraft. Failures in wire harnesses have exhibited arcing and burning that will propagate drastically, to the interruption of many electrical circuits from a fault initiated by the failure of deteriorating wires. There is an urgent need for a capability to schedule aircraft rewiring in an orderly manner with a logically derived determination of which aircraft have aged to the point of absolute necessity. Excessive maintenance was demonstrated to result from the accelerated aging due to the parameters of moisture, temperature, and strain that exist in the Naval Aircraft environment. Laboratory studies have demonstrated that MIL-W-81381 wire insulation when aged at high humidities followed the classical Arrhenius thermal aging relationship. In an extension of the project a multifactor formula was developed that is now capable of predicting life under varying conditions of these service parameters. An automated test system has also been developed to analyze the degree of deterioration that has occurred in wires taken from an aircraft in order to obtain an assessment of remaining life. Since it is both physically and financially impossible to replace the wiring in all the Navy's aircraft at once, this system will permit expedient scheduling so that those aircraft that are most probable to have wiring failure problems can be overhauled first. Author

N95-16072*# Applied Research Associates, Inc., Raleigh, NC.
PORTABLE PARALLEL STOCHASTIC OPTIMIZATION FOR
THE DESIGN OF AEROPROPULSION COMPONENTS Final
Report
ROBERT H. SUES and G. S. RHODES Cleveland, OH NASA Oct. 1994 62 p Original contains color illustrations (Contract(s)/Grant(s): NAS3-26839; RTOP 324-01-00) (NASA-CR-195312; E-8725; NAS 1.26:195312) Avail: CASI HC A04/

MF A01; 2 functional color pages

This report presents the results of Phase 1 research to develop a methodology for performing large-scale Multi-disciplinary Stochastic Optimization (MSO) for the design of aerospace systems ranging from aeropropulsion components to complete aircraft configurations. The current research recognizes that such design optimization problems are computationally expensive, and require the use of either massively parallel or multiple-processor computers. The methodology also recognizes that many operational and performance parameters are uncertain, and that uncertainty must be considered explicitly to achieve optimum performance and cost. The objective of this Phase 1 research was to initialize the development of an MSO methodology that is portable to a wide variety of hardware platforms, while achieving efficient, large-scale parallelism when multiple processors are available. The first effort in the project was a literature review of available computer hardware, as well as review of portable, parallel programming environments. The first effort was to implement the MSO methodology for a problem using the portable parallel programming language, Parallel Virtual Machine (PVM). The third and final effort was to demonstrate the example on a variety of computers, including a distributed-memory multiprocessor, a distributed-memory network of workstations, and a single-processor workstation. Results indicate the MSO methodology can be well-applied towards large-scale aerospace design problems. Nearly perfect linear speedup was demonstrated for computation of optimization sensitivity coefficients on both a 128-node distributed-memory multiprocessor (the Intel iPSC/860) and a network of workstations (speedups of almost 19 times achieved for 20 workstations). Very high parallel efficiencies (75 percent for 31 processors and 60 percent for 50 processors) were also achieved for computation of aerodynamic influence coefficients on the Intel. Finally, the multi-level parallelization strategy that will be needed for large-scale MSO problems was demonstrated to be highly efficient. The same parallel code instructions were used on both platforms, demonstrating portability. There are many applications for which MSO can be applied, including NASA's High-Speed-Civil Transport, and advanced propulsion systems. The use of MSO will reduce design and development time and testing costs dramatically. Author

N95-16097 Massachusetts Inst. of Tech., Lexington.
SOLID STATE RADAR DEMONSTRATION TEST RESULTS AT
THE FAA TECHNICAL CENTER
RICHARD L. FERRANTI 17 Jun. 1994 39 p Limited Reproducibility: More than 20% of this document may be affected by microfiche quality (Contract(s)/Grant(s): DTFA01-93-Z-02012) (AD-A281520; ATC-221) Avail: Issuing Activity (Defense Technical Information Center (DTIC))

In 1992 and 1993 ITT Gilfillan teamed with Thomson CSF to develop a solid state transmitter system for airport surveillance radar applications. Because of the low peak power limitations of the solid state transmitter, the radar uses pulse compression techniques to obtain 55 nmi detection performance. In the fall of 1992 ITT/Thompson executed a Cooperative Research and Development Agreement with the FAA's Terminal Area Surveillance System (TASS) program office to demonstrate the transmitter at the FAA Technical Center using the FAATC's ASR-9. The laboratory participated in these tests, which were completed in April 1993. The laboratory test plan included an assessment of the solid state radar's time sidelobe levels, stability, susceptibility to short pulse interference, and target detection performance. Although the tests were limited in scope and the data required several post-collection processing corrections, the radar exhibited very low time sidelobe levels, had excellent stability, and showed adequate detection performance. The pulse compression receiver was vulnerable to short pulse interference and will require specialized processing techniques to minimize its effects. It was not possible to take weather data, and the FAA Technical Center radar environment has no stressing clutter. Recommendations are made for the follow-on effort at a mountainous site to more completely characterize the solid state ATC radar. DTIC

N95-16163# Massachusetts Inst. of Tech., Cambridge. Turbine Lab.
**UNSTEADY FLOW PHENOMENA IN DISCRETE PASSAGE
 DIFFUSERS FOR CENTRIFUGAL COMPRESSORS** Final
 Report, 8 Jul. 1990 - 8 Jan. 1994
 V. FILIPENCO, J. M. JOHNSTON, and E. M. GREITZER 6 May 1994
 39 p

(Contract(s)/Grant(s): DAAL03-90-G-0138)
 (AD-A281412; ARO-27627.3-EG) Avail: CASI HC A03/MF A01

Research is described on the fluid dynamic behavior of high performance diffusers for centrifugal compressors, with particular application to small gas turbine engine applications. Using a unique swirl generator, experiments have been carried out to define the performance and stall onset behavior of a modern discrete passage diffuser as a function of inlet conditions. Two diffusers were examined, one with 30 passages and one with 38 passages. Inlet blockage and axial asymmetry were varied over Mach numbers up to unity and over a range of inlet swirl angles. Diffuser pressure recovery and operating range were calculated using traverse measurements made upstream of the diffuser. It was found that the performance of the diffuser under different inlet conditions could be expressed to a high degree of accuracy as a single curve of nondimensional static pressure recovery coefficient, based on availability averaged inlet stagnation pressure, and momentum-averaged inlet flow angle. Unsteady pressure measurements showed that the diffuser entered rotating stall at reduced flow rates. No long wavelength stall precursor was determined from the measurements.

DTIC

N95-16250# Nanjing Univ. of Aeronautics and Astronautics, Nanjing, Jiangsu (China). Research Inst. of Helicopter Technique.
**INVESTIGATION OF DYNAMIC INFLOW'S INFLUENCE ON
 ROTOR CONTROL DERIVATIVES**

XIAOGU ZHANG and JINSONG BAO *In its* Joint Proceedings on Aeronautics and Astronautics (JPAA) p 1-10 May 1993 Sponsored by the Aeronautical Science Foundation of China
 Avail: CASI HC A02/MF A03

A method including dynamic inflow model is developed to analyze rotor force and moments. Rotor model tests are performed to measure rotor control derivatives. The dynamic inflow model is verified through the comparative study between analytical results and test data. The influence of dynamic inflow on different conditions is investigated. A simplified analytical model is used to investigate the influence of dynamic inflow on the different rotor configurations. The correlation between theoretical predictions with dynamic inflow and test results is excellent.

Author

N95-16268# Nanjing Univ. of Aeronautics and Astronautics, Nanjing, Jiangsu (China). Dept. of Electronic Engineering.
**LINEAR PREDICTION DATA EXTRAPOLATION
 SUPERRESOLUTION RADAR IMAGING**

ZHAODA ZHU, ZHENRU YE, and XIAOQING WU *In its* Joint Proceedings on Aeronautics and Astronautics (JPAA) p 125-130 May 1993 Sponsored by the Aeronautical Science Foundation of China
 Avail: CASI HC A02/MF A03

Range resolution and cross-range resolution of range-doppler imaging radars are related to the effective bandwidth of transmitted signal and the angle through which the object rotates relatively to the radar line of sight (RLOS) during the coherent processing time, respectively. In this paper, linear prediction data extrapolation discrete Fourier transform (LPDEDFT) superresolution imaging method is investigated for the purpose of surpassing the limitation imposed by the conventional FFT range-doppler processing and improving the resolution capability of range-doppler imaging radar. The LPDEDFT superresolution imaging method, which is conceptually simple, consists of extrapolating observed data beyond the observation windows by means of linear prediction, and then performing the conventional IDFT of the extrapolated data. The live data of a metalized scale model B-52 aircraft mounted on a rotating platform in a microwave anechoic chamber and a flying Boeing-727

aircraft were processed. It is concluded that, compared to the conventional Fourier method, either higher resolution for the same effective bandwidth of transmitted signals and total rotation angle of the object or equal-quality images from smaller bandwidth and total angle may be obtained by LPDEDFT.

Author

N95-16278# Nanjing Univ. of Aeronautics and Astronautics, Nanjing, Jiangsu (China). Dept. of Automatic Control.

**THE COMPUTER ANALYSIS OF THE PREDICTION OF
 AIRCRAFT ELECTRICAL POWER SUPPLY SYSTEM
 RELIABILITY**

XINHUA MU, YANGGUANG YAN, and JIBING PEN *In its* Joint Proceedings on Aeronautics and Astronautics (JPAA) p 191-197 May 1993 See also A92-37958

Avail: CASI HC A02/MF A03

With the fast development of aviation technique, the requirements of the aircraft electrical power supply system reliability become much higher. In view of this, the reliability prediction method of simple systems can not meet the need of the research on modern aircraft electrical power supply systems. Therefore, the reliability prediction of complex systems by computers is significant. In this paper a network model of aircraft electrical power supply system is analyzed according to the reliability theory. The minimal path non-coherent technique and the computer realization process are discussed. The program flow-chart is given in detail. The reliability of an example aircraft DC electrical power supply system is calculated. Curves of system reliability are obtained by which the basis for the system reliability design is provided.

Author

N95-16281# Kazan Aviation Inst. (USSR).
**DEVELOPMENT OF PROCESSES, MEANS, AND
 THEORETICAL PRINCIPLES OF THIN-WALLED DETAIL
 PLASTIC FORMING AT KAZAN AVIATION INSTITUTE**

I. M. ZAKIROV *In* Nanjing Univ. of Aeronautics and Astronautics, Joint Proceedings on Aeronautics and Astronautics (JPAA) p 214-216 May 1993

Avail: CASI HC A01/MF A03

The scientific school of thin-walled detail plastic forming was established at Kazan Aviation Institute in the transition period from wood to metal aircraft construction. High precision requirements to thin walled detail plastic forming drove the development of new processes to secure high productivity and a work culture under conditions of low volume production.

Author (revised)

N95-16322# Wright Lab., Wright-Patterson AFB, OH.
**AN ENGINEERING CODE TO ANALYZE HYPERSONIC
 THERMAL MANAGEMENT SYSTEMS**

VALERIE J. VANGRIETHUYSEN and CLARK E. WALLACE *In* JHU The 1993 JANNAF Propulsion Meeting, Volume 1 p 319-333 Nov. 1993

(Contract(s)/Grant(s): F33615-91-C-2169)

Avail: CPIA, 10630 Little Patuxent Pkwy., Suite 202, Columbia, MD 21044-3200 HC

This paper will describe an effort that is underway within the Advanced Propulsion Division of the Aero Propulsion and Power Directorate at Wright Patterson AFB to develop an engineering computer code to aid in the development of hypersonic thermal management systems. The goal of the Vehicle Integrated Thermal Management Code (VITMAC), is to thermally model the entire thermal management system on an integrated basis for an entire vehicle. A further goal is for it to be a stand-alone code. In other words, to predict the aerodynamic heating on the vehicle surface during the trajectory, to the heat loads from the propulsion system, subsystems and avionics, and to the heat transfer through the structure and insulation. In addition, VITMAC will be able to model the flow of the coolant through the network. All this is to determine if the vehicle is thermally balanced and if there are any areas in risk of melting or thermal degradation. The code also has the option to accept user data for aerodynamic heating, heat loads and user-specific components. To aid the user while inputting the vehicle configuration, geometry, components, and 'plumbing' data, a graphical

12 ENGINEERING

user interface is being incorporated within the code. This will enable the user, even those with little experience in the area, with the aid of a mouse, to literally see the network on the screen as it is being inputted. This capability will speed up the input process, particularly for complex systems, as well as aid in error detection. This paper will further discuss the architecture of VITMAC. Also discussed will be its developmental status and capabilities, computer system that supports the code, its relevancy to other types of vehicles and applications, expansion capability and future plans. Author

N95-16349# Marotta Scientific Controls, Inc., Montville, NJ.

A LIFTING BALL VALVE FOR CRYOGENIC FLUID APPLICATIONS

JOSEPH M. CARDIN, ROBERT H. REINICKE, and STEPHEN D. BRUNEAU *In* JHU, The 1993 JANNAF Propulsion Meeting, Volume 2 p 297-312 Nov. 1993
Avail: CASI HC A03/MF A04

Marotta Scientific Controls, Inc. has designed a Lifting Ball Valve (LBV) capable of both flow modulation and tight shutoff for cryogenic and other applications. The LBV features a thin-walled visor valving element that lifts off the seal with near axial motion before rotating completely out of the flow path. This is accomplished with a simple, robust mechanism that minimizes cost and weight. Conventional spherical rotating seats are plagued by leakage due to 'scuffing' as the seal and seat slide against one another while opening. Cryogenic valves, which typically utilize plastic seals, are particularly susceptible to this type of damage. The seal in the LBV lifts off the seal without 'scuffing' making it immune to this failure mode. In addition, the LBV lifting mechanism is capable of applying the very high seating loads required to seal at cryogenic temperatures. These features make the LBV ideally suited for cryogenic valve applications. Another major feature of the LBV is the fact that the visor rotates completely out of the flow path. This allows for a smaller, lighter valve for a given flow capacity, especially for line sizes above one inch. The LBV is operated by a highly integrated 'wetted' DC brushless motor. The motor rotor is 'wetted' in that it is immersed in the fluid. To ensure compatibility, the motor rotor is encased in a thin-walled CRES weldment. The motor stator is outside the fluid containment weldment and therefore is not in direct contact with the fluid. To preclude the potential for external leakage there are no static or dynamic seals or bellows across the pressure boundary. The power required to do the work of operating the valving mechanism is transmitted across the pressure boundary by electromagnetic interaction between the motor rotor and the stator. Commutation of the motor is accomplished using the output of a special 'wetted' resolver. This paper describes the design, operation, and element testing of the LBV. Author

N95-16448# Naval Postgraduate School, Monterey, CA.

SPREAD SPECTRUM APPLICATIONS IN UNMANNED AERIAL VEHICLES M.S. Thesis

PHILIP K. BESS Jun. 1994 99 p
(AD-A281035) Avail: CASI HC A05/MF A02

This thesis is part of an ongoing Naval Postgraduate School research project to develop unmanned aerial vehicles (UAV's) using current off the shelf (COTS) technology. This thesis specifically evaluated a spread spectrum UHF data link between a UAV and ground terminal. The command and control (C2) process and its role as the fundamental premise of the warfare commander were discussed. A review of the Pioneer remotely piloted vehicle (RPV), which gained such wide recognition during Operations Desert Storm and Desert Shield, was provided to the reader for familiarization with the workings of a generic UAV. An investigation of two common spread spectrum techniques and their associated benefits was made. A link budget calculation was made. The choice of a spread spectrum radio transceiver was reviewed. The requirements and design of the UAV and ground terminal antenna were discussed. A link budget analysis was performed. An atmospheric path propagation prediction was performed. The details of an actual flight test and

the data gathered were examined. Future changes to enhance the data link performance and increase its capabilities were introduced. The COTS spread spectrum data link will enhance the role of the UAV in its command and control mission for the warfare commander. DTIC

N95-16461*# National Aeronautics and Space Administration. Langley Research Center, Hampton, VA.

APPLICATIONS OF AUTOMATIC DIFFERENTIATION IN COMPUTATIONAL FLUID DYNAMICS

LAWRENCE L. GREEN, A. CARLE, C. BISCHOF, KARA J. HAIGLER, and PERRY A. NEWMAN *In* The Role of Computers in Research and Development at Langley Research Center p 168-180 Oct. 1994
Avail: CASI HC A03/MF A06

Automatic differentiation (AD) is a powerful computational method that provides for computing exact sensitivity derivatives (SD) from existing computer programs for multidisciplinary design optimization (MDO) or in sensitivity analysis. A pre-compiler AD tool for FORTRAN programs called ADIFOR has been developed. The ADIFOR tool has been easily and quickly applied by NASA Langley researchers to assess the feasibility and computational impact of AD in MDO with several different FORTRAN programs. These include a state-of-the-art three dimensional multigrid Navier-Stokes flow solver for wings or aircraft configurations in transonic turbulent flow. With ADIFOR the user specifies sets of independent and dependent variables with an existing computer code. ADIFOR then traces the dependency path throughout the code, applies the chain rule to formulate derivative expressions, and generates new code to compute the required SD matrix. The resulting codes have been verified to compute exact non-geometric and geometric SD for a variety of cases. In less time than is required to compute the SD matrix using centered divided differences. Author (revised)

N95-16588*# Toledo Univ., OH. Dept. of Mechanical Engineering. FPCAS2D USER'S GUIDE, VERSION 1.0 Final Report
MILIND A. BAKHLE Cleveland, OH NASA Dec. 1994 58 p
(Contract(s)/Grant(s): NAG3-1234; RTOP 538-03-11)
(NASA-CR-195413; E-9299; NAS 1.26:195413) Avail: CASI HC A04/MF A01

The FPCAS2D computer code has been developed for aeroelastic stability analysis of bladed disks such as those in fans, compressors, turbines, propellers, or propfans. The aerodynamic analysis used in this code is based on the unsteady two-dimensional full potential equation which is solved for a cascade of blades. The structural analysis is based on a two degree-of-freedom rigid typical section model for each blade. Detailed explanations of the aerodynamic analysis, the numerical algorithms, and the aeroelastic analysis are not given in this report. This guide can be used to assist in the preparation of the input data required by the FPCAS2D code. A complete description of the input data is provided in this report. In addition, four test cases, including inputs and outputs, are provided. Author

N95-16621# Rome Lab., Griffiss AFB, NY.

A VHF/UHF ANTENNA FOR THE PRECISION ANTENNA MEASUREMENT SYSTEM (PAMS)

DANIEL E. WARREN Jul. 1994 33 p
(Contract(s)/Grant(s): AF PROJ. 3321)
(AD-A285673; RL-TR-94-85) Avail: CASI HC A03/MF A01

This report describes the development of an antenna concept that is to be used to extend the lower frequency limit of the Precision Antenna Measurement System (PAMS) down to 30 MHz. It includes a discussion of the concepts of reflection ranges, log periodic antennas, half space antennas, non-steerable antennas, and numerical definition of antenna patterns in two dimensions. PAMS is located at the Verona Research Facility, and is a system for measuring the radiation patterns of antennas on aircraft while they are in flight. DTIC

N95-16736# North Carolina State Univ., Raleigh, NC. Dept. of Mechanical and Aerospace Engineering.

TIME ACCURATE COMPUTATION OF UNSTEADY INLET FLOWS WITH A DYNAMIC FLOW ADAPTIVE MESH Final Report, 15 Mar. 1992 - 30 Jun. 1994

D. S. MCRAE and RUSTY A. BENSON 7 Sep. 1994 52 p
(Contract(s)/Grant(s): F49620-92-J-0189)
(AD-A285498; AFOSR-94-0625TR) Avail: CASI HC A04/MF A01

Research has been performed to obtain very accurate dynamic simulations of supersonic inlet unstart using CFD codes and a dynamic solution adaptive mesh algorithm developed at NCSU. The codes use Runge-Kutta time differencing and Advective Upwind Split Method spatial differencing in finite volume form. Other changes have been incorporated to improve the time accuracy when the computational mesh is dynamically adapted. Solutions have been obtained and animated for unstart of generic 2-D mixed compressions and fully supersonic inlets. Analysis of results revealed that laminar viscous flow unstart occurs by a separation/oblique shock mechanism rather than movement of a normal shock. Turbulent flow simulations reveal that initial shock motion occurs initially but then reverts to the separation/oblique shock mechanisms. 3-D steady and unsteady simulations are presented and conclusions drawn concerning the role of separation in inlet unstart. DTIC

N95-16828*# National Aeronautics and Space Administration. Langley Research Center, Hampton, VA.

APPLICATIONS OF AUTOMATIC DIFFERENTIATION IN CFD

A. CARLE (Rice Univ., Houston, TX.), L. L. GREEN, P. A. NEWMAN, and C. H. BISCHOF (Argonne National Lab., IL.) 1994 13 p
Presented at the 24th International Fluid Dynamics, Plasma Dynamics and Laser Conference, Colorado Springs, CO, 20-23 Jun. 1994
(Contract(s)/Grant(s): W-31-109-ENG-38)

(NASA-TM-109948; NAS 1.15:109948; DE94-013400; ANL/MCS/CP-82980; CONF-940662-1) Avail: CASI HC A03/MF A01

Automated multidisciplinary design of aircraft requires the optimization of complex performance objectives with respect to a number of design parameters and constraints. The effect of these independent design variables on the system performance criteria can be quantified in terms of sensitivity derivatives for the individual discipline simulation codes. Typical advanced CFD codes do not provide such derivatives as part of a flow solution. These derivatives are expensive to obtain by divided differences from perturbed solutions, and may be unreliable, particularly for noisy functions. In this paper, automatic differentiation has been investigated as a means of extending iterative CFD codes with sensitivity derivatives. In particular, the ADIFOR automatic differentiator has been applied to the 3-D, thin-layer Navier-Stokes, multigrid flow solver called TLNS3D coupled with the WTCC wing grid generator. Results of a sequence of efforts in which TLNS3D has been successfully augmented to compute a variety of sensitivities are presented. It is shown that sensitivity derivatives can be obtained accurately and efficiently using ADIFOR, although significant advances are necessary for the efficiency of ADIFOR-generated derivative code to become truly competitive with hand-differentiated code. DOE

N95-16911*# National Aeronautics and Space Administration. Lewis Research Center, Cleveland, OH.

OPTIMIZATION OF ADAPTIVE INTRAPLY HYBRID FIBER COMPOSITES WITH RELIABILITY CONSIDERATIONS

MICHAEL C. SHIAO (NYMA, Inc., Brook Park, OH.) and CHRISTOS C. CHAMIS Dec. 1994 16 p
Presented at 1994 North American Conference on Smart Structures and Materials, Orlando, FL, 13-18 Feb. 1994; sponsored by IEEE

Contract(s)/Grant(s): NAS3-27186; RTOP 505-62-10)
(NASA-TM-106632; E-8933; NAS 1.15:106632) Avail: CASI HC A03/MF A01

The reliability with bounded distribution parameters (mean, standard deviation) was maximized and the reliability-based cost was minimized for adaptive intra-ply hybrid fiber composites by using a probabilistic method. The probabilistic method accounts for

all naturally occurring uncertainties including those in constituent material properties, fabrication variables, structure geometry, and control-related parameters. Probabilistic sensitivity factors were computed and used in the optimization procedures. For actuated change in the angle of attack of an airfoil-like composite shell structure with an adaptive torque plate, the reliability was maximized to 0.9999 probability, with constraints on the mean and standard deviation of the actuation material volume ratio (percentage of actuation composite material in a ply) and the actuation strain coefficient. The reliability-based cost was minimized for an airfoil-like composite shell structure with an adaptive skin and a mean actuation material volume ratio as the design parameter. At a 0.9-mean actuation material volume ratio, the minimum cost was obtained. Author

N95-16939# National Renewable Energy Lab., Golden, CO.
STRUCTURAL EFFECTS OF UNSTEADY AERODYNAMIC FORCES ON HORIZONTAL-AXIS WIND TURBINES

M. S. MILLER and D. E. SHIPLEY Aug. 1994 9 p
Presented at the AIAA Region 5 Student Conference, Saint Louis, MO, 8-11 Apr. 1992
Prepared in cooperation with Colorado Univ., Boulder, CO
(Contract(s)/Grant(s): DE-AC36-83CH-10093)
(DE94-011863; NREL/TP-441-7078; CONF-9204294-1) Avail: CASI HC A02/MF A01

Due to its renewable nature and abundant resources, wind energy has the potential to fulfill a large portion of this nation's energy needs. The simplest means of utilizing wind energy is through the use of downwind, horizontal-axis wind turbines (HAWT) with fixed-pitch rotors. This configuration regulates the peak power by allowing the rotor blade to aerodynamically stall. The stall point, the point of maximum coefficient of lift, is currently predicted using data obtained from wind tunnel tests. Unfortunately, these tests do not accurately simulate conditions encountered in the field. Flow around the tower and nacelle coupled with inflow turbulence and rotation of the turbine blades create unpredicted aerodynamic forces. Dynamic stall is hypothesized to occur. Such aerodynamic loads are transmitted into the rotor and tower causing structural resonance that drastically reduces the design lifetime of the wind turbine. The current method of alleviating this problem is to structurally reinforce the tower and blades. However, this adds unneeded mass and, therefore, cost to the turbines. A better understanding of the aerodynamic forces and the manner in which they affect the structure would allow for the design of more cost effective and durable wind turbines. Data compiled by the National Renewable Energy Laboratory (NREL) for a downwind HAWT with constant chord, untwisted, fixed-pitch rotors is analyzed. From these data, the actual aerodynamic characteristics of the rotor are being portrayed and the potential effects upon the structure can for the first time be fully analyzed. Based upon their understanding, solutions to the problem of structural resonance are emerging. DOE

N95-17418*# California Univ., Los Angeles, CA.
IN-FLIGHT IMAGING OF TRANSVERSE GAS JETS INJECTED INTO TRANSONIC AND SUPERSONIC CROSSFLOWS: DESIGN AND DEVELOPMENT M.S. Thesis, Mar. 1993

KON-SHENG CHARLES WANG Nov. 1994 88 p
(Contract(s)/Grant(s): NCC2-374; RTOP 505-68-53)
(NASA-CR-186031; H-2027; NAS 1.26:186031) Avail: CASI HC A05/MF A01

The design and development of an airborne flight-test experiment to study nonreacting gas jets injected transversely into transonic and supersonic crossflows is presented. Free-stream/crossflow Mach numbers range from 0.8 to 2.0. Planar laser-induced fluorescence (PLIF) of an iodine-seeded nitrogen jet is used to visualize the jet flow. Time-dependent images are obtained with a high-speed intensified video camera synchronized to the laser pulse rate. The entire experimental assembly is configured compactly inside a unique flight-test-fixture (FTF) mounted under the fuselage of the F-104G research aircraft, which serves as a 'flying wind tunnel' at NASA Dryden Flight Research Center. The aircraft is flown at

predetermined speeds and altitudes to permit a perfectly expanded (or slightly underexpanded) gas jet to form just outside the FTF at each free-stream Mach number. Recorded gas jet images are then digitized to allow analysis of jet trajectory, spreading, and mixing characteristics. Comparisons will be made with analytical and numerical predictions. This study shows the viability of applying highly sophisticated groundbased flow diagnostic techniques to flight-test vehicle platforms that can achieve a wide range of thermo/fluid dynamic conditions. Realistic flow environments, high enthalpies, unconstrained flowfields, and moderate operating costs are also realized, in contrast to traditional wind-tunnel testing. Author

N95-17490* National Aeronautics and Space Administration. Hugh L. Dryden Flight Research Center, Edwards, CA.

SHEAR BUCKLING ANALYSIS OF A HAT-STIFFENED PANEL
WILLIAM L. KO and RAYMOND H. JACKSON Washington Nov. 1994 20 p
(Contract(s)/Grant(s): RTOP 505-63-40)
(NASA-TM-4644; H-2019; NAS 1.15:4644) Avail: CASI HC A03/MF A01

A buckling analysis was performed on a hat-stiffened panel subjected to shear loading. Both local buckling and global buckling were analyzed. The global shear buckling load was found to be several times higher than the local shear buckling load. The classical shear buckling theory for a flat plate was found to be useful in predicting the local shear buckling load of the hat-stiffened panel, and the predicted local shear buckling loads thus obtained compare favorably with the results of finite element analysis. Author

N95-17507 Northrop Corp., Pico Rivera, CA. B-2 Div.
EDDY CURRENT FOR DETECTING SECOND LAYER CRACKS UNDER INSTALLED FASTENERS Final Report, 1 Oct. 1991 - 1 Nov. 1993

WILLIAM R. SHEPPARD Apr. 1994 64 p Limited Reproducibility: More than 20% of this document may be affected by microfiche quality
(Contract(s)/Grant(s): F33615-91-C-5660)
(AD-A282412; WL-TR-94-4006) Avail: CASI HC A04

The detection of second layer Cracks Under Fasteners (CUF) persists as an Air Force Logistics need. This work seeks to extend technology developed for detecting cracks in aluminum alloy substructure below graphite-epoxy skins, to structures with an aluminum first layer. Improvements to the design of the Northrop Low Frequency Eddy Current Array (LFECA) system are identified to improve sensitivity to CUFs in aluminum-over-aluminum structures. The probe core shape, dimensions, and coil configurations were optimized for detection with installed fasteners and metallic skin. A multiparameter analysis algorithm is applied to enable flaw discrimination from centering variations, edge responses and other sources of noise. The study also quantifies the capabilities and limitations of the LFECA system. DTIC

N95-17847* Deutsche Forschungsanstalt fuer Luft- und Raumfahrt, Brunswick (Germany). Inst. fuer Entwurfsaerodynamik.
2-D AIRFOIL TESTS INCLUDING SIDE WALL BOUNDARY LAYER MEASUREMENTS

W. BARTELHEIMER, K. H. HORSTMANN, and W. PUFFERT-MEISSNER In AGARD, A Selection of Experimental Test Cases for the Validation of CFD Codes, Volume 2 11 p Aug. 1994
Copyright Avail: CASI HC A03/MF A06

The data presented in this contribution were obtained in the DLR Transonic Wind Tunnel Braunschweig. The intent of the experiment was to provide data giving information on the development of the TWB-side wall boundary layer in the presence of a typical transonic airfoil model for further investigation of the influence of the side wall boundary layer on 2-D airfoil measurements. For this purpose boundary layer pitot pressure were measured in 13 different side wall positions around the airfoil. Airfoil pressure distributions were obtained in several spanwise positions by sliding the airfoil

model in a spanwise direction. The test cases investigated correspond to the design conditions of the airfoil ($Ma = 0.73$, $\alpha = 1.5$ deg) and to a slow ($\alpha = 0$ deg) and a high ($\alpha = 3.0$ deg) lift value at the same Mach number. For these cases wall pressure distributions were measured on the center slot of the top and bottom walls. Additionally to the pressure measurements some oil flow pictures were made on the upper airfoil surface and the adjacent wind tunnel side wall to get more insight in the structure of the flow. In order to have well defined wind tunnel boundary conditions for the evaluation by computational methods, the slotted top and bottom walls of the test section were closed for these specific tests. This means, of course, that the presented airfoil pressure distributions do not correspond to free flight conditions and are not comparable to wind tunnel results obtained in slotted or perforated transonic test sections. Author

N95-17867* Deutsche Forschungsanstalt fuer Luft- und Raumfahrt, Goettingen (Germany). Inst. fuer Stroemungsmechanik.
THREE-DIMENSIONAL BOUNDARY LAYER AND FLOW FIELD DATA OF AN INCLINED PROLATE SPHEROID
H.-P. KREPLIN In AGARD, A Selection of Experimental Test Cases for the Validation of CFD Codes, Volume 2 12 p Aug. 1994
Copyright Avail: CASI HC A03/MF A06

A research project on the investigation of three-dimensional boundary layers on inclined bodies of revolution has been carried out. Experimental data for such flows were provided which can be used for the validation of calculation methods and the testing and development of turbulence models for three-dimensional flows. Problems of laminar-turbulent boundary layer separation have been studied for a range of angles of incidence and Reynolds number.

Derived from text

N95-17869* Office National d'Etudes et de Recherches Aerospatiales, Paris (France).

ELLIPSOID-CYLINDER MODEL
D. BARBERIS In AGARD, A Selection of Experimental Test Cases for the Validation of CFD Codes, Volume 2 11 p Aug. 1994
Copyright Avail: CASI HC A03/MF A06

The data presented in this contribution were obtained in the F2 subsonic wind tunnel of the ONERA Fauga-Mauzac Center. The objective of this work was to obtain detailed experimental data on a separated vortex flow. The model shape has been chosen to be as simple as possible in order to facilitate the mathematical modeling. This model has been defined after preliminary studies in a water tunnel. The present document reports the results obtained with an axisymmetric model at incidence. Attention has been focused on the boundary layer evolution in the zone of separation and on the mechanism leading to the formation of a well detached primary vortex. The flow has been investigated in great detail by using several experimental techniques: surface flow visualizations, surface pressure measurements, field explorations by multihole pressure probes, and an LDV system. Derived from text

N95-17871* Office National d'Etudes et de Recherches Aerospatiales, Paris (France).

TEST DATA ON A NON-CIRCULAR BODY FOR SUBSONIC, TRANSONIC AND SUPERSONIC MACH NUMBERS
P. CHAMPIGNY In AGARD, A Selection of Experimental Test Cases for the Validation of CFD Codes, Volume 2 11 p Aug. 1994
Copyright Avail: CASI HC A03/MF A06

Measurements on a non-circular body were made in ONERA wind tunnels. This body, representative of non-conventional missile shapes, was studied for Mach numbers from 0.4 to 3.0 (S2MA wind-tunnel) and 4.5 (S3MA wind-tunnel), angles of attack up to 20 deg and sideslip angles up to 10 deg, with a free transition. The data base consists of static pressure measurements. The intent of the experiment was to provide data for evaluation of three-dimensional flow computation methods, as part of a research program sponsored by

the 'Direction des Recherches, Etudes et Techniques' of the French Ministry of Defense. The flow exhibits large separation regions and strong vortices, even at low angles of attack, due to the particular shape of the body (lenticular cross-section). Author

N95-18042*# College of William and Mary, Williamsburg, VA. Program in Applied Science.

A SPECTRALLY ACCURATE BOUNDARY-LAYER CODE FOR INFINITE SWEEP WINGS Interim Report

C. DAVID PRUETT Dec. 1994 36 p

(Contract(s)/Grant(s): NAS1-19656; RTOP 505-59-50-02)

(NASA-CR-195014; NAS 1.26:195014) Avail: CASI HC A03/MF A01

This report documents the development, validation, and application of a spectrally accurate boundary-layer code, WINGBL2, which has been designed specifically for use in stability analyses of swept-wing configurations. Currently, we consider only the quasi-three-dimensional case of an infinitely long wing of constant cross section. The effects of streamwise curvature, streamwise pressure gradient, and wall suction and/or blowing are taken into account in the governing equations and boundary conditions. The boundary-layer equations are formulated both for the attachment-line flow and for the evolving boundary layer. The boundary-layer equations are solved by marching in the direction perpendicular to the leading edge, for which high-order (up to fifth) backward differencing techniques are used. In the wall-normal direction, a spectral collocation method, based upon Chebyshev polynomial approximations, is exploited. The accuracy, efficiency, and user-friendliness of WINGBL2 make it well suited for applications to linear stability theory, parabolized stability equation methodology, direct numerical simulation, and large-eddy simulation. The method is validated against existing schemes for three test cases, including incompressible swept Hiemenz flow and Mach 2.4 flow over an airfoil swept at 70 deg to the free stream. Author

N95-18190*# Institute for Computer Applications in Science and Engineering, Hampton, VA.

THE STABILITY OF TWO-PHASE FLOW OVER A SWEEP-WING Final Report

ADRIAN COWARD (Manchester Univ., England.) and PHILIP HALL (Manchester Univ., England.) Oct. 1994 44 p Submitted for publication Sponsored by Science Research Council

(Contract(s)/Grant(s): NAS1-19480; RTOP 505-90-52-01)

(NASA-CR-194994; NAS 1.26:194994; ICASE-94-86) Avail: CASI HC A03/MF A01

We use numerical and asymptotic techniques to study the stability of a two-phase air/water flow above a flat porous plate. This flow is a model of the boundary layer which forms on a yawed cylinder and can be used as a useful approximation to the air flow over swept wings during heavy rainfall. We show that the interface between the water and air layers can significantly destabilize the flow, leading to traveling wave disturbances which move along the attachment line. This instability occurs for lower Reynolds numbers than in the case of the absence of a water layer. We also investigate the instability of inviscid stationary modes. We calculate the effective wavenumber and orientation of the stationary disturbance when the fluids have identical physical properties. Using perturbation methods we obtain corrections due to a small stratification in viscosity, thus quantifying the interfacial effects. Our analytical results are in agreement with the numerical solution which we obtain for arbitrary fluid properties. Author

N95-18191*# Institute for Computer Applications in Science and Engineering, Hampton, VA.

ON THE LIGHTHILL RELATIONSHIP AND SOUND GENERATION FROM ISOTROPIC TURBULENCE Final Report

YE ZHOU, ALEXANDER PRASKOVSKY (National Center for Atmospheric Research, Boulder, CO.), and STEVEN ONCLEY (National Center for Atmospheric Research, Boulder, CO.) Nov.

1994 19 p Submitted for publication Sponsored by NSF (Contract(s)/Grant(s): NAS1-19480; RTOP 505-90-52-01) (NASA-CR-195005; NAS 1.26:195005; ICASE-94-92) Avail: CASI HC A03/MF A01

In 1952, Lighthill developed a theory for determining the sound generated by a turbulent motion of a fluid. With some statistical assumptions, Proudman applied this theory to estimate the acoustic power of isotropic turbulence. Recently, Lighthill established a simple relationship that relates the fourth-order retarded time and space covariance of his stress tensor to the corresponding second-order covariance and the turbulent flatness factor, without making statistical assumptions for a homogeneous turbulence. Lilley revisited Proudman's work and applied the Lighthill relationship to evaluate directly the radiated acoustic power from isotropic turbulence. After choosing the time separation dependence in the two-point velocity time and space covariance based on the insights gained from direct numerical simulations, Lilley concluded that the Proudman constant is determined by the turbulent flatness factor and the second-order spatial velocity covariance. In order to estimate the Proudman constant at high Reynolds numbers, we analyzed a unique data set of measurements in a large wind tunnel and atmospheric surface layer that covers a range of the Taylor microscale based on Reynolds numbers $2.0 \times 10^{(exp 3)}$ less than or equal to $R(\text{sub } \lambda)$ less than or equal to $12.7 \times 10^{(exp 3)}$. Our measurements demonstrate that the Lighthill relationship is a good approximation, providing additional support to Lilley's approach. The flatness factor is found between 2.7 - 3.3 and the second order spatial velocity covariance is obtained. Based on these experimental data, the Proudman constant is estimated to be 0.68 - 3.68. Author

N95-18193*# Institute for Computer Applications in Science and Engineering, Hampton, VA.

EFFECT OF CROSSFLOW ON GOERTLER INSTABILITY IN INCOMPRESSIBLE BOUNDARY LAYERS Final Report

Y. H. ZURIGAT (Jordan Univ., Amman.) and M. R. MALIK (High Technology Corp., Hampton, VA.) Nov. 1994 20 p Submitted for publication

(Contract(s)/Grant(s): NAS1-19480; NAS1-19299; RTOP 505-90-52-01)

(NASA-CR-195007; NAS 1.26:195007; ICASE-94-94) Avail: CASI HC A03/MF A01

Linear stability theory is used to study the effect of crossflow on Goertler instability in incompressible boundary layers. The results cover a wide range of sweep angle, pressure gradient, and wall curvature parameters. It is shown that the crossflow stabilizes Goertler disturbances by reducing the maximum growth rate and shrinking the unstable band of spanwise wave numbers. On the other hand, the effect of concave wall curvature on crossflow instability is destabilizing. Calculations show that the changeover from Goertler to crossflow instabilities is a function of Goertler number, pressure gradient, and sweep angle. The results demonstrate that Goertler instability may still be relevant in the transition process on swept wings even at large angles of sweep if the pressure gradient is sufficiently small. The influence of pressure gradient and sweep can be combined by defining a crossflow Reynolds number. Thus, the changeover from Goertler to crossflow instability takes place at some critical crossflow Reynolds number whose value increases with Goertler number. Author

N95-18325* National Aeronautics and Space Administration. Marshall Space Flight Center, Huntsville, AL.

TUNED MASS DAMPER FOR INTEGRALLY BLADED TURBINE ROTOR Patent

JOHN J. MARRA, inventor (to NASA) 20 Dec. 1994 6 p Filed 12 Oct. 1993 Supersedes N94-29353 (32 - 8, p 3298)

(NASA-CASE-MFS-28697-1; US-PATENT-5,373,922; US-PATENT-APPL-SN-134443; US-PATENT-CLASS-188-379; US-PATENT-CLASS-416-144; US-PATENT-CLASS-74-573R; US-PATENT-CLASS-74-574; INT-PATENT-CLASS-F16F-7/10) Avail: US Patent and

Trademark Office

The invention is directed to a damper ring for damping the natural vibration of the rotor blades of an integrally bladed rocket turbine rotor. The invention consists of an integral damper ring which is fixed to the underside of the rotor blade platform of a turbine rotor. The damper ring includes integral supports which extend radially outwardly therefrom. The supports are located adjacent to the base portion and directly under each blade of the rotor. Vibration damping is accomplished by action of tuned mass damper beams attached at each end to the supports. These beams vibrate at a predetermined frequency during operation. The vibration of the beams enforce a local node of zero vibratory amplitude at the interface between the supports and the beam. The vibration of the beams create forces upon the supports which forces are transmitted through the rotor blade mounting platform to the base of each rotor blade. When these forces attain a predetermined design frequency and magnitude and are directed to the base of the rotor blades, vibration of the rotor blades is effectively counteracted.

Official Gazette of the U.S. Patent and Trademark Office

N95-18388* Virginia Polytechnic Inst. and State Univ., Blacksburg, VA. Dept. of Aerospace and Ocean Engineering.

COMPRESSION STRENGTH OF COMPOSITE PRIMARY STRUCTURAL COMPONENTS Semiannual Report, 1 May - 31 Oct. 1994

ERIC R. JOHNSON Dec. 1994 65 p

(Contract(s)/Grant(s): NAG1-537)

(NASA-CR-197554; NAS 1.26:197554) Avail: CASI HC A04/MF A01

The linear elastic response is determined for an internally pressurized, long circular cylindrical shell stiffened on the inside by a regular arrangement of identical stringers and identical rings. Periodicity of this configuration permits the analysis of a portion of the shell wall centered over a generic stringer-ring joint; i.e., a unit cell model. The stiffeners are modeled as discrete beams, and the stringer is assumed to have a symmetrical cross section and the ring an asymmetrical section. Asymmetry causes out-of-plane bending and torsion of the ring. Displacements are assumed as truncated double Fourier series plus simple terms in the axial coordinate to account for the closed and pressure vessel effect (a non-periodic effect). The interacting line loads between the stiffeners and the inside shell wall are Lagrange multipliers in the formulation, and they are also assumed as truncated Fourier series. Displacement continuity constraints between the stiffeners and shell along the contact lines are satisfied point-wise. Equilibrium is imposed by the principle of virtual work. A composite material crown panel from the fuselage of a large transport aircraft is the numerical example. The distributions of the interacting line loads, and the out-of-plane bending moment and torque in the ring, are strongly dependent on modeling the deformations due to transverse shear and cross-sectional warping of the ring in torsion. This paper contains the results from the semiannual report on research on 'Pressure Pillowing of an Orthogonally Stiffened Cylindrical Shell'. The results of the new work are illustrated in the included appendix. Author (revised)

N95-18436 Federal Aviation Administration, Cambridge, MA. National Transportation Systems Center.

AN ANALYSIS OF TOWER (LOCAL) CONTROLLER-PILOT VOICE COMMUNICATIONS Final Report

KIM M. CARDOSI Jun. 1994 28 p Limited Reproducibility: More

than 20% of this document may be affected by microfiche quality (AD-A283718; DOT-VNTSC-FAA-94-11; DOT/FAA/RD-94/15) Avail: Issuing Activity (Defense Technical Information Center (DTIC))

The purpose was to examine current pilot-controller communication practices in the terminal environment. Forty-nine hours of voice tapes from local positions in ten air traffic control towers (ATCTs) were examined. There were 8444 controller-to-pilot messages (e.g., clearances to takeoff or land, instructions to hold short or change radio frequencies, etc.) examined. The complexity of the controller's message (i.e., the number of pieces of information) was examined and the number of erroneous readbacks and pilot re-

quests for repeats were analyzed as a function of message complexity. Pilot acknowledgements were also analyzed; the numbers of full and partial readbacks and acknowledgements only (i.e., 'roger') were tallied. Fewer than one percent of the messages resulted in communications errors. Among the error factors examined were: complexity of the message, type of acknowledgement, use of call sign in the acknowledgement, type of information in error, and whether or not the controller responded to the readback error. Instances in which the controller contacted the aircraft with one call sign and the pilot acknowledged the transmission with another call sign were also examined. The report concludes with recommendations to further reduce the probability of communication errors.

DTIC

N95-18461# Department of the Navy, Washington, DC.

HYDROFOIL FORCE BALANCE Patent Application

PAUL J. LEFEBVRE, inventor (to Navy) and WILLIAM P. BARKER, inventor (to Navy) 20 Jul. 1994 22 p

(AD-D016475; US-PATENT-APPL-SN-279037; NAVY-CASE-74885) Avail: CASI HC A02/MF A01

The present invention relates to a measuring device for measuring a component of a force acting on a test body, such as a hydrofoil, positioned within a testing apparatus. The measuring device has a test body formed by a foil shaped center section and two adjacent end sections. Each end section is joined to the center section by a flexure member having sufficient stiffness so that there is negligible relative motion between the center section and the end sections as a fluid medium flows past the center section. At least one strain gauge is mounted to at least one flexure member to measure the forces acting on the center section. A method for measuring the load on a test body is also described. DTIC

N95-18660 Johnson Controls, Inc., Milwaukee, WI. Battery Group. **DEVELOPMENT OF A BIPOLAR LEAD/ACID BATTERY FOR THE MORE ELECTRIC AIRCRAFT** Interim Report, 1 Sep. 1991 - 1 Mar. 1993

DOUGLAS C. PIERCE Mar. 1994 43p Limited Reproducibility: More than 20% of this document may be affected by microfiche quality (Contract(s)/Grant(s): F33615-91-C-2142)

(AD-A284050; WL-TR-94-2025) Avail: Issuing Activity (Defense Technical Information Center (DTIC))

This report summarizes the development work completed under contract F33615-91-C-2142 for the time period of September 1991 through March 1993. The focus of the work was on the development of a filled polymeric composite substrate for use in a true bipolar lead acid battery. The contract goals for the development of the substrate material are as follows: Resistivity: less than or equal to 2 ohm-cm; Thickness: less than or equal to 0.064 cm; Weight: less than or equal to 150 mg/sq cm; Area: more than or equal to 400 sq cm. This report presents information towards achieving those goals. DTIC

N95-18737* Research Inst. for Advanced Computer Science, Moffett Field, CA.

MESH QUALITY CONTROL FOR MULTIPLY-REFINED TETRAHEDRAL GRIDS

RUPAK BISWAS and ROGER STRAWN (Army Aviation Systems Command, Moffett Field, CA.) Nov. 1994 16 p Submitted for publication

(Contract(s)/Grant(s): NAS2-13721)

(NASA-CR-197595; NAS 1.26:197595; RIACS-TR-94-19) Avail: CASI HC A03/MF A01

A new algorithm for controlling the quality of multiply-refined tetrahedral meshes is presented in this paper. The basic dynamic mesh adaption procedure allows localized grid refinement and coarsening to efficiently capture aerodynamic flow features in computational fluid dynamics problems; however, repeated application of the procedure may significantly deteriorate the quality of the mesh. Results presented show the effectiveness of this mesh quality algorithm and its potential in the area of helicopter aerodynamics and acoustics. Author

N95-18901 Cornell Univ., Ithaca, NY.
WAVE CYCLE DESIGN FOR WAVE ROTOR ENGINES WITH LIMITED NITROGEN OXIDE EMISSIONS Ph.D. Thesis
 MOHAMED RAZI NALIM 1994 200 p
 Avail: Univ. Microfilms Order No. DA9416705

Direct work exchange between gases in wave rotors can be used to create topping cycles for gas turbine engines with peak temperatures and pressures exceeding the limits that restrict the performance of present day turbomachinery. Analytical methods are used for preliminary design and evaluation of a class of wave rotor cycles that involve large-amplitude nonsteady expansions of hot combustion products in the wave channels. A computer code is then employed to calculate the detailed time-evolution of the channel flow field. It uses the method of characteristics for one-dimensional inviscid flow, extended to treat strong shocks, entropy gradients and discontinuities, and their interactions. Several wave rotor engine cycles are designed suitable for supersonic aircraft propulsion at Mach 2.6. One is a five-port topping cycle with wave expansion provided to accommodate both the temperature limit imposed by a low-NO(x) combustor, and the limit for cooled turbine blades. Performance improvement equivalent to a 50-150 K increase in turbine inlet temperature is obtained, for turboshaft core engines. Reverse-flow expansion of the hot gas is found to be superior for this cycle. A second type of cycle involves staged rich-lean combustion with expansion-wave cooling of very hot primary rich (ϕ approximately equal to 1.2-1.5) combustion products to a temperature (below 2000 K) permitting NO(x) reduction through hydrocarbon addition when necessary. Combustion is completed by rapid mixing of secondary air, similar to the two-stage rich-quench-lean (RQL) low-NO(x) combustor being evaluated at NASA Lewis for high speed propulsion, but at a lower temperature. This cycle provides an equivalent turbine-inlet-temperature improvement of about 250 K, while reducing peak temperature in the critical mixing zone by 250-400 K, compared to an equally efficient conventional cycle with RQL combustion. A through-flow expansion wave cycle is presented for this scheme. Both types of engine cycles involve bypass flows for optimal performance. Dissert. Abstr.

N95-18938* McDonnell-Douglas Aerospace, Saint Louis, MO.
FIBER OPTIC CONTROL SYSTEM INTEGRATION FOR ADVANCED AIRCRAFT. ELECTRO-OPTIC AND SENSOR FABRICATION, INTEGRATION, AND ENVIRONMENTAL TESTING FOR FLIGHT CONTROL SYSTEMS: LABORATORY TEST RESULTS Final Report
 BRADLEY L. KESSLER Nov. 1994 388 p
 (Contract(s)/Grant(s): NAS3-25796; RTOP 505-62-50)
 (NASA-CR-195408; E-9265; NAS 1.26:195408) Avail: CASI HC A17/MF A04

This report presents the data obtained in laboratory testing of the optical sensors and multiplexing architecture developed for flight testing in the NASA F-18 systems research aircraft. Author

N95-18955* Eidetics International, Inc., Torrance, CA.
DEVELOPMENT OF A MULTICOMPONENT FORCE AND MOMENT BALANCE FOR WATER TUNNEL APPLICATIONS, VOLUME 1
 CARLOS J. SUAREZ, GERALD N. MALCOLM, BRIAN R. KRAMER, BROOKE C. SMITH, and BERT F. AYERS Washington NASA Dec. 1994 103 p Original contains color illustrations
 (Contract(s)/Grant(s): NAS2-13571; RTOP 505-59-53)
 (NASA-CR-4642-VOL-1; H-2030-VOL-1; NAS 1.26:4642-VOL-1) Avail: CASI HC A06/MF A02; 3 functional color pages

The principal objective of this research effort was to develop a multicomponent strain gauge balance to measure forces and moments on models tested in flow visualization water tunnels. An internal balance was designed that allows measuring normal and side forces, and pitching, yawing and rolling moments (no axial force). The five-components to applied loads, low interactions between the sections and no hysteresis. Static experiments (which are discussed in this Volume) were conducted in the Eidetics water tunnel with delta wings and a

model of the F/A-18. Experiments with the F/A-18 model included a thorough baseline study and investigations of the effect of control surface deflections and of several Forebody Vortex Control (FVC) techniques. Results were compared to wind tunnel data and, in general, the agreement is very satisfactory. The results of the static tests provide confidence that loads can be measured accurately in the water tunnel with a relatively simple multicomponent internal balance. Dynamic experiments were also performed using the balance, and the results are discussed in detail in Volume 2 of this report. Author

N95-18956* Eidetics International, Inc., Torrance, CA.
DEVELOPMENT OF A MULTICOMPONENT FORCE AND MOMENT BALANCE FOR WATER TUNNEL APPLICATIONS, VOLUME 2
 CARLOS J. SUAREZ, GERALD N. MALCOLM, BRIAN R. KRAMER, BROOKE C. SMITH, and BERT F. AYERS Washington NASA Dec. 1994 131 p Original contains color illustrations
 (Contract(s)/Grant(s): NAS2-13571; RTOP 505-59-53)
 (NASA-CR-4642-VOL-2; H-2030-VOL-2; NAS 1.26:4642-VOL-2) Avail: CASI HC A07/MF A02; 2 functional color pages

The principal objective of this research effort was to develop a multicomponent strain gauge balance to measure forces and moments on models tested in flow visualization water tunnels. Static experiments (which are discussed in Volume 1 of this report) were conducted, and the results showed good agreement with wind tunnel data on similar configurations. Dynamic experiments, which are the main topic of this Volume, were also performed using the balance. Delta wing models and two F/A-18 models were utilized in a variety of dynamic tests. This investigation showed that, as expected, the values of the inertial tares are very small due to the low rotating rates required in a low-speed water tunnel and can, therefore, be ignored. Oscillations in pitch, yaw and roll showed hysteresis loops that compared favorably to data from dynamic wind tunnel experiments. Pitch-up and hold maneuvers revealed the long persistence, or time-lags, of some of the force components in response to the motion. Rotary-balance experiments were also successfully performed. The good results obtained in these dynamic experiments bring a whole new dimension to water tunnel testing and emphasize the importance of having the capability to perform simultaneous flow visualization and force/moment measurements during dynamic situations. Author

N95-19019# Central Inst. of Aviation Motors, Moscow (Russia).
SOLUTION OF NAVIER-STOKES EQUATIONS USING HIGH ACCURACY MONOTONE SCHEMES
 VLADISLAV G. KRUPA and MIKHAIL J. IVANOV In AGARD, *Mathematical Models of Gas Turbine Engines and their Components* 16 p Dec. 1994
 Copyright Avail: CASI HC A03/MF A02

Numerical monotone methods for integration of the Reynolds averaged Navier-Stokes equations are presented. These methods employ finite volume formulation, implicit high-order accuracy Godunov type scheme and two-equation ($q - \omega$) turbulence model, based on integration up to the wall. To illustrate the typical peculiarities of these methods the computations of viscous flows in curvilinear ducts, around 2D airfoils and 3D shock-wave boundary layer interaction are considered. Available experimental data are used for verification of the computed results. Author

N95-19035 Naval Air Warfare Center, Patuxent River, MD. Aircraft Div.
WAVEFORM BOUNDING AND COMBINATION TECHNIQUES FOR DIRECT DRIVE TESTING
 SAMUEL FRAZIER, EDWARD PARIMUHA, MURALI TUMMALA, and THOMAS F. WINNENBERG 1994 8 p Limited Reproducibility: More than 20% of this document may be affected by microfiche quality (AD-A284075) Avail: Issuing Activity (Defense Technical Information Center (DTIC))

This paper presents various methods to combine a set of measured test signals into a composite signal. The composite signal represents the set of measured test signals by retaining the significant

12 ENGINEERING

attributes of the original set of measured test data. The composite waveforms are generated to obtain rigorous direct drive waveforms used during aircraft lightning and EMP assessments. Here we propose two techniques and a hybrid method to synthesize the composite waveforms. DTIC

N95-19125* National Aeronautics and Space Administration, Lewis Research Center, Cleveland, OH.

DETECTING GEAR TOOTH FRACTURE IN A HIGH CONTACT RATIO FACE GEAR MESH

JAMES J. ZAKRAJSEK, ROBERT F. HANDSCHUH (Army Research Lab., Cleveland, OH.), DAVID G. LEWICKI (Army Research Lab., Cleveland, OH.), and HARRY J. DECKER (Army Research Lab., Cleveland, OH.) Jan. 1995 13 p Presented at the 49th Meeting of the Society for Machinery Failure Prevention Technology, Virginia Beach, VA, 18-20 Apr. 1995; sponsored by Vibration Inst., ONR, and ARL Prepared in cooperation with Army Research Lab., Cleveland, OH

(Contract(s)/Grant(s): RTOP 505-62-36; DA PROJ. 1L1-62211-A-47-A)

(NASA-TM-106822; E-9366; NAS 1.15:106822; ARL-TR-600) Avail: CASI HC A03/MF A01

This paper summarized the results of a study in which three different vibration diagnostic methods were used to detect gear tooth fracture in a high contact ratio face gear mesh. The NASA spiral bevel gear fatigue test rig was used to produce unseeded fault, natural failures of four face gear specimens. During the fatigue tests, which were run to determine load capacity and primary failure mechanisms for face gears, vibration signals were monitored and recorded for gear diagnostic purposes. Gear tooth bending fatigue and surface pitting were the primary failure modes found in the tests. The damage ranged from partial tooth fracture on a single tooth in one test to heavy wear, severe pitting, and complete tooth fracture of several teeth on another test. Three gear fault detection techniques, FM4, NA4*, and NB4, were applied to the experimental data. These methods use the signal average in both the time and frequency domain. Method NA4* was able to conclusively detect the gear tooth fractures in three out of the four fatigue tests, along with gear tooth surface pitting and heavy wear. For multiple tooth fractures, all of the methods gave a clear indication of the damage. It was also found that due to the high contact ratio of the face gear mesh, single tooth fractures did not significantly affect the vibration signal, making this type of failure difficult to detect. Author

N95-19161* Wright Lab., Wright-Patterson AFB, OH. Acoustics and Sonic Fatigue Section.

THERMO-ACOUSTIC FATIGUE DESIGN FOR HYPERSONIC VEHICLE SKIN PANELS

KENNETH R. WENTZ, ROBERT D. BLEVINS (Rohr Industries, Inc., Chula Vista, CA.), and IAN HOLEHOUSE (Rohr Industries, Inc., Chula Vista, CA.) In AGARD, Impact of Acoustic Loads on Aircraft Structures 9 p Sep. 1994

Copyright Avail: CASI HC A02/MF A03

Thermo-vibro-acoustic analysis and test of skin panels for airbreathing hypersonic vehicles is made for a generic vehicle and trajectory. Aerothermal analysis shows that impingement of the bow shock wave on the vehicle and engine noise produce high fluctuating pressures and local heat fluxes. Maximum temperatures will exceed 2700 F (1480 C) at the top of the ascent trajectory and engine sound levels will exceed 170 dB at takeoff. As a result, loads due to engine acoustics and shock impingement dominate the design of many transatmospheric vehicle skin panels. Author

N95-19236* McDonnell-Douglas Aerospace, Saint Louis, MO.

FIBER OPTIC CONTROL SYSTEM INTEGRATION FOR ADVANCED AIRCRAFT. ELECTRO-OPTIC AND SENSOR FABRICATION, INTEGRATION, AND ENVIRONMENTAL

TESTING FOR FLIGHT CONTROL SYSTEMS Final Report

DANIEL W. SEAL, THOMAS L. WEAVER, BRADLEY L. KESSLER, CARLOS A. BEDOYA, and ROBERT E. MATTES Nov. 1994 127 p

(Contract(s)/Grant(s): NAS3-25796; RTOP 505-62-50) (NASA-CR-191194; E-8151; NAS 1.26:191194) Avail: CASI HC A07/MF A02

This report describes the design, development, and testing of passive fiber optic sensors and a multiplexing electro-optic architecture (EOA) for installation and flight test on a NASA-owned F-18 aircraft. This hardware was developed under the Fiber Optic Control Systems for Advanced Aircraft program, part of a multiyear NASA initiative to design, develop, and demonstrate through flight test 'fly-by-light' systems for application to advanced aircraft flight and propulsion control. This development included the design and production of 10 passive optical sensors and associated multiplexed EOA hardware based on wavelength division multiplexed (WDM) technology. A variety of sensor types (rotary position, linear position, temperature, and pressure) incorporating a broad range of sensor technologies (WDM analog, WDM digital, analog microbend, and fluorescent time rate of decay) were obtained from different manufacturers and functionally integrated with an independently designed EOA. The sensors were built for installation in a variety of aircraft locations, placing the sensors in a variety of harsh environments. The sensors and EOA were designed and built to have the resulting devices be as close as practical to a production system. The integrated system was delivered to NASA for flight testing on a NASA-owned F-18 aircraft. Development and integration testing of the system provided valuable information as to which sensor types were simplest to design and build for a military aircraft environment and which types were simplest to operate with a multiplexed EOA. Not all sensor types met the full range of performance and environmental requirements. EOA development problems provided information on directions to pursue in future fly-by-light flight control development programs. Lessons learned in the development of the EOA and sensor hardware are summarized. Author (revised)

N95-19251* Advisory Group for Aerospace Research and Development, Neuilly-Sur-Seine (France). Fluid Dynamics Panel.

WALL INTERFERENCE, SUPPORT INTERFERENCE AND FLOW FIELD MEASUREMENTS [LES EFFETS DE PAROI ET DE SUPPORT ET LES MESURES DES CHAMPS D'ECOULEMENT]

Jul. 1994 439 p In ENGLISH and FRENCH Symposium held in Brussels, Belgium, 4-7 Oct. 1993 Original contains color illustrations

(AGARD-CP-535; ISBN-92-835-0756-8) Copyright Avail: CASI HC A19/MF A04

The 31 papers prepared for the AGARD Fluid Dynamics Panel (FDP) Symposium on 'Wall Interference, Support Interference, and Flow Field Measurements' are contained in this report. In addition, a Technical Evaluator's Report assessing the success of the Symposium in meeting its objectives, and an edited transcript of the General Discussion held at the end of the meeting are also included. The primary objective of this Symposium was to report on recent developments from research and technology programs aimed at reducing test data errors caused by wind tunnel walls, model supports, and intrusive flow field measurement devices. The scope of papers included wall interference correction methods based on measured data at the walls and methods to eliminate wall interference through adaptive and/or ventilated walls, support interference calculations and correction methods, and recent advances in flow field measurement techniques. For individual titles, see N95-19252 through N95-19282.

N95-19252* McDonnell-Douglas Aerospace, Long Beach, CA. Transport Aircraft.

THE CRUCIAL ROLE OF WALL INTERFERENCE, SUPPORT INTERFERENCE AND FLOW FIELD MEASUREMENTS IN THE DEVELOPMENT OF ADVANCED AIRCRAFT CONFIGURATIONS

F. T. LYNCH, R. C. CRITES (McDonnell-Douglas Aerospace, Saint Louis, MO.), and F. W. SPAID (McDonnell-Douglas Aerospace, Saint Louis, MO.) In AGARD, Wall Interference, Support Interfer-

ence and Flow Field Measurements 38 p Jul. 1994
Copyright Avail: CASI HC A03/MF A04

The requirements, current technology status, and future needs for methodologies to assess wall and support interference effects, and for flow field measurement capabilities, are addressed from an aircraft industry perspective. The requirement for higher Reynolds number testing, especially for transport aircraft, places a much greater burden on the development of the respective technologies. Accurate wall interference estimation methods, including modeling of the tunnel wall flow, are required to assure that models are sized such that wall effects are correctable. Limitations of wall-interference correction methodologies, which occur as a consequence of current CFD inadequacies, are addressed. Flow field correction methods, as well as surface pressure correction methods, are covered. Three techniques for estimating model support interference are reviewed, namely, the use of dummy stings in experimental tests, use of empirically-based methods for similar installations, and use of CFD-based methods. The need to design support system concepts that minimize interference, and, in the process, permit the effective application of CFD-based methods, is highlighted. Flow diagnostic techniques needed to permit extrapolation of sub-scale wind-tunnel-measured aerodynamic characteristics to full-scale conditions, and to provide the understanding to allow deficiencies to be addressed and corrected, or to guide the design of improved-performance concepts, are reviewed. Both surface flow measurement/visualization and off-body measurements are considered. Noteworthy results obtained with current intrusive devices are reviewed, but the emphasis for the future is clearly shown to reside with optical, non-intrusive techniques such as pressure sensitive paint, infrared imaging, particle image velocimetry, and Doppler global velocimetry. Author

N95-19255# Institute for Aerospace Research, Ottawa (Ontario).
**APPLICATIONS OF THE FIVE-HOLE PROBE TECHNIQUE
FOR FLOW FIELD SURVEYS AT THE INSTITUTE FOR
AEROSPACE RESEARCH**

L. H. OHMAN (De Havilland Aircraft Co. of Canada Ltd., Downsview, Ontario.) and V. D. NGUYEN *In* AGARD, Wall Interference, Support Interference and Flow Field Measurements 15 p Jul. 1994 Original contains color illustrations
Copyright Avail: CASI HC A03/MF A04

This paper deals with calibrations and uses of the five-hole probes for flow field survey. Two applications are given: one in transonic regime in the near slipstream of a powered propfan mounted on a half-model wing configuration and the other behind a generic submarine model at subsonic speeds. The acquired data have been analyzed in terms of flow angles, total and dynamic pressures and Mach number and velocity vector in a probe fixed coordinate system. These parameters were necessary in determining the flow field characteristics of the studied configurations which are presented and discussed. Author

N95-19257# Von Karman Inst. for Fluid Dynamics, Rhode-Saint-Genese (Belgium). Turbomachinery Dept.
**AERODYNAMIC INVESTIGATION OF THE FLOW FIELD IN A
180 DEG TURN CHANNEL WITH SHARP BEND**
GUIDO RAU and TONY ARTS *In* AGARD, Wall Interference, Support Interference and Flow Field Measurements 8 p Jul. 1994
Copyright Avail: CASI HC A02/MF A04

The internal cooling of gas turbine blades is generally ensured by secondary air flowing through narrow passages existing inside the airfoils. These internal channels are usually connected by 180 deg turns with sharp bends. The aerodynamic and associated convective heat transfer characteristics observed in this type of geometry are significantly influenced by strong secondary flows and flow separations. The purpose of the present experimental effort is to give a detailed description of some aerodynamic aspects of this particular flow pattern. Detailed measurements of the three-dimensional velocity field were performed by means of a two-component

Laser Doppler Velocimeter. The third velocity component was obtained by repeating the measurements at two different orientations of the emitting optics with respect to the test section. Author

N95-19258# Centre d'Etudes et de Recherches, Toulouse (France). Dept. d'Etudes et de Recherches en Aero-Thermodynamique.
**EXPERIMENTAL TECHNIQUES FOR MEASURING
TRANSONIC FLOW WITH A THREE DIMENSIONAL LASER
VELOCIMETRY SYSTEM. APPLICATION TO DETERMINING
THE DRAG OF A FUSELAGE [TECHNIQUE EXPERIMENTALE
DE MESURE EN ECOULEMENT TRANSSONIQUE AVEC UN
SYSTEME DE VELOCIMETRIE LASER TRIDIMENSIONNEL.
APPLICATION A LA DETERMINATION DE LA TRAINEE D'UN
FUSELAGE]**

A. SERAUDIE, A. MIGNOSI, J. B. DOR, and S. PRUDHOMME *In* AGARD, Wall Interference, Support Interference and Flow Field Measurements 6 p Jul. 1994 *In* FRENCH Original contains color illustrations
Copyright Avail: CASI HC A02/MF A04

Recent developments in laser anemometry have been used to design a three dimensional laser system which has been in operation at the CERT ONERA's T2 wind tunnel since December 1989: fiber optics (to lead the light between the source and the emitting optics), Fast FOURIER Transfer Doppler processors (to analyze the Doppler signals), high power transmission system (to provide color separation), digital control of displacement motors and real time operation (to move the measuring point during the run). This device works well for the short run times of the T2 wind tunnel, providing a good accuracy which allows 30 to 50 measurement points during 60 to 120 seconds of the test. After a complete description of the 3D laser velocimetry system, the present paper will develop some typical measurements which have been performed. For each case we will present some test results obtained under transonic conditions: shock wave probing (shape and location on the upper side of a 2D transonic model); and 3D velocity measurements in forward and backward scatter configurations with the wall approach for areas without good accessibility. In order to obtain the drag of a fuselage, a vertical plane located downstream of the model was measured with two devices: laser velocimetry in order to obtain the three components of velocity; and a pressure rake providing the static and total pressures. The combination of these measurements (pressure and velocity) allowed the calculation of the total drag of the 3D model. Author

N95-19262# Defence Research Agency, Bedford (England).
**BOUNDARY-FLOW MEASUREMENT METHODS FOR WALL
INTERFERENCE ASSESSMENT AND CORRECTION:
CLASSIFICATION AND REVIEW**

P. R. ASHILL *In* AGARD, Wall Interference, Support Interference and Flow Field Measurements 21 p Jul. 1994 Sponsored by Dept. of Trade and Industry
Copyright Avail: CASI HC A03/MF A04

The development of methods of determining wind-tunnel wall interference from measurements of the flow at a boundary adjacent to the wind-tunnel walls has required the collaboration of theoreticians and experimenters. After these methods are classified and reviewed, techniques for making the measurements are discussed and the concept of correcting wind-tunnel flows to equivalent free-air conditions is examined. Three classes of method are identified, two needing a model representation ('one-variable' and 'wall-signature' types) and a third needing no simulation of the flow around the model ('two-variable' methods). All three classes are related and the need for accuracy in the model representation in 'one-variable' methods can be relaxed by a suitable choice of 'mixed' boundary conditions. Further work is needed to establish non-intrusive techniques and to develop improved methods for determining the normal component of velocity at or just away from the measurement surface. The need for research to establish allowable limits on variations in wall-induced velocity in the region of the model is highlighted. Author

N95-19263# Deutsche Forschungsanstalt fuer Luft- und Raumfahrt, Brunswick (Germany).

WALL CORRECTION METHOD WITH MEASURED BOUNDARY CONDITIONS FOR LOW SPEED WIND TUNNELS

A. KUEPPER *In* AGARD, Wall Interference, Support Interference and Flow Field Measurements 10 p Jul. 1994

Copyright Avail: CASI HC A02/MF A04

In the wind tunnel division of DLR in Braunschweig a wall correction method based on measured boundary conditions was developed. The verification of the method was made with theoretically calculated boundary conditions and with experimental test data. The calculation of the wall interferences from theoretical boundary conditions are in good agreement with exact reference data of the wall interferences. The advantage of the wall pressure correction method is shown by the results of the experimental tests where the measured coefficients of the force and the moments are compared with the corrected coefficients and the coefficients of free-flight. In this comparison the classical correction method is shown too. The wall correction method is easy to use because no information of the model is required and can be applied into an on-line processing. Particular attention should be paid to the wall pressure measurement system because wrong wall pressure data can have an influence on the calculated wall interferences. Author

N95-19264# Aeronautical Research Inst. of Sweden, Bromma. Aerodynamics Dept.

COMPUTATIONAL SIMULATIONS FOR SOME TESTS IN TRANSONIC WIND TUNNELS

NADA AGRELL *In* AGARD, Wall Interference, Support Interference and Flow Field Measurements 13 p Jul. 1994 Sponsored by FFV and Defence Material Dept.

Copyright Avail: CASI HC A03/MF A04

Two large models with swept wings have been investigated in two rather similar tunnels, whose cross sectional areas differ by a factor of 9. The tunnels are configured with slotted walls. The larger of the tunnels has a ventilation of 8.3 percent, while the ventilation of the smaller tunnel has been varied between 4.2 percent and 8.3 percent for this investigation. The blockage of the tested models in the tunnels varied from approximately 0.2 percent to 1.7 percent. For the case with blockage of 1.7 percent the ratio of span to the width (equals to the height) of the tunnel was 0.8. For the configuration blocking 0.6 percent in the larger of the two wind tunnels the comparison of Mach number signatures on the tunnel walls between experiments and computations is very good at both Mach numbers, 0.9 and 0.95, and both angles of attack, 0 and 10 degrees. The position of the 'shock' is very well predicted in the computations. Most of the computational simulations for the model blocking 1.7 percent in the smaller of the two tunnels have so far been performed at Mach number 0.8 and at angles of attack of 0 and 2 degrees. This presentation has been concentrated on Mach number 0.8 and angle of attack of 2 degrees. However, a limited number of comparisons is given for other cases, like Mach number 0.8 with angle of attack 5 degrees and Mach number 0.95 with angle of attack 2 degrees. As can be seen the agreement is excellent for all Mach numbers and related angles of attack that have been investigated. Author

N95-19265# Nangia Associates, Bristol (England).

ESTIMATING WIND TUNNEL INTERFERENCE DUE TO VECTORED JET FLOWS

R. K. NANGIA *In* AGARD, Wall Interference, Support Interference and Flow Field Measurements 14 p Jul. 1994 Sponsored by Defence Research Agency

Copyright Avail: CASI HC A03/MF A04

An important consideration in the testing of aircraft models with vectored jets is the allowance to be made for wind tunnel interference on jet flows. Depending on the cross-section dimensions, the wind tunnel interference, can be particularly severe at high incidences or for high jet velocities and large jet deflections. For assessment of these effects, either 'Wall pressure signature' or 'Direct' methods can be used. The wall pressure methods, although

requiring dedicated instrumentation, have the advantage that model flow simulation is not required. The direct methods allow calculations of interference prior to the tests and can therefore assist in optimization of model geometry for a particular wind tunnel. A 'Direct' method for estimating wind tunnel interference due to jet flows is described. A semi-empirical model of the jet plume, imaged in walls has been used to represent the tunnel constraint. Comparisons with results from a 'wall pressure signature' method are very encouraging. The results emphasize the large magnitudes of effects which can arise, particularly in experiments with 2, 3 or 4 vectoring nozzles on multi-surface aircraft configurations. For 4 nozzles with jet velocity ratio near 10, the vertical velocity flow angle can be near 6 - 8 degrees. The present technique offers the capability of guiding the design of acceptable experiments, or for checking the validity of existing information. Several aspects of future work have been proposed. Author

N95-19266*# Wright Lab., Wright-Patterson AFB, OH. Aero-Instrumentation Group.

DETERMINATION OF SOLID/POROUS WALL BOUNDARY CONDITIONS FROM WIND TUNNEL DATA FOR COMPUTATIONAL FLUID DYNAMICS CODES

THOMAS J. BEUTNER, ZEKI Z. CELIK (Stanford Univ., CA.), and LEONARD ROBERTS (Stanford Univ., CA.) *In* AGARD, Wall Interference, Support Interference and Flow Field Measurements 19 p Jul. 1994

(Contract(s)/Grant(s): NCC2-55)

Copyright Avail: CASI HC A03/MF A04

A computational and experimental study has been undertaken to investigate methods of modelling solid and porous wall boundary conditions in computational fluid dynamics (CFD) codes. The procedure utilizes experimental measurements at the walls to develop a flow field solution based on the method of singularities. This flow field solution is then imposed as a pressure boundary condition in a CFD simulation of the internal flow field. The effectiveness of this method in describing the boundary conditions at the wind tunnel walls using only sparse experimental measurements has been investigated. Verification of the approach using computational studies has been carried out using an incompressible flow solver. The current work demonstrates this technique for low speed flows and compares the result with experimental data obtained from a heavily instrumented variable porosity test section. Position and refinement of experimental measurements required to describe porous wall boundary conditions have also been considered for application to other porous wall wind tunnels. The approach developed is simple, computationally inexpensive, and does not require extensive or intrusive measurements. It may be applied to both solid and porous wall wind tunnel tests. Some consideration is given to the extension of this method to three dimensions. Author

N95-19273# Aeronautical Research Inst. of Sweden, Bromma.

CALCULATION OF LOW SPEED WIND TUNNEL WALL INTERFERENCE FROM STATIC PRESSURE PIPE MEASUREMENTS

LARS FERNKRANS *In* AGARD, Wall Interference, Support Interference and Flow Field Measurements 7 p Jul. 1994 Sponsored by FMV

Copyright Avail: CASI HC A02/MF A04

A wall interference prediction tool based on a boundary condition method is developed. The correction method, based on Green's theorem, gives the interference velocity potential field in the control volume from the velocities on a control surface around the model of interest without the need to model the flow field. The boundary velocities around separated wake flows are measured with static pressure pipes. This is done with both solid and partially open test section walls. The results are used for validation of the tool and to evaluate the possibilities to use static pressure pipes in low speed flows as a means to get the perturbation velocities needed to calculate blockage effects in nonsolid walls cases. This paper also describes some problems in estimating flow properties that are not

measured. The results presented show that if the static pressure measurements are made carefully it is possible to resolve small cross flow velocities with the necessary accuracy for the correction method. Author

N95-19275# Tsentrlnl Aerogldrodlnamicheskll Inst., Moscow (USSR). Aerodynamics Dept.

THE TRADITIONAL AND NEW METHODS OF ACCOUNTING FOR THE FACTORS DISTORTING THE FLOW OVER A MODEL IN LARGE TRANSONIC WIND TUNNELS

V. M. NEYLAND *In* AGARD, Wall Interference, Support Interference and Flow Field Measurements 10 p Jul. 1994
Copyright Avail: CASI HC A02/MF A04

The report presents a brief review of the investigation methods and results obtained for the key problems of the test procedure in the industrial sub- and transonic TSAGI wind tunnels. Among these are the flow calibration in 'empty wind tunnels', the wall interference minimization, and the interference with supporting devices. These problems can be solved only in the combination of the calculation and theoretical investigations with the tests carried out first in pilot facilities and then in large wind tunnels. As examples are given the results of the flow calibration both in the conventional conditions of a uniform test section flow and in a flow with the side wall boundary layer suction which is typical for two-dimensional model tests. The flow boundary influence is investigated by the calculation and experimental method of corrections which works well at angles of attack up to 50 degrees at $M = 0.9$. Good results are also obtained owing to the application of the adaptive perforation to reduce the wall interference on a large-scale civil plane model (blockage is 3.16 percent). The introduction of corrections for the sting-induced flow distortion over the model afterbody is discussed shortly. Author

N95-19276# Centre d'Etudes et de Recherches, Toulouse (France). Dept. d'Etudes et de Recherches en Aero-Thermodynamique.

ANALYSIS OF TEST SECTION SIDEWALL EFFECTS ON A TWO DIMENSIONAL AIRFOIL: EXPERIMENTAL AND NUMERICAL INVESTIGATIONS [EFFETS LATERAUX DANS UNE VEINE D'ESSAIS AUTOUR D'UN PROFIL D'AILE BIDIMENSIONNEL: ETUDES EXPERIMENTALE ET NUMERIQUE]

J. P. ARCHAMBAUD, J. F. MICHONNEAU, and A. MIGNOSI *In* AGARD, Wall Interference, Support Interference and Flow Field Measurements 8 p Jul. 1994 *In* FRENCH
Copyright Avail: CASI HC A02/MF A04

Sidewall effects affect the pressure field around a 2D airfoil tested in wind tunnel, even on its central section. First, laser measurement results show the 3D boundary condition near sidewalls. Then, another experimental investigation points out on the model the perturbation due to sidewall effects. In the second part a numerical method is described (coupling between inviscid flow and sidewall boundary layer computations) which allows taking into account sidewall effects. Comparisons with experiments are shown. Finally, the numerical method is used to estimate the Mach number correction due to sidewall effects. Author

N95-19277# Office National d'Etudes et de Recherches Aerospatiales, Modane (France). Centre d'Essais de Modane-Avrieux.

CALCULATION OF WALL EFFECTS OF FLOW ON A PERFORATED WALL WITH A CODE OF SURFACE SINGULARITIES [CALCULS DES EFFETS DE PAROIS DANS DES VEINES A PAROIS PERFOREES AVEC UN CODE DE SINGULARITES SURFACIQUES]

J. F. PIAT *In* AGARD, Wall Interference, Support Interference and Flow Field Measurements 12 p Jul. 1994 *In* FRENCH
Copyright Avail: CASI HC A03/MF A04

Simplifying assumptions are inherent in the analytic method previously used for the determination of wall interferences on a model in a wind tunnel. To eliminate these assumptions, a new code based on the vortex lattice method was developed. It is suitable for processing any shape of test sections with limited areas of porous

wall, the characteristic of which can be nonlinear. Calculation of wall effects in S3MA wind tunnel, whose test section is rectangular 0.78 m x 0.56 m, and fitted with two or four perforated walls, have been performed. Wall porosity factors have been adjusted to obtain the best fit between measured and computed pressure distributions on the test section walls. The code was checked by measuring nearly equal drag coefficients for a model tested in S3MA wind tunnel (after wall corrections) and in S2MA wind tunnel whose test section is seven times larger (negligible wall corrections). Author

N95-19444# National Aerospace Lab., Bangalore (India). Computational and Theoretical Fluid Dynamics Div.

CFD: ADVANCES AND APPLICATIONS, PART 1

Oct. 1993 216 p Lecture series held in Bangalore, India, 19-21 Oct. 1993

(NAL-SP-9322-PT-1) Avail: CASI HC A10/MF A03

The important topics covered in this series of lectures include governing equations for aerodynamic flow, grid generation techniques, potential flow methods, accurate high resolution discretization schemes for hyperbolic conservation laws, principle and application of multigrid techniques for convergence acceleration, and finally the efficient and robust finite-volume algorithms for computation of high speed flows in complex aerodynamic configurations. For individual titles, see N95-19445 through N95-19454.

N95-19447# National Aerospace Lab., Bangalore (India). Computational and Theoretical Fluid Dynamics Div.

COMPUTATION OF INVISCID FLOWS: FULL POTENTIAL METHOD

R. RANGARAJAN *In* its CFD: Advances and Applications, Part 1 p 23-50 Oct. 1993

Avail: CASI HC A03/MF A03

Various forms of FP (full potential) equation, spatial differencing schemes, and iterative schemes are briefly discussed. The finite difference method of solution of FP equation in cartesian coordinates is discussed in some detail. Applications of this code to a variety of flow situations like those on airfoils, axisymmetric bodies, wing, and wing-body combinations are presented. The note concludes with some general remarks on the state-of-the-art in this field. Derived from text

N95-19448# National Aerospace Lab., Bangalore (India). Computational and Theoretical Fluid Dynamics Div.

PANEL METHODS

ASHOK SRIVASTAVA *In* its CFD: Advances and Applications, Part 1 p 51-75 Oct. 1993

Avail: CASI HC A03/MF A03

A comprehensive description of panel methods has been given to enable an understanding of the underlying theory and the basic structure of the panel codes for aerodynamic applications. Panel methods have seen peak activity in the industry and remain as yet the sole technique for efficient and practical computations on complex-aircraft configurations. The method of the linearized approach of solving flow problems is well proven and till the turn of the century panel methods will continue to remain as the workhorse for computing aerodynamic characteristics of aircraft shapes in the industry. The alternative Euler and Navier-Stokes solvers have yet to mature for applications to complex shapes, hence panel methods will be in the light for at least another decade. Derived from text

N95-19462# National Aerospace Lab., Bangalore (India). Computational and Theoretical Fluid Dynamics Div.

COMPUTATION OF VORTEX BREAKDOWN

VIDYADHAR Y. MUDKAVI *In* its CFD: Advances and Applications, 1994 p 241-280 Oct. 1994

Avail: CASI HC A03/MF A04

Vortex breakdown is a deceptively simple looking, complex and poorly understood phenomenon. According to Benjamin (1962), vortex breakdown or bursting is an abrupt and drastic change of

structure which sometimes occurs in swirling flows. This phenomenon is commonly found to occur on leading edge vortices over delta wings and on trailing vortices in aircraft wakes. While it is necessary to prevent vortex breakdown over a delta wing, since it results in loss of lift, it is desirable to allow vortices to burst in aircraft wakes since it reduces hazard to follower aircraft. Vortex breakdown is also useful in chemically reacting flows where it is employed as a flame holder. But, more than anything, this phenomenon is studied because it is one of the basic problems in fluid dynamics. What follows is the authors own limited perspective of the problem. The reader will find that he/she is not introduced to the problem directly. Instead, a whole lot of material is devoted to the development of the equations of vortex dynamics with special emphasis on the motion of a vortex filament. The intention here is to motivate the reader about the merits of describing fluid flows using vortex elements as building blocks rather than velocity and pressure. Model equations of vortex breakdown are derived next using these equations. Other theoretical descriptions of the phenomenon are also stated, Benjamin's theory being of prime importance. Author

N95-19470*# Rockwell International Corp., Downey, CA. Space Systems Div.

FATIGUE LOADS SPECTRA DERIVATION FOR THE SPACE SHUTTLE: SECOND CYCLE

RAPHAEL ORTASSE In NASA. Langley Research Center, FAA/NASA International Symposium on Advanced Structural Integrity Methods for Airframe Durability and Damage Tolerance, Part 2 p 517-545 Sep. 1994

Avail: CASI HC A03/MF A04

Some of the environments and loads experienced by the Space Shuttle or future reusable space vehicles are unique, while others are similar to those encountered by commercial and/or military aircraft. Prior to the Space Transportation System (STS) flights, fatigue loads spectra were generated for the Space Shuttle based on anticipated environments and assumptions that were shown not to be applicable to the actual flight environments the vehicle experienced. This resulted in the need to generate a new cycle of fatigue loads spectra, which was based on measured flight data as well as mission profiles, reflecting the various types of service and operations the vehicle and payloads experienced. Author

N95-19471*# Laboratory for Strength of Materials Components and Structures, Puspipstek (Indonesia).

PREDICTION OF FATIGUE CRACK GROWTH UNDER FLIGHT-SIMULATION LOADING WITH THE MODIFIED CORPUS MODEL

U. H. PADMADINATA and J. SCHIJVE (Technische Hogeschool, Delft, Netherlands.) In NASA. Langley Research Center, FAA/NASA International Symposium on Advanced Structural Integrity Methods for Airframe Durability and Damage Tolerance, Part 2 p 547-562 Sep. 1994

Avail: CASI HC A03/MF A04

The CORPUS (Computation Of Retarded Propagation Under Spectrum loading) crack growth prediction model for variable-amplitude loading, as introduced by De Koning, was based on crack closure. It includes a multiple-overload effect and a transition from plane strain to plane stress. In the modified CORPUS model an underload affected zone (ULZ) is introduced, which is significant for flight-simulation loading in view of the once per flight compressive ground load. The ULZ is associated with reversed plastic deformation induced by the underloads after crack closure has already occurred. Predictions of the crack growth fatigue life are presented for a large variety of flight-simulation test series on 2024-T3 sheet specimens in order to reveal the effects of a number of variables: the design stress level, the gust spectrum severity, the truncation level (clipping), omission of small cycles, and the ground stress level. Tests with different load sequences are also included. The trends of the effects induced by the variables are correctly predicted. The quantitative agreement between the predictions and the test results is also satisfactory. Author

N95-19472*# National Aeronautics and Space Administration. Langley Research Center, Hampton, VA.

THE CHARACTERIZATION OF WIDESPREAD FATIGUE DAMAGE IN FUSELAGE STRUCTURE

ROBERT S. PIASCIK, SCOTT A. WILLARD (Lockheed Engineering and Sciences Co., Hampton, VA.), and **MATTHEW MILLER** (Boeing Commercial Airplane Co., Seattle, WA.) In its FAA/NASA International Symposium on Advanced Structural Integrity Methods for Airframe Durability and Damage Tolerance, Part 2 p 563-579 Sep. 1994

Avail: CASI HC A03/MF A04

The characteristics of widespread fatigue damage (WSFD) in fuselage riveted structure were established by detailed nondestructive and destructive examinations of fatigue damage contained in a full size fuselage test article. The objectives of this work were to establish an experimental data base for validating emerging WSFD analytical prediction methodology and to identify first order effects that contribute to fatigue crack initiation and growth. Detailed examinations were performed on a test panel containing four bays of a riveted lap splice joint. The panel was removed from a full scale fuselage test article after receiving 60,000 full pressurization cycles. The results of in situ examinations document the progression of fuselage skin fatigue crack growth through crack linkup. Detailed tear down examinations and fractography of the lap splice joint region revealed fatigue crack initiation sites, crack morphology and crack linkup geometry. From this large data base, distributions of crack size and locations are presented and discussions of operative damage mechanisms are offered. Author

N95-19473*# Georgia Inst. of Tech., Atlanta, GA. Computational Modeling Center.

DISCRETE CRACK GROWTH ANALYSIS METHODOLOGY FOR THROUGH CRACKS IN PRESSURIZED FUSELAGE STRUCTURES

DAVID O. POTYONDY, PAUL A. WAWRZYNEK (Cornell Univ., Ithaca, NY.), and **ANTHONY R. INGRAFFEA** (Cornell Univ., Ithaca, NY.) In NASA. Langley Research Center, FAA/NASA International Symposium on Advanced Structural Integrity Methods for Airframe Durability and Damage Tolerance, Part 2 p 581-601 Sep. 1994 (Contract(s)/Grant(s): NAG1-1184)

Avail: CASI HC A03/MF A04

A methodology for simulating the growth of long through cracks in the skin of pressurized aircraft fuselage structures is described. Crack trajectories are allowed to be arbitrary and are computed as part of the simulation. The interaction between the mechanical loads acting on the superstructure and the local structural response near the crack tips is accounted for by employing a hierarchical modeling strategy. The structural response for each cracked configuration is obtained using a geometrically nonlinear shell finite element analysis procedure. Four stress intensity factors, two for membrane behavior and two for bending using Kirchhoff plate theory, are computed using an extension of the modified crack closure integral method. Crack trajectories are determined by applying the maximum tangential stress criterion. Crack growth results in localized mesh deletion, and the deletion regions are remeshed automatically using a newly developed all-quadrilateral meshing algorithm. The effectiveness of the methodology and its applicability to performing practical analyses of realistic structures is demonstrated by simulating curvilinear crack growth in a fuselage panel that is representative of a typical narrow-body aircraft. The predicted crack trajectory and fatigue life compare well with measurements of these same quantities from a full-scale pressurized panel test. Author

N95-19477*# Foster-Miller Associates, Inc., Waltham, MA.

EVALUATION OF THE FUSELAGE LAP JOINT FATIGUE AND TERMINATING ACTION REPAIR

GOPAL SAMAVEDAM, DOUGLAS THOMSON, and DAVID Y. JEONG (Department of Transportation, Cambridge, MA.) In NASA. Langley Research Center, FAA/NASA International Symposium on Advanced

Structural Integrity Methods for Airframe Durability and Damage Tolerance, Part 2 p 653-663 Sep. 1994 Sponsored by FAA
 Avail: CASI HC A03/MF A04

Terminating action is a remedial repair which entails the replacement of shear head countersunk rivets with universal head rivets which have a larger shank diameter. The procedure was developed to eliminate the risk of widespread fatigue damage (WFD) in the upper rivet row of a fuselage lap joint. A test and evaluation program has been conducted by Foster-Miller, Inc. (FMI) to evaluate the terminating action repair of the upper rivet row of a commercial aircraft fuselage lap splice. Two full scale fatigue tests were conducted on fuselage panels using the growth of fatigue cracks in the lap joint. The second test was performed to evaluate the effectiveness of the terminating action repair. In both tests, cyclic pressurization loading was applied to the panels while crack propagation was recorded at all rivet locations at regular intervals to generate detailed data on conditions of fatigue crack initiation, ligament link-up, and fuselage fracture. This program demonstrated that the terminating action repair substantially increases the fatigue life of a fuselage panel structure and effectively eliminates the occurrence of cracking in the upper rivet row of the lap joint. While high cycle crack growth was recorded in the middle rivet row during the second test, failure was not imminent when the test was terminated after cycling to well beyond the service life. The program also demonstrated that the initiation, propagation, and linkup of WFD in full-scale fuselage structures can be simulated and quantitatively studied in the laboratory. This paper presents an overview of the testing program and provides a detailed discussion of the data analysis and results. Crack distribution and propagation rates and directions as well as frequency of cracking are presented for both tests. The progression of damage to linkup of adjacent cracks and to eventual overall panel failure is discussed. In addition, an assessment of the effectiveness of the terminating action repair and the occurrence of cracking in the middle rivet row is provided, and conclusions of practical interest are drawn. Author

N95-19483*# Boeing Commercial Airplane Co., Seattle, WA.
THE APPLICATION OF NEWMAN CRACK-CLOSURE MODEL TO PREDICTING FATIGUE CRACK GROWTH
 ERJIAN SI (Shanghai Aircraft Research Inst., Shanghai, China.) In NASA. Langley Research Center, FAA/NASA International Symposium on Advanced Structural Integrity Methods for Airframe Durability and Damage Tolerance, Part 2 p 741-753 Sep. 1994
 Avail: CASI HC A03/MF A04

Newman crack-closure model and the relevant crack growth program were applied to the analysis of crack growth under constant amplitude and aircraft spectrum loading on a number of aluminum alloy materials. The analysis was performed for available test data of 2219-T851, 2024-T3, 2024-T351, 7075-T651, 2324-T39, and 7150-T651 aluminum materials. The results showed that the constraint factor is a significant factor in the method. The determination of the constraint factor is discussed. For constant amplitude loading, satisfactory crack growth lives could be predicted. For the above aluminum specimens, the ratio of predicted to experimental lives, N_p/N_t , ranged from 0.74 to 1.36. The mean value of N_p/N_t was 0.97. For a specified complex spectrum loading, predicted crack growth lives are not in very good agreement with the test data. Further effort is needed to correctly simulate the transition between plane strain and plane stress conditions, existing near the crack tip. Author (revised)

N95-19496*# Aluminum Co. of America, Alcoa Center, PA.
PREDICTION OF R-CURVES FROM SMALL COUPON TESTS
 J. R. YEH, G. H. BRAY, R. J. BUCCI, and Y. MACHERET In NASA. Langley Research Center, FAA/NASA International Symposium on Advanced Structural Integrity Methods for Airframe Durability and Damage Tolerance, Part 2 p 999-1013 Sep. 1994
 Avail: CASI HC A03/MF A04

R-curves were predicted for Alclad 2024-T3 and C188-T3 sheet using the results of small-coupon Kahn tear tests in combination with

two-dimensional elastic-plastic finite element stress analyses. The predictions were compared to experimental R-curves from 6.3, 16 and 60-inch wide M(T) specimens and good agreement was obtained. The method is an inexpensive alternative to wide panel testing for characterizing the fracture toughness of damage-tolerant sheet alloys. The usefulness of this approach was demonstrated by performing residual strength calculations for a two-bay crack in a representative fuselage structure. C188-T3 was predicted to have a 24 percent higher load carrying capability than 2024-T3 in this application as a result of its superior fracture toughness. Author

N95-19501*# National Aeronautics and Space Administration. Lewis Research Center, Cleveland, OH.
TECHNOLOGY BENEFIT ESTIMATOR (T/BEST): USER'S MANUAL
 EDWARD R. GENERAZIO, CHRISTOS C. CHAMIS, and GALIB ABUMERI (NYMA, Inc., Brook Park, OH.) Dec. 1994 214 p
 (Contract(s)/Grant(s): NAS3-27186; RTOP 505-63-5B)
 (NASA-TM-106785; E-9239; NAS 1.15:106785) Avail: CASI HC A10/MF A03

The Technology Benefit Estimator (T/BEST) system is a formal method to assess advanced technologies and quantify the benefit contributions for prioritization. T/BEST may be used to provide guidelines to identify and prioritize high payoff research areas, help manage research and limited resources, show the link between advanced concepts and the bottom line, i.e., accrued benefit and value, and to communicate credibly the benefits of research. The T/BEST software computer program is specifically designed to estimating benefits, and benefit sensitivities, of introducing new technologies into existing propulsion systems. Key engine cycle, structural, fluid, mission and cost analysis modules are used to provide a framework for interfacing with advanced technologies. An open-ended, modular approach is used to allow for modification and addition of both key and advanced technology modules. T/BEST has a hierarchical framework that yields varying levels of benefit estimation accuracy that are dependent on the degree of input detail available. This hierarchical feature permits rapid estimation of technology benefits even when the technology is at the conceptual stage. As knowledge of the technology details increases the accuracy of the benefit analysis increases. Included in T/BEST's framework are correlations developed from a statistical data base that is relied upon if there is insufficient information given in a particular area, e.g., fuel capacity or aircraft landing weight. Statistical predictions are not required if these data are specified in the mission requirements. The engine cycle, structural fluid, cost, noise, and emissions analyses interact with the default or user material and component libraries to yield estimates of specific global benefits: range, speed, thrust, capacity, component life, noise, emissions, specific fuel consumption, component and engine weights, pre-certification test, mission performance engine cost, direct operating cost, life cycle cost, manufacturing cost, development cost, risk, and development time. Currently, T/BEST operates on stand-alone or networked workstations, and uses a UNIX shell or script to control the operation of interfaced FORTRAN based analyses. T/BEST's interface structure works equally well with non-FORTRAN or mixed software analysis. This interface structure is designed to maintain the integrity of the expert's analyses by interfacing with expert's existing input and output files. Parameter input and output data (e.g., number of blades, hub diameters, etc.) are passed via T/BEST's neutral file, while copious data (e.g., finite element models, profiles, etc.) are passed via file pointers that point to the expert's analyses output files. In order to make the communications between the T/BEST's neutral file and attached analyses codes simple, only two software commands, PUT and GET, are required. This simplicity permits easy access to all input and output variables contained within the neutral file. Both public domain and proprietary analyses codes may be attached with a minimal amount of effort, while maintaining full data and analysis integrity, and security. T/BEST's software framework, status, beginner-to-expert operation, interface

13 GEOSCIENCES

architecture, analysis module addition, and key analysis modules are discussed. Representative examples of T/BEST benefit analyses are shown. Author

13 GEOSCIENCES

Includes geosciences (general); earth resources; energy production and conversion; environment pollution; geophysics; meteorology and climatology; and oceanography.

N95-16506# Pennsylvania State Univ., University Park, PA. Dept. of Physics.

ANISOTROPIC HEAT EXCHANGERS/STACK CONFIGURATIONS FOR THERMOACOUSTIC HEAT ENGINES

Summary Report, 1 Oct. 1993 - 31 May 1994

JULIAN D. MAYNARD 21 Jun. 1994 8 p

(Contract(s)/Grant(s): N00014-93-1-1127)

(AD-A280974) Avail: CASI HC A02/MF A01

The goal of this project is to explore novel configurations of heat exchangers and the stack (heat pumping) section of thermoacoustic heat engines. The approach will be to use anisotropic systems, such as made possible by glass capillary array technology. A part of the project will involve the development of high power drives and acoustic resonators for testing the new systems. DTIC

N95-18093# Alabama Univ., Huntsville, AL. Earth System Science Lab.

FIELD AND DATA ANALYSIS STUDIES RELATED TO THE ATMOSPHERIC ENVIRONMENT Final Report, 21 Feb. 1991 - 1 Mar. 1994

STANLEY KIDDER, DOUGLAS MACH, JEFF BAILEY, MICHAEL STEWART, DAVE SLATON, DENNIS BUECHLER, MICHAEL BOTTS, and LAURIE COLLINS Mar. 1994 7 p

(Contract(s)/Grant(s): NAS8-38776)

(NASA-CR-196543; NAS 1.26:196543) Avail: CASI HC A02/MF A01

This report summarizes work on a broad array of projects including: (1) applications of meteorological and/or oceanographic satellites; (2) improvement of the current set of NASA/USAF lightning related launch commit criteria rules; (3) the design, building, testing and deployment of a set of cylindrical field mills for aircraft use; (4) the study of marginal electrification storm conditions in relationship to the current launch commit rules for the space shuttle and various other launch vehicles using an instrumented aircraft; (5) support of the DC-8 and ER-2 lightning instrument package as part of both the Tropical Ocean - Global Atmospheric/Coupled Ocean-Atmospheric Response Experiment and the Convection and Moisture Experiment; (6) design of electronic circuitry and microprocessor firmware for the NASA Advanced Ground Based Field Mill; (7) design and testing of electronic and computer instrumentation for atmospheric electricity measurements; (8) simulating observations from a lightning imaging sensor on the Tropical Rainfall Measuring satellite; and (9) supporting scientific visualization and the development of computer software tools. Derived from text

N95-18722 Royal Netherlands Meteorological Inst., De Bilt. **ATMOSPHERIC EFFECTS OF HIGH-FLYING SUBSONIC AIRCRAFT: A CATALOGUE OF PERTURBING INFLUENCES** WIEGER FRANSEN Jun. 1994 97 p Sponsored by Ministry of Transport (ISSN 0169-1651) (KNMI-SR-94-03; ISBN-90-369-2054-X) Copyright Avail: Issuing Activity

Forecasts of global air transport demand predict an average annual growth rate between 5 and 7 percent until 2010. This implies that in 2005 the number of passenger-kilometers performed will at least be doubled compared to the situation in 1990. Since aircraft emit components which are both greenhouse gases and ozone precursors, this forecast of a substantial world-wide increase in air traffic aroused new interest, from both scientists and policy-makers, in

the atmospheric effects of aircraft exhaust. But although a great deal of work in both fields has been done on investigating and how to deal with the effects of air traffic at and around airports and of future supersonic flights in the stratosphere, little is known about the effects of subsonic aircraft during cruise. This reports' objective is to contribute to fill this gap. By merging the results of many studies which directly or indirectly aimed at elucidating one aspect of the complex problem of how high-flying aircraft influence atmospheric processes, an attempt is made to give the readers some insight in, and sense of the seriousness of, the effects of high-flying aircraft. Author

15

MATHEMATICAL AND COMPUTER SCIENCES

Includes mathematical and computer sciences (general); computer operations and hardware; computer programming and software; computer systems; cybernetics; numerical analysis; statistics and probability; systems analysis; and theoretical mathematics.

A95-63636

SELECTION OF OPTIMAL PARAMETERS FOR A SYSTEM, CONTROLLING THE FLIGHT HEIGHT, WHEN INFORMATION ABOUT THE STATE VECTOR IS INCOMPLETE

L. G. ROMANENKO KGTU, Kazan (Russia) Izvestiya VUZ: Aviatsionnaya Tekhnika (ISSN 0579-2975) no. 1 January-March 1994 p. 17-23 In RUSSIAN

(BTN-94-EIX94461408753) Copyright

The synthesis of optimal control systems is not very difficult, when the state vector can be completely measured. But in most cases, not all variables of the state vector are measurable. It is necessary therefore to select only some variables that should be sufficient for controlling purposes. Equations have been derived and analytical dependences have been obtained to determine gear ratio for a system, controlling the flight height. EI

A95-64580

NONSMOOTH TRAJECTORY OPTIMIZATION: AN APPROACH USING CONTINUOUS SIMULATED ANNEALING

PING LU Iowa State Univ., Ames, IA and M. ASIF KHAN Journal of Guidance, Control, and Dynamics (ISSN 0731-5090) vol. 17, no. 4 July-August 1994 p. 685-691 refs

(BTN-94-EIX94511433914) Copyright

A continuous simulated annealing algorithm is introduced as a new global trajectory optimization tool for nonsmooth dynamic systems. Its properties are discussed. The algorithm is implemented in a trajectory optimization program. The difficult problem of nonsmooth trajectory optimization for a high-performance, rigid-body aircraft is successfully solved using this approach. The results show that the simulated annealing algorithm outperforms some other well-known conventional algorithms by a large margin. Author (EI)

A95-64582

OUTPUT FEEDBACK CONTROL UNDER RANDOMLY VARYING DISTRIBUTED DELAYS

RAY ASOK Pennsylvania State Univ., University Park, PA Journal of Guidance, Control, and Dynamics (ISSN 0731-5090) vol. 17, no. 4 July-August 1994 p. 701-711 refs (BTN-94-EIX94511433916) Copyright

An output feedback control law has been formulated in a stochastic setting, based on the principles of minimum variance filtering and dynamic programming, for application to processes that are subjected to randomly varying distributed delays. The proposed estimation and control law for delay compensation is built on the concept of the conventional linear quadratic Gaussian (LQG), called delay compensated linear quadratic Gaussian (DCLQG). Although the certainty equivalence property of LQG does not hold for DCLQG in general, the combined state estimation and state feedback ap-

proach of DCLQG offers a suboptimal solution to the control problem under randomly varying distributed delays. DCLQG is potentially applicable to analysis and synthesis of control systems for vehicle management of future generation aircraft where a computer network is employed for distributed processing and on-line information exchange between diverse control and decision-making functions. Results of simulation experiments are presented to demonstrate efficacy of the proposed DCLQG algorithm for flight control of an advanced aircraft. Author (EI)

A95-64585

TEST BENCH FOR ROTORCRAFT HOVER CONTROL

MARTIN F. WEILENMANN ETH Swiss Federal Inst of Technology, Zurich (Switzerland) and HANS P. GEERING Journal of Guidance, Control, and Dynamics (ISSN 0731-5090) vol. 17, no. 4 July-August 1994 p. 729-736 refs (BTN-94-EIX94511433919) Copyright

This paper describes an indoor stand for a computer-controlled model helicopter. This stand was built to verify modern multivariable controller algorithms in real-world tests rather than in simulations. A commercial radio-controlled helicopter (not a scale model) is mounted on a mechanical structure allowing 6-degree of freedom flight conditions in a 2-m cube. The symmetrical geometry of the frame reduces its physical influence on the rotorcraft to be equivalent to a concentrated mass near the center of gravity. Including the dynamics of the driving motor and some unsteady aspects of the aerodynamics, an unstable 18th order mathematical model results. In addition, the radio controller causes a significant time delay. For this system, several control algorithms have been applied (channelwise proportional differential (PD) controller used for system identification, Linear Quadratic Gaussian/Loop Transfer Recovery (LQG/LTR) approaches, modal controller). The quality of the test results and some aspects of design problems are described and compared in the second part of the paper. Author (EI)

A95-64588

INTELLIGENT CONTROL LAW TUNING FOR AIAA CONTROLS DESIGN CHALLENGE

YING-JYI PAUL WEI Lockheed Fort Worth Co, Fort Worth, TX Journal of Guidance, Control, and Dynamics (ISSN 0731-5090) vol. 17, no. 4 July-August 1994 p. 753-758 refs (BTN-94-EIX94511433922) Copyright

Constrained optimization is used as the basis of the intelligent control law tuning applied to the AIAA Controls Design Challenge. A tuning rule is formulated by translating multiple control system design requirements into a cost function and a set of constraints. During the tuning process, constrained optimization is employed to search for control laws that minimize the cost function subject to the constraints. Simulation results are presented to demonstrate the successful applications of the method. Author (EI)

N95-15988*# National Aeronautics and Space Administration. Lyndon B. Johnson Space Center, Houston, TX.

VIRTUAL ENVIRONMENT APPLICATION WITH PARTIAL GRAVITY SIMULATION

DAVID M. RAY and MICHAEL N. VANCHAU In its ISMCR 1994: Topical Workshop on Virtual Reality. Proceedings of the Fourth International Symposium on Measurement and Control in Robotics p 114-122 Nov. 1994 Avail: CASI HC A02/MF A02

To support manned missions to the surface of Mars and missions requiring manipulation of payloads and locomotion in space, a training facility is required to simulate the conditions of both partial and microgravity. A partial gravity simulator (Pogo) which uses pneumatic suspension is being studied for use in virtual reality training. Pogo maintains a constant partial gravity simulation with a variation of simulated body force between 2.2 and 10 percent, depending on the type of locomotion inputs. This paper is based on the concept and application of a virtual environment system with Pogo including a head-mounted display and glove. The reality

engine consists of a high end SGI workstation and PC's which drive Pogo's sensors and data acquisition hardware used for tracking and control. The tracking system is a hybrid of magnetic and optical trackers integrated for this application. Author (revised)

N95-16272# Kazan Aviation Inst. (USSR).

GENERALIZED METHOD OF SOLVING TOPOLOGICAL OPTIMIZATION PROBLEMS FOR ELECTRICAL AIRPLANE EQUIPMENT SYSTEMS IN COMPUTER-AIDED DESIGN

V. S. TERESHCHUK In Nanjing Univ. of Aeronautics and Astronautics, Joint Proceedings on Aeronautics and Astronautics (JPAA) p 152-156 May 1993 Avail: CASI HC A01/MF A03

In developing a computer-aided design system for electric airborne equipment used by an aircraft design bureau, a number of optimization topological and parametric problems must be solved. We represent a set of all the components of the electric equipment systems arranged on board in accordance with their functional features or special requirements. The set of components can either be united into electrical structures or subject to the arrangement only. A system model of a multi-level structure of airborne equipment in the process of its disintegration is proposed and an algorithm of the electric equipment synthesis that makes it possible to find a solution for a number of separately unsolvable problems is given. Author (revised)

N95-16458*# National Aeronautics and Space Administration. Langley Research Center, Hampton, VA.

RAPID SOLUTION OF LARGE-SCALE SYSTEMS OF EQUATIONS

OLAF O. STORAASLI In its The Role of Computers in Research and Development at Langley Research Center p 130-146 Oct. 1994 Avail: CASI HC A03/MF A06

The analysis and design of complex aerospace structures requires the rapid solution of large systems of linear and nonlinear equations, eigenvalue extraction for buckling, vibration and flutter modes, structural optimization and design sensitivity calculation. Computers with multiple processors and vector capabilities can offer substantial computational advantages over traditional scalar computer for these analyses. These computers fall into two categories: shared memory computers and distributed memory computers. This presentation covers general-purpose, highly efficient algorithms for generation/assembly or element matrices, solution of systems of linear and nonlinear equations, eigenvalue and design sensitivity analysis and optimization. All algorithms are coded in FORTRAN for shared memory computers and many are adapted to distributed memory computers. The capability and numerical performance of these algorithms will be addressed. Author

N95-16474*# National Aeronautics and Space Administration. Langley Research Center, Hampton, VA.

MATLAB AS A ROBUST CONTROL DESIGN TOOL

IRENE M. GREGORY In its The Role of Computers in Research and Development at Langley Research Center p 485-496 Oct. 1994 Avail: CASI HC A03/MF A06

This presentation introduces Matlab as a tool used in flight control research. The example used to illustrate some of the capabilities of this software is a robust controller designed for a single stage to orbit air breathing vehicles's ascent to orbit. The global requirements of the controller are to stabilize the vehicle and follow a trajectory in the presence of atmospheric disturbances and strong dynamic coupling between airframe and propulsion. Author (revised)

N95-16864# Massachusetts Inst. of Tech., Cambridge.

WORKSHOP ON FORMAL MODELS FOR INTELLIGENT CONTROL Final Report, 1 Sep. - 31 Dec. 1993

SANJOY K. MITTER Apr. 1994 16 p (Contract(s)/Grant(s): DAAH04-93-G-0500) (AD-A281399; ARO-32483.1-MA-CF) Avail: CASI HC A03/MF A01

15 MATHEMATICAL AND COMPUTER SCIENCES

A workshop on Formal Models for Intelligent Control, jointly funded by the Army Office (ARO) and the National Aeronautics and Space Administration (NASA), and jointly sponsored by the Center for Intelligent Control Systems (CICS) and the University of California at Berkeley's Intelligent Machines and Robotics Laboratory, was held at M.I.T. during 30 September—2 October 1993. The workshop brought together a large number of researchers and specialists from universities, the government, and industry, providing a stage for interesting presentations as well as lively discussion. A number of papers discussed general characteristics of intelligent control systems, and several presented case studies. DTIC

N95-16897*# Institute for Computer Applications in Science and Engineering, Hampton, VA.
ALGORITHMS FOR BILEVEL OPTIMIZATION Final Report
NATALIA ALEXANDROV and J. E. DENNIS, JR. NASA Sep. 1994
13 p Submitted for publication
(Contract(s)/Grant(s): NAS1-19480; RTOP 505-90-52-01)
(NASA-CR-194980; NAS 1.26:194980; ICASE-94-77) Avail: CASI HC A03/MF A01

General multilevel nonlinear optimization problems arise in design of complex systems and can be used as a means of regularization for multi-criteria optimization problems. Here, for clarity in displaying our ideas, we restrict ourselves to general bilevel optimization problems, and we present two solution approaches. Both approaches use a trust-region globalization strategy, and they can be easily extended to handle the general multilevel problem. We make no convexity assumptions, but we do assume that the problem has a nondegenerate feasible set. We consider necessary optimality conditions for the bi-level problem formulations and discuss results that can be extended to obtain multilevel optimization formulations with constraints at each level. Author

N95-16898*# Institute for Computer Applications in Science and Engineering, Hampton, VA.
ICASE Semiannual Report, 1 Apr. - 30 Sep. 1994
NASA Oct. 1994 122 p
(Contract(s)/Grant(s): NAS1-19480; NAS1-18605; NAS1-18107; NAS1-17070; NAS1-17130; NAS1-15810; NAS1-16394; NAS1-14101; NAS1-14472; RTOP 505-90-52-01)
(NASA-CR-195001; NAS 1.26:195001) Avail: CASI HC A06/MF A02

This report summarizes research conducted at the Institute for Computer Applications in Science and Engineering in the areas of (1) applied and numerical mathematics, including numerical analysis and algorithm development; (2) theoretical and computational research in fluid mechanics in selected areas of interest, including acoustics and combustion; (3) experimental research in transition and turbulence and aerodynamics involving Langley facilities and scientists; and (4) computer science. Author (revised)

N95-16906*# National Aeronautics and Space Administration. Lewis Research Center, Cleveland, OH.
A WORKSTATION BASED SIMULATOR FOR TEACHING COMPRESSIBLE AERODYNAMICS
THOMAS J. BENSON Dec. 1994 15 p Presented at the 33rd Aerospace Sciences Meeting, Reno, NV, 9-12 Jan. 1995; sponsored by AIAA
(Contract(s)/Grant(s): RTOP 505-62-52)
(NASA-TM-106799; E-9275; NAS 1.15:106799; AIAA PAPER 95-0070) Avail: CASI HC A03/MF A01

A workstation-based interactive flow simulator has been developed to aid in the teaching of undergraduate compressible aerodynamics. By solving the equations found in NACA 1135, the simulator models three basic fluids problems encountered in supersonic flow: flow past a compression corner, flow past two wedges in series, and flow past two opposed wedges. The study can vary the geometry or flow conditions through a graphical user interface and the new conditions are calculated immediately. Various graphical formats

present the results of the flow calculations to the student. The simulator includes interactive questions and answers to aid in both the use of the tool and to develop an understanding of some of the complexities of compressible aerodynamics. A series of help screens make the simulator easy to learn and use. Author

N95-17264*# National Aeronautics and Space Administration. Lewis Research Center, Cleveland, OH.
INTERACTIVE COMPUTER GRAPHICS APPLICATIONS FOR COMPRESSIBLE AERODYNAMICS
THOMAS J. BENSON Dec. 1994 17 p Presented at the 33rd Aerospace Sciences Meeting, Reno, NV, 9-12 Jan. 1995; sponsored by AIAA
(Contract(s)/Grant(s): RTOP 505-62-52)
(NASA-TM-106802; E-9279; NAS 1.15:106802; AIAA PAPER 95-0119) Avail: CASI HC A03/MF A01

Three computer applications have been developed to solve inviscid compressible fluids problems using interactive computer graphics. The first application is a compressible flow calculator which solves for isentropic flow, normal shocks, and oblique shocks or centered expansions produced by two dimensional ramps. The second application couples the solutions generated by the first application to a more graphical presentation of the results to produce a desk top simulator of three compressible flow problems: 1) flow past a single compression ramp; 2) flow past two ramps in series; and 3) flow past two opposed ramps. The third application extends the results of the second to produce a design tool which solves for the flow through supersonic external or mixed compression inlets. The applications were originally developed to run on SGI or IBM workstations running GL graphics. They are currently being extended to solve additional types of flow problems and modified to operate on any X-based workstation. Author

N95-18018 Naval Postgraduate School, Monterey, CA.
A PLATFORM INDEPENDENT APPLICATION OF LUX ILLUMINATION PREDICTION ALGORITHMS M.S. Thesis
MICHAEL T. LESTER Jun. 1994 126 p Limited Reproducibility: More than 20% of this document may be affected by microfiche quality (AD-A283669) Avail: CASI HC A07

Naval Aviators require prior knowledge of the time and location of astronomical phenomena in order to properly plan and execute combat and training operations during the hours of darkness using Night Vision Devices (NVD's). This thesis presents a computer application of illumination prediction algorithms which predict the time of selected astronomical phenomena. This computer program is platform independent (given the proper libraries), event-driven, object-oriented, and utilizes a Graphical User Interface (GUI). Using this application, operators in the field will be able to determine the time of selected phenomena and the quantity of illumination, measured in Lux, for a given time and date. DTIC

N95-18110*# Institute for Computer Applications in Science and Engineering, Hampton, VA.
FLOATING SHOCK FITTING VIA LAGRANGIAN ADAPTIVE MESHES Final Report
JOHN VANROSENDALE Nov. 1994 24 p Submitted for publication
(Contract(s)/Grant(s): NAS1-19480; RTOP 505-90-52-01)
(NASA-CR-194997; NAS 1.26:194997; ICASE-94-89) Avail: CASI HC A03/MF A01

In recent works we have formulated a new approach to compressible flow simulation, combining the advantages of shock-fitting and shock-capturing. Using a cell-centered Roe scheme discretization on unstructured meshes, we warp the mesh while marching to steady state, so that mesh edges align with shocks and other discontinuities. This new algorithm, the Shock-fitting Lagrangian Adaptive Method (SLAM) is, in effect, a reliable shock-capturing algorithm which yields shock-fitted accuracy at convergence. Shock-capturing algorithms like this, which warp the mesh to yield shock-fitted accuracy, are new and relatively untried. However, their

potential is clear. In the context of sonic booms, accurate calculation of near-field sonic boom signatures is critical to the design of the High Speed Civil Transport (HSCT). SLAM should allow computation of accurate N-wave pressure signatures on comparatively coarse meshes, significantly enhancing our ability to design low-boom configurations for high-speed aircraft. Author

N95-18365# Wright Lab., Wright-Patterson AFB, OH.
UNIVERSAL WIND TUNNEL DATA ACQUISITION AND REDUCTION SOFTWARE Final Report, Jan. 1990 - Apr. 1993
GLENN W. WILLIAMS Jan. 1994 128 p
(Contract(s)/Grant(s): AF PROJ. 2404)
(AD-A283897; WL-TR-94-3063) Avail: CASI HC A07/MF A02

A software system was designed to support the data acquisition and reduction requirements of six wind tunnels (three continuous flow and three blow down) and a force/pressure laboratory. In order to make it easier for users to identify and select the command options available, a drop down menu was developed for use as the primary interface between the operator and the software. This drop down menu was developed before window terminals were available, and thus it works on VT100 type terminals. Because some operations/procedures are recurring during a specific test and include a series of menu commands, a macro feature was included as a user maintainable function in order to reduce a set of commands/operations to a single keystroke. The facility hardware configuration and data output formats are coded into the system by editing text files, no compilation or linking is required. DTC

N95-18564# California Univ., Los Angeles, CA. Flight Systems Research Center.

MINIMAL TIME DETECTION. ALGORITHMS AND APPLICATIONS TO FLIGHT SYSTEMS

ALEXANDER TARTAKOVSKY Dec. 1993 86 p
(TR-2-FSRC-93) Avail: CASI HC A05/MF A01

The report focuses on sequential algorithms to detect changes in statistical models of observed random data when these occur at unknown points in time and statistical properties of observations after change occurrence depend on change time. Besides it is assumed that the samples are non-identically distributed and the amount of a change is unknown. The development of well-known results in change-point detection problems for such a model has great importance for various applications, for example for testing of flight systems. A maximum likelihood detection algorithm (with respect to an unknown change time) is investigated for independent non-identically distributed observations. It is proved that this procedure is asymptotically optimal with respect to expect detection delay (i.e., is a minimal time-detection algorithm) when the mean time until false alarm (or between false detections) tends to infinity. Several asymptotically optimal and non-optimal simple modifications of the maximum likelihood algorithm are also considered. For the case of an unknown amount of change two approaches are proposed. The first one consists of the testing of multiple hypotheses. The second approach is based on the use of the double maximum likelihood principle both for unknown change in time and unknown parameter after change. An asymptotically optimal (minimal time) multialternative sequential algorithm is constructed and analyzed. In contrast to the adaptive algorithm the multialternative one ensures minimal detection delay only for several isolated points, but does not require estimation of an unknown amount and hence can be used for moderate sample size. Finally, proposed minimal time detection algorithms are applied in the problem of identification of aircraft system parameters from flight test data during flight control. Author

N95-18899*# National Aeronautics and Space Administration. Langley Research Center, Hampton, VA.

DYNAMIC STABILITY INSTRUMENTATION SYSTEM (DSIS). VOLUME 1: HARDWARE DESCRIPTION

T. L. JORDAN, T. S. DANIELS, D. A. HARE, R. P. BOYDEN, and D. A. DRESS Nov. 1994 91 p
(Contract(s)/Grant(s): RTOP 505-59-54-02)

(NASA-TM-109160-VOL-1; NAS 1.15:109160-VOL-1) Avail: CASI HC A05/MF A01

This paper is a hardware description manual for the Dynamic Stability Instrumentation System that is used in specific NASA Langley wind tunnels. The instrumentation system performs either a synchronous demodulation or a fast Fourier transform on dynamic balance strain gage signals, and ultimately computes aerodynamic coefficients. The DSIS consists of a double rack of instruments, a remote motor-generator set, two special stings each with motor driven shafts, and specially designed balances. The major components in the instrumentation rack include a personal computer, digital signal processor microcomputers, computer-controlled signal conditioners, function generator, digital multimeter, and an optional fast Fourier transform analyzer. Author

16 PHYSICS

Includes physics (general); acoustics; atomic and molecular physics; nuclear and high-energy physics; optics; plasma physics; solid-state physics; and thermodynamics and statistical physics.

A95-63522

THE EFFECTS OF AIRCRAFT (B-52) OVERFLIGHTS ON ANCIENT STRUCTURES

J. C. BATTIS Phillips Lab., Hanscom Air Force Base, MA Journal of Sound and Vibration (ISSN 0022-460X) vol. 171, no. 2 March 24, 1994 p. 267-283 refs

(BTN-94-EIX94341340070) Copyright

To simulate combat missions for the American bomber force, the Air Combat Command conducts low altitude training flights along routes throughout the U.S.A. This paper presents the results of an effort to evaluate the effect of these overflights on the many archaeologically significant structures located beneath the training routes. This study has shown that: (1) low overflights can induce measurable vibrations in these ancient structures; (2) the overflight induced motions do not constitute an appreciable threat to the sites; and (3) the observed levels of motion are no greater than those induced by sources in the natural environment. Although these findings are specific to overflights by B-52s, comparison of the low frequency acoustic signature of the B-52 and that of the B-1B overflights should not pose a significantly greater threat to the structures than B-52 overflights. Author (EI)

A95-63639

ON THE PARTICULAR FEATURES OF DYNAMIC PROCESSES IN SOLIDS WITH VARYING BOUNDARY DURING INTERACTION WITH INTENSIVE HEAT FLOWS

E. M. KARTASHOV Akademiya Tonkoj Khimicheskoi Tekhnologii, Moscow (Russia), A. A. RKHIMA, and A. G. RUBIN Izvestiya VUZ: Aviatsonnaya Tekhnika (ISSN 0579-2975) no. 1 January-March 1994 p. 30-34 In RUSSIAN refs
(BTN-94-EIX94461408756) Copyright

Dynamic thermoelastic reaction of a solid during heat shock has been studied. The movement in time of the boundary of the thermal stressed state was considered. This movement may take place due to the burn out of the material on the surface, caused by the melting, with the melted area being blown away continuously. This may be explained by the surface destruction and other processes associated with high temperatures. It has been shown that as the velocity of the movement of the boundary grows, compressing stresses, temperature, and deformations increase. EI

N95-16226# Army Aeromedical Research Lab., Fort Rucker, AL.
THE ASSESSMENT OF THE AH-64D, LONGBOW, MAST-MOUNTED ASSEMBLY NOISE HAZARD FOR MAINTENANCE PERSONNEL Final Report
BEN T. MOZO and ELMAREE GORDON Jul. 1994 40 p

16 PHYSICS

(AD-A284971; USAARL-94-37) Avail: CASI HC A03/MF A01

Noise levels around the AH-64 helicopter exceed safe limits. Maintenance personnel are required to wear hearing protection to reduce hazard to hearing while performing maintenance procedures. This evaluation was directed at determining the contribution to noise levels by the auxiliary power unit (APU), auxiliary ground power unit (AGPU), environmental control system (ECS), and mast mounted assembly (MMA) at a variety of maintenance positions and establish protection capabilities of standard protectors for those noise levels. DTIC

N95-16401*# Missouri Univ., Rolla, MO. Dept. of Mechanical and Aerospace Engineering and Engineering Mechanics.

DUCTED FAN ACOUSTIC RADIATION INCLUDING THE EFFECTS OF NONUNIFORM MEAN FLOW AND ACOUSTIC TREATMENT Final Technical Report, 31 Aug. 1981 - 30 Jun. 1993

WALTER EVERSMA and INDRANIL DANDA ROY Jul. 1993 80 p

(Contract(s)/Grant(s): NAG3-178)

(NASA-CR-197449; NAS 1.26:197449) Avail: CASI HC A05/MF A01

Forward and aft acoustic propagation and radiation from a ducted fan is modeled using a finite element discretization of the acoustic field equations. The fan noise source is introduced as equivalent body forces representing distributed blade loading. The flow in and around the nacelle is assumed to be nonuniform, reflecting the effects of forward flight and flow into the inlet. Refraction due to the fan exit jet shear layer is not represented. Acoustic treatment on the inlet and exhaust duct surfaces provides a mechanism for attenuation. In a region enclosing the fan a pressure formulation is used with the assumption of locally uniform flow. Away from the fan a velocity potential formulation is used and the flow is assumed nonuniform but irrotational. A procedure is developed for matching the two regions by making use of local duct modal amplitudes as transition state variables and determining the amplitudes by enforcing natural boundary conditions at the interface between adjacent regions in which pressure and velocity potential are used. Simple models of rotor alone and rotor/exit guide vane generated noise are used to demonstrate the calculation of the radiated acoustic field and to show the effect of acoustic treatment. The model has been used to assess the success of four techniques for acoustic lining optimization in reducing far field noise. Author

N95-16848*# Pennsylvania State Univ., State College, PA. Applied Research Lab.

ACTIVE MINIMIZATION OF ENERGY DENSITY IN THREE-DIMENSIONAL ENCLOSURES Performance Report, Dec. 1993 - Dec. 1994

SCOTT D. SOMMERFELDT 23 Nov. 1994 8 p

(Contract(s)/Grant(s): NAG1-1557)

(NASA-CR-197213; NAS 1.26:197213) Avail: CASI HC A02/MF A01

The objective of this research project is to further investigate and develop a novel approach for actively controlling the sound field in enclosures. Typically the acoustic field in an enclosure has been controlled by minimizing the sum of the squared pressures from several microphones distributed throughout the enclosure. The approach being investigated in this project involves minimizing the acoustic energy density at the sensor locations, rather than the squared pressure. Previous research in a simple one-dimensional enclosure showed that improved global attenuation of the acoustic field is often obtained by minimizing the energy density, rather than the pressure. The current project builds on the previous research by extending the method of controlling the acoustic energy density to three-dimensional enclosures. The results will establish if improved control can still be expected in a more general enclosure. Pending successful results, the method could be applied to control problems such as attenuating the acoustic noise in an aircraft fuselage, an automobile cabin, or other general enclosures. The research project was set up as a two-year project designed to achieve both numerical and experimental results. The primary focus of the first year of

research (now being completed) was on the analytical/numerical modeling of the method of controlling the acoustic energy density. During the second year, the research focuses on experimental verification of the approach and extending our understanding of the method. Derived from text

N95-17334# Army Aeromedical Research Lab., Fort Rucker, AL. **FACTORS AFFECTING THE VISUAL FRAGMENTATION OF THE FIELD-OF-VIEW IN PARTIAL BINOCULAR OVERLAP DISPLAYS** Final Report

VICTOR KLYMENKO, ROBERT W. VERONA, HOWARD H. BEASLEY, JOHN S. MARTIN, and WILLIAM E. MCLEAN (Universal Energy Systems, Inc., Daleville, AL.) Jun. 1994 55 p

(Contract(s)/Grant(s): DA PROJ. 3E1-62787-A-879)

(AD-A283081; USAARL-94-29) Avail: CASI HC A04/MF A01

Small fields-of-view (FOV) are detrimental to the visual tasks required of military pilots. In order to increase the extent of the visual world available to U.S. Army helicopter pilots using helmet mounted displays (HMD), without incurring increases in size or weight or losses in central resolution, an unusual method of display - partial binocular overlap - has been proposed. Two flanking monocular regions and a central binocular overlap region constitute the FOV in partial binocular overlap displays. DTIC

N95-18542 Duke Univ., Durham, NC.

ACOUSTIC RADIATION DAMPING OF FLAT RECTANGULAR PLATES SUBJECTED TO SUBSONIC FLOWS Ph.D. Thesis

KAREN HEITMAN LYLE 1993 118 p

Avail: Univ. Microfilms Order No. DA9414114

The acoustic radiation damping for various isotropic and laminated composite plates and semi-infinite strips subjected to a uniform subsonic and steady flow has been predicted. The predictions are based on the linear vibration of a flat plate. The fluid loading is characterized as the perturbation pressure derived from the linearized Bernoulli and continuity equations. Parameters varied in the analysis include Mach number, mode number and plate size, aspect ratio and mass. The predictions are compared with existing theoretical results and experimental data. The analytical results show that the fluid loading can significantly affect realistic plate responses. Generally, graphite/epoxy and carbon/carbon plates have higher acoustic radiation damping values than similar aluminum plates, except near plate divergence conditions resulting from aeroelastic instability. Universal curves are presented where the acoustic radiation damping normalized by the mass ratio is a linear function of the reduced frequency. A separate curve is required for each Mach number and plate aspect ratio. In addition, acoustic radiation damping values can be greater than or equal to the structural component of the modal critical damping ratio (assumed as 0.01) for the higher subsonic Mach numbers. New experimental data were acquired for comparison with the analytical results.

Dissert. Abstr.

N95-18912# Deutsche Forschungsanstalt fuer Luft- und Raumfahrt, Goettingen (Germany). Inst. fuer Stroemungsmechanik.

FLOW FIELD INVESTIGATION IN A FREE JET - FREE JET CORE SYSTEM FOR THE GENERATION OF HIGH INTENSITY MOLECULAR BEAMS Ph.D. Thesis [UNTERSUCHUNG DER STROEMUNG IN EINEM FREISTRABL-KERNFREISTRABL-SYSTEM ZUR ERZEUGUNG INTENSIVER MOLEKULARSTRAHLEN]

BENT FRITSCHKE 1994 219 p In GERMAN Original contains color illustrations (ISSN 0939-2963)

(DLR-FB-94-11) Avail: CASI HC A10/MF A03

In a free jet - free jet core system the first skimmer is (unlike in conventional molecular beam systems) operated in continuum flow. This until now rarely examined concept is treated in detail experimentally and theoretically. Investigated are the influence of skimmer geometry, pumping capacity, gas properties, Mach and Knudsen number, skimmer boundary layer and condensation. The main emphasis of the work is put on the treatment of the arising shocks.

This leads to criteria for optimizing the system as a source for molecular beams with previously not achieved intensities and as a wind tunnel for the experimental investigation of gas-surface interactions under orbital conditions. Author

N95-19142# Advisory Group for Aerospace Research and Development, Neuilly-Sur-Seine (France). Structures and Materials Panel. IMPACT OF ACOUSTIC LOADS ON AIRCRAFT STRUCTURES [IMPACT DES SOLICITATIONS ACOUSTIQUES SUR LES STRUCTURES D'AERONEFS]

Sep. 1994 265 p In ENGLISH and FRENCH Symposium held in Lillehammer, Norway, May 1994 Original contains color illustrations (AGARD-CP-549; ISBN-92-836-0001-0) Copyright Avail: CASI HC A12/MF A03

A broad band of different activities was addressed in the Specialists' Meeting held by the Structures and Materials Panel of AGARD in May 1994: Topics dealt with the acoustic environment in subsonic and hypersonic flow regimes, innovative structural design techniques and materials for fatigue resistant structures, and experimental and analytical tools for evaluation of the behavior of structures in an acoustically and thermally adverse environment. For individual titles, see N95-19143 through N95-19167.

N95-19143# British Aerospace Aircraft Group, Warton (England). Military Aircraft Div.

CURRENT AND FUTURE PROBLEMS IN STRUCTURAL ACOUSTIC FATIGUE

P. D. GREEN In AGARD, Impact of Acoustic Loads on Aircraft Structures 5 p Sep. 1994

Copyright Avail: CASI HC A01/MF A03

Acoustic fatigue failures can be caused by the dynamic response of aircraft structures to unsteady pressure loading from aerodynamic and engine acoustic sources. The life of structures is often difficult to assess accurately and may be greatly affected by steady thermal, in-plane and out-of-plane loads. Furthermore, currently available methods do not enable fatigue life assessment of the substructure to be made, despite these failures occurring regularly in service. This paper discusses current problems associated with structural acoustic fatigue and extends upon this to account for likely clearance philosophies and configurations for future aircraft. Author

N95-19144# Eurocopter Deutschland G.m.b.H., Munich (Germany). HELICOPTER INTERNAL NOISE

G. NIESL and E. LAUDIEN (Daimler-Benz A.G., Munich, Germany.) In AGARD, Impact of Acoustic Loads on Aircraft Structures 12 p Sep. 1994 Sponsored in part by BRITE/EURAM (Contract(s)/Grant(s): PROJ. RHINO)

Copyright Avail: CASI HC A03/MF A03

Compared to fixed wing aircraft, helicopter interior noise is higher, and subjectively more annoying. This is mainly due to discrete frequencies by the main transmission system, and also from other components like main and tail rotor, engines, or cooling fans. Up to now, mainly passive measures have been used for interior noise reduction. Despite intensive experimental and theoretical investigation to improve acoustic treatment, their weight penalties remain high especially in the low frequency range. Here, active noise control offers additional capacities without excessive weight efforts. Loud-speaker based systems are sufficiently well developed for implementing a prototype system in the helicopter. Two other principles are in development: active panel control which introduces mechanical actuators to excite the cabin walls, and active control of gearbox struts with actuators in the load path between gearbox and fuselage. Author

N95-19145# Dassault Aviation, Saint-Cloud (France). AEROACOUSTIC QUALIFICATION OF HERMES SHINGLES [DIMENSIONNEMENT ET QUALIFICATION

AEROACOUSTIQUE DES TUILES HERMES]

C. PETIAU and A. PARET In AGARD, Impact of Acoustic Loads on Aircraft Structures 17 p Sep. 1994 In ENGLISH and FRENCH Copyright Avail: CASI HC A03/MF A03

General problems of aeroacoustic analysis are presented, taking as an example shingle studies of the HERMES space shuttle. Analysis of shingle behavior meets this problem in a particularly difficult way (very hard environment, specific difficulties due to design of shingles). Available analysis tools include: (1) calculation means, which are mainly those of aeroelasticity, and (2) ground test means (wind tunnel, progressive wave tubes, shaker,...). None of these means can alone satisfy the needs of structural dimensioning and qualification; in particular the calculation of turbulent sources is not possible today, and they are very difficult to simulate with ground testing of actual structural parts. In spite of these difficulties, and referring to the preliminary tests and calculations of HERMES shingles, a rational strategy is proposed for aeroacoustic dimensioning and qualification of structural parts. This leads to a succession of tests, the conditions of which are determined by calculations, calculation models being themselves validated by comparison with test results. Author

N95-19146# Wright Lab., Wright-Patterson AFB, OH. Structural Dynamics Branch.

WEAPONS BAY ACOUSTIC ENVIRONMENT

L. L. SHAW and R. M. SHIMOVETZ In AGARD, Impact of Acoustic Loads on Aircraft Structures 10 p Sep. 1994

Copyright Avail: CASI HC A02/MF A03

An aircraft weapons bay exposed to freestream flow experiences an intense aeroacoustic environment in and around the bay. Experience has taught that the intensity of this environment can be severe enough to result in damage to a store, its internal equipment, or the structure of the weapons bay itself. To ensure that stores and sensitive internal equipment can withstand this hazardous environment and successfully complete the mission, they must be qualified to the most severe sound pressure levels anticipated for the mission. If the qualification test levels are too high, the store and its internal equipment will be over designed, resulting in unnecessary costs and possible performance penalties. If the qualification levels are below those experienced in flight, the store or its internal equipment may catastrophically fail during performance of the mission. Thus, it is desirable that the expected levels in weapons bays be accurately predicted. A large number of research efforts have been directed toward understanding flow-induced cavity oscillations. However, the phenomena are still not adequately understood to allow one to predict the fluctuating pressure levels for various configurations and flow conditions. This is especially true at supersonic flow speeds, where only a small amount of data are available. This paper will give a background of flow induced cavity oscillations and discuss predictions, control and suppression, and the future of weapons bay acoustic environments. A large number of research efforts have been directed toward understanding flow-induced cavity oscillations. However, the phenomena are still not adequately understood to allow one to predict the fluctuating pressure levels for various configurations and flow conditions. This is especially true at supersonic flow speeds, where only a small amount of data are available. This paper will give a background of flow induced cavity oscillations and discuss predictions, control and suppression, and the future of weapons bay acoustic environments. Author

N95-19147# Alenia, Turin (Italy).

IMPACT OF NOISE ENVIRONMENT ON ENGINE NACELLE DESIGN

R. GIUZIO, E. DALLE-MURA, and G. GIUFFRE In AGARD, Impact of Acoustic Loads on Aircraft Structures 11 p Sep. 1994

Copyright Avail: CASI HC A03/MF A03

The present paper describes the general philosophy and the followed methodology in engine nacelle design, usually resulting in the embodiment of acoustic treatment in intake and exhaust ducts

to make the relevant aircraft compliant with noise certification requirements. A general description of conventional acoustic liners currently in service, and liners of innovative design currently being investigated is also included, giving emphasis to the methodology for the selection of the proper acoustic treatment. Finally the Alenia software package (ALNOIS), ad hoc developed to cover the complete engine nacelle acoustic design and to support the acoustic panels manufacturing, is briefly described. Author

N95-19148*# National Aeronautics and Space Administration. Langley Research Center, Hampton, VA.
IMPACT OF DYNAMIC LOADS ON PROPULSION INTEGRATION

J. M. SEINER *In* AGARD, Impact of Acoustic Loads on Aircraft Structures 14 p Sep. 1994
 Copyright Avail: CASI HC A03/MF A03

Aircraft dynamic loads produced by engine exhaust plumes are examined for a class of military fighter and bomber configurations in model and full scale. The configurations examined are associated with the USAF F-15 and B-1B aircraft, and the US F-18 HARV and ASTOVL programs. The experience gained as a result of these studies is used to formulate a level of understanding concerning this phenomena that could be useful at the preliminary stage of propulsion/airframe design. Author

N95-19149# Wright Lab., Wright-Patterson AFB, OH. Chief, Structural Integrity Branch.
HIGH-TEMPERATURE ACOUSTIC TEST FACILITIES AND METHODS

JEROME PEARSON *In* AGARD, Impact of Acoustic Loads on Aircraft Structures 9 p Sep. 1994
 Copyright Avail: CASI HC A02/MF A03

The Wright Laboratory is the Air Force center for air vehicles, responsible for developing advanced technology and incorporating it into new flight vehicles and for continuous technological improvement of operational air vehicles. Part of that responsibility is the problem of acoustic fatigue. With the advent of jet aircraft in the 1950's, acoustic fatigue of aircraft structure became a significant problem. In the 1960's the Wright Laboratory constructed the first large acoustic fatigue test facilities in the United States, and the laboratory has been a dominant factor in high-intensity acoustic testing since that time. This paper discusses some of the intense environments encountered by new and planned Air Force flight vehicles, and describes three new acoustic test facilities of the Wright Laboratory designed for testing structures in these dynamic environments. These new test facilities represent the state of the art in high-temperature, high-intensity acoustic testing and random fatigue testing. They will allow the laboratory scientists and engineers to test the new structures and materials required to withstand the severe environments of captive-carry missiles, augmented lift wings and flaps, exhaust structures of stealth aircraft, and hyper-sonic vehicle structures well into the twenty-first century. Author

N95-19156# Deutsche Aerospace A.G., Bremen (Germany).
ACOUSTIC FATIGUE TESTING ON DIFFERENT MATERIALS AND SKIN-STRINGER ELEMENTS

KLAUS KOENIG *In* AGARD, Impact of Acoustic Loads on Aircraft Structures 11 p Sep. 1994
 Copyright Avail: CASI HC A03/MF A03

Within a comparative study, 29 different coupons covering 8 different designs and 6 different materials were fatigued by an excitation of 30 g (exp 2)/Hz on a shaker. The selected designs and materials represent realistic alternatives of an aircraft surface structure. The investigation led to the following conclusion: (1) Besides classical aluminium, CFRP is the best material with regard to sonic fatigue. (2) Al/Li, ARALL and Al layer materials showed shorter life times than the classical Al. (3) The most striking improvement in design for the dimensions selected here was achieved with separate doublers between skin and stringer. (4) The modal damping found was most often smaller than the 1.7 percent of the critical as known

from ESDU for Al. (5) Pure CFRP without rivets showed the smallest damping: 0.6 - 0.9 percent. Author

N95-19157# McDonnell-Douglas Corp., Saint Louis, MO.
ACOUSTIC FATIGUE CHARACTERISTICS OF ADVANCED MATERIALS AND STRUCTURES

J. H. JACOBS and M. A. FERMAN (Saint Louis Univ., Cahokia, IL.)
In AGARD, Impact of Acoustic Loads on Aircraft Structures 9 p Sep. 1994

Copyright Avail: CASI HC A02/MF A03

A summary of McDonnell Douglas Aerospace's (MDA) capability for treating acoustic loading on modern fighter aircraft structure is given. A brief overview of techniques that have been developed since the mid-70's are presented. In metallic structure fabrication concepts such as Super Plastic Formed/Diffusion Bonding (SPF/DB) suddenly required new analysis procedures. In addition, the 1980's brought the additional complications of structures exposed to high thermal and acoustic environments on such vehicles as the AV-8B Harrier II and National Aerospace Plane (NASP). Methods developed to handle these new material forms, intense noise, and thermal loads are discussed. The influences of nonlinear structural responses on fatigue life due to combined load environments are also discussed. Additional developments in thermal-acoustic testing capability are also discussed. Author

N95-19159# Dassault Aviation, Saint-Cloud (France). Structures Div.
BRITE-EURAM PROGRAMME: ACOUFAT ACOUSTIC FATIGUE AND RELATED DAMAGE TOLERANCE OF ADVANCED COMPOSITE AND METALLIC STRUCTURES

D. TOUGARD *In* AGARD, Impact of Acoustic Loads on Aircraft Structures 12 p Sep. 1994 Sponsored in cooperation with the European Community and ACOUFAT
 Copyright Avail: CASI HC A03/MF A03

The Brite/Euram programme ACOUFAT is concerned with 'Acoustic fatigue and related damage tolerance of advanced composite and metallic structure'. Three main fields of the ACOUFAT results are discussed: (1) The use of a 'frequency degradation' criterion, usually applied to classical metallic materials and early Carbon Fiber Reinforced Plastic (CFRP) materials, is not considered suitable, as the only parameter, for determination of CFRP specimen 'failure' in acoustic fatigue. It is suggested that a suitable criterion should be based, in further work, upon the degradation of the mechanical properties of the specimens; (2) On the basis of Wind-Tunnel (WT) calibration tests, a semi-empirical model of the spatio-temporal characteristics of the aero-acoustic loads exerted on a flat panel by the turbulent field created by a flap has been developed and utilized as 'Load Data Input' for Finite Element (FE) calculations. The WT tests have been reasonably well presented: the development of this semi-empirical model is an encouraging initial success. The results from the initial modelling suggest that this can be extended to the modelling of the acoustic loads in Progressive Wave Tubes (PWT); and (3) The excitation of structures by aero-acoustic loads may not be simulated fully in PWT by simply modifying and correctly shaping the spectral content. The effect of the spatial distribution of the loading is clearly different in both cases and the tested specimen endurance may be significantly different. It is clear that a theoretical approach based on a correct prediction of the responses to both types of environment is required. Author

N95-19162# British Aerospace Aircraft Group, Bristol (England).
APPLICATION OF SUPERPLASTICALLY FORMED AND DIFFUSION BONDED STRUCTURES IN HIGH INTENSITY NOISE ENVIRONMENTS

R. J. CUMMINS and J. P. C. WONG *In* AGARD, Impact of Acoustic Loads on Aircraft Structures 10 p Sep. 1994
 Copyright Avail: CASI HC A02/MF A03

Two specimens, representing an aircraft control surface and an access door, have been tested under high intensity acoustic excitation. The access door was also subjected to an elevated temperature environment of 150 C during this test. These specimens were

manufactured as multi-cell box configurations by superplastic forming and diffusion bonding (SPFDB) to a similar structural weight as existing aircraft components produced by alternative means of construction. The influence of the spandrel-shaped void, formed at the skin/stringer intersection, on the acoustic fatigue performance is considered. Author (revised)

**N95-19163# Alenia Spazio S.p.A., Turin (Italy).
AN OVERALL APPROACH OF COCKPIT NOISE
VERIFICATION IN A MILITARY AIRCRAFT**

R. GIUZIO and M. NORESE (Aeronautica Macchi S.p.A., Varese, Italy.) *In* AGARD, Impact of Acoustic Loads on Aircraft Structures 12 p Sep. 1994

Copyright Avail: CASI HC A03/MF A03

The present paper describes the applicable concepts for cockpit noise verification in military aircraft. A design-to-noise procedure is outlined and the overall requirements for medical, intelligibility and operational aspects are discussed, including the proposition of an adequate index to quantify the quality of noise at the pilot's ear. Guidelines for cockpit noise control, to be applied during the design phase of the project, are given together with the expected benefits. Advanced noise control measures and noise measuring techniques are also dealt with and a specific case of cockpit noise verification is described. Author (revised)

**N95-19164# National Research Council of Canada, Ottawa (Ontario).
Inst. for Aerospace Research.**

**NOISE TRANSMISSION AND REDUCTION IN TURBOPROP
AIRCRAFT**

DOUGLAS G. MACMARTIN, GORDON L. BASSO, and BARRY LEIGH (De Havilland Aircraft Co. of Canada Ltd., Downsview, Ontario.) *In* AGARD, Impact of Acoustic Loads on Aircraft Structures 9 p Sep. 1994

Copyright Avail: CASI HC A02/MF A03

There is considerable interest in reducing the cabin noise environment in turboprop aircraft. Various approaches have been considered at deHaviland Inc., including passive tuned-vibration absorbers, speaker-based noise cancellation, and structural vibration control of the fuselage. These approaches will be discussed briefly. In addition to controlling the noise, a method of predicting the internal noise is required both to evaluate potential noise reduction approaches, and to validate analytical design models. Instead of costly flight tests, or carrying out a ground simulation of the propeller pressure field, a much simpler reciprocal technique can be used. A capacitive scanner is used to measure the fuselage vibration response on a deHaviland Dash-8 fuselage, due to an internal noise source. The approach is validated by comparing this reciprocal noise transmission measurement with the direct measurement. The fuselage noise transmission information is then combined with computer predictions of the propeller pressure field data to predict the internal noise at two points. Author

**N95-19274# Central Aerohydrodynamics Inst., Zhukovskiy (Russia).
OPTICAL SURFACE PRESSURE MEASUREMENTS:**

ACCURACY AND APPLICATION FIELD EVALUATION

A. BUKOV, V. MOSHAROV, A. ORLOV, V. PESETSKY, V. RADCHENKO, S. PHONOV, S. MATYASH, M. KUZMIN (Moscow M. V. Lomonosov Inst. of the Technology of Fine Chemicals, USSR.), and N. SADOVSKII (Moscow M. V. Lomonosov Inst. of the Technology of Fine Chemicals, USSR.) *In* AGARD, Wall Interference, Support Interference and Flow Field Measurements 9 p Jul. 1994

Copyright Avail: CASI HC A02/MF A04

Optical pressure measurement (OPM) is a new pressure measurement method rapidly developed in several aerodynamic research centers: TsAGI (Russia), Boeing, NASA, McDonnell Douglas (all USA), and DLR (Germany). Present level of OPM-method provides its practice as standard experimental method of aerodynamic investigations in definite application fields. Applications of OPM-method are determined mainly by its accuracy. The accuracy

of OPM-method is determined by the errors of three following groups: (1) errors of the luminescent pressure sensor (LPS) itself, such as uncompensated temperature influence, photo degradation, temperature and pressure hysteresis, variation of the LPS parameters from point to point on the model surface, etc.; (2) errors of the measurement system, such as noise of the photodetector, nonlinearity and nonuniformity of the photodetector, time and temperature offsets, etc.; and (3) methodological errors, owing to displacement and deformation of the model in an airflow, a contamination of the model surface, scattering of the excitation and luminescent light from the model surface and test section walls, etc. OPM-method allows getting total error of measured pressure not less than 1 percent. This accuracy is enough to visualize the pressure field and allows determining total and distributed aerodynamic loads and solving some problems of local aerodynamic investigations at transonic and supersonic velocities. OPM is less effective at low subsonic velocities (M less than 0.4), and for precise measurements, for example, an airfoil optimization. Current limitations of the OPM-method are discussed on an example of the surface pressure measurements and calculations of the integral loads on the wings of canard-aircraft model. The pressure measurement system and data reduction methods used on these tests are also described. Author

17

SOCIAL SCIENCES

Includes social sciences (general); administration and management; documentation and information science; economics and cost analysis; law and political science; and urban technology and transportation.

A95-63656

ON A PROGRAM-INFORMATION SYSTEM TDSoft

A. F. DREGALIN KGTU, Kazan (Russia), R. R. NAZYROVA, T. R. SITDIKOV, and I. N. BALASHOV *Izvestiya VUZ: Aviatsonnaya Tekhnika* (ISSN 0579-2975) no.1 January-March 1994 p. 102-106 *In* RUSSIAN refs (BTN-94-EIX94461408773) Copyright

The program-information system TDsoft is designed to investigate heat processes in engines of flying vehicles. The analysis of processes in engines of flying vehicles is based on high-temperature thermodynamics methods. These methods are using characteristics of individual compounds and components. Unlike the programs designed for thermodynamic calculations and developed for computers of preceding generations, the TDsoft system provides more reliable methods of making thermodynamic calculations of low-temperature systems. Besides, the system is provided with a dialogue interface 'man - computer' for both regular and irregular users. EI

A95-64855

THE ICAO CNS/ATM SYSTEM: NEW KING, NEW LAW?

B. D. K. HENAKU Univ. of Leiden, Netherlands *Air and Space Law* (ISSN 0927-3379) vol. 19, no. 3 June 1994 p. 146-151 (HTN-95-50218) Copyright

The International Civil Aviation Organization (ICAO) Communication Navigation Surveillance/Air Traffic Management (CNS/ATM) system is designed to improve air navigation facilities and systems. With the implementation of this system, the impact of space satellites will not only be felt in the technical side of air navigation but also in the legal framework designed to regulate that sector. Some introductory observations are made regarding the fields of law that may have to be taken into consideration in the quest to govern this new air navigation system. Questions are: What law should govern the satellite-based air navigation system; and what are some of the legal approaches that may have to be readdressed? Relevant aspects of space law are examined along with telecommunication law and air law. Hemer

17 SOCIAL SCIENCES

A95-64856

AIRCRAFT ACCIDENT INVESTIGATION AND AIRWORTHINESS — A PRACTICAL EXAMPLE OF THE INTERACTION OF TWO DISCIPLINES WITH SOME REFLECTIONS ON POSSIBLE LEGAL CONSEQUENCES

PETER MARTIN *Air and Space Law* (ISSN 0927-3379) vol. 19, no. 3 June 1994 p. 158-163 (HTN-95-50219) Copyright

The fundamental purpose of the investigation of air accidents is to determine the circumstances and causes of the accident with a view to the preservation of life and the avoidance of accident in the future. In the United Kingdom (UK), an air accident report usually incorporates recommendations made to the authority entitled to receive the report concerning the preservation of life and accident prevention. It is the duty of the Civil Aviation Authority to evaluate, and if it chooses, to implement the safety recommendations made by the Air Accident Investigation Branch to the Secretary of State for Transport. The interaction of these two entities as examined along with the legal ramifications of their actions. Hemer

A95-64857

WORLD TRENDS IN AIR TRANSPORT POLICIES. (APPROACHING THE 21ST CENTURY)

HENRI A. WASSENBERGH *Leiden Univ., Netherlands Air and Space Law* (ISSN 0927-3379) vol. 19, no. 3 June 1994 p. 174-178

(HTN-95-50220) Copyright

An alternative solution is sought to the continued participation in international air transport by all countries of the world, and especially the countries in stages of development. The alternative to international cross-border inter-air carrier cooperation for developing nations, is enlightened protection. This is an air policy, which does not isolate the national airline industry from the world air traffic market, does not freeze the capacity of the foreign air carriers, nor make the growth of foreign capacity on a route dependent on the growth of the capacity of the national air carrier on that route; a policy which allows for and stimulates growth of the market. Hemer

A95-64860

EC AVIATION SCENE

BEREND J. H. CRANS *De Brauw Blackstone, Westbroek, Amsterdam, Netherlands* and STEVEN P. CRAS *De Brauw Blackstone, Westbroek, Amsterdam, Netherlands Air and Space Law* (ISSN 0927-3379) vol. 19, no. 1 February 1994 p. 31-39 (HTN-95-50223) Copyright

Some of the developments are addressed in European Community (EC) air transport law that have taken place since the last issue of this journal. The following matters are discussed: (1) Common rules for the allotment of slots at Community airports; (2) A procedure relating to a Commission decision to the application of Regulation (EEC) No 2408/92; and (3) The agreement between the EC and the government of the USA concerning the application of the GATT agreement on trade in civil aircraft on trade in large civil aircraft. The Agreement tries to prevent disputes between the USA (Boeing) and the EC (Airbus) regarding government support to the manufacture and trade in large civil aircraft. Hemer

N95-18573*# National Aeronautics and Space Administration, Washington, DC.

NASA HIGH PERFORMANCE COMPUTING AND COMMUNICATIONS PROGRAM Annual Report, 1993

LEE HOLCOMB, PAUL SMITH, and PAUL HUNTER Nov. 1994 121 p (NASA-TM-4653; NAS 1.15:4653) Avail: CASI HC A06/MF A02

The National Aeronautics and Space Administration's HPCC program is part of a new Presidential initiative aimed at producing a 1000-fold increase in supercomputing speed and a 1(X)-fold improvement in available communications capability by 1997. As more advanced technologies are developed under the HPCC program, they will be used to solve NASA's 'Grand Challenge' problems,

which include improving the design and simulation of advanced aerospace vehicles, allowing people at remote locations to communicate more effectively and share information, increasing scientists' abilities to model the Earth's climate and forecast global environmental trends, and improving the development of advanced spacecraft. NASA's HPCC program is organized into three projects which are unique to the agency's mission: the Computational Aerosciences (CAS) project, the Earth and Space Sciences (ESS) project, and the Remote Exploration and Experimentation (REE) project. An additional project, the Basic Research and Human Resources (BRHR) project, exists to promote long term research in computer science and engineering and to increase the pool of trained personnel in a variety of scientific disciplines. This document presents an overview of the objectives and organization of these projects, as well as summaries of early accomplishments and the significance, status, and plans for individual research and development programs within each project. Areas of emphasis include benchmarking, testbeds, software and simulation methods. Author

N95-18578# General Accounting Office, Washington, DC. National Security and International Affairs Div.

EUROPEAN AERONAUTICS: STRONG GOVERNMENT PRESENCE IN INDUSTRY STRUCTURE AND RESEARCH AND DEVELOPMENT SUPPORT. REPORT TO CONGRESSIONAL REQUESTERS

Mar. 1994 60 p

(GAO/NSIAD-94-71; B-255687; AD-A279220) Avail: CASI HC A04/MF A01; GAO, PO Box 6015, Gaithersburg, MD 20884-6015 HC

The structure of the aeronautical industries of France, Germany, and the United Kingdom, their government's support towards aeronautical research and development, and the organization of each country's respective aeronautical research and development establishments are the topics of this GAO report. Information on aeronautical research and development efforts by the European community and its member nations are also included. Due to industrial consolidation, it was found that there is only one major assembler/airframe manufacturer of large civil transport aircraft in each of the three major countries studied. Also, each country had only one or two large civil aircraft engine manufacturers, again due to industrial consolidation. Although there are international collaborative efforts by each of the manufacturers, these efforts do not generally involve joint research nor information sharing of aeronautical information, perhaps due to national security concerns and/or from the companies' unwillingness to share data due to competition within the industry. Derived from text

19

GENERAL

A95-65764

TWO PROJECTS OF V. M. MYASISHCHEV

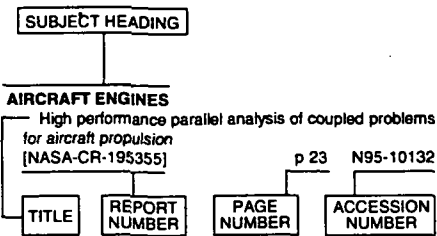
V. M. PETRAKOV *British Interplanetary Society Journal* (ISSN 0007-094X) vol. 47, no. 9 September 1994 p. 347-354 (HTN-95-50269) Copyright

Until recently the name of Vladimir M. Myasishchev was known only to specialists in aviation technology, although he is regarded in that number of distinguished aviation-constructors of world class. Jets, created under the leadership of V. M. Myasishchev in the 50s, remained in use for many years and are still in service at the present time. The years have since passed but memories remain of his achievements, actions and plans. He died in the autumn of 1978 and in 1981 his name was given to an experimental machine building factory, where he worked in his latter years and where, under his leadership, was created the transport jet 3M-T, since named in his memory and a creation of his already done in the mid-50s. This jet conveyed to the Baikonur Cosmodrome the reusable spacecraft

'Buran' and blocks of the 'Energiya' carrier-rocket and in 1990 a memorial stone was laid at one of the buildings of the 'Salyut' construction bureau. The names of most of the constructors in Soviet space rocket technology are widely know but there are still many blank spots in the history of aviation and space rocket technology. For example, it has become known only in the last year that, work was carried out in space rocket themes in the OKB-23 under the leadership of V. M. Myasishev. The two major projects of V. M. Myasishchev are examined in detail.

Author (revised by Hemer)

Typical Subject Index Listing



The subject heading is a key to the subject content of the document. The title is used to provide a description of the subject matter. When the title is insufficiently descriptive of document content, a title extension is added, separated from the title by three hyphens. The accession number and the page number are included in each entry to assist the user in locating the abstract in the abstract section. If applicable, a report number is also included as an aid in identifying the document. Under any one subject heading, the accession numbers are arranged in sequence.

A

ABLATION

On the particular features of dynamic processes in solids with varying boundary during interaction with intensive heat flows
[BTN-94-EIX94461408756] p 171 A95-63639

Thermal chemical energy of ablating silica surfaces in air breathing solid rocket engines p 148 N95-16316

ABLATIVE MATERIALS

Thermal chemical energy of ablating silica surfaces in air breathing solid rocket engines p 148 N95-16316

ABRASION

Quality optimization of thermally sprayed coatings produced by the JP-5000 (HVOP) gun using mathematical modeling p 152 N95-19008

ABRASION RESISTANCE

Evaluation of alternate F-14 wing lug coating [AD-A283207] p 129 N95-17631

ACCELERATED LIFE TESTS

An artificial corrosion protocol for lap-splices in aircraft skin p 152 N95-19482

ACCIDENT INVESTIGATION

Annual review of aircraft accident data: US Air carrier operations, calendar year 1992 [PB95-100319] p 123 N95-17748

ACCIDENT PREVENTION

Aircraft safety evaluation [BTN-94-EIX94511309382] p 103 A95-64608

ACCUMULATIONS

Collection efficiency and ice accretion calculations for a sphere, a swept MS(1)-317 wing, a swept NACA-0012 wing tip, an axisymmetric inlet, and a Boeing 737-300 [NASA-TM-106831] p 123 N95-18582

ACOUSTIC ATTENUATION

Active minimization of energy density in three-dimensional enclosures [NASA-CR-197213] p 172 N95-16848

ACOUSTIC EXCITATION

Impact of Acoustic Loads on Aircraft Structures

[AGARD-CP-549] p 173 N95-19142

Nonlinear dynamic response of aircraft structures to acoustic excitation p 135 N95-19151

Brite-Euram programme: ACOUFAT acoustic fatigue and related damage tolerance of advanced composite and metallic structures p 174 N95-19159

ACOUSTIC FATIGUE

Impact of Acoustic Loads on Aircraft Structures

[AGARD-CP-549] p 173 N95-19142

Current and future problems in structural acoustic fatigue p 173 N95-19143

High-temperature acoustic test facilities and methods p 174 N95-19149

Nonlinear dynamic response of aircraft structures to acoustic excitation p 135 N95-19151

Acoustic fatigue testing on different materials and skin-stringer elements p 174 N95-19156

Acoustic fatigue characteristics of advanced materials and structures p 174 N95-19157

Brite-Euram programme: ACOUFAT acoustic fatigue and related damage tolerance of advanced composite and metallic structures p 174 N95-19159

Thermo-acoustic fatigue design for hypersonic vehicle skin panels p 162 N95-19161

Application of superplastically formed and diffusion bonded structures in high intensity noise environments p 174 N95-19162

ACOUSTIC PROPAGATION

Ducted fan acoustic radiation including the effects of nonuniform mean flow and acoustic treatment

[NASA-CR-197449] p 172 N95-16401

ACOUSTIC SIMULATION

Design and operation of a thermoacoustic test facility p 147 N95-19150

ACOUSTICS

Anisotropic heat exchangers/stack configurations for thermoacoustic heat engines [AD-A280974] p 168 N95-16506

Active minimization of energy density in three-dimensional enclosures [NASA-CR-197213] p 172 N95-16848

ACTIVE CONTROL

A computational investigation of wake-induced airfoil flutter in incompressible flow and active flutter control [AD-A281534] p 142 N95-16109

Active load control during rolling maneuvers -- performed in the Langley Transonic Dynamics Tunnel [NASA-TP-3455] p 129 N95-17397

Microgravity isolation system design: A case study [NASA-TM-106804] p 104 N95-17657

Helicopter internal noise p 173 N95-19144

ADAPTATION

Adaptive wind tunnel walls versus wall interference correction methods in 2D flows at high blockage ratios p 147 N95-19267

ADAPTIVE CONTROL

A feedforward control approach to the local navigation problem for autonomous vehicles [AD-A282787] p 126 N95-17706

ADDITIVES

Evaluation of an unlighted swinging airport sign [AD-A284763] p 146 N95-18087

ADHESIVE BONDING

Ultrasonic techniques for repair of aircraft structures with bonded composite patches p 136 N95-19486

AEROACOUSTICS

On the Lighthill relationship and sound generation from isotropic turbulence [NASA-CR-195005] p 159 N95-18191

Aeroacoustic qualification of HERMES shingles p 173 N95-19145

Weapons bay acoustic environment p 173 N95-19146

Impact of noise environment on engine nacelle design p 173 N95-19147

Impact of dynamic loads on propulsion integration p 174 N95-19148

Modelling structurally damaging twin-jet screech p 135 N95-19154

Unsteady aerodynamic analyses for turbomachinery aeroelastic predictions p 141 N95-19381

AEROASSIST

Numerical optimization of synergetic maneuvers [AD-A283398] p 109 N95-17435

AERODYNAMIC CHARACTERISTICS

Joint Proceedings on Aeronautics and Astronautics (JPAA) [ISBN-7-80-046602-7] p 104 N95-16249

An approach to aerodynamic characteristics of low radar cross-section fuselages p 106 N95-16251

FPCAS2D user's guide, version 1.0 [NASA-CR-195413] p 156 N95-16588

Twin engine afterbody model p 115 N95-17880

Investigation into the aerodynamic characteristics of a combat aircraft research model fitted with a forward swept wing p 116 N95-17884

Documentation and archiving of the Space Shuttle wind tunnel test data base. Volume 1: Background and description [NASA-TM-104806-VOL-1] p 151 N95-19237

Aerodynamic investigation of the flow field in a 180 deg turn channel with sharp bend p 163 N95-19257

Interaction of a three strut support on the aerodynamic characteristics of a civil aviation model p 122 N95-19279

AERODYNAMIC COEFFICIENTS

Error propagation equations for estimating the uncertainty in high-speed wind tunnel test results [DE94-014136] p 145 N95-16509

Measurements on a two-dimensional aerofoil with high-lift devices p 109 N95-17848

Two-dimensional 18.5 percent thick supercritical airfoil NLR 7301 p 110 N95-17854

Sectional prediction of 3D effects for separated flow on rotating blades [PB94-201696] p 117 N95-18503

Static aerodynamics CFD analysis for 120-mm hypersonic KE projectile design [ARL-MR-184] p 118 N95-18611

Dynamic Stability Instrumentation System (DSIS). Volume 1: Hardware description [NASA-TM-109160-VOL-1] p 171 N95-18899

2-D and 3-D oscillating wing aerodynamics for a range of angles of attack including stall [NASA-TM-4632] p 120 N95-19119

AERODYNAMIC CONFIGURATIONS

Calculation of geometry of stamps with small allowances for pieces of the aerodynamic profile [BTN-94-EIX94461408772] p 103 A95-63655

Optimum Design Methods for Aerodynamics [AGARD-R-803] p 127 N95-16562

Single-pass method for the solution of inverse potential and rotational problems. Part 1: 2-D and quasi 3-D theory and application p 107 N95-16563

Single-pass method for the solution of inverse potential and rotational problems. Part 2: Fully 3-D potential theory and applications p 107 N95-16564

Optimum aerodynamic design via boundary control p 127 N95-16565

Residual-correction type and related computational methods for aerodynamic design. Part 1: Airfoil and wing design p 128 N95-16566

Tools for applied engineering optimization p 128 N95-16570

Automation of reverse engineering process in aircraft modeling and related optimization problems [NASA-CR-197109] p 129 N95-16899

A selection of experimental test cases for the validation of CFD codes, volume 2 [AGARD-AR-303-VOL-2] p 109 N95-17846

A selection of experimental test cases for the validation of CFD codes. Supplement: Datasets A-E [AGARD-AR-303-SUPPL] p 117 N95-18539

Documentation and archiving of the Space Shuttle wind tunnel test data base. Volume 1: Background and description [NASA-TM-104806-VOL-1] p 151 N95-19237

Interference corrections for a centre-line plate mount in a porous-walled transonic wind tunnel p 122 N95-19280

Panel methods p 165 N95-19448

AERODYNAMIC DRAG

- An investigation of the transonic pressure drag coefficient for axis-symmetric bodies
[AD-A280990] p 105 N95-15994
- Measurements on a two-dimensional aerofoil with high-lift devices p 109 N95-17848
- Experimental techniques for measuring transonic flow with a three dimensional laser velocimetry system. Application to determining the drag of a fuselage p 163 N95-19258

AERODYNAMIC FORCES

- Structural effects of unsteady aerodynamic forces on horizontal-axis wind turbines
[DE94-011863] p 157 N95-16939
- Force and pressure data of an ogive-nosed slender body at high angles of attack and different Reynolds numbers p 113 N95-17868
- Subsonic flow around US-orbiter model FALKE in the DNW p 115 N95-17877
- Hydrofoil force balance
[AD-D016475] p 160 N95-18461
- Gyroscopic and propeller aerodynamic effects on engine mounts dynamic loads in turbulence conditions p 132 N95-18599

AERODYNAMIC HEAT TRANSFER

- On the particular features of dynamic processes in solids with varying boundary during interaction with intensive heat flows
[BTN-94-EIX94461408756] p 171 A95-63639
- An analysis code for the Rapid Engineering Estimation of Momentum and Energy Losses (REMEL)
[NASA-CR-191178] p 108 N95-16887
- Documentation and archiving of the Space Shuttle wind tunnel test data base. Volume 1: Background and description
[NASA-TM-104806-VOL-1] p 151 N95-19237

AERODYNAMIC HEATING

- An engineering code to analyze hypersonic thermal management systems p 155 N95-16322
- Numerical optimization of synergetic maneuvers
[AD-A283398] p 109 N95-17435

AERODYNAMIC INTERFERENCE

- Wall-signature methods for high speed wind tunnel wall interference corrections p 107 N95-16257
- 2-D aileron effectiveness study p 110 N95-17851
- Data from the GARTEur (AD) Action Group 02 airfoil CAST 7/DOA1 experiments p 111 N95-17856
- Single-engine tail interference model p 115 N95-17879
- Low speed propeller slipstream aerodynamic effects p 116 N95-17882
- Background noise levels measured in the NASA Lewis 9- by 15-foot low-speed wind tunnel
[NASA-TM-106817] p 145 N95-18054
- Wall Interference, Support Interference and Flow Field Measurements
[AGARD-CP-535] p 162 N95-19251
- The crucial role of wall interference, support interference and flow field measurements in the development of advanced aircraft configurations p 162 N95-19252
- Boundary-flow measurement methods for wall interference assessment and correction: Classification and review p 163 N95-19262
- Estimating wind tunnel interference due to vectored jet flows p 164 N95-19265
- Adaptive wind tunnel walls versus wall interference correction methods in 2D flows at high blockage ratios p 147 N95-19267
- Interference determination for wind tunnels with slotted walls p 147 N95-19269
- Transonic wind tunnel boundary interference correction p 147 N95-19271
- Calculation of low speed wind tunnel wall interference from static pressure pipe measurements p 164 N95-19273
- The traditional and new methods of accounting for the factors distorting the flow over a model in large transonic wind tunnels p 165 N95-19275
- Calculation of wall effects of flow on a perforated wall with a code of surface singularities p 165 N95-19277
- Evaluation of combined wall- and support-interference on wind tunnel models p 122 N95-19278
- Interaction of a three strut support on the aerodynamic characteristics of a civil aviation model p 122 N95-19279

AERODYNAMIC LOADS

- Engineering methods for the evaluation of transonic flutter characteristics for aerodynamic control surfaces
[BTN-94-EIX94461408589] p 141 A95-63064
- Residual-correction type and related computational methods for aerodynamic design. Part 2: Multi-point airfoil design p 128 N95-16567
- Optimal shape design for aerodynamics p 128 N95-16568
- Airfoil optimization by the one-shot method p 128 N95-16569

Aerodynamic shape optimization p 128 N95-16572

- Active load control during rolling maneuvers — performed in the Langley Transonic Dynamics Tunnel
[NASA-TP-3455] p 129 N95-17397
- Aircraft Loads due to Turbulence and their impact on Design and Certification
[AGARD-R-798] p 143 N95-18597
- Design limit loads based upon statistical discrete gust methodology p 133 N95-18603
- Pressure measurements on an F/A-18 twin vertical tail in buffeting flow. Volume 4, part 2: Buffet cross spectral densities
[AD-A285555] p 143 N95-18641
- Wind turbine blade aerodynamics: The combined experiment
[DE94-011866] p 118 N95-18645
- Wind turbine blade aerodynamics: The analysis of field test data
[DE94-011867] p 118 N95-18646
- Determination of stores pointing error due to wing flexibility under flight load
[NASA-TM-4646] p 134 N95-19044
- The accuracy of parameter estimation in system identification of noisy aircraft load measurement
[NASA-CR-197516] p 134 N95-19130
- Brite-Euram programme: ACOUFAT acoustic fatigue and related damage tolerance of advanced composite and metallic structures p 174 N95-19159
- Prediction of fatigue crack growth under flight-simulation loading with the modified CORPUS model p 166 N95-19471
- Development of load spectra for Airbus A330/A340 full scale fatigue tests p 135 N95-19479

AERODYNAMIC NOISE

- Ducted fan acoustic radiation including the effects of nonuniform mean flow and acoustic treatment
[NASA-CR-197449] p 172 N95-16401
- On the Lighthill relationship and sound generation from isotropic turbulence
[NASA-CR-195005] p 159 N95-18191

AERODYNAMIC STABILITY

- Investigation of dynamic inflow's influence on rotor control derivatives p 155 N95-16250
- A spectrally accurate boundary-layer code for infinite swept wings
[NASA-CR-195014] p 159 N95-18042
- Integrated aerodynamic fin and stowable TVC vane system
[AD-D016457] p 151 N95-19073

AERODYNAMIC STALLING

- Structural effects of unsteady aerodynamic forces on horizontal-axis wind turbines
[DE94-011863] p 157 N95-16939
- Aircraft accident report: Stall and loss of control on final approach, Atlantic Coast Airlines, Inc./United Express Flight 6291, Jetstream 4101, N304UE Columbus, OH, 7 January 1994
[PB94-910409] p 123 N95-17646
- Numerical simulation of dynamic-stall suppression by tangential blowing
[AD-A284887] p 120 N95-19110
- 2-D and 3-D oscillating wing aerodynamics for a range of angles of attack including stall
[NASA-TM-4632] p 120 N95-19119

AERODYNAMICS

- Aircraft model for the AIAA controls design challenge
[BTN-94-EIX94511433921] p 142 A95-64587
- Aerodynamic design and calculation of flow around the plane cascade of turbine
[BTN-94-EIX94481415357] p 104 A95-65347
- A workstation based simulator for teaching compressible aerodynamics p 170 N95-16906
- Interactive computer graphics applications for compressible aerodynamics p 170 N95-17264
- Low speed propeller slipstream aerodynamic effects p 116 N95-17882
- Parachute inflation: A problem in aeroelasticity
[AD-A284375] p 117 N95-18340
- CFD: Advances and Applications, part 1
[NAL-SP-9322-PT-1] p 165 N95-19444

AEROELASTICITY

- On the dynamics of aeroelastic oscillators with one degree of freedom
[BTN-94-EIX94501431527] p 153 A95-64524
- Measurements of unsteady pressure and structural response for an elastic supercritical wing
[NASA-TP-3443] p 104 N95-16560
- FPAS2D user's guide, version 1.0
[NASA-CR-195413] p 156 N95-16588
- Parachute inflation: A problem in aeroelasticity
[AD-A284375] p 117 N95-18340
- A linear system identification and validation of an AH-64 Apache aeroelastic simulation model p 146 N95-18903

Unsteady aerodynamic analyses for turbomachinery aeroelastic predictions p 141 N95-19381

AEROMANEUVERING

- Numerical optimization of synergetic maneuvers
[AD-A283398] p 109 N95-17435

AERONAUTICAL ENGINEERING

- Calculation of geometry of stamps with small allowances for pieces of the aerodynamic profile
[BTN-94-EIX94461408772] p 103 A95-63655

AEROSPACE ENGINEERING

- Optimum Design Methods for Aerodynamics
[AGARD-R-803] p 127 N95-16562
- Tools for applied engineering optimization p 128 N95-16570
- NASA High Performance Computing and Communications program p 176 N95-18573
- [NASA-TM-4653]
- NASA Lewis Research Center Workshop on Forced Response in Turbomachinery
[NASA-CP-10147] p 141 N95-19380

AEROSPACE INDUSTRY

- A study of software standards used in the avionics industry p 137 N95-16456
- The global aircraft shape p 128 N95-16571
- Review of the EUROPT Project AERO-0026 p 129 N95-16573
- Military aviation maintenance industry in Western Europe: Concentration and internationalization
[PB94-189180] p 104 N95-17451
- European aeronautics: Strong government presence in industry structure and research and development support. Report to Congressional Requesters
[GAO/NSIAD-94-71] p 176 N95-18578

AEROSPACE MEDICINE

- A surgical support system for Space Station Freedom p 149 N95-16776

AEROSPACE SYSTEMS

- Conference on Aerospace Transparent Materials and Enclosures, volume 1
[AD-A283925] p 133 N95-18677

AEROSPACE TECHNOLOGY TRANSFER

- Revitalizing general aviation
[NASA-TM-110113] p 129 N95-16982

AEROTHERMOCHEMISTRY

- Improved analytical solution for varying specific heat parallel stream mixing
[BTN-94-EIX94481415349] p 103 A95-65339

AEROTHERMODYNAMICS

- A model for preliminary facility design including simulation issues p 144 N95-16318
- Hypersonic wind tunnel test techniques
[AD-A284057] p 118 N95-18663
- Design and operation of a thermoacoustic test facility p 147 N95-19150
- Thermo-acoustic fatigue design for hypersonic vehicle skin panels p 162 N95-19161

AEROZINE

- Regenerative cooling for liquid propellant rocket thrust chambers
[INPE-5565-TDI/540] p 150 N95-18720

AFTERBODIES

- An investigation of the transonic pressure drag coefficient for axis-symmetric bodies
[AD-A280990] p 105 N95-15994
- Single-engine tail interference model p 115 N95-17879
- Twin engine afterbody model p 115 N95-17880
- Numerical computations of supersonic base flow with special emphasis on turbulence modeling
[AD-A283688] p 119 N95-18670
- Transonic and supersonic flowfield measurements about axisymmetric afterbodies for validation of advanced CFD codes p 121 N95-19260

AFTERBURNING

- Single-engine tail interference model p 115 N95-17879

AGING (MATERIALS)

- Problems with aging wiring in Naval aircraft p 154 N95-16048

AH-64 HELICOPTER

- The assessment of the AH-64D, longbow, mast-mounted assembly noise hazard for maintenance personnel
[AD-A284971] p 171 N95-16226
- A linear system identification and validation of an AH-64 Apache aeroelastic simulation model p 146 N95-18903

AILERONS

- 2-D aileron effectiveness study p 110 N95-17851

AIR BREATHING ENGINES

- Hypersonic air-breathing aeropropulsion facility test support requirements p 144 N95-16319

AIR FLOW

- A selection of experimental test cases for the validation of CFD codes, volume 2
[AGARD-AR-303-VOL-2] p 109 N95-17846

- The stability of two-phase flow over a swept-wing
[NASA-CR-194994] p 159 N95-18190
- A selection of experimental test cases for the validation of CFD codes. Supplement: Datasets A-E
[AGARD-AR-303-SUPPL] p 117 N95-18539
- AIR INTAKES**
- Numerical simulation of helicopter engine plume in forward flight
[NASA-CR-197488] p 107 N95-16589
- Data acquisition and processing software for the Low Speed Wind Tunnel tests of the Jindivik auxiliary air intake
[AD-A285455] p 108 N95-17178
- AIR LAW**
- The ICAO CNS/ATM system: New king, new law?
[HTN-95-50218] p 175 A95-64855
- World trends in air transport policies. (Approaching the 21st century)
[HTN-95-50220] p 176 A95-64857
- AIR NAVIGATION**
- Commentary on Walton correspondence relating to the ILS glide slope
[BTN-94-EIX94441380856] p 125 A95-64288
- The ICAO CNS/ATM system: New king, new law?
[HTN-95-50218] p 175 A95-64855
- AIR POLLUTION**
- Atmospheric effects of high-flying subsonic aircraft: A catalogue of perturbing influences
[KNMI-SR-94-03] p 168 N95-18722
- AIR TO SURFACE MISSILES**
- Application of photogrammetry of F-14D store separation
[AD-A284154] p 132 N95-18417
- AIR TRAFFIC**
- Atmospheric effects of high-flying subsonic aircraft: A catalogue of perturbing influences
[KNMI-SR-94-03] p 168 N95-18722
- On-line handling of air traffic: Management, guidance and control
[AGARD-AG-321] p 126 N95-18927
- AIR TRAFFIC CONTROL**
- The ICAO CNS/ATM system: New king, new law?
[HTN-95-50218] p 175 A95-64855
- Solid state radar demonstration test results at the FAA Technical Center
[AD-A281520] p 154 N95-16097
- Modeling of Instrument Landing System (ILS) localizer signal on runway 25L at Los Angeles International Airport
[NASA-TM-4588] p 125 N95-17384
- Heliport/vertiport MLS precision approaches
[AD-A283505] p 126 N95-18059
- An analysis of tower (local) controller-pilot voice communications
[AD-A283718] p 160 N95-18436
- On-line handling of air traffic: Management, guidance and control
[AGARD-AG-321] p 126 N95-18927
- AIR TRAFFIC CONTROLLERS (PERSONNEL)**
- An analysis of tower (local) controller-pilot voice communications
[AD-A283718] p 160 N95-18436
- AIR TRANSPORTATION**
- World trends in air transport policies. (Approaching the 21st century)
[HTN-95-50220] p 176 A95-64857
- EC Aviation Scene
[HTN-95-50223] p 176 A95-64860
- AIRBORNE EQUIPMENT**
- Generalized method of solving topological optimization problems for electrical airplane equipment systems in computer-aided design
[AD-A283700] p 133 N95-18621
- AIRCRAFT ACCIDENT INVESTIGATION**
- Commentary on Walton correspondence relating to the ILS glide slope
[BTN-94-EIX94441380856] p 125 A95-64288
- Aircraft accident investigation and airworthiness - A practical example of the interaction of two disciplines with some reflections on possible legal consequences
[HTN-95-50219] p 176 A95-64856
- A correlative investigation of simulated occupant motion and accident report in a helicopter crash
[AD-A285190] p 123 N95-16404
- Aircraft accident report: Stall and loss of control on final approach, Atlantic Coast Airlines, Inc./United Express Flight 6291 Jetstream 4101, N304UE Columbus, OH, 7 January 1994
[PB94-910409] p 123 N95-17646
- Spectrogram diagnosis of aircraft disasters
[AD-A285673] p 124 N95-19167
- AIRCRAFT ACCIDENTS**
- Commentary on Walton correspondence relating to the ILS glide slope
[BTN-94-EIX94441380856] p 125 A95-64288
- Aircraft accident report: Stall and loss of control on final approach, Atlantic Coast Airlines, Inc./United Express Flight 6291 Jetstream 4101, N304UE Columbus, OH, 7 January 1994
[PB94-910409] p 123 N95-17646
- Annual review of aircraft accident data: US Air carrier operations, calendar year 1992
[PB95-100319] p 123 N95-17748
- Spectrogram diagnosis of aircraft disasters
[AD-A285673] p 124 N95-19167
- AIRCRAFT ANTENNAS**
- A VHF/UHF antenna for the Precision Antenna Measurement System (PAMS)
[AD-A285673] p 156 N95-16621
- AIRCRAFT COMMUNICATION**
- Spread spectrum applications in unmanned aerial vehicles
[AD-A281035] p 156 N95-16448
- AIRCRAFT COMPARTMENTS**
- Generalized method of solving topological optimization problems for electrical airplane equipment systems in computer-aided design
[AD-A283700] p 133 N95-18621
- Helicopter internal noise
[AD-A283700] p 133 N95-18621
- Weapons bay acoustic environment
[AD-A283700] p 133 N95-18621
- Noise transmission and reduction in turboprop aircraft
[AD-A283700] p 133 N95-18621
- AIRCRAFT CONFIGURATIONS**
- Portable parallel stochastic optimization for the design of aeropropulsion components
[NASA-CR-195312] p 154 N95-16072
- STOVL CFD model test case
[AD-A283700] p 133 N95-18621
- Comparison of stochastic and deterministic nonlinear gust analysis methods to meet continuous turbulence criteria
[AD-A283700] p 133 N95-18621
- Panel methods
[AD-A283700] p 133 N95-18621
- AIRCRAFT CONSTRUCTION MATERIALS**
- Analytical description of and forecast for stress relaxation of aviation materials under the vibration conditions
[BTN-94-EIX94461408751] p 126 A95-63634
- Calculation of geometry of stamps with small allowances for pieces of the aerodynamic profile
[BTN-94-EIX94461408772] p 103 A95-63655
- Shear buckling analysis of a hat-stiffened panel
[NASA-TM-4644] p 158 N95-17490
- Conference on Aerospace Transparent Materials and Enclosures, Volume 2: Sessions 5-9
[AD-A283926] p 131 N95-18162
- Conference on Aerospace Transparent Materials and Enclosures, volume 1
[AD-A283925] p 133 N95-18677
- Thermo-acoustic fatigue design for hypersonic vehicle skin panels
[AD-A283926] p 131 N95-18162
- AIRCRAFT CONTROL**
- Aircraft model for the AIAA controls design challenge
[BTN-94-EIX94511433921] p 142 A95-64587
- Time-optimal turn to a heading: An analytic solution
[BTN-94-EIX94511433940] p 142 A95-64606
- Plant and controller optimization by convex methods
[AD-A283700] p 133 N95-18621
- Fiber Optic Control System integration for advanced aircraft. Electro-optic and sensor fabrication, integration, and environmental testing for flight control systems: Laboratory test results
[NASA-CR-195408] p 161 N95-18938
- Fiber Optic Control System integration for advanced aircraft. Electro-optic and sensor fabrication, integration, and environmental testing for flight control systems
[NASA-CR-191194] p 162 N95-19236
- AIRCRAFT DESIGN**
- Joint Proceedings on Aeronautics and Astronautics (JPAA)
[ISBN-7-80-046602-7] p 104 N95-16249
- An improved method of airfoil design
[AD-A283700] p 133 N95-18621
- Development of strength analysis methods and design model for aircraft constructions in Kazan Aviation Institute
[AD-A283700] p 133 N95-18621
- Evaluation of the dynamic stability characteristics of the NAL Light Transport Aircraft
[NAL-PD-CA-9217] p 142 N95-16392
- Optimum Design Methods for Aerodynamics
[AGARD-R-803] p 127 N95-16562
- Optimum aerodynamic design via boundary control
[AD-A283700] p 133 N95-18621
- Residual-correction type and related computational methods for aerodynamic design. Part 1: Airfoil and wing design
[AD-A283700] p 133 N95-18621
- Residual-correction type and related computational methods for aerodynamic design. Part 2: Multi-point airfoil design
[AD-A283700] p 133 N95-18621
- Optimal shape design for aerodynamics
[AD-A283700] p 133 N95-18621
- Airfoil optimization by the one-shot method
[AD-A283700] p 133 N95-18621
- Tools for applied engineering optimization**
p 128 N95-16570
- The global aircraft shape
p 128 N95-16571
- Applications of automatic differentiation in CFD
[NASA-TM-109948] p 157 N95-16828
- Multi-lab comparison on R-curve methodologies: Alloy 2024-T3
[NASA-CR-195004] p 151 N95-16860
- Automation of reverse engineering process in aircraft modeling and related optimization problems
[NASA-CR-197109] p 129 N95-16899
- Cooperative control theory and integrated flight and propulsion control
[NASA-CR-197493] p 142 N95-17404
- OAT15A airfoil data
p 111 N95-17857
- Measurements of the flow over a low aspect-ratio wing in the Mach number range 0.6 to 0.87 for the purpose of validation of computational methods. Part 1: Wing design, model construction, surface flow. Part 2: Mean flow in the boundary layer and wake, 4 test cases
p 112 N95-17860
- Investigation into the aerodynamic characteristics of a combat aircraft research model fitted with a forward swept wing
p 116 N95-17884
- Wing design for a civil tiltrotor transport aircraft
[NASA-CR-197523] p 130 N95-18090
- Aircraft Loads due to Turbulence and their Impact on Design and Certification
[AGARD-R-798] p 143 N95-18597
- Design limit loads based upon statistical discrete gust methodology
p 133 N95-18603
- A review of gust load calculation methods at de Havilland
p 118 N95-18604
- Ageing nuclear power plant management: An aeronautical viewpoint
[NAL-PD-SN-9306] p 105 N95-18606
- Course module for AA201: Wing structural design project
[AD-A283618] p 133 N95-18616
- Plant and controller optimization by convex methods
[AD-A283700] p 133 N95-18621
- E-6A hardness assurance, maintenance and surveillance program
[AD-A283994] p 134 N95-19067
- Impact of noise environment on engine nacelle design
p 173 N95-19147
- Modelling structurally damaging twin-jet screech
p 135 N95-19154
- AIRCRAFT ENGINES**
- Gas-turbine engines with increased efficiency of two circuits, due to the use of the utilizing steam-turbine circuit
[BTN-94-EIX94461408755] p 153 A95-63638
- On a program-information system TDSoft
[BTN-94-EIX94461408773] p 175 A95-63656
- Portable parallel stochastic optimization for the design of aeropropulsion components
[NASA-CR-195312] p 154 N95-16072
- Theoretical fundamentals of the aircraft GTE tests
p 138 N95-16265
- Hypersonic air-breathing aeropropulsion facility test support requirements
p 144 N95-16319
- The global aircraft shape
p 128 N95-16571
- Gyroscopic and propeller aerodynamic effects on engine mounts dynamic loads in turbulence conditions
p 132 N95-18599
- Wave cycle design for wave rotor engines with limited nitrogen oxide emissions
p 161 N95-18901
- Quality optimization of thermally sprayed coatings produced by the JP-5000 (HVOF) gun using mathematical modeling
p 152 N95-19008
- Mathematical Models of Gas Turbine Engines and their Components
[AGARD-LS-198] p 139 N95-19017
- AIRCRAFT EQUIPMENT**
- Bicarbonate of soda blasting technology for aircraft wheel depainting
[PB94-193323] p 104 N95-17466
- Preliminary evaluation of the F/A-18 quantity/multiple envelope expansion
[AD-A284119] p 132 N95-18407
- AIRCRAFT GUIDANCE**
- Modeling of Instrument Landing System (ILS) localizer signal on runway 25L at Los Angeles International Airport
[NASA-TM-4588] p 125 N95-17384
- On-line handling of air traffic: Management, guidance and control
[AGARD-AG-321] p 126 N95-18927
- AIRCRAFT ICING**
- Collection efficiency and ice accretion calculations for a sphere, a swept MS(1)-317 wing, a swept NACA-0012 wing tip, an axisymmetric inlet, and a Boeing 737-300
[NASA-TM-106831] p 123 N95-18582
- Methods for scaling icing test conditions
[NASA-TM-106827] p 124 N95-19284

AIRCRAFT INDUSTRY

Development of processes, means, and theoretical principles of thin-walled detail plastic forming at Kazan Aviation Institute p 155 N95-16281

AIRCRAFT INSTRUMENTS

Flight parameters monitoring system for tracking structural integrity of rotary-wing aircraft p 135 N95-19469

AIRCRAFT LANDING

Application of GPS/SINS/RA integrated system to aircraft approach landing p 125 N95-16277

AIRCRAFT MAINTENANCE

Aircraft accident investigation and airworthiness -- A practical example of the interaction of two disciplines with some reflections on possible legal consequences [HTN-95-50219] p 176 A95-64856

Problems with aging wiring in Naval aircraft p 154 N95-16048

Military aviation maintenance industry in Western Europe: Concentration and internationalization [PB94-189180] p 104 N95-17451

Ultrasonic techniques for repair of aircraft structures with bonded composite patches p 136 N95-19486

AIRCRAFT MANEUVERS

Time-optimal turn to a heading: An analytic solution [BTN-94-EIX94511433940] p 142 A95-64606

AIRCRAFT MODELS

Aircraft model for the AIAA controls design challenge [BTN-94-EIX94511433921] p 142 A95-64587

Linear prediction data extrapolation superresolution radar imaging p 155 N95-16268

Automation of reverse engineering process in aircraft modeling and related optimization problems [NASA-CR-197109] p 129 N95-16899

Measurements on a two-dimensional aerofoil with high-lift devices p 109 N95-17848

Two-dimensional 16.5 percent thick supercritical airfoil NLR 7301 p 110 N95-17854

Low-speed surface pressure and boundary layer measurement data for the NLR 7301 airfoil section with trailing edge flap p 111 N95-17855

Data from the GARTEur (AD) Action Group 02 airfoil CAST 7/DOA1 experiments p 111 N95-17856

A supercritical airfoil experiment p 111 N95-17858

Two-dimensional high-lift airfoil data for CFD code validation p 112 N95-17859

Measurements of the flow over a low aspect-ratio wing in the Mach number range 0.6 to 0.87 for the purpose of validation of computational methods. Part 1: Wing design, model construction, surface flow. Part 2: Mean flow in the boundary layer and wake, 4 test cases p 112 N95-17860

Detailed study at supersonic speeds of the flow around delta wings p 112 N95-17861

Investigation into the aerodynamic characteristics of a combat aircraft research model fitted with a forward swept wing p 116 N95-17884

Interaction, bursting and control of vortices of a cropped double-delta wing at high angle of attack [AD-A283656] p 119 N95-18669

Estimating wind tunnel interference due to vectored jet flows p 164 N95-19265

AIRCRAFT NOISE

The effects of aircraft (B-52) overflights on ancient structures [BTN-94-EIX94341340070] p 171 A95-63522

The assessment of the AH-64D, longbow, mast-mounted assembly noise hazard for maintenance personnel [AD-A284971] p 171 N95-16226

Helicopter internal noise p 173 N95-19144

Impact of noise environment on engine nacelle design p 173 N95-19147

Modelling structurally damaging twin-jet screech p 135 N95-19154

An overall approach of cockpit noise verification in a military aircraft p 175 N95-19163

Noise transmission and reduction in turboprop aircraft p 175 N95-19164

AIRCRAFT PARTS

Automation of reverse engineering process in aircraft modeling and related optimization problems [NASA-CR-197109] p 129 N95-16899

AIRCRAFT PERFORMANCE

Six degree of freedom flight dynamic and performance simulation of a remotely-piloted vehicle [AERO-TN-9301] p 131 N95-18097

Design limit loads based upon statistical discrete gust methodology p 133 N95-18603

AIRCRAFT PILOTS

A correlative investigation of simulated occupant motion and accident report in a helicopter crash [AD-A285190] p 123 N95-16404

AIRCRAFT POWER SUPPLIES

The computer analysis of the prediction of aircraft electrical power supply system reliability p 155 N95-16278

AIRCRAFT PRODUCTION

Low rate initial production in Army Aviation systems development [AD-A281871] p 127 N95-16356

Composite chronicles: A study of the lessons learned in the development, production, and service of composite structures [NASA-CR-4620] p 151 N95-16859

AIRCRAFT RELIABILITY

Aircraft safety evaluation [BTN-94-EIX94511309382] p 103 A95-64608

Aircraft accident investigation and airworthiness -- A practical example of the interaction of two disciplines with some reflections on possible legal consequences [HTN-95-50219] p 176 A95-64856

Residual life and strength estimates of aircraft structural components with MSD/MED p 136 N95-19485

AIRCRAFT SAFETY

Aircraft safety evaluation [BTN-94-EIX94511309382] p 103 A95-64608

Aircraft accident report: Stall and loss of control on final approach, Atlantic Coast Airlines, Inc./United Express Flight 6291 Jetstream 4101, N304UE Columbus, OH, 7 January 1994 [PB94-910409] p 123 N95-17646

A study of the effect of store unsteady aerodynamics on gust and turbulence loads p 133 N95-18601

Ageing nuclear power plant management: An aeronautical viewpoint [NAL-PD-SN-9306] p 105 N95-18606

On-line handling of air traffic: Management, guidance and control [AGARD-AG-321] p 126 N95-18927

Safety study: Commuter airline safety [PB94-917004] p 124 N95-19132

AIRCRAFT SPECIFICATIONS

Six degree of freedom flight dynamic and performance simulation of a remotely-piloted vehicle [AERO-TN-9301] p 131 N95-18097

AIRCRAFT STRUCTURES

Development of strength analysis methods and design model for aircraft constructions in Kazan Aviation Institute p 127 N95-16264

Development of processes, means, and theoretical principles of thin-walled detail plastic forming at Kazan Aviation Institute p 155 N95-16281

The use of electrochemistry and ellipsometry for identifying and evaluating corrosion on aircraft [AD-A285323] p 151 N95-16371

Rapid solution of large-scale systems of equations p 169 N95-16458

Composite chronicles: A study of the lessons learned in the development, production, and service of composite structures [NASA-CR-4620] p 151 N95-16859

Course module for AA201: Wing structural design project [AD-A283618] p 133 N95-18616

Pressure measurements on an F/A-18 twin vertical tail in buffet flow. Volume 4, part 2: Buffet cross spectral densities [AD-A285555] p 143 N95-18641

The accuracy of parameter estimation in system identification of noisy aircraft load measurement [NASA-CR-197516] p 134 N95-19130

Impact of Acoustic Loads on Aircraft Structures [AGARD-CP-549] p 173 N95-19142

Current and future problems in structural acoustic fatigue p 173 N95-19143

Impact of noise environment on engine nacelle design p 173 N95-19147

High-temperature acoustic test facilities and methods p 174 N95-19149

Nonlinear dynamic response of aircraft structures to acoustic excitation p 135 N95-19151

Acoustic fatigue testing on different materials and skin-stringer elements p 174 N95-19156

Acoustic fatigue characteristics of advanced materials and structures p 174 N95-19157

Application of superplastically formed, and diffusion bonded structures in high intensity noise environments p 174 N95-19162

FAA/NASA International Symposium on Advanced Structural Integrity Methods for Airframe Durability and Damage Tolerance, part 2 [NASA-CP-3274-PT-2] p 124 N95-19468

Discrete crack growth analysis methodology for through cracks in pressurized fuselage structures p 166 N95-19473

Aircraft stress sequence development: A complex engineering process made simple p 136 N95-19480

Residual life and strength estimates of aircraft structural components with MSD/MED p 136 N95-19485

Ultrasonic techniques for repair of aircraft structures with bonded composite patches p 136 N95-19486

Widespread fatigue damage monitoring: Issues and concerns p 136 N95-19488

Aircraft fatigue and crack growth considering loads by structural component p 137 N95-19497

AIRCRAFT SURVIVABILITY

Assessing aircraft survivability to high frequency transient threats [AD-A283999] p 134 N95-18726

AIRCRAFT WAKES

Aircraft wake vortex takeoff tests at O'Hara International Airport [AD-A283828] p 118 N95-18624

AIRFIELD SURFACE MOVEMENTS

Development of an Automated Airfield Dynamic Cone Penetrometer (AADCP) prototype and the evaluation of unsurfaced airfield seismic surveying using Spectral Analysis of Surface Waves (SASW) technology [AD-A281985] p 145 N95-17444

AIRFOIL OSCILLATIONS

Unsteady flow testing in a passive low-correction wind tunnel p 147 N95-19272

AIRFOIL PROFILES

Measurements on a two-dimensional aerofoil with high-lift devices p 109 N95-17848

Investigation of the flow over a series of 14 percent-thick supercritical aerofoils with significant rear camber p 109 N95-17849

Surface pressure and wake drag measurements on the Boeing A4 airfoil in the IAR 1.5X1.5m Wind Tunnel Facility p 110 N95-17850

Low-speed surface pressure and boundary layer measurement data for the NLR 7301 airfoil section with trailing edge flap p 111 N95-17855

In-flight lift-drag characteristics for a forward-swept wing aircraft and comparisons with contemporary aircraft [NASA-TP-3414] p 117 N95-18565

AIRFOILS

A computational investigation of wake-induced airfoil flutter in incompressible flow and active flutter control [AD-A281534] p 142 N95-16109

An improved method of airfoil design p 106 N95-16252

Residual-correction type and related computational methods for aerodynamic design. Part 1: Airfoil and wing design p 128 N95-16566

Residual-correction type and related computational methods for aerodynamic design. Part 2: Multi-point airfoil design p 128 N95-16567

Optimal shape design for aerodynamics p 128 N95-16568

Airfoil optimization by the one-shot method p 128 N95-16569

Review of the EUROPT Project AERO-0026 p 129 N95-16573

2-D airfoil tests including side wall boundary layer measurements p 158 N95-17847

Measurements on a two-dimensional aerofoil with high-lift devices p 109 N95-17848

Surface pressure and wake drag measurements on the Boeing A4 airfoil in the IAR 1.5X1.5m Wind Tunnel Facility p 110 N95-17850

Investigation of an NLF(1)-0416 airfoil in compressible subsonic flow p 110 N95-17852

Experiments in the trailing edge flow of an NLR 7702 airfoil p 110 N95-17853

Two-dimensional 16.5 percent thick supercritical airfoil NLR 7301 p 110 N95-17854

Data from the GARTEur (AD) Action Group 02 airfoil CAST 7/DOA1 experiments p 111 N95-17856

OAT15A airfoil data p 111 N95-17857

Two-dimensional high-lift airfoil data for CFD code validation p 112 N95-17859

Fatigue in single crystal nickel superalloys [AD-A285727] p 152 N95-18068

Hydrofoil force balance p 160 N95-18461

Solution of full potential equation on an airfoil by multigrad technique [AD-D016475] p 160 N95-18461

Numerical simulation of dynamic-stall suppression by tangential blowing [AD-A284887] p 120 N95-19110

2-D and 3-D oscillating wing aerodynamics for a range of angles of attack including stall [NASA-TM-4632] p 120 N95-19119

Development of pneumatic test techniques for subsonic high-lift and in-ground-effect wind tunnel investigations p 121 N95-19268

Analysis of test section sidewall effects on a two dimensional airfoil: Experimental and numerical investigations p 165 N95-19276

Ice accretion with varying surface tension [NASA-TM-106826] p 124 N95-19285

AIRFRAME MATERIALS

Static and dynamic friction behavior of candidate high temperature airframe seal materials [NASA-TM-106571] p 152 N95-16905
Acoustic fatigue testing on different materials and skin-stringer elements p 174 N95-19156
Acoustic fatigue characteristics of advanced materials and structures p 174 N95-19157

AIRFRAMES

Cooperative control theory and integrated flight and propulsion control [NASA-CR-197493] p 142 N95-17404
Experimental data on the aerodynamic interactions between a helicopter rotor and an airframe p 116 N95-17883
The generic simulation executive at Manned Flight Simulator [AD-A283997] p 146 N95-18724
FAA/NASA International Symposium on Advanced Structural Integrity Methods for Airframe Durability and Damage Tolerance, part 2 [NASA-CP-3274-PT-2] p 124 N95-19468
Development of load spectra for Airbus A330/A340 full scale fatigue tests p 135 N95-19479

AIRLINE OPERATIONS

Aircraft accident report: Stall and loss of control on final approach, Atlantic Coast Airlines, Inc./United Express Flight 6291 Jetstream 4101, N304UE Columbus, OH, 7 January 1994 [PB94-910409] p 123 N95-17646
Safety study: Commuter airline safety [PB94-917004] p 124 N95-19132

AIRPORTS

Modeling of Instrument Landing System (ILS) localizer signal on runway 25L at Los Angeles International Airport [NASA-TM-4588] p 125 N95-17384
Evaluation of an unlighted swinging airport sign [AD-A284763] p 146 N95-18087
Aircraft wake vortex takeoff tests at O'Hara International Airport [AD-A283828] p 118 N95-18624
On-line handling of air traffic: Management, guidance and control [AGARD-AG-321] p 126 N95-18927

ALGORITHMS

A grid generation and flow solution method for the Euler equations on unstructured grids [HTN-95-20003] p 153 A95-63201
Generalized method of solving topological optimization problems for electrical airplane equipment systems in computer-aided design p 169 N95-16272
Optimum Design Methods for Aerodynamics [AGARD-R-803] p 127 N95-16562
FPCAS2D user's guide, version 1.0 [NASA-CR-195413] p 156 N95-16588
Algorithms for bilevel optimization [NASA-CR-194980] p 170 N95-16897
Eddy current for detecting second layer cracks under installed fasteners [AD-A282412] p 158 N95-17507
A platform independent application of Lux illumination prediction algorithms [AD-A283669] p 170 N95-18018
Minimal time detection algorithms and applications to flight systems [TR-2-FSRC-93] p 171 N95-18564
Mesh quality control for multiply-refined tetrahedral grids [NASA-CR-197595] p 160 N95-18737
An assessment of the adaptive unstructured tetrahedral grid, Euler Flow Solver Code FELISA [NASA-TP-3526] p 119 N95-19041

ALL-WEATHER AIR NAVIGATION

A PC-based interactive simulation of the F-111C Pavé Tack system and related sensor, avionics and aircraft aspects [AD-A285500] p 129 N95-16969

ALTERNATING CURRENT

The use of electrochemistry and ellipsometry for identifying and evaluating corrosion on aircraft [AD-A285323] p 151 N95-16371

ALTITUDE

Evaluation of an autopilot based multimodelling [PB94-190725] p 142 N95-17454

ALTITUDE CONTROL

Selection of optimal parameters for a system, controlling the flight height, when information about the state vector is incomplete [BTN-94-EIX94461408753] p 168 A95-63636

ALUMINUM ALLOYS

Multi-lab comparison on R-curve methodologies: Alloy 2024-T3 [NASA-CR-195004] p 151 N95-18660
The application of Newman crack-closure model to predicting fatigue crack growth p 167 N95-19483

Fatigue crack growth in 2024-T3 aluminum under tensile and transverse shear stresses p 153 N95-19490
Prediction of R-curves from small coupon tests p 167 N95-19496

ANECHOIC CHAMBERS

Background noise levels measured in the NASA Lewis 9- by 15-foot low-speed wind tunnel [NASA-TM-106817] p 145 N95-18054

ANEMOMETERS

Aircraft wake vortex takeoff tests at O'Hara International Airport [AD-A283828] p 118 N95-18624

ANGLE OF ATTACK

X-29 high-angle-of-attack [BTN-94-EIX94511309383] p 127 A95-64609
An approach to aerodynamic characteristics of low radar cross-section fuselages p 106 N95-16251
An improved method of airfoil design p 106 N95-16252
Residual-correction type and related computational methods for aerodynamic design. Part 2: Multi-point airfoil design p 128 N95-16567
Numerical simulation of transient vortex breakdown above a pitching delta wing p 107 N95-16808
DLR-F4 wing body configuration p 130 N95-17863
DLR-F5: Test wing for CFD and applied aerodynamics p 113 N95-17864
Low aspect ratio wing experiment p 113 N95-17865

Wind tunnel investigations of the appearance of shocks in the windward region of bodies with circular cross section at angle of attack p 113 N95-17866
Three-dimensional boundary layer and flow field data of an inclined prolate spheroid p 158 N95-17867
Force and pressure data of an ogive-nosed slender body at high angles of attack and different Reynolds numbers p 113 N95-17868
Ellipsoid-cylinder model p 158 N95-17869

Wind tunnel performance comparative test results of a circular cylinder and 50 percent ellipse tailboom for circulation control antitorque applications [AD-A283335] p 130 N95-18008
Interaction, bursting and control of vortices of a cropped double-delta wing at high angle of attack [AD-A283656] p 119 N95-18669
2-D and 3-D oscillating wing aerodynamics for a range of angles of attack including stall [NASA-TM-4632] p 120 N95-19119
Velocity measurements with hot-wires in a vortex-dominated flowfield p 121 N95-19261

ANNULAR FLOW

Measurement of gust response on a turbine cascade [NASA-TM-106776] p 117 N95-18457

ANTENNA DESIGN

A VHF/UHF antenna for the Precision Antenna Measurement System (PAMS) [AD-A285673] p 156 N95-16621
Field verification of the wind tunnel coefficients p 109 N95-17291

ANTENNA RADIATION PATTERNS

A VHF/UHF antenna for the Precision Antenna Measurement System (PAMS) [AD-A285673] p 156 N95-16621

APPLICATIONS PROGRAMS (COMPUTERS)

Applications of automatic differentiation in computational fluid dynamics p 156 N95-16461
An analysis code for the Rapid Engineering Estimation of Momentum and Energy Losses (REMEL) [NASA-CR-191178] p 108 N95-16887
Interactive computer graphics applications for compressible aerodynamics [NASA-TM-106802] p 170 N95-17264
A platform independent application of Lux illumination prediction algorithms [AD-A283669] p 170 N95-18018
The generic simulation executive at Manned Flight Simulator [AD-A283997] p 146 N95-18724
Enhanced capabilities and modified users manual for axial-flow compressor conceptual design code CSPAN [NASA-TM-106833] p 119 N95-18933
Aircraft stress sequence development: A complex engineering process made simple p 136 N95-19480

APPROACH

Heliport/vertiport MLS precision approaches [AD-A283505] p 126 N95-18059

APPROACH CONTROL

Modeling of Instrument Landing System (ILS) localizer signal on runway 25L at Los Angeles International Airport [NASA-TM-4588] p 125 N95-17384

ARC JET ENGINES

Arcjet thruster research and technology, phase 2 [NASA-CR-182276] p 105 N95-18044

ARCHAEOLOGY

The effects of aircraft (B-52) overflights on ancient structures [BTN-94-EIX94341340070] p 171 A95-63522

ARCHITECTURE (COMPUTERS)

Portable parallel stochastic optimization for the design of aeropropulsion components [NASA-CR-195312] p 154 N95-16072
NASA High Performance Computing and Communications program [NASA-TM-4653] p 176 N95-18573

ARTIFICIAL INTELLIGENCE

Workshop on Formal Models for Intelligent Control [AD-A281399] p 169 N95-16864
Identification of Artificial Intelligence (AI) applications for maintenance, monitoring, and control of airway facilities [AD-A282479] p 125 N95-17373

ASCENT

Matlab as a robust control design tool p 169 N95-16474

ASPECT RATIO

Measurements of the flow over a low aspect-ratio wing in the Mach number range 0.6 to 0.87 for the purpose of validation of computational methods. Part 1: Wing design, model construction, surface flow. Part 2: Mean flow in the boundary layer and wake, 4 test cases p 112 N95-17860

ASTRONOMICAL COORDINATES

A platform independent application of Lux illumination prediction algorithms [AD-A283669] p 170 N95-18018

ASYMMETRY

Compression strength of composite primary structural components [NASA-CR-197554] p 160 N95-18388

ASYMPTOTIC SERIES

Studies on high pressure and unsteady flame phenomena [AD-A284126] p 152 N95-18410

ATMOSPHERIC EFFECTS

Matlab as a robust control design tool p 169 N95-16474
Atmospheric effects of high-flying subsonic aircraft: A catalogue of perturbing influences [KNMI-SR-94-03] p 168 N95-18722

ATMOSPHERIC MODELS

Microburst vertical wind estimation from horizontal wind measurements [NASA-TP-3460] p 131 N95-18198

ATMOSPHERIC PRESSURE

Studies on high pressure and unsteady flame phenomena [AD-A284126] p 152 N95-18410

ATMOSPHERIC TURBULENCE

Aircraft Loads due to Turbulence and their Impact on Design and Certification [AGARD-R-798] p 143 N95-18597
The impact of non-linear flight control systems on the prediction of aircraft loads due to turbulence p 143 N95-18598
Gyroscopic and propeller aerodynamic effects on engine mounts dynamic loads in turbulence conditions p 132 N95-18599
Treatment of non-linear systems by timeplane-transformed CT methods: The spectral gust method p 143 N95-18600
A study of the effect of store unsteady aerodynamics on gust and turbulence loads p 133 N95-18601
Comparison of stochastic and deterministic nonlinear gust analysis methods to meet continuous turbulence criteria p 133 N95-18602
Special effects of gust loads on military aircraft p 133 N95-18605

AUGMENTATION

Aeromechanics technology, volume 1. Task 1: Three-dimensional Euler/Navier-Stokes Aerodynamic Method (TEAM) enhancements [AD-A285713] p 132 N95-18483

AUTOMATIC CONTROL

Operational And Supportability Implementation System (OASIS) test and evaluation master plan [AD-A284765] p 126 N95-18088
VSTOL Systems Research Aircraft (VSRA) Harrier [NASA-TM-110117] p 126 N95-18347
NASA develops new digital flight control system [NASA-NEWS-RELEASE-94-47] p 144 N95-19029

AUTOMATIC PILOTS

Evaluation of an autopilot based multimodelling [PB94-190725] p 142 N95-17454

AUTONOMOUS NAVIGATION

A feedforward control approach to the local navigation problem for autonomous vehicles [AD-A282787] p 126 N95-17706

AVIATION METEOROLOGY

Microburst vertical wind estimation from horizontal wind measurements
[NASA-TP-3460] p 131 N95-18198

AVIONICS

The computer analysis of the prediction of aircraft electrical power supply system reliability p 155 N95-16278
A study of software standards used in the avionics industry p 137 N95-16456
New technologies for space avionics [NASA-CR-197574] p 150 N95-18196
KC-135 cockpit modernization study. Phase 1: Equipment evaluation [AD-A284099] p 131 N95-18398
Strategic avionics technology definition studies. Subtask 3-1A3: Electrical Actuation (ELA) Systems Test Facility [NASA-CR-188360] p 143 N95-18567

AXIAL LOADS

A Lifting Ball Valve for cryogenic fluid applications p 156 N95-16349
Results of uniaxial and biaxial tests on riveted fuselage lap joint specimens p 136 N95-19491

AXISYMMETRIC BODIES

An investigation of the transonic pressure drag coefficient for axis-symmetric bodies [AD-A280990] p 105 N95-15994
Pressure distributions on research wing W4 mounted on an axisymmetric body p 112 N95-17862
Ellipsoid-cylinder model p 158 N95-17869

B

B-52 AIRCRAFT

The effects of aircraft (B-52) overflights on ancient structures [BTN-94-EIX94341340070] p 171 A95-63522

BACKGROUND NOISE

Background noise levels measured in the NASA Lewis 9- by 15-foot low-speed wind tunnel [NASA-TM-106817] p 145 N95-18054

BACKWARD DIFFERENCING

A spectrally accurate boundary-layer code for infinite swept wings [NASA-CR-195014] p 159 N95-18042

BALANCE

Helicopter Performance Evaluation (HELPE) computer model [AD-A284319] p 131 N95-18381
Hydrofoil force balance [AD-D016475] p 160 N95-18461

BALL BEARINGS

A Lifting Ball Valve for cryogenic fluid applications p 156 N95-16349

BASE FLOW

Numerical computations of supersonic base flow with special emphasis on turbulence modeling [AD-A283688] p 119 N95-18670

BASE PRESSURE

Investigation of the flow development on a highly swept canard/wing research model with segmented leading- and trailing-edge flaps p 114 N95-17876

BAYS (STRUCTURAL UNITS)

Weapons bay acoustic environment p 173 N95-19146

BENDING

Discrete crack growth analysis methodology for through cracks in pressurized fuselage structures p 166 N95-19473

BENDING FATIGUE

Detecting gear tooth fracture in a high contact ratio face gear mesh [NASA-TM-106822] p 162 N95-19125

BENDING MOMENTS

Investigation of dynamic inflow's influence on rotor control derivatives p 155 N95-16250

BERNOULLI THEOREM

Acoustic radiation damping of flat rectangular plates subjected to subsonic flows p 172 N95-18542

BIBLIOGRAPHIES

Documentation and archiving of the Space Shuttle wind tunnel test data base. Volume 1: Background and description [NASA-TM-104806-VOL-1] p 151 N95-19237

BINOCULARS

Factors affecting the visual fragmentation of the field-of-view in partial binocular overlap displays [AD-A283081] p 172 N95-17334

BIPOLARITY

Development of a bipolar lead/acid battery for the more electric aircraft [AD-A284050] p 160 N95-18660

BLOCKING

Adaptive wind tunnel walls versus wall interference correction methods in 2D flows at high blockage ratios p 147 N95-19267

BLOWDOWN WIND TUNNELS

Free-jet testing at Mach 3.44 in GASL's aero/thermo test facility p 145 N95-16320
Operating capability and current status of the reactivated NASA Lewis Research Center Hypersonic Tunnel Facility [NASA-TM-106808] p 148 N95-19286

BLUNT BODIES

Ellipsoid-cylinder model p 158 N95-17869

BODY-WING CONFIGURATIONS

Wing-body juncture flows [AD-A281526] p 106 N95-16099
Aerodynamic shape optimization p 128 N95-16572
Review of the EUROPT Project AERO-0026 p 129 N95-16573
Pressure distributions on research wing W4 mounted on an axisymmetric body p 112 N95-17862
DLR-F4 wing body configuration p 130 N95-17863

BONDED JOINTS

Application of superplastically formed and diffusion bonded structures in high intensity noise environments p 174 N95-19162

BOOSTER ROCKET ENGINES

The 1993 JANNAF Propulsion Meeting, volume 1 [CPIA-PUBL-602-VOL-1] p 148 N95-16312

BORON-EPOXY COMPOSITES

Ultrasonic techniques for repair of aircraft structures with bonded composite patches p 136 N95-19486

BOUNDARIES

Waveform bounding and combination techniques for direct drive testing [AD-A284075] p 161 N95-19035
Boundary-flow measurement methods for wall interference assessment and correction: Classification and review p 163 N95-19262
Transonic wind tunnel boundary interference correction p 147 N95-19271

BOUNDARY CONDITIONS

2-D airfoil tests including side wall boundary layer measurements p 158 N95-17847
Data from the GARTEur (AD) Action Group 02 airfoil CAST 7/DOA1 experiments p 111 N95-17856
Low aspect ratio wing experiment p 113 N95-17865

A spectrally accurate boundary-layer code for infinite swept wings [NASA-CR-195014] p 159 N95-18042
Wall correction method with measured boundary conditions for low speed wind tunnels p 164 N95-19263

Determination of solid/porous wall boundary conditions from wind tunnel data for computational fluid dynamics codes p 164 N95-19266
Analysis of test section sidewall effects on a two dimensional airfoil: Experimental and numerical investigations p 165 N95-19276

BOUNDARY ELEMENT METHOD

Linear instability waves in supersonic jets confined in circular and non-circular ducts [BTN-94-EIX94341340068] p 103 A95-63520

BOUNDARY LAYER COMBUSTION

Service and physical properties of liquid-jet fuels p 151 N95-16256

BOUNDARY LAYER CONTROL

Optimum aerodynamic design via boundary control p 127 N95-16565
Parametric study on laminar flow for finite wings at supersonic speeds [NASA-TM-108852] p 116 N95-18101

BOUNDARY LAYER EQUATIONS

A spectrally accurate boundary-layer code for infinite swept wings [NASA-CR-195014] p 159 N95-18042

BOUNDARY LAYER FLOW

Mach number, flow angle, and loss measurements downstream of a transonic fan-blade cascade [AD-A280907] p 108 N95-16824
Experiments in the trailing edge flow of an NLR 7702 airfoil p 110 N95-17853
Data from the GARTEur (AD) Action Group 02 airfoil CAST 7/DOA1 experiments p 111 N95-17856
The stability of two-phase flow over a swept-wing [NASA-CR-194994] p 159 N95-18190
Effect of crossflow on Goertler instability in incompressible boundary layers [NASA-CR-195007] p 159 N95-18193
Solution of Navier-Stokes equations using high accuracy monotone schemes p 161 N95-19019
Boundary-flow measurement methods for wall interference assessment and correction: Classification and review p 163 N95-19262

Viscous flow past aerofoils axisymmetric bodies and wings p 123 N95-19457

BOUNDARY LAYER SEPARATION

Wing-body juncture flows [AD-A281526] p 106 N95-16099
Time accurate computation of unsteady inlet flows with a dynamic flow adaptive mesh [AD-A285498] p 157 N95-16736
Mach number, flow angle, and loss measurements downstream of a transonic fan-blade cascade [AD-A280907] p 108 N95-16824
Low-speed surface pressure and boundary layer measurement data for the NLR 7301 airfoil section with trailing edge flap p 111 N95-17855
Three-dimensional boundary layer and flow field data of an inclined prolate spheroid p 158 N95-17867
Ellipsoid-cylinder model p 158 N95-17869
Supersonic vortex flow around a missile body p 114 N95-17870

Test data on a non-circular body for subsonic, transonic and supersonic Mach numbers p 158 N95-17871
Experimental investigation of the vortex flow over a 76/60-deg double delta wing p 114 N95-17874
Wind tunnel test on a 65 deg delta wing with rounded leading edges: The International Vortex Flow Experiment p 114 N95-17875

Subsonic flow around US-orbiter model FALKE in the DNW p 115 N95-17877
Sectional prediction of 3D effects for separated flow on rotating blades [PB94-201696] p 117 N95-18503
Theoretical investigations of shock/boundary layer interactions on a Ma(infinity) = 8 waverider [DLR-FB-94-12] p 119 N95-18910

BOUNDARY LAYER STABILITY

Parametric study on laminar flow for finite wings at supersonic speeds [NASA-TM-108852] p 116 N95-18101
Effect of crossflow on Goertler instability in incompressible boundary layers [NASA-CR-195007] p 159 N95-18193

BOUNDARY LAYER TRANSITION

Wind tunnel test on a 65 deg delta wing with a sharp or rounded leading edge: The international vortex flow experiment p 114 N95-17872
Hypersonic wind tunnel test techniques [AD-A284057] p 118 N95-18663

BOUNDARY LAYERS

Aerodynamic shape optimization p 128 N95-16572
2-D airfoil tests including side wall boundary layer measurements p 158 N95-17847
Low-speed surface pressure and boundary layer measurement data for the NLR 7301 airfoil section with trailing edge flap p 111 N95-17855
Measurements of the flow over a low aspect-ratio wing in the Mach number range 0.6 to 0.87 for the purpose of validation of computational methods. Part 1: Wing design model construction, surface flow. Part 2: Mean flow in the boundary layer and wake, 4 test cases p 112 N95-17860

BREADBOARD MODELS

Eddy current for detecting second layer cracks under installed fasteners [AD-A282412] p 158 N95-17507

BUBBLES

Low-speed surface pressure and boundary layer measurement data for the NLR 7301 airfoil section with trailing edge flap p 111 N95-17855

BUCKLING

Shear buckling analysis of a hat-stiffened panel [NASA-TM-4644] p 158 N95-17490

BUFFETING

Pressure measurements on an F/A-18 twin vertical tail in buffeting flow. Volume 4, part 2: Buffet cross spectral densities [AD-A285555] p 143 N95-18641

BURNING RATE

Studies on high pressure and unsteady flame phenomena [AD-A284126] p 152 N95-18410

C

C-135 AIRCRAFT

KC-135 cockpit modernization study. Phase 1: Equipment evaluation [AD-A284099] p 131 N95-18398
An artificial corrosion protocol for lap-splices in aircraft skin p 152 N95-19482

CALIBRATING

An investigation of polynomial calibrations methods for wind tunnel balances p 144 N95-16258

- Aeromechanics technology, volume 1. Task 1: Three-dimensional Euler/Navier-Stokes Aerodynamic Method (TEAM) enhancements [AD-A285713] p 132 N95-18483
- Applications of the five-hole probe technique for flow field surveys at the Institute for Aerospace Research p 163 N95-19255
- CAMBER**
Investigation of the flow over a series of 14 percent-thick supercritical aerofoils with significant rear camber p 109 N95-17849
- CANARD CONFIGURATIONS**
Experimental study at low supersonic speeds of a missile concept having opposing wraparound tails [NASA-TM-4582] p 106 N95-16069
Wind tunnel test on a 65 deg delta wing with a sharp or rounded leading edge: The international vortex flow experiment p 114 N95-17872
Wind tunnel test on a 65 deg delta wing with rounded leading edges: The International Vortex Flow Experiment p 114 N95-17875
Investigation of the flow development on a highly swept canard/wing research model with segmented leading- and trailing-edge flaps p 114 N95-17876
Velocity measurements with hot-wires in a vortex-dominated flowfield p 121 N95-19261
- CAPTURE EFFECT**
Floating shock fitting via Lagrangian adaptive meshes [NASA-CR-194997] p 170 N95-18110
- CARBON FIBER REINFORCED PLASTICS**
Brite-Euram programme: ACOUFAT acoustic fatigue and related damage tolerance of advanced composite and metallic structures p 174 N95-19159
- CARBONATES**
Bicarbonate of soda blasting technology for aircraft wheel depainting [PB94-193323] p 104 N95-17466
- CASCADE FLOW**
Aerodynamic design and calculation of flow around the plane cascade of turbine [BTN-94-EIX94481415357] p 104 A95-65347
Mach number, flow angle, and loss measurements downstream of a transonic fan-blade cascade [AD-A280907] p 108 N95-16824
Measurement of gust response on a turbine cascade [NASA-TM-106776] p 117 N95-18457
Enhanced capabilities and modified users manual for axial-flow compressor conceptual design code CSPAN [NASA-TM-106833] p 119 N95-18933
Simulation of steady and unsteady viscous flows in turbomachinery p 140 N95-19023
- CATHODE RAY TUBES**
An evaluation of aircraft CRT and dot-matrix display legibility requirements [AD-A283933] p 138 N95-18164
- CAVITY FLOW**
Weapons bay acoustic environment p 173 N95-19146
- CENTRIFUGAL COMPRESSORS**
Unsteady flow phenomena in discrete passage diffusers for centrifugal compressors [AD-A281412] p 155 N95-16163
- CERAMIC MATRIX COMPOSITES**
A CMC database for use in the next generation launch vehicles (rockets) p 150 N95-18993
- CERTIFICATION**
Aircraft and sub-system certification by piloted simulation [AGARD-AR-278] p 145 N95-17388
- CH-47 HELICOPTER**
Design and flight test of a simplified control system for a transport helicopter p 144 N95-18902
- CHANGE DETECTION**
Minimal time detection algorithms and applications to flight systems [TR-2-FSRC-93] p 171 N95-18564
- CHANNEL FLOW**
Aerodynamic investigation of the flow field in a 180 deg turn channel with sharp bend p 163 N95-19257
- CHEMICAL COMPOSITION**
Solid fuel ramjet composition [AD-D016458] p 152 N95-19090
- CIRCULAR CYLINDERS**
Wind tunnel investigations of the appearance of shocks in the windward region of bodies with circular cross section at angle of attack p 113 N95-17866
Force and pressure data of an ogive-nosed slender body at high angles of attack and different Reynolds numbers p 113 N95-17868
Wind tunnel performance comparative test results of a circular cylinder and 50 percent ellipse tailboom for circulation control antitorque applications [AD-A283335] p 130 N95-18008
- CIRCULATION CONTROL AIRFOILS**
Wind tunnel performance comparative test results of a circular cylinder and 50 percent ellipse tailboom for circulation control antitorque applications [AD-A283335] p 130 N95-18008
- CIVIL AVIATION**
The ICAO CNS/ATM system: New king, new law? [HTN-95-50218] p 175 A95-64855
Aircraft accident investigation and airworthiness -- A practical example of the interaction of two disciplines with some reflections on possible legal consequences [HTN-95-50219] p 176 A95-64856
World trends in air transport policies. (Approaching the 21st century) [HTN-95-50220] p 176 A95-64857
EC Aviation Scene [HTN-95-50223] p 176 A95-64860
European aeronautics: Strong government presence in industry structure and research and development support. Report to Congressional Requesters [GAO/NSIAD-94-71] p 176 N95-18578
- CLASSIFICATIONS**
Hypersonic flow-field measurements: Intrusive and nonintrusive [AD-A283867] p 119 N95-18674
- CLEARANCES**
Aircraft and sub-system certification by piloted simulation [AGARD-AR-278] p 145 N95-17388
- CLOSED CYCLES**
Ultimate characteristics of a rocket engine with a turbo-pump supply system [BTN-94-EIX94461408757] p 148 A95-63640
- COANDA EFFECT**
Wind tunnel performance comparative test results of a circular cylinder and 50 percent ellipse tailboom for circulation control antitorque applications [AD-A283335] p 130 N95-18008
Static investigation of two fluidic thrust-vectoring concepts on a two-dimensional convergent-divergent nozzle [NASA-TM-4574] p 120 N95-19042
- COCKPITS**
Industry review of a crew-centered cockpit design process and toolset [AD-A282966] p 130 N95-17661
KC-135 cockpit modernization study. Phase 1: Equipment evaluation [AD-A284099] p 131 N95-18398
The generic simulation executive at Manned Flight Simulator [AD-A283997] p 146 N95-18724
An overall approach of cockpit noise verification in a military aircraft p 175 N95-19163
- COMBUSTION CHAMBERS**
Development and application of the double V type flame stabilizer [BTN-94-EIX94481415355] p 154 A95-65345
A model for preliminary facility design including simulation issues p 144 N95-16318
One-dimensional flow description for the combustion chamber of a scramjet [DLR-FB-94-06] p 139 N95-18911
- COMBUSTION EFFICIENCY**
Combustor kinetic energy efficiency analysis of the hypersonic research engine data p 148 N95-16321
Experimental and analytical methods for the determination of connected-pipe ramjet and ducted rocket internal performance [AGARD-AR-323] p 149 N95-17278
- COMBUSTION PRODUCTS**
Wave cycle design for wave rotor engines with limited nitrogen oxide emissions p 161 N95-18901
- COMBUSTION TEMPERATURE**
Ultimate characteristics of a rocket engine with a turbo-pump supply system [BTN-94-EIX94461408757] p 148 A95-63640
- COMMAND AND CONTROL**
Spread spectrum applications in unmanned aerial vehicles [AD-A281035] p 156 N95-16448
Workshop on Formal Models for Intelligent Control [AD-A281399] p 169 N95-16864
Packet utilisation definitions for the ESA XMM mission p 150 N95-17596
- COMMAND GUIDANCE**
Safety aspects of spacecraft commanding p 149 N95-17248
- COMMERCIAL AIRCRAFT**
Annual review of aircraft accident data: US Air carrier operations, calendar year 1992 [PB95-100319] p 123 N95-17748
DLR-F4 wing body configuration p 130 N95-17863
- COMMUTER AIRCRAFT**
Safety study: Commuter airline safety [PB94-917004] p 124 N95-19132
- COMPLEX SYSTEMS**
Algorithms for bilevel optimization [NASA-CR-194980] p 170 N95-16897
- COMPONENT RELIABILITY**
Residual life and strength estimates of aircraft structural components with MSD/MED p 136 N95-19485
- COMPOSITE MATERIALS**
Fatigue in single crystal nickel superalloys [AD-A285727] p 152 N95-18068
Conference on Aerospace Transparent Materials and Enclosures. Volume 2: Sessions 5-9 [AD-A283926] p 131 N95-18162
Conference on Aerospace Transparent Materials and Enclosures, volume 1 [AD-A283925] p 133 N95-18677
- COMPOSITE STRUCTURES**
Service and physical properties of liquid-jet fuels p 151 N95-16256
Composite chronicles: A study of the lessons learned in the development, production, and service of composite structures [NASA-CR-4620] p 151 N95-16859
Optimization of adaptive intraply hybrid fiber composites with reliability considerations [NASA-TM-106632] p 157 N95-16911
Wing design for a civil tiltrotor transport aircraft [NASA-CR-197523] p 130 N95-18090
Compression strength of composite primary structural components [NASA-CR-197554] p 160 N95-18388
Impact of Acoustic Loads on Aircraft Structures [AGARD-CP-549] p 173 N95-19142
- COMPRESSIBILITY**
Investigation of an NLF(1)-0416 airfoil in compressible subsonic flow p 110 N95-17852
- COMPRESSIBLE BOUNDARY LAYER**
A spectrally accurate boundary-layer code for infinite swept wings [NASA-CR-195014] p 159 N95-18042
- COMPRESSIBLE FLOW**
A workstation based simulator for teaching compressible aerodynamics [NASA-TM-106799] p 170 N95-16906
Three dimensional compressible turbulent flow computations for a diffusing S-duct with/without vortex generators [NASA-CR-195390] p 138 N95-17402
Investigation of an NLF(1)-0416 airfoil in compressible subsonic flow p 110 N95-17852
Floating shock fitting via Lagrangian adaptive meshes [NASA-CR-194997] p 170 N95-18110
Numerical simulation of dynamic-stall suppression by tangential blowing [AD-A284887] p 120 N95-19110
- COMPRESSIBLE FLUIDS**
Interactive computer graphics applications for compressible aerodynamics [NASA-TM-106802] p 170 N95-17264
- COMPRESSION LOADS**
Shear buckling analysis of a hat-stiffened panel [NASA-TM-4644] p 158 N95-17490
- COMPRESSIVE STRENGTH**
Development of an Automated Airfield Dynamic Cone Penetrometer (AADCP) prototype and the evaluation of unsurfaced airfield seismic surveying using Spectral Analysis of Surface Waves (SASW) technology [AD-A281985] p 145 N95-17444
Compression strength of composite primary structural components [NASA-CR-197554] p 160 N95-18388
- COMPUTATIONAL FLUID DYNAMICS**
A grid generation and flow solution method for the Euler equations on unstructured grids [HTN-95-20003] p 153 A95-63201
Improved analytical solution for varying specific heat parallel stream mixing [BTN-94-EIX94481415349] p 103 A95-65339
Numerical simulation of supersonic compression corners and hypersonic inlet flows using the RPLUS2D code [NASA-TM-106580] p 105 N95-16038
High altitude hypersonic flowfield radiation [AD-A281386] p 106 N95-16160
Applications of automatic differentiation in computational fluid dynamics p 156 N95-16461
Optimum Design Methods for Aerodynamics [AGARD-R-803] p 127 N95-16562
Time accurate computation of unsteady inlet flows with a dynamic flow adaptive mesh [AD-A285498] p 157 N95-16736
Applications of automatic differentiation in CFD [NASA-TM-109948] p 157 N95-16828
Interactive computer graphics applications for compressible aerodynamics [NASA-TM-106802] p 170 N95-17264

Three dimensional compressible turbulent flow computations for a diffusing S-duct with/without vortex generators
 [NASA-CR-195390] p 138 N95-17402
 A selection of experimental test cases for the validation of CFD codes, volume 2
 [AGARD-AR-303-VOL-2] p 109 N95-17846
 Low-speed surface pressure and boundary layer measurement data for the NLR 7301 airfoil section with trailing edge flap p 111 N95-17855
 Data from the GARTEur (AD) Action Group 02 airfoil CAST 7/DOA1 experiments p 111 N95-17856
 A supercritical airfoil experiment p 111 N95-17858
 Two-dimensional high-lift airfoil data for CFD code validation p 112 N95-17859
 Measurements of the flow over a low aspect-ratio wing in the Mach number range 0.6 to 0.87 for the purpose of validation of computational methods. Part 1: Wing design, model construction, surface flow. Part 2: Mean flow in the boundary layer and wake, 4 test cases p 112 N95-17860
 Detailed study at supersonic speeds of the flow around delta wings p 112 N95-17861
 STOVL CFD model test case p 115 N95-17881
 Low speed propeller slipstream aerodynamic effects p 116 N95-17882
 Parachute inflation: A problem in aerelasticity [AD-A284375] p 117 N95-18340
 Aeromechanics technology, volume 1. Task 1: Three-dimensional Euler/Navier-Stokes Aerodynamic Method (TEAM) enhancements p 132 N95-18483
 A selection of experimental test cases for the validation of CFD codes. Supplement: Datasets A-E [AGARD-AR-303-SUPPL] p 117 N95-18539
 NASA High Performance Computing and Communications program [NASA-TM-4653] p 176 N95-18573
 Static aerodynamics CFD analysis for 120-mm hypersonic KE projectile design [ARL-MR-184] p 118 N95-18611
 Numerical computations of supersonic base flow with special emphasis on turbulence modeling [AD-A283688] p 119 N95-18670
 Hypersonic flow-field measurements: Intrusive and nonintrusive [AD-A283867] p 119 N95-18674
 Mesh quality control for multiply-refined tetrahedral grids [NASA-CR-197595] p 160 N95-18737
 Solution of full potential equation on an airfoil by multigrid technique [NAL-TM-CSS-9303] p 119 N95-18904
 Theoretical investigations of shock/boundary layer interactions on a Ma(infinity) = 8 waverider [DLR-FB-94-12] p 119 N95-18910
 One-dimensional flow description for the combustion chamber of a scramjet [DLR-FB-94-06] p 139 N95-18911
 Flow field investigation in a free jet - free jet core system for the generation of high intensity molecular beams [DLR-FB-94-11] p 172 N95-18912
 Solution of Navier-Stokes equations using high accuracy monotone schemes p 161 N95-19019
 An assessment of the adaptive unstructured tetrahedral grid, Euler Flow Solver Code FELISA [NASA-TP-3526] p 119 N95-19041
 Static investigation of two fluidic thrust-vectoring concepts on a two-dimensional convergent-divergent nozzle [NASA-TM-4574] p 120 N95-19042
 Determination of stores pointing error due to wing flexibility under flight load [NASA-TM-4646] p 134 N95-19044
 Numerical simulation of dynamic-stall suppression by tangential blowing [AD-A284887] p 120 N95-19110
 Navier-Stokes, flight, and wind tunnel flow analysis for the F/A-18 aircraft [NASA-TP-3478] p 120 N95-19114
 Determination of solid/porous wall boundary conditions from wind tunnel data for computational fluid dynamics codes p 164 N95-19266
 Unsteady aerodynamic analyses for turbomachinery aeroelastic predictions p 141 N95-19381
 Steady potential solver for unsteady aerodynamic analyses p 141 N95-19382
 CFD: Advances and Applications, part 1 [NAL-SP-9322-PT-1] p 165 N95-19444
 Computation of inviscid flows: Full potential method p 165 N95-19447
 Panel methods p 165 N95-19448
 Viscous flow past aerofoils axisymmetric bodies and wings p 123 N95-19457

COMPUTATIONAL GRIDS

A grid generation and flow solution method for the Euler equations on unstructured grids [HTN-95-20003] p 153 A95-63201
 Time accurate computation of unsteady inlet flows with a dynamic flow adaptive mesh [AD-A285498] p 157 N95-16736
 Floating shock fitting via Lagrangian adaptive meshes [NASA-CR-194997] p 170 N95-18110
 Mesh quality control for multiply-refined tetrahedral grids [NASA-CR-197595] p 160 N95-18737
 The mathematical models of flow passage for gas turbine engines and their components p 140 N95-19020
 Application of multicomponent models to flow passage simulation in multistage turbomachines and whole gas turbine engines p 140 N95-19022
 An assessment of the adaptive unstructured tetrahedral grid, Euler Flow Solver Code FELISA [NASA-TP-3526] p 119 N95-19041
 Numerical simulation of dynamic-stall suppression by tangential blowing [AD-A284887] p 120 N95-19110
 CFD: Advances and Applications, part 1 [NAL-SP-9322-PT-1] p 165 N95-19444
COMPUTER AIDED DESIGN
 Generalized method of solving topological optimization problems for electrical airplane equipment systems in computer-aided design p 169 N95-16272
 An engineering code to analyze hypersonic thermal management systems p 155 N95-16322
 Applications of automatic differentiation in CFD [NASA-TM-109948] p 157 N95-16828
 Wing design for a civil tiltrotor transport aircraft [NASA-CR-197523] p 130 N95-18090
 Enhanced capabilities and modified users manual for axial-flow compressor conceptual design code CSPAN [NASA-TM-106833] p 119 N95-18933
 Application of multidisciplinary models to the cooled turbine rotor design p 140 N95-19024
 Perspective problems of gas turbine engines simulation p 140 N95-19026
 Modelling structurally damaging twin-jet screech p 135 N95-19154
COMPUTER ASSISTED INSTRUCTION
 A workstation based simulator for teaching compressible aerodynamics [NASA-TM-106799] p 170 N95-16906
COMPUTER GRAPHICS
 Interactive computer graphics applications for compressible aerodynamics [NASA-TM-106802] p 170 N95-17264
 An evaluation of aircraft CRT and dot-matrix display legibility requirements [AD-A283933] p 138 N95-18164
COMPUTER PROGRAM INTEGRITY
 A study of software standards used in the avionics industry p 137 N95-16456
COMPUTER PROGRAMMING
 A study of software standards used in the avionics industry p 137 N95-16456
 Applications of automatic differentiation in computational fluid dynamics p 156 N95-16461
COMPUTER PROGRAMS
 On a program-information system TDsoft [BTN-94-EI194461408773] p 175 A95-63656
 Evaluation of the dynamic stability characteristics of the NAL Light Transport Aircraft [NAL-PD-CA-9217] p 142 N95-16392
 A study of software standards used in the avionics industry p 137 N95-16456
 FPCAS2D user's guide, version 1.0 [NASA-CR-195413] p 156 N95-16588
 Demonstration of the Dynamic Flowgraph Methodology using the Titan 2 Space Launch Vehicle Digital Flight Control System [NASA-CR-197517] p 150 N95-17493
 Data from the GARTEur (AD) Action Group 02 airfoil CAST 7/DOA1 experiments p 111 N95-17856
 OAT15A airfoil data p 111 N95-17857
 Two-dimensional high-lift airfoil data for CFD code validation p 112 N95-17859
 A platform independent application of Lux illumination prediction algorithms p 170 N95-18018
 Operational And Supportability Implementation System (OASIS) test and evaluation master plan [AD-A284765] p 126 N95-18088
 Regenerative cooling for liquid propellant rocket thrust chambers [INPE-5565-TDI/540] p 150 N95-18720
 Hypersonic flight testing [AD-A283981] p 134 N95-18891
 An assessment of the adaptive unstructured tetrahedral grid, Euler Flow Solver Code FELISA [NASA-TP-3526] p 119 N95-19041

Evaluation of scanners for C-scan imaging in nondestructive inspection of aircraft [DE94-012473] p 152 N95-19100
 Unsteady aerodynamic analyses for turbomachinery aeroelastic predictions p 141 N95-19381
 Technology Benefit Estimator (T/BEST): User's manual [NASA-TM-106785] p 167 N95-19501
COMPUTER SYSTEMS PERFORMANCE
 The ICAO CNS/ATM system: New king, new law? [HTN-95-50218] p 175 A95-64855
COMPUTER SYSTEMS PROGRAMS
 The generic simulation executive at Manned Flight Simulator [AD-A283997] p 146 N95-18724
 Technology Benefit Estimator (T/BEST): User's manual [NASA-TM-106785] p 167 N95-19501
COMPUTER TECHNIQUES
 Portable parallel stochastic optimization for the design of aeropropulsion components [NASA-CR-195312] p 154 N95-16072
 Joint Proceedings on Aeronautics and Astronautics (JPAA) [ISBN-7-80-046602-7] p 104 N95-16249
 The computer analysis of the prediction of aircraft electrical power supply system reliability p 155 N95-16278
 Rapid solution of large-scale systems of equations p 169 N95-16458
 Interactive computer graphics applications for compressible aerodynamics [NASA-TM-106802] p 170 N95-17264
 Identification of Artificial Intelligence (AI) applications for maintenance, monitoring, and control of airway facilities [AD-A282479] p 125 N95-17373
 A platform independent application of Lux illumination prediction algorithms [AD-A283669] p 170 N95-18018
COMPUTERIZED SIMULATION
 Matlab as a robust control design tool p 169 N95-16474
 Numerical simulation of helicopter engine plume in forward flight [NASA-CR-197488] p 107 N95-16589
 Applications of automatic differentiation in CFD [NASA-TM-109948] p 157 N95-16828
 A workstation based simulator for teaching compressible aerodynamics [NASA-TM-106799] p 170 N95-16906
 A PC-based interactive simulation of the F-111C Pavé Tack system and related sensor, avionics and aircraft aspects [AD-A285500] p 129 N95-16969
 Interactive computer graphics applications for compressible aerodynamics [NASA-TM-106802] p 170 N95-17264
 Demonstration of the Dynamic Flowgraph Methodology using the Titan 2 Space Launch Vehicle Digital Flight Control System [NASA-CR-197517] p 150 N95-17493
 Low-speed surface pressure and boundary layer measurement data for the NLR 7301 airfoil section with trailing edge flap p 111 N95-17855
 Data from the GARTEur (AD) Action Group 02 airfoil CAST 7/DOA1 experiments p 111 N95-17856
 OAT15A airfoil data p 111 N95-17857
 A supercritical airfoil experiment p 111 N95-17858
 Two-dimensional high-lift airfoil data for CFD code validation p 112 N95-17859
 Six degree of freedom flight dynamic and performance simulation of a remotely-piloted vehicle [AERO-TN-9301] p 131 N95-18097
 Helicopter Performance Evaluation (HELPE) computer model [AD-A284319] p 131 N95-18381
 Studies on high pressure and unsteady flame phenomena [AD-A284126] p 152 N95-18410
 Aeromechanics technology, volume 1. Task 1: Three-dimensional Euler/Navier-Stokes Aerodynamic Method (TEAM) enhancements [AD-A285713] p 132 N95-18483
 NASA High Performance Computing and Communications program [NASA-TM-4653] p 176 N95-18573
 The generic simulation executive at Manned Flight Simulator [AD-A283997] p 146 N95-18724
 Perspective problems of gas turbine engines simulation p 140 N95-19026
 Fatigue loads spectra derivation for the Space Shuttle: Second cycle p 166 N95-19470

- COMPUTERS**
Evaluation of scanners for C-scan imaging in nondestructive inspection of aircraft [DE94-012473] p 152 N95-19100
- CONCURRENT ENGINEERING**
New technologies for space avionics [NASA-CR-197574] p 150 N95-18196
- CONFERENCES**
The 1993 JANNAP Propulsion Meeting, volume 1 [CPIA-PUBL-602-VOL-1] p 148 N95-16312
Workshop on Formal Models for Intelligent Control [AD-A281399] p 169 N95-16864
Conference on Aerospace Transparent Materials and Enclosures, Volume 2: Sessions 5-9 [AD-A283926] p 131 N95-18162
Aircraft Loads due to Turbulence and their Impact on Design and Certification [AGARD-R-798] p 143 N95-18597
Conference on Aerospace Transparent Materials and Enclosures, volume 1 [AD-A283925] p 133 N95-18677
Mathematical Models of Gas Turbine Engines and their Components [AGARD-LS-198] p 139 N95-19017
Wall Interference, Support Interference and Flow Field Measurements [AGARD-CP-535] p 162 N95-19251
NASA Lewis Research Center Workshop on Forced Response in Turbomachinery [NASA-CP-10147] p 141 N95-19380
FAA/NASA International Symposium on Advanced Structural Integrity Methods for Airframe Durability and Damage Tolerance, part 2 [NASA-CP-3274-PT-2] p 124 N95-19468
- CONFINEMENT**
Numerical mixing calculations of confined reacting jet flows in a cylindrical duct [NASA-TM-106736] p 139 N95-18133
- CONFORMAL MAPPING**
Optimum aerodynamic design via boundary control p 127 N95-16565
- CONSERVATION LAWS**
CFD: Advances and Applications, part 1 [NAL-SP-9322-PT-1] p 165 N95-19444
- CONTAMINANTS**
Bicarbonate of soda blasting technology for aircraft wheel repainting [PB94-193323] p 104 N95-17466
- CONTINUITY EQUATION**
Acoustic radiation damping of flat rectangular plates subjected to subsonic flows p 172 N95-18542
- CONTINUUM FLOW**
Hypersonic wind tunnel test techniques [AD-A284057] p 118 N95-18663
Flow field investigation in a free jet - free jet core system for the generation of high intensity molecular beams [DLR-FB-94-11] p 172 N95-18912
- CONTOURS**
New approach to geometric profiling of the design elements of the passage part in turbo-machines [BTN-94-EIX94461408769] p 153 A95-63652
An approach to aerodynamic characteristics of low radar cross-section fuselages p 106 N95-16251
- CONTROL**
Strategic avionics technology definition studies, Subtask 3-1A3: Electrical Actuation (ELA) Systems Test Facility [NASA-CR-188360] p 143 N95-18567
- CONTROL BOARDS**
On-line handling of air traffic: Management, guidance and control [AGARD-AG-321] p 126 N95-18927
- CONTROL SURFACES**
Engineering methods for the evaluation of transonic flutter characteristics for aerodynamic control surfaces [BTN-94-EIX94461408589] p 141 A95-63064
Modelling for optimal operations of line milling of aerodynamic surfaces [BTN-94-EIX94461408774] p 138 A95-63657
Active load control during rolling maneuvers — performed in the Langley Transonic Dynamics Tunnel [NASA-TP-3455] p 129 N95-17397
Plant and controller optimization by convex methods [AD-A283700] p 133 N95-18621
- CONTROL SYSTEMS DESIGN**
Selection of optimal parameters for a system, controlling the flight height, when information about the state vector is incomplete [BTN-94-EIX94461408753] p 168 A95-63636
Nonsmooth trajectory optimization: An approach using continuous simulated annealing [BTN-94-EIX94511433914] p 168 A95-64580
H(sup 2)/H(sup INF) controller design for a two-dimensional thin airfoil flutter suppression [BTN-94-EIX94511433918] p 141 A95-64584
Test bench for rotorcraft hover control [BTN-94-EIX94511433919] p 169 A95-64585
Aircraft model for the AIAA controls design challenge [BTN-94-EIX94511433921] p 142 A95-64587
Intelligent control law tuning for AIAA controls design challenge [BTN-94-EIX94511433922] p 169 A95-64588
Sensor fault detection and diagnosis simulation of a helicopter engine in an intelligent control framework [NASA-TM-106784] p 137 N95-15970
Matlab as a robust control design tool [AGARD-AR-278] p 145 N95-17388
Cooperative control theory and integrated flight and propulsion control [NASA-CR-197493] p 142 N95-17404
Microgravity isolation system design: A case study [NASA-TM-106804] p 104 N95-17657
Microgravity isolation system design: A modern control synthesis framework [NASA-TM-106805] p 105 N95-18197
Microgravity isolation system design: A modern control analysis framework [NASA-TM-106803] p 105 N95-18486
The impact of non-linear flight control systems on the prediction of aircraft loads due to turbulence p 143 N95-18598
Plant and controller optimization by convex methods [AD-A283700] p 133 N95-18621
Design and flight test of a simplified control system for a transport helicopter p 144 N95-18902
- CONTROL THEORY**
Output feedback control under randomly varying distributed delays [BTN-94-EIX94511433916] p 168 A95-64582
Design of nonlinear control laws for high-angle-of-attack flight [BTN-94-EIX94511433920] p 141 A95-64586
Aircraft model for the AIAA controls design challenge [BTN-94-EIX94511433921] p 142 A95-64587
Intelligent control law tuning for AIAA controls design challenge [BTN-94-EIX94511433922] p 169 A95-64588
Optimum aerodynamic design via boundary control p 127 N95-16565
Cooperative control theory and integrated flight and propulsion control [NASA-CR-197493] p 142 N95-17404
- CONTROLLERS**
H(sup 2)/H(sup INF) controller design for a two-dimensional thin airfoil flutter suppression [BTN-94-EIX94511433918] p 141 A95-64584
Test bench for rotorcraft hover control [BTN-94-EIX94511433919] p 169 A95-64585
Design of nonlinear control laws for high-angle-of-attack flight [BTN-94-EIX94511433920] p 141 A95-64586
New technologies for space avionics [NASA-CR-197574] p 150 N95-18196
Microgravity isolation system design: A modern control analysis framework [NASA-TM-106803] p 105 N95-18486
Plant and controller optimization by convex methods [AD-A283700] p 133 N95-18621
- CONVECTIVE HEAT TRANSFER**
Verification of multidisciplinary models for turbomachines p 140 N95-19025
- CONVERGENT NOZZLES**
Single-engine tail interference model p 115 N95-17879
- CONVERGENT-DIVERGENT NOZZLES**
Static investigation of two fluidic thrust-vectoring concepts on a two-dimensional convergent-divergent nozzle [NASA-TM-4574] p 120 N95-19042
- CONVEXITY**
Plant and controller optimization by convex methods [AD-A283700] p 133 N95-18621
- COOLING SYSTEMS**
Regenerative cooling for liquid propellant rocket thrust chambers [INPE-5565-TDI/540] p 150 N95-18720
Application of multidisciplinary models to the cooled turbine rotor design p 140 N95-19024
- CORNER FLOW**
Numerical simulation of supersonic compression corners and hypersonic inlet flows using the RPLUS2D code [NASA-TM-106580] p 105 N95-16038
Corner vortex suppressor [AD-D016423] p 116 N95-18337
- CORRECTION**
Wall-signature methods for high speed wind tunnel wall interference corrections p 107 N95-16257
Boundary-flow measurement methods for wall interference assessment and correction: Classification and review p 163 N95-19262
Wall correction method with measured boundary conditions for low speed wind tunnels p 164 N95-19263
Adaptive wind tunnel walls versus wall interference correction methods in 2D flows at high blockage ratios p 147 N95-19267
Transonic wind tunnel boundary interference correction p 147 N95-19271
Calculation of wall effects of flow on a perforated wall with a code of surface singularities p 165 N95-19277
Interference corrections for a centre-line plate mount in a porous-walled transonic wind tunnel p 122 N95-19280
Correction of support influences on measurements with sting mounted wind tunnel models p 122 N95-19281
- CORROSION RESISTANCE**
A CMC database for use in the next generation launch vehicles (rockets) p 150 N95-18993
FAA/NASA International Symposium on Advanced Structural Integrity Methods for Airframe Durability and Damage Tolerance, part 2 [NASA-CP-3274-PT-2] p 124 N95-19468
- CORROSION TESTS**
The use of electrochemistry and ellipsometry for identifying and evaluating corrosion on aircraft [AD-A285323] p 151 N95-16371
An artificial corrosion protocol for lap-splices in aircraft skin p 152 N95-19482
- COST ANALYSIS**
Technology Benefit Estimator (T/BEST): User's manual [NASA-TM-106785] p 167 N95-19501
- COST EFFECTIVENESS**
Optimum Design Methods for Aerodynamics [AGARD-R-803] p 127 N95-16562
Review of the EUROPT Project AERO-0026 p 129 N95-16573
- COST ESTIMATES**
Technology Benefit Estimator (T/BEST): User's manual [NASA-TM-106785] p 167 N95-19501
- COST REDUCTION**
Optimization of adaptive intraply hybrid fiber composites with reliability considerations [NASA-TM-106632] p 157 N95-16911
- CRACK CLOSURE**
Prediction of fatigue crack growth under flight-simulation loading with the modified CORPUS model p 166 N95-19471
Discrete crack growth analysis methodology for through cracks in pressurized fuselage structures p 166 N95-19473
The application of Newman crack-closure model to predicting fatigue crack growth p 167 N95-19483
- CRACK INITIATION**
The characterization of widespread fatigue damage in fuselage structure p 166 N95-19472
Evaluation of the fuselage lap joint fatigue and terminating action repair p 166 N95-19477
Fatigue life until small cracks in aircraft structures: Durability and damage tolerance p 135 N95-19478
Results of uniaxial and biaxial tests on riveted fuselage lap joint specimens p 136 N95-19491
Aircraft fatigue and crack growth considering loads by structural component p 137 N95-19497
- CRACK OPENING DISPLACEMENT**
Fatigue life until small cracks in aircraft structures: Durability and damage tolerance p 135 N95-19478
- CRACK PROPAGATION**
Multi-lab comparison on R-curve methodologies: Alloy 2024-T3 [NASA-CR-195004] p 151 N95-16860
Prediction of fatigue crack growth under flight-simulation loading with the modified CORPUS model p 166 N95-19471
The characterization of widespread fatigue damage in fuselage structure p 166 N95-19472
Discrete crack growth analysis methodology for through cracks in pressurized fuselage structures p 166 N95-19473
Evaluation of the fuselage lap joint fatigue and terminating action repair p 166 N95-19477
Fatigue life until small cracks in aircraft structures: Durability and damage tolerance p 135 N95-19478
The application of Newman crack-closure model to predicting fatigue crack growth p 167 N95-19483
Fatigue crack growth in 2024-T3 aluminum under tensile and transverse shear stresses p 153 N95-19490
Fatigue and residual strength investigation of ARALL(R) -3 and GLARE(R) -2 panels with bonded stringers p 137 N95-19495
Aircraft fatigue and crack growth considering loads by structural component p 137 N95-19497

CRACK TIPS

CRACK TIPS

Discrete crack growth analysis methodology for through cracks in pressurized fuselage structures p 166 N95-19473

The application of Newman crack-closure model to predicting fatigue crack growth p 167 N95-19483

CRACKING (FRACTURING)

Eddy current for detecting second layer cracks under installed fasteners

[AD-A282412] p 158 N95-17507

Evaluation of the fuselage lap joint fatigue and terminating action repair p 166 N95-19477

CRACKS

Eddy current for detecting second layer cracks under installed fasteners

[AD-A282412] p 158 N95-17507

Evaluation of the fuselage lap joint fatigue and terminating action repair p 166 N95-19477

Nonlinear analysis of damaged stiffened fuselage shells subjected to combined loads p 137 N95-19499

CRASH LANDING

Aircraft accident report: Stall and loss of control on final approach, Atlantic Coast Airlines, Inc./United Express Flight 6291 Jetstream 4101, N304UE Columbus, OH, 7 January 1994

[PB94-910409] p 123 N95-17646

CRASHES

Commentary on Walton correspondence relating to the ILS glide slope

[BTN-94-EIX94441380856] p 125 A95-64288

A correlative investigation of simulated occupant motion and accident report in a helicopter crash

[AD-A285190] p 123 N95-16404

CREEP ANALYSIS

Analytical description of and forecast for stress relaxation of aviation materials under the vibration conditions

[BTN-94-EIX94461408751] p 126 A95-63634

CREW PROCEDURES (INFLIGHT)

Federal aviation regulations, part 91. General operating and flight rules. Change 5

[PB94-194883] p 123 N95-17476

CREW WORKSTATIONS

Industry review of a crew-centered cockpit design process and toolset

[AD-A282966] p 130 N95-17661

CRITICAL LOADING

Fatigue loads spectra derivation for the Space Shuttle: Second cycle

p 166 N95-19470

CRITICAL VELOCITY

Effect of crossflow on Goertler instability in incompressible boundary layers

[NASA-CR-195007] p 159 N95-18193

CROSS FLOW

On the dynamics of aeroelastic oscillators with one degree of freedom

[BTN-94-EIX94501431527] p 153 A95-64524

Wall-signature methods for high speed wind tunnel wall interference corrections

p 107 N95-16257

In-flight imaging of transverse gas jets injected into transonic and supersonic crossflows: Design and development

[NASA-CR-186031] p 157 N95-17418

Effect of crossflow on Goertler instability in incompressible boundary layers

[NASA-CR-195007] p 159 N95-18193

CRYOGENIC FLUIDS

A Lifting Ball Valve for cryogenic fluid applications

p 156 N95-16349

CRYOGENIC ROCKET PROPELLANTS

Airborne rotary separator study

[NASA-CR-191045] p 150 N95-18743

CULTURAL RESOURCES

The effects of aircraft (B-52) overflights on ancient structures

[BTN-94-EIX94341340070] p 171 A95-63522

CUMULATIVE DAMAGE

An artificial corrosion protocol for lap-splices in aircraft skin

p 152 N95-19482

CURING

Ultrasonic techniques for repair of aircraft structures with bonded composite patches

p 136 N95-19486

CURVED PANELS

Shear buckling analysis of a hat-stiffened panel

[NASA-TM-4644] p 158 N95-17490

Evaluation of the fuselage lap joint fatigue and terminating action repair

p 166 N95-19477

CUTTING

Modelling for optimal operations of line milling of aerodynamic surfaces

[BTN-94-EIX94461408774] p 138 A95-63657

CYCLIC LOADS

Fatigue crack growth in 2024-T3 aluminum under tensile and transverse shear stresses

p 153 N95-19490

CYLINDRICAL BODIES

Wind tunnel investigations of the appearance of shocks in the windward region of bodies with circular cross section at angle of attack p 113 N95-17866

Force and pressure data of an ogive-nosed slender body at high angles of attack and different Reynolds numbers p 113 N95-17868

Supersonic vortex flow around a missile body p 114 N95-17870

Field and data analysis studies related to the atmospheric environment [NASA-CR-196543] p 168 N95-18093

Numerical mixing calculations of confined reacting jet flows in a cylindrical duct [NASA-TM-106736] p 139 N95-18133

Numerical computations of supersonic base flow with special emphasis on turbulence modeling [AD-A283688] p 119 N95-18670

CYLINDRICAL SHELLS

Development of strength analysis methods and design model for aircraft constructions in Kazan Aviation Institute p 127 N95-16264

Compression strength of composite primary structural components [NASA-CR-197554] p 160 N95-18388

D

DAMAGE

Brite-Euram programme: ACOUFAT acoustic fatigue and related damage tolerance of advanced composite and metallic structures p 174 N95-19159

Widespread fatigue damage monitoring: Issues and concerns p 136 N95-19488

DATA ACQUISITION

Virtual environment application with partial gravity simulation p 169 N95-15988

Data acquisition and processing software for the Low Speed Wind Tunnel tests of the Jindivik auxiliary air intake

[AD-A285455] p 108 N95-17178

Universal wind tunnel data acquisition and reduction software [AD-A283897] p 171 N95-18365

Strategic avionics technology definition studies. Subtask 3-1A3: Electrical Actuation (ELA) Systems Test Facility [NASA-CR-188360] p 143 N95-18567

Dynamic Stability Instrumentation System (DSIS). Volume 1: Hardware description [NASA-TM-109160-VOL-1] p 171 N95-18899

Flight parameters monitoring system for tracking structural integrity of rotary-wing aircraft p 135 N95-19469

DATA BASES

A supercritical airfoil experiment p 111 N95-17858

A selection of experimental test cases for the validation of CFD codes. Supplement: Datasets A-E [AGARD-AR-303-SUPPL] p 117 N95-18539

A CMC database for use in the next generation launch vehicles (rockets) p 150 N95-18993

DATA CORRELATION

Data from the GARTEur (AD) Action Group 02 airfoil CAST 7/DOA1 experiments p 111 N95-17856

DATA LINKS

Spread spectrum applications in unmanned aerial vehicles [AD-A281035] p 156 N95-16448

DATA PROCESSING

Automation of reverse engineering process in aircraft modeling and related optimization problems [NASA-CR-197109] p 129 N95-16899

A processing centre for the CNES CE-GPS experimentation OAT15A airfoil data p 111 N95-17857

Flight parameters monitoring system for tracking structural integrity of rotary-wing aircraft p 135 N95-19469

DC 8 AIRCRAFT

Aircraft wake vortex takeoff tests at O'Hara International Airport

[AD-A283828] p 118 N95-18624

DC 9 AIRCRAFT

Users guide for NASA Lewis Research Center DC-9 Reduced-Gravity Aircraft Program

[NASA-TM-106755] p 146 N95-18586

DECISION MAKING

Output feedback control under randomly varying distributed delays [BTN-94-EIX94511433916] p 168 A95-64582

On-line handling of air traffic: Management, guidance and control [AGARD-AG-321] p 126 N95-18927

DECOMPOSITION

Single-pass method for the solution of inverse potential and rotational problems. Part 1: 2-D and quasi 3-D theory and application p 107 N95-16563

DEFENSE PROGRAM

Assessing aircraft survivability to high frequency transient threats [AD-A283999] p 134 N95-18726

DEFLECTION

Evaluation of an unlighted swinging airport sign [AD-A284763] p 146 N95-18087

Determination of stores pointing error due to wing flexibility under flight load [NASA-TM-4646] p 134 N95-19044

Estimating wind tunnel interference due to vectored jet flows p 164 N95-19265

DEGREES OF FREEDOM

On the dynamics of aeroelastic oscillators with one degree of freedom [BTN-94-EIX94501431527] p 153 A95-64524

FPCAS2D user's guide, version 1.0 [NASA-CR-195413] p 156 N95-16588

Six degree of freedom flight dynamic and performance simulation of a remotely-piloted vehicle [AERO-TN-9301] p 131 N95-18097

Application of photogrammetry of F-14D store separation [AD-A284154] p 132 N95-18417

DELTA WINGS

Numerical simulation of transient vortex breakdown above a pitching delta wing [AD-A281075] p 107 N95-16808

Transonic Navier-Stokes calculations about a 65 deg delta wing [NASA-CR-4635] p 108 N95-17273

Detailed study at supersonic speeds of the flow around delta wings p 112 N95-17861

Wind tunnel test on a 65 deg delta wing with a sharp or rounded leading edge: The international vortex flow experiment p 114 N95-17872

Delta-wing model p 114 N95-17873

Experimental investigation of the vortex flow over a 76/60-deg double delta wing p 114 N95-17874

Wind tunnel test on a 65 deg delta wing with rounded leading edges: The International Vortex Flow Experiment p 114 N95-17875

STOVL CFD model test case p 115 N95-17881

Overview of unsteady transonic wind tunnel test on a semispan straked delta wing oscillating in pitch [AD-A284097] p 117 N95-18380

Aeromechanics technology, volume 1. Task 1: Three-dimensional Euler/Navier-Stokes Aerodynamic Method (TEAM) enhancements [AD-A285713] p 132 N95-18483

Interaction, bursting and control of vortices of a cropped double-delta wing at high angle of attack [AD-A283656] p 119 N95-18669

The utilization of a high speed reflective visualization system in the study of transonic flow over a delta wing p 121 N95-19259

Velocity measurements with hot-wires in a vortex-dominated flowfield p 121 N95-19261

DEPENDENT VARIABLES

Single-pass method for the solution of inverse potential and rotational problems. Part 2: Fully 3-D potential theory and applications p 107 N95-16564

DEPLOYMENT

EURECA mission control experience and messages for the future p 149 N95-17252

DERIVATION

Investigation of dynamic inflow's influence on rotor control derivatives p 155 N95-16250

DESIGN ANALYSIS

Portable parallel stochastic optimization for the design of aeropropulsion components [NASA-CR-195312] p 154 N95-16072

An improved method of airfoil design p 106 N95-16252

Small turbojets: Designs and installations p 138 N95-16323

Rapid solution of large-scale systems of equations p 169 N95-16458

Matlab as a robust control design tool p 169 N95-16474

Optimum Design Methods for Aerodynamics [AGARD-R-803] p 127 N95-16562

Airfoil optimization by the one-shot method p 128 N95-16569

FPCAS2D user's guide, version 1.0 [NASA-CR-195413] p 156 N95-16588

Applications of automatic differentiation in CFD [NASA-TM-109948] p 157 N95-16828

Algorithms for bilevel optimization [NASA-CR-194980] p 170 N95-16897

- Eddy current for detecting second layer cracks under installed fasteners
[AD-A282412] p 158 N95-17507
Conference on Aerospace Transparent Materials and Enclosures. Volume 2: Sessions 5-9
[AD-A283926] p 131 N95-18162
Microgravity isolation system design: A modern control analysis framework
[NASA-TM-106803] p 105 N95-18486
Strategic avionics technology definition studies. Subtask 3-1A3: Electrical Actuation (ELA) Systems Test Facility
[NASA-CR-188360] p 143 N95-18567
Design limit loads based upon statistical discrete gust methodology
p 133 N95-18603
Conference on Aerospace Transparent Materials and Enclosures, volume 1
[AD-A283925] p 133 N95-18677
- DETERIORATION**
Problems with aging wiring in Naval aircraft
p 154 N95-16048
- DIFFERENTIAL EQUATIONS**
Single-pass method for the solution of inverse potential and rotational problems. Part 2: Fully 3-D potential theory and applications
p 107 N95-16564
Optimum aerodynamic design via boundary control
p 127 N95-16565
- DIFFERENTIAL GEOMETRY**
Single-pass method for the solution of inverse potential and rotational problems. Part 1: 2-D and quasi 3-D theory and application
p 107 N95-16563
- DIFFERENTIAL PRESSURE**
Pressure measurements on an F/A-18 twin vertical tail in buffeting flow. Volume 4, part 2: Buffet cross spectral densities
[AD-A285555] p 143 N95-18641
- DIFFUSION FLAMES**
Studies on high pressure and unsteady flame phenomena
[AD-A284126] p 152 N95-18410
- DIGITAL COMPUTERS**
A PC-based interactive simulation of the F-111C Pave Tack system and related sensor, avionics and aircraft aspects
[AD-A285500] p 129 N95-16969
- DIGITAL SYSTEMS**
NASA develops new digital flight control system
[NASA-NEWS-RELEASE-94-47] p 144 N95-19029
- DISCRETE FUNCTIONS**
Design limit loads based upon statistical discrete gust methodology
p 133 N95-18603
- DISPLAY DEVICES**
An evaluation of aircraft CRT and dot-matrix display legibility requirements
[AD-A283933] p 138 N95-18164
- DISTRIBUTED PROCESSING**
Rapid solution of large-scale systems of equations
p 169 N95-16458
- DIVERGENT NOZZLES**
Single-engine tail interference model
p 115 N95-17879
- DOPPLER RADAR**
Linear prediction data extrapolation superresolution radar imaging
p 155 N95-16268
- DOWNWASH**
Numerical simulation of helicopter engine plume in forward flight
[NASA-CR-197488] p 107 N95-16589
- DRAG**
Investigation of the influence of pylons and stores on the wing lower surface flow
p 116 N95-17885
In-flight lift-drag characteristics for a forward-swept wing aircraft and comparisons with contemporary aircraft
[NASA-TP-3414] p 117 N95-18565
- DRAG COEFFICIENTS**
An investigation of the transonic pressure drag coefficient for axis-symmetric bodies
[AD-A280990] p 105 N95-15994
Static aerodynamics CFD analysis for 120-mm hypersonic KE projectile design
[ARL-MR-184] p 118 N95-18611
- DRAG MEASUREMENT**
Surface pressure and wake drag measurements on the Boeing A4 airfoil in the IAR 1.5X1.5m Wind Tunnel Facility
p 110 N95-17850
Interference corrections for a centre-line plate mount in a porous-walled transonic wind tunnel
p 122 N95-19280
- DRAG REDUCTION**
An investigation of the transonic pressure drag coefficient for axis-symmetric bodies
[AD-A280990] p 105 N95-15994
- DROOPED AIRFOILS**
Wind tunnel test on a 65 deg delta wing with a sharp or rounded leading edge: The international vortex flow experiment
p 114 N95-17872
- DUCT GEOMETRY**
Linear instability waves in supersonic jets confined in circular and non-circular ducts
[BTN-94-EIX94341340068] p 103 A95-63520
Three dimensional compressible turbulent flow computations for a diffusing S-duct with/without vortex generators
[NASA-CR-195390] p 138 N95-17402
- DUCTED FAN ENGINES**
Ducted fan acoustic radiation including the effects of nonuniform mean flow and acoustic treatment
[NASA-CR-197449] p 172 N95-16401
- DUCTED FLOW**
Linear instability waves in supersonic jets confined in circular and non-circular ducts
[BTN-94-EIX94341340068] p 103 A95-63520
Solution of Navier-Stokes equations using high accuracy monotone schemes
p 161 N95-19019
- DUCTED ROCKET ENGINES**
Experimental and analytical methods for the determination of connected-pipe ramjet and ducted rocket internal performance
[AGARD-AR-323] p 149 N95-17278
- DURABILITY**
Mathematical modelling concerning the development of a system of similar installations, taking into account their operational intensity (an aircraft-helicopter fleet taken as an example)
[BTN-94-EIX94461408783] p 103 A95-63646
FAA/NASA International Symposium on Advanced Structural Integrity Methods for Airframe Durability and Damage Tolerance, part 2
[NASA-CP-3274-PT-2] p 124 N95-19468
- DYNAMIC CHARACTERISTICS**
Static and dynamic friction behavior of candidate high temperature airframe seal materials
[NASA-TM-106571] p 152 N95-16905
- DYNAMIC CONTROL**
Design of nonlinear control laws for high-angle-of-attack flight
[BTN-94-EIX94511433920] p 141 A95-64586
Development of a multicomponent force and moment balance for water tunnel applications, volume 1
[NASA-CR-4642-VOL-1] p 161 N95-18955
- DYNAMIC LOADS**
Matlab as a robust control design tool
p 169 N95-16474
Gyroscopic and propeller aerodynamic effects on engine mounts dynamic loads in turbulence conditions
p 132 N95-18599
Impact of dynamic loads on propulsion integration
p 174 N95-19148
- DYNAMIC MODELS**
Investigation of dynamic inflow's influence on rotor control derivatives
p 155 N95-16250
A review of gust load calculation methods at de Havilland
p 118 N95-18604
A linear system identification and validation of an AH-64 Apache aeroelastic simulation model
p 146 N95-18903
- DYNAMIC PRESSURE**
Pressure measurements on an F/A-18 twin vertical tail in buffeting flow. Volume 4, part 2: Buffet cross spectral densities
[AD-A285555] p 143 N95-18641
- DYNAMIC RESPONSE**
Measurements of unsteady pressure and structural response for an elastic supercritical wing
[NASA-TP-3443] p 104 N95-16560
Parachute inflation: A problem in aeroelasticity
[AD-A284375] p 117 N95-18340
A review of gust load calculation methods at de Havilland
p 118 N95-18604
Special effects of gust loads on military aircraft
p 133 N95-18605
Current and future problems in structural acoustic fatigue
p 173 N95-19143
Nonlinear dynamic response of aircraft structures to acoustic excitation
p 135 N95-19151
Forced response of mistuned bladed disks
p 141 N95-19383
- DYNAMIC STABILITY**
Evaluation of the dynamic stability characteristics of the NAL Light Transport Aircraft
[NAL-PD-CA-9217] p 142 N95-16392
Dynamic Stability Instrumentation System (DSIS). Volume 1: Hardware description
[NASA-TM-109160-VOL-1] p 171 N95-18899
- DYNAMIC STRUCTURAL ANALYSIS**
Parachute inflation: A problem in aeroelasticity
[AD-A284375] p 117 N95-18340
- DYNAMIC TESTS**
Investigation of dynamic inflow's influence on rotor control derivatives
p 155 N95-16250
- Development of a multicomponent force and moment balance for water tunnel applications, volume 2
[NASA-CR-4642-VOL-2] p 161 N95-18956
Calculation of support interference in dynamic wind-tunnel tests
p 122 N95-19282
- E**
- EARTH (PLANET)**
Conversion of Earth-centered Earth-fixed coordinates to geodetic coordinates
[BTN-94-EIX94441380862] p 125 A95-64294
- EARTH ORBITAL RENDEZVOUS**
EURECA mission control experience and messages for the future
p 149 N95-17252
- EDDY CURRENTS**
Eddy current for detecting second layer cracks under installed fasteners
[AD-A282412] p 158 N95-17507
Evaluation of scanners for C-scan imaging in nondestructive inspection of aircraft
[DE94-012473] p 152 N95-19100
- EDUCATION**
A workstation based simulator for teaching compressible aerodynamics
[NASA-TM-106799] p 170 N95-16906
- EJECTION SEATS**
Preliminary evaluation of the F/A-18 quantity/multiple envelope expansion
[AD-A284119] p 132 N95-18407
- ELASTIC DEFORMATION**
Determination of stores pointing error due to wing flexibility under flight load
[NASA-TM-4646] p 134 N95-19044
- ELECTRIC BATTERIES**
Development of a bipolar lead/acid battery for the more electric aircraft
[AD-A284050] p 160 N95-18660
- ELECTRIC EQUIPMENT**
Generalized method of solving topological optimization problems for electrical airplane equipment systems in computer-aided design
p 169 N95-16272
- ELECTRIC PROPULSION**
Arcjet thruster research and technology, phase 2
[NASA-CR-182276] p 105 N95-18044
- ELECTRIC WIRE**
Problems with aging wiring in Naval aircraft
p 154 N95-16048
- ELECTRICAL INSULATION**
Problems with aging wiring in Naval aircraft
p 154 N95-16048
- ELECTRIFICATION**
Field and data analysis studies related to the atmospheric environment
[NASA-CR-196543] p 168 N95-18093
- ELECTRO-OPTICS**
Fiber Optic Control System integration for advanced aircraft. Electro-optic and sensor fabrication, integration and environmental testing for flight control systems
[NASA-CR-191194] p 162 N95-19236
- ELECTROCHEMICAL CORROSION**
The use of electrochemistry and ellipsometry for identifying and evaluating corrosion on aircraft
[AD-A285323] p 151 N95-16371
- ELECTROCHEMISTRY**
The use of electrochemistry and ellipsometry for identifying and evaluating corrosion on aircraft
[AD-A285323] p 151 N95-16371
- ELECTROMAGNETIC INTERACTIONS**
A Lifting Ball Valve for cryogenic fluid applications
p 156 N95-16349
- ELECTROMAGNETIC PULSES**
Assessing aircraft survivability to high frequency transient threats
[AD-A283999] p 134 N95-18726
Waveform bounding and combination techniques for direct drive testing
[AD-A284075] p 161 N95-19035
E-6A hardness assurance, maintenance and surveillance program
[AD-A283994] p 134 N95-19067
- ELECTROMAGNETIC RADIATION**
Hypersonic wind tunnel test techniques
[AD-A284057] p 118 N95-18663
- ELECTROMAGNETISM**
Hypersonic wind tunnel test techniques
[AD-A284057] p 118 N95-18663
- ELECTRONIC AIRCRAFT**
E-6A hardness assurance, maintenance and surveillance program
[AD-A283994] p 134 N95-19067
- ELLIPSONOMETRY**
The use of electrochemistry and ellipsometry for identifying and evaluating corrosion on aircraft
[AD-A285323] p 151 N95-16371

ELLIPTICAL CYLINDERS

Ellipsoid-cylinder model p 158 N95-17869

ENCLOSURE

Active minimization of energy density in three-dimensional enclosures [NASA-CR-197213] p 172 N95-16848

ENERGY BUDGETS

Helicopter Performance Evaluation (HELPE) computer model [AD-A284319] p 131 N95-18381

ENERGY CONVERSION EFFICIENCY

Gas-turbine engines with increased efficiency of two circuits, due to the use of the utilizing steam-turbine circuit [BTN-94-EIX94461408755] p 153 A95-63638

ENERGY DISSIPATION

An analysis code for the Rapid Engineering Estimation of Momentum and Energy Losses (REMEL) [NASA-CR-191178] p 108 N95-16887

ENGINE AIRFRAME INTEGRATION

Cooperative control theory and integrated flight and propulsion control [NASA-CR-197493] p 142 N95-17404
Impact of dynamic loads on propulsion integration p 174 N95-19148

ENGINE CONTROL

Cooperative control theory and integrated flight and propulsion control [NASA-CR-197493] p 142 N95-17404

ENGINE DESIGN

Gas-turbine engines with increased efficiency of two circuits, due to the use of the utilizing steam-turbine circuit [BTN-94-EIX94461408755] p 153 A95-63638
Two projects of V. M. Myasishchev [HTN-95-50269] p 176 A95-65764
Small turbojets: Designs and installations p 138 N95-16323
Experimental and analytical methods for the determination of connected-pipe ramjet and ducted rocket internal performance [AGARD-AR-323] p 149 N95-17278
Wave cycle design for wave rotor engines with limited nitrogen oxide emissions p 161 N95-18901
Application of multidisciplinary models to the cooled turbine rotor design p 140 N95-19024
Perspective problems of gas turbine engines simulation p 140 N95-19026

ENGINE INLETS

Three dimensional compressible turbulent flow computations for a diffusing S-duct with/without vortex generators [NASA-CR-195390] p 138 N95-17402
Collection efficiency and ice accretion calculations for a sphere, a swept MS(1)-317 wing, a swept NACA-0012 wing tip, an axisymmetric inlet, and a Boeing 737-300 [NASA-TM-106831] p 123 N95-18582

ENGINE MONITORING INSTRUMENTS

An artificial neural network system for diagnosing gas turbine engine fuel faults [DE94-013960] p 138 N95-17371

ENGINE PARTS

Quality optimization of thermally sprayed coatings produced by the JP-5000 (HVOF) gun using mathematical modeling p 152 N95-19008
Mathematical Models of Gas Turbine Engines and their Components [AGARD-LS-198] p 139 N95-19017

ENGINE TESTS

Theoretical fundamentals of the aircraft GTE tests p 138 N95-16265
Scramjet testing guidelines p 138 N95-16317
Hypersonic air-breathing aer propulsion facility test support requirements p 144 N95-16319
Free-jet testing at Mach 3.44 in GASL's aero/thermo test facility p 145 N95-16320
Unmanned aerial vehicle heavy fuel engine test [AD-A284332] p 139 N95-18383
Airborne rotary separator study [NASA-CR-191045] p 150 N95-18743

ENGINEERS

Development of strength analysis methods and design model for aircraft constructions in Kazan Aviation Institute p 127 N95-16264
ICASE [NASA-CR-195001] p 170 N95-16898

ENVIRONMENTAL TESTS

High-temperature acoustic test facilities and methods p 174 N95-19149
Design and operation of a thermoacoustic test facility p 147 N95-19150

EQUATIONS OF MOTION

Evaluation of the dynamic stability characteristics of the NAL Light Transport Aircraft [NAL-PO-CA-9217] p 142 N95-16392

ERROR ANALYSIS

Error propagation equations for estimating the uncertainty in high-speed wind tunnel test results [DE94-014136] p 145 N95-16509
Field verification of the wind tunnel coefficients p 109 N95-17291
An analysis of tower (local) controller-pilot voice communications [AD-A283718] p 160 N95-18436
Optical surface pressure measurements: Accuracy and application field evaluation p 175 N95-19274

ERRORS

Determination of stores pointing error due to wing flexibility under flight load [NASA-TM-4646] p 134 N95-19044
Development of pneumatic test techniques for subsonic high-lift and in-ground-effect wind tunnel investigations p 121 N95-19268

ESTIMATING

The accuracy of parameter estimation in system identification of noisy aircraft load measurement [NASA-CR-197516] p 134 N95-19130
Estimating wind tunnel interference due to vectored jet flows p 164 N95-19265

EUCLIDEAN GEOMETRY

Single-pass method for the solution of inverse potential and rotational problems. Part 2: Fully 3-D potential theory and applications p 107 N95-16564

EULER EQUATIONS OF MOTION

A grid generation and flow solution method for the Euler equations on unstructured grids [HTN-95-20003] p 153 A95-63201
Theoretical investigations of shock/boundary layer interactions on a Ma(infinity) = 8 waverider [DLR-FB-94-12] p 119 N95-18910
The mathematical models of flow passage for gas turbine engines and their components p 140 N95-19020
An assessment of the adaptive unstructured tetrahedral grid, Euler Flow Solver Code FELISA [NASA-TP-3526] p 119 N95-19041

EURECA (ESA)

EURECA mission control experience and messages for the future p 149 N95-17252

EUROPE

EC Aviation Scene [HTN-95-50223] p 176 A95-64860

EVALUATION

Helicopter Performance Evaluation (HELPE) computer model [AD-A284319] p 131 N95-18381
Evaluation of scanners for C-scan imaging in nondestructive inspection of aircraft [DE94-012473] p 152 N95-19100

EXHAUST DIFFUSERS

Unsteady flow phenomena in discrete passage diffusers for centrifugal compressors [AD-A281412] p 155 N95-16163

EXHAUST EMISSION

Atmospheric effects of high-flying subsonic aircraft: A catalogue of perturbing influences [KNMI-SR-94-03] p 168 N95-18722
Wave cycle design for wave rotor engines with limited nitrogen oxide emissions p 161 N95-18901

EXHAUST GASES

Numerical simulation of helicopter engine plume in forward flight [NASA-CR-197488] p 107 N95-16589
Atmospheric effects of high-flying subsonic aircraft: A catalogue of perturbing influences [KNMI-SR-94-03] p 168 N95-18722
Impact of dynamic loads on propulsion integration p 174 N95-19148

EXHAUST NOZZLES

Small turbojets: Designs and installations p 138 N95-16323

EXPENDABLE STAGES (SPACECRAFT)

Program test objectives milestone 3 -- Integrated Propulsion Technology Demonstrator [NASA-CR-197030] p 127 N95-15971

EXPERIMENT DESIGN

A study of software standards used in the avionics industry p 137 N95-16456
Experimental and analytical methods for the determination of connected-pipe ramjet and ducted rocket internal performance [AGARD-AR-323] p 149 N95-17278

EXPERT SYSTEMS

Identification of Artificial Intelligence (AI) applications for maintenance, monitoring, and control of airway facilities [AD-A282479] p 125 N95-17373

EXTERNAL STORES

Flight testing high lateral asymmetries on highly augmented Fighter/Attack aircraft [AD-A284206] p 130 N95-17953
A study of the effect of store unsteady aerodynamics on gust and turbulence loads p 133 N95-18601

EXTRAPOLATION

Linear prediction data extrapolation superresolution radar imaging p 155 N95-16268
Hypersonic flight testing [AD-A283981] p 134 N95-18891

EXTRATERRESTRIAL ENVIRONMENTS

Fatigue loads spectra derivation for the Space Shuttle: Second cycle p 166 N95-19470

F

F-111 AIRCRAFT

A PC-based interactive simulation of the F-111C Pave Tack system and related sensor, avionics and aircraft aspects [AD-A285500] p 129 N95-16969

F-14 AIRCRAFT

Evaluation of alternate F-14 wing lug coating [AD-A283207] p 129 N95-17631
Application of photogrammetry of F-14D store separation [AD-A284154] p 132 N95-18417

F-15 AIRCRAFT

Development of a low-aspect ratio fin for flight research experiments [NASA-TM-4596] p 108 N95-16858

F-18 AIRCRAFT

Flight testing high lateral asymmetries on highly augmented Fighter/Attack aircraft [AD-A284206] p 130 N95-17953
Pressure measurements on an F/A-18 twin vertical tail in buffeting flow. Volume 4, part 2: Buffet cross spectral densities [AD-A285555] p 143 N95-18641
Fiber Optic Control System integration for advanced aircraft. Electro-optic and sensor fabrication, integration, and environmental testing for flight control systems: Laboratory test results [NASA-CR-195408] p 161 N95-18938
Navier-Stokes, flight, and wind tunnel flow analysis for the F/A-18 aircraft [NASA-TP-3478] p 120 N95-19114

F-4 AIRCRAFT

Application of photogrammetry of F-14D store separation [AD-A284154] p 132 N95-18417

FABRICATION

Optimization of adaptive intraply hybrid fiber composites with reliability considerations [NASA-TM-106632] p 157 N95-16911

FAILURE ANALYSIS

A study of software standards used in the avionics industry p 137 N95-16456

FAILURE MODES

A Lifting Ball Valve for cryogenic fluid applications p 156 N95-16349
Detecting gear tooth fracture in a high contact ratio face gear mesh [NASA-TM-106822] p 162 N95-19125

FAN BLADES

Ducted fan acoustic radiation including the effects of nonuniform mean flow and acoustic treatment [NASA-CR-197449] p 172 N95-16401
Mach number, flow angle, and loss measurements downstream of a transonic fan-blade cascade [AD-A280907] p 108 N95-16824

FAN FIELDS

Ducted fan acoustic radiation including the effects of nonuniform mean flow and acoustic treatment [NASA-CR-197449] p 172 N95-16401
Correction of support influences on measurements with sting mounted wind tunnel models p 122 N95-19281

FAST FOURIER TRANSFORMATIONS

Linear prediction data extrapolation superresolution radar imaging p 155 N95-16268
Waveform bounding and combination techniques for direct drive testing [AD-A284075] p 161 N95-19035

FASTENERS

Eddy current for detecting second layer cracks under installed fasteners [AD-A282412] p 158 N95-17507

FATIGUE (MATERIALS)

Fatigue in single crystal nickel superalloys [AD-A285727] p 152 N95-18068
FAA/NASA International Symposium on Advanced Structural Integrity Methods for Airframe Durability and Damage Tolerance, part 2 p 124 N95-19468
Fatigue loads spectra derivation for the Space Shuttle: Second cycle p 166 N95-19470
Prediction of fatigue crack growth under flight-simulation loading with the modified CORPUS model p 166 N95-19471

- The characterization of widespread fatigue damage in fuselage structure p 166 N95-19472
- Residual life and strength estimates of aircraft structural components with MSD/MED p 136 N95-19485
- Widespread fatigue damage monitoring: Issues and concerns p 136 N95-19488
- Fatigue crack growth in 2024-T3 aluminum under tensile and transverse shear stresses p 153 N95-19490
- Fatigue and residual strength investigation of ARALL(R) -3 and GLARE(R) -2 panels with bonded stringers p 137 N95-19495
- Aircraft fatigue and crack growth considering loads by structural component p 137 N95-19497
- FATIGUE LIFE**
- Current and future problems in structural acoustic fatigue p 173 N95-19143
- Brite-Euram programme: ACOUFAT acoustic fatigue and related damage tolerance of advanced composite and metallic structures p 174 N95-19159
- Prediction of fatigue crack growth under flight-simulation loading with the modified CORPUS model p 166 N95-19471
- Discrete crack growth analysis methodology for through cracks in pressurized fuselage structures p 166 N95-19473
- Fatigue life until small cracks in aircraft structures: Durability and damage tolerance p 135 N95-19478
- The application of Newman crack-closure model to predicting fatigue crack growth p 167 N95-19483
- Residual life and strength estimates of aircraft structural components with MSD/MED p 136 N95-19485
- FATIGUE TESTS**
- Detecting gear tooth fracture in a high contact ratio face gear mesh [NASA-TM-106822] p 162 N95-19125
- High-temperature acoustic test facilities and methods p 174 N95-19149
- Acoustic fatigue testing on different materials and skin-stringer elements p 174 N95-19156
- Brite-Euram programme: ACOUFAT acoustic fatigue and related damage tolerance of advanced composite and metallic structures p 174 N95-19159
- Prediction of fatigue crack growth under flight-simulation loading with the modified CORPUS model p 166 N95-19471
- Evaluation of the fuselage lap joint fatigue and terminating action repair p 166 N95-19477
- Development of load spectra for Airbus A330/A340 full scale fatigue tests p 135 N95-19479
- An artificial corrosion protocol for lap-splices in aircraft skin p 152 N95-19482
- Ultrasonic techniques for repair of aircraft structures with bonded composite patches p 136 N95-19486
- Results of uniaxial and biaxial tests on riveted fuselage lap joint specimens p 136 N95-19491
- FAULT DETECTION**
- Sensor fault detection and diagnosis simulation of a helicopter engine in an intelligent control framework [NASA-TM-106784] p 137 N95-15970
- An artificial neural network system for diagnosing gas turbine engine fuel faults [DE94-013960] p 138 N95-17371
- Eddy current for detecting second layer cracks under installed fasteners [AD-A282412] p 158 N95-17507
- Detecting gear tooth fracture in a high contact ratio face gear mesh [NASA-TM-106822] p 162 N95-19125
- FEEDBACK CONTROL**
- Output feedback control under randomly varying distributed delays [BTN-94-EIX94511433916] p 168 A95-64582
- H(sup 2)/H(sup INF) controller design for a two-dimensional thin airfoil flutter suppression [BTN-94-EIX94511433918] p 141 A95-64584
- Time-optimal turn to a heading: An analytic solution [BTN-94-EIX94511433940] p 142 A95-64606
- Cooperative control theory and integrated flight and propulsion control [NASA-CR-197493] p 142 N95-17404
- Microgravity isolation system design: A case study [NASA-TM-106804] p 104 N95-17657
- Simulation investigation on system identification of gas turbine [PB95-104238] p 139 N95-17749
- Microgravity isolation system design: A modern control analysis framework [NASA-TM-106803] p 105 N95-18486
- Plant and controller optimization by convex methods [AD-A283700] p 133 N95-18621
- FEEDFORWARD CONTROL**
- A feedforward control approach to the local navigation problem for autonomous vehicles [AD-A282787] p 126 N95-17706
- FIBER COMPOSITES**
- Optimization of adaptive intraply hybrid fiber composites with reliability considerations [NASA-TM-106632] p 157 N95-16911
- A CMC database for use in the next generation launch vehicles (rockets) p 150 N95-18993
- FIBER OPTICS**
- Fiber-optic technology for transport aircraft [BTN-94-EIX94511309384] p 103 A95-64610
- Fiber Optic Control System integration for advanced aircraft. Electro-optic and sensor fabrication, integration, and environmental testing for flight control systems: Laboratory test results [NASA-CR-195408] p 161 N95-18938
- Fiber Optic Control System integration for advanced aircraft. Electro-optic and sensor fabrication, integration, and environmental testing for flight control systems [NASA-CR-191194] p 162 N95-19236
- FIELD OF VIEW**
- Factors affecting the visual fragmentation of the field-of-view in partial binocular overlap displays [AD-A283081] p 172 N95-17334
- FIGHTER AIRCRAFT**
- Design of nonlinear control laws for high-angle-of-attack flight [BTN-94-EIX94511433920] p 141 A95-64586
- Investigation into the aerodynamic characteristics of a combat aircraft research model fitted with a forward swept wing p 116 N95-17884
- Application of photogrammetry of F-14D store separation [AD-A284154] p 132 N95-18417
- Aircraft stress sequence development: A complex engineering process made simple p 136 N95-19480
- FILAMENT WINDING**
- Recent advances in graphite/epoxy motor cases p 149 N95-16333
- FINITE DIFFERENCE THEORY**
- Static aerodynamics CFD analysis for 120-mm hypersonic KE projectile design [ARL-MR-184] p 118 N95-18611
- Computation of inviscid flows: Full potential method p 165 N95-19447
- FINITE ELEMENT METHOD**
- Shear buckling analysis of a hat-stiffened panel [NASA-TM-4644] p 158 N95-17490
- A review of gust load calculation methods at de Havilland p 118 N95-18604
- Simulation of multidisciplinary problems for the thermostress state of cooled high temperature turbines p 140 N95-19021
- Discrete crack growth analysis methodology for through cracks in pressurized fuselage structures p 166 N95-19473
- Widespread fatigue damage monitoring: Issues and concerns p 136 N95-19488
- Fatigue crack growth in 2024-T3 aluminum under tensile and transverse shear stresses p 153 N95-19490
- Prediction of R-curves from small coupon tests p 167 N95-19496
- FINITE VOLUME METHOD**
- Three dimensional compressible turbulent flow computations for a diffusing S-curt with/without vortex generators [NASA-CR-195390] p 138 N95-17402
- FINS**
- Modelling for optimal operations of line milling of aerodynamic surfaces [BTN-94-EIX94461408774] p 138 A95-63657
- Development of a low-aspect ratio fin for flight research experiments [NASA-TM-4596] p 108 N95-16858
- Integrated aerodynamic fin and stowable TVC vane system [AD-D016457] p 151 N95-19073
- FITTING**
- Floating shock fitting via Lagrangian adaptive meshes [NASA-CR-194997] p 170 N95-18110
- FLAME HOLDERS**
- Computation of vortex breakdown p 165 N95-19462
- FLAME STABILITY**
- Development and application of the double V type flame stabilizer [BTN-94-EIX94481415355] p 154 A95-65345
- FLAMES**
- Development and application of the double V type flame stabilizer [BTN-94-EIX94481415355] p 154 A95-65345
- FLAT PLATES**
- The stability of two-phase flow over a swept-wing [NASA-CR-194994] p 159 N95-18190
- Acoustic radiation damping of flat rectangular plates subjected to subsonic flows p 172 N95-18542
- FLEXIBILITY**
- Determination of stores pointing error due to wing flexibility under flight load [NASA-TM-4646] p 134 N95-19044
- FLEXIBLE WINGS**
- Active load control during rolling maneuvers — performed in the Langley Transonic Dynamics Tunnel [NASA-TP-3455] p 129 N95-17397
- FLEXING**
- Hydrofoil force balance [AD-D016475] p 160 N95-18461
- FLIGHT ALTITUDE**
- Selection of optimal parameters for a system, controlling the flight height, when information about the state vector is incomplete [BTN-94-EIX94461408753] p 168 A95-63636
- Atmospheric effects of high-flying subsonic aircraft: A catalogue of perturbing influences [KNMI-SR-94-03] p 168 N95-18722
- FLIGHT CHARACTERISTICS**
- Design of nonlinear control laws for high-angle-of-attack flight [BTN-94-EIX94511433920] p 141 A95-64586
- Evaluation of the dynamic stability characteristics of the NAL Light Transport Aircraft [NAL-PD-CA-9217] p 142 N95-16392
- STOVL CFD model test case p 115 N95-17881
- Six degree of freedom flight dynamic and performance simulation of a remotely-piloted vehicle [AERO-TN-9301] p 131 N95-18097
- Flight parameters monitoring system for tracking structural integrity of rotary-wing aircraft p 135 N95-19469
- FLIGHT CONDITIONS**
- Numerical simulation of helicopter engine plume in forward flight [NASA-CR-197488] p 107 N95-16589
- Helicopter Performance Evaluation (HELPE) computer model [AD-A284319] p 131 N95-18381
- Comparison of frequency response and perturbation methods to extract linear models from a nonlinear simulation [AD-A284115] p 146 N95-18405
- Flight parameters monitoring system for tracking structural integrity of rotary-wing aircraft p 135 N95-19469
- FLIGHT CONTROL**
- Selection of optimal parameters for a system, controlling the flight height, when information about the state vector is incomplete [BTN-94-EIX94461408753] p 168 A95-63636
- Output feedback control under randomly varying distributed delays [BTN-94-EIX94511433916] p 168 A95-64582
- Design of nonlinear control laws for high-angle-of-attack flight [BTN-94-EIX94511433920] p 141 A95-64586
- Time-optimal turn to a heading: An analytic solution [BTN-94-EIX94511433940] p 142 A95-64606
- Matlab as a robust control design tool p 169 N95-16474
- Workshop on Formal Models for Intelligent Control [AD-A281399] p 169 N95-16864
- EURECA mission control experience and messages for the future p 149 N95-17252
- Aircraft and sub-system certification by piloted simulation [AGARD-AR-278] p 145 N95-17388
- Packet utilisation definitions for the ESA XMM mission p 150 N95-17596
- Flight testing high lateral asymmetries on highly augmented Fighter/Attack aircraft [AD-A284206] p 130 N95-17953
- VSTOL Systems Research Aircraft (VSRA) Harrier [NASA-TM-110117] p 126 N95-18347
- The impact of non-linear flight control systems on the prediction of aircraft loads due to turbulence p 143 N95-18598
- Treatment of non-linear systems by timeplane-transformed CT methods: The spectral gust method p 143 N95-18600
- Design and flight test of a simplified control system for a transport helicopter p 144 N95-18902
- Integrated aerodynamic fin and stowable TVC vane system [AD-D016457] p 151 N95-19073
- FLIGHT ENVELOPES**
- Aircraft and sub-system certification by piloted simulation [AGARD-AR-278] p 145 N95-17388
- Flight testing high lateral asymmetries on highly augmented Fighter/Attack aircraft [AD-A284206] p 130 N95-17953

Course module for AA201: Wing structural design project
[AD-A283618] p 133 N95-18616

FLIGHT HAZARDS
Waveform bounding and combination techniques for direct drive testing
[AD-A284075] p 161 N95-19035

FLIGHT SAFETY
Federal aviation regulations, part 91. General operating and flight rules. Change 5
[PB94-194883] p 123 N95-17476
Annual review of aircraft accident data: US Air carrier operations, calendar year 1992
[PB95-100319] p 123 N95-17748
Users guide for NASA Lewis Research Center DC-9 Reduced-Gravity Aircraft Program
[NASA-TM-106755] p 146 N95-18586
A study of the effect of store unsteady aerodynamics on gust and turbulence loads p 133 N95-18601
On-line handling of air traffic: Management, guidance and control
[AGARD-AG-321] p 126 N95-18927
Safety study: Commuter airline safety
[PB94-917004] p 124 N95-19132

FLIGHT SIMULATION
Six degree of freedom flight dynamic and performance simulation of a remotely-piloted vehicle
[AERO-TN-9301] p 131 N95-18097
KC-135 cockpit modernization study. Phase 1: Equipment evaluation
[AD-A284099] p 131 N95-18398
Comparison of frequency response and perturbation methods to extract linear models from a nonlinear simulation
[AD-A284115] p 146 N95-18405
Development of load spectra for Airbus A330/A340 full scale fatigue tests p 135 N95-19479

FLIGHT SIMULATORS
ADST system test report for the rotary wing aircraft airmen aeromodel and weapon model merge with the ATAC 2 baseline
[AD-A281580] p 127 N95-16171
Aircraft and sub-system certification by piloted simulation
[AGARD-AR-278] p 145 N95-17388
Comparison of frequency response and perturbation methods to extract linear models from a nonlinear simulation
[AD-A284115] p 146 N95-18405
The generic simulation executive at Manned Flight Simulator
[AD-A283997] p 146 N95-18724
Helicopter in-flight simulation development and use in test pilot training
[AD-A283998] p 146 N95-18725
Assessing aircraft survivability to high frequency transient threats
[AD-A283999] p 134 N95-18726
A linear system identification and validation of an AH-64 Apache aeroelastic simulation model p 146 N95-18903

FLIGHT TEST VEHICLES
Development of a low-aspect ratio fin for flight research experiments
[NASA-TM-4596] p 108 N95-16858
In-flight imaging of transverse gas jets injected into transonic and supersonic crossflows: Design and development
[NASA-CR-186031] p 157 N95-17418

FLIGHT TESTS
X-29 high-angle-of-attack
[BTN-94-EIX94511309383] p 127 A95-64609
A VHF/UHF antenna for the Precision Antenna Measurement System (PAMS)
[AD-A285673] p 156 N95-16621
Development of a low-aspect ratio fin for flight research experiments
[NASA-TM-4596] p 108 N95-16858
Modeling of Instrument Landing System (ILS) localizer signal on runway 25L at Los Angeles International Airport
[NASA-TM-4588] p 125 N95-17384
Flight testing high lateral asymmetries on highly augmented Fighter/Attack aircraft
[AD-A284206] p 130 N95-17953
KC-135 cockpit modernization study. Phase 1: Equipment evaluation
[AD-A284099] p 131 N95-18398
Preliminary evaluation of the F/A-18 quantity/multiple envelope expansion
[AD-A284119] p 132 N95-18407
Tilt Rotor Unmanned Air Vehicle System (TRUS) demonstrator flight test program
[AD-A284151] p 132 N95-18415

Helicopter in-flight simulation development and use in test pilot training
[AD-A283998] p 146 N95-18725

Hypersonic flight testing
[AD-A283981] p 134 N95-18891
Design and flight test of a simplified control system for a transport helicopter p 144 N95-18902
Navier-Stokes, flight, and wind tunnel flow analysis for the F/A-18 aircraft
[NASA-TP-3478] p 120 N95-19114
Fiber Optic Control System integration for advanced aircraft. Electro-optic and sensor fabrication, integration, and environmental testing for flight control systems
[NASA-CR-191194] p 162 N95-19236

FLOW CHARACTERISTICS
A selection of experimental test cases for the validation of CFD codes, volume 2
[AGARD-AR-303-VOL-2] p 109 N95-17846
Experiments in the trailing edge flow of an NLR 7702 airfoil p 110 N95-17853
Delta-wing model p 114 N95-17873
STOVL CFD model test case p 115 N95-17881
Numerical mixing calculations of confined reacting jet flows in a cylindrical duct
[NASA-TM-106736] p 139 N95-18133
A selection of experimental test cases for the validation of CFD codes. Supplement: Datasets A-E
[AGARD-AR-303-SUPPL] p 117 N95-18539
Navier-Stokes, flight, and wind tunnel flow analysis for the F/A-18 aircraft
[NASA-TP-3478] p 120 N95-19114

FLOW DISTORTION
The traditional and new methods of accounting for the factors distorting the flow over a model in large transonic wind tunnels p 165 N95-19275

FLOW DISTRIBUTION
Residual-correction type and related computational methods for aerodynamic design. Part 1: Airfoil and wing design p 128 N95-16566
Airfoil optimization by the one-shot method p 128 N95-16569
Numerical simulation of helicopter engine plume in forward flight
[NASA-CR-197488] p 107 N95-16589
Numerical simulation of transient vortex breakdown above a pitching delta wing
[AD-A281075] p 107 N95-16808
Three-dimensional boundary layer and flow field data of an inclined prolate spheroid p 158 N95-17867
Force and pressure data of an ogive-nosed slender body at high angles of attack and different Reynolds numbers p 113 N95-17868
Pressure distribution measurements on an isolated TPS 441 nacelle p 115 N95-17878
Low speed propeller slipstream aerodynamic effects p 116 N95-17882
Floating shock fitting via Lagrangian adaptive meshes
[NASA-CR-194997] p 170 N95-18110
Numerical mixing calculations of confined reacting jet flows in a cylindrical duct
[NASA-TM-106736] p 139 N95-18133
Hypersonic flow-field measurements: Intrusive and nonintrusive
[AD-A283867] p 119 N95-18674
The crucial role of wall interference, support interference and flow field measurements in the development of advanced aircraft configurations p 162 N95-19252
Applications of the five-hole probe technique for flow field surveys at the Institute for Aerospace Research p 163 N95-19255
Aerodynamic investigation of the flow field in a 180 deg turn channel with sharp bend p 163 N95-19257
The utilization of a high speed reflective visualization system in the study of transonic flow over a delta wing p 121 N95-19259
Transonic and supersonic flowfield measurements about axisymmetric afterbodies for validation of advanced CFD codes p 121 N95-19260
Velocity measurements with hot-wires in a vortex-dominated flowfield p 121 N95-19261
Determination of solid/porous wall boundary conditions from wind tunnel data for computational fluid dynamics codes p 164 N95-19266
Calculation of low speed wind tunnel wall interference from static pressure pipe measurements p 164 N95-19273
Parabolized Navier-Stokes solution of supersonic/hypersonic flows p 123 N95-19464

FLOW EQUATIONS
Steady potential solver for unsteady aerodynamic analyses p 141 N95-19382

FLOW GEOMETRY
Application of multicomponent models to flow passage simulation in multistage turbomachines and whole gas turbine engines p 140 N95-19022

FLOW MEASUREMENT
Mach number, flow angle, and loss measurements downstream of a transonic fan-blade cascade
[AD-A280907] p 108 N95-16824
Detailed study at supersonic speeds of the flow around delta wings p 112 N95-17861
Wall Interference, Support Interference and Flow Field Measurements p 162 N95-19251
The crucial role of wall interference, support interference and flow field measurements in the development of advanced aircraft configurations p 162 N95-19252
Applications of the five-hole probe technique for flow field surveys at the Institute for Aerospace Research p 163 N95-19255
Aerodynamic investigation of the flow field in a 180 deg turn channel with sharp bend p 163 N95-19257
Experimental techniques for measuring transonic flow with a three dimensional laser velocimetry system. Application to determining the drag of a fuselage p 163 N95-19258
Transonic and supersonic flowfield measurements about axisymmetric afterbodies for validation of advanced CFD codes p 121 N95-19260

FLOW STABILITY
Linear instability waves in supersonic jets confined in circular and non-circular ducts
[BTN-94-EIX94341340068] p 103 A95-63520
The stability of two-phase flow over a swept-wing
[NASA-CR-194994] p 159 N95-18190

FLOW VISUALIZATION
In-flight imaging of transverse gas jets injected into transonic and supersonic crossflows: Design and development
[NASA-CR-186031] p 157 N95-17418
Subsonic flow around US-orbiter model FALKE in the DNW p 115 N95-17877
Overview of unsteady transonic wind tunnel test on a semispan straked delta wing oscillating in pitch
[AD-A284097] p 117 N95-18380
Hypersonic flow-field measurements: Intrusive and nonintrusive
[AD-A283867] p 119 N95-18674
Static investigation of two fluidic thrust-vectoring concepts on a two-dimensional convergent-divergent nozzle
[NASA-TM-4574] p 120 N95-19042
The crucial role of wall interference, support interference and flow field measurements in the development of advanced aircraft configurations p 162 N95-19252
The utilization of a high speed reflective visualization system in the study of transonic flow over a delta wing p 121 N95-19259

FLUID DYNAMICS
Unsteady flow phenomena in discrete passage diffusers for centrifugal compressors
[AD-A281412] p 155 N95-16163
An analysis code for the Rapid Engineering Estimation of Momentum and Energy Losses (REMEL)
[NASA-CR-191178] p 108 N95-16887
Computation of vortex breakdown p 165 N95-19462

FLUID FLOW
New approach to geometric profiling of the design elements of the passage part in turbo-machines
[BTN-94-EIX94461408769] p 153 A95-63652
Hydrofoil force balance
[AD-D016475] p 160 N95-18461
Computation of vortex breakdown p 165 N95-19462

FLUID MECHANICS
Aeromechanics technology, volume 1. Task 1: Three-dimensional Euler/Navier-Stokes Aerodynamic Method (TEAM) enhancements
[AD-A285713] p 132 N95-18483

FLUIDICS
Static investigation of two fluidic thrust-vectoring concepts on a two-dimensional convergent-divergent nozzle
[NASA-TM-4574] p 120 N95-19042

FLUTTER
H(sup 2)/H(sup INF) controller design for a two-dimensional thin airfoil flutter suppression
[BTN-94-EIX94511433918] p 141 A95-64584
A computational investigation of wake-induced airfoil flutter in incompressible flow and active flutter control
[AD-A281534] p 142 N95-16109

FLUTTER ANALYSIS
Engineering methods for the evaluation of transonic flutter characteristics for aerodynamic control surfaces
[BTN-94-EIX94461408589] p 141 A95-63064
A computational investigation of wake-induced airfoil flutter in incompressible flow and active flutter control
[AD-A281534] p 142 N95-16109

FLUX DENSITY
Active minimization of energy density in three-dimensional enclosures [NASA-CR-197213] p 172 N95-16848

FLY BY LIGHT CONTROL
Fiber-optic technology for transport aircraft [BTN-94-EIX94511309384] p 103 A95-64610
Fiber Optic Control System integration for advanced aircraft. Electro-optic and sensor fabrication, integration, and environmental testing for flight control systems: Laboratory test results [NASA-CR-195408] p 161 N95-18938
Fiber Optic Control System integration for advanced aircraft. Electro-optic and sensor fabrication, integration, and environmental testing for flight control systems [NASA-CR-191194] p 162 N95-19236

FLY BY WIRE CONTROL
Development of a bipolar lead/acid battery for the more electric aircraft [AD-A284050] p 160 N95-18660
NASA develops new digital flight control system [NASA-NEWS-RELEASE-94-47] p 144 N95-19029

FORCE DISTRIBUTION
2-D aileron effectiveness study p 110 N95-17851
Hydrofoil force balance [AD-D016475] p 160 N95-18461

FORCED VIBRATION
Forced response of mistuned bladed disks p 141 N95-19383

FORTRAN
Applications of automatic differentiation in computational fluid dynamics p 156 N95-16461

FOURIER SERIES
Compression strength of composite primary structural components [NASA-CR-197554] p 160 N95-18388

FRACTOGRAPHY
The characterization of widespread fatigue damage in fuselage structure p 166 N95-19472

FRACTURE MECHANICS
FAA/NASA International Symposium on Advanced Structural Integrity Methods for Airframe Durability and Damage Tolerance, part 2 [NASA-CP-3274-PT-2] p 124 N95-19468
The application of Newman crack-closure model to predicting fatigue crack growth p 167 N95-19483

FRACTURE STRENGTH
Multi-lab comparison on R-curve methodologies: Alloy 2024-T3 [NASA-CR-195004] p 151 N95-16860
A CMC database for use in the next generation launch vehicles (rockets) p 150 N95-18993
Prediction of R-curves from small coupon tests p 167 N95-19496

FRACTURES (MATERIALS)
Detecting gear tooth fracture in a high contact ratio face gear mesh [NASA-TM-106822] p 162 N95-19125

FRACTURING
Multi-lab comparison on R-curve methodologies: Alloy 2024-T3 [NASA-CR-195004] p 151 N95-16860

FREE FLOW
Investigation of the flow over a series of 14 percent-thick supercritical aerofoils with significant rear camber
OAT15A airfoil data p 109 N95-17849
p 111 N95-17857
Two-dimensional high-lift airfoil data for CFD code validation p 112 N95-17859

FREE JETS
Flow field investigation in a free jet - free jet core system for the generation of high intensity molecular beams [DLR-FB-94-11] p 172 N95-18912

FREQUENCY RESPONSE
Comparison of frequency response and perturbation methods to extract linear models from a nonlinear simulation [AD-A284115] p 146 N95-18405
Comparison of stochastic and deterministic nonlinear gust analysis methods to meet continuous turbulence criteria p 133 N95-18602

FRICTION FACTOR
Static and dynamic friction behavior of candidate high temperature airframe seal materials [NASA-TM-106571] p 152 N95-16905

FUEL COMBUSTION
Combustor kinetic energy efficiency analysis of the hypersonic research engine data p 148 N95-16321

FUEL CONTROL
Ultimate characteristics of a rocket engine with a turbo-pump supply system [BTN-94-EIX94461408757] p 148 A95-63640
New technologies for space avionics [NASA-CR-197574] p 150 N95-18196

FUEL TESTS
Unmanned aerial vehicle heavy fuel engine test [AD-A284332] p 139 N95-18383

FUEL VALVES
A Lifting Ball Valve for cryogenic fluid applications p 156 N95-16349

FUELS
Unmanned aerial vehicle heavy fuel engine test [AD-A284332] p 139 N95-18383

FULL SCALE TESTS
Wall interaction effects for a full-scale helicopter rotor in the NASA Ames 80- by 120-foot wind tunnel p 121 N95-19270
Evaluation of the fuselage lap joint fatigue and terminating action repair p 166 N95-19477
Development of load spectra for Airbus A330/A340 full scale fatigue tests p 135 N95-19479

FUNCTIONAL DESIGN SPECIFICATIONS
New approach to geometric profiling of the design elements of the passage part in turbo-machines [BTN-94-EIX94461408769] p 153 A95-63652
Generalized method of solving topological optimization problems for electrical airplane equipment systems in computer-aided design p 169 N95-16272
The impact of non-linear flight control systems on the prediction of aircraft loads due to turbulence p 143 N95-18598
Design limit loads based upon statistical discrete gust methodology p 133 N95-18603

FUSELAGES
An approach to aerodynamic characteristics of low radar cross-section fuselages p 106 N95-16251
Numerical simulation of helicopter engine plume in forward flight [NASA-CR-197488] p 107 N95-16589
Wind tunnel investigations of the appearance of shocks in the windward region of bodies with circular cross section at angle of attack p 113 N95-17866
STOVL CFD model test case p 115 N95-17881
Investigation of the influence of pylons and stores on the wing lower surface flow p 116 N95-17885
Application of photogrammetry of F-14D store separation [AD-A284154] p 132 N95-18417
Experimental techniques for measuring transonic flow with a three dimensional laser velocimetry system. Application to determining the drag of a fuselage p 163 N95-19258
The characterization of widespread fatigue damage in fuselage structure p 166 N95-19472
Discrete crack growth analysis methodology for through cracks in pressurized fuselage structures p 166 N95-19473
Evaluation of the fuselage lap joint fatigue and terminating action repair p 166 N95-19477
Development of load spectra for Airbus A330/A340 full scale fatigue tests p 135 N95-19479
Results of uniaxial and biaxial tests on riveted fuselage lap joint specimens p 136 N95-19491
Prediction of R-curves from small coupon tests p 167 N95-19496
Nonlinear analysis of damaged stiffened fuselage shells subjected to combined loads p 137 N95-19499

FUZZY SYSTEMS
Workshop on Formal Models for Intelligent Control [AD-A281399] p 169 N95-16864

G

GAS DYNAMICS
Simulation of multidisciplinary problems for the thermosress state of cooled high temperature turbines p 140 N95-19021
Application of multidisciplinary models to the cooled turbine rotor design p 140 N95-19024

GAS FLOW
Flow field investigation in a free jet - free jet core system for the generation of high intensity molecular beams [DLR-FB-94-11] p 172 N95-18912
Mathematical Models of Gas Turbine Engines and their Components [AGARD-LS-198] p 139 N95-19017
The mathematical models of flow passage for gas turbine engines and their components p 140 N95-19020
Application of multicomponent models to flow passage simulation in multistage turbomachines and whole gas turbine engines p 140 N95-19022
Application of multidisciplinary models to the cooled turbine rotor design p 140 N95-19024
Parabolized Navier-Stokes solution of supersonic/hypersonic flows p 123 N95-19464

GAS INJECTION
In-flight imaging of transverse gas jets injected into transonic and supersonic crossflows: Design and development [NASA-CR-186031] p 157 N95-17418

GAS JETS
Linear instability waves in supersonic jets confined in circular and non-circular ducts [BTN-94-EIX94341340068] p 103 A95-63520

GAS TEMPERATURE
Ultimate characteristics of a rocket engine with a turbo-pump supply system [BTN-94-EIX94461408757] p 148 A95-63640

GAS TURBINE ENGINES
Gas-turbine engines with increased efficiency of two circuits, due to the use of the utilizing steam-turbine circuit [BTN-94-EIX94461408755] p 153 A95-63638
Modelling for optimal operations of line milling of aerodynamic surfaces [BTN-94-EIX94461408774] p 138 A95-63657
Theoretical fundamentals of the aircraft GTE tests p 138 N95-16265
An artificial neural network system for diagnosing gas turbine engine fuel faults [DE94-013960] p 138 N95-17371
Simulation investigation on system identification of gas turbine [PB95-104238] p 139 N95-17749
Wave cycle design for wave rotor engines with limited nitrogen oxide emissions p 161 N95-18901
Mathematical Models of Gas Turbine Engines and their Components [AGARD-LS-198] p 139 N95-19017
The mathematical models of flow passage for gas turbine engines and their components p 140 N95-19020
Application of multicomponent models to flow passage simulation in multistage turbomachines and whole gas turbine engines p 140 N95-19022

GAS TURBINES
Fatigue in single crystal nickel superalloys [AD-A285727] p 152 N95-18068
Numerical mixing calculations of confined reacting jet flows in a cylindrical duct [NASA-TM-106736] p 139 N95-18133

GAS-SOLID INTERACTIONS
On the particular features of dynamic processes in solids with varying boundary during interaction with intensive heat flows [BTN-94-EIX94461408756] p 171 A95-63639

GAS-SOLID INTERFACES
On the particular features of dynamic processes in solids with varying boundary during interaction with intensive heat flows [BTN-94-EIX94461408756] p 171 A95-63639

GEAR TEETH
Detecting gear tooth fracture in a high contact ratio face gear mesh [NASA-TM-106822] p 162 N95-19125

GEARS
Detecting gear tooth fracture in a high contact ratio face gear mesh [NASA-TM-106822] p 162 N95-19125

GENERAL AVIATION AIRCRAFT
Revitalizing general aviation [NASA-TM-110113] p 129 N95-16982
Annual review of aircraft accident data: US Air carrier operations, calendar year 1992 [PB95-100319] p 123 N95-17748

GENERAL OVERVIEWS
Composite chronicles: A study of the lessons learned in the development, production, and service of composite structures [NASA-CR-4620] p 151 N95-16859

GENETIC ALGORITHMS
Review of the EUROPT Project AERO-0026 p 129 N95-16573

GEODESY
Conversion of Earth-centered Earth-fixed coordinates to geodetic coordinates [BTN-94-EIX94441380862] p 125 A95-64294

GEODETC COORDINATES
Conversion of Earth-centered Earth-fixed coordinates to geodetic coordinates [BTN-94-EIX94441380862] p 125 A95-64294

GLARE
An evaluation of aircraft CRT and dot-matrix display legibility requirements [AD-A283933] p 138 N95-18164

GLIDE PATHS
Commentary on Walton correspondence relating to the ILS glide slope [BTN-94-EIX94441380856] p 125 A95-64288
Application of GPS/SINS/RA integrated system to aircraft approach landing p 125 N95-16277

- GLOBAL POSITIONING SYSTEM**
Application of GPS/SINS/RA integrated system to aircraft approach landing p 125 N95-16277
A processing centre for the CNES CE-GPS experimentation p 125 N95-17196
Heliport/vertiport MLS precision approaches [AD-A283505] p 126 N95-18059
- GOERTLER INSTABILITY**
Effect of crossflow on Goertler instability in incompressible boundary layers [NASA-CR-195007] p 159 N95-18193
- GOVERNMENT/INDUSTRY RELATIONS**
EC Aviation Scene [HTN-95-50223] p 176 A95-64860
European aeronautics: Strong government presence in industry structure and research and development support. Report to Congressional Requesters [GAO/NSIAD-94-71] p 176 N95-18578
- GRAPHICAL USER INTERFACE**
A workstation based simulator for teaching compressible aerodynamics [NASA-TM-106799] p 170 N95-16906
A platform independent application of Lux illumination prediction algorithms [AD-A283669] p 170 N95-18018
- GRAPHITE-EPOXY COMPOSITES**
Recent advances in graphite/epoxy motor cases p 149 N95-16333
- GRAVITATIONAL PHYSIOLOGY**
Virtual environment application with partial gravity simulation p 169 N95-15988
A surgical support system for Space Station Freedom p 149 N95-16776
- GRID GENERATION (MATHEMATICS)**
A grid generation and flow solution method for the Euler equations on unstructured grids [HTN-95-20003] p 153 A95-63201
Mesh quality control for multiply-refined tetrahedral grids [NASA-CR-197595] p 160 N95-18737
Simulation of multidisciplinary problems for the thermostress state of cooled high temperature turbines p 140 N95-19021
An assessment of the adaptive unstructured tetrahedral grid, Euler Flow Solver Code FELISA [NASA-TP-3526] p 119 N95-19041
CFD: Advances and Applications, part 1 [NAL-SP-9322-PT-1] p 165 N95-19444
- GROUND BASED CONTROL**
EURECA mission control experience and messages for the future p 149 N95-17252
- GROUND EFFECT (AERODYNAMICS)**
Tilt Rotor Unmanned Air Vehicle System (TRUS) demonstrator flight test program [AD-A284151] p 132 N95-18415
Development of pneumatic test techniques for subsonic high-lift and in-ground-effect wind tunnel investigations p 121 N95-19268
- GROUND STATIONS**
A VHF/UHF antenna for the Precision Antenna Measurement System (PAMS) [AD-A285673] p 156 N95-16621
A processing centre for the CNES CE-GPS experimentation p 125 N95-17196
- GROUND TESTS**
A model for preliminary facility design including simulation issues p 144 N95-16318
Hypersonic air-breathing aeropropulsion facility test support requirements p 144 N95-16319
Development of a low-aspect ratio fin for flight research experiments [NASA-TM-4596] p 108 N95-16858
Hypersonic flight testing [AD-A283981] p 134 N95-18891
- GROUND TRUTH**
Field verification of the wind tunnel coefficients p 109 N95-17291
- GUN PROPELLANTS**
The 1993 JANNAF Propulsion Meeting, volume 1 [CPIA-PUBL-602-VOL-1] p 148 N95-16312
- GUST LOADS**
The impact of non-linear flight control systems on the prediction of aircraft loads due to turbulence p 143 N95-18598
A study of the effect of store unsteady aerodynamics on gust and turbulence loads p 133 N95-18601
Comparison of stochastic and deterministic nonlinear gust analysis methods to meet continuous turbulence criteria p 133 N95-18602
A review of gust load calculation methods at de Havilland p 118 N95-18604
Special effects of gust loads on military aircraft p 133 N95-18605
- GUSTS**
H(sup 2)/H(sup INF) controller design for a two-dimensional thin airfoil flutter suppression [BTN-94-EIX94511433918] p 141 A95-64584
Field verification of the wind tunnel coefficients p 109 N95-17291
Measurement of gust response on a turbine cascade [NASA-TM-106776] p 117 N95-18457
Treatment of non-linear systems by timeplane-transformed CT methods: The spectral gust method p 143 N95-18600
Design limit loads based upon statistical discrete gust methodology p 133 N95-18603
A review of gust load calculation methods at de Havilland p 118 N95-18604
Special effects of gust loads on military aircraft p 133 N95-18605
- GYROSCOPIC STABILITY**
Gyroscopic and propeller aerodynamic effects on engine mounts dynamic loads in turbulence conditions p 132 N95-18599

H

- HARDNESS**
A CMC database for use in the next generation launch vehicles (rockets) p 150 N95-18993
E-6A hardness assurance, maintenance and surveillance program [AD-A283994] p 134 N95-19067
- HARRIER AIRCRAFT**
VSTOL Systems Research Aircraft (VSRA) Harrier [NASA-TM-110117] p 126 N95-18347
- HAZARDS**
The assessment of the AH-64D, longbow, mast-mounted assembly noise hazard for maintenance personnel [AD-A284971] p 171 N95-16226
- HEAD-UP DISPLAYS**
VSTOL Systems Research Aircraft (VSRA) Harrier [NASA-TM-110117] p 126 N95-18347
- HEARING**
The assessment of the AH-64D, longbow, mast-mounted assembly noise hazard for maintenance personnel [AD-A284971] p 171 N95-16226
- HEAT ENGINES**
On a program-information system TDsoft [BTN-94-EIX94461408773] p 175 A95-63656
Anisotropic heat exchangers/stack configurations for thermoacoustic heat engines [AD-A280974] p 168 N95-16506
- HEAT EXCHANGERS**
Anisotropic heat exchangers/stack configurations for thermoacoustic heat engines [AD-A280974] p 168 N95-16506
Airborne rotary separator study [NASA-CR-191045] p 150 N95-18743
- HEAT RESISTANT ALLOYS**
Fatigue in single crystal nickel superalloys [AD-A285727] p 152 N95-18068
- HEAT TRANSFER**
Investigation of heat transfer between rotating shafts of transmissions of turbojet engines [BTN-94-EIX94461408760] p 138 A95-63643
Service and physical properties of liquid-jet fuels p 151 N95-16256
An engineering code to analyze hypersonic thermal management systems p 155 N95-16322
Hypersonic wind tunnel test techniques [AD-A284057] p 118 N95-18663
Hypersonic flight testing [AD-A283981] p 134 N95-18891
Application of multidisciplinary models to the cooled turbine rotor design p 140 N95-19024
- HELICOPTER CONTROL**
Test bench for rotorcraft hover control [BTN-94-EIX94511433919] p 169 A95-64585
Design and flight test of a simplified control system for a transport helicopter p 144 N95-18902
- HELICOPTER ENGINES**
Sensor fault detection and diagnosis simulation of a helicopter engine in an intelligent control framework [NASA-TM-106784] p 137 N95-15970
Numerical simulation of helicopter engine plume in forward flight [NASA-CR-197488] p 107 N95-16589
- HELICOPTER PERFORMANCE**
Helicopter Performance Evaluation (HELPE) computer model [AD-A284319] p 131 N95-18381
- HELICOPTERS**
Test bench for rotorcraft hover control [BTN-94-EIX94511433919] p 169 A95-64585
A correlative investigation of simulated occupant motion and accident report in a helicopter crash [AD-A285190] p 123 N95-16404
Experimental data on the aerodynamic interactions between a helicopter rotor and an airframe p 116 N95-17883
Heliport/vertiport MLS precision approaches [AD-A283505] p 126 N95-18059
Helicopter Performance Evaluation (HELPE) computer model [AD-A284319] p 131 N95-18381
Tilt Rotor Unmanned Air Vehicle System (TRUS) demonstrator flight test program [AD-A284151] p 132 N95-18415
Helicopter in-flight simulation development and use in test pilot training [AD-A283998] p 146 N95-18725
Helicopter internal noise p 173 N95-19144
- HELIPORTS**
Heliport/vertiport MLS precision approaches [AD-A283505] p 126 N95-18059
- HELMET MOUNTED DISPLAYS**
Factors affecting the visual fragmentation of the field-of-view in partial binocular overlap displays [AD-A283081] p 172 N95-17334
- HERMES MANNED SPACEPLANE**
Aeroacoustic qualification of HERMES shingles p 173 N95-19145
- HIGH ENERGY FUELS**
Solid fuel ramjet composition [AD-D016458] p 152 N95-19090
- HIGH FREQUENCIES**
Assessing aircraft survivability to high frequency transient threats [AD-A283999] p 134 N95-18726
- HIGH PRESSURE**
Twin engine afterbody model p 115 N95-17880
Studies on high pressure and unsteady flame phenomena [AD-A284126] p 152 N95-18410
- HIGH REYNOLDS NUMBER**
Detailed study at supersonic speeds of the flow around delta wings p 112 N95-17861
On the Lighthill relationship and sound generation from isotropic turbulence [NASA-CR-195005] p 159 N95-18191
Unsteady aerodynamic analyses for turbomachinery aeroelastic predictions p 141 N95-19381
- HIGH SPEED**
Error propagation equations for estimating the uncertainty in high-speed wind tunnel test results [DE94-014136] p 145 N95-16509
Two-dimensional 16.5 percent thick supercritical airfoil NLR 7301 p 110 N95-17854
Hypersonic flight testing [AD-A283981] p 134 N95-18891
- HIGH TEMPERATURE TESTS**
High-temperature acoustic test facilities and methods p 174 N95-19149
Design and operation of a thermoacoustic test facility p 147 N95-19150
- HOLDERS**
Background noise levels measured in the NASA Lewis 9- by 15-foot low-speed wind tunnel [NASA-TM-106817] p 145 N95-18054
- HORIZONTAL FLIGHT**
Time-optimal turn to a heading: An analytic solution [BTN-94-EIX94511433940] p 142 A95-64606
Numerical simulation of helicopter engine plume in forward flight [NASA-CR-197488] p 107 N95-16589
- HORSESHOE VORTICES**
Wing-body juncture flows [AD-A281526] p 106 N95-16099
- HUMAN FACTORS ENGINEERING**
Industry review of a crew-centered cockpit design process and toolset [AD-A282966] p 130 N95-17661
Conference on Aerospace Transparent Materials and Enclosures, volume 1 [AD-A283925] p 133 N95-18677
An overall approach of cockpit noise verification in a military aircraft p 175 N95-19163
- HYBRID COMPOSITES**
Optimization of adaptive intraply hybrid fiber composites with reliability considerations [NASA-TM-106632] p 157 N95-16911
- HYDRAULIC ANALOGIES**
Verification of multidisciplinary models for turbomachines p 140 N95-19025
- HYDRAULIC TEST TUNNELS**
Corner vortex suppressor [AD-D016423] p 116 N95-18337
Development of a multicomponent force and moment balance for water tunnel applications, volume 1 [NASA-CR-4642-VOL-1] p 161 N95-18955
Development of a multicomponent force and moment balance for water tunnel applications, volume 2 [NASA-CR-4642-VOL-2] p 161 N95-18956

- HYDROFOILS**
Hydrofoil force balance
[AD-D016475] p 160 N95-18461
- HYDROGEN FUELS**
Airborne rotary separator study
[NASA-CR-191045] p 150 N95-18743
- HYPERSONIC AIRCRAFT**
Static and dynamic friction behavior of candidate high temperature airframe seal materials
[NASA-TM-106571] p 152 N95-16905
- HYPERSONIC FLIGHT**
Hypersonic flight testing
[AD-A283981] p 134 N95-18891
- HYPERSONIC FLOW**
High altitude hypersonic flowfield radiation
[AD-A281386] p 106 N95-16160
In-flight imaging of transverse gas jets injected into transonic and supersonic crossflows: Design and development
[NASA-CR-186031] p 157 N95-17418
Hypersonic flow-field measurements: Intrusive and nonintrusive
[AD-A283867] p 119 N95-18674
Theoretical investigations of shock/boundary layer interactions on a Ma(infinity) = 8 waverider
[DLR-FB-94-12] p 119 N95-18910
Parabolized Navier-Stokes solution of supersonic/hypersonic flows
p 123 N95-19464
- HYPERSONIC INLETS**
Numerical simulation of supersonic compression corners and hypersonic inlet flows using the RPLUS2D code
[NASA-TM-106580] p 105 N95-16038
- HYPERSONIC SPEED**
Numerical simulation of supersonic compression corners and hypersonic inlet flows using the RPLUS2D code
[NASA-TM-106580] p 105 N95-16038
Scramjet testing guidelines
p 138 N95-16317
- HYPERSONIC TEST APPARATUS**
A model for preliminary facility design including simulation issues
p 144 N95-16318
Hypersonic air-breathing aer propulsion facility test support requirements
p 144 N95-16319
- HYPERSONIC VEHICLES**
Ultraviolet emissions occurring about hypersonic vehicles in rarefied flows
[AD-A281452] p 106 N95-16076
Hypersonic wind tunnel test techniques
[AD-A284057] p 118 N95-18663
Thermo-acoustic fatigue design for hypersonic vehicle skin panels
p 162 N95-19161
- HYPERSONIC WIND TUNNELS**
Wall-signature methods for high speed wind tunnel wall interference corrections
p 107 N95-16257
A model for preliminary facility design including simulation issues
p 144 N95-16318
Hypersonic air-breathing aer propulsion facility test support requirements
p 144 N95-16319
Hypersonic wind tunnel test techniques
[AD-A284057] p 118 N95-18663
Operating capability and current status of the reactivated NASA Lewis Research Center Hypersonic Tunnel Facility
[NASA-TM-106808] p 148 N95-19286
- HYPERSONICS**
High altitude hypersonic flowfield radiation
[AD-A281386] p 106 N95-16160
An engineering code to analyze hypersonic thermal management systems
p 155 N95-16322
Static aerodynamics CFD analysis for 120-mm hypersonic KE projectile design
[ARL-MR-184] p 118 N95-18611
- ICE**
Ice accretion with varying surface tension
[NASA-TM-106826] p 124 N95-19285
- ICE FORMATION**
Ice accretion with varying surface tension
[NASA-TM-106826] p 124 N95-19285
- IDENTIFYING**
The use of electrochemistry and ellipsometry for identifying and evaluating corrosion on aircraft
[AD-A285323] p 151 N95-16371
- ILLUMINATION**
A platform independent application of Lux illumination prediction algorithms
[AD-A283669] p 170 N95-18018
- IMAGE PROCESSING**
Joint Proceedings on Aeronautics and Astronautics (JPAA)
[ISBN-7-80-046602-7] p 104 N95-16249
- IMAGING RADAR**
Linear prediction data extrapolation superresolution radar imaging
p 155 N95-16268
- IMAGING TECHNIQUES**
Linear prediction data extrapolation superresolution radar imaging
p 155 N95-16268
In-flight imaging of transverse gas jets injected into transonic and supersonic crossflows: Design and development
[NASA-CR-186031] p 157 N95-17418
Evaluation of scanners for C-scan imaging in nondestructive inspection of aircraft
[DE94-012473] p 152 N95-19100
- IMPACT RESISTANCE**
Conference on Aerospace Transparent Materials and Enclosures. Volume 2: Sessions 5-9
[AD-A283926] p 131 N95-18162
- IMPEDANCE MEASUREMENT**
The use of electrochemistry and ellipsometry for identifying and evaluating corrosion on aircraft
[AD-A285323] p 151 N95-16371
- IN-FLIGHT MONITORING**
Flight parameters monitoring system for tracking structural integrity of rotary-wing aircraft
p 135 N95-19469
- INCOMPRESSIBLE BOUNDARY LAYER**
Effect of crossflow on Goertler instability in incompressible boundary layers
[NASA-CR-195007] p 159 N95-18193
- INCOMPRESSIBLE FLOW**
A computational investigation of wake-induced airfoil flutter in incompressible flow and active flutter control
[AD-A281534] p 142 N95-16109
- INDUSTRIES**
Military aviation maintenance industry in Western Europe: Concentration and internationalization
[PB94-189180] p 104 N95-17451
- INERTIAL NAVIGATION**
Application of GPS/SINS/RA integrated system to aircraft approach landing
p 125 N95-16277
- INFORMATION DISSEMINATION**
ICASE
[NASA-CR-195001] p 170 N95-16898
- INFORMATION RETRIEVAL**
On a program information system TDsoft
[BTN-94-EIX94461408773] p 175 A95-63656
- INFRARED RADIATION**
Application of photogrammetry of F-14D store separation
[AD-A284154] p 132 N95-18417
- INLET FLOW**
Numerical simulation of supersonic compression corners and hypersonic inlet flows using the RPLUS2D code
[NASA-TM-106580] p 105 N95-16038
Unsteady flow phenomena in discrete passage diffusers for centrifugal compressors
[AD-A281412] p 155 N95-16163
Time accurate computation of unsteady inlet flows with a dynamic flow adaptive mesh
[AD-A285498] p 157 N95-16736
Three dimensional compressible turbulent flow computations for a diffusing S-duct with/without vortex generators
[NASA-CR-195390] p 138 N95-17402
Wind turbine blade aerodynamics: The combined experiment
[DE94-011866] p 118 N95-18645
Wind turbine blade aerodynamics: The analysis of field test data
[DE94-011867] p 118 N95-18646
- INLET NOZZLES**
Combustor kinetic energy efficiency analysis of the hypersonic research engine data
p 148 N95-16321
Small turbojets: Designs and installations
p 138 N95-16323
- INMARSAT SATELLITES**
A processing centre for the CNES CE-GPS experimentation
p 125 N95-17196
- INSTALLING**
Mathematical modelling concerning the development of a system of similar installations, taking into account their operational intensity (an aircraft-helicopter fleet taken as an example)
[BTN-94-EIX94461408763] p 103 A95-63646
- INSTRUMENT APPROACH**
Helioport/vertiport MLS precision approaches
[AD-A283505] p 126 N95-18059
- INSTRUMENT LANDING SYSTEMS**
Commentary on Walton correspondence relating to the ILS glide slope
[BTN-94-EIX94441380856] p 125 A95-64288
Modeling of Instrument Landing System (ILS) localizer signal on runway 25L at Los Angeles International Airport
[NASA-TM-4588] p 125 N95-17384
- INSTRUMENT PACKAGES**
Field and data analysis studies related to the atmospheric environment
[NASA-CR-196543] p 168 N95-18093
- INTEGRATED MISSION CONTROL CENTER**
EURECA mission control experience and messages for the future
p 149 N95-17252
- INTERACTIONAL AERODYNAMICS**
Wing-body juncture flows
[AD-A281526] p 106 N95-16099
A computational investigation of wake-induced airfoil flutter in incompressible flow and active flutter control
[AD-A281534] p 142 N95-16109
Single-engine tail interference model
p 115 N95-17879
Sectional prediction of 3D effects for separated flow on rotating blades
[PB94-201696] p 117 N95-18503
Pressure measurements on an F/A-18 twin vertical tail in buffeting flow. Volume 4, part 2: Buffet cross spectral densities
[AD-A285555] p 143 N95-18641
- INTERFACIAL TENSION**
Ice accretion with varying surface tension
[NASA-TM-106826] p 124 N95-19285
- INTERFERENCE DRAG**
Single-engine tail interference model
p 115 N95-17879
- INTERNAL COMBUSTION ENGINES**
A stationary flow of a viscous liquid in radial clearances of rotor bearings in the turbocompressor of an internal combustion engine
[BTN-94-EIX94461408765] p 153 A95-63648
- INTERNAL FLOW**
One-dimensional flow description for the combustion chamber of a scramjet
[DLR-FB-94-06] p 139 N95-18911
Determination of solid/porous wall boundary conditions from wind tunnel data for computational fluid dynamics codes
p 164 N95-19266
- INTERNAL PRESSURE**
Experimental and analytical methods for the determination of connected-pipe ramjet and ducted rocket internal performance
[AGARD-AR-323] p 149 N95-17278
Nonlinear analysis of damaged stiffened fuselage shells subjected to combined loads
p 137 N95-19499
- INTERNATIONAL COOPERATION**
World trends in air transport policies. (Approaching the 21st century)
[HTN-95-50220] p 176 A95-64857
Aircraft and sub-system certification by piloted simulation
[AGARD-AR-278] p 145 N95-17388
Military aviation maintenance industry in Western Europe: Concentration and internationalization
[PB94-189180] p 104 N95-17451
European aeronautics: Strong government presence in industry structure and research and development support. Report to Congressional Requesters
[GAO/NSIAD-94-71] p 176 N95-18578
- INTERNATIONAL SPACE STATION**
Assessment of the Space Station program
p 149 N95-16352
- INTERORBITAL TRAJECTORIES**
Numerical optimization of synergetic maneuvers
[AD-A283398] p 109 N95-17435
- INTERPOLATION**
New approach to geometric profiling of the design elements of the passage part in turbo-machines
[BTN-94-EIX94461408769] p 153 A95-63652
Evaluation of an autopilot based multimodelling
[PB94-190725] p 142 N95-17454
- INVENTORIES**
The generic simulation executive at Manned Flight Simulator
[AD-A283997] p 146 N95-18724
- INVISCID FLOW**
Improved analytical solution for varying specific heat parallel stream mixing
[BTN-94-EIX94481415349] p 103 A95-65339
Interactive computer graphics applications for compressible aerodynamics
[NASA-TM-106802] p 170 N95-17264
Computation of inviscid flows: Full potential method
p 165 N95-19447
Viscous flow past aerofoils axisymmetric bodies and wings
p 123 N95-19457
- ISOTROPIC TURBULENCE**
On the Lighthill relationship and sound generation from isotropic turbulence
[NASA-CR-195005] p 159 N95-18191
- ISOTROPY**
Fatigue in single crystal nickel superalloys
[AD-A285727] p 152 N95-18068

J

J INTEGRAL

- Multi-lab comparison on R-curve methodologies: Alloy 2024-T3 [NASA-CR-195004] p 151 N95-16860
- JET AIRCRAFT**
Preliminary evaluation of the F/A-18 quantity/multiple envelope expansion [AD-A284119] p 132 N95-18407
- JET CONTROL**
New technologies for space avionics [NASA-CR-197574] p 150 N95-18196
- JET ENGINE FUELS**
Service and physical properties of liquid-jet fuels p 151 N95-16256
- JET ENGINES**
Pressure distribution measurements on an isolated TPS 441 nacelle p 115 N95-17878
- JET FLOW**
Numerical mixing calculations of confined reacting jet flows in a cylindrical duct [NASA-TM-106736] p 139 N95-18133
Flow field investigation in a free jet - free jet core system for the generation of high intensity molecular beams [DLR-FB-94-11] p 172 N95-18912
- JET MIXING FLOW**
One-dimensional flow description for the combustion chamber of a scramjet [DLR-FB-94-06] p 139 N95-18911
- JET PROPULSION**
Twin engine afterbody model p 115 N95-17880
- JET VANES**
Integrated aerodynamic fin and stowable TVC vane system [AD-D016457] p 151 N95-19073
- JETSTREAM AIRCRAFT**
Aircraft accident report: Stall and loss of control on final approach, Atlantic Coast Airlines, Inc./United Express Flight 6291 Jetstream 4101, N304UE Columbus, OH, 7 January 1994 [PB94-910409] p 123 N95-17646
- JINDIVIK TARGET AIRCRAFT**
Data acquisition and processing software for the Low Speed Wind Tunnel tests of the Jindivik auxiliary air intake [AD-A285455] p 108 N95-17178
- JOINTS (JUNCTIONS)**
Evaluation of scanners for C-scan imaging in nondestructive inspection of aircraft [DE94-012473] p 152 N95-19100
- JP-4 JET FUEL**
Regenerative cooling for liquid propellant rocket thrust chambers [INPE-5565-TDI/540] p 150 N95-18720
Airborne rotary separator study [NASA-CR-191045] p 150 N95-18743
- JP-5 JET FUEL**
Unmanned aerial vehicle heavy fuel engine test [AD-A284332] p 139 N95-18383
Regenerative cooling for liquid propellant rocket thrust chambers [INPE-5565-TDI/540] p 150 N95-18720
- JP-8 JET FUEL**
Unmanned aerial vehicle heavy fuel engine test [AD-A284332] p 139 N95-18383
- K**
- K-EPSILON TURBULENCE MODEL**
Numerical computations of supersonic base flow with special emphasis on turbulence modeling [AD-A283688] p 119 N95-18670
- KALMAN FILTERS**
Application of GPS/SINS/RA integrated system to aircraft approach landing p 125 N95-16277
- KAPTON (TRADEMARK)**
Problems with aging wiring in Naval aircraft p 154 N95-16048
- KELVIN-HELMHOLTZ INSTABILITY**
Linear instability waves in supersonic jets confined in circular and non-circular ducts [BTN-94-EIX94341340068] p 103 A95-63520
- KINETIC ENERGY**
Combustor kinetic energy efficiency analysis of the hypersonic research engine data p 148 N95-16321
An analysis code for the Rapid Engineering Estimation of Momentum and Energy Losses (REMEL) [NASA-CR-191178] p 108 N95-16887
Static aerodynamics CFD analysis for 120-mm hypersonic KE projectile design [ARL-MR-184] p 118 N95-18611

L

LAGRANGE MULTIPLIERS

- Compression strength of composite primary structural components [NASA-CR-197554] p 160 N95-18388
- LAGRANGIAN FUNCTION**
Floating shock fitting via Lagrangian adaptive meshes [NASA-CR-194997] p 170 N95-18110
- LAMINAR BOUNDARY LAYER**
Three-dimensional boundary layer and flow field data of an inclined prolate spheroid p 158 N95-17867
Parametric study on laminar flow for finite wings at supersonic speeds [NASA-TM-108852] p 116 N95-18101
- LAMINAR FLOW**
Parametric study on laminar flow for finite wings at supersonic speeds [NASA-TM-108852] p 116 N95-18101
Studies on high pressure and unsteady flame phenomena [AD-A284126] p 152 N95-18410
Numerical simulation of dynamic-stall suppression by tangential blowing [AD-A284887] p 120 N95-19110
- LANDING AIDS**
Commentary on Walton correspondence relating to the ILS glide slope [BTN-94-EIX94441380856] p 125 A95-64288
Joint Proceedings on Aeronautics and Astronautics (JPAA) [ISBN-7-80-046602-7] p 104 N95-16249
Application of GPS/SINS/RA integrated system to aircraft approach landing p 125 N95-16277
- LANDING SIMULATION**
Development of load spectra for Airbus A330/A340 full scale fatigue tests p 135 N95-19479
- LANDING SITES**
Development of an Automated Airfield Dynamic Cone Penetrometer (AADCP) prototype and the evaluation of unsurfaced airfield seismic surveying using Spectral Analysis of Surface Waves (SASW) technology [AD-A281985] p 145 N95-17444
- LAP JOINTS**
Evaluation of the fuselage lap joint fatigue and terminating action repair p 166 N95-19477
Fatigue life until small cracks in aircraft structures: Durability and damage tolerance p 135 N95-19478
An artificial corrosion protocol for lap-splices in aircraft skin p 152 N95-19482
Results of uniaxial and biaxial tests on riveted fuselage lap joint specimens p 136 N95-19491
Nonlinear analysis of damaged stiffened fuselage shells subjected to combined loads p 137 N95-19499
- LASER ANEMOMETERS**
Transonic and supersonic flowfield measurements about axisymmetric afterbodies for validation of advanced CFD codes p 121 N95-19260
- LASER DOPPLER VELOCIMETERS**
Aerodynamic investigation of the flow field in a 180 deg turn channel with sharp bend p 163 N95-19257
Experimental techniques for measuring transonic flow with a three dimensional laser velocimetry system. Application to determining the drag of a fuselage p 163 N95-19258
Transonic and supersonic flowfield measurements about axisymmetric afterbodies for validation of advanced CFD codes p 121 N95-19260
- LASERS**
Aircraft wake vortex takeoff tests at O'Hara International Airport [AD-A283828] p 118 N95-18624
- LATERAL CONTROL**
Evaluation of an autopilot based multimodelling [PB94-190725] p 142 N95-17454
- LAUNCH VEHICLES**
Field and data analysis studies related to the atmospheric environment [NASA-CR-196543] p 168 N95-18093
- LAUNCHING**
Field and data analysis studies related to the atmospheric environment [NASA-CR-196543] p 168 N95-18093
- LAW (JURISPRUDENCE)**
Aircraft accident investigation and airworthiness -- A practical example of the interaction of two disciplines with some reflections on possible legal consequences [HTN-95-50219] p 176 A95-64856
EC Aviation Scene [HTN-95-50223] p 176 A95-64860
- LEAD ACID BATTERIES**
Development of a bipolar lead/acid battery for the more electric aircraft [AD-A284050] p 160 N95-18660

LEADING EDGE FLAPS

Investigation of the flow development on a highly swept canard/wing research model with segmented leading- and trailing-edge flaps p 114 N95-17876

LEADING EDGES

- Transonic Navier-Stokes calculations about a 65 deg delta wing [NASA-CR-4635] p 108 N95-17273
Two-dimensional high-lift airfoil data for CFD code validation p 112 N95-17859
Wind tunnel test on a 65 deg delta wing with a sharp or rounded leading edge: The international vortex flow experiment p 114 N95-17872
Wind tunnel test on a 65 deg delta wing with rounded leading edges: The International Vortex Flow Experiment p 114 N95-17875

LEAST SQUARES METHOD

The accuracy of parameter estimation in system identification of noisy aircraft load measurement [NASA-CR-197516] p 134 N95-19130

LEGIBILITY

An evaluation of aircraft CRT and dot-matrix display legibility requirements [AD-A283933] p 138 N95-18164

LENTICULAR BODIES

Test data on a non-circular body for subsonic, transonic and supersonic Mach numbers p 158 N95-17871

LIFE (DURABILITY)

FAA/NASA International Symposium on Advanced Structural Integrity Methods for Airframe Durability and Damage Tolerance, part 2 [NASA-CP-3274-PT-2] p 124 N95-19468

LIFE CYCLE COSTS

Aerodynamic shape optimization p 128 N95-16572

LIFT

Measurements on a two-dimensional aerofoil with high-lift devices p 109 N95-17848
In-flight lift-drag characteristics for a forward-swept wing aircraft and comparisons with contemporary aircraft [NASA-TP-3414] p 117 N95-18565

LIFT DRAG RATIO

An approach to aerodynamic characteristics of low radar cross-section fuselages p 106 N95-16251
Residual-correction type and related computational methods for aerodynamic design. Part 2: Multi-point airfoil design p 128 N95-16567
The global aircraft shape p 128 N95-16571
Aerodynamic shape optimization p 128 N95-16572

LIGHT TRANSPORT AIRCRAFT

Evaluation of the dynamic stability characteristics of the NAL Light Transport Aircraft [NAL-PD-CA-9217] p 142 N95-16392

LIGHTHILL METHOD

On the Lighthill relationship and sound generation from isotropic turbulence [NASA-CR-195005] p 159 N95-18191

LIGHTNING

Field and data analysis studies related to the atmospheric environment [NASA-CR-196543] p 168 N95-18093

LINEAR EQUATIONS

Rapid solution of large-scale systems of equations p 169 N95-16458

LINEAR PREDICTION

Linear prediction data extrapolation superresolution radar imaging p 155 N95-16268

LINEAR QUADRATIC GAUSSIAN CONTROL

Output feedback control under randomly varying distributed delays [BTN-94-EIX94511433916] p 168 A95-64582

LINEAR VIBRATION

Acoustic radiation damping of flat rectangular plates subjected to subsonic flows p 172 N95-18542

LIQUID OXYGEN

Airborne rotary separator study [NASA-CR-191045] p 150 N95-18743

LIQUID PROPELLANT ROCKET ENGINES

Ultimate characteristics of a rocket engine with a turbo-pump supply system [BTN-94-EIX94461408757] p 148 A95-63640

LISTS

ICASE [NASA-CR-195001] p 170 N95-16898

LOAD TESTS

Development of load spectra for Airbus A330/A340 full scale fatigue tests p 135 N95-19479

LOADS (FORCES)

An investigation of polynomial calibrations methods for wind tunnel balances p 144 N95-16258
Field verification of the wind tunnel coefficients p 109 N95-17291
Aircraft fatigue and crack growth considering loads by structural component p 137 N95-19497
Nonlinear analysis of damaged stiffened fuselage shells subjected to combined loads p 137 N95-19499

LOG PERIODIC ANTENNAS

A VHF/UHF antenna for the Precision Antenna Measurement System (PAMS)
[AD-A285673] p 156 N95-16621

LOGIC DESIGN

Workshop on Formal Models for Intelligent Control
[AD-A281399] p 169 N95-16864

LOGISTICS

E-6A hardness assurance, maintenance and surveillance program
[AD-A283994] p 134 N95-19067

LOW ASPECT RATIO

Development of a low-aspect ratio fin for flight research experiments
[NASA-TM-4596] p 108 N95-16858

LOW ASPECT RATIO WINGS

An approach to aerodynamic characteristics of low radar cross-section fuselages p 106 N95-16251
Low aspect ratio wing experiment p 113 N95-17865

LOW CONDUCTIVITY

Quality optimization of thermally sprayed coatings produced by the JP-5000 (HVOF) gun using mathematical modeling p 152 N95-19008

LOW COST

Assessing aircraft survivability to high frequency transient threats
[AD-A283999] p 134 N95-18726

LOW SPEED

Two-dimensional 16.5 percent thick supercritical airfoil NLR 7301 p 110 N95-17854
Low-speed surface pressure and boundary layer measurement data for the NLR 7301 airfoil section with trailing edge flap p 111 N95-17855
Force and pressure data of an ogive-nosed slender body at high angles of attack and different Reynolds numbers p 113 N95-17868
Low speed propeller slipstream aerodynamic effects p 116 N95-17882
Velocity measurements with hot-wires in a vortex-dominated flowfield p 121 N95-19261

LOW SPEED WIND TUNNELS

Data acquisition and processing software for the Low Speed Wind Tunnel tests of the Jindivik auxiliary air intake
[AD-A285455] p 108 N95-17178
Low speed propeller slipstream aerodynamic effects p 116 N95-17882
Background noise levels measured in the NASA Lewis 9- by 15-foot low-speed wind tunnel
[NASA-TM-106817] p 145 N95-18054
Wall correction method with measured boundary conditions for low speed wind tunnels p 164 N95-19263
Calculation of low speed wind tunnel wall interference from static pressure pipe measurements p 164 N95-19273

LUBRICANTS

A stationary flow of a viscous liquid in radial clearances of rotor bearings in the turbocompressor of an internal combustion engine
[BTN-94-EIX94461408765] p 153 A95-63648

LUGS

Evaluation of alternate F-14 wing lug coating
[AD-A283207] p 129 N95-17631

LUMINESCENCE

Optical surface pressure measurements: Accuracy and application field evaluation p 175 N95-19274

M

MACH NUMBER

Unsteady flow phenomena in discrete passage diffusers for centrifugal compressors
[AD-A281412] p 155 N95-16163
Scramjet testing guidelines p 138 N95-16317
Error propagation equations for estimating the uncertainty in high-speed wind tunnel test results
[DE94-014136] p 145 N95-16509
Mach number, flow angle, and loss measurements downstream of a transonic fan-blade cascade
[AD-A280907] p 108 N95-16824
Comparison of computational and experimental results for a supercritical airfoil
[NASA-TM-4601] p 108 N95-16908
2-D aileron effectiveness study p 110 N95-17851
Investigation of an NLF(1)-0416 airfoil in compressible subsonic flow p 110 N95-17852
OAT15A airfoil data p 111 N95-17857
Measurements of the flow over a low aspect-ratio wing in the Mach number range 0.6 to 0.87 for the purpose of validation of computational methods. Part 1: Wing design, model construction, surface flow. Part 2: Mean flow in the boundary layer and wake, 4 test cases p 112 N95-17860

Pressure distributions on research wing W4 mounted on an axisymmetric body p 112 N95-17862
DLR-F4 wing body configuration p 130 N95-17863
Low aspect ratio wing experiment p 113 N95-17865

MACHINE TOOLS

Measurement of gust response on a turbine cascade
[NASA-TM-106776] p 117 N95-18457

MAGNETIC DISKS

A selection of experimental test cases for the validation of CFD codes. Supplement: Datasets A-E
[AGARD-AR-303-SUPPL] p 117 N95-18539

MAINTAINABILITY

KC-135 cockpit modernization study. Phase 1: Equipment evaluation
[AD-A284099] p 131 N95-18398

MAINTENANCE

The assessment of the AH-64D, longbow, mast-mounted assembly noise hazard for maintenance personnel
[AD-A284971] p 171 N95-16226
Identification of Artificial Intelligence (AI) applications for maintenance, monitoring, and control of airway facilities
[AD-A282479] p 125 N95-17373
E-6A hardness assurance, maintenance and surveillance program
[AD-A283994] p 134 N95-19067

MAN MACHINE SYSTEMS

Industry review of a crew-centered cockpit design process and toolset
[AD-A282966] p 130 N95-17661

MANAGEMENT METHODS

Technology Benefit Estimator (T/BEST): User's manual
[NASA-TM-106785] p 167 N95-19501

MANAGEMENT SYSTEMS

An engineering code to analyze hypersonic thermal management systems p 155 N95-16322
Packet utilisation definitions for the ESA XMM mission p 150 N95-17596

On-line handling of air traffic: Management, guidance and control
[AGARD-AG-321] p 126 N95-18927

MANNED SPACE FLIGHT

Virtual environment application with partial gravity simulation p 169 N95-15988

MANUFACTURING

European aeronautics: Strong government presence in industry structure and research and development support. Report to Congressional Requesters
[GAO/NSIAD-94-71] p 176 N95-18578

MARINE PROPULSION

Simulation investigation on system identification of gas turbine
[PB95-104238] p 139 N95-17749

MARKET RESEARCH

Quality optimization of thermally sprayed coatings produced by the JP-5000 (HVOF) gun using mathematical modeling p 152 N95-19008

MARS SURFACE

Virtual environment application with partial gravity simulation p 169 N95-15988

MASS FLOW

Simulation of multidisciplinary problems for the thermostress state of cooled high temperature turbines p 140 N95-19021

MASSIVELY PARALLEL PROCESSORS

Portable parallel stochastic optimization for the design of aeropropulsion components
[NASA-CR-185312] p 154 N95-16072

MATERIALS TESTS

Regenerative cooling for liquid propellant rocket thrust chambers
[INPE-5565-TDI/540] p 150 N95-18720

MATHEMATICAL MODELS

Mathematical modelling concerning the development of a system of similar installations, taking into account their operational intensity (an aircraft-helicopter fleet taken as an example)
[BTN-94-EIX94461408763] p 103 A95-63646
On the dynamics of aeroelastic oscillators with one degree of freedom
[BTN-94-EIX94501431527] p 153 A95-64524
Nonsmooth trajectory optimization: An approach using continuous simulated annealing
[BTN-94-EIX94511433914] p 168 A95-64580
H(sup 2)/H(sup INF) controller design for a two-dimensional thin airfoil flutter suppression
[BTN-94-EIX94511433918] p 141 A95-64584
Test bench for rotorcraft hover control
[BTN-94-EIX94511433919] p 169 A95-64585
Aircraft model for the AIAA controls design challenge
[BTN-94-EIX94511433921] p 142 A95-64587

Joint Proceedings on Aeronautics and Astronautics (JPAA)

[ISBN-7-80-046602-7] p 104 N95-16249
An investigation of polynomial calibrations methods for wind tunnel balances p 144 N95-16258

Evaluation of the dynamic stability characteristics of the NAL Light Transport Aircraft
[NAL-PD-CA-9217] p 142 N95-16392

Numerical simulation of helicopter engine plume in forward flight
[NASA-CR-197488] p 107 N95-16589

Algorithms for bilevel optimization
[NASA-CR-194980] p 170 N95-16897

Evaluation of an autopilot based multimodelling
[PB94-190725] p 142 N95-17454

Demonstration of the Dynamic Flowgraph Methodology using the Titan 2 Space Launch Vehicle Digital Flight Control System
[NASA-CR-197517] p 150 N95-17493

Numerical mixing calculations of confined reacting jet flows in a cylindrical duct
[NASA-TM-106736] p 139 N95-18133

Compression strength of composite primary structural components
[NASA-CR-197554] p 160 N95-18388

Aeromechanics technology, volume 1. Task 1. Three-dimensional Euler/Navier-Stokes Aerodynamic Method (TEAM) enhancements
[AD-A285713] p 132 N95-18483

Minimal time detection algorithms and applications to flight systems
[TR-2-FSRC-93] p 171 N95-18564

The impact of non-linear flight control systems on the prediction of aircraft loads due to turbulence p 143 N95-18598

Regenerative cooling for liquid propellant rocket thrust chambers
[INPE-5565-TDI/540] p 150 N95-18720

A linear system identification and validation of an AH-64 Apache aeroelastic simulation model p 146 N95-18903

Mathematical Models of Gas Turbine Engines and their Components
[AGARD-LS-198] p 139 N95-19017

The mathematical models of flow passage for gas turbine engines and their components p 140 N95-19020

Simulation of multidisciplinary problems for the thermostress state of cooled high temperature turbines p 140 N95-19021

Application of multicomponent models to flow passage simulation in multistage turbomachines and whole gas turbine engines p 140 N95-19022

Application of multidisciplinary models to the cooled turbine rotor design p 140 N95-19024

Unsteady aerodynamic analyses for turbomachinery aeroelastic predictions p 141 N95-19381

Forced response of mistuned bladed disks p 141 N95-19383

Prediction of fatigue crack growth under flight-simulation loading with the modified CORPUS model p 166 N95-19471

Discrete crack growth analysis methodology for through cracks in pressurized fuselage structures p 166 N95-19473

MATRICES (MATHEMATICS)

Direct splitting of coefficient matrix for numerical calculation of transonic nozzle flow
[BTN-94-EIX94481415356] p 103 A95-65346

Plant and controller optimization by convex methods
[AD-A283700] p 133 N95-18621

MAXIMUM LIKELIHOOD ESTIMATES

Minimal time detection algorithms and applications to flight systems
[TR-2-FSRC-93] p 171 N95-18564

MCDONNELL DOUGLAS AIRCRAFT

Fiber-optic technology for transport aircraft
[BTN-94-EIX94511309384] p 103 A95-64610

MEASURING INSTRUMENTS

Hypersonic flight testing
[AD-A283981] p 134 N95-18891

MECHANICAL ENGINEERING

Strategic avionics technology definition studies. Subtask 3-1A3: Electrical Actuation (ELA) Systems Test Facility
[NASA-CR-188260] p 143 N95-18567

MECHANICAL OSCILLATORS

On the dynamics of aeroelastic oscillators with one degree of freedom
[BTN-94-EIX94501431527] p 153 A95-64524

MECHANICAL PROPERTIES

Engineering methods for the evaluation of transonic flutter characteristics for aerodynamic control surfaces
[BTN-94-EIX94461408589] p 141 A95-63064

Course module for AA201: Wing structural design project
[AD-A283618] p 133 N95-18616

MEDICAL SERVICES

MEDICAL SERVICES

A surgical support system for Space Station Freedom
p 149 N95-16776

MEMORY (COMPUTERS)

Rapid solution of large-scale systems of equations
p 169 N95-16458

METAL BONDING

Application of superplastically formed and diffusion bonded structures in high intensity noise environments
p 174 N95-19162

METAL FATIGUE

Evaluation of the fuselage lap joint fatigue and terminating action repair p 166 N95-19477
The application of Newman crack-closure model to predicting fatigue crack growth p 167 N95-19483

METAL SHEETS

Prediction of R-curves from small coupon tests
p 167 N95-19496

METAL WORKING

Development of processes, means, and theoretical principles of thin-walled detail plastic forming at Kazan Aviation Institute p 155 N95-16281

METALS

Bicarbonate of soda blasting technology for aircraft wheel depainting
[PB94-19323] p 104 N95-17466

METEOROLOGICAL SATELLITES

Field and data analysis studies related to the atmospheric environment
[NASA-CR-196543] p 168 N95-18093

METHANE

Airborne rotary separator study
[NASA-CR-191045] p 150 N95-18743

MICROBURSTS (METEOROLOGY)

Microburst vertical wind estimation from horizontal wind measurements
[NASA-TP-3460] p 131 N95-18198

MICROCRACKS

Fatigue life until small cracks in aircraft structures: Durability and damage tolerance p 135 N95-19478

MICROGRAVITY

Virtual environment application with partial gravity simulation p 169 N95-15988
A surgical support system for Space Station Freedom p 149 N95-16776

Microgravity isolation system design: A case study
[NASA-TM-106804] p 104 N95-17657

Microgravity isolation system design: A modern control synthesis framework
[NASA-TM-106805] p 105 N95-18197

Microgravity isolation system design: A modern control analysis framework
[NASA-TM-106803] p 105 N95-18486

Users guide for NASA Lewis Research Center DC-9 Reduced-Gravity Aircraft Program
[NASA-TM-106755] p 146 N95-18586

MICROPHONES

Background noise levels measured in the NASA Lewis 9- by 15-foot low-speed wind tunnel
[NASA-TM-106817] p 145 N95-18054

MICROWAVE LANDING SYSTEMS

Heliport/vertiport MLS precision approaches
[AD-A283505] p 126 N95-18059

MILITARY AIRCRAFT

The effects of aircraft (B-52) overflights on ancient structures
[BTN-94-EIX94341340070] p 171 A95-63522
Military aviation maintenance industry in Western Europe: Concentration and internationalization
[PB94-189180] p 104 N95-17451

MILITARY AVIATION

Low rate initial production in Army Aviation systems development
[AD-A281871] p 127 N95-16356

MILLING (MACHINING)

Modelling for optimal operations of line milling of aerodynamic surfaces
[BTN-94-EIX94461408774] p 138 A95-63657

MISSILE BODIES

Supersonic vortex flow around a missile body
p 114 N95-17870

MISSILE CONFIGURATIONS

Experimental study at low supersonic speeds of a missile concept having opposing wraparound tails
[NASA-TM-4582] p 106 N95-16069
Evaluation of an autopilot based multimodelling
[PB94-190725] p 142 N95-17454

A selection of experimental test cases for the validation of CFD codes, volume 2
[AGARD-AR-303-VOL-2] p 109 N95-17846

A selection of experimental test cases for the validation of CFD codes. Supplement: Datasets A-E
[AGARD-AR-303-SUPPL] p 117 N95-18539

MISSILE CONTROL

Experimental study at low supersonic speeds of a missile concept having opposing wraparound tails
[NASA-TM-4582] p 106 N95-16069

Evaluation of an autopilot based multimodelling
[PB94-190725] p 142 N95-17454
Integrated aerodynamic fin and stowable TVC vane system
[AD-D016457] p 151 N95-19073

MISSILES

Evaluation of an autopilot based multimodelling
[PB94-190725] p 142 N95-17454
Solid fuel ramjet composition
[AD-D016458] p 152 N95-19090

MISSION PLANNING

EURECA mission control experience and messages for the future p 149 N95-17252
Fatigue loads spectra derivation for the Space Shuttle: Second cycle p 166 N95-19470

MIXING LAYERS (FLUIDS)

Numerical mixing calculations of confined reacting jet flows in a cylindrical duct p 139 N95-18133
Studies on high pressure and unsteady flame phenomena
[AD-A284126] p 152 N95-18410

MOLECULAR BEAMS

Flow field investigation in a free jet - free jet core system for the generation of high intensity molecular beams
[DLR-FB-94-11] p 172 N95-18912

MULTIDISCIPLINARY DESIGN OPTIMIZATION

NASA High Performance Computing and Communications program
[NASA-TM-4653] p 176 N95-18573

MULTIGRID METHODS

Solution of full potential equation on an airfoil by multigrid technique
[NAL-TM-CSS-9303] p 119 N95-18904
CFD: Advances and Applications, part 1
[NAL-SP-9322-PT-1] p 165 N95-19444

MULTIPLEXING

Fiber Optic Control System integration for advanced aircraft. Electro-optic and sensor fabrication, integration, and environmental testing for flight control systems: Laboratory test results
[NASA-CR-195408] p 161 N95-18938

MULTIPROCESSING (COMPUTERS)

Portable parallel stochastic optimization for the design of aeropropulsion components
[NASA-CR-195312] p 154 N95-16072

N

NACELLES

Ducted fan acoustic radiation including the effects of nonuniform mean flow and acoustic treatment
[NASA-CR-197449] p 172 N95-16401
Pressure distribution measurements on an isolated TPS 441 nacelle p 115 N95-17878
Low speed propeller slipstream aerodynamic effects p 116 N95-17882
Impact of noise environment on engine nacelle design p 173 N95-19147

NASA PROGRAMS

Assessment of the Space Station program
p 149 N95-16352

ICASE

[NASA-CR-195001] p 170 N95-16898
NASA High Performance Computing and Communications program
[NASA-TM-4653] p 176 N95-18573

NATIONAL AIRSPACE SYSTEM

Identification of Artificial Intelligence (AI) applications for maintenance, monitoring, and control of airway facilities
[AD-A282479] p 125 N95-17373
Operational And Supportability Implementation System (OASIS) test and evaluation master plan
[AD-A284765] p 126 N95-18088

NAVIER-STOKES EQUATION

Comparison of computational and experimental results for a supercritical airfoil
[NASA-TM-4601] p 108 N95-16908
Three dimensional compressible turbulent flow computations for a diffusing S-duct with/without vortex generators
[NASA-CR-195390] p 138 N95-17402
Static aerodynamics CFD analysis for 120-mm hypersonic KE projectile design
[ARL-MR-184] p 118 N95-18611
Numerical computations of supersonic base flow with special emphasis on turbulence modeling
[AD-A283688] p 119 N95-18670
Theoretical investigations of shock/boundary layer interactions on a Ma(infinity) = 8 waverider
[DLR-FB-94-12] p 119 N95-18910

Solution of Navier-Stokes equations using high accuracy monotone schemes p 161 N95-19019
Simulation of steady and unsteady viscous flows in turbomachinery p 140 N95-19023
Numerical simulation of dynamic-stall suppression by tangential blowing p 120 N95-19110
[AD-A284887]
Unsteady aerodynamic analyses for turbomachinery aeroelastic predictions p 141 N95-19381
Parabolized Navier-Stokes solution of supersonic/hypersonic flows p 123 N95-19464

NAVIGATION AIDS

Conversion of Earth-centered Earth-fixed coordinates to geodetic coordinates
[BTN-94-EIX94441380862] p 125 A95-64294

NEAR FIELDS

Correction of support influences on measurements with sting mounted wind tunnel models p 122 N95-19281

NEURAL NETS

An artificial neural network system for diagnosing gas turbine engine fuel faults
[DE94-013960] p 138 N95-17371
The accuracy of parameter estimation in system identification of noisy aircraft load measurement
[NASA-CR-197516] p 134 N95-19130

NEWTON-RAPHSON METHOD

Demonstration of the Dynamic Flowgraph Methodology using the Titan 2 Space Launch Vehicle Digital Flight Control System
[NASA-CR-197517] p 150 N95-17493

NICKEL ALLOYS

Fatigue in single crystal nickel superalloys
[AD-A285727] p 152 N95-18068

NIGHT VISION

A platform independent application of Lux illumination prediction algorithms
[AD-A283669] p 170 N95-18018

NITROGEN OXIDES

Numerical mixing calculations of confined reacting jet flows in a cylindrical duct p 139 N95-18133
[NASA-TM-106736]
Wave cycle design for wave rotor engines with limited nitrogen oxide emissions p 161 N95-18901

NOISE

The accuracy of parameter estimation in system identification of noisy aircraft load measurement
[NASA-CR-197516] p 134 N95-19130

NOISE (SOUND)

The assessment of the AH-64D, longbow, mast-mounted assembly noise hazard for maintenance personnel
[AD-A284971] p 171 N95-16226

NOISE GENERATORS

Ducted fan acoustic radiation including the effects of nonuniform mean flow and acoustic treatment
[NASA-CR-197449] p 172 N95-16401

NOISE INTENSITY

The assessment of the AH-64D, longbow, mast-mounted assembly noise hazard for maintenance personnel
[AD-A284971] p 171 N95-16226
An overall approach of cockpit noise verification in a military aircraft p 175 N95-19163

NOISE MEASUREMENT

Background noise levels measured in the NASA Lewis 9- by 15-foot low-speed wind tunnel
[NASA-TM-106817] p 145 N95-18054

NOISE PREDICTION

On the Lighthill relationship and sound generation from isotropic turbulence
[NASA-CR-195005] p 159 N95-18191
NOISE PREDICTION (AIRCRAFT)
Modelling structurally damaging twin-jet screech p 135 N95-19154

NOISE PROPAGATION

Noise transmission and reduction in turboprop aircraft
p 175 N95-19164

NOISE REDUCTION

Background noise levels measured in the NASA Lewis 9- by 15-foot low-speed wind tunnel
[NASA-TM-106817] p 145 N95-18054
Helicopter internal noise p 173 N95-19144
Impact of noise environment on engine nacelle design p 173 N95-19147

An overall approach of cockpit noise verification in a military aircraft p 175 N95-19163
Noise transmission and reduction in turboprop aircraft p 175 N95-19164

NONEQUILIBRIUM FLOW

High altitude hypersonic flowfield radiation
[AD-A281386] p 106 N95-16160

NONINTRUSIVE MEASUREMENT

Wall Interference, Support Interference and Flow Field Measurements
[AGARD-CP-535] p 162 N95-19251
The crucial role of wall interference, support interference and flow field measurements in the development of advanced aircraft configurations p 162 N95-19252

NONLINEAR EQUATIONS

Rapid solution of large-scale systems of equations
p 169 N95-16458

NONLINEAR SYSTEMS

Design of nonlinear control laws for high-angle-of-attack flight
[BTN-94-EIX94511433920] p 141 A95-64586

Aircraft model for the AIAA controls design challenge
[BTN-94-EIX94511433921] p 142 A95-64587

2-D aileron effectiveness study p 110 N95-17851
The impact of non-linear flight control systems on the prediction of aircraft loads due to turbulence
p 143 N95-18598

Treatment of non-linear systems by timeplane-transformed CT methods: The spectral gust method p 143 N95-18600

Nonlinear dynamic response of aircraft structures to acoustic excitation p 135 N95-19151

NONLINEARITY

Algorithms for bilevel optimization
[NASA-CR-194980] p 170 N95-16897

Comparison of stochastic and deterministic nonlinear gust analysis methods to meet continuous turbulence criteria p 133 N95-18602

Unsteady aerodynamic analyses for turbomachinery aeroelastic predictions p 141 N95-19381

Nonlinear analysis of damaged stiffened fuselage shells subjected to combined loads p 137 N95-19499

NONUNIFORM FLOW

Ducted fan acoustic radiation including the effects of nonuniform mean flow and acoustic treatment
[NASA-CR-197449] p 172 N95-16401

NOZZLE DESIGN

A model for preliminary facility design including simulation issues p 144 N95-16318

NOZZLE EFFICIENCY

Combustor kinetic energy efficiency analysis of the hypersonic research engine data p 148 N95-16321

NOZZLE FLOW

Direct splitting of coefficient matrix for numerical calculation of transonic nozzle flow
[BTN-94-EIX94481415356] p 103 A95-65346

Flow field investigation in a free jet - free jet core system for the generation of high intensity molecular beams
[DLR-FB-94-11] p 172 N95-18912

NUCLEAR POWER REACTORS

Ageing nuclear power plant management: An aeronautical viewpoint
[NAL-PD-SN-9306] p 105 N95-18606

NUMERICAL ANALYSIS

On the dynamics of aeroelastic oscillators with one degree of freedom
[BTN-94-EIX94501431527] p 153 A95-64524

Optimum Design Methods for Aerodynamics
[AGARD-R-803] p 127 N95-16562

Optimal shape design for aerodynamics
p 128 N95-16568

Review of the EUROPT Project AERO-0026
p 129 N95-16573

NUMERICAL CONTROL

Test bench for rotorcraft hover control
[BTN-94-EIX94511433919] p 169 A95-64585

OASES

Operational And Supportability Implementation System (OASIS) test and evaluation master plan
[AD-A284765] p 126 N95-18088

OBJECT-ORIENTED PROGRAMMING

Safety aspects of spacecraft commanding
p 149 N95-17248

OBLIQUE SHOCK WAVES

Direct splitting of coefficient matrix for numerical calculation of transonic nozzle flow
[BTN-94-EIX94481415356] p 103 A95-65346

OCEANOGRAPHY

Field and data analysis studies related to the atmospheric environment
[NASA-CR-196543] p 168 N95-18093

OILS

Bicarbonate of soda blasting technology for aircraft wheel depainting
[PB94-193323] p 104 N95-17466

ON-LINE SYSTEMS

Sensor fault detection and diagnosis simulation of a helicopter engine in an intelligent control framework
[NASA-TM-106784] p 137 N95-15970

On-line handling of air traffic: Management, guidance and control
[AGARD-AG-321] p 126 N95-18927

ONBOARD DATA PROCESSING

Packet utilisation definitions for the ESA XMM mission
p 150 N95-17596

ONE DIMENSIONAL FLOW

One-dimensional flow description for the combustion chamber of a scramjet
[DLR-FB-94-06] p 139 N95-18911

OPERATING SYSTEMS (COMPUTERS)

The generic simulation executive at Manned Flight Simulator
[AD-A283997] p 146 N95-18724

OPTICAL MEASUREMENT

Optical surface pressure measurements: Accuracy and application field evaluation p 175 N95-19274

OPTICAL MEASURING INSTRUMENTS

Fiber Optic Control System integration for advanced aircraft. Electro-optic and sensor fabrication, integration, and environmental testing for flight control systems
[NASA-CR-191194] p 162 N95-19236

OPTIMAL CONTROL

Selection of optimal parameters for a system, controlling the flight height, when information about the state vector is incomplete
[BTN-94-EIX94461408753] p 168 A95-63636

Modelling for optimal operations of line milling of aerodynamic surfaces
[BTN-94-EIX94461408774] p 138 A95-63657

Nonsmooth trajectory optimization: An approach using continuous simulated annealing
[BTN-94-EIX94511433914] p 168 A95-64580

Time-optimal turn to a heading: An analytic solution
[BTN-94-EIX94511433940] p 142 A95-64606

Microgravity isolation system design: A case study
[NASA-TM-106804] p 104 N95-17657

A feedforward control approach to the local navigation problem for autonomous vehicles
[AD-A282787] p 126 N95-17706

Microgravity isolation system design: A modern control synthesis framework
[NASA-TM-106805] p 105 N95-18197

OPTIMIZATION

Intelligent control law tuning for AIAA controls design challenge
[BTN-94-EIX94511433922] p 169 A95-64588

Portable parallel stochastic optimization for the design of aeropropulsion components
[NASA-CR-195312] p 154 N95-16072

Optimum Design Methods for Aerodynamics
[AGARD-R-803] p 127 N95-16562

Optimum aerodynamic design via boundary control
p 127 N95-16565

Optimal shape design for aerodynamics
p 128 N95-16568

Airfoil optimization by the one-shot method
p 128 N95-16569

Tools for applied engineering optimization
p 128 N95-16570

The global aircraft shape p 128 N95-16571
Aerodynamic shape optimization p 128 N95-16572

Review of the EUROPT Project AERO-0026
p 129 N95-16573

ORBITAL MANEUVERS

Numerical optimization of synergetic maneuvers
[AD-A283398] p 109 N95-17435

OSCILLATING FLOW

A computational investigation of wake-induced airfoil flutter in incompressible flow and active flutter control
[AD-A281534] p 142 N95-16109

OSCILLATION DAMPERS

Tuned mass damper for integrally bladed turbine rotor
[NASA-CASE-MFS-28697-1] p 159 N95-18325

OSCILLATIONS

On the dynamics of aeroelastic oscillators with one degree of freedom
[BTN-94-EIX94501431527] p 153 A95-64524

Overview of unsteady transonic wind tunnel test on a semispan straked delta wing oscillating in pitch
[AD-A284097] p 117 N95-18380

Development of a multicomponent force and moment balance for water tunnel applications, volume 2
[NASA-CR-4642-VOL-2] p 161 N95-18956

P**PACKETS (COMMUNICATION)**

Packet utilisation definitions for the ESA XMM mission
p 150 N95-17596

PAINTS

Bicarbonate of soda blasting technology for aircraft wheel depainting
[PB94-193323] p 104 N95-17466

PANEL METHOD (FLUID DYNAMICS)

A computational investigation of wake-induced airfoil flutter in incompressible flow and active flutter control
[AD-A281534] p 142 N95-16109

Course module for AA201: Wing structural design project
[AD-A283618] p 133 N95-18616

Calculation of support interference in dynamic wind-tunnel tests p 122 N95-19282

CFD: Advances and Applications, part 1
[NAL-SP-9322-PT-1] p 165 N95-19444

Panel methods p 165 N95-19448

PANELS

Thermo-acoustic fatigue design for hypersonic vehicle skin panels p 162 N95-19161

PARABOLIC FLIGHT

A surgical support system for Space Station Freedom
p 149 N95-16776

Users guide for NASA Lewis Research Center DC-9 Reduced-Gravity Aircraft Program
[NASA-TM-106755] p 146 N95-18586

PARACHUTES

Parachute inflation: A problem in aeroelasticity
[AD-A284375] p 117 N95-18340

PARALLEL PROCESSING (COMPUTERS)

Portable parallel stochastic optimization for the design of aeropropulsion components
[NASA-CR-195312] p 154 N95-16072

Rapid solution of large-scale systems of equations
p 169 N95-16458

PARALLEL PROGRAMMING

Portable parallel stochastic optimization for the design of aeropropulsion components
[NASA-CR-195312] p 154 N95-16072

NASA High Performance Computing and Communications program
[NASA-TM-4653] p 176 N95-18573

PARAMETER IDENTIFICATION

Minimal time detection algorithms and applications to flight systems
[TR-2-FSRC-93] p 171 N95-18564

PAYLOADS

Virtual environment application with partial gravity simulation
p 169 N95-15988

Parachute inflation: A problem in aeroelasticity
[AD-A284375] p 117 N95-18340

PENDULUMS

On the dynamics of aeroelastic oscillators with one degree of freedom
[BTN-94-EIX94501431527] p 153 A95-64524

PENETRATION

Development of an Automated Airfield Dynamic Cone Penetrometer (AADCP) prototype and the evaluation of unsurfaced airfield seismic surveying using Spectral Analysis of Surface Waves (SASW) technology
[AD-A281985] p 145 N95-17444

PENETROMETERS

Development of an Automated Airfield Dynamic Cone Penetrometer (AADCP) prototype and the evaluation of unsurfaced airfield seismic surveying using Spectral Analysis of Surface Waves (SASW) technology
[AD-A281985] p 145 N95-17444

PERFORMANCE PREDICTION

Aerodynamic design and calculation of flow around the plane cascade of turbine
[BTN-94-EIX94481415357] p 104 A95-65347

The computer analysis of the prediction of aircraft electrical power supply system reliability
p 155 N95-16278

Six degree of freedom flight dynamic and performance simulation of a remotely-piloted vehicle
[AERO-TN-9301] p 131 N95-18097

PERFORMANCE TESTS

Solid state radar demonstration test results at the FAA Technical Center
[AD-A281520] p 154 N95-16097

ADST system test report for the rotary wing aircraft airnet aeromodel and weapon model merge with the ATAC 2 baseline
[AD-A281580] p 127 N95-16171

Wind tunnel performance comparative test results of a circular cylinder and 50 percent ellipse tailboom for circulation control antitorque applications
[AD-A283335] p 130 N95-18008

Conference on Aerospace Transparent Materials and Enclosures. Volume 2: Sessions 5-9
[AD-A283926] p 131 N95-18162

Helicopter Performance Evaluation (HELPE) computer model
[AD-A284319] p 131 N95-18381

PERIODIC VARIATIONS

Compression strength of composite primary structural components
[NASA-CR-197554] p 160 N95-18388

PERSONNEL MANAGEMENT

Development of strength analysis methods and design model for aircraft constructions in Kazan Aviation Institute p 127 N95-16264

PERTURBATION

Airfoil optimization by the one-shot method p 128 N95-16569

Comparison of frequency response and perturbation methods to extract linear models from a nonlinear simulation [AD-A284115] p 146 N95-18405

PHOTOCHROMISM

Conference on Aerospace Transparent Materials and Enclosures, volume 1 [AD-A283925] p 133 N95-18677

PHOTOGRAMMETRY

Application of photogrammetry of F-14D store separation [AD-A284154] p 132 N95-18417

PILOT ERROR

Aircraft accident report: Stall and loss of control on final approach, Atlantic Coast Airlines, Inc./United Express Flight 6291 Jetstream 4101, N304UE Columbus, OH, 7 January 1994 [PB94-910409] p 123 N95-17646

PILOT INDUCED OSCILLATION

Aircraft and sub-system certification by piloted simulation [AGARD-AR-278] p 145 N95-17388

PILOT PERFORMANCE

Aircraft and sub-system certification by piloted simulation [AGARD-AR-278] p 145 N95-17388

PILOT TRAINING

Helicopter in-flight simulation development and use in test pilot training [AD-A283998] p 146 N95-18725

PILOTLESS AIRCRAFT

Spread spectrum applications in unmanned aerial vehicles [AD-A281035] p 156 N95-16448
Unmanned aerial vehicle heavy fuel engine test [AD-A284332] p 139 N95-18383

PILOTS (PERSONNEL)

An analysis of tower (local) controller-pilot voice communications [AD-A283718] p 160 N95-18436

PITCH (INCLINATION)

Numerical simulation of transient vortex breakdown above a pitching delta wing [AD-A281075] p 107 N95-16808
Development of a multicomponent force and moment balance for water tunnel applications, volume 2 [NASA-CR-4642-VOL-2] p 161 N95-18956

PITCHING MOMENTS

Measurements on a two-dimensional aerofoil with high-lift devices p 109 N95-17848
Static aerodynamics CFD analysis for 120-mm hypersonic KE projectile design [ARL-MR-184] p 118 N95-18611
Development of a multicomponent force and moment balance for water tunnel applications, volume 1 [NASA-CR-4642-VOL-1] p 161 N95-18955

PITOT TUBES

Hypersonic flow-field measurements: Intrusive and nonintrusive [AD-A283867] p 119 N95-18674

PITTING

Detecting gear tooth fracture in a high contact ratio face gear mesh [NASA-TM-106822] p 162 N95-19125

PLASTIC DEFORMATION

Development of processes, means, and theoretical principles of thin-walled detail plastic forming at Kazan Aviation Institute p 155 N95-16281
Prediction of fatigue crack growth under flight-simulation loading with the modified CORPUS model p 166 N95-19471

PLATE THEORY

Discrete crack growth analysis methodology for through cracks in pressurized fuselage structures p 166 N95-19473

PLENUM CHAMBERS

Unsteady flow testing in a passive low-correction wind tunnel p 147 N95-19272

PLUMES

Numerical simulation of helicopter engine plume in forward flight [NASA-CR-197488] p 107 N95-16589
Impact of dynamic loads on propulsion integration p 174 N95-19148
Estimating wind tunnel interference due to vectored jet flows p 164 N95-19265

PNEUMATICS

Development of pneumatic test techniques for subsonic high-lift and in-ground-effect wind tunnel investigations p 121 N95-19268

POLYBUTADIENE

Solid fuel ramjet composition [AD-D016458] p 152 N95-19090

POLYNOMIALS

An investigation of polynomial calibrations methods for wind tunnel balances p 144 N95-16258

POLYURETHANE RESINS

Evaluation of alternate F-14 wing lug coating [AD-A283207] p 129 N95-17631

POROUS MATERIALS

Service and physical properties of liquid-jet fuels p 151 N95-16256

POROUS PLATES

The stability of two-phase flow over a swept-wing [NASA-CR-194994] p 159 N95-18190

POROUS WALLS

Determination of solid/porous wall boundary conditions from wind tunnel data for computational fluid dynamics codes p 164 N95-19266

Calculation of wall effects of flow on a perforated wall with a code of surface singularities p 165 N95-19277

POTENTIAL FLOW

Single-pass method for the solution of inverse potential and rotational problems. Part 1: 2-D and quasi 3-D theory and application p 107 N95-16563

Solution of full potential equation on an airfoil by multigrid technique [NAL-TM-CSS-9303] p 119 N95-18904

CFD: Advances and Applications, part 1 [NAL-SP-9322-PT-1] p 165 N95-19444

Computation of inviscid flows: Full potential method p 165 N95-19447

Viscous flow past aerofoils axisymmetric bodies and wings p 123 N95-19457

POTENTIAL THEORY

Single-pass method for the solution of inverse potential and rotational problems. Part 2: Fully 3-D potential theory and applications p 107 N95-16564

POWER CONDITIONING

Strategic avionics technology definition studies. Subtask 3-1A3: Electrical Actuation (ELA) Systems Test Facility [NASA-CR-188360] p 143 N95-18567

POWERED LIFT AIRCRAFT

STOVL CFD model test case p 115 N95-17881

PRECISION

Development of processes, means, and theoretical principles of thin-walled detail plastic forming at Kazan Aviation Institute p 155 N95-16281

PREDICTION ANALYSIS TECHNIQUES

The computer analysis of the prediction of aircraft electrical power supply system reliability p 155 N95-16278
Forced response of mistuned bladed disks p 141 N95-19383

PREMIXED FLAMES

Studies on high pressure and unsteady flame phenomena [AD-A284126] p 152 N95-18410

PRESSURE

Investigation of the influence of pylons and stores on the wing lower surface flow p 116 N95-17885

PRESSURE DISTRIBUTION

An improved method of airfoil design p 106 N95-16252

Wall-signature methods for high speed wind tunnel wall interference corrections p 107 N95-16257
Measurements of unsteady pressure and structural response for an elastic supercritical wing [NASA-TP-3443] p 104 N95-16560

Residual-correction type and related computational methods for aerodynamic design. Part 1: Airfoil and wing design p 128 N95-16566

Aerodynamic shape optimization p 128 N95-16572
Review of the EUROPT Project AERO-0026 p 129 N95-16573

2-D airfoil tests including side wall boundary layer measurements p 158 N95-17847
Measurements on a two-dimensional aerofoil with high-lift devices p 109 N95-17848

2-D airfoil effectiveness study p 110 N95-17851
Two-dimensional 16.5 percent thick supercritical airfoil NLR 7301 p 110 N95-17854

Low-speed surface pressure and boundary layer measurement data for the NLR 7301 airfoil section with trailing edge flap p 111 N95-17855
Measurements of the flow over a low aspect-ratio wing in the Mach number range 0.6 to 0.87 for the purpose of validation of computational methods. Part 1: Wing design, model construction, surface flow. Part 2: Mean flow in the boundary layer and wake, 4 test cases p 112 N95-17860

Detailed study at supersonic speeds of the flow around delta wings p 112 N95-17861
Pressure distributions on research wing W4 mounted on an axisymmetric body p 112 N95-17862
DLR-F5: Test wing for CFD and applied aerodynamics p 113 N95-17864

Wind tunnel investigations of the appearance of shocks in the windward region of bodies with circular cross section at angle of attack p 113 N95-17866
Force and pressure data of an ogive-nosed slender body at high angles of attack and different Reynolds numbers p 113 N95-17868

Pressure distribution measurements on an isolated TPS 441 nacelle p 115 N95-17878
Measurement of gust response on a turbine cascade [NASA-TM-106776] p 117 N95-18457
Aeromechanics technology, volume 1. Task 1: Three-dimensional Euler/Navier-Stokes Aerodynamic Method (TEAM) enhancements [AD-A285713] p 132 N95-18483

2-D and 3-D oscillating wing aerodynamics for a range of angles of attack including stall [NASA-TM-4632] p 120 N95-19119
Analysis of test section sidewall effects on a two dimensional airfoil: Experimental and numerical investigations p 165 N95-19276

PRESSURE DRAG

An investigation of the transonic pressure drag coefficient for axis-symmetric bodies [AD-A280990] p 105 N95-15994

PRESSURE GRADIENTS

Airfoil optimization by the one-shot method p 128 N95-16569
Tools for applied engineering optimization p 128 N95-16570

Mach number, flow angle, and loss measurements downstream of a transonic fan-blade cascade [AD-A280907] p 108 N95-16824
Investigation of the flow over a series of 14 percent-thick supercritical aerofoils with significant rear camber p 109 N95-17849

Effect of crossflow on Goertler instability in incompressible boundary layers [NASA-CR-195007] p 159 N95-18193

PRESSURE MEASUREMENT

Data acquisition and processing software for the Low Speed Wind Tunnel tests of the Jindivik auxiliary air intake [AD-A285455] p 108 N95-17178

Measurements on a two-dimensional aerofoil with high-lift devices p 109 N95-17848
Surface pressure and wake drag measurements on the Boeing A4 airfoil in the IAR 1.5X1.5m Wind Tunnel Facility p 110 N95-17850

Pressure distribution measurements on an isolated TPS 441 nacelle p 115 N95-17878
Applications of the five-hole probe technique for flow field surveys at the Institute for Aerospace Research p 163 N95-19255

Calculation of low speed wind tunnel wall interference from static pressure pipe measurements p 164 N95-19273
Optical surface pressure measurements: Accuracy and application field evaluation p 175 N95-19274

PRESSURE RATIO

Error propagation equations for estimating the uncertainty in high-speed wind tunnel test results [DE94-014136] p 145 N95-16509

PRESSURE SENSORS

Single-engine tail interference model p 115 N95-17879
Overview of unsteady transonic wind tunnel test on a semispan straked delta wing oscillating in pitch [AD-A284097] p 117 N95-18380

Applications of the five-hole probe technique for flow field surveys at the Institute for Aerospace Research p 163 N95-19255
Optical surface pressure measurements: Accuracy and application field evaluation p 175 N95-19274

PRESSURE VESSELS

Compression strength of composite primary structural components [NASA-CR-197554] p 160 N95-18388

PROBABILITY THEORY

Aircraft wake vortex takeoff tests at O'Hara International Airport [AD-A283828] p 118 N95-18624

PROBES

Eddy current for detecting second layer cracks under installed fasteners [AD-A282412] p 158 N95-17507

PROBLEM SOLVING

Optimum Design Methods for Aerodynamics [AGARD-R-803] p 127 N95-16562
Review of the EUROPT Project AERO-0026 p 129 N95-16573

PROCUREMENT POLICY
 Low rate initial production in Army Aviation systems development
 [AD-A281871] p 127 N95-16356

PRODUCT DEVELOPMENT
 Eddy current for detecting second layer cracks under installed fasteners
 [AD-A282412] p 158 N95-17507

PRODUCTIVITY
 Modelling for optimal operations of line milling of aerodynamic surfaces
 [BTN-94-EIX94461408774] p 138 A95-63657
 Development of processes, means, and theoretical principles of thin-walled detail plastic forming at Kazan Aviation Institute p 155 N95-16281
 The global aircraft shape p 128 N95-16571

PROGRAMMING ENVIRONMENTS
 Portable parallel stochastic optimization for the design of aeropropulsion components
 [NASA-CR-195312] p 154 N95-16072

PROJECT MANAGEMENT
 Review of the EUROPT Project AERO-0026
 p 129 N95-16573

PROJECTILES
 Static aerodynamics CFD analysis for 120-mm hypersonic KE projectile design
 [ARL-MR-184] p 118 N95-18611

PROLATE SPHEROIDS
 Three-dimensional boundary layer and flow field data of an inclined prolate spheroid p 158 N95-17867

PROP-FAN TECHNOLOGY
 FPCAS2D user's guide, version 1.0
 [NASA-CR-195413] p 156 N95-16588

PROPELLANT TESTS
 Airborne rotary separator study
 [NASA-CR-191045] p 150 N95-18743

PROPELLER FANS
 FPCAS2D user's guide, version 1.0
 [NASA-CR-195413] p 156 N95-16588

PROPELLER NOISE
 Noise transmission and reduction in turboprop aircraft
 p 175 N95-19164

PROPELLER SLIPSTREAMS
 Low speed propeller slipstream aerodynamic effects
 p 116 N95-17882

PROPELLERS
 Gyroscopic and propeller aerodynamic effects on engine mounts dynamic loads in turbulence conditions
 p 132 N95-18599

PROPULSION
 The 1993 JANNAF Propulsion Meeting, volume 1
 [CPIA-PUBL-602-VOL-1] p 148 N95-16312
 Operating capability and current status of the reactivated NASA Lewis Research Center Hypersonic Tunnel Facility
 [NASA-TM-106808] p 148 N95-19286

PROPULSION SYSTEM CONFIGURATIONS
 Small turbojets: Designs and installations
 p 138 N95-16323
 The global aircraft shape p 128 N95-16571
 Technology Benefit Estimator (T/BEST): User's manual
 [NASA-TM-106785] p 167 N95-19501

PROPULSION SYSTEM PERFORMANCE
 Development and application of the double V type flame stabilizer
 [BTN-94-EIX94481415355] p 154 A95-65345
 Aerodynamic design and calculation of flow around the plane cascade of turbine
 [BTN-94-EIX94481415357] p 104 A95-65347
 Joint Proceedings on Aeronautics and Astronautics (JPAA)
 [ISBN-7-80-046602-7] p 104 N95-16249
 Service and physical properties of liquid-jet fuels
 p 151 N95-16256
 Theoretical fundamentals of the aircraft GTE tests
 p 138 N95-16265
 Experimental and analytical methods for the determination of connected-pipe ramjet and ducted rocket internal performance
 [AGARD-AR-323] p 149 N95-17278
 Cooperative control theory and integrated flight and propulsion control
 [NASA-CR-197493] p 142 N95-17404
 Airborne rotary separator study
 [NASA-CR-191045] p 150 N95-18743

PROTECTION
 The assessment of the AH-64D, longbow, mast-mounted assembly noise hazard for maintenance personnel
 [AD-A284971] p 171 N95-16226

PROTECTIVE COATINGS
 Evaluation of alternate F-14 wing lug coating
 [AD-A283207] p 129 N95-17631
 Quality optimization of thermally sprayed coatings produced by the JP-5000 (HVOF) gun using mathematical modeling p 152 N95-19008

PROTOTYPES
 A surgical support system for Space Station Freedom
 p 149 N95-16776
 New technologies for space avionics
 [NASA-CR-197574] p 150 N95-18196

PULSE RADAR
 Solid state radar demonstration test results at the FAA Technical Center
 [AD-A281520] p 154 N95-16097

PYLONS
 Investigation of the influence of pylons and stores on the wing lower surface flow
 p 116 N95-17885

Q

QUADRATIC PROGRAMMING
 Automation of reverse engineering process in aircraft modeling and related optimization problems
 [NASA-CR-197109] p 129 N95-16899

QUALITY CONTROL
 Mesh quality control for multiply-refined tetrahedral grids
 [NASA-CR-197595] p 160 N95-18737

R

RADAR CROSS SECTIONS
 An approach to aerodynamic characteristics of low radar cross-section fuselages p 106 N95-16251

RADAR MEASUREMENT
 Microburst vertical wind estimation from horizontal wind measurements
 [NASA-TP-3460] p 131 N95-18198

RADAR TRANSMITTERS
 Solid state radar demonstration test results at the FAA Technical Center
 [AD-A281520] p 154 N95-16097

RADIATION MEASURING INSTRUMENTS
 A VHF/UHF antenna for the Precision Antenna Measurement System (PAMS)
 [AD-A285673] p 156 N95-16621

RADIATION SPECTRA
 High altitude hypersonic flowfield radiation
 [AD-A281386] p 106 N95-16160

RADIO ALTIMETERS
 Application of GPS/SINS/RA integrated system to aircraft approach landing p 125 N95-16277

RADIO FREQUENCIES
 Hypersonic wind tunnel test techniques
 [AD-A284057] p 118 N95-18663

RAMJET ENGINES
 The 1993 JANNAF Propulsion Meeting, volume 1
 [CPIA-PUBL-602-VOL-1] p 148 N95-16312
 Thermal chemical energy of ablating silica surfaces in air breathing solid rocket engines p 148 N95-16316
 Free-jet testing at Mach 3.44 in GASL's aero/thermo test facility p 145 N95-16320
 Experimental and analytical methods for the determination of connected-pipe ramjet and ducted rocket internal performance
 [AGARD-AR-323] p 149 N95-17278
 Solid fuel ramjet composition
 [AD-D016458] p 152 N95-19090

RAREFIED GAS DYNAMICS
 Ultraviolet emissions occurring about hypersonic vehicles in rarefied flows
 [AD-A281452] p 106 N95-16076

REACTING FLOW
 Numerical mixing calculations of confined reacting jet flows in a cylindrical duct
 [NASA-TM-106736] p 139 N95-18133
 Computation of vortex breakdown
 p 165 N95-19462

REACTOR DESIGN
 Ageing nuclear power plant management: An aeronautical viewpoint
 [NAL-PD-SN-9306] p 105 N95-18606

REACTOR SAFETY
 Ageing nuclear power plant management: An aeronautical viewpoint
 [NAL-PD-SN-9306] p 105 N95-18606

REAL TIME OPERATION
 Sensor fault detection and diagnosis simulation of a helicopter engine in an intelligent control framework
 [NASA-TM-106784] p 137 N95-15970

RECONNAISSANCE AIRCRAFT
 Spread spectrum applications in unmanned aerial vehicles
 [AD-A281035] p 156 N95-16448

RECOVERABLE LAUNCH VEHICLES
 Program test objectives milestone 3 --- Integrated Propulsion Technology Demonstrator
 [NASA-CR-197030] p 127 N95-15971

RECTANGULAR PLATES
 Acoustic radiation damping of flat rectangular plates subjected to subsonic flows p 172 N95-18542

RECTANGULAR WIND TUNNELS
 Corner vortex suppressor
 [AD-D016423] p 116 N95-18337

REFRACTORY MATERIALS
 Static and dynamic friction behavior of candidate high temperature airframe seal materials
 [NASA-TM-106571] p 152 N95-16905

REGENERATIVE COOLING
 Regenerative cooling for liquid propellant rocket thrust chambers
 [INPE-5565-TDI/540] p 150 N95-18720

REGULATIONS
 Application of GPS/SINS/RA integrated system to aircraft approach landing p 125 N95-16277
 Evaluation of the dynamic stability characteristics of the NAL Light Transport Aircraft
 [NAL-PD-CA-9217] p 142 N95-16392
 Federal aviation regulations, part 91. General operating and flight rules. Change 5
 [PB94-194883] p 123 N95-17476
 Safety study: Commuter airline safety
 [PB94-917004] p 124 N95-19132

RELIABILITY
 Problems with aging wiring in Naval aircraft
 p 154 N95-16048
 Optimization of adaptive intraply hybrid fiber composites with reliability considerations
 [NASA-TM-106632] p 157 N95-16911

RELIABILITY ANALYSIS
 Aircraft safety evaluation
 [BTN-94-EIX94511309382] p 103 A95-64608
 The computer analysis of the prediction of aircraft electrical power supply system reliability
 p 155 N95-16278
 Residual life and strength estimates of aircraft structural components with MSD/MED p 136 N95-19485

RELIABILITY ENGINEERING
 The computer analysis of the prediction of aircraft electrical power supply system reliability
 p 155 N95-16278

REMOTELY PILOTED VEHICLES
 Six degree of freedom flight dynamic and performance simulation of a remotely-piloted vehicle
 [AERO-TN-9301] p 131 N95-18097

REMOVAL
 Bicarbonate of soda blasting technology for aircraft wheel depainting
 [PB94-193323] p 104 N95-17466

REPLACING
 Application of photogrammetry of F-14D store separation
 [AD-A284154] p 132 N95-18417

REPORTS
 ICASE
 [NASA-CR-195001] p 170 N95-16898

RESEARCH AIRCRAFT
 VSTOL Systems Research Aircraft (VSRA) Harrier
 [NASA-TM-110117] p 126 N95-18347
 Fiber Optic Control System integration for advanced aircraft. Electro-optic and sensor fabrication, integration, and environmental testing for flight control systems: Laboratory test results
 [NASA-CR-195408] p 161 N95-18938

RESEARCH AND DEVELOPMENT
 ICASE
 [NASA-CR-195001] p 170 N95-16898
 NASA High Performance Computing and Communications program
 [NASA-TM-4653] p 176 N95-18573
 European aeronautics: Strong government presence in industry structure and research and development support. Report to Congressional Requesters
 [GAO/NSIAD-94-71] p 176 N95-18578

RESEARCH FACILITIES
 Development of strength analysis methods and design model for aircraft constructions in Kazan Aviation Institute p 127 N95-16264
 A study of software standards used in the avionics industry p 137 N95-16456
 A VHF/UHF antenna for the Precision Antenna Measurement System (PAMS)
 [AD-A285673] p 156 N95-16621
 ICASE
 [NASA-CR-195001] p 170 N95-16898

RESIDUAL STRENGTH
 Residual life and strength estimates of aircraft structural components with MSD/MED p 136 N95-19485
 Widespread fatigue damage monitoring: Issues and concerns p 136 N95-19488
 Fatigue and residual strength investigation of ARALL(R) -3 and GLARE(R) -2 panels with bonded stringers
 p 137 N95-19495

Prediction of R-curves from small coupon tests p 167 N95-19496

RESONATORS
Anisotropic heat exchangers/stack configurations for thermoacoustic heat engines [AD-A280974] p 168 N95-16506

REVERBERATION CHAMBERS
Design and operation of a thermoacoustic test facility p 147 N95-19150

REVERSE ENGINEERING
Automation of reverse engineering process in aircraft modeling and related optimization problems [NASA-CR-197109] p 129 N95-16899

REVIEWING
Boundary-flow measurement methods for wall interference assessment and correction: Classification and review p 163 N95-19262

REYNOLDS NUMBER
Transonic Navier-Stokes calculations about a 65 deg delta wing [NASA-CR-4635] p 108 N95-17273
2-D airfoil effectiveness study p 110 N95-17851
Two-dimensional 16.5 percent thick supercritical airfoil NLR 7301 p 110 N95-17854
OAT15A airfoil data p 111 N95-17857
Pressure distributions on research wing W4 mounted on an axisymmetric body p 112 N95-17862
Three-dimensional boundary layer and flow field data of an inclined prolate spheroid p 158 N95-17867
Force and pressure data of an ogive-nosed slender body at high angles of attack and different Reynolds numbers p 113 N95-17868
Effect of crossflow on Goertler instability in incompressible boundary layers [NASA-CR-195007] p 159 N95-18193
Hypersonic flow-field measurements: Intrusive and nonintrusive [AD-A283867] p 119 N95-18674
Velocity measurements with hot-wires in a vortex-dominated flowfield p 121 N95-19261
Unsteady flow testing in a passive low-correction wind tunnel p 147 N95-19272

RIPPLES
Preliminary evaluation of the F/A-18 quantity/multiple envelope expansion [AD-A284119] p 132 N95-18407

RIVETED JOINTS
Fatigue life until small cracks in aircraft structures: Durability and damage tolerance p 135 N95-19478
Results of uniaxial and biaxial tests on riveted fuselage lap joint specimens p 136 N95-19491

RIVETS
Evaluation of the fuselage lap joint fatigue and terminating action repair p 166 N95-19477

ROBOTICS
Joint Proceedings on Aeronautics and Astronautics (JPAA) [ISBN-7-80-046602-7] p 104 N95-16249
A feedforward control approach to the local navigation problem for autonomous vehicles [AD-A282787] p 126 N95-17706

ROBUSTNESS (MATHEMATICS)
Tools for applied engineering optimization p 128 N95-16570

ROCKET ENGINE CONTROL
New technologies for space avionics [NASA-CR-197574] p 150 N95-18196

ROCKET ENGINE DESIGN
Program test objectives milestone 3 — Integrated Propulsion Technology Demonstrator [NASA-CR-197030] p 127 N95-15971
Arcjet thruster research and technology, phase 2 [NASA-CR-182276] p 105 N95-18044

ROCKET ENGINES
Integrated aerodynamic fin and stowable TVC vane system [AD-D016457] p 151 N95-19073

ROCKET THRUST
Regenerative cooling for liquid propellant rocket thrust chambers [INPE-5565-TDI/540] p 150 N95-18720

ROLL
Active load control during rolling maneuvers — performed in the Langley Transonic Dynamics Tunnel [NASA-TP-3455] p 129 N95-17397
Development of a multicomponent force and moment balance for water tunnel applications, volume 2 [NASA-CR-4642-VOL-2] p 161 N95-18956

ROLLING MOMENTS
Experimental study at low supersonic speeds of a missile concept having opposing wraparound tails [NASA-TM-4582] p 106 N95-16069
Development of a multicomponent force and moment balance for water tunnel applications, volume 1 [NASA-CR-4642-VOL-1] p 161 N95-18955

ROTARY ENGINES
Unmanned aerial vehicle heavy fuel engine test [AD-A284332] p 139 N95-18383

ROTARY WING AIRCRAFT
ADST system test report for the rotary wing aircraft airmet aeromodel and weapon model merge with the ATAC 2 baseline [AD-A281580] p 127 N95-16171
Experimental data on the aerodynamic interactions between a helicopter rotor and an airframe p 116 N95-17883
Flight parameters monitoring system for tracking structural integrity of rotary-wing aircraft p 135 N95-19469

ROTARY WINGS
Experimental data on the aerodynamic interactions between a helicopter rotor and an airframe p 116 N95-17883
A linear system identification and validation of an AH-64 Apache aeroelastic simulation model p 146 N95-18903
2-D and 3-D oscillating wing aerodynamics for a range of angles of attack including stall [NASA-TM-4632] p 120 N95-19119
Wall interaction effects for a full-scale helicopter rotor in the NASA Ames 80- by 120-foot wind tunnel p 121 N95-19270

ROTATING BODIES
A Lifting Ball Valve for cryogenic fluid applications p 156 N95-16349

ROTATING SHAFTS
Investigation of heat transfer between rotating shafts of transmissions of turbojet engines [BTN-94-EIX94461408760] p 138 A95-63643

ROTATING STALLS
Unsteady flow phenomena in discrete passage diffusers for centrifugal compressors [AD-A281412] p 155 N95-16163

ROTOR AERODYNAMICS
Investigation of dynamic inflow's influence on rotor control derivatives p 155 N95-16250
Measurement of gust response on a turbine cascade [NASA-TM-106776] p 117 N95-18457
Sectional prediction of 3D effects for separated flow on rotating blades [PB94-201696] p 117 N95-18503
Wind turbine blade aerodynamics: The combined experiment [DE94-011866] p 118 N95-18645
Wind turbine blade aerodynamics: The analysis of field test data [DE94-011867] p 118 N95-18646

ROTOR BLADES
Investigation of dynamic inflow's influence on rotor control derivatives p 155 N95-16250

ROTOR BLADES (TURBOMACHINERY)
Tuned mass damper for integrally bladed turbine rotor [NASA-CASE-MFS-28697-1] p 159 N95-18325
Measurement of gust response on a turbine cascade [NASA-TM-106776] p 117 N95-18457
Verification of multidisciplinary models for turbomachines p 140 N95-19025

ROTOR BODY INTERACTIONS
Experimental data on the aerodynamic interactions between a helicopter rotor and an airframe p 116 N95-17883

ROTOR DYNAMICS
Tuned mass damper for integrally bladed turbine rotor [NASA-CASE-MFS-28697-1] p 159 N95-18325
A linear system identification and validation of an AH-64 Apache aeroelastic simulation model p 146 N95-18903

ROTORS
A stationary flow of a viscous liquid in radial clearances of rotor bearings in the turbocompressor of an internal combustion engine [BTN-94-EIX94461408765] p 153 A95-63648
A Lifting Ball Valve for cryogenic fluid applications p 156 N95-16349
Numerical simulation of helicopter engine plume in forward flight [NASA-CR-197488] p 107 N95-16589
Structural effects of unsteady aerodynamic forces on horizontal-axis wind turbines [DE94-011863] p 157 N95-16939
Wave cycle design for wave rotor engines with limited nitrogen oxide emissions p 161 N95-18901

RUNWAYS
Modeling of Instrument Landing System (ILS) localizer signal on runway 25L at Los Angeles International Airport [NASA-TM-4588] p 125 N95-17384
Aircraft wake vortex takeoff tests at O'Hara International Airport [AD-A283828] p 118 N95-18624

RUSSIAN FEDERATION
Development of strength analysis methods and design model for aircraft constructions in Kazan Aviation Institute p 127 N95-16264

S

SAFETY FACTORS
Aircraft accident investigation and airworthiness — A practical example of the interaction of two disciplines with some reflections on possible legal consequences [HTN-95-50219] p 176 A95-64856
The global aircraft shape p 128 N95-16571
Safety aspects of spacecraft commanding p 149 N95-17248
Aircraft and sub-system certification by piloted simulation [AGARD-AR-278] p 145 N95-17388

SAFETY MANAGEMENT
Safety aspects of spacecraft commanding p 149 N95-17248
Safety study: Commuter airline safety [PB94-917004] p 124 N95-19132

SCALE EFFECT
Methods for scaling icing test conditions [NASA-TM-106827] p 124 N95-19284

SCALE MODELS
Methods for scaling icing test conditions [NASA-TM-106827] p 124 N95-19284

SCALING LAWS
Methods for scaling icing test conditions [NASA-TM-106827] p 124 N95-19284

SCANNERS
Evaluation of scanners for C-scan imaging in nondestructive inspection of aircraft [DE94-012473] p 152 N95-19100

SCHLIEREN PHOTOGRAPHY
Wind tunnel investigations of the appearance of shocks in the windward region of bodies with circular cross section at angle of attack p 113 N95-17866

SCIENTISTS
Two projects of V. M. Myasishchev [HTN-95-50269] p 176 A95-65764
ICASE [NASA-CR-195001] p 170 N95-16898

SEATS
A correlative investigation of simulated occupant motion and accident report in a helicopter crash [AD-A285190] p 123 N95-16404

SECONDARY FLOW
Static investigation of two fluidic thrust-vectoring concepts on a two-dimensional convergent-divergent nozzle [NASA-TM-4574] p 120 N95-19042

SEMISPAN MODELS
2-D and 3-D oscillating wing aerodynamics for a range of angles of attack including stall [NASA-TM-4632] p 120 N95-19119

SENSITIVITY
Applications of automatic differentiation in computational fluid dynamics p 156 N95-16461

SENSORS
Determination of stores pointing error due to wing flexibility under flight load [NASA-TM-4646] p 134 N95-19044

SEPARATED FLOW
Numerical simulation of helicopter engine plume in forward flight [NASA-CR-197488] p 107 N95-16589

SEPARATORS
Airborne rotary separator study [NASA-CR-191045] p 150 N95-18743

SERVICE LIFE
Problems with aging wiring in Naval aircraft p 154 N95-16048
Service and physical properties of liquid-jet fuels p 151 N95-16256

SHAFTS (MACHINE ELEMENTS)
Wall interaction effects for a full-scale helicopter rotor in the NASA Ames 80- by 120-foot wind tunnel p 121 N95-19270

SHAPES
Optimum aerodynamic design via boundary control p 127 N95-16565
Residual-correction type and related computational methods for aerodynamic design. Part 1: Airfoil and wing design p 128 N95-16566
Optimal shape design for aerodynamics p 128 N95-16568
Airfoil optimization by the one-shot method p 128 N95-16569
The global aircraft shape p 128 N95-16571
Review of the EUROPT Project AERO-0026 p 129 N95-16573

- Ice accretion with varying surface tension
[NASA-TM-106826] p 124 N95-19285
- SHARP LEADING EDGES**
Wind tunnel test on a 65 deg delta wing with a sharp or rounded leading edge: The international vortex flow experiment p 114 N95-17872
Delta-wing model p 114 N95-17873
Experimental investigation of the vortex flow over a 76/60-deg double delta wing p 114 N95-17874
Interaction, bursting and control of vortices of a cropped double-delta wing at high angle of attack
[AD-A283656] p 119 N95-18669
- SHEAR STRESS**
An analysis code for the Rapid Engineering Estimation of Momentum and Energy Losses (REMEL)
[NASA-CR-191178] p 108 N95-16887
Shear buckling analysis of a hat-stiffened panel
[NASA-TM-4644] p 158 N95-17490
Fatigue crack growth in 2024-T3 aluminum under tensile and transverse shear stresses p 153 N95-19490
- SHOCK RESISTANCE**
Quality optimization of thermally sprayed coatings produced by the JP-5000 (HVOF) gun using mathematical modeling p 152 N95-19008
- SHOCK WAVE INTERACTION**
Numerical simulation of supersonic compression corners and hypersonic inlet flows using the RPLUS2D code
[NASA-TM-106580] p 105 N95-16038
Mach number, flow angle, and loss measurements downstream of a transonic fan-blade cascade
[AD-A280907] p 108 N95-16824
Theoretical investigations of shock/boundary layer interactions on a Ma(infinity) = 8 waverider
[DLR-FB-94-12] p 119 N95-18910
- SHOCK WAVES**
Aerodynamic design and calculation of flow around the plane cascade of turbine
[BTN-94-EIX94481415357] p 104 A95-65347
Time accurate computation of unsteady inlet flows with a dynamic flow adaptive mesh
[AD-A285498] p 157 N95-16736
Investigation of the flow over a series of 14 percent-thick supercritical aerofoils with significant rear camber p 109 N95-17849
Wind tunnel investigations of the appearance of shocks in the windward region of bodies with circular cross section at angle of attack p 113 N95-17866
Aeromechanics technology, volume 1. Task 1: Three-dimensional Euler/Navier-Stokes Aerodynamic Method (TEAM) enhancements p 132 N95-18483
Flow field investigation in a free jet - free jet core system for the generation of high intensity molecular beams
[DLR-FB-94-11] p 172 N95-18912
Spectrogram diagnosis of aircraft disasters p 124 N95-19167
- SHORT CRACKS**
Widespread fatigue damage monitoring: Issues and concerns p 136 N95-19488
- SIGNAL PROCESSING**
Joint Proceedings on Aeronautics and Astronautics (JPAA)
[ISBN-7-80-046602-7] p 104 N95-16249
Dynamic Stability Instrumentation System (DSIS). Volume 1: Hardware description p 171 N95-18899
[NASA-TM-109160-VOL-1] p 171 N95-18899
Waveform bounding and combination techniques for direct drive testing p 161 N95-19035
- SIGNATURES**
The use of electrochemistry and ellipsometry for identifying and evaluating corrosion on aircraft
[AD-A285323] p 151 N95-16371
An assessment of the adaptive unstructured tetrahedral grid, Euler Flow Solver Code FELISA
[NASA-TP-3526] p 119 N95-19041
- SILICON DIOXIDE**
Thermal chemical energy of ablating silica surfaces in air breathing solid rocket engines p 148 N95-16316
- SIMULATED ANNEALING**
Nonsmooth trajectory optimization: An approach using continuous simulated annealing
[BTN-94-EIX94511433914] p 168 A95-64580
- SIMULATION**
A correlative investigation of simulated occupant motion and accident report in a helicopter crash
[AD-A285190] p 123 N95-16404
A surgical support system for Space Station Freedom p 149 N95-16776
Simulation of multidisciplinary problems for the thermostress state of cooled high temperature turbines p 140 N95-19021
Simulation of steady and unsteady viscous flows in turbomachinery p 140 N95-19023
Computational simulations for some tests in transonic wind tunnels p 164 N95-19264
- Determination of solid/porous wall boundary conditions from wind tunnel data for computational fluid dynamics codes p 164 N95-19266
- SINGLE CRYSTALS**
Fatigue in single crystal nickel superalloys
[AD-A285727] p 152 N95-18068
- SINGLE STAGE TO ORBIT VEHICLES**
Matlab as a robust control design tool p 169 N95-16474
- SINGULARITY (MATHEMATICS)**
Determination of solid/porous wall boundary conditions from wind tunnel data for computational fluid dynamics codes p 164 N95-19266
- SKIN (STRUCTURAL MEMBER)**
Acoustic fatigue testing on different materials and skin-stringer elements p 174 N95-19156
Thermo-acoustic fatigue design for hypersonic vehicle skin panels p 162 N95-19161
An artificial corrosion protocol for lap-splices in aircraft skin p 152 N95-19482
- SKIN FRICTION**
An analysis code for the Rapid Engineering Estimation of Momentum and Energy Losses (REMEL)
[NASA-CR-191178] p 108 N95-16887
- SLENDER BODIES**
Force and pressure data of an ogive-nosed slender body at high angles of attack and different Reynolds numbers p 113 N95-17868
- SLOTS**
Interference determination for wind tunnels with slotted walls p 147 N95-19269
- SLOTTED WIND TUNNELS**
Interference determination for wind tunnels with slotted walls p 147 N95-19269
- SOFTWARE ENGINEERING**
A study of software standards used in the avionics industry p 137 N95-16456
Rapid solution of large-scale systems of equations p 169 N95-16458
Applications of automatic differentiation in computational fluid dynamics p 156 N95-16461
Data acquisition and processing software for the Low Speed Wind Tunnel tests of the Jindivik auxiliary air intake
[AD-A285455] p 108 N95-17178
NASA High Performance Computing and Communications program
[NASA-TM-4653] p 176 N95-18573
- SOFTWARE TOOLS**
Applications of automatic differentiation in computational fluid dynamics p 156 N95-16461
Matlab as a robust control design tool p 169 N95-16474
Tools for applied engineering optimization p 128 N95-16570
Data acquisition and processing software for the Low Speed Wind Tunnel tests of the Jindivik auxiliary air intake
[AD-A285455] p 108 N95-17178
Interactive computer graphics applications for compressible aerodynamics
[NASA-TM-106802] p 170 N95-17264
Demonstration of the Dynamic Flowgraph Methodology using the Titan 2 Space Launch Vehicle Digital Flight Control System
[NASA-CR-197517] p 150 N95-17493
Universal wind tunnel data acquisition and reduction software
[AD-A283897] p 171 N95-18365
- SOIL MAPPING**
Development of an Automated Airfield Dynamic Cone Penetrometer (AADCP) prototype and the evaluation of unroofed airfield seismic surveying using Spectral Analysis of Surface Waves (SASW) technology
[AD-A281985] p 145 N95-17444
- SOLID PROPELLANT COMBUSTION**
Solid fuel ramjet composition p 152 N95-19090
- SOLID PROPELLANT ROCKET ENGINES**
The 1993 JANNAF Propulsion Meeting, volume 1
[CPIA-PUBL-602-VOL-1] p 148 N95-16312
Thermal chemical energy of ablating silica surfaces in air breathing solid rocket engines p 148 N95-16316
Recent advances in graphite/epoxy motor cases p 149 N95-16333
- SOLID STATE DEVICES**
Solid state radar demonstration test results at the FAA Technical Center
[AD-A281520] p 154 N95-16097
- SOLID WASTES**
Bicarbonate of soda blasting technology for aircraft wheel depainting
[PB94-193323] p 104 N95-17466
- SOLIDS**
On the particular features of dynamic processes in solids with varying boundary during interaction with intensive heat flows
[BTN-94-EIX94461408756] p 171 A95-63639
- SONIC BOOMS**
Floating shock fitting via Lagrangian adaptive meshes
[NASA-CR-194997] p 170 N95-18110
An assessment of the adaptive unstructured tetrahedral grid, Euler Flow Solver Code FELISA
[NASA-TP-3526] p 119 N95-19041
- SOUND FIELDS**
Active minimization of energy density in three-dimensional enclosures
[NASA-CR-197213] p 172 N95-16848
- SOUND GENERATORS**
Anisotropic heat exchangers/stack configurations for thermoacoustic heat engines
[AD-A280974] p 168 N95-16506
- SOUND PRESSURE**
Weapons bay acoustic environment p 173 N95-19146
Modelling structurally damaging twin-jet screech p 135 N95-19154
- SOUND WAVES**
Ducted fan acoustic radiation including the effects of nonuniform mean flow and acoustic treatment
[NASA-CR-197449] p 172 N95-16401
Active minimization of energy density in three-dimensional enclosures
[NASA-CR-197213] p 172 N95-16848
Acoustic radiation damping of flat rectangular plates subjected to subsonic flow p 172 N95-18542
- SPACE ENVIRONMENT SIMULATION**
Virtual environment application with partial gravity simulation p 169 N95-15988
- SPACE LAW**
The ICAO CNS/ATM system: New king, new law?
[HTN-95-50218] p 175 A95-64855
World trends in air transport policies. (Approaching the 21st century)
[HTN-95-50220] p 176 A95-64857
- SPACE PROCESSING**
Microgravity isolation system design: A modern control analysis framework
[NASA-TM-106803] p 105 N95-18486
- SPACE SHUTTLE BOOSTERS**
Documentation and archiving of the Space Shuttle wind tunnel test data base. Volume 1: Background and description
[NASA-TM-104806-VOL-1] p 151 N95-19237
- SPACE SHUTTLE ORBITERS**
Hypersonic flight testing
[AD-A283981] p 134 N95-18891
Documentation and archiving of the Space Shuttle wind tunnel test data base. Volume 1: Background and description
[NASA-TM-104806-VOL-1] p 151 N95-19237
- SPACE SHUTTLES**
Ultraviolet emissions occurring about hypersonic vehicles in rarefied flows
[AD-A281452] p 106 N95-16076
Field and data analysis studies related to the atmospheric environment
[NASA-CR-196543] p 168 N95-18093
Hypersonic flight testing
[AD-A283981] p 134 N95-18891
Documentation and archiving of the Space Shuttle wind tunnel test data base. Volume 1: Background and description
[NASA-TM-104806-VOL-1] p 151 N95-19237
Fatigue loads spectra derivation for the Space Shuttle: Second cycle p 166 N95-19470
- SPACE STATION FREEDOM**
A surgical support system for Space Station Freedom p 149 N95-16776
- SPACEBORNE EXPERIMENTS**
Microgravity isolation system design: A modern control synthesis framework
[NASA-TM-106805] p 105 N95-18197
- SPACECRAFT CONFIGURATIONS**
Fatigue loads spectra derivation for the Space Shuttle: Second cycle p 166 N95-19470
- SPACECRAFT CONSTRUCTION MATERIALS**
Recent advances in graphite/epoxy motor cases p 149 N95-16333
Conference on Aerospace Transparent Materials and Enclosures. Volume 2: Sessions 5-9
[AD-A283926] p 131 N95-18162
Conference on Aerospace Transparent Materials and Enclosures, volume 1
[AD-A283925] p 133 N95-18677
A CMC database for use in the next generation launch vehicles (rockets) p 150 N95-18993

- SPACECRAFT CONTROL**
Safety aspects of spacecraft commanding p 149 N95-17248
Packet utilisation definitions for the ESA XMM mission p 150 N95-17596
- SPACECRAFT DESIGN**
Two projects of V. M. Myasishchev [HTN-95-50269] p 176 A95-65764
- SPACECRAFT GLOW**
Ultraviolet emissions occurring about hypersonic vehicles in rarefied flows [AD-A281452] p 106 N95-16076
- SPACECRAFT LAUNCHING**
Program test objectives milestone 3 --- Integrated Propulsion Technology Demonstrator [NASA-CR-197030] p 127 N95-15971
- SPACECRAFT MODELS**
Safety aspects of spacecraft commanding p 149 N95-17248
- SPACECRAFT PERFORMANCE**
Safety aspects of spacecraft commanding p 149 N95-17248
- SPACECRAFT PROPULSION**
Arcjet thruster research and technology, phase 2 [NASA-CR-182276] p 105 N95-18044
- SPACECRAFT STRUCTURES**
Aeroacoustic qualification of HERMES shingles p 173 N95-19145
- SPACECREWS**
Virtual environment application with partial gravity simulation p 169 N95-15988
- SPECIFIC HEAT**
Improved analytical solution for varying specific heat parallel stream mixing [BTN-94-EIX94481415349] p 103 A95-65339
- SPECTRAL METHODS**
A spectrally accurate boundary-layer code for infinite swept wings [NASA-CR-195014] p 159 N95-18042
Treatment of non-linear systems by timeplane-transformed CT methods: The spectral gust method p 143 N95-18600
- SPECTRUM ANALYSIS**
Development of an Automated Airfield Dynamic Cone Penetrometer (AADCP) prototype and the evaluation of unsurfaced airfield seismic surveying using Spectral Analysis of Surface Waves (SASW) technology [AD-A281985] p 145 N95-17444
Spectrogram diagnosis of aircraft disasters p 124 N95-19167
- SPEED REGULATORS**
Simulation investigation on system identification of gas turbine [PB95-104238] p 139 N95-17749
- SPHERES**
Collection efficiency and ice accretion calculations for a sphere, a swept MS(1)-317 wing, a swept NACA-0012 wing tip, an axisymmetric inlet, and a Boeing 737-300 [NASA-TM-106831] p 123 N95-18582
- SPHERICAL COORDINATES**
Single-pass method for the solution of inverse potential and rotational problems. Part 2: Fully 3-D potential theory and applications p 107 N95-16564
- SPRAYED COATINGS**
Quality optimization of thermally sprayed coatings produced by the JP-5000 (HVOF) gun using mathematical modeling p 152 N95-19008
- SPREAD SPECTRUM TRANSMISSION**
Spread spectrum applications in unmanned aerial vehicles [AD-A281035] p 156 N95-16448
- STABILITY**
Helicopter in-flight simulation development and use in test pilot training [AD-A283998] p 146 N95-18725
- STABILITY DERIVATIVES**
Evaluation of the dynamic stability characteristics of the NAL Light Transport Aircraft [NAL-PD-CA-9217] p 142 N95-16392
Error propagation equations for estimating the uncertainty in high-speed wind tunnel test results [DE94-014136] p 145 N95-16509
- STABILITY TESTS**
FPCAS2D user's guide, version 1.0 [NASA-CR-195413] p 156 N95-16588
- STABILIZATION**
Microgravity isolation system design: A modern control analysis framework [NASA-TM-106803] p 105 N95-18486
- STABILIZERS (FLUID DYNAMICS)**
Twin engine afterbody model p 115 N95-17880
- STAMPING**
Calculation of geometry of stamps with small allowances for pieces of the aerodynamic profile [BTN-94-EIX94461408772] p 103 A95-63655
- STANDARD DEVIATION**
Optimization of adaptive intraply hybrid fiber composites with reliability considerations [NASA-TM-106632] p 157 N95-16911
- STANDARDS**
A study of software standards used in the avionics industry p 137 N95-16456
Field verification of the wind tunnel coefficients p 109 N95-17291
Aircraft and sub-system certification by piloted simulation [AGARD-AR-278] p 145 N95-17388
- STATE VECTORS**
Selection of optimal parameters for a system, controlling the flight height, when information about the state vector is incomplete [BTN-94-EIX94461408753] p 168 A95-63636
- STATIC FRICTION**
Static and dynamic friction behavior of candidate high temperature airframe seal materials [NASA-TM-106571] p 152 N95-16905
- STATIC LOADS**
Course module for AA201: Wing structural design project [AD-A283618] p 133 N95-18616
- STATIC MODELS**
Verification of multidisciplinary models for turbomachines p 140 N95-19025
- STATIC PRESSURE**
Hypersonic flow-field measurements: Intrusive and nonintrusive [AD-A283867] p 119 N95-18674
Calculation of low speed wind tunnel wall interference from static pressure pipe measurements p 164 N95-19273
- STATIC STABILITY**
Plant and controller optimization by convex methods [AD-A283700] p 133 N95-18621
Hypersonic wind tunnel test techniques [AD-A284057] p 118 N95-18663
- STATIC TESTS**
Development of a multicomponent force and moment balance for water tunnel applications, volume 1 [NASA-CR-4642-VOL-1] p 161 N95-18955
Static investigation of two fluidic thrust-vectoring concepts on a two-dimensional convergent-divergent nozzle [NASA-TM-4574] p 120 N95-19042
- STATIONKEEPING**
Arcjet thruster research and technology, phase 2 [NASA-CR-182276] p 105 N95-18044
- STATISTICAL DISTRIBUTIONS**
Minimal time detection algorithms and applications to flight systems [TR-2-FSRC-93] p 171 N95-18564
- STATORS**
A Lifting Ball Valve for cryogenic fluid applications p 156 N95-16349
- STEADY FLOW**
Acoustic radiation damping of flat rectangular plates subjected to subsonic flows p 172 N95-18542
Simulation of steady and unsteady viscous flows in turbomachinery p 140 N95-19023
Steady potential solver for unsteady aerodynamic analyses p 141 N95-19382
- STEAM TURBINES**
Gas-turbine engines with increased efficiency of two circuits, due to the use of the utilizing steam-turbine circuit [BTN-94-EIX94461408755] p 153 A95-63638
- STIFFENING**
Compression strength of composite primary structural components [NASA-CR-197554] p 160 N95-18388
- STIFFNESS**
A CMC database for use in the next generation launch vehicles (rockets) p 150 N95-18993
- STOCHASTIC PROCESSES**
Output feedback control under randomly varying distributed delays [BTN-94-EIX94511433916] p 168 A95-64582
Portable parallel stochastic optimization for the design of aeropropulsion components [NASA-CR-195312] p 154 N95-16072
Comparison of stochastic and deterministic nonlinear gust analysis methods to meet continuous turbulence criteria p 133 N95-18602
Forced response of mistuned bladed disks p 141 N95-19383
- STRAIN GAGE BALANCES**
Dynamic Stability Instrumentation System (DSIS). Volume 1: Hardware description [NASA-TM-109160-VOL-1] p 171 N95-18899
Development of a multicomponent force and moment balance for water tunnel applications, volume 1 [NASA-CR-4642-VOL-1] p 161 N95-18955
Development of a multicomponent force and moment balance for water tunnel applications, volume 2 [NASA-CR-4642-VOL-2] p 161 N95-18956
- STRAIN GAGES**
Hydrofoil force balance [AD-D016475] p 160 N95-18461
- STRAKES**
Experimental investigation of the vortex flow over a 76/60-deg double delta wing p 114 N95-17874
- STRESS ANALYSIS**
Analytical description of and forecast for stress relaxation of aviation materials under the vibration conditions [BTN-94-EIX94461408751] p 126 A95-63634
Aircraft stress sequence development: A complex engineering process made simple p 136 N95-19480
Prediction of R-curves from small coupon tests p 167 N95-19496
- STRESS DISTRIBUTION**
Prediction of R-curves from small coupon tests p 167 N95-19496
- STRESS INTENSITY FACTORS**
Multi-lab comparison on R-curve methodologies: Alloy 2024-T3 [NASA-CR-195004] p 151 N95-16860
Discrete crack growth analysis methodology for through cracks in pressurized fuselage structures p 166 N95-19473
- STRESS RELAXATION**
Analytical description of and forecast for stress relaxation of aviation materials under the vibration conditions [BTN-94-EIX94461408751] p 126 A95-63634
- STRINGERS**
Acoustic fatigue testing on different materials and skin-stringer elements p 174 N95-19156
Fatigue and residual strength investigation of ARALL(R) -3 and GLARE(R) -2 panels with bonded stringers p 137 N95-19495
- STRUCTURAL ANALYSIS**
FPCAS2D user's guide, version 1.0 [NASA-CR-195413] p 156 N95-16588
Measurements on a two-dimensional aerofoil with high-lift devices p 109 N95-17848
FAA/NASA International Symposium on Advanced Structural Integrity Methods for Airframe Durability and Damage Tolerance, part 2 [NASA-CP-3274-PT-2] p 124 N95-19468
Flight parameters monitoring system for tracking structural integrity of rotary-wing aircraft p 135 N95-19469
Technology Benefit Estimator (T/BEST): User's manual [NASA-TM-106785] p 167 N95-19501
- STRUCTURAL DESIGN**
A Lifting Ball Valve for cryogenic fluid applications p 156 N95-16349
Rapid solution of large-scale systems of equations p 169 N95-16458
Wing design for a civil tiltrotor transport aircraft [NASA-CR-197523] p 130 N95-18090
Course module for AA201: Wing structural design project [AD-A283618] p 133 N95-18616
Impact of Acoustic Loads on Aircraft Structures [AGARD-CP-549] p 173 N95-19142
Current and future problems in structural acoustic fatigue p 173 N95-19143
Aeroacoustic qualification of HERMES shingles p 173 N95-19145
- STRUCTURAL DESIGN CRITERIA**
Aircraft Loads due to Turbulence and their Impact on Design and Certification [AGARD-R-798] p 143 N95-18597
- STRUCTURAL ENGINEERING**
NASA Lewis Research Center Workshop on Forced Response in Turbomachinery [NASA-CP-10147] p 141 N95-19380
- STRUCTURAL FAILURE**
Forced response of mistuned bladed disks p 141 N95-19383
FAA/NASA International Symposium on Advanced Structural Integrity Methods for Airframe Durability and Damage Tolerance, part 2 [NASA-CP-3274-PT-2] p 124 N95-19468
Results of uniaxial and biaxial tests on riveted fuselage lap joint specimens p 136 N95-19491
- STRUCTURAL RELIABILITY**
Current and future problems in structural acoustic fatigue p 173 N95-19143
- STRUCTURAL STABILITY**
Application of superplastically formed and diffusion bonded structures in high intensity noise environments p 174 N95-19162

STRUCTURAL VIBRATION

- The effects of aircraft (B-52) overflights on ancient structures
[BTN-94-EIX9431340070] p 171 A95-63522
- Analytical description of and forecast for stress relaxation of aviation materials under the vibration conditions
[BTN-94-EIX94461408751] p 126 A95-63634
- Pressure measurements on an F/A-18 twin vertical tail in buffeting flow. Volume 4, part 2: Buffet cross spectral densities
[AD-A265555] p 143 N95-18641
- Nonlinear dynamic response of aircraft structures to acoustic excitation p 135 N95-19151
- Spectrogram diagnosis of aircraft disasters p 124 N95-19167

STRUTS

- Interaction of a three strut support on the aerodynamic characteristics of a civil aviation model p 122 N95-19279

STUDENTS

- A workstation based simulator for teaching compressible aerodynamics
[NASA-TM-106799] p 170 N95-16906

SUBCRITICAL FLOW

- An improved method of airfoil design p 106 N95-16252

SUBROUTINES

- Demonstration of the Dynamic Flowgraph Methodology using the Titan 2 Space Launch Vehicle Digital Flight Control System
[NASA-CR-197517] p 150 N95-17493
- Steady potential solver for unsteady aerodynamic analyses p 141 N95-19382

SUBSONIC AIRCRAFT

- Atmospheric effects of high-flying subsonic aircraft: A catalogue of perturbing influences
[KNMI-SR-94-03] p 168 N95-18722

SUBSONIC FLOW

- Three dimensional compressible turbulent flow computations for a diffusing S-duct with/without vortex generators
[NASA-CR-195390] p 138 N95-17402
- Investigation of an NLF(1)-0416 airfoil in compressible subsonic flow p 110 N95-17852
- Measurements of the flow over a low aspect-ratio wing in the Mach number range 0.6 to 0.87 for the purpose of validation of computational methods. Part 1: Wing design, model construction, surface flow. Part 2: Mean flow in the boundary layer and wake, 4 test cases p 112 N95-17860
- Pressure distributions on research wing W4 mounted on an axisymmetric body p 112 N95-17862
- Three-dimensional boundary layer and flow field data of an inclined prolate spheroid p 158 N95-17867
- Ellipsoid-cylinder model p 158 N95-17869
- Delta-wing model p 114 N95-17873
- Wind tunnel test on a 65 deg delta wing with rounded leading edges: The International Vortex Flow Experiment p 114 N95-17875
- Investigation of the flow development on a highly swept canard/wing research model with segmented leading- and trailing-edge flaps p 114 N95-17876
- Subsonic flow around US-orbiter model FALKE in the DNW p 115 N95-17877
- Measurement of gust response on a turbine cascade
[NASA-TM-106776] p 117 N95-18457
- Acoustic radiation damping of flat rectangular plates subjected to subsonic flows p 172 N95-18542
- Solution of full potential equation on an airfoil by multigrid technique
[NAL-TM-CSS-9303] p 119 N95-18904
- Calculation of support interference in dynamic wind-tunnel tests p 122 N95-19282
- SUBSONIC SPEED**
- Measurements of the flow over a low aspect-ratio wing in the Mach number range 0.6 to 0.87 for the purpose of validation of computational methods. Part 1: Wing design, model construction, surface flow. Part 2: Mean flow in the boundary layer and wake, 4 test cases p 112 N95-17860
- DLR-F4 wing body configuration p 130 N95-17863
- Low aspect ratio wing experiment p 113 N95-17865
- Test data on a non-circular body for subsonic, transonic and supersonic Mach numbers p 158 N95-17871
- Wind tunnel test on a 65 deg delta wing with a sharp or rounded leading edge: The international vortex flow experiment p 114 N95-17872
- SUBSONIC WIND TUNNELS**
- Unsteady flow testing in a passive low-correction wind tunnel p 147 N95-19272
- Evaluation of combined wall- and support-interference on wind tunnel models p 122 N95-19278

SUBSTRATES

- Development of a bipolar lead/acid battery for the more electric aircraft
[AD-A284050] p 160 N95-18660

SUPERCOMPUTERS

- NASA High Performance Computing and Communications program
[NASA-TM-4653] p 176 N95-18573

SUPERCritical AIRFOILS

- Comparison of computational and experimental results for a supercritical airfoil
[NASA-TM-4601] p 108 N95-16908
- A supercritical airfoil experiment p 111 N95-17858

SUPERCritical WINGS

- Measurements of unsteady pressure and structural response for an elastic supercritical wing
[NASA-TP-3443] p 104 N95-16560

SUPERPLASTIC FORMING

- Application of superplastically formed and diffusion bonded structures in high intensity noise environments p 174 N95-19162

SUPERSONIC COMBUSTION

- Studies on high pressure and unsteady flame phenomena
[AD-A284126] p 152 N95-18410

SUPERSONIC COMBUSTION RAMJET ENGINES

- Scramjet testing guidelines p 138 N95-16317
- Combustor kinetic energy efficiency analysis of the hypersonic research engine data p 148 N95-16321
- One-dimensional flow description for the combustion chamber of a scramjet
[DLR-FB-94-06] p 139 N95-18911
- Operating capability and current status of the reactivated NASA Lewis Research Center Hypersonic Tunnel Facility
[NASA-TM-106808] p 148 N95-19286

SUPERSONIC FLOW

- In-flight imaging of transverse gas jets injected into transonic and supersonic crossflows: Design and development
[NASA-CR-186031] p 157 N95-17418
- Detailed study at supersonic speeds of the flow around delta wings p 112 N95-17861
- Wind tunnel investigations of the appearance of shocks in the windward region of bodies with circular cross section at angle of attack p 113 N95-17866
- Supersonic vortex flow around a missile body p 114 N95-17870
- Numerical computations of supersonic base flow with special emphasis on turbulence modeling
[AD-A283688] p 119 N95-18670
- An assessment of the adaptive unstructured tetrahedral grid, Euler Flow Solver Code FELISA
[NASA-TP-3526] p 119 N95-19041
- Transonic and supersonic flowfield measurements about axisymmetric afterbodies for validation of advanced CFD codes p 121 N95-19260
- Parabolized Navier-Stokes solution of supersonic/hypersonic flows p 123 N95-19464

SUPERSONIC INLETS

- Time accurate computation of unsteady inlet flows with a dynamic flow adaptive mesh
[AD-A285498] p 157 N95-16736

SUPERSONIC JET FLOW

- Linear instability waves in supersonic jets confined in circular and non-circular ducts
[BTN-94-EIX9431340068] p 103 A95-63520

SUPERSONIC SPEED

- Numerical simulation of supersonic compression corners and hypersonic inlet flows using the RPLUS2D code
[NASA-TM-106580] p 105 N95-16038
- Experimental study at low supersonic speeds of a missile concept having opposing wraparound tails
[NASA-TM-4582] p 106 N95-16069
- Detailed study at supersonic speeds of the flow around delta wings p 112 N95-17861
- Test data on a non-circular body for subsonic, transonic and supersonic Mach numbers p 158 N95-17871
- Wind tunnel test on a 65 deg delta wing with a sharp or rounded leading edge: The international vortex flow experiment p 114 N95-17872
- Parametric study on laminar flow for finite wings at supersonic speeds
[NASA-TM-108852] p 116 N95-18101

SUPERSONIC TRANSPORTS

- Aerodynamic shape optimization p 128 N95-16572
- Multi-lab comparison on R-curve methodologies: Alloy 2024-T3
[NASA-CR-195004] p 151 N95-16860

SUPERSONIC WIND TUNNELS

- Free-jet testing at Mach 3.44 in GASL's aero/thermo test facility p 145 N95-16320

SUPPORT INTERFERENCE

- Wall Interference, Support Interference and Flow Field Measurements
[AGARD-CP-535] p 162 N95-19251

- The crucial role of wall interference, support interference and flow field measurements in the development of advanced aircraft configurations p 162 N95-19252
- Evaluation of combined wall- and support-interference on wind tunnel models p 122 N95-19278
- Interaction of a three strut support on the aerodynamic characteristics of a civil aviation model p 122 N95-19279
- Interference corrections for a centre-line plate mount in a porous-walled transonic wind tunnel p 122 N95-19280
- Correction of support influences on measurements with sting mounted wind tunnel models p 122 N95-19281
- Calculation of support interference in dynamic wind-tunnel tests p 122 N95-19282

SUPPORT SYSTEMS

- A surgical support system for Space Station Freedom p 149 N95-16776

SUPPRESSORS

- Corner vortex suppressor
[AD-D016423] p 116 N95-18337

SURFACE TEMPERATURE

- Verification of multidisciplinary models for turbomachines p 140 N95-19025

SURFACE TREATMENT

- Modelling for optimal operations of line milling of aerodynamic surfaces
[BTN-94-EIX94461408774] p 138 A95-63657

SURFACE WAVES

- Development of an Automated Airfield Dynamic Cone Penetrometer (AADCP) prototype and the evaluation of unsurfaced airfield seismic surveying using Spectral Analysis of Surface Waves (SASW) technology
[AD-A281985] p 145 N95-17444

SURGERY

- A surgical support system for Space Station Freedom p 149 N95-16776

SURVEILLANCE

- E-6A hardness assurance, maintenance and surveillance program
[AD-A283994] p 134 N95-19067

SURVEILLANCE RADAR

- Solid state radar demonstration test results at the FAA Technical Center
[AD-A281520] p 154 N95-16097

SURVEYS

- Industry review of a crew-centered cockpit design process and toolset
[AD-A282966] p 130 N95-17661

SWEEP ANGLE

- Effect of crossflow on Goertler instability in incompressible boundary layers
[NASA-CR-195007] p 159 N95-18193

SWEEP FORWARD WINGS

- Investigation into the aerodynamic characteristics of a combat aircraft research model fitted with a forward swept wing p 116 N95-17884
- In-flight lift-drag characteristics for a forward-swept wing aircraft and comparisons with contemporary aircraft
[NASA-TP-3414] p 117 N95-18565

SWEEP WINGS

- Investigation of the flow development on a highly swept canard/wing research model with segmented leading- and trailing-edge flaps p 114 N95-17876
- A spectrally accurate boundary-layer code for infinite swept wings
[NASA-CR-195014] p 159 N95-18042
- Collection efficiency and ice accretion calculations for a sphere, a swept MS(1)-317 wing, a swept NACA-0012 wing tip, an axisymmetric inlet, and a Boeing 737-300
[NASA-TM-106831] p 123 N95-18582
- The utilization of a high speed reflective visualization system in the study of transonic flow over a delta wing p 121 N95-19259
- Velocity measurements with hot-wires in a vortex-dominated flowfield p 121 N95-19261
- Computational simulations for some tests in transonic wind tunnels p 164 N95-19264

SWEEPBACK WINGS

- Measurements of the flow over a low aspect-ratio wing in the Mach number range 0.6 to 0.87 for the purpose of validation of computational methods. Part 1: Wing design, model construction, surface flow. Part 2: Mean flow in the boundary layer and wake, 4 test cases p 112 N95-17860
- Pressure distributions on research wing W4 mounted on an axisymmetric body p 112 N95-17862
- DLR-F4 wing body configuration p 130 N95-17863
- DLR-F5: Test wing for CFD and applied aerodynamics p 113 N95-17864
- Delta-wing model p 114 N95-17873
- Wind tunnel test on a 65 deg delta wing with rounded leading edges: The International Vortex Flow Experiment p 114 N95-17875

SWITCHING CIRCUITS

- SWITCHING CIRCUITS**
 Demonstration of the Dynamic Flowgraph Methodology using the Titan 2 Space Launch Vehicle Digital Flight Control System [NASA-CR-197517] p 150 N95-17493
- SYNTHETIC APERTURE RADAR**
 Linear prediction data extrapolation superresolution radar imaging p 155 N95-16268
- SYSTEM IDENTIFICATION**
 Comparison of frequency response and perturbation methods to extract linear models from a nonlinear simulation [AD-A284115] p 146 N95-18405
 A linear system identification and validation of an AH-64 Apache aeroelastic simulation model p 146 N95-18903
 The accuracy of parameter estimation in system identification of noisy aircraft load measurement [NASA-CR-197516] p 134 N95-19130
- SYSTEMS ANALYSIS**
 Demonstration of the Dynamic Flowgraph Methodology using the Titan 2 Space Launch Vehicle Digital Flight Control System [NASA-CR-197517] p 150 N95-17493
- SYSTEMS ENGINEERING**
 Mathematical modelling concerning the development of a system of similar installations, taking into account their operational intensity (an aircraft-helicopter fleet taken as an example) [BTN-94-EIX94461408763] p 103 A95-63646
 Program test objectives milestone 3 --- Integrated Propulsion Technology Demonstrator [NASA-CR-197030] p 127 N95-15971
 Generalized method of solving topological optimization problems for electrical airplane equipment systems in computer-aided design p 169 N95-16272
 The computer analysis of the prediction of aircraft electrical power supply system reliability p 155 N95-16278
 Cooperative control theory and integrated flight and propulsion control [NASA-CR-197493] p 142 N95-17404
 Packet utilisation definitions for the ESA XMM mission p 150 N95-17596
 Simulation investigation on system identification of gas turbine [PB95-104238] p 139 N95-17749
 Strategic avionics technology definition studies. Subtask 3-1A3: Electrical Actuation (ELA) Systems Test Facility [NASA-CR-188360] p 143 N95-18567
 Hypersonic flight testing [AD-A283981] p 134 N95-18891
- T**
- TAIL ASSEMBLIES**
 Single-engine tail interference model p 115 N95-17879
 Twin engine afterbody model p 115 N95-17880
 Pressure measurements on an F/A-18 twin vertical tail in buffeting flow. Volume 4, part 2: Buffet cross spectral densities [AD-A285555] p 143 N95-18641
- TAKEOFF**
 STOVL CFD model test case p 115 N95-17881
 Tilt Rotor Unmanned Air Vehicle System (TRUS) demonstrator flight test program [AD-A284151] p 132 N95-18415
 Aircraft wake vortex takeoff tests at O'Hara International Airport [AD-A283828] p 118 N95-18624
- TANKER AIRCRAFT**
 KC-135 cockpit modernization study. Phase 1: Equipment evaluation [AD-A284099] p 131 N95-18398
- TECHNICAL WRITING**
 ICASE [NASA-CR-195001] p 170 N95-16898
- TECHNOLOGY UTILIZATION**
 Program test objectives milestone 3 --- Integrated Propulsion Technology Demonstrator [NASA-CR-197030] p 127 N95-15971
 Revitalizing general aviation [NASA-TM-110113] p 129 N95-16982
- TELEMETRY**
 Packet utilisation definitions for the ESA XMM mission p 150 N95-17596
- TEMPERATURE CONTROL**
 An engineering code to analyze hypersonic thermal management systems p 155 N95-16322
- TEMPERATURE DISTRIBUTION**
 Simulation of multidisciplinary problems for the thermostress state of cooled high temperature turbines p 140 N95-19021

- Verification of multidisciplinary models for turbomachines p 140 N95-19025
- TEMPERATURE EFFECTS**
 Static and dynamic friction behavior of candidate high temperature airframe seal materials [NASA-TM-106571] p 152 N95-16905
- TEMPERATURE PROBES**
 Hypersonic flow-field measurements: Intrusive and nonintrusive [AD-A283867] p 119 N95-18674
- TENSILE STRESS**
 Fatigue crack growth in 2024-T3 aluminum under tensile and transverse shear stresses p 153 N95-19490
- TENSOR ANALYSIS**
 Single-pass method for the solution of inverse potential and rotational problems. Part 1: 2-D and quasi 3-D theory and application p 107 N95-16563
- TEST CHAMBERS**
 High-temperature acoustic test facilities and methods p 174 N95-19149
 Development of pneumatic test techniques for subsonic high-lift and in-ground-effect wind tunnel investigations p 121 N95-19268
 Unsteady flow testing in a passive low-correction wind tunnel p 147 N95-19272
- TEST FACILITIES**
 Experimental and analytical methods for the determination of connected-pipe ramjet and ducted rocket internal performance [AGARD-AR-323] p 149 N95-17278
 Strategic avionics technology definition studies. Subtask 3-1A3: Electrical Actuation (ELA) Systems Test Facility [NASA-CR-188360] p 143 N95-18567
 High-temperature acoustic test facilities and methods p 174 N95-19149
 Development of pneumatic test techniques for subsonic high-lift and in-ground-effect wind tunnel investigations p 121 N95-19268
 Operating capability and current status of the reactivated NASA Lewis Research Center Hypersonic Tunnel Facility [NASA-TM-106808] p 148 N95-19286
- TEST FIRING**
 Program test objectives milestone 3 --- Integrated Propulsion Technology Demonstrator [NASA-CR-197030] p 127 N95-15971
- TEST PILOTS**
 Preliminary evaluation of the F/A-18 quantity/multiple envelope expansion [AD-A284119] p 132 N95-18407
 Helicopter in-flight simulation development and use in test pilot training [AD-A283998] p 146 N95-18725
- TEST STANDS**
 NASA High Performance Computing and Communications program [NASA-TM-4653] p 176 N95-18573
- TETRAHEDRONS**
 Mesh quality control for multiply-refined tetrahedral grids [NASA-CR-197595] p 160 N95-18737
 An assessment of the adaptive unstructured tetrahedral grid, Euler Flow Solver Code FELISA [NASA-TP-3526] p 119 N95-19041
- THERMAL ANALYSIS**
 Thermo-acoustic fatigue design for hypersonic vehicle skin panels p 162 N95-19161
 Technology Benefit Estimator (T/BEST): User's manual [NASA-TM-106785] p 167 N95-19501
- THERMAL CONDUCTIVITY**
 Quality optimization of thermally sprayed coatings produced by the JP-5000 (HVOF) gun using mathematical modeling p 152 N95-19008
- THERMAL CONTROL COATINGS**
 Quality optimization of thermally sprayed coatings produced by the JP-5000 (HVOF) gun using mathematical modeling p 152 N95-19008
- THERMAL ENVIRONMENTS**
 Hypersonic wind tunnel test techniques [AD-A284057] p 118 N95-18663
- THERMAL INSULATION**
 Thermal chemical energy of ablating silica surfaces in air breathing solid rocket engines p 148 N95-16316
- THERMAL PROTECTION**
 Thermal chemical energy of ablating silica surfaces in air breathing solid rocket engines p 148 N95-16316
- THERMAL RADIATION**
 High altitude hypersonic flowfield radiation [AD-A281386] p 106 N95-16160
- THERMAL RESISTANCE**
 A CMC database for use in the next generation launch vehicles (rockets) p 150 N95-18993

- THERMAL SHOCK**
 On the particular features of dynamic processes in solids with varying boundary during interaction with intensive heat flows [BTN-94-EIX94461408756] p 171 A95-63639
 Quality optimization of thermally sprayed coatings produced by the JP-5000 (HVOF) gun using mathematical modeling p 152 N95-19008
- THERMAL STRESSES**
 On the particular features of dynamic processes in solids with varying boundary during interaction with intensive heat flows [BTN-94-EIX94461408756] p 171 A95-63639
 Simulation of multidisciplinary problems for the thermostress state of cooled high temperature turbines p 140 N95-19021
 Application of multidisciplinary models to the cooled turbine rotor design p 140 N95-19024
- THERMOCHEMISTRY**
 Thermal chemical energy of ablating silica surfaces in air breathing solid rocket engines p 148 N95-16316
- THERMODYNAMIC CYCLES**
 Wave cycle design for wave rotor engines with limited nitrogen oxide emissions p 161 N95-18901
- THERMODYNAMIC PROPERTIES**
 Anisotropic heat exchangers/stack configurations for thermoacoustic heat engines [AD-A280974] p 168 N95-16506
 Single-pass method for the solution of inverse potential and rotational problems. Part 1: 2-D and quasi 3-D theory and application p 107 N95-16563
 Single-pass method for the solution of inverse potential and rotational problems. Part 2: Fully 3-D potential theory and applications p 107 N95-16564
- THERMODYNAMICS**
 On a program-information system TDsoft [BTN-94-EIX94461408773] p 175 A95-63656
- THERMOELASTICITY**
 On the particular features of dynamic processes in solids with varying boundary during interaction with intensive heat flows [BTN-94-EIX94461408756] p 171 A95-63639
- THIN AIRFOILS**
 H(sup 2)/H(sup INF) controller design for a two-dimensional thin airfoil flutter suppression [BTN-94-EIX94511433918] p 141 A95-64584
 Wing-body juncture flows [AD-A281526] p 106 N95-16099
- THIN PLATES**
 Fatigue crack growth in 2024-T3 aluminum under tensile and transverse shear stresses p 153 N95-19490
- THIN WALLED SHELLS**
 Development of strength analysis methods and design model for aircraft constructions in Kazan Aviation Institute p 127 N95-16264
- THIN WALLS**
 Development of processes, means, and theoretical principles of thin-walled detail plastic forming at Kazan Aviation Institute p 155 N95-16281
- THREE DIMENSIONAL BOUNDARY LAYER**
 Three-dimensional boundary layer and flow field data of an inclined prolate spheroid p 158 N95-17867
 A spectrally accurate boundary-layer code for infinite swept wings [NASA-CR-195014] p 159 N95-18042
 Effect of crossflow on Goertler instability in incompressible boundary layers [NASA-CR-195007] p 159 N95-18193
 Sectional prediction of 3D effects for separated flow on rotating blades [PB94-201696] p 117 N95-18503
- THREE DIMENSIONAL FLOW**
 Wing-body juncture flows [AD-A281526] p 106 N95-16099
 Three dimensional compressible turbulent flow computations for a diffusing S-duct with/without vortex generators [NASA-CR-195390] p 138 N95-17402
 Test data on a non-circular body for subsonic, transonic and supersonic Mach numbers p 158 N95-17871
 Low speed propeller slipstream aerodynamic effects p 116 N95-17882
 Sectional prediction of 3D effects for separated flow on rotating blades [PB94-201696] p 117 N95-18503
 An assessment of the adaptive unstructured tetrahedral grid, Euler Flow Solver Code FELISA [NASA-TP-3526] p 119 N95-19041
- THRUST CHAMBERS**
 Regenerative cooling for liquid propellant rocket thrust chambers [INPE-5565-TDI/540] p 150 N95-18720
- THRUST VECTOR CONTROL**
 VSTOL Systems Research Aircraft (VSRA) Harrier [NASA-TM-110117] p 126 N95-18347

Static investigation of two fluidic thrust-vectoring concepts on a two-dimensional convergent-divergent nozzle
[NASA-TM-4574] p 120 N95-19042

Integrated aerodynamic fin and stowable TVC vane system
[AD-D016457] p 151 N95-19073

TILES
Aeroacoustic qualification of HERMES shingles p 173 N95-19145

TILT ROTOR AIRCRAFT
Wing design for a civil tiltrotor transport aircraft
[NASA-CR-197523] p 130 N95-18090

Tilt Rotor Unmanned Air Vehicle System (TRUS) demonstrator flight test program
[AD-A284151] p 132 N95-18415

TIME DEPENDENCE
Demonstration of the Dynamic Flowgraph Methodology using the Titan 2 Space Launch Vehicle Digital Flight Control System
[NASA-CR-197517] p 150 N95-17493

Minimal time detection algorithms and applications to flight systems
[TR-2-FSRC-93] p 171 N95-18564

Velocity measurements with hot-wires in a vortex-dominated flowfield p 121 N95-19261

TIME MARCHING
Numerical computations of supersonic base flow with special emphasis on turbulence modeling
[AD-A283688] p 119 N95-18670

TOLERANCES (MECHANICS)
Brite-Euram programme: ACOUFAT acoustic fatigue and related damage tolerance of advanced composite and metallic structures p 174 N95-19159

FAA/NASA International Symposium on Advanced Structural Integrity Methods for Airframe Durability and Damage Tolerance, part 2
[NASA-CP-3274-PT-2] p 124 N95-19468

Fatigue life until small cracks in aircraft structures: Durability and damage tolerance p 135 N95-19478

TOPOLOGY
Generalized method of solving topological optimization problems for electrical airplane equipment systems in computer-aided design p 169 N95-16272

TORSION
Course module for AA201: Wing structural design project
[AD-A283618] p 133 N95-18616

TRAILING EDGE FLAPS
Low-speed surface pressure and boundary layer measurement data for the NLR 7301 airfoil section with trailing edge flap p 111 N95-17855

Two-dimensional high-lift airfoil data for CFD code validation p 112 N95-17859

Investigation of the flow development on a highly swept canard/wing research model with segmented leading- and trailing-edge flaps p 114 N95-17876

TRAILING EDGES
Experiments in the trailing edge flow of an NLR 7702 airfoil p 110 N95-17853

TRAINING AIRCRAFT
Aircraft stress sequence development: A complex engineering process made simple p 136 N95-19480

TRAINING DEVICES
Helicopter in-flight simulation development and use in test pilot training
[AD-A283998] p 146 N95-18725

TRAJECTORY CONTROL
Matlab as a robust control design tool p 169 N95-16474

TRAJECTORY OPTIMIZATION
Nonsmooth trajectory optimization: An approach using continuous simulated annealing
[BTN-94-EIX94511433914] p 168 A95-64580

Numerical optimization of synergetic maneuvers
[AD-A283398] p 109 N95-17435

TRANSATMOSPHERIC VEHICLES
Thermo-acoustic fatigue design for hypersonic vehicle skin panels p 162 N95-19161

TRANSFER ORBITS
Numerical optimization of synergetic maneuvers
[AD-A283398] p 109 N95-17435

TRANSFORMATIONS (MATHEMATICS)
Conversion of Earth-centered Earth-fixed coordinates to geodetic coordinates
[BTN-94-EIX94441380862] p 125 A95-64294

An improved method of airfoil design p 106 N95-16252

TRANSITION FLIGHT
STOVL CFD model test case p 115 N95-17881

TRANSITION FLOW
Experimental investigation of the vortex flow over a 76/60-deg double delta wing p 114 N95-17874

TRANSMISSIONS (MACHINE ELEMENTS)
Investigation of heat transfer between rotating shafts of transmissions of turbojet engines
[BTN-94-EIX94461408760] p 138 A95-63643

TRANSONIC FLOW
Engineering methods for the evaluation of transonic flutter characteristics for aerodynamic control surfaces
[BTN-94-EIX94461408589] p 141 A95-63064

Aerodynamic design and calculation of flow around the plane cascade of turbine
[BTN-94-EIX94481415357] p 104 A95-65347

An investigation of the transonic pressure drag coefficient for axis-symmetric bodies
[AD-A280990] p 105 N95-15994

Mach number, flow angle, and loss measurements downstream of a transonic fan-blade cascade
[AD-A280907] p 108 N95-16824

Comparison of computational and experimental results for a supercritical airfoil
[NASA-TM-4601] p 108 N95-16908

Transonic Navier-Stokes calculations about a 65 deg delta wing
[NASA-CR-4635] p 108 N95-17273

2-D airfoil tests including side wall boundary layer measurements p 158 N95-17847

Investigation of an NLF(1)-0416 airfoil in compressible subsonic flow p 110 N95-17852

OAT15A airfoil data p 111 N95-17857

DLR-F5: Test wing for CFD and applied aerodynamics p 113 N95-17864

Wind tunnel test on a 65 deg delta wing with rounded leading edges: The International Vortex Flow Experiment p 114 N95-17875

Investigation of the flow development on a highly swept canard/wing research model with segmented leading- and trailing-edge flaps p 114 N95-17876

Overview of unsteady transonic wind tunnel test on a semispan straked delta wing oscillating in pitch
[AD-A284097] p 117 N95-18380

Experimental techniques for measuring transonic flow with a three dimensional laser velocimetry system. Application to determining the drag of a fuselage p 163 N95-19258

The utilization of a high speed reflective visualization system in the study of transonic flow over a delta wing p 121 N95-19259

Transonic and supersonic flowfield measurements about axisymmetric afterbodies for validation of advanced CFD codes p 121 N95-19260

Transonic wind tunnel boundary interference correction p 147 N95-19271

TRANSONIC FLUTTER
Engineering methods for the evaluation of transonic flutter characteristics for aerodynamic control surfaces
[BTN-94-EIX94461408589] p 141 A95-63064

TRANSONIC NOZZLES
Direct splitting of coefficient matrix for numerical calculation of transonic nozzle flow
[BTN-94-EIX94481415356] p 103 A95-65346

TRANSONIC SPEED
Measurements of unsteady pressure and structural response for an elastic supercritical wing
[NASA-TP-3443] p 104 N95-16560

Two-dimensional 16.5 percent thick supercritical airfoil NLR 7301 p 110 N95-17854

DLR-F4 wing body configuration p 130 N95-17863

Low aspect ratio wing experiment p 113 N95-17865

Test data on a non-circular body for subsonic, transonic and supersonic Mach numbers p 158 N95-17871

Wind tunnel test on a 65 deg delta wing with a sharp or rounded leading edge: The international vortex flow experiment p 114 N95-17872

In-flight lift-drag characteristics for a forward-swept wing aircraft and comparisons with contemporary aircraft
[NASA-TP-3414] p 117 N95-18565

Computational simulations for some tests in transonic wind tunnels p 164 N95-19264

TRANSONIC WIND TUNNELS
Wall-signature methods for high speed wind tunnel wall interference corrections p 107 N95-16257

Comparison of computational and experimental results for a supercritical airfoil
[NASA-TM-4601] p 108 N95-16908

Single-engine tail interference model p 115 N95-17879

Overview of unsteady transonic wind tunnel test on a semispan straked delta wing oscillating in pitch
[AD-A284097] p 117 N95-18380

Computational simulations for some tests in transonic wind tunnels p 164 N95-19264

Interference determination for wind tunnels with slotted walls p 147 N95-19269

Transonic wind tunnel boundary interference correction p 147 N95-19271

The traditional and new methods of accounting for the factors distorting the flow over a model in large transonic wind tunnels p 165 N95-19275

Interference corrections for a centre-line plate mount in a porous-walled transonic wind tunnel p 122 N95-19280

TRANSPARENCY
Conference on Aerospace Transparent Materials and Enclosures. Volume 2: Sessions 5-9
[AD-A283926] p 131 N95-18162

Conference on Aerospace Transparent Materials and Enclosures, volume 1
[AD-A283925] p 133 N95-18677

TRANSPORT AIRCRAFT
Fiber-optic technology for transport aircraft
[BTN-94-EIX94511309384] p 103 A95-64610

DLR-F4 wing body configuration p 130 N95-17863

Wing design for a civil tiltrotor transport aircraft
[NASA-CR-197523] p 130 N95-18090

European aeronautics: Strong government presence in industry structure and research and development support. Report to Congressional Requesters
[GAO/NSIAD-94-71] p 176 N95-18578

TRISONIC WIND TUNNELS
Interference corrections for a centre-line plate mount in a porous-walled transonic wind tunnel p 122 N95-19280

TROPICAL REGIONS
Field and data analysis studies related to the atmospheric environment
[NASA-CR-196543] p 168 N95-18093

TUNGSTEN CARBIDES
Quality optimization of thermally sprayed coatings produced by the JP-5000 (HVOF) gun using mathematical modeling p 152 N95-19008

TUNING
Intelligent control law tuning for AIAA controls design challenge
[BTN-94-EIX94511433922] p 169 A95-64588

Forced response of mistuned bladed disks p 141 N95-19383

TURBINE BLADES
Ultimate characteristics of a rocket engine with a turbo-pump supply system
[BTN-94-EIX94461408757] p 148 A95-63640

Modelling for optimal operations of line milling of aerodynamic surfaces
[BTN-94-EIX94461408774] p 138 A95-63657

Structural effects of unsteady aerodynamic forces on horizontal-axis wind turbines p 157 N95-16939

Measurement of gust response on a turbine cascade
[NASA-TM-106776] p 117 N95-18457

Wind turbine blade aerodynamics: The combined experiment
[DE94-011866] p 118 N95-18645

Wind turbine blade aerodynamics: The analysis of field test data
[DE94-011867] p 118 N95-18646

Simulation of multidisciplinary problems for the thermostress state of cooled high temperature turbines p 140 N95-19021

Application of multidisciplinary models to the cooled turbine rotor design p 140 N95-19024

Aerodynamic investigation of the flow field in a 180 deg turn channel with sharp bend p 163 N95-19257

TURBINE PUMPS
Ultimate characteristics of a rocket engine with a turbo-pump supply system
[BTN-94-EIX94461408757] p 148 A95-63640

TURBINES
Aerodynamic design and calculation of flow around the plane cascade of turbine
[BTN-94-EIX94481415357] p 104 A95-65347

Simulation of multidisciplinary problems for the thermostress state of cooled high temperature turbines p 140 N95-19021

TURBOCOMPRESSORS
A stationary flow of a viscous liquid in radial clearances of rotor bearings in the turbocompressor of an internal combustion engine
[BTN-94-EIX94461408765] p 153 A95-63648

Enhanced capabilities and modified users manual for axial-flow compressor conceptual design code CSPAN
[NASA-TM-106833] p 119 N95-18933

TURBOJET ENGINES
Investigation of heat transfer between rotating shafts of transmissions of turbojet engines
[BTN-94-EIX94461408760] p 138 A95-63643

Development and application of the double V type flame stabilizer
[BTN-94-EIX94481415355] p 154 A95-65345

Small turbojets: Designs and installations p 138 N95-16323

Perspective problems of gas turbine engines simulation p 140 N95-19026

TURBOMACHINE BLADES

- NASA Lewis Research Center Workshop on Forced Response in Turbomachinery
[NASA-CP-10147] p 141 N95-19380
Forced response of mistuned bladed disks p 141 N95-19383

TURBOMACHINERY

- New approach to geometric profiling of the design elements of the passage part in turbo-machines
[BTN-94-EIX94461408769] p 153 A95-63652
Application of multicomponent models to flow passage simulation in multistage turbomachines and whole gas turbine engines p 140 N95-19022
Simulation of steady and unsteady viscous flows in turbomachinery p 140 N95-19023
Verification of multidisciplinary models for turbomachines p 140 N95-19025
NASA Lewis Research Center Workshop on Forced Response in Turbomachinery
[NASA-CP-10147] p 141 N95-19380
Unsteady aerodynamic analyses for turbomachinery aeroelastic predictions p 141 N95-19381
Steady potential solver for unsteady aerodynamic analyses p 141 N95-19382
Forced response of mistuned bladed disks p 141 N95-19383

TURBOPROP AIRCRAFT

- Noise transmission and reduction in turboprop aircraft p 175 N95-19164

TURBOSHAPTS

- Sensor fault detection and diagnosis simulation of a helicopter engine in an intelligent control framework
[NASA-TM-106784] p 137 N95-15970

TURBULENCE

- Structural effects of unsteady aerodynamic forces on horizontal-axis wind turbines
[DE94-011863] p 157 N95-16939
Experiments in the trailing edge flow of an NLR 7702 airfoil p 110 N95-17853

TURBULENCE EFFECTS

- A study of the effect of store unsteady aerodynamics on gust and turbulence loads p 133 N95-18601
Comparison of stochastic and deterministic nonlinear gust analysis methods to meet continuous turbulence criteria p 133 N95-18602
Design limit loads based upon statistical discrete gust methodology p 133 N95-18603
Pressure measurements on an F/A-18 twin vertical tail in buffeting flow. Volume 4, part 2: Buffet cross spectral densities p 143 N95-18641

TURBULENCE MODELS

- Transonic Navier-Stokes calculations about a 65 deg delta wing
[NASA-CR-4635] p 108 N95-17273
A supercritical airfoil experiment p 111 N95-17858
Aeromechanics technology, volume 1, Task 1: Three-dimensional Euler/Navier-Stokes Aerodynamic Method (TEAM) enhancements p 132 N95-18483
Solution of Navier-Stokes equations using high accuracy monotone schemes p 161 N95-19019
Simulation of steady and unsteady viscous flows in turbomachinery p 140 N95-19023

TURBULENT BOUNDARY LAYER

- Numerical simulation of supersonic compression corners and hypersonic inlet flows using the RPLUS2D code
[NASA-TM-106580] p 105 N95-16038
Three-dimensional boundary layer and flow field data of an inclined prolate spheroid p 158 N95-17867
Sectional prediction of 3D effects for separated flow on rotating blades p 117 N95-18503
[PB94-201696]
Theoretical investigations of shock/boundary layer interactions on a $M(\infty) = 8$ waverider
[DLR-FB-94-12] p 119 N95-18910
Flow field investigation in a free jet - free jet core system for the generation of high intensity molecular beams
[DLR-FB-94-11] p 172 N95-18912

TURBULENT FLOW

- Time accurate computation of unsteady inlet flows with a dynamic flow adaptive mesh
[AD-A285498] p 157 N95-16736
Three dimensional compressible turbulent flow computations for a diffusing S-duct with/without vortex generators
[NASA-CR-195390] p 138 N95-17402
Interaction, bursting and control of vortices of a cropped double-delta wing at high angle of attack
[AD-A283656] p 119 N95-18669
Numerical computations of supersonic base flow with special emphasis on turbulence modeling
[AD-A283688] p 119 N95-18670
Simulation of steady and unsteady viscous flows in turbomachinery p 140 N95-19023

- Velocity measurements with hot-wires in a vortex-dominated flowfield p 121 N95-19261
Viscous flow past aerofoils axisymmetric bodies and wings p 123 N95-19457

TURBULENT WAKES

- A supercritical airfoil experiment p 111 N95-17858

TURNING FLIGHT

- Time-optimal turn to a heading: An analytic solution
[BTN-94-EIX94511433940] p 142 A95-64606

TWISTED WINGS

- Determination of stores pointing error due to wing flexibility under flight load
[NASA-TM-4646] p 134 N95-19044

TWO DIMENSIONAL BODIES

- 2-D airfoil tests including side wall boundary layer measurements p 158 N95-17847
2-D airfoil effectiveness study p 110 N95-17851

TWO DIMENSIONAL FLOW

- A grid generation and flow solution method for the Euler equations on unstructured grids
[HTN-95-20003] p 153 A95-63201
Numerical simulation of supersonic compression corners and hypersonic inlet flows using the RPLUS2D code
[NASA-TM-106580] p 105 N95-16038
Two-dimensional high-lift airfoil data for CFD code validation p 112 N95-17859
Numerical simulation of dynamic-stall suppression by tangential blowing
[AD-A284887] p 120 N95-19110

TWO DIMENSIONAL MODELS

- Measurements on a two-dimensional airfoil with high-lift devices p 109 N95-17848
Investigation of the flow over a series of 14 percent-thick supercritical aerofoils with significant rear camber p 109 N95-17849
Experiments in the trailing edge flow of an NLR 7702 airfoil p 110 N95-17853
Two-dimensional 16.5 percent thick supercritical airfoil NLR 7301 p 110 N95-17854
Low-speed surface pressure and boundary layer measurement data for the NLR 7301 airfoil section with trailing edge flap p 111 N95-17855
OAT15A airfoil data p 111 N95-17857
A supercritical airfoil experiment p 111 N95-17858
Two-dimensional high-lift airfoil data for CFD code validation p 112 N95-17859
Static investigation of two fluidic thrust-vectoring concepts on a two-dimensional convergent-divergent nozzle
[NASA-TM-4574] p 120 N95-19042
Interference determination for wind tunnels with slotted walls p 147 N95-19269

TWO FLUID MODELS

- Static investigation of two fluidic thrust-vectoring concepts on a two-dimensional convergent-divergent nozzle
[NASA-TM-4574] p 120 N95-19042

TWO PHASE FLOW

- The stability of two-phase flow over a swept-wing
[NASA-CR-194994] p 159 N95-18190

U

U.S.S.R. SPACE PROGRAM

- Two projects of V. M. Myasishchev
[HTN-95-50269] p 176 A95-65764

U-2 AIRCRAFT

- Field and data analysis studies related to the atmospheric environment
[NASA-CR-196543] p 168 N95-18093

ULTRAHIGH FREQUENCIES

- A VHF/UHF antenna for the Precision Antenna Measurement System (PAMS)
[AD-A285673] p 156 N95-16621

ULTRASONICS

- Ultrasonic techniques for repair of aircraft structures with bonded composite patches p 136 N95-19486

ULTRAVIOLET EMISSION

- Ultraviolet emissions occurring about hypersonic vehicles in rarefied flows
[AD-A281452] p 106 N95-16076

UMBILICAL CONNECTORS

- Microgravity isolation system design: A modern control synthesis framework
[NASA-TM-106805] p 105 N95-18197

UNIFORM FLOW

- Acoustic radiation damping of flat rectangular plates subjected to subsonic flows p 172 N95-18542

UNITED STATES

- EC Aviation Scene
[HTN-95-50223] p 176 A95-64860
Annual review of aircraft accident data: US Air carrier operations, calendar year 1992
[PB95-100319] p 123 N95-17748

UNSTEADY AERODYNAMICS

- A computational investigation of wake-induced airfoil flutter in incompressible flow and active flutter control
[AD-A281534] p 142 N95-16109
Numerical simulation of transient vortex breakdown above a pitching delta wing p 107 N95-16808
[AD-A281075]
Structural effects of unsteady aerodynamic forces on horizontal-axis wind turbines p 157 N95-16939
[DE94-011863]
Overview of unsteady transonic wind tunnel test on a semispan straked delta wing oscillating in pitch
[AD-A284097] p 117 N95-18380
Sectional prediction of 3D effects for separated flow on rotating blades p 117 N95-18503
[PB94-201696]
A study of the effect of store unsteady aerodynamics on gust and turbulence loads p 133 N95-18601
Pressure measurements on an F/A-18 twin vertical tail in buffeting flow. Volume 4, part 2: Buffet cross spectral densities p 143 N95-18641
[AD-A285555]
Wind turbine blade aerodynamics: The combined experiment p 118 N95-18645
[DE94-011866]
Wind turbine blade aerodynamics: The analysis of field test data p 118 N95-18646
[DE94-011867]
Unsteady aerodynamic analyses for turbomachinery aeroelastic predictions p 141 N95-19381
Steady potential solver for unsteady aerodynamic analyses p 141 N95-19382

UNSTEADY FLOW

- Unsteady flow phenomena in discrete passage diffusers for centrifugal compressors p 155 N95-16163
[AD-A281421]
Measurements of unsteady pressure and structural response for an elastic supercritical wing
[NASA-TP-3443] p 104 N95-16560
Time accurate computation of unsteady inlet flows with a dynamic flow adaptive mesh
[AD-A285498] p 157 N95-16736
A supercritical airfoil experiment p 111 N95-17858
Overview of unsteady transonic wind tunnel test on a semispan straked delta wing oscillating in pitch
[AD-A284097] p 117 N95-18380
Pressure measurements on an F/A-18 twin vertical tail in buffeting flow. Volume 4, part 2: Buffet cross spectral densities p 143 N95-18641
[AD-A285555]
Wind turbine blade aerodynamics: The combined experiment p 118 N95-18645
[DE94-011866]
Wind turbine blade aerodynamics: The analysis of field test data p 118 N95-18646
[DE94-011867]
The mathematical models of flow passage for gas turbine engines and their components p 140 N95-19020
Simulation of steady and unsteady viscous flows in turbomachinery p 140 N95-19023
Unsteady flow testing in a passive low-correction wind tunnel p 147 N95-19272
Calculation of support interference in dynamic wind-tunnel tests p 122 N95-19282

UPPER SURFACE BLOWING

- Numerical simulation of dynamic-stall suppression by tangential blowing
[AD-A284887] p 120 N95-19110

USER MANUALS (COMPUTER PROGRAMS)

- FPCAS2D user's guide, version 1.0
[NASA-CR-195413] p 156 N95-16588
Users guide for NASA Lewis Research Center DC-9 Reduced-Gravity Aircraft Program
[NASA-TM-106755] p 146 N95-18586
Enhanced capabilities and modified users manual for axial-flow compressor conceptual design code CSPAN
[NASA-TM-106833] p 119 N95-18933
Technology Benefit Estimator (T/BEST): User's manual
[NASA-TM-106785] p 167 N95-19501
- USER REQUIREMENTS
- On a program-information system Tdsoft
[BTN-94-EIX94461408773] p 175 A95-63656
Universal wind tunnel data acquisition and reduction software
[AD-A283897] p 171 N95-18365

V

V/STOL AIRCRAFT

- Cooperative control theory and integrated flight and propulsion control
[NASA-CR-197493] p 142 N95-17404
STOVL CFD model test case p 115 N95-17881

VSTOL Systems Research Aircraft (VSRA) Harrier [NASA-TM-110117] p 126 N95-18347
 NASA develops new digital flight control system [NASA-NEWS-RELEASE-94-47] p 144 N95-19029

VANES
 Application of multidisciplinary models to the cooled turbine rotor design p 140 N95-19024

VARIABLE AMPLITUDE LOADING
 Prediction of fatigue crack growth under flight-simulation loading with the modified CORPUS model p 166 N95-19471

VELOCITY DISTRIBUTION
 Single-pass method for the solution of inverse potential and rotational problems. Part 1: 2-D and quasi 3-D theory and application p 107 N95-16563
 Residual-correction type and related computational methods for aerodynamic design. Part 1: Airfoil and wing design p 128 N95-16566
 Residual-correction type and related computational methods for aerodynamic design. Part 2: Multi-point airfoil design p 128 N95-16567
 Measurement of gust response on a turbine cascade [NASA-TM-106776] p 117 N95-18457
 Aerodynamic investigation of the flow field in a 180 deg turn channel with sharp bend p 163 N95-19257

VELOCITY MEASUREMENT
 Aerodynamic investigation of the flow field in a 180 deg turn channel with sharp bend p 163 N95-19257
 Experimental techniques for measuring transonic flow with a three dimensional laser velocimetry system. Application to determining the drag of a fuselage p 163 N95-19258
 Velocity measurements with hot-wires in a vortex-dominated flowfield p 121 N95-19261

VENTILATION
 Computational simulations for some tests in transonic wind tunnels p 164 N95-19264

VERBAL COMMUNICATION
 An analysis of tower (local) controller-pilot voice communications [AD-A283718] p 160 N95-18436

VERTICAL AIR CURRENTS
 Microburst vertical wind estimation from horizontal wind measurements [NASA-TP-3460] p 131 N95-18198

VERTICAL LANDING
 STOVL CFD model test case p 115 N95-17881
 Heliport/vertiport MLS precision approaches [AD-A283505] p 126 N95-18059
 VSTOL Systems Research Aircraft (VSRA) Harrier [NASA-TM-110117] p 126 N95-18347

VERTICAL TAKEOFF
 VSTOL Systems Research Aircraft (VSRA) Harrier [NASA-TM-110117] p 126 N95-18347

VERY HIGH FREQUENCIES
 A VHF/UHF antenna for the Precision Antenna Measurement System (PAMS) [AD-A285673] p 156 N95-16621

VIBRATION DAMPING
 H(sup 2)/H(sup INF) controller design for a two-dimensional thin airfoil flutter suppression [BTN-94-EIX94511433918] p 141 A95-64584
 Tuned mass damper for integrally bladed turbine rotor [NASA-CASE-MFS-28697-1] p 159 N95-18325
 Acoustic radiation damping of flat rectangular plates subjected to subsonic flow p 172 N95-18542

VIBRATION ISOLATORS
 Microgravity isolation system design: A case study [NASA-TM-106804] p 104 N95-17657
 Microgravity isolation system design: A modern control synthesis framework [NASA-TM-106805] p 105 N95-18197
 Tuned mass damper for integrally bladed turbine rotor [NASA-CASE-MFS-28697-1] p 159 N95-18325
 Microgravity isolation system design: A modern control analysis framework [NASA-TM-106803] p 105 N95-18486

VIBRATION TESTS
 High-temperature acoustic test facilities and methods p 174 N95-19149
 Nonlinear dynamic response of aircraft structures to acoustic excitation p 135 N95-19151

VIBRATORY LOADS
 Analytical description of and forecast for stress relaxation of aviation materials under the vibration conditions [BTN-94-EIX94461408751] p 126 A95-63634

VIRTUAL REALITY
 Virtual environment application with partial gravity simulation p 169 N95-15988

VISCOUS DRAG
 An analysis code for the Rapid Engineering Estimation of Momentum and Energy Losses (REMEL) [NASA-CR-191178] p 108 N95-16887

VISCOUS FLOW
 A stationary flow of a viscous liquid in radial clearances of rotor bearings in the turbocompressor of an internal combustion engine [BTN-94-EIX94461408765] p 153 A95-63648
 Time accurate computation of unsteady inlet flows with a dynamic flow adaptive mesh [AD-A285498] p 157 N95-16736
 Three dimensional compressible turbulent flow computations for a diffusing S-duct with/without vortex generators [NASA-CR-195390] p 138 N95-17402
 Investigation of the flow over a series of 14 percent-thick supercritical aerofoils with significant rear camber p 109 N95-17849
 Measurements of the flow over a low aspect-ratio wing in the Mach number range 0.6 to 0.87 for the purpose of validation of computational methods. Part 1: Wing design, model construction, surface flow. Part 2: Mean flow in the boundary layer and wake, 4 test cases p 112 N95-17860
 Solution of Navier-Stokes equations using high accuracy monotone schemes p 161 N95-19019
 Simulation of steady and unsteady viscous flows in turbomachinery p 140 N95-19023
 Viscous flow past aerofoils axisymmetric bodies and wings p 123 N95-19457

VISCOUS FLUIDS
 A stationary flow of a viscous liquid in radial clearances of rotor bearings in the turbocompressor of an internal combustion engine [BTN-94-EIX94461408765] p 153 A95-63648

VISUAL FIELDS
 Factors affecting the visual fragmentation of the field-of-view in partial binocular overlap displays [AD-A283081] p 172 N95-17334

VISUAL FLIGHT RULES
 Federal aviation regulations, part 91. General operating and flight rules. Change 5 [PB94-194883] p 123 N95-17476

VISUAL PERCEPTION
 Factors affecting the visual fragmentation of the field-of-view in partial binocular overlap displays [AD-A283081] p 172 N95-17334

VOICE COMMUNICATION
 An analysis of tower (local) controller-pilot voice communications [AD-A283718] p 160 N95-18436

VORTEX ALLEVIATION
 Corner vortex suppressor [AD-D016423] p 116 N95-18337

VORTEX BREAKDOWN
 Numerical simulation of transient vortex breakdown above a pitching delta wing [AD-A281075] p 107 N95-16808
 Navier-Stokes, flight, and wind tunnel flow analysis for the F/A-18 aircraft [NASA-TP-3478] p 120 N95-19114
 Computation of vortex breakdown p 165 N95-19462

VORTEX FILAMENTS
 Computation of vortex breakdown p 165 N95-19462

VORTEX GENERATORS
 Mach number, flow angle, and loss measurements downstream of a transonic fan-blade cascade [AD-A280907] p 108 N95-16824
 Three dimensional compressible turbulent flow computations for a diffusing S-duct with/without vortex generators [NASA-CR-195390] p 138 N95-17402

VORTEX LATTICE METHOD
 Panel methods p 165 N95-19448

VORTEX SHEDDING
 Interaction, bursting and control of vortices of a cropped double-delta wing at high angle of attack [AD-A283656] p 119 N95-18669

VORTICES
 Numerical simulation of transient vortex breakdown above a pitching delta wing [AD-A281075] p 107 N95-16808
 Transonic Navier-Stokes calculations about a 65 deg delta wing [NASA-CR-4635] p 108 N95-17273
 Three dimensional compressible turbulent flow computations for a diffusing S-duct with/without vortex generators [NASA-CR-195390] p 138 N95-17402
 Ellipsoid-cylinder model p 158 N95-17869
 Supersonic vortex flow around a missile body p 114 N95-17870
 Test data on a non-circular body for subsonic, transonic and supersonic Mach numbers p 158 N95-17871
 Wind tunnel test on a 65 deg delta wing with a sharp or rounded leading edge: The international vortex flow experiment p 114 N95-17872

Delta-wing model p 114 N95-17873
 Experimental investigation of the vortex flow over a 76/60-deg double delta wing p 114 N95-17874
 Wind tunnel test on a 65 deg delta wing with rounded leading edges: The International Vortex Flow Experiment p 114 N95-17875
 Investigation of the flow development on a highly swept canard/wing research model with segmented leading- and trailing-edge flaps p 114 N95-17876
 Subsonic flow around US-orbiter model FALKE in the DNW p 115 N95-17877
 Corner vortex suppressor [AD-D016423] p 116 N95-18337
 Aircraft wake vortex takeoff tests at O'Hara International Airport [AD-A283828] p 118 N95-18624
 Interaction, bursting and control of vortices of a cropped double-delta wing at high angle of attack [AD-A283656] p 119 N95-18669
 Development of a multicomponent force and moment balance for water tunnel applications, volume 1 [NASA-CR-4642-VOL-1] p 161 N95-18955
 Navier-Stokes, flight, and wind tunnel flow analysis for the F/A-18 aircraft [NASA-TP-3478] p 120 N95-19114
 Velocity measurements with hot-wires in a vortex-dominated flowfield p 121 N95-19261
 Computation of vortex breakdown p 165 N95-19462

W

WAKES
 Surface pressure and wake drag measurements on the Boeing A4 airfoil in the IAR 1.5X1.5m Wind Tunnel Facility p 110 N95-17850
 Aircraft wake vortex takeoff tests at O'Hara International Airport [AD-A283828] p 118 N95-18624

WALL FLOW
 Wall-signature methods for high speed wind tunnel wall interference corrections p 107 N95-16257
 2-D airfoil tests including side wall boundary layer measurements p 158 N95-17847
 Data from the GARTEur (AD) Action Group 02 airfoil CAST 7/DOA1 experiments p 111 N95-17856
 A supercritical airfoil experiment p 111 N95-17858
 Boundary-flow measurement methods for wall interference assessment and correction: Classification and review p 163 N95-19262
 Adaptive wind tunnel walls versus wall interference correction methods in 2D flows at high blockage ratios p 147 N95-19267
 Interference determination for wind tunnels with slotted walls p 147 N95-19269
 Calculation of low speed wind tunnel wall interference from static pressure pipe measurements p 164 N95-19273
 Analysis of test section sidewall effects on a two dimensional airfoil: Experimental and numerical investigations p 165 N95-19276
 Calculation of wall effects of flow on a perforated wall with a code of surface singularities p 165 N95-19277

WALL PRESSURE
 Wall correction method with measured boundary conditions for low speed wind tunnels p 164 N95-19263
 Estimating wind tunnel interference due to vectored jet flows p 164 N95-19265
 Wall interaction effects for a full-scale helicopter rotor in the NASA Ames 80- by 120-foot wind tunnel p 121 N95-19270

WALL TEMPERATURE
 Regenerative cooling for liquid propellant rocket thrust chambers [INPE-5565-TDI/540] p 150 N95-18720

WALLS
 Wall correction method with measured boundary conditions for low speed wind tunnels p 164 N95-19263
 Computational simulations for some tests in transonic wind tunnels p 164 N95-19264
 Wall interaction effects for a full-scale helicopter rotor in the NASA Ames 80- by 120-foot wind tunnel p 121 N95-19270

WAR GAMES
 ADST system test report for the rotary wing aircraft airmet aeromodel and weapon model merge with the ATAC 2 baseline [AD-A281580] p 127 N95-16171

WASTE ENERGY UTILIZATION
 Gas-turbine engines with increased efficiency of two circuits, due to the use of the utilizing steam-turbine circuit [BTN-94-EIX94461408755] p 153 A95-63638

- WATER FLOW**
The stability of two-phase flow over a swept-wing
[NASA-CR-194994] p 159 N95-18190
- WATER TUNNEL TESTS**
Interaction, bursting and control of vortices of a cropped double-delta wing at high angle of attack
[AD-A283656] p 119 N95-18669
Development of a multicomponent force and moment balance for water tunnel applications, volume 1
[NASA-CR-4642-VOL-1] p 161 N95-18955
Development of a multicomponent force and moment balance for water tunnel applications, volume 2
[NASA-CR-4642-VOL-2] p 161 N95-18956
- WAVE DRAG**
In-flight lift-drag characteristics for a forward-swept wing aircraft and comparisons with contemporary aircraft
[NASA-TP-3414] p 117 N95-18565
- WAVEFORMS**
Waveform bounding and combination techniques for direct drive testing
[AD-A284075] p 161 N95-19035
- WAVEGUIDE ANTENNAS**
Field verification of the wind tunnel coefficients
p 109 N95-17291
- WAVELENGTH DIVISION MULTIPLEXING**
Fiber Optic Control System integration for advanced aircraft. Electro-optic and sensor fabrication, integration, and environmental testing for flight control systems
[NASA-CR-191194] p 162 N95-19236
- WAVRIDERS**
Theoretical investigations of shock/boundary layer interactions on a $Ma(\infty) = 8$ waverider
[DLR-FB-94-12] p 119 N95-18910
- WEAPON SYSTEMS**
ADST system test report for the rotary wing aircraft aimed aeromodel and weapon model merge with the ATAC 2 baseline
[AD-A281580] p 127 N95-16171
Low rate initial production in Army Aviation systems development
[AD-A281871] p 127 N95-16356
- WEAPONS DELIVERY**
A PC-based interactive simulation of the F-111C Pavé Tack system and related sensor, avionics and aircraft aspects
[AD-A285500] p 129 N95-16969
- WEAPONS DEVELOPMENT**
Low rate initial production in Army Aviation systems development
[AD-A281871] p 127 N95-16356
- WEAR**
Static and dynamic friction behavior of candidate high temperature airframe seal materials
[NASA-TM-106571] p 152 N95-16905
- WEAR RESISTANCE**
A CMC database for use in the next generation launch vehicles (rockets)
p 150 N95-18993
- WEAR TESTS**
Evaluation of alternate F-14 wing lug coating
[AD-A283207] p 129 N95-17631
- WEATHER**
Field verification of the wind tunnel coefficients
p 109 N95-17291
- WEIGHT INDICATORS**
An investigation of polynomial calibrations methods for wind tunnel balances
p 144 N95-16258
- WEIGHTING FUNCTIONS**
Plant and controller optimization by convex methods
[AD-A283700] p 133 N95-18621
- WEIGHTLESSNESS**
Virtual environment application with partial gravity simulation
p 169 N95-15988
- WEIGHTLESSNESS SIMULATION**
Users guide for NASA Lewis Research Center DC-9 Reduced-Gravity Aircraft Program
[NASA-TM-106755] p 146 N95-18586
- WHEELS**
Bicarbonate of soda blasting technology for aircraft wheel depainting
[PB94-193323] p 104 N95-17466
- WIND DIRECTION**
Structural effects of unsteady aerodynamic forces on horizontal-axis wind turbines
[DE94-011863] p 157 N95-16939
Field verification of the wind tunnel coefficients
p 109 N95-17291
- WIND EFFECTS**
 $H(\text{sup } 2)/H(\text{sup } 1)$ controller design for a two-dimensional thin airfoil flutter suppression
[BTN-94-EIX94511433918] p 141 A95-64584
- WIND SHEAR**
Microburst vertical wind estimation from horizontal wind measurements
[NASA-TP-3460] p 131 N95-18198
- WIND TUNNEL APPARATUS**
An investigation of polynomial calibrations methods for wind tunnel balances
p 144 N95-16258
Dynamic Stability Instrumentation System (DSIS).
Volume 1: Hardware description
[NASA-TM-109160-VOL-1] p 171 N95-18899
- WIND TUNNEL CALIBRATION**
Free-jet testing at Mach 3.44 in GASL's aero/thermo test facility
p 145 N95-16320
Error propagation equations for estimating the uncertainty in high-speed wind tunnel test results
[DE94-014136] p 145 N95-16509
The traditional and new methods of accounting for the factors distorting the flow over a model in large transonic wind tunnels
p 165 N95-19275
Analysis of test section sidewall effects on a two dimensional airfoil: Experimental and numerical investigations
p 165 N95-19276
Calculation of wall effects of flow on a perforated wall with a code of surface singularities
p 165 N95-19277
Interference corrections for a centre-line plate mount in a porous-walled transonic wind tunnel
p 122 N95-19280
Correction of support influences on measurements with sting mounted wind tunnel models
p 122 N95-19281
- WIND TUNNEL MODELS**
Comparison of computational and experimental results for a supercritical airfoil
[NASA-TM-4601] p 108 N95-16908
Evaluation of combined wall- and support-interference on wind tunnel models
p 122 N95-19278
Interaction of a three strut support on the aerodynamic characteristics of a civil aviation model
p 122 N95-19279
Interference corrections for a centre-line plate mount in a porous-walled transonic wind tunnel
p 122 N95-19280
Correction of support influences on measurements with sting mounted wind tunnel models
p 122 N95-19281
Calculation of support interference in dynamic wind-tunnel tests
p 122 N95-19282
- WIND TUNNEL TESTS**
Experimental study at low supersonic speeds of a missile concept having opposing wraparound tails
[NASA-TM-4582] p 106 N95-16069
An approach to aerodynamic characteristics of low radar cross-section fuselages
p 106 N95-16251
Wall-signature methods for high speed wind tunnel wall interference corrections
p 107 N95-16257
Hypersonic air-breathing aeropropulsion facility test support requirements
p 144 N95-16319
Free-jet testing at Mach 3.44 in GASL's aero/thermo test facility
p 145 N95-16320
Error propagation equations for estimating the uncertainty in high-speed wind tunnel test results
[DE94-014136] p 145 N95-16509
Measurements of unsteady pressure and structural response for an elastic supercritical wing
[NASA-TP-3443] p 104 N95-16560
Structural effects of unsteady aerodynamic forces on horizontal-axis wind turbines
[DE94-011863] p 157 N95-16939
Data acquisition and processing software for the Low Speed Wind Tunnel tests of the Jindivik auxiliary air intake
[AD-A285455] p 108 N95-17178
Field verification of the wind tunnel coefficients
p 109 N95-17291
Active load control during rolling maneuvers — performed in the Langley Transonic Dynamics Tunnel
[NASA-TP-3455] p 129 N95-17397
A selection of experimental test cases for the validation of CFD codes, volume 2
[AGARD-AR-303-VOL-2] p 109 N95-17846
2-D airfoil tests including side wall boundary layer measurements
p 158 N95-17847
Measurements on a two-dimensional aerofoil with high-lift devices
p 109 N95-17848
Investigation of the flow over a series of 14 percent-thick supercritical aerofoils with significant rear camber
p 109 N95-17849
Surface pressure and wake drag measurements on the Boeing A4 airfoil in the IAR 1.5X1.5m Wind Tunnel Facility
p 110 N95-17850
2-D airfoil effectiveness study
p 110 N95-17851
Investigation of an NLF(1)-0416 airfoil in compressible subsonic flow
p 110 N95-17852
Experiments in the trailing edge flow of an NLR 7702 airfoil
p 110 N95-17853
Two-dimensional 16.5 percent thick supercritical airfoil NLR 7301
p 110 N95-17854
Low-speed surface pressure and boundary layer measurement data for the NLR 7301 airfoil section with trailing edge flap
p 111 N95-17855
Data from the GARTEur (AD) Action Group 02 airfoil CAST 7/DOA1 experiments
p 111 N95-17856
- OAT15A airfoil data
p 111 N95-17857
A supercritical airfoil experiment
p 111 N95-17858
Two-dimensional high-lift airfoil data for CFD code validation
p 112 N95-17859
Measurements of the flow over a low aspect-ratio wing in the Mach number range 0.6 to 0.87 for the purpose of validation of computational methods. Part 1: Wing design, model construction, surface flow. Part 2: Mean flow in the boundary layer and wake, 4 test cases
p 112 N95-17860
Detailed study at supersonic speeds of the flow around delta wings
p 112 N95-17861
Pressure distributions on research wing W4 mounted on an axisymmetric body
p 112 N95-17862
DLR-F4 wing body configuration
p 130 N95-17863
DLR-F5: Test wing for CFD and applied aerodynamics
p 113 N95-17864
Low aspect ratio wing experiment
p 113 N95-17865
Wind tunnel investigations of the appearance of shocks in the windward region of bodies with circular cross section at angle of attack
p 113 N95-17866
Three-dimensional boundary layer and flow field data of an inclined prolate spheroid
p 158 N95-17867
Force and pressure data of an ogive-nosed slender body at high angles of attack and different Reynolds numbers
p 113 N95-17868
Ellipsoid-cylinder model
p 158 N95-17869
Supersonic vortex flow around a missile body
p 114 N95-17870
Test data on a non-circular body for subsonic, transonic and supersonic Mach numbers
p 158 N95-17871
Wind tunnel test on a 65 deg delta wing with a sharp or rounded leading edge: The international vortex flow experiment
p 114 N95-17872
Delta-wing model
p 114 N95-17873
Experimental investigation of the vortex flow over a 76/60-deg double delta wing
p 114 N95-17874
Wind tunnel test on a 65 deg delta wing with rounded leading edges: The International Vortex Flow Experiment
p 114 N95-17875
Investigation of the flow development on a highly swept canard/wing research model with segmented leading- and trailing-edge flaps
p 114 N95-17876
Subsonic flow around US-orbiter model FALKE in the DNW
p 115 N95-17877
Low speed propeller slipstream aerodynamic effects
p 116 N95-17882
Wind tunnel performance comparative test results of a circular cylinder and 50 percent ellipse tailboom for circulation control antitorque applications
[AD-A283335] p 130 N95-18008
Overview of unsteady transonic wind tunnel test on a semispan straked delta wing oscillating in pitch
[AD-A284097] p 117 N95-18380
A selection of experimental test cases for the validation of CFD codes. Supplement: Datasets A-E
[AGARD-AR-303-SUPPL] p 117 N95-18539
Pressure measurements on an F/A-18 twin vertical tail in buffeting flow. Volume 4, part 2: Buffet cross spectral densities
[AD-A285555] p 143 N95-18641
Hypersonic wind tunnel test techniques
[AD-A284057] p 118 N95-18663
Static investigation of two fluidic thrust-vectoring concepts on a two-dimensional convergent-divergent nozzle
[NASA-TM-4574] p 120 N95-19042
Navier-Stokes, flight, and wind tunnel flow analysis for the F/A-18 aircraft
[NASA-TP-3478] p 120 N95-19114
2-D and 3-D oscillating wing aerodynamics for a range of angles of attack including stall
[NASA-TM-4632] p 120 N95-19119
Documentation and archiving of the Space Shuttle wind tunnel test data base. Volume 1: Background and description
[NASA-TM-104806-VOL-1] p 151 N95-19237
Wall Interference, Support Interference and Flow Field Measurements
[AGARD-CP-535] p 162 N95-19251
The crucial role of wall interference, support interference and flow field measurements in the development of advanced aircraft configurations
p 162 N95-19252
The utilization of a high speed reflective visualization system in the study of transonic flow over a delta wing
p 121 N95-19259
Transonic and supersonic flowfield measurements about axisymmetric afterbodies for validation of advanced CFD codes
p 121 N95-19260
Determination of solid/porous wall boundary conditions from wind tunnel data for computational fluid dynamics codes
p 164 N95-19266
Adaptive wind tunnel walls versus wall interference correction methods in 2D flows at high blockage ratios
p 147 N95-19267

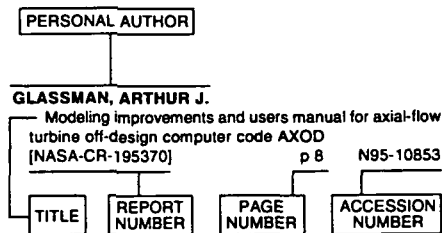
- Development of pneumatic test techniques for subsonic high-lift and in-ground-effect wind tunnel investigations p 121 N95-19268
- Interference determination for wind tunnels with slotted walls p 147 N95-19269
- Wall interaction effects for a full-scale helicopter rotor in the NASA Ames 80- by 120-foot wind tunnel p 121 N95-19270
- Unsteady flow testing in a passive low-correction wind tunnel p 147 N95-19272
- Calculation of low speed wind tunnel wall interference from static pressure pipe measurements p 164 N95-19273
- The traditional and new methods of accounting for the factors distorting the flow over a model in large transonic wind tunnels p 165 N95-19275
- Analysis of test section sidewall effects on a two dimensional airfoil: Experimental and numerical investigations p 165 N95-19276
- Calculation of wall effects of flow on a perforated wall with a code of surface singularities p 165 N95-19277
- Evaluation of combined wall- and support-interference on wind tunnel models p 122 N95-19278
- Interaction of a three strut support on the aerodynamic characteristics of a civil aviation model p 122 N95-19279
- Interference corrections for a centre-line plate mount in a porous-walled transonic wind tunnel p 122 N95-19280
- Correction of support influences on measurements with sting mounted wind tunnel models p 122 N95-19281
- Calculation of support interference in dynamic wind-tunnel tests p 122 N95-19282
- Methods for scaling icing test conditions [NASA-TM-106827] p 124 N95-19284
- WIND TUNNEL WALLS**
- Wall-signature methods for high speed wind tunnel wall interference corrections p 107 N95-16257
- Surface pressure and wake drag measurements on the Boeing A4 airfoil in the IAR 1.5X1.5m Wind Tunnel Facility p 110 N95-17850
- 2-D aileron effectiveness study p 110 N95-17851
- Data from the GARTEur (AD) Action Group 02 airfoil CAST 7/DOA1 experiments p 111 N95-17856
- OAT15A airfoil data p 111 N95-17857
- A supercritical airfoil experiment p 111 N95-17858
- Two-dimensional high-lift airfoil data for CFD code validation p 112 N95-17859
- Wall Interference, Support Interference and Flow Field Measurements [AGARD-CP-535] p 162 N95-19251
- The crucial role of wall interference, support interference and flow field measurements in the development of advanced aircraft configurations p 162 N95-19252
- Boundary-flow measurement methods for wall interference assessment and correction: Classification and review p 163 N95-19262
- Estimating wind tunnel interference due to vectored jet flows p 164 N95-19265
- Determination of solid/porous wall boundary conditions from wind tunnel data for computational fluid dynamics codes p 164 N95-19266
- Adaptive wind tunnel walls versus wall interference correction methods in 2D flows at high blockage ratios p 147 N95-19267
- Interference determination for wind tunnels with slotted walls p 147 N95-19269
- Unsteady flow testing in a passive low-correction wind tunnel p 147 N95-19272
- Analysis of test section sidewall effects on a two dimensional airfoil: Experimental and numerical investigations p 165 N95-19276
- Calculation of wall effects of flow on a perforated wall with a code of surface singularities p 165 N95-19277
- Evaluation of combined wall- and support-interference on wind tunnel models p 122 N95-19278
- WIND TUNNELS**
- STOVL CFD model test case p 115 N95-17881
- Universal wind tunnel data acquisition and reduction software [AD-A283897] p 171 N95-18365
- Hypersonic flight testing [AD-A283981] p 134 N95-18891
- Wall correction method with measured boundary conditions for low speed wind tunnels p 164 N95-19263
- Estimating wind tunnel interference due to vectored jet flows p 164 N95-19265
- Development of pneumatic test techniques for subsonic high-lift and in-ground-effect wind tunnel investigations p 121 N95-19268
- Wall interaction effects for a full-scale helicopter rotor in the NASA Ames 80- by 120-foot wind tunnel p 121 N95-19270
- WIND TURBINES**
- Structural effects of unsteady aerodynamic forces on horizontal-axis wind turbines [DE94-011863] p 157 N95-16939
- Wind turbine blade aerodynamics: The combined experiment [DE94-011866] p 118 N95-18645
- Wind turbine blade aerodynamics: The analysis of field test data [DE94-011867] p 118 N95-18646
- WIND VELOCITY**
- Evaluation of an unlighted swinging airport sign [AD-A284763] p 146 N95-18087
- WIND VELOCITY MEASUREMENT**
- Microburst vertical wind estimation from horizontal wind measurements [NASA-TP-3460] p 131 N95-18198
- WINDPOWER UTILIZATION**
- Structural effects of unsteady aerodynamic forces on horizontal-axis wind turbines [DE94-011863] p 157 N95-16939
- WIND FLAPS**
- Low-speed surface pressure and boundary layer measurement data for the NLR 7301 airfoil section with trailing edge flap p 111 N95-17855
- WING LOADING**
- Active load control during rolling maneuvers — performed in the Langley Transonic Dynamics Tunnel [NASA-TP-3455] p 129 N95-17397
- 2-D aileron effectiveness study p 110 N95-17851
- Fight testing high lateral asymmetries on highly augmented Fighter/Attack aircraft [AD-A284206] p 130 N95-17953
- Determination of stores pointing error due to wing flexibility under flight load [NASA-TM-4646] p 134 N95-19044
- Development of load spectra for Airbus A330/A340 full scale fatigue tests p 135 N95-19479
- WING OSCILLATIONS**
- A computational investigation of wake-induced airfoil flutter in incompressible flow and active flutter control [AD-A281534] p 142 N95-16109
- 2-D and 3-D oscillating wing aerodynamics for a range of angles of attack including stall [NASA-TM-4632] p 120 N95-19119
- WING PANELS**
- Fatigue and residual strength investigation of ARALL(R) -3 and GLARE(R) -2 panels with bonded stringers p 137 N95-19495
- WING SLOTS**
- Numerical simulation of dynamic-stall suppression by tangential blowing [AD-A284887] p 120 N95-19110
- WING TANKS**
- Determination of stores pointing error due to wing flexibility under flight load [NASA-TM-4646] p 134 N95-19044
- WINGS**
- Aerodynamic shape optimization p 128 N95-16572
- Investigation of the influence of pylons and stores on the wing lower surface flow p 116 N95-17885
- Wing design for a civil tiltrotor transport aircraft [NASA-CR-197523] p 130 N95-18090
- Parametric study on laminar flow for finite wings at supersonic speeds [NASA-TM-108852] p 116 N95-18101
- Course module for AA201: Wing structural design project [AD-A283618] p 133 N95-18616
- The accuracy of parameter estimation in system identification of noisy aircraft load measurement [NASA-CR-197516] p 134 N95-19130
- Development of load spectra for Airbus A330/A340 full scale fatigue tests p 135 N95-19479
- WIRING**
- Problems with aging wiring in Naval aircraft p 154 N95-16048
- WOOD**
- Development of processes, means, and theoretical principles of thin-walled detail plastic forming at Kazan Aviation Institute p 155 N95-16281
- WORKSTATIONS**
- A workstation based simulator for teaching compressible aerodynamics [NASA-TM-106799] p 170 N95-16906
- Operational And Supportability Implementation System (OASIS) test and evaluation master plan [AD-A284765] p 126 N95-18088
- X**
- X-29 AIRCRAFT**
- X-29 high-angle-of-attack [BTN-94-EI94511309383] p 127 A95-64609
- In-flight lift-drag characteristics for a forward-swept wing aircraft and comparisons with contemporary aircraft [NASA-TP-3414] p 117 N95-18565
- Y**
- YAW**
- Development of a multicomponent force and moment balance for water tunnel applications, volume 2 [NASA-CR-4642-VOL-2] p 161 N95-18956
- YAWING MOMENTS**
- Static aerodynamics CFD analysis for 120-mm hypersonic KE projectile design [ARL-MR-184] p 118 N95-18611
- Development of a multicomponent force and moment balance for water tunnel applications, volume 1 [NASA-CR-4642-VOL-1] p 161 N95-18955
- YIELD POINT**
- Fatigue life until small cracks in aircraft structures: Durability and damage tolerance p 135 N95-19478
- Z**
- ZIRCONIUM OXIDES**
- Quality optimization of thermally sprayed coatings produced by the JP-5000 (HVOF) gun using mathematical modeling p 152 N95-19008

PERSONAL AUTHOR INDEX

AERONAUTICAL ENGINEERING / A Continuing Bibliography (Supplement 316)

April 1995

Typical Personal Author Index Listing



Listings in this index are arranged alphabetically by personal author. The title of the document is used to provide a brief description of the subject matter. The report number helps to indicate the type of document (e.g., NASA report, translation, NASA contractor report). The page and accession numbers are located beneath and to the right of the title. Under any one author's name the accession numbers are arranged in sequence.

A

- ABSIL, L. H. J.**
Experiments in the trailing edge flow of an NLR 7702 airfoil p 110 N95-17853
- ABUMERI, GALIB**
Technology Benefit Estimator (T/BEST): User's manual [NASA-TM-106785] p 167 N95-19501
- ADAMS, RICHARD J.**
Design of nonlinear control laws for high-angle-of-attack flight [BTN-94-EIX94511433920] p 141 A95-64586
- ADKISSON, LORI**
Identification of Artificial Intelligence (AI) applications for maintenance, monitoring, and control of airway facilities [AD-A282479] p 125 N95-17373
- AFANAS'EV, I. V.**
New approach to geometric profiling of the design elements of the passage part in turbo-machines [BTN-94-EIX94461408769] p 153 A95-63652
- AGARWAL, R. K.**
Aeromechanics technology, volume 1. Task 1: Three-dimensional Euler/Navier-Stokes Aerodynamic Method (TEAM) enhancements [AD-A285713] p 132 N95-18483
Transonic wind tunnel boundary interference correction p 147 N95-19271
- AGRELL, JOHAN**
Transonic and supersonic flowfield measurements about axisymmetric afterbodies for validation of advanced CFD codes p 121 N95-19260
- AGRELL, NADA**
Computational simulations for some tests in transonic wind tunnels p 164 N95-19264
- AIBEL, DAVID W.**
New technologies for space avionics [NASA-CR-197574] p 150 N95-18196
- ALEM, NABIH M.**
A correlative investigation of simulated occupant motion and accident report in a helicopter crash [AD-A285190] p 123 N95-16404
- ALEXANDROV, NATALIA**
Algorithms for bilevel optimization [NASA-CR-194980] p 170 N95-16897

- ALKHOZAM, ABDULLAH M.**
Interaction, bursting and control of vortices of a cropped double-delta wing at high angle of attack [AD-A283656] p 119 N95-18669
- ALLAIRE, P. E.**
Microgravity isolation system design: A case study [NASA-TM-106804] p 104 N95-17657
Microgravity isolation system design: A modern control synthesis framework [NASA-TM-106805] p 105 N95-18197
Microgravity isolation system design: A modern control analysis framework [NASA-TM-106803] p 105 N95-18486
- ALLEN, JERRY M.**
Experimental study at low supersonic speeds of a missile concept having opposing wraparound tails [NASA-TM-4582] p 106 N95-16069
- ALMANZA, JOE**
ADST system test report for the rotary wing aircraft airnet aeromodel and weapon model merge with the ATAC 2 baseline [AD-A281580] p 127 N95-16171
- ALMOSONO, D.**
Calculation of support interference in dynamic wind-tunnel tests p 122 N95-19282
- ANDERSON, BERNHARD H.**
Numerical simulation of supersonic compression corners and hypersonic inlet flows using the RPLUS2D code [NASA-TM-106580] p 105 N95-16038
- ANDERSON, DAVID N.**
Methods for scaling icing test conditions [NASA-TM-106827] p 124 N95-19284
Ice accretion with varying surface tension [NASA-TM-106826] p 124 N95-19285
- ANDERSON, W. KYLE**
A grid generation and flow solution method for the Euler equations on unstructured grids [HTN-95-20003] p 153 A95-63201
- ANKENY, ALAN E.**
Evaluation of alternate F-14 wing lug coating [AD-A283207] p 129 N95-17631
- ANNIS, CHARLES**
Fatigue in single crystal nickel superalloys [AD-A285727] p 152 N95-18068
- ANON**
Aircraft safety evaluation [BTN-94-EIX94511309382] p 103 A95-64608
X-29 high-angle-of-attack [BTN-94-EIX94511309383] p 127 A95-64609
Fiber-optic technology for transport aircraft [BTN-94-EIX94511309384] p 103 A95-64610
- ANTLEY, MICHAEL**
Assessing aircraft survivability to high frequency transient threats [AD-A283999] p 134 N95-18726
- APOSTOLAKIS, G.**
Demonstration of the Dynamic Flowgraph Methodology using the Titan 2 Space Launch Vehicle Digital Flight Control System [NASA-CR-197517] p 150 N95-17493
- ARCHAMBAUD, J. P.**
Data from the GARTEur (AD) Action Group 02 airfoil CAST 7/DQA1 experiments p 111 N95-17856
OAT15A airfoil data p 111 N95-17857
Analysis of test section sidewall effects on a two dimensional airfoil: Experimental and numerical investigations p 165 N95-19276
- ARTS, TONY**
Aerodynamic investigation of the flow field in a 180 deg turn channel with sharp bend p 163 N95-19257
- ASHILL, P. R.**
Investigation of the flow over a series of 14 percent-thick supercritical aerofoils with significant rear camber p 109 N95-17849
- Boundary-flow measurement methods for wall interference assessment and correction: Classification and review p 163 N95-19262
- ASOK, RAY**
Output feedback control under randomly varying distributed delays [BTN-94-EIX94511433916] p 168 A95-64582

- ATLURI, SATYA N.**
Residual life and strength estimates of aircraft structural components with MSD/MED p 136 N95-19485
- AUSTIN, JEFFREY G.**
Mach number, flow angle, and loss measurements downstream of a transonic fan-blade cascade [AD-A280907] p 108 N95-16824
- AYER, T. C.**
Unsteady aerodynamic analyses for turbomachinery aeroelastic predictions p 141 N95-19381
- AYERS, BERT F.**
Development of a multicomponent force and moment balance for water tunnel applications, volume 1 [NASA-CR-4642-VOL-1] p 161 N95-18955
Development of a multicomponent force and moment balance for water tunnel applications, volume 2 [NASA-CR-4642-VOL-2] p 161 N95-18956

B

- BACHMANN, GLEN R.**
H(sup 2)/H(sup INF) controller design for a two-dimensional thin airfoil flutter suppression [BTN-94-EIX94511433918] p 141 A95-64584
- BAECKLUND, K.**
Military aviation maintenance industry in Western Europe: Concentration and internationalization [PB94-189180] p 104 N95-17451
- BAHM, CATHERINE M.**
Determination of stores pointing error due to wing flexibility under flight load [NASA-TM-4646] p 134 N95-19044
- BAILEY, JEFF**
Field and data analysis studies related to the atmospheric environment [NASA-CR-196543] p 168 N95-18093
- BAINS, JANE C.**
Nonlinear analysis of damaged stiffened fuselage shells subjected to combined loads p 137 N95-19499
- BAKHLE, MILIND A.**
FPCAS2D user's guide, version 1.0 [NASA-CR-195413] p 156 N95-16588
- BALASHOV, I. N.**
On a program-information system TDsoft [BTN-94-EIX94461408773] p 175 A95-63656
- BALDERSON, KEITH A.**
Comparison of frequency response and perturbation methods to extract linear models from a nonlinear simulation [AD-A284115] p 146 N95-18405
- BANDA, SIVA S.**
Design of nonlinear control laws for high-angle-of-attack flight [BTN-94-EIX94511433920] p 141 A95-64586
- BANDYOPADHYAY, PROMODE R.**
Corner vortex suppressor [AD-D016423] p 116 N95-18337
- BANFORD, MICHAEL**
Pressure measurements on an F/A-18 twin vertical tail in buffeting flow. Volume 4, part 2: Buffet cross spectral densities [AD-A285555] p 143 N95-18641
- BANNINK, W. J.**
The utilization of a high speed reflective visualization system in the study of transonic flow over a delta wing p 121 N95-19259
- BAO, JINSONG**
Investigation of dynamic inflow's influence on rotor control derivatives p 155 N95-16250
- BARBERIS, D.**
Ellipsoid-cylinder model p 158 N95-17869
Supersonic vortex flow around a missile body p 114 N95-17870
- Delta-wing model p 114 N95-17873
- BARKER, WILLIAM P.**
Hydrofoil force balance [AD-D016475] p 160 N95-18461
- BARNETT, M.**
Unsteady aerodynamic analyses for turbomachinery aeroelastic predictions p 141 N95-19381

BARTELHEIMER, W.
2-D airfoil tests including side wall boundary layer measurements p 158 N95-17847

BASCIANI, M.
Adaptive wind tunnel walls versus wall interference correction methods in 2D flows at high blockage ratios p 147 N95-19267

BASHKIRTSEV, A. V.
Modelling for optimal operations of line milling of aerodynamic surfaces [BTN-94-EIX94461408774] p 138 A95-63657

BASSO, GORDON L.
Noise transmission and reduction in turboprop aircraft p 175 N95-19164

BATTIS, J. C.
The effects of aircraft (B-52) overflights on ancient structures [BTN-94-EIX94341340070] p 171 A95-63522

BAUMERT, W.
Pressure distribution measurements on an isolated TPS 441 nacelle p 115 N95-17878

BAYERDOERFER, G.
Design and operation of a thermoacoustic test facility p 147 N95-19150

BEALE, DAVID G.
A correlative investigation of simulated occupant motion and accident report in a helicopter crash [AD-A285190] p 123 N95-16404

BEASLEY, HOWARD H.
Factors affecting the visual fragmentation of the field-of-view in partial binocular overlap displays [AD-A283081] p 172 N95-17334

BEDOYA, CARLOS A.
Fiber Optic Control System integration for advanced aircraft. Electro-optic and sensor fabrication, integration, and environmental testing for flight control systems [NASA-CR-191194] p 162 N95-19236

BENNER, WILLIAM E.
Operational And Supportability Implementation System (OASIS) test and evaluation master plan [AD-A284765] p 126 N95-18088

BENNEY, RICHARD J.
Parachute inflation: A problem in aeroelasticity [AD-A284375] p 117 N95-18340

BENOIT, ANDRE
On-line handling of air traffic: Management, guidance and control [AGARD-AG-321] p 126 N95-18927

BENSON, RUSTY A.
Time accurate computation of unsteady inlet flows with a dynamic flow adaptive mesh [AD-A285498] p 157 N95-16736

BENSON, THOMAS J.
A workstation based simulator for teaching compressible aerodynamics [NASA-TM-106799] p 170 N95-16906
Interactive computer graphics applications for compressible aerodynamics [NASA-TM-106802] p 170 N95-17264

BERRIER, BOBBY L.
Single-engine tail interference model p 115 N95-17879

BESS, PHILIP K.
Spread spectrum applications in unmanned aerial vehicles [AD-A281035] p 156 N95-16448

BEUTNER, THOMAS J.
Determination of solid/porous wall boundary conditions from wind tunnel data for computational fluid dynamics codes p 164 N95-19266

BI, NAI-PEI
Experimental data on the aerodynamic interactions between a helicopter rotor and an airframe p 116 N95-17883

BIDWELL, COLIN S.
Collection efficiency and ice accretion calculations for a sphere, a swept MS(1)-317 wing, a swept NACA-0012 wing tip, an axisymmetric inlet, and a Boeing 737-300 [NASA-TM-106831] p 123 N95-18582

BILANIN, ALAN J.
Ice accretion with varying surface tension [NASA-TM-106826] p 124 N95-19285

BILLICA, R. D.
A surgical support system for Space Station Freedom p 149 N95-16776

BISCHOF, C.
Applications of automatic differentiation in computational fluid dynamics p 156 N95-16461

BISCHOF, C. H.
Applications of automatic differentiation in CFD [NASA-TM-109948] p 157 N95-16828

BISWAS, RUPAK
Mesh quality control for multiply-refined tetrahedral grids [NASA-CR-197595] p 160 N95-18737

BLEVINS, ROBERT D.
Thermo-acoustic fatigue design for hypersonic vehicle skin panels p 162 N95-19161

BODONYI, RICHARD J.
Wing-body juncture flows [AD-A281526] p 106 N95-16099

BOER, RUUD G. DEN
Overview of unsteady transonic wind tunnel test on a semispan straked delta wing oscillating in pitch [AD-A284097] p 117 N95-18380

BONNET, A.
Interaction of a three strut support on the aerodynamic characteristics of a civil aviation model p 122 N95-19279

BOTTS, MICHAEL
Field and data analysis studies related to the atmospheric environment [NASA-CR-196543] p 168 N95-18093

BOWDEN, FRED D.
A PC-based interactive simulation of the F-111C Pavé Tack system and related sensor, avionics and aircraft aspects [AD-A285500] p 129 N95-16969

BOYDEN, R. P.
Dynamic Stability Instrumentation System (DSIS). Volume 1: Hardware description [NASA-TM-109160-VOL-1] p 171 N95-18899

BRAY, G. H.
Prediction of R-curves from small coupon tests p 167 N95-19496

BREITSAMTER, CHRISTIAN
Velocity measurements with hot-wires in a vortex-dominated flowfield p 121 N95-19261

BRINK-SPALINK, J.
Treatment of non-linear systems by timeplane-transformed CT methods: The spectral gust method p 143 N95-18600

BRITT, VICKI O.
Nonlinear analysis of damaged stiffened fuselage shells subjected to combined loads p 137 N95-19499

BROWN, DANSEN
Pressure measurements on an F/A-18 twin vertical tail in buffeting flow. Volume 4, part 2: Buffet cross spectral densities [AD-A285555] p 143 N95-18641

BROWN, STEVE WESLEY
Documentation and archiving of the Space Shuttle wind tunnel test data base. Volume 1: Background and description [NASA-TM-104806-VOL-1] p 151 N95-19237

BRUCATO, ROBERT
Unmanned aerial vehicle heavy fuel engine test [AD-A284332] p 139 N95-18383

BRUMBAUGH, RANDAL W.
Aircraft model for the AIAA controls design challenge [BTN-94-EIX94511433921] p 142 A95-64587

BRUNE, G. W.
Two-dimensional high-lift airfoil data for CFD code validation p 112 N95-17859

BRUNEAU, STEPHEN D.
A Lifting Ball Valve for cryogenic fluid applications p 156 N95-16349

BUCCI, R. J.
Prediction of R-curves from small coupon tests p 167 N95-19496

BUECHLER, DENNIS
Field and data analysis studies related to the atmospheric environment [NASA-CR-196543] p 168 N95-18093

BUETEFISCH, K. A.
Wind tunnel test on a 65 deg delta wing with rounded leading edges: The International Vortex Flow Experiment p 114 N95-17875

BUFFINGTON, JAMES M.
Design of nonlinear control laws for high-angle-of-attack flight [BTN-94-EIX94511433920] p 141 A95-64586

BUKOV, A.
Optical surface pressure measurements: Accuracy and application field evaluation p 175 N95-19274

BURDETTE, GEORGE W.
Solid fuel ramjet composition [AD-D016458] p 152 N95-19090

BURNETTE, KEITH T.
An evaluation of aircraft CRT and dot-matrix display legibility requirements [AD-A283933] p 138 N95-18164

BURNHAM, D.
Aircraft wake vortex takeoff tests at O'Hara International Airport [AD-A283828] p 118 N95-18624

BURRIS, STEPHEN A.
Course module for AA201: Wing structural design project [AD-A283618] p 133 N95-18616

BURT, MARTIN
Transonic and supersonic flowfield measurements about axisymmetric afterbodies for validation of advanced CFD codes p 121 N95-19260

BUTLER, BARCLAY P.
A correlative investigation of simulated occupant motion and accident report in a helicopter crash [AD-A285190] p 123 N95-16404

BUTTS, D. G.
Aircraft stress sequence development: A complex engineering process made simple p 136 N95-19480

C

CAIN, ALAN B.
Modelling structurally damaging twin-jet screech p 135 N95-19154

CALEDONIA, GEORGE E.
Ultraviolet emissions occurring about hypersonic vehicles in rarefied flows [AD-A281452] p 106 N95-16076

CAMACHO, Y.
A study of the effect of store unsteady aerodynamics on gust and turbulence loads p 133 N95-18601

CAMPBELL, FRANK J.
Problems with aging wiring in Naval aircraft p 154 N95-16048

CAMPBELL, M. R.
A surgical support system for Space Station Freedom p 149 N95-16776

CARDIN, JOSEPH M.
A Lifting Ball Valve for cryogenic fluid applications p 156 N95-16349

CARDOSI, KIM M.
An analysis of tower (local) controller-pilot voice communications [AD-A283718] p 160 N95-18436

CARLE, A.
Applications of automatic differentiation in computational fluid dynamics p 156 N95-16461
Applications of automatic differentiation in CFD [NASA-TM-109948] p 157 N95-16828

CASALENGUA, J.
A study of the effect of store unsteady aerodynamics on gust and turbulence loads p 133 N95-18601

CELIK, ZEKI Z.
Determination of solid/porous wall boundary conditions from wind tunnel data for computational fluid dynamics codes p 164 N95-19266

CHAMIS, CHRISTOS C.
Optimization of adaptive intraply hybrid fiber composites with reliability considerations p 157 N95-16911
Technology Benefit Estimator (T/BEST): User's manual [NASA-TM-106785] p 167 N95-19501

CHAMPIGNY, P.
Test data on a non-circular body for subsonic, transonic and supersonic Mach numbers p 158 N95-17871

CHAPMAN, DEAN R.
High altitude hypersonic flowfield radiation [AD-A281386] p 106 N95-16160

CHAVIARPOPOULOS, P.
Single-pass method for the solution of inverse potential and rotational problems. Part 1: 2-D and quasi 3-D theory and application p 107 N95-16563
Single-pass method for the solution of inverse potential and rotational problems. Part 2: Fully 3-D potential theory and applications p 107 N95-16564

CHEN, A. S. C.
Bicarbonate of soda blasting technology for aircraft wheel depainting [PB94-193323] p 104 N95-17466

CHEN, FULIAN
Direct splitting of coefficient matrix for numerical calculation of transonic nozzle flow [BTN-94-EIX94481415356] p 103 A95-65346

CHEN, G.
Linear instability waves in supersonic jets confined in circular and non-circular ducts [BTN-94-EIX94341340068] p 103 A95-63520

CHIN, V. D.
2-D airfoil effectiveness study p 110 N95-17851

CHO, SOO-YONG
Three dimensional compressible turbulent flow computations for a diffusing S-duct with/without vortex generators [NASA-CR-195390] p 138 N95-17402

CHRISTENSEN, PAUL E.
Recent advances in graphite/epoxy motor cases p 149 N95-16333

CLARK, C. M.
Flight testing high lateral asymmetries on highly augmented Fighter/Attack aircraft [AD-A284206] p 130 N95-17953

- CLARK, E. L.**
Error propagation equations for estimating the uncertainty in high-speed wind tunnel test results [DE94-014136] p 145 N95-16509
- CLIMENT, H.**
A study of the effect of store unsteady aerodynamics on gust and turbulence loads p 133 N95-18601
- COLLINS, LAURIE**
Field and data analysis studies related to the atmospheric environment [NASA-CR-196543] p 168 N95-18093
- CORNWELL, MICHAEL D.**
Thermal chemical energy of ablating silica surfaces in air breathing solid rocket engines p 148 N95-16316
- COWARD, ADRIAN**
The stability of two-phase flow over a swept-wing [NASA-CR-194994] p 159 N95-18190
- CRANS, BEREND J. H.**
EC Aviation Scene [HTN-95-50223] p 176 A95-64860
- CRAS, STEVEN P.**
EC Aviation Scene [HTN-95-50223] p 176 A95-64860
- CREASMAN, F.**
Transonic wind tunnel boundary interference correction p 147 N95-19271
- CRESCI, D.**
Free-jet testing at Mach 3.44 in GASL's aero/thermo test facility p 145 N95-16320
- CRITES, R. C.**
The crucial role of wall interference, support interference and flow field measurements in the development of advanced aircraft configurations p 162 N95-19252
Transonic wind tunnel boundary interference correction p 147 N95-19271
- CUI, JIYA**
Improved analytical solution for varying specific heat parallel stream mixing [BTN-94-EIX94481415349] p 103 A95-65339
- CUMMINS, R. J.**
Application of superplastically formed and diffusion bonded structures in high intensity noise environments p 174 N95-19162
- CUNNINGHAM, ATLEE M., JR.**
Overview of unsteady transonic wind tunnel test on a semispan straked delta wing oscillating in pitch [AD-A284097] p 117 N95-18380
- CURETON, K. L.**
Strategic avionics technology definition studies. Subtask 3-1A3: Electrical Actuation (ELA) Systems Test Facility [NASA-CR-188360] p 143 N95-18567
- D**
- DACRES, CHESTER M.**
The use of electrochemistry and ellipsometry for identifying and evaluating corrosion on aircraft [AD-A285323] p 151 N95-16371
- DALLE-MURA, E.**
Impact of noise environment on engine nacelle design p 173 N95-19147
- DANIELS, T. S.**
Dynamic Stability Instrumentation System (DSIS). Volume 1: Hardware description [NASA-TM-109160-VOL-1] p 171 N95-18899
- DANIELSON, ARNOLD O.**
Integrated aerodynamic fin and stowable TVC vane system [AD-D016457] p 151 N95-19073
- DAVIES, MIKE**
A PC-based interactive simulation of the F-111C Pave Tack system and related sensor, avionics and aircraft aspects [AD-A285500] p 129 N95-16969
- DECHANT, LAWRENCE J.**
An analysis code for the Rapid Engineering Estimation of Momentum and Energy Losses (REMEL) [NASA-CR-191178] p 108 N95-16887
- DECKER, HARRY J.**
Detecting gear tooth fracture in a high contact ratio face gear mesh [NASA-TM-106822] p 162 N95-19125
- DEDOUSSIS, V.**
Single-pass method for the solution of inverse potential and rotational problems. Part 1: 2-D and quasi 3-D theory and application p 107 N95-16563
Single-pass method for the solution of inverse potential and rotational problems. Part 2: Fully 3-D potential theory and applications p 107 N95-16564
- DEESE, J. E.**
Transonic wind tunnel boundary interference correction p 147 N95-19271
- DEGTYAREV, G. L.**
Joint Proceedings on Aeronautics and Astronautics (JPAA) [ISBN-7-80-046602-7] p 104 N95-16249
- DELFRATE, JOHN H.**
Development of a low-aspect ratio fin for flight research experiments [NASA-TM-4596] p 108 N95-16858
- DELLACORTE, C.**
Static and dynamic friction behavior of candidate high temperature airframe seal materials [NASA-TM-106571] p 152 N95-16905
- DELUCA, DANIEL P.**
Fatigue in single crystal nickel superalloys [AD-A285727] p 152 N95-18068
- DENNIS, J. E., JR.**
Algorithms for bilevel optimization [NASA-CR-194980] p 170 N95-16897
- DEPASQUALE, WILLIAM**
E-6A hardness assurance, maintenance and surveillance program [AD-A283994] p 134 N95-19067
- DESAI, S. S.**
Viscous flow past aerofoils axisymmetric bodies and wings p 123 N95-19457
- DIETZ, G.**
Investigation of an NLF(1)-0416 airfoil in compressible subsonic flow p 110 N95-17852
- DIMANLIG, ARSENIO C. B.**
Numerical simulation of helicopter engine plume in forward flight [NASA-CR-197488] p 107 N95-16589
- DINGUS, PETER**
New technologies for space avionics [NASA-CR-197574] p 150 N95-18196
- DITTMAR, JAMES H.**
Background noise levels measured in the NASA Lewis 9- by 15-foot low-speed wind tunnel [NASA-TM-106817] p 145 N95-18054
- DJOMEHRI, M. JAHED**
An assessment of the adaptive unstructured tetrahedral grid, Euler Flow Solver Code FELISA [NASA-TP-3526] p 119 N95-19041
- DOMINIK, C. J.**
2-D airfoil effectiveness study p 110 N95-17851
- DONOHUE, S. R.**
The utilization of a high speed reflective visualization system in the study of transonic flow over a delta wing p 121 N95-19259
- DONTAS, KEJITAN**
Identification of Artificial Intelligence (AI) applications for maintenance, monitoring, and control of airway facilities [AD-A282479] p 125 N95-17373
- DOR, J. B.**
Experimental techniques for measuring transonic flow with a three dimensional laser velocimetry system. Application to determining the drag of a fuselage p 163 N95-19258
- DREGALIN, A. F.**
On a program-information system TDsoft [BTN-94-EIX94461408773] p 175 A95-63656
Service and physical properties of liquid-jet fuels p 151 N95-16256
- DRESS, D. A.**
Dynamic Stability Instrumentation System (DSIS). Volume 1: Hardware description [NASA-TM-109160-VOL-1] p 171 N95-18899
- DRNEVICH, R. F.**
Airborne rotary separator study [NASA-CR-191045] p 150 N95-16743
- DUNGAN, G. D.**
Flight testing high lateral asymmetries on highly augmented Fighter/Attack aircraft [AD-A284206] p 130 N95-17953
- DUQUE, EARL P. N.**
Numerical simulation of helicopter engine plume in forward flight [NASA-CR-197488] p 107 N95-16589
- DURAND, JEAN-CLAUDE**
A processing centre for the CNES CE-GPS experimentation p 125 N95-17196
- DUYAR, AHMET**
Sensor fault detection and diagnosis simulation of a helicopter engine in an intelligent control framework [NASA-TM-106784] p 137 N95-15970
- E**
- ECKERT, D.**
Correction of support influences on measurements with sting mounted wind tunnel models p 122 N95-19281
- ECKSTROM, CLINTON V.**
Measurements of unsteady pressure and structural response for an elastic supercritical wing [NASA-TP-3443] p 104 N95-16560
- EGGLESTON, DEBRA S.**
The 1993 JANNAF Propulsion Meeting, volume 1 [CPIA-PUBL-602-VOL-1] p 148 N95-16312
- EHRHART, JOHN E., JR.**
KC-135 cockpit modernization study. Phase 1: Equipment evaluation [AD-A284099] p 131 N95-18398
- ELSENAAR, A.**
Wind tunnel test on a 65 deg delta wing with a sharp or rounded leading edge: The international vortex flow experiment p 114 N95-17872
- EMIN, O. N.**
Gas-turbine engines with increased efficiency of two circuits, due to the use of the utilizing steam-turbine circuit [BTN-94-EIX94461408755] p 153 A95-63638
- ENGLAR, ROBERT J.**
Development of pneumatic test techniques for subsonic high-lift and in-ground-effect wind tunnel investigations p 121 N95-19268
- ERICKSON, LARRY L.**
An assessment of the adaptive unstructured tetrahedral grid, Euler Flow Solver Code FELISA [NASA-TP-3526] p 119 N95-19041
- ESCH, H.**
Wind tunnel investigations of the appearance of shocks in the windward region of bodies with circular cross section at angle of attack p 113 N95-17866
- EVERETT, WIN**
Preliminary evaluation of the F/A-18 quantity/multiple envelope expansion [AD-A284119] p 132 N95-18407
- EVERSMAN, WALTER**
Ducted fan acoustic radiation including the effects of nonuniform mean flow and acoustic treatment [NASA-CR-197449] p 172 N95-16401
- F**
- FERGUSON, CHRIS J.**
Application of photogrammetry of F-14D store separation [AD-A284154] p 132 N95-18417
- FERMAN, M. A.**
Acoustic fatigue characteristics of advanced materials and structures p 174 N95-19157
- FERNKRANS, LARS**
Calculation of low speed wind tunnel wall interference from static pressure pipe measurements p 164 N95-19273
- FERRANTI, RICHARD L.**
Solid state radar demonstration test results at the FAA Technical Center [AD-A281520] p 154 N95-16097
- FERRI, P.**
EURECA mission control experience and messages for the future p 149 N95-17252
- FILIPENCO, V.**
Unsteady flow phenomena in discrete passage diffusers for centrifugal compressors [AD-A281412] p 155 N95-16163
- FIRMIN, M. C. P.**
Measurements of the flow over a low aspect-ratio wing in the Mach number range 0.6 to 0.87 for the purpose of validation of computational methods. Part 1: Wing design, model construction, surface flow. Part 2: Mean flow in the boundary layer and wake, 4 test cases p 112 N95-17860
- FISHER, DAVID T.**
Wind tunnel performance comparative test results of a circular cylinder and 50 percent ellipse tailboom for circulation control antitorque applications [AD-A283355] p 130 N95-18008
- FOGG, DAVID A.**
A PC-based interactive simulation of the F-111C Pave Tack system and related sensor, avionics and aircraft aspects [AD-A285500] p 129 N95-16969
- FRANCINI, R. B.**
Ultrasonic techniques for repair of aircraft structures with bonded composite patches p 136 N95-19486
- FRANSEN, WIEGER**
Atmospheric effects of high-flying subsonic aircraft: A catalogue of perturbing influences [KNMI-SR-94-03] p 168 N95-18722
- FRAZIER, SAMUEL**
Waveform bounding and combination techniques for direct drive testing [AD-A284075] p 161 N95-19035
- FRAZIER, SAMUEL J.**
Assessing aircraft survivability to high frequency transient threats [AD-A283999] p 134 N95-18726

FREESTONE, M. M.

FREESTONE, M. M.
Interference determination for wind tunnels with slotted walls p 147 N95-19269

FREYBERG, L.
Design and operation of a thermoacoustic test facility p 147 N95-19150

FRITSCH, BENT
Flow field investigation in a free jet - free jet core system for the generation of high intensity molecular beams [DLR-FB-94-11] p 172 N95-18912

FULKER, J. L.
Pressure distributions on research wing W4 mounted on an axisymmetric body p 112 N95-17862

G

GALWAY, ROBIN D.
Interference corrections for a centre-line plate mount in a porous-walled transonic wind tunnel p 122 N95-19280

GARCIA-AVELLO, C.
On-line handling of air traffic: Management, guidance and control [AGARD-AG-321] p 126 N95-18927

GARCIA, JOSEPH AVILA
Parametric study on laminar flow for finite wings at supersonic speeds [NASA-TM-108852] p 116 N95-18101

GAUNTNER, JIM W.
NASA Lewis Research Center Workshop on Forced Response in Turbomachinery [NASA-CP-10147] p 141 N95-19380

GAWRONSKI, W. K.
Field verification of the wind tunnel coefficients p 109 N95-17291

GAYNOR, T. L.
Program test objectives milestone 3 [NASA-CR-197030] p 127 N95-15971

GEERING, HANS P.
Test bench for rotorcraft hover control [BTN-94-EIX94511433919] p 169 A95-64585

GENERAZIO, EDWARD R.
Technology Benefit Estimator (T/BEST): User's manual [NASA-TM-106785] p 167 N95-19501

GETSON, E. S.
Application of photogrammetry of F-14D store separation [AD-A284154] p 132 N95-18417

GHAFFARI, FARHAD
Navier-Stokes, flight, and wind tunnel flow analysis for the F/A-18 aircraft [NASA-TP-3478] p 120 N95-19114

GIELDA, T. P.
Aeromechanics technology, volume 1. Task 1: Three-dimensional Euler/Navier-Stokes Aerodynamic Method (TEAM) enhancements [AD-A285713] p 132 N95-18483

GIESKE, J. H.
Evaluation of scanners for C-scan imaging in nondestructive inspection of aircraft [DE94-012473] p 152 N95-19100

GIUFFRE, G.
Impact of noise environment on engine nacelle design p 173 N95-19147

GIUZIO, R.
Impact of noise environment on engine nacelle design p 173 N95-19147

An overall approach of cockpit noise verification in a military aircraft p 175 N95-19163

GLASER, JOHN
A review of gust load calculation methods at de Havilland p 118 N95-18604

GLASSMAN, ARTHUR J.
Enhanced capabilities and modified users manual for axial-flow compressor conceptual design code CSPAN [NASA-TM-106833] p 119 N95-18933

GOGGIN, PATRICK J.
Comparison of stochastic and deterministic nonlinear gust analysis methods to meet continuous turbulence criteria p 133 N95-18602

GOODEN, J. H. M.
Low-speed surface pressure and boundary layer measurement data for the NLR 7301 airfoil section with trailing edge flap p 111 N95-17855

GORDON, ELMAREE
The assessment of the AH-64D, longbow, mast-mounted assembly noise hazard for maintenance personnel [AD-A284971] p 171 N95-16226

GRANOVSKII, A. V.
Application of multidisciplinary models to the cooled turbine rotor design p 140 N95-19024

GREBER, ISAAC
Three dimensional compressible turbulent flow computations for a diffusing S-duct with/without vortex generators [NASA-CR-195390] p 138 N95-17402

GREEN, L. L.
Applications of automatic differentiation in CFD [NASA-TM-109948] p 157 N95-16828

GREEN, LAWRENCE L.
Applications of automatic differentiation in computational fluid dynamics p 156 N95-16461

GREEN, P. D.
Current and future problems in structural acoustic fatigue p 173 N95-19143

GREGORY, IRENE M.
Matlab as a robust control design tool p 169 N95-16474

GREITZER, E. M.
Unsteady flow phenomena in discrete passage diffusers for centrifugal compressors [AD-A281412] p 155 N95-16163

GREITZER, F. L.
An artificial neural network system for diagnosing gas turbine engine fuel faults [DE94-013960] p 138 N95-17371

GRODSINSKY, C. M.
Microgravity isolation system design: A case study [NASA-TM-106804] p 104 N95-17657

Microgravity isolation system design: A modern control synthesis framework [NASA-TM-106805] p 105 N95-18197

Microgravity isolation system design: A modern control analysis framework [NASA-TM-106803] p 105 N95-18486

GUARRO, S.
Demonstration of the Dynamic Flowgraph Methodology using the Titan 2 Space Launch Vehicle Digital Flight Control System [NASA-CR-197517] p 150 N95-17493

GUIDOS, BERNARD J.
Static aerodynamics CFD analysis for 120-mm hypersonic KE projectile design [ARL-MR-184] p 118 N95-18611

GUNTERMANN, P.
Investigation of an NLF(1)-0416 airfoil in compressible subsonic flow p 110 N95-17852

GUREVICH, INNA
New technologies for space avionics [NASA-CR-197574] p 150 N95-18196

H

HAAKER, T. I.
On the dynamics of aeroelastic oscillators with one degree of freedom [BTN-94-EIX94501431527] p 153 A95-64524

HADCOCK, RICHARD N.
Composite chronicles: A study of the lessons learned in the development, production, and service of composite structures [NASA-CR-4620] p 151 N95-16859

HAIGLER, KARA J.
Applications of automatic differentiation in computational fluid dynamics p 156 N95-16461

HAINES, JOEL
E-6A hardness assurance, maintenance and surveillance program [AD-A283994] p 134 N95-19067

HALL, DAVID G.
Background noise levels measured in the NASA Lewis 9- by 15-foot low-speed wind tunnel [NASA-TM-106817] p 145 N95-18054

HALL, PHILIP
The stability of two-phase flow over a swept-wing [NASA-CR-194994] p 159 N95-18190

HALTURIN, V. A.
Simulation of multidisciplinary problems for the thermostress state of cooled high temperature turbines p 140 N95-19021

HAMPTON, R. D.
Microgravity isolation system design: A case study [NASA-TM-106804] p 104 N95-17657

Microgravity isolation system design: A modern control synthesis framework [NASA-TM-106805] p 105 N95-18197

Microgravity isolation system design: A modern control analysis framework [NASA-TM-106803] p 105 N95-18486

HAN, BUZHANG
An investigation of polynomial calibrations methods for wind tunnel balances p 144 N95-16258

HAN, S. O. T. H.
Two-dimensional 16.5 percent thick supercritical airfoil NLR 7301 p 110 N95-17854

HAND, LAWRENCE A.
A supercritical airfoil experiment p 111 N95-17858

HANDSCHUH, ROBERT F.
Detecting gear tooth fracture in a high contact ratio face gear mesh [NASA-TM-106822] p 162 N95-19125

HARE, D. A.
Dynamic Stability Instrumentation System (DSIS). Volume 1: Hardware description [NASA-TM-109160-VOL-1] p 171 N95-18899

HARRIS, CHARLES E.
FAA/NASA International Symposium on Advanced Structural Integrity Methods for Airframe Durability and Damage Tolerance, part 2 [NASA-CP-3274-PT-2] p 124 N95-19468

HARTMANN, K.
Force and pressure data of an ogive-nosed slender body at high angles of attack and different Reynolds numbers p 113 N95-17868

Wind tunnel test on a 65 deg delta wing with rounded leading edges: The International Vortex Flow Experiment p 114 N95-17875

HAYHURST, KELLY J.
A study of software standards used in the avionics industry p 137 N95-16456

HEINLE, ROBERT A.
Determination of stores pointing error due to wing flexibility under flight load [NASA-TM-4646] p 134 N95-19044

HENAKU, B. D. K.
The ICAO CNS/ATM system: New king, new law? [HTN-95-50218] p 175 A95-64855

HICKS, JOHN W.
In-flight lift-drag characteristics for a forward-swept wing aircraft and comparisons with contemporary aircraft [NASA-TP-3414] p 117 N95-18565

HOADLEY, SHERWOOD T.
Active load control during rolling maneuvers [NASA-TP-3455] p 129 N95-17397

HOLCOMB, LEE
NASA High Performance Computing and Communications program [NASA-TM-4653] p 176 N95-18573

HOLDEMAN, J. D.
Numerical mixing calculations of confined reacting jet flows in a cylindrical duct [NASA-TM-106736] p 139 N95-18133

HOLEHOUSE, IAN
Thermo-acoustic fatigue design for hypersonic vehicle skin panels p 162 N95-19161

HOOSE, K. V.
Combustor kinetic energy efficiency analysis of the hypersonic research engine data p 148 N95-16321

HORSTMANN, K. H.
2-D airfoil tests including side wall boundary layer measurements p 158 N95-17847

HOUBOLT, JOHN C.
Special effects of gust loads on military aircraft p 133 N95-18605

HOUWINK, R.
Sectional prediction of 3D effects for separated flow on rotating blades [PB94-201696] p 117 N95-18503

HOYNIK, DAN
NASA Lewis Research Center Workshop on Forced Response in Turbomachinery [NASA-CP-10147] p 141 N95-19380

Steady potential solver for unsteady aerodynamic analyses p 141 N95-19382

HUEBNER, H.
EURECA mission control experience and messages for the future p 149 N95-17252

HUESCHEN, RICHARD M.
Modeling of Instrument Landing System (ILS) localizer signal on runway 25L at Los Angeles International Airport [NASA-TM-4588] p 125 N95-17384

HUGHES, THOMAS C.
KC-135 cockpit modernization study. Phase 1: Equipment evaluation [AD-A284099] p 131 N95-18398

HULL, D. L.
Design limit loads based upon statistical discrete gust methodology p 133 N95-18603

HUNTER, PAUL
NASA High Performance Computing and Communications program [NASA-TM-4653] p 176 N95-18573

HURDLEBRINK, DEBRA
New technologies for space avionics [NASA-CR-197574] p 150 N95-18196

- ILLI, O. J., JR.**
An artificial neural network system for diagnosing gas turbine engine fuel faults [DE94-013960] p 138 N95-17371
- INGRAFFEA, ANTHONY R.**
Discrete crack growth analysis methodology for through cracks in pressurized fuselage structures p 166 N95-19473
- IVANOV, MIKHAIL J.**
Solution of Navier-Stokes equations using high accuracy monotone schemes p 161 N95-19019
The mathematical models of flow passage for gas turbine engines and their components p 140 N95-19020
Perspective problems of gas turbine engines simulation p 140 N95-19026
- JACKSON, KATHERINE**
Industry review of a crew-centered cockpit design process and toolset [AD-A282966] p 130 N95-17661
- JACKSON, RAYMOND H.**
Shear buckling analysis of a hat-stiffened panel [NASA-TM-4644] p 158 N95-17490
- JACOBS, J. H.**
Acoustic fatigue characteristics of advanced materials and structures p 174 N95-19157
- JAMESON, ANTONY**
Optimum aerodynamic design via boundary control p 127 N95-16565
- JANUS, RAY**
A PC-based interactive simulation of the F-111C Pavé Tack system and related sensor, avionics and aircraft aspects [AD-A285500] p 129 N95-16969
- JEONG, DAVID Y.**
Evaluation of the fuselage lap joint fatigue and terminating action repair p 166 N95-19477
- JIANG, XINGHONG**
Direct splitting of coefficient matrix for numerical calculation of transonic nozzle flow [BTN-94-EIX94481415356] p 103 A95-65346
- JOHNSON, ERIC R.**
Compression strength of composite primary structural components [NASA-CR-197554] p 160 N95-18388
- JOHNSON, INGMAR**
An investigation of polynomial calibrations methods for wind tunnel balances p 144 N95-16258
- JOHNSTON, J. M.**
Unsteady flow phenomena in discrete passage diffusers for centrifugal compressors [AD-A281412] p 155 N95-16163
- JOHNSTON, S. L.**
A surgical support system for Space Station Freedom p 149 N95-16776
- JONES, D. J.**
Surface pressure and wake drag measurements on the Boeing A4 airfoil in the IAR 1.5X1.5m Wind Tunnel Facility p 110 N95-17850
- JORDAN, T. L.**
Dynamic Stability Instrumentation System (DSIS). Volume 1: Hardware description [NASA-TM-109160-VOL-1] p 171 N95-18899
- KANGAS, L. J.**
An artificial neural network system for diagnosing gas turbine engine fuel faults [DE94-013960] p 138 N95-17371
- KANNAN, S. M.**
Evaluation of the dynamic stability characteristics of the NAL Light Transport Aircraft [NAL-PD-CA-9217] p 142 N95-16392
- KAPOOR, KAMLESH**
Numerical simulation of supersonic compression corners and hypersonic inlet flows using the RPLUS2D code [NASA-TM-106580] p 105 N95-16038
- KARNA, ANITA**
Identification of Artificial Intelligence (AI) applications for maintenance, monitoring, and control of airway facilities [AD-A282479] p 125 N95-17373
- KARNA, KAMAL**
Identification of Artificial Intelligence (AI) applications for maintenance, monitoring, and control of airway facilities [AD-A282479] p 125 N95-17373
- KARTASHOV, E. M.**
On the particular features of dynamic processes in solids with varying boundary during interaction with intensive heat flows [BTN-94-EIX94461408756] p 171 A95-63639
- KATAEV, YU. P.**
Analytical description of and forecast for stress relaxation of aviation materials under the vibration conditions [BTN-94-EIX94461408751] p 126 A95-63634
- KATZ, DONALD**
Identification of Artificial Intelligence (AI) applications for maintenance, monitoring, and control of airway facilities [AD-A282479] p 125 N95-17373
- KATZ, ERIC S.**
Evaluation of an unlighted swinging airport sign [AD-A284763] p 146 N95-18087
- KEE-BOWLING, BONNIE**
Background noise levels measured in the NASA Lewis 9- by 15-foot low-speed wind tunnel [NASA-TM-106817] p 145 N95-18054
- KELLY, ALONZO**
A feedforward control approach to the local navigation problem for autonomous vehicles [AD-A282787] p 126 N95-17706
- KERREBROCK, JACK L.**
Assessment of the Space Station program p 149 N95-16352
- KESSLER, BRADLEY L.**
Fiber Optic Control System integration for advanced aircraft. Electro-optic and sensor fabrication, integration, and environmental testing for flight control systems: Laboratory test results [NASA-CR-195408] p 161 N95-18938
Fiber Optic Control System integration for advanced aircraft. Electro-optic and sensor fabrication, integration, and environmental testing for flight control systems [NASA-CR-191194] p 162 N95-19236
- KHAN, M. ASIF**
Nonsmooth trajectory optimization: An approach using continuous simulated annealing [BTN-94-EIX94511433914] p 168 A95-64580
- KHINOO, L. A.**
Helicopter in-flight simulation development and use in test pilot training [AD-A283998] p 146 N95-18725
- KIDDER, STANLEY**
Field and data analysis studies related to the atmospheric environment [NASA-CR-196543] p 168 N95-18093
- KIOCK, R.**
Pressure distribution measurements on an isolated TPS 441 nacelle p 115 N95-17878
- KIWAN, ABDUL R.**
Helicopter Performance Evaluation (HELPE) computer model [AD-A284319] p 131 N95-18381
- KLYMENKO, VICTOR**
Factors affecting the visual fragmentation of the field-of-view in partial binocular overlap displays [AD-A283081] p 172 N95-17334
- KNOSPE, C. R.**
Microgravity isolation system design: A case study [NASA-TM-106804] p 104 N95-17657
Microgravity isolation system design: A modern control synthesis framework [NASA-TM-106805] p 105 N95-18197
Microgravity isolation system design: A modern control analysis framework [NASA-TM-106803] p 105 N95-18486
- KNOX, CHARLES E.**
Modeling of Instrument Landing System (ILS) localizer signal on runway 25L at Los Angeles International Airport [NASA-TM-4588] p 125 N95-17384
- KO, WILLIAM L.**
Shear buckling analysis of a hat-stiffened panel [NASA-TM-4644] p 158 N95-17490
- KOENIG, KLAUS**
Acoustic fatigue testing on different materials and skin-stringer elements p 174 N95-19156
- KOMEL', S. V.**
Ultimate characteristics of a rocket engine with a turbo-pump supply system [BTN-94-EIX94461408757] p 148 A95-63640
- KONG, JEFFREY**
The accuracy of parameter estimation in system identification of noisy aircraft load measurement [NASA-CR-197516] p 134 N95-19130
- KONG, L.**
Unsteady flow testing in a passive low-correction wind tunnel p 147 N95-19272
- KOONTZ, S.**
Free-jet testing at Mach 3.44 in GASL's aero/thermo test facility p 145 N95-16320
- KOROVIN, E. M.**
Modelling for optimal operations of line milling of aerodynamic surfaces [BTN-94-EIX94461408774] p 138 A95-63657
- KOSTEGE, VALEREY K.**
Simulation of multidisciplinary problems for the thermostress state of cooled high temperature turbines p 140 N95-19021
Verification of multidisciplinary models for turbomachines p 140 N95-19025
- KOSTEGE, VALERY K.**
Application of multidisciplinary models to the cooled turbine rotor design p 140 N95-19024
- KOZHEVNIKOV, YU. V.**
Theoretical fundamentals of the aircraft GTE tests p 138 N95-16265
- KRAMER, BRIAN R.**
Development of a multicomponent force and moment balance for water tunnel applications, volume 1 [NASA-CR-4642-VOL-1] p 161 N95-18955
Development of a multicomponent force and moment balance for water tunnel applications, volume 2 [NASA-CR-4642-VOL-2] p 161 N95-18956
- KRECH, ROBERT H.**
Ultraviolet emissions occurring about hypersonic vehicles in rarefied flows [AD-A281452] p 106 N95-16076
- KREMER, FRANS G. J.**
One-dimensional flow description for the combustion chamber of a scramjet [DLR-FB-94-06] p 139 N95-18911
- KREPLIN, H.-P.**
Three-dimensional boundary layer and flow field data of an inclined prolate spheroid p 158 N95-17867
- KRUCK, MARY**
ADST system test report for the rotary wing aircraft airnet aeromodel and weapon model merge with the ATAC 2 baseline [AD-A281580] p 127 N95-16171
- KRUPA, VLADISLAV G.**
Solution of Navier-Stokes equations using high accuracy monotone schemes p 161 N95-19019
Simulation of steady and unsteady viscous flows in turbomachinery p 140 N95-19023
- KUEPPER, A.**
Wall correction method with measured boundary conditions for low speed wind tunnels p 164 N95-19263
- KULWICKI, PHILIP**
Industry review of a crew-centered cockpit design process and toolset [AD-A282966] p 130 N95-17661
- KURKOV, A. P.**
Measurement of gust response on a turbine cascade [NASA-TM-106776] p 117 N95-18457
- KURTKEYA, MEHMET**
Sensor fault detection and diagnosis simulation of a helicopter engine in an intelligent control framework [NASA-TM-106784] p 137 N95-15970
- KURUVILA, G.**
Airfoil optimization by the one-shot method p 128 N95-16569
- KUTSCHENREUTER, P.**
Scramjet testing guidelines p 138 N95-16317
- KUZMIN, M.**
Optical surface pressure measurements: Accuracy and application field evaluation p 175 N95-19274
- KUZNETSOV, V. I.**
Gas-turbine engines with increased efficiency of two circuits, due to the use of the utilizing steam-turbine circuit [BTN-94-EIX94461408755] p 153 A95-63638
- LABRUJERE, TH. E.**
Residual-correction type and related computational methods for aerodynamic design. Part 1: Airfoil and wing design p 128 N95-16566
Residual-correction type and related computational methods for aerodynamic design. Part 2: Multi-point airfoil design p 128 N95-16567
- LAM, S. S.**
Data acquisition and processing software for the Low Speed Wind Tunnel tests of the Jindivik auxiliary air intake [AD-A285455] p 108 N95-17178
- LANCIAULT, MARK**
New technologies for space avionics [NASA-CR-197574] p 150 N95-18196
- LASCHKA, BORIS**
Velocity measurements with hot-wires in a vortex-dominated flowfield p 121 N95-19261
- LAUDIEN, E.**
Helicopter internal noise p 173 N95-19144

- LAVELLE, THOMAS M.**
Enhanced capabilities and modified users manual for axial-flow compressor conceptual design code CSPAN [NASA-TM-106833] p 119 N95-18933
- LAW, C. K.**
Studies on high pressure and unsteady flame phenomena [AD-A284126] p 152 N95-18410
- LAWTON, JOSEPH**
Unmanned aerial vehicle heavy fuel engine test [AD-A284332] p 139 N95-18383
- LEFEBVRE, PAUL J.**
Hydrofoil force balance [AD-D016475] p 160 N95-18461
- LEHMAN, EDWARD**
Industry review of a crew-centered cockpit design process and toolset [AD-A282966] p 130 N95-17661
- LEIGH, BARRY**
Noise transmission and reduction in turboprop aircraft p 175 N95-19164
- LEISHMAN, J. G.**
Experimental data on the aerodynamic interactions between a helicopter rotor and an airframe p 116 N95-17883
- LEMAITRE, J.**
On-line handling of air traffic: Management, guidance and control [AGARD-AG-321] p 126 N95-18927
- LESTER, MICHAEL T.**
A platform independent application of Lux illumination prediction algorithms [AD-A283669] p 170 N95-18018
- LEWICKI, DAVID G.**
Detecting gear tooth fracture in a high contact ratio face gear mesh [NASA-TM-106822] p 162 N95-19125
- LI, W.**
Automation of reverse engineering process in aircraft modeling and related optimization problems [NASA-CR-197109] p 129 N95-16899
- LITT, JONATHAN**
Sensor fault detection and diagnosis simulation of a helicopter engine in an intelligent control framework [NASA-TM-106784] p 137 N95-15970
- LIU, JIANYE**
Application of GPS/SINS/RA integrated system to aircraft approach landing p 125 N95-16277
- LOCKWOOD, MARY KAE**
Modelling structurally damaging twin-jet screech p 135 N95-19154
- LOKOS, WILLIAM A.**
Determination of stores pointing error due to wing flexibility under flight load [NASA-TM-4646] p 134 N95-19044
- LONDENBERG, W. KELLY**
Transonic Navier-Stokes calculations about a 65 deg delta wing [NASA-CR-4635] p 108 N95-17273
- LU, PING**
Nonsmooth trajectory optimization: An approach using continuous simulated annealing [BTN-94-EIX94511433914] p 168 A95-64580
- LUBOSCH, BERND**
E-6A hardness assurance, maintenance and surveillance program [AD-A283994] p 134 N95-19067
- LUCCI, B. L.**
Measurement of gust response on a turbine cascade [NASA-TM-106776] p 117 N95-18457
- LUKASZEWICZ, V.**
Static and dynamic friction behavior of candidate high temperature airframe seal materials [NASA-TM-106571] p 152 N95-16905
- LUKE, SUE**
In-flight lift-drag characteristics for a forward-swept wing aircraft and comparisons with contemporary aircraft [NASA-TP-3414] p 117 N95-18565
- LUNEV, A. N.**
Calculation of geometry of stamps with small allowances for pieces of the aerodynamic profile [BTN-94-EIX94461408772] p 103 A95-63655
- LUSEBRINK, H.**
Treatment of non-linear systems by timeplane-transformed CT methods: The spectral gust method p 143 N95-18600
- LUTTGES, M. W.**
Wind turbine blade aerodynamics: The combined experiment [DE94-011866] p 118 N95-18645
Wind turbine blade aerodynamics: The analysis of field test data [DE94-011867] p 118 N95-18646
- LYLE, KAREN HEITMAN**
Acoustic radiation damping of flat rectangular plates subjected to subsonic flows p 172 N95-18542
- LYNCH, F. T.**
2-D aileron effectiveness study p 110 N95-17851
The crucial role of wall interference, support interference and flow field measurements in the development of advanced aircraft configurations p 162 N95-19252

M

- MACCORMACK, ROBERT W.**
High altitude hypersonic flowfield radiation [AD-A281386] p 106 N95-16160
- MACH, DOUGLAS**
Field and data analysis studies related to the atmospheric environment [NASA-CR-196543] p 168 N95-18093
- MACHERET, Y.**
Prediction of R-curves from small coupon tests p 167 N95-19496
- MACMARTIN, DOUGLAS G.**
Noise transmission and reduction in turboprop aircraft p 175 N95-19164
- MADERUELO, C.**
A study of the effect of store unsteady aerodynamics on gust and turbulence loads p 133 N95-18601
- MAGGIO, ANTHONY**
Unmanned aerial vehicle heavy fuel engine test [AD-A284332] p 139 N95-18383
- MAHANTA, KAMALA**
A CMC database for use in the next generation launch vehicles (rockets) p 150 N95-18993
- MALCOLM, GERALD N.**
Development of a multicomponent force and moment balance for water tunnel applications, volume 1 [NASA-CR-4642-VOL-1] p 161 N95-18955
Development of a multicomponent force and moment balance for water tunnel applications, volume 2 [NASA-CR-4642-VOL-2] p 161 N95-18956
- MALIK, M. R.**
Effect of crossflow on Goertler instability in incompressible boundary layers [NASA-CR-195007] p 159 N95-18193
- MALLORY, MARK**
E-6A hardness assurance, maintenance and surveillance program [AD-A283994] p 134 N95-19067
- MANTEL, B.**
Review of the EUROPT Project AERO-0026 p 129 N95-16573
- MAROLO, SAMUEL A.**
Conference on Aerospace Transparent Materials and Enclosures. Volume 2: Sessions 5-9 [AD-A283926] p 131 N95-18162
Conference on Aerospace Transparent Materials and Enclosures, volume 1 [AD-A283925] p 133 N95-18677
- MARRA, JOHN J.**
Tuned mass damper for integrally bladed turbine rotor [NASA-CASE-MFS-28697-1] p 159 N95-18325
- MARTIN, JOHN S.**
Factors affecting the visual fragmentation of the field-of-view in partial binocular overlap displays [AD-A283081] p 172 N95-17334
- MARTIN, PETER**
Aircraft accident investigation and airworthiness -- A practical example of the interaction of two disciplines with some reflections on possible legal consequences [HTN-95-50219] p 176 A95-64856
- MASELAND, J. E. J.**
Experimental investigation of the vortex flow over a 76/60-deg double delta wing p 114 N95-17874
- MATEER, GEORGE G.**
A supercritical airfoil experiment p 111 N95-17858
- MATTES, ROBERT E.**
Fiber Optic Control System integration for advanced aircraft. Electro-optic and sensor fabrication, integration, and environmental testing for flight control systems [NASA-CR-191194] p 162 N95-19236
- MATTHEWS, R. K.**
Hypersonic wind tunnel test techniques [AD-A284057] p 118 N95-18663
Hypersonic flow-field measurements: Intrusive and nonintrusive [AD-A283867] p 119 N95-18674
Hypersonic flight testing [AD-A283981] p 134 N95-18891
- MATYASH, S.**
Optical surface pressure measurements: Accuracy and application field evaluation p 175 N95-19274
- MAUS, J. R.**
Hypersonic flight testing [AD-A283981] p 134 N95-18891
- MAYNARD, JULIAN D.**
Anisotropic heat exchangers/stack configurations for thermocoustic heat engines [AD-A280974] p 168 N95-16506
- MCCULLOUGH, JAMES A.**
Operational And Supportability Implementation System (OASIS) test and evaluation master plan [AD-A284765] p 126 N95-18088
- MCDONALD, M. A.**
Measurements of the flow over a low aspect-ratio wing in the Mach number range 0.6 to 0.87 for the purpose of validation of computational methods. Part 1: Wing design, model construction, surface flow. Part 2: Mean flow in the boundary layer and wake, 4 test cases p 112 N95-17860
- MC FARLAND, RICHARD H.**
Commentary on Walton correspondence relating to the ILS glide slope [BTN-94-EIX94441380856] p 125 A95-64288
- MCGOVERN, JANET L.**
Evaluation of alternate F-14 wing lug coating [AD-A283207] p 129 N95-17631
- MCCLEAN, WILLIAM E.**
Factors affecting the visual fragmentation of the field-of-view in partial binocular overlap displays [AD-A283081] p 172 N95-17334
- MCCLEMORE, DONALD**
Assessing aircraft survivability to high frequency transient threats [AD-A283999] p 134 N95-18726
- MCRAE, D. S.**
Time accurate computation of unsteady inlet flows with a dynamic flow adaptive mesh [AD-A285498] p 157 N95-16736
- MEDLER, LAWRENCE P.**
Low rate initial production in Army Aviation systems development [AD-A281871] p 127 N95-16356
- MELLSTROM, J. A.**
Field verification of the wind tunnel coefficients p 109 N95-17291
- MEWHINNEY, MICHAEL**
NASA develops new digital flight control system [NASA-NEWS-RELEASE-94-47] p 144 N95-19029
- MEYERS, GARY W.**
Solid fuel ramjet composition [AD-D016458] p 152 N95-19090
- MEYERS, MICHAEL J.**
Tilt Rotor Unmanned Air Vehicle System (TRUS) demonstrator flight test program [AD-A284151] p 132 N95-18415
- MICHONNEAU, J. F.**
Analysis of test section sidewall effects on a two dimensional airfoil: Experimental and numerical investigations p 165 N95-19276
- MIGNOSI, A.**
Data from the GARTEur (AD) Action Group 02 airfoil CAST 7/DOA1 experiments p 111 N95-17856
Experimental techniques for measuring transonic flow with a three dimensional laser velocimetry system. Application to determining the drag of a fuselage p 163 N95-19258
Analysis of test section sidewall effects on a two dimensional airfoil: Experimental and numerical investigations p 165 N95-19276
- MILLER, M. S.**
Structural effects of unsteady aerodynamic forces on horizontal-axis wind turbines [DE94-011863] p 157 N95-16939
Wind turbine blade aerodynamics: The combined experiment [DE94-011866] p 118 N95-18645
Wind turbine blade aerodynamics: The analysis of field test data [DE94-011867] p 118 N95-18646
- MILLER, MATTHEW**
The characterization of widespread fatigue damage in fuselage structure p 166 N95-19472
- MILLER, PHILIP**
Transonic and supersonic flowfield measurements about axisymmetric afterbodies for validation of advanced CFD codes p 121 N95-19260
- MILLER, R. V.**
Helicopter in-flight simulation development and use in test pilot training [AD-A283998] p 146 N95-18725
- MITTER, SANJOY K.**
Workshop on Formal Models for Intelligent Control [AD-A281399] p 169 N95-16864
- MOHAMMADI, JAMSHID**
Flight parameters monitoring system for tracking structural integrity of rotary-wing aircraft p 135 N95-19469
- MOHAN, S. R.**
Interference determination for wind tunnels with slotted walls p 147 N95-19269

- MOHLER, STANLEY R., JR.**
Collection efficiency and ice accretion calculations for a sphere, a swept MS(1)-317 wing, a swept NACA-0012 wing tip, an axisymmetric inlet, and a Boeing 737-300 [NASA-TM-106831] p 123 N95-18582
- MOIR, I. R. M.**
Measurements on a two-dimensional aerofoil with high-lift devices p 109 N95-17848
- MOISEEVA, L. T.**
Calculation of geometry of stamps with small allowances for pieces of the aerodynamic profile [BTN-94-EIX94461408772] p 103 A95-63655
- MOKRY, M.**
Evaluation of combined wall- and support-interference on wind tunnel models p 122 N95-19278
- MOREL, MICHAEL**
NASA Lewis Research Center Workshop on Forced Response in Turbomachinery [NASA-CP-10147] p 141 N95-19380
- MORRIS, D. E.**
Static and dynamic friction behavior of candidate high temperature airframe seal materials [NASA-TM-106571] p 152 N95-16905
- MORRIS, P. J.**
Linear instability waves in supersonic jets confined in circular and non-circular ducts [BTN-94-EIX94341340068] p 103 A95-63520
- MOSHAROV, V.**
Optical surface pressure measurements: Accuracy and application field evaluation p 175 N95-19274
- MOZO, BEN T.**
The assessment of the AH-64D, longbow, mast-mounted assembly noise hazard for maintenance personnel [AD-A284971] p 171 N95-16226
- MU, XINHUA**
The computer analysis of the prediction of aircraft electrical power supply system reliability p 155 N95-16278
- MUDKAVI, VIDYADHAR Y.**
Computation of vortex breakdown p 165 N95-19462
- MURTHY, DURBHA V.**
NASA Lewis Research Center Workshop on Forced Response in Turbomachinery [NASA-CP-10147] p 141 N95-19380
- N**
- NALIM, MOHAMED RAZI**
Wave cycle design for wave rotor engines with limited nitrogen oxide emissions p 161 N95-18901
- NANGIA, R. K.**
Estimating wind tunnel interference due to vectored jet flows p 164 N95-19265
- HAZYROVA, R. R.**
On a program-information system Tdsoft [BTN-94-EIX94461408773] p 175 A95-63656
- NEWMAN, D. M.**
Six degree of freedom flight dynamic and performance simulation of a remotely-piloted vehicle [AERO-TN-9301] p 131 N95-18097
- NEWMAN, P. A.**
Applications of automatic differentiation in CFD [NASA-TM-109948] p 157 N95-16828
- NEWMAN, PERRY A.**
Applications of automatic differentiation in computational fluid dynamics p 156 N95-16461
- NEYLAND, V. M.**
The traditional and new methods of accounting for the factors distorting the flow over a model in large transonic wind tunnels p 165 N95-19275
- NGUYEN, V. D.**
Applications of the five-hole probe technique for flow field surveys at the Institute for Aerospace Research p 163 N95-19255
- NI, YONGXI**
Application of GPS/SINS/RA integrated system to aircraft approach landing p 125 N95-16277
- NICHOLS, JAMES**
The generic simulation executive at Manned Flight Simulator [AD-A283997] p 146 N95-18724
- NICHOLSON, JOHN C.**
Numerical optimization of synergistic maneuvers [AD-A283398] p 109 N95-17435
- NIELSEN, THOMAS**
Development of load spectra for Airbus A330/A340 full scale fatigue tests p 135 N95-19479
- NIESL, G.**
Helicopter internal noise p 173 N95-19144
- NIEWOEHNER, ROBERT J., JR.**
Plant and controller optimization by convex methods [AD-A283700] p 133 N95-18621
- NIGMATULLIN, RAVIL Z.**
The mathematical models of flow passage for gas turbine engines and their components p 140 N95-19020
Application of multicomponent models to flow passage simulation in multistage turbomachines and whole gas turbine engines p 140 N95-19022
- NISHIMURA, Y.**
Surface pressure and wake drag measurements on the Boeing A4 airfoil in the IAR 1.5X1.5m Wind Tunnel Facility p 110 N95-17850
- NORESE, M.**
An overall approach of cockpit noise verification in a military aircraft p 175 N95-19163
- NOWOBILSKI, J. J.**
Airborne rotary separator study [NASA-CR-191045] p 150 N95-18743
- NYBLOM, K.**
Military aviation maintenance industry in Western Europe: Concentration and internationalization [PB94-189180] p 104 N95-17451
- NYE, H. R.**
Packet utilisation definitions for the ESA XMM mission p 150 N95-17596
- O**
- OECHSLE, VICTOR L.**
Numerical mixing calculations of confined reacting jet flows in a cylindrical duct [NASA-TM-106736] p 139 N95-18133
- OEZBAY, HITAY**
H(sup 2)/H(sup INF) controller design for a two-dimensional thin airfoil flutter suppression [BTN-94-EIX94511433918] p 141 A95-64584
- OHMAN, L. H.**
Applications of the five-hole probe technique for flow field surveys at the Institute for Aerospace Research p 163 N95-19255
- OLFENBUTTEL, R. F.**
Bicarbonate of soda blasting technology for aircraft wheel repainting [PB94-193323] p 104 N95-17466
- OLIVER, M.**
A study of the effect of store unsteady aerodynamics on gust and turbulence loads p 133 N95-18601
- OLKIEWICZ, CRAIG**
Flight parameters monitoring system for tracking structural integrity of rotary-wing aircraft p 135 N95-19469
- OLSEN, J. R.**
Strategic avionics technology definition studies. Subtask 3-1A3: Electrical Actuation (ELA) Systems Test Facility [NASA-CR-188360] p 143 N95-18567
- OLSEN, MIKE**
Low aspect ratio wing experiment p 113 N95-17865
- ONCLEY, STEVEN**
On the Lighthill relationship and sound generation from isotropic turbulence [NASA-CR-195005] p 159 N95-18191
- ORLOV, A.**
Optical surface pressure measurements: Accuracy and application field evaluation p 175 N95-19274
- ORTASSE, RAPHAEL**
Fatigue loads spectra derivation for the Space Shuttle: Second cycle p 166 N95-19470
- OISOPOV, I. L.**
New approach to geometric profiling of the design elements of the passage part in turbo-machines [BTN-94-EIX94461408769] p 153 A95-63652
- OSTER, JOHN**
Preliminary evaluation of the F/A-18 quantity/multiple envelope expansion [AD-A284119] p 132 N95-18407
- P**
- PACK, WILLIAM D.**
Operating capability and current status of the reactivated NASA Lewis Research Center Hypersonic Tunnel Facility [NASA-TM-106808] p 148 N95-19286
- PADMADINATA, U. H.**
Prediction of fatigue crack growth under flight-simulation loading with the modified CORPUS model p 166 N95-19471
- PAN, JIAZHENG**
An approach to aerodynamic characteristics of low radar cross-section fuselages p 106 N95-16251
- PAPAILIOU, K. D.**
Single-pass method for the solution of inverse potential and rotational problems. Part 1: 2-D and quasi 3-D theory and application p 107 N95-16563
- Single-pass method for the solution of inverse potential and rotational problems. Part 2: Fully 3-D potential theory and applications p 107 N95-16564
- PARET, A.**
Aeroacoustic qualification of HERMES shingles p 173 N95-19145
- PARIMUHA, EDWARD**
Waveform bounding and combination techniques for direct drive testing [AD-A284075] p 161 N95-19035
- PARIMUHA, EDWARD M.**
Assessing aircraft survivability to high frequency transient threats [AD-A283999] p 134 N95-18726
- PARK, JAI H.**
Residual life and strength estimates of aircraft structural components with MSD/MED p 136 N95-19485
- PARKINSON, G. V.**
Unsteady flow testing in a passive low-correction wind tunnel p 147 N95-19272
- PASSCHIER, D. M.**
Experiments in the trailing edge flow of an NLR 7702 airfoil p 110 N95-17853
- PEARSON, JEROME**
High-temperature acoustic test facilities and methods p 174 N95-19149
- PECCIA, N.**
Safety aspects of spacecraft commanding p 149 N95-17248
- PEISEN, DEBORAH**
Heliport/vertiport MLS precision approaches [AD-A283505] p 126 N95-18059
- PELEGRIN, M.**
On-line handling of air traffic: Management, guidance and control [AGARD-AG-321] p 126 N95-18927
- PEN, JIBING**
The computer analysis of the prediction of aircraft electrical power supply system reliability p 155 N95-16278
- PENDLETON, ED**
Pressure measurements on an F/A-18 twin vertical tail in buffeting flow. Volume 4, part 2: Buffet cross spectral densities [AD-A285555] p 143 N95-18641
- PERIAUX, J.**
Review of the EUROPT Project AERO-0026 p 129 N95-16573
- PESETSKY, V.**
Optical surface pressure measurements: Accuracy and application field evaluation p 175 N95-19274
- PETIAU, C.**
Aeroacoustic qualification of HERMES shingles p 173 N95-19145
- PETRAKOV, V. M.**
Two projects of V. M. Myasishchev [HTN-95-50269] p 176 A95-65764
- PETRE, E.**
On-line handling of air traffic: Management, guidance and control [AGARD-AG-321] p 126 N95-18927
- PETTIT, CHRIS**
Pressure measurements on an F/A-18 twin vertical tail in buffeting flow. Volume 4, part 2: Buffet cross spectral densities [AD-A285555] p 143 N95-18641
- PHONOV, S.**
Optical surface pressure measurements: Accuracy and application field evaluation p 175 N95-19274
- PIASCIK, ROBERT S.**
The characterization of widespread fatigue damage in fuselage structure p 166 N95-19472
- PIAT, J. F.**
Calculation of wall effects of flow on a perforated wall with a code of surface singularities p 165 N95-19277
- PIERCE, DOUGLAS C.**
Development of a bipolar lead/acid battery for the more electric aircraft [AD-A284050] p 160 N95-18660
- PIERRE, CHRISTOPHE**
Forced response of mistuned bladed disks p 141 N95-19383
- PIERS, W. J.**
Sectional prediction of 3D effects for separated flow on rotating blades [PB94-201696] p 117 N95-18503
- PIRONNEAU, O.**
Optimal shape design for aerodynamics p 128 N95-16568
- PIZIALI, R. A.**
2-D and 3-D oscillating wing aerodynamics for a range of angles of attack including stall [NASA-TM-4632] p 120 N95-19119

POOLE, RICHARD J. D.
Interference corrections for a centre-line plate mount in a porous-walled transonic wind tunnel p 122 N95-19280

POTOTZKY, ANTHONY S.
Active load control during rolling maneuvers [NASA-TP-3455] p 129 N95-17397

POTYONDY, DAVID O.
Discrete crack growth analysis methodology for through cracks in pressurized fuselage structures p 166 N95-19473

POWELL, E. S.
A model for preliminary facility design including simulation issues p 144 N95-16318

PRABHU, DINESH K.
Parabolized Navier-Stokes solution of supersonic/hypersonic flows p 123 N95-19464

PRASKOVSKY, ALEXANDER
On the Lighthill relationship and sound generation from isotropic turbulence [NASA-CR-195005] p 159 N95-18191

PRATHER, WILLIAM
Assessing aircraft survivability to high frequency transient threats [AD-A283999] p 134 N95-18726

PRYONO, EDDY
An investigation of the transonic pressure drag coefficient for axi-symmetric bodies [AD-A280990] p 105 N95-15994

PRUDHOMME, S.
Experimental techniques for measuring transonic flow with a three dimensional laser velocimetry system. Application to determining the drag of a fuselage p 163 N95-19258

PRUETT, C. DAVID
A spectrally accurate boundary-layer code for infinite swept wings [NASA-CR-195014] p 159 N95-18042

PSZOLLA, H.
Wind tunnel test on a 65 deg delta wing with rounded leading edges: The International Vortex Flow Experiment p 114 N95-17875

PUFFERT-MEISSNER, W.
2-D airfoil tests including side wall boundary layer measurements p 158 N95-17847

PURVIS, CHRISTOPHER REECE
Design and flight test of a simplified control system for a transport helicopter p 144 N95-18902

Q

QUAST, A.
Subsonic flow around US-orbiter model FALKE in the DNW p 115 N95-17877

QUEMARD, C.
Interaction of a three strut support on the aerodynamic characteristics of a civil aviation model p 122 N95-19279

R

RADCHENKO, V.
Optical surface pressure measurements: Accuracy and application field evaluation p 175 N95-19274

RADESPIEL, R.
Subsonic flow around US-orbiter model FALKE in the DNW p 115 N95-17877

RAIS-ROHANI, MASOUD
Wing design for a civil tiltrotor transport aircraft [NASA-CR-197523] p 130 N95-18090

RANGARAJAN, R.
Computation of inviscid flows: Full potential method p 165 N95-19447

RANKIN, CHARLES C.
Nonlinear analysis of damaged stiffened fuselage shells subjected to combined loads p 137 N95-19499

RAU, GUIDO
Aerodynamic investigation of the flow field in a 180 deg turn channel with sharp bend p 163 N95-19257

RAY, DAVID M.
Virtual environment application with partial gravity simulation p 169 N95-15988

REDDY, S. V.
Fatigue and residual strength investigation of ARALL(R) -3 and GLARE(R) -2 panels with bonded stringers p 137 N95-19495

REDEKER, G.
DLR-F4 wing body configuration p 130 N95-17863

REEVE, T.
An artificial neural network system for diagnosing gas turbine engine fuel faults [DE94-013960] p 138 N95-17371

REINICKE, ROBERT H.
A Lifting Ball Valve for cryogenic fluid applications p 156 N95-16349

REYNOLDS, ANTHONY P.
Multi-lab comparison on R-curve methodologies: Alloy 2024-T3 [NASA-CR-195004] p 151 N95-16860

RHODES, G. S.
Portable parallel stochastic optimization for the design of aeropropulsion components [NASA-CR-195312] p 154 N95-16072

RHUDY, R. W.
Hypersonic wind tunnel test techniques [AD-A284057] p 118 N95-18663

RICHWINE, DAVID M.
Development of a low-aspect ratio fin for flight research experiments [NASA-TM-4596] p 108 N95-16858

RIVERS, MELISSA B.
Comparison of computational and experimental results for a supercritical airfoil [NASA-TM-4601] p 108 N95-16908

RKHIMA, A. A.
On the particular features of dynamic processes in solids with varying boundary during interaction with intensive heat flows [BTN-94-EIX94461408756] p 171 A95-63639

ROBERTS, LEONARD
Determination of solid/porous wall boundary conditions from wind tunnel data for computational fluid dynamics codes p 164 N95-19266

ROBINSON, M. C.
Wind turbine blade aerodynamics: The combined experiment [DE94-011866] p 118 N95-18645
Wind turbine blade aerodynamics: The analysis of field test data [DE94-011867] p 118 N95-18646

RODDE, A. M.
OAT15A airfoil data p 111 N95-17857

RODGERS, C.
Small turbojets: Designs and installations p 138 N95-16323

RODRIGUEZ, D. L.
2-D aileron effectiveness study p 110 N95-17851

ROGERS, J. P.
Strategic avionics technology definition studies. Subtask 3-1A3: Electrical Actuation (ELA) Systems Test Facility [NASA-CR-188360] p 143 N95-18567

ROMANENKO, L. G.
Selection of optimal parameters for a system, controlling the flight height, when information about the state vector is incomplete [BTN-94-EIX94461408753] p 168 A95-63636

ROMERE, PAUL O.
Documentation and archiving of the Space Shuttle wind tunnel test data base. Volume 1: Background and description [NASA-TM-104806-VOL-1] p 151 N95-19237

ROTH, KARLJN R.
STOVL CFD model test case p 115 N95-17881

ROUNTREE, MICHAEL
Industry review of a crew-centered cockpit design process and toolset [AD-A282966] p 130 N95-17661

ROY, INDRANIL DANDA
Ducted fan acoustic radiation including the effects of nonuniform mean flow and acoustic treatment [NASA-CR-197449] p 172 N95-16401

RUBIN, A. G.
On the particular features of dynamic processes in solids with varying boundary during interaction with intensive heat flows [BTN-94-EIX94461408756] p 171 A95-63639

RUBIN, RAFAEL LEVY
Regenerative cooling for liquid propellant rocket thrust chambers [INPE-5565-TDI/540] p 150 N95-18720

RUEGER, M. L.
Transonic wind tunnel boundary interference correction p 147 N95-19271

RUSSO, G. P.
Adaptive wind tunnel walls versus wall interference correction methods in 2D flows at high blockage ratios p 147 N95-19267

S

SADOVSKII, N.
Optical surface pressure measurements: Accuracy and application field evaluation p 175 N95-19274

SAFRONOV, A. V.
Engineering methods for the evaluation of transonic flutter characteristics for aerodynamic control surfaces [BTN-94-EIX94461408589] p 141 A95-63064

SAFRONOV, V. A.
Engineering methods for the evaluation of transonic flutter characteristics for aerodynamic control surfaces [BTN-94-EIX94461408589] p 141 A95-63064

SAHU, JUBARAJ
Numerical computations of supersonic base flow with special emphasis on turbulence modeling [AD-A283688] p 119 N95-18670

SALAS, M. D.
Airfoil optimization by the one-shot method p 128 N95-16569

SALOV, N. N.
Investigation of heat transfer between rotating shafts of transmissions of turbojet engines [BTN-94-EIX94461408760] p 138 A95-63643

SALTZMAN, EDWIN J.
In-flight lift-drag characteristics for a forward-swept wing aircraft and comparisons with contemporary aircraft [NASA-TP-3414] p 117 N95-18565

SAMAVEDAM, GOPAL
Evaluation of the fuselage lap joint fatigue and terminating action repair p 166 N95-19477

SAMUELSSON, I.
Low speed propeller slipstream aerodynamic effects p 116 N95-17882

SANDFORD, MAYNARD C.
Measurements of unsteady pressure and structural response for an elastic supercritical wing [NASA-TP-3443] p 104 N95-16560

SAUCRAY, J. M.
Gyroscopic and propeller aerodynamic effects on engine mounts dynamic loads in turbulence conditions p 132 N95-18599

SAWYER, BRIAN
Heliport/vertiport MLS precision approaches [AD-A283505] p 126 N95-18059

SCHIERMAN, JOHN D.
Cooperative control theory and integrated flight and propulsion control [NASA-CR-197493] p 142 N95-17404

SCHJIVE, J.
Prediction of fatigue crack growth under flight-simulation loading with the modified CORPUS model p 166 N95-19471
Fatigue life until small cracks in aircraft structures: Durability and damage tolerance p 135 N95-19478

SCHMIDT, DAVID K.
Cooperative control theory and integrated flight and propulsion control [NASA-CR-197493] p 142 N95-17404

SCHMIDT, H.-J.
Development of load spectra for Airbus A330/A340 full scale fatigue tests p 135 N95-19479

SCHRADER, K. H.
Aircraft stress sequence development: A complex engineering process made simple p 136 N95-19480

SEAL, DANIEL W.
Fiber Optic Control System integration for advanced aircraft. Electro-optic and sensor fabrication, integration, and environmental testing for flight control systems [NASA-CR-191194] p 162 N95-19236

SEEGMILLER, H. LEE
A supercritical airfoil experiment p 111 N95-17858
Low aspect ratio wing experiment p 113 N95-17865

SEIDEL, DAVID A.
Measurements of unsteady pressure and structural response for an elastic supercritical wing [NASA-TP-3443] p 104 N95-16560

SEINER, J. M.
Impact of dynamic loads on propulsion integration p 174 N95-19148

SENAPATI, N.
Ultrasonic techniques for repair of aircraft structures with bonded composite patches p 136 N95-19486

SERAUDIE, A.
Experimental techniques for measuring transonic flow with a three dimensional laser velocimetry system. Application to determining the drag of a fuselage p 163 N95-19258

SERGIENKO, A. A.
Ultimate characteristics of a rocket engine with a turbo-pump supply system [BTN-94-EIX94461408757] p 148 A95-63640

SHAW, BEVIL J.
An artificial corrosion protocol for lap-splices in aircraft skin p 152 N95-19482

SHAW, L. L.
Weapons bay acoustic environment p 173 N95-19146

SHAW, ROBERT J.
Numerical simulation of supersonic compression corners and hypersonic inlet flows using the RPLUS2D code [NASA-TM-106580] p 105 N95-16038

- SHEPPARD, WILLIAM R.**
Eddy current for detecting second layer cracks under installed fasteners
[AD-A282412] p 158 N95-17507
- SHIAO, MICHAEL C.**
Optimization of adaptive intraply hybrid fiber composites with reliability considerations
[NASA-TM-106632] p 157 N95-16911
- SHIMOVETZ, R. M.**
Weapons bay acoustic environment
p 173 N95-19146
- SHINODA, PATRICK M.**
Wall interaction effects for a full-scale helicopter rotor in the NASA Ames 80- by 120-foot wind tunnel
p 121 N95-19270
- SHIPLEY, D. E.**
Structural effects of unsteady aerodynamic forces on horizontal-axis wind turbines
[DE94-011863] p 157 N95-16939
Wind turbine blade aerodynamics: The combined experiment
[DE94-011866] p 118 N95-18645
Wind turbine blade aerodynamics: The analysis of field test data
[DE94-011867] p 118 N95-18646
- SHORE, CHARLES P.**
Nonlinear analysis of damaged stiffened fuselage shells subjected to combined loads
p 137 N95-19499
- SI, ERJUAN**
The application of Newman crack-closure model to predicting fatigue crack growth
p 167 N95-19483
- SIMMONS, M. J.**
Detailed study at supersonic speeds of the flow around delta wings
p 112 N95-17861
- SINGH, RIPUDAMAN**
Residual life and strength estimates of aircraft structural components with MSD/MED
p 136 N95-19485
- SIRAZETDINOV, R. T.**
Mathematical modelling concerning the development of a system of similar installations, taking into account their operational intensity (an aircraft-helicopter fleet taken as an example)
[BTN-94-EIX94461408763] p 103 A95-63646
- SITDIKOV, T. R.**
On a program-information system TDsoft
[BTN-94-EIX94461408773] p 175 A95-63656
- SKOMOROKHOV, V. I.**
Service and physical properties of liquid-jet fuels
p 151 N95-16256
- SLATON, DAVE**
Field and data analysis studies related to the atmospheric environment
[NASA-CR-196543] p 168 N95-18093
- SLINGERLAND, F. W.**
Spectrogram diagnosis of aircraft disasters
p 124 N95-19167
- SMITH, BROOKE C.**
Development of a multicomponent force and moment balance for water tunnel applications, volume 1
[NASA-CR-4642-VOL-1] p 161 N95-18955
Development of a multicomponent force and moment balance for water tunnel applications, volume 2
[NASA-CR-4642-VOL-2] p 161 N95-18956
- SMITH, L. A.**
Bicarbonate of soda blasting technology for aircraft wheel depainting
[PB94-193323] p 104 N95-17466
- SMITH, PAUL**
NASA High Performance Computing and Communications program
[NASA-TM-4653] p 176 N95-18573
- SMITH, S. H.**
Ultrasonic techniques for repair of aircraft structures with bonded composite patches
p 136 N95-19486
- SMITH, V. K.**
Hypersonic flight testing
[AD-A283981] p 134 N95-18891
- SNEL, H.**
Sectional prediction of 3D effects for separated flow on rotating blades
[PB94-201696] p 117 N95-18503
- SOBIECZKY, H.**
DLR-F5: Test wing for CFD and applied aerodynamics
p 113 N95-17864
- SOMMERFELDT, SCOTT D.**
Active minimization of energy density in three-dimensional enclosures
[NASA-CR-197213] p 172 N95-16848
- SPAID, F. W.**
The crucial role of wall interference, support interference and flow field measurements in the development of advanced aircraft configurations
p 162 N95-19252
- SPARKS, W. A.**
Aircraft stress sequence development: A complex engineering process made simple
p 136 N95-19480
- SRINIVASA, C.**
Solution of full potential equation on an airfoil by multigrad technique
[NAL-TM-CSS-9303] p 119 N95-18904
- SRIVASTAVA, ASHOK**
Panel methods
p 165 N95-19448
- STANEWSKY, E.**
Data from the GARTEur (AD) Action Group 02 airfoil CAST 7/DOA1 experiments
p 111 N95-17856
- STANNILAND, D.**
Investigation of the flow development on a highly swept canard/wing research model with segmented leading- and trailing-edge flaps
p 114 N95-17876
Investigation into the aerodynamic characteristics of a combat aircraft research model fitted with a forward swept wing
p 116 N95-17884
Investigation of the influence of pylons and stores on the wing lower surface flow
p 116 N95-17885
- STARNES, JAMES H., JR.**
Nonlinear analysis of damaged stiffened fuselage shells subjected to combined loads
p 137 N95-19499
- STEFKO, GEORGE L.**
NASA Lewis Research Center Workshop on Forced Response in Turbomachinery
[NASA-CP-10147] p 141 N95-19380
- STEIN, KEITH R.**
Parachute inflation: A problem in aeroelasticity
[AD-A284375] p 117 N95-18340
- STEINETZ, B. M.**
Static and dynamic friction behavior of candidate high temperature airframe seal materials
[NASA-TM-106571] p 152 N95-16905
- STEWART, MICHAEL**
Field and data analysis studies related to the atmospheric environment
[NASA-CR-196543] p 168 N95-18093
- STORAASLI, OLAF O.**
Rapid solution of large-scale systems of equations
p 169 N95-16458
- STOREY, BRETT**
Industry review of a crew-centered cockpit design process and toolset
[AD-A282966] p 130 N95-17661
- STOUFFLET, B.**
Review of the EUROPT Project AERO-0026
p 129 N95-16573
- STRAWN, ROGER**
Mesh quality control for multiply-refined tetrahedral grids
[NASA-CR-197595] p 160 N95-18737
- STURISKY, SELWYN HOWARD**
A linear system identification and validation of an AH-64 Apache aeroelastic simulation model
p 146 N95-18903
- SU, M.**
Simulation investigation on system identification of gas turbine
[PB95-104238] p 139 N95-17749
- SUARD, NORBERT**
A processing centre for the CNES CE-GPS experimentation
p 125 N95-17196
- SUAZES, CARLOS J.**
Development of a multicomponent force and moment balance for water tunnel applications, volume 1
[NASA-CR-4642-VOL-1] p 161 N95-18955
Development of a multicomponent force and moment balance for water tunnel applications, volume 2
[NASA-CR-4642-VOL-2] p 161 N95-18956
- SUES, ROBERT H.**
Portable parallel stochastic optimization for the design of aeropropulsion components
[NASA-CR-195312] p 154 N95-16072
- SUI, JUNYOU**
Aerodynamic design and calculation of flow around the plane cascade of turbine
[BTN-94-EIX94481415357] p 104 A95-65347
- SUNDER, R.**
Ageing nuclear power plant management: An aeronautical viewpoint
[NAL-PD-SN-9306] p 105 N95-18606
- SUNDURIN, V. G.**
Simulation of multidisciplinary problems for the thermostress state of cooled high temperature turbines
p 140 N95-19021
- SWETTIS, J.**
Automation of reverse engineering process in aircraft modeling and related optimization problems
[NASA-CR-197109] p 129 N95-16899
- SWIERTRA, S.**
On-line handling of air traffic: Management, guidance and control
[AGARD-AG-321] p 126 N95-18927
- SWIFT, T.**
Widespread fatigue damage monitoring: Issues and concerns
p 136 N95-19488
- SZODRUCH, JOACHIM**
A supercritical airfoil experiment
p 111 N95-17858

T

- TAASAN, SHLOMO**
Airfoil optimization by the one-shot method
p 128 N95-16569
- TALBOT, T.**
Aircraft wake vortex takeoff tests at O'Hara International Airport
[AD-A283828] p 118 N95-18624
- TARTAKOVSKY, ALEXANDER**
Minimal time detection algorithms and applications to flight systems
[TR-2-FSRC-93] p 171 N95-18564
- TAWFIK, HAZEM**
Quality optimization of thermally sprayed coatings produced by the JP-5000 (HVOF) gun using mathematical modeling
p 152 N95-19008
- TERESHCHUK, V. S.**
Generalized method of solving topological optimization problems for electrical airplane equipment systems in computer-aided design
p 169 N95-16272
- THOMAS, SCOTT R.**
Operating capability and current status of the reactivated NASA Lewis Research Center Hypersonic Tunnel Facility
[NASA-TM-106808] p 148 N95-19286
- THOMPSON, LYNN**
ADST system test report for the rotary wing aircraft airmet aeromodel and weapon model merge with the ATAC 2 baseline
[AD-A281580] p 127 N95-16171
- THOMSON, DOUGLAS**
Evaluation of the fuselage lap joint fatigue and terminating action repair
p 166 N95-19477
- TOUGARD, D.**
Brite-Euram programme: ACQUFAT acoustic fatigue and related damage tolerance of advanced composite and metallic structures
p 174 N95-19159
- TOWNE, MATTHEW C.**
Numerical simulation of dynamic-stall suppression by tangential blowing
[AD-A284887] p 120 N95-19110
- TREFNY, CHARLES J.**
Operating capability and current status of the reactivated NASA Lewis Research Center Hypersonic Tunnel Facility
[NASA-TM-106808] p 148 N95-19286
- TSAI, C. Y.**
Free-jet testing at Mach 3.44 in GASL's aero/thermo test facility
p 145 N95-16320
- TUMMALA, MURALI**
Waveform bounding and combination techniques for direct drive testing
[AD-A284075] p 161 N95-19035
- TURNER, MARK A.**
A computational investigation of wake-induced airfoil flutter in incompressible flow and active flutter control
[AD-A281534] p 142 N95-16109

V

- VAKHITOV, M. V.**
Development of strength analysis methods and design model for aircraft constructions in Kazan Aviation Institute
p 127 N95-16264
- VANCHAU, MICHAEL N.**
Virtual environment application with partial gravity simulation
p 169 N95-15988
- VANDAM, CORNELIS P.**
Numerical simulation of helicopter engine plume in forward flight
[NASA-CR-197488] p 107 N95-16589
- VANDENBERG, B.**
Low-speed surface pressure and boundary layer measurement data for the NLR 7301 airfoil section with trailing edge flap
p 111 N95-17855
- VANDERBURGH, A. H. P.**
On the dynamics of aeroelastic oscillators with one degree of freedom
[BTN-94-EIX94501431527] p 153 A95-64524
- VANDERVELDEN, A.**
Tools for applied engineering optimization
p 128 N95-16570
The global aircraft shape
p 128 N95-16571
Aerodynamic shape optimization
p 128 N95-16572
- VANGRIETHUYSEN, VALERIE J.**
An engineering code to analyze hypersonic thermal management systems
p 155 N95-16322
- VANROSENDALE, JOHN**
Floating shock fitting via Lagrangian adaptive meshes
[NASA-CR-194997] p 170 N95-18110

- VASIL'EV, G. V.**
Analytical description of and forecast for stress relaxation of aviation materials under the vibration conditions
[BTN-94-EIX94461408751] p 126 A95-63634
- VENEDIKTOV, V. D.**
Application of multidisciplinary models to the cooled turbine rotor design p 140 N95-19024
- VERDON, JOSEPH M.**
Unsteady aerodynamic analyses for turbomachinery aeroelastic predictions p 141 N95-19381
- VERHAAGEN, N. G.**
Experimental investigation of the vortex flow over a 76/60-deg double delta wing p 114 N95-17874
- VERONA, ROBERT W.**
Factors affecting the visual fragmentation of the field-of-view in partial binocular overlap displays
[AD-A283081] p 172 N95-17334
- VICROY, DAN D.**
Microburst vertical wind estimation from horizontal wind measurements
[NASA-TP-3460] p 131 N95-18198
- VISBAL, MIGUEL R.**
Numerical simulation of transient vortex breakdown above a pitching delta wing
[AD-A281075] p 107 N95-16808
- VISWANATHAN, K.**
Linear instability waves in supersonic jets confined in circular and non-circular ducts
[BTN-94-EIX94341340068] p 103 A95-63520
- VIZ, MARK J.**
Fatigue crack growth in 2024-T3 aluminum under tensile and transverse shear stresses p 153 N95-19490
- VLEJGER, H.**
Results of uniaxial and biaxial tests on riveted fuselage lap joint specimens p 136 N95-19491
- VOSTEEN, LOUIS F.**
Composite chronicles: A study of the lessons learned in the development, production, and service of composite structures
[NASA-CR-4620] p 151 N95-16859
- ## W
- WAHLS, RICHARD A.**
Comparison of computational and experimental results for a supercritical airfoil
[NASA-TM-4601] p 108 N95-16908
- WAIBEL, MICHAEL**
Theoretical investigations of shock/boundary layer interactions on a Ma(infinity) = 8 waverider
[DLR-FB-94-12] p 119 N95-18910
- WALDEN, RAINER**
Time-optimal turn to a heading: An analytic solution
[BTN-94-EIX94511433940] p 142 A95-64606
- WALKER, STEVEN H.**
Modelling structurally damaging twin-jet screech p 135 N95-19154
- WALLACE, CLARK E.**
An engineering code to analyze hypersonic thermal management systems p 155 N95-16322
- WANG, JIGEN**
Development and application of the double V type flame stabilizer
[BTN-94-EIX94481415355] p 154 A95-65345
- WANG, KON-SHENG CHARLES**
In-flight imaging of transverse gas jets injected into transonic and supersonic crossflows: Design and development
[NASA-CR-186031] p 157 N95-17418
- WANG, YIFEI**
An approach to aerodynamic characteristics of low radar cross-section fuselages p 106 N95-16251
- WARMAN, R. M.**
The impact of non-linear flight control systems on the prediction of aircraft loads due to turbulence p 143 N95-18598
- WARREN, DANIEL E.**
A VHF/UHF antenna for the Precision Antenna Measurement System (PAMS)
[AD-A285673] p 156 N95-16621
- WASSENBERGH, HENRI A.**
World trends in air transport policies. (Approaching the 21st century)
[HTN-95-50220] p 176 A95-64857
- WATSON, CAROLYN B.**
Experimental study at low supersonic speeds of a missile concept having opposing wraparound tails
[NASA-TM-4582] p 106 N95-16069
- WAWRZYNEK, PAUL A.**
Discrete crack growth analysis methodology for through cracks in pressurized fuselage structures p 166 N95-19473

- WEATHERS, JEFFREY T.**
Comparison of frequency response and perturbation methods to extract linear models from a nonlinear simulation
[AD-A284115] p 146 N95-18405
- WEAVER, THOMAS L.**
Fiber Optic Control System integration for advanced aircraft. Electro-optic and sensor fabrication, integration, and environmental testing for flight control systems
[NASA-CR-191194] p 162 N95-19236
- WEI, YING-JYI PAUL**
Intelligent control law tuning for AIAA controls design challenge
[BTN-94-EIX94511433922] p 169 A95-64588
- WEILENMANN, MARTIN F.**
Test bench for rotorcraft hover control
[BTN-94-EIX94511433919] p 169 A95-64585
- WEINTRAUB, DAVID**
Development of an Automated Airfield Dynamic Cone Penetrometer (AADCP) prototype and the evaluation of unsurfaced airfield seismic surveying using Spectral Analysis of Surface Waves (SASW) technology
[AD-A281985] p 145 N95-17444
- WEIRICH, R. F.**
Transonic wind tunnel boundary interference correction p 147 N95-19271
- WENGLAR, LYDIA**
New technologies for space avionics
[NASA-CR-197574] p 150 N95-18196
- WENTZ, KENNETH R.**
Thermo-acoustic fatigue design for hypersonic vehicle skin panels p 162 N95-19161
- WETTLAUFER, BRIAN**
Hypersonic air-breathing aeropropulsion facility test support requirements p 144 N95-16319
- WHITE, R. G.**
Nonlinear dynamic response of aircraft structures to acoustic excitation p 135 N95-19151
- WILLARD, SCOTT A.**
The characterization of widespread fatigue damage in fuselage structure p 166 N95-19472
- WILLAUME, J.**
Interaction of a three strut support on the aerodynamic characteristics of a civil aviation model p 122 N95-19279
- WILLIAMS, GLENN W.**
Universal wind tunnel data acquisition and reduction software
[AD-A283897] p 171 N95-18365
- WILLIAMS, W. D.**
Hypersonic flow-field measurements: Intrusive and nonintrusive
[AD-A283867] p 119 N95-18674
- WILSON, DALE A.**
Fatigue and residual strength investigation of ARALL(R) -3 and GLARE(R) -2 panels with bonded stringers p 137 N95-19495
- WILSON, WILLIAM G.**
Recent advances in graphite/epoxy motor cases p 149 N95-16333
- WIMMER, W.**
EURECA mission control experience and messages for the future p 149 N95-17252
- WING, DAVID J.**
Twin engine afterbody model p 115 N95-17880
Static investigation of two fluidic thrust-vectoring concepts on a two-dimensional convergent-divergent nozzle
[NASA-TM-4574] p 120 N95-19042
- WINNENBERG, THOMAS F.**
Waveform bounding and combination techniques for direct drive testing
[AD-A284075] p 161 N95-19035
- WIRKANDER, S. L.**
Evaluation of an autopilot based multimodelling
[PB94-190725] p 142 N95-17454
- WOLFE, H. F.**
Nonlinear dynamic response of aircraft structures to acoustic excitation p 135 N95-19151
- WONG, J. P. C.**
Application of superplastically formed and diffusion bonded structures in high intensity noise environments p 174 N95-19162
- WONG, K. C.**
Six degree of freedom flight dynamic and performance simulation of a remotely-piloted vehicle
[AERO-TN-9301] p 131 N95-18097
- WOODS-VEDELER, JESSICA A.**
Active load control during rolling maneuvers
[NASA-TP-3455] p 129 N95-17397
- WOODWARD, RICHARD P.**
Background noise levels measured in the NASA Lewis 9- by 15-foot low-speed wind tunnel
[NASA-TM-106817] p 145 N95-18054

- WRIGHT, A.**
Aircraft wake vortex takeoff tests at O'Hara International Airport
[AD-A283828] p 118 N95-18624
- WU, MING**
Fatigue and residual strength investigation of ARALL(R) -3 and GLARE(R) -2 panels with bonded stringers p 137 N95-19495
- WU, XIAOQING**
Linear prediction data extrapolation superresolution radar imaging p 155 N95-16268
- WU, XINGPING**
Direct splitting of coefficient matrix for numerical calculation of transonic nozzle flow
[BTN-94-EIX94481415356] p 103 A95-65346

Y

- YAN, YANGGUANG**
The computer analysis of the prediction of aircraft electrical power supply system reliability p 155 N95-16278
- YANIEC, JOHN S.**
Users guide for NASA Lewis Research Center DC-9 Reduced-Gravity Aircraft Program
[NASA-TM-106755] p 146 N95-18586
- YANO, STEVE E.**
Arcjet thruster research and technology, phase 2
[NASA-CR-182276] p 105 N95-18044
- YARMUS, J.**
Aircraft wake vortex takeoff tests at O'Hara International Airport
[AD-A283828] p 118 N95-18624
- YAU, M.**
Demonstration of the Dynamic Flowgraph Methodology using the Titan 2 Space Launch Vehicle Digital Flight Control System
[NASA-CR-197517] p 150 N95-17493
- YE, ZHENRU**
Linear prediction data extrapolation superresolution radar imaging p 155 N95-16268
- YEH, J. R.**
Prediction of R-curves from small coupon tests p 167 N95-19496
- YORK, JAMES L.**
Recent advances in graphite/epoxy motor cases p 149 N95-16333
- YOST, J. D.**
Aircraft fatigue and crack growth considering loads by structural component p 137 N95-19497
- YOUNG, RICHARD D.**
Nonlinear analysis of damaged stiffened fuselage shells subjected to combined loads p 137 N95-19499
- YOUNG, T. S.**
Wind turbine blade aerodynamics: The combined experiment
[DE94-011866] p 118 N95-18645
Wind turbine blade aerodynamics: The analysis of field test data
[DE94-011867] p 118 N95-18646
- YUAN, XIN**
Application of GPS/SINS/RA integrated system to aircraft approach landing p 125 N95-16277

Z

- ZAKIROV, I. M.**
Development of processes, means, and theoretical principles of thin-walled detail plastic forming at Kazan Aviation Institute p 155 N95-16281
- ZAKRAJSEK, JAMES J.**
Detecting gear tooth fracture in a high contact ratio face gear mesh
[NASA-TM-106822] p 162 N95-19125
- ZEHNDE, ALAN T.**
Fatigue crack growth in 2024-T3 aluminum under tensile and transverse shear stresses p 153 N95-19490
- ZHANG, CAIWEN**
An approach to aerodynamic characteristics of low radar cross-section fuselages p 106 N95-16251
An improved method of airfoil design p 106 N95-16252
- ZHANG, HONGBIN**
Development and application of the double V type flame stabilizer
[BTN-94-EIX94481415355] p 154 A95-65345
- ZHANG, QIWEI**
Wall-signature methods for high speed wind tunnel wall interference corrections p 107 N95-16257
- ZHANG, XIAOQIU**
Investigation of dynamic inflow's influence on rotor control derivatives p 155 N95-16250

PERSONAL AUTHOR INDEX

ZURIGAT, Y. H.

ZHARINOV, V. G.

A stationary flow of a viscous liquid in radial clearances
of rotor bearings in the turbocompressor of an internal
combustion engine
[BTN-94-EIX94461408765] p 153 A95-63648

ZHOU, YE

On the Lighthill relationship and sound generation from
isotropic turbulence
[NASA-CR-195005] p 159 N95-18191

ZHU, JIANYING

Joint Proceedings on Aeronautics and Astronautics
(JPAA)
[ISBN-7-80-046602-7] p 104 N95-16249

ZHU, ZHAODA

Linear prediction data extrapolation superresolution
radar imaging p 155 N95-16268

ZUPPARDI, G.

Adaptive wind tunnel walls versus wall interference
correction methods in 2D flows at high blockage ratios
p 147 N95-19267

ZURIGAT, Y. H.

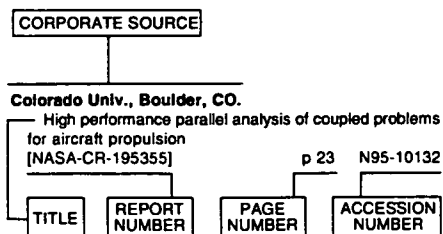
Effect of crossflow on Goertler instability in
incompressible boundary layers
[NASA-CR-195007] p 159 N95-18193

CORPORATE SOURCE INDEX

AERONAUTICAL ENGINEERING / A Continuing Bibliography (Supplement 316)

April 1995

Typical Corporate Source Index Listing



Listings in this index are arranged alphabetically by corporate source. The title of the document is used to provide a brief description of the subject matter. The page number and the accession number are included in each entry to assist the user in locating the abstract in the abstract section. If applicable, a report number is also included as an aid in identifying the document.

A

Advisory Group for Aerospace Research and Development, Neuilly-Sur-Seine (France).

- Optimum Design Methods for Aerodynamics
[AGARD-R-803] p 127 N95-16562
- Experimental and analytical methods for the determination of connected-pipe ramjet and ducted rocket internal performance
[AGARD-AR-323] p 149 N95-17278
- Aircraft and sub-system certification by piloted simulation
[AGARD-AR-278] p 145 N95-17388
- A selection of experimental test cases for the validation of CFD codes, volume 2
[AGARD-AR-303-VOL-2] p 109 N95-17846
- A selection of experimental test cases for the validation of CFD codes. Supplement: Datasets A-E
[AGARD-AR-303-SUPPL] p 117 N95-18539
- Aircraft Loads due to Turbulence and their Impact on Design and Certification
[AGARD-R-798] p 143 N95-18597
- On-line handling of air traffic: Management, guidance and control
[AGARD-AG-321] p 126 N95-18927
- Mathematical Models of Gas Turbine Engines and their Components
[AGARD-LS-198] p 139 N95-19017
- Impact of Acoustic Loads on Aircraft Structures
[AGARD-CP-549] p 173 N95-19142
- Wall Interference, Support Interference and Flow Field Measurements
[AGARD-CP-535] p 162 N95-19251
- Aeronautical Research Inst. of Sweden, Bromma.**
- Low speed propeller slipstream aerodynamic effects
p 116 N95-17882
- Computational simulations for some tests in transonic wind tunnels
p 164 N95-19264
- Calculation of low speed wind tunnel wall interference from static pressure pipe measurements
p 164 N95-19273

- Aeronautical Systems Div., Wright-Patterson AFB, OH.**
- KC-135 cockpit modernization study. Phase 1: Equipment evaluation
[AD-A284099] p 131 N95-18398
- Aerospaiale, Toulouse (France).**
- Gyroscopic and propeller aerodynamic effects on engine mounts dynamic loads in turbulence conditions
p 132 N95-18599
- Interaction of a three strut support on the aerodynamic characteristics of a civil aviation model
p 122 N95-19279
- Air Force Inst. of Tech., Wright-Patterson AFB, OH.**
- Development of an Automated Airfield Dynamic Cone Penetrometer (AADCP) prototype and the evaluation of unsurfaced airfield seismic surveying using Spectral Analysis of Surface Waves (SASW) technology
[AD-A281985] p 145 N95-17444
- Numerical simulation of dynamic-stall suppression by tangential blowing
[AD-A284887] p 120 N95-19110
- Aircraft Research Association Ltd., Bedford (England).**
- Investigation of the flow development on a highly swept canard/wing research model with segmented leading- and trailing-edge flaps
p 114 N95-17876
- Investigation into the aerodynamic characteristics of a combat aircraft research model fitted with a forward swept wing
p 116 N95-17884
- Investigation of the influence of pylons and stores on the wing lower surface flow
p 116 N95-17885
- Alabama Univ., Huntsville, AL.**
- Field and data analysis studies related to the atmospheric environment
[NASA-CR-196543] p 168 N95-18093
- Alcoa Technical Center, Alcoa Center, PA.**
- An artificial corrosion protocol for lap-splices in aircraft skin
p 152 N95-19482
- Alenia, Turin (Italy).**
- Impact of noise environment on engine nacelle design
p 173 N95-19147
- Alenia Spazio S.p.A., Turin (Italy).**
- An overall approach of cockpit noise verification in a military aircraft
p 175 N95-19163
- Aluminum Co. of America, Alcoa Center, PA.**
- Prediction of R-curves from small coupon tests
p 167 N95-19496
- Analytical Methods, Inc., Redmond, WA.**
- Calculation of support interference in dynamic wind-tunnel tests
p 122 N95-19282
- Analytical Services and Materials, Inc., Hampton, VA.**
- Composite chronicles: A study of the lessons learned in the development, production, and service of composite structures
[NASA-CR-4620] p 151 N95-16859
- Multi-lab comparison on R-curve methodologies: Alloy 2024-T3
[NASA-CR-195004] p 151 N95-16860
- Applied Research Associates, Inc., Raleigh, NC.**
- Portable parallel stochastic optimization for the design of aeropropulsion components
[NASA-CR-195312] p 154 N95-16072
- Applied Thermal Sciences, Orono, ME.**
- Combustor kinetic energy efficiency analysis of the hypersonic research engine data
p 148 N95-16321
- Army Aeromedical Research Lab., Fort Rucker, AL.**
- The assessment of the AH-64D, longbow, mast-mounted assembly noise hazard for maintenance personnel
[AD-A284971] p 171 N95-16226
- A correlative investigation of simulated occupant motion and accident report in a helicopter crash
[AD-A285190] p 123 N95-16404
- Factors affecting the visual fragmentation of the field-of-view in partial binocular overlap displays
[AD-A283081] p 172 N95-17334
- Army Aviation Research and Development Command, Moffett Field, CA.**
- Wall interaction effects for a full-scale helicopter rotor in the NASA Ames 80- by 120-foot wind tunnel
p 121 N95-19270
- Army Aviation Systems Command, Moffett Field, CA.**
- 2-D and 3-D oscillating wing aerodynamics for a range of angles of attack including stall
[NASA-TM-4632] p 120 N95-19119

- Army Natick Research and Development Command, MA.**
- Parachute inflation: A problem in aeroelasticity
[AD-A284375] p 117 N95-18340
- Army Research Lab., Aberdeen Proving Ground, MD.**
- Helicopter Performance Evaluation (HELPE) computer model
[AD-A284319] p 131 N95-18381
- Static aerodynamics CFD analysis for 120-mm hypersonic KE projectile design
[ARL-MR-184] p 118 N95-18611
- Numerical computations of supersonic base flow with special emphasis on turbulence modeling
[AD-A283688] p 119 N95-18670
- Army Research Lab., Cleveland, OH.**
- Sensor fault detection and diagnosis simulation of a helicopter engine in an intelligent control framework
[NASA-TM-106784] p 137 N95-15970
- Detecting gear tooth fracture in a high contact ratio face gear mesh
[NASA-TM-106822] p 162 N95-19125
- Arnold Engineering Development Center, Arnold AFS, TN.**
- A model for preliminary facility design including simulation issues
p 144 N95-16318
- Hypersonic air-breathing aeropropulsion facility test support requirements
p 144 N95-16319
- Hypersonic wind tunnel test techniques
[AD-A284057] p 118 N95-18663
- Hypersonic flow-field measurements: Intrusive and nonintrusive
[AD-A283867] p 119 N95-18674
- Hypersonic flight testing
[AD-A283981] p 134 N95-18891
- Avions Marcel Dassault-Breguet Aviation, Saint-Cloud (France).**
- Review of the EUROPT Project AERO-0026
p 129 N95-16573

B

- Battelle Columbus Labs., OH.**
- Bicarbonate of soda blasting technology for aircraft wheel depainting
[PB94-193323] p 104 N95-17466
- Ultrasonic techniques for repair of aircraft structures with bonded composite patches
p 136 N95-19486
- Boeing Commercial Airplane Co., Seattle, WA.**
- Two-dimensional high-lift airfoil data for CFD code validation
p 112 N95-17859
- The application of Newman crack-closure model to predicting fatigue crack growth
p 167 N95-19483
- British Aerospace Airbus Ltd., Bristol (England).**
- The impact of non-linear flight control systems on the prediction of aircraft loads due to turbulence
p 143 N95-18598
- British Aerospace Aircraft Group, Bristol (England).**
- Application of superplastically formed and diffusion bonded structures in high intensity noise environments
p 174 N95-19162
- British Aerospace Aircraft Group, Preston (England).**
- Transonic and supersonic flowfield measurements about axisymmetric afterbodies for validation of advanced CFD codes
p 121 N95-19260
- British Aerospace Aircraft Group, Watton (England).**
- Current and future problems in structural acoustic fatigue
p 173 N95-19143
- British Columbia Univ., Vancouver (British Columbia).**
- Unsteady flow testing in a passive low-correction wind tunnel
p 147 N95-19272
- Burnette Engineering, Fairborn, OH.**
- An evaluation of aircraft CRT and dot-matrix display legibility requirements
[AD-A283933] p 138 N95-18164

C

- California Univ., Davis, CA.**
- Numerical simulation of helicopter engine plume in forward flight
[NASA-CR-197488] p 107 N95-16589

- California Univ., Los Angeles, CA.**
In-flight imaging of transverse gas jets injected into transonic and supersonic crossflows: Design and development
[NASA-CR-186031] p 157 N95-17418
Demonstration of the Dynamic Flowgraph Methodology using the Titan 2 Space Launch Vehicle Digital Flight Control System
[NASA-CR-197517] p 150 N95-17493
Minimal time detection algorithms and applications to flight systems
[TR-2-FSRC-93] p 171 N95-18564
The accuracy of parameter estimation in system identification of noisy aircraft load measurement
[NASA-CR-197516] p 134 N95-19130
- Carnegie-Mellon Univ., Pittsburgh, PA.**
A feedforward control approach to the local navigation problem for autonomous vehicles
[AD-A282787] p 126 N95-17706
- Case Western Reserve Univ., Cleveland, OH.**
Three dimensional compressible turbulent flow computations for a diffusing S-duct with/without vortex generators
[NASA-CR-195390] p 138 N95-17402
- CCG Associates, Inc., Silver Spring, MD.**
Identification of Artificial Intelligence (AI) applications for maintenance, monitoring, and control of airway facilities
[AD-A282479] p 125 N95-17373
- Central Aerohydrodynamics Inst., Zhukovsky (Russia).**
Optical surface pressure measurements: Accuracy and application field evaluation
p 175 N95-19274
- Central Inst. of Aviation Motors, Moscow (Russia).**
Solution of Navier-Stokes equations using high accuracy monotone schemes
p 161 N95-19019
The mathematical models of flow passage for gas turbine engines and their components
p 140 N95-19020
Simulation of multidisciplinary problems for the thermostress state of cooled high temperature turbines
p 140 N95-19021
Application of multicomponent models to flow passage simulation in multistage turbomachines and whole gas turbine engines
p 140 N95-19022
Simulation of steady and unsteady viscous flows in turbomachinery
p 140 N95-19023
Application of multidisciplinary models to the cooled turbine rotor design
p 140 N95-19024
Verification of multidisciplinary models for turbomachines
p 140 N95-19025
Perspective problems of gas turbine engines simulation
p 140 N95-19026
- Centre d'Etudes et de Recherches, Toulouse (France).**
Experimental techniques for measuring transonic flow with a three dimensional laser velocimetry system. Application to determining the drag of a fuselage
p 163 N95-19258
Analysis of test section sidewall effects on a two dimensional airfoil: Experimental and numerical investigations
p 165 N95-19276
- Centre National d'Etudes Spatiales, Toulouse (France).**
A processing centre for the CNES CE-GPS experimentation
p 125 N95-17196
- Cessna Aircraft Co., Wichita, KS.**
Design limit loads based upon statistical discrete gust methodology
p 133 N95-18603
- City Univ., London (England).**
Interference determination for wind tunnels with slotted walls
p 147 N95-19269
- College of William and Mary, Williamsburg, VA.**
A spectrally accurate boundary-layer code for infinite swept wings
[NASA-CR-195014] p 159 N95-18042
- Colorado Univ., Boulder, CO.**
Structural effects of unsteady aerodynamic forces on horizontal-axis wind turbines
[DE94-011863] p 157 N95-16939
- Construcciones Aeronauticas S.A., Madrid (Spain).**
A study of the effect of store unsteady aerodynamics on gust and turbulence loads
p 133 N95-18601
- Cornell Univ., Ithaca, NY.**
Wave cycle design for wave rotor engines with limited nitrogen oxide emissions
p 161 N95-18901
Fatigue crack growth in 2024-T3 aluminum under tensile and transverse shear stresses
p 153 N95-19490
- D**
- DACC SCI, Inc., Columbia, MD.**
The use of electrochemistry and ellipsometry for identifying and evaluating corrosion on aircraft
[AD-A285323] p 151 N95-16371
- Dassault Aviation, Saint-Cloud (France).**
Aeroacoustic qualification of HERMES shingles
p 173 N95-19145
- Brite-Euram programme: ACOUFAT acoustic fatigue and related damage tolerance of advanced composite and metallic structures**
p 174 N95-19159
- Dayton Univ., OH.**
Conference on Aerospace Transparent Materials and Enclosures, volume 1
[AD-A283925] p 133 N95-18677
- Dayton Univ. Research Inst., OH.**
Conference on Aerospace Transparent Materials and Enclosures. Volume 2: Sessions 5-9
[AD-A283926] p 131 N95-18162
- De Havilland Aircraft Co. of Canada Ltd., Downsview (Ontario).**
A review of gust load calculation methods at de Havilland
p 118 N95-18604
Interference corrections for a centre-line plate mount in a porous-walled transonic wind tunnel
p 122 N95-19280
- Defence Research Agency, Bedford (England).**
Investigation of the flow over a series of 14 percent-thick supercritical aerofoils with significant rear camber
p 109 N95-17849
Detailed study at supersonic speeds of the flow around delta wings
p 112 N95-17861
Pressure distributions on research wing W4 mounted on an axisymmetric body
p 112 N95-17862
Boundary-flow measurement methods for wall interference assessment and correction: Classification and review
p 163 N95-19262
- Defence Research Agency, Farnborough, Hampshire (England).**
Measurements on a two-dimensional aerofoil with high-lift devices
p 109 N95-17848
Measurements of the flow over a low aspect-ratio wing in the Mach number range 0.6 to 0.87 for the purpose of validation of computational methods. Part 1: Wing design, model construction, surface flow. Part 2: Mean flow in the boundary layer and wake, 4 test cases
p 112 N95-17860
- Defence Science and Technology Organization, Melbourne (Australia).**
Data acquisition and processing software for the Low Speed Wind Tunnel tests of the Jindivik auxiliary air intake
[AD-A285455] p 108 N95-17178
- Delavan, Inc., West Des Moines, IA.**
Thermal chemical energy of ablating silica surfaces in air breathing solid rocket engines
p 148 N95-16316
- Department of the Navy, Washington, DC.**
Corner vortex suppressor
[AD-D016423] p 116 N95-18337
Hydrofoil force balance
[AD-D016475] p 160 N95-18461
Integrated aerodynamic fin and stowable TVC vane system
[AD-D016457] p 151 N95-19073
Solid fuel ramjet composition
[AD-D016458] p 152 N95-19090
- Deutsche Aerospace A.G., Bremen (Germany).**
Acoustic fatigue testing on different materials and skin-stringer elements
p 174 N95-19156
- Deutsche Airbus G.m.b.H., Bremen (Germany).**
Tools for applied engineering optimization
p 128 N95-16570
The global aircraft shape
p 128 N95-16571
Aerodynamic shape optimization
p 128 N95-16572
- Deutsche Airbus G.m.b.H., Hamburg (Germany).**
Treatment of non-linear systems by timeplane-transformed CT methods: The spectral gust method
p 143 N95-18600
Development of load spectra for Airbus A330/A340 full scale fatigue tests
p 135 N95-19479
- Deutsche Forschungsanstalt fuer Luft- und Raumfahrt, Brunswick (Germany).**
2-D airfoil tests including side wall boundary layer measurements
p 158 N95-17847
DLR-F4 wing body configuration
p 130 N95-17863
Subsonic flow around US-orbiter model FALKE in the DNW
p 115 N95-17877
Pressure distribution measurements on an isolated TPS 441 nacelle
p 115 N95-17878
Theoretical investigations of shock/boundary layer interactions on a Ma(infinity) = 8 waverider
[DLR-FB-94-12] p 119 N95-18910
Wall correction method with measured boundary conditions for low speed wind tunnels
p 164 N95-19263
- Deutsche Forschungsanstalt fuer Luft- und Raumfahrt, Cologne (Germany).**
Wind tunnel investigations of the appearance of shocks in the windward region of bodies with circular cross section at angle of attack
p 113 N95-17866
One-dimensional flow description for the combustion chamber of a scramjet
[DLR-FB-94-06] p 139 N95-18911
- Deutsche Forschungsanstalt fuer Luft- und Raumfahrt, Goettingen (Germany).**
DLR-F5: Test wing for CFD and applied aerodynamics
p 113 N95-17864
Three-dimensional boundary layer and flow field data of an inclined prolate spheroid
p 158 N95-17867
Force and pressure data of an ogive-nosed slender body at high angles of attack and different Reynolds numbers
p 113 N95-17868
Wind tunnel test on a 65 deg delta wing with rounded leading edges: The International Vortex Flow Experiment
p 114 N95-17875
Flow field investigation in a free jet - free jet core system for the generation of high intensity molecular beams
[DLR-FB-94-11] p 172 N95-18912
- Duke Univ., Durham, NC.**
Acoustic radiation damping of flat rectangular plates subjected to subsonic flows
p 172 N95-18542
- E**
- Eidetics International, Inc., Torrance, CA.**
Development of a multicomponent force and moment balance for water tunnel applications, volume 1
[NASA-CR-4642-VOL-1] p 161 N95-18955
Development of a multicomponent force and moment balance for water tunnel applications, volume 2
[NASA-CR-4642-VOL-2] p 161 N95-18956
- Electronics Research Lab., Salisbury (Australia).**
A PC-based interactive simulation of the F-111C Pavé Tack system and related sensor, avionics and aircraft aspects
[AD-A285500] p 129 N95-16969
- Environmental Protection Agency, Cincinnati, OH.**
Bicarbonate of soda blasting technology for aircraft wheel decontamination
[PB94-193323] p 104 N95-17466
- Eurocopter Deutschland G.m.b.H., Munich (Germany).**
Helicopter internal noise
p 173 N95-19144
- European Space Agency, European Space Operations Center, Darmstadt (Germany).**
Safety aspects of spacecraft commanding
p 149 N95-17248
EURECA mission control experience and messages for the future
p 149 N95-17252
Packet utilisation definitions for the ESA XMM mission
p 150 N95-17596
- F**
- Federal Aviation Administration, Atlanta, GA.**
Evaluation of an unlighted swinging airport sign
[AD-A284763] p 146 N95-18087
Operational And Supportability Implementation System (OASIS) test and evaluation master plan
[AD-A284765] p 126 N95-18088
- Federal Aviation Administration, Cambridge, MA.**
An analysis of tower (local) controller-pilot voice communications
[AD-A283718] p 160 N95-18436
Aircraft wake vortex takeoff tests at O'Hara International Airport
[AD-A283828] p 118 N95-18624
- Federal Aviation Administration, Long Beach, CA.**
Widespread fatigue damage monitoring: Issues and concerns
p 136 N95-19488
- Federal Aviation Administration, Washington, DC.**
Federal aviation regulations, part 91. General operating and flight rules. Change 5
[PB94-194883] p 123 N95-17476
- Foster-Miller Associates, Inc., Waltham, MA.**
Evaluation of the fuselage lap joint fatigue and terminating action repair
p 166 N95-19477
- G**
- General Accounting Office, Washington, DC.**
European aeronautics: Strong government presence in industry structure and research and development support. Report to Congressional Requesters
[GAO/NSIAD-94-71] p 176 N95-18578
- General Applied Science Labs., Inc., Ronkonkoma, NY.**
Free-jet testing at Mach 3.44 in GASL's aero/thermo test facility
p 145 N95-16320
- General Electric Co., Cincinnati, OH.**
Scramjet testing guidelines
p 138 N95-16317
- Georgia Inst. of Tech., Atlanta, GA.**
A linear system identification and validation of an AH-64 Apache aeroelastic simulation model
p 146 N95-18903
Development of pneumatic test techniques for subsonic high-lift and in-ground-effect wind tunnel investigations
p 121 N95-19268

- Discrete crack growth analysis methodology for through cracks in pressurized fuselage structures p 166 N95-19473
- Residual life and strength estimates of aircraft structural components with MSD/MED p 136 N95-19485
- German-Dutch Wind Tunnel, North East Polder (Netherlands).**
Correction of support influences on measurements with sting mounted wind tunnel models p 122 N95-19281
- H**
- Hercules Aerospace Co., Magna, UT.**
Recent advances in graphite/epoxy motor cases p 149 N95-16333

- I**
- Industrieanlagen-Betriebsgesellschaft m.b.H., Ottobrunn (Germany).**
Design and operation of a thermoacoustic test facility p 147 N95-19150
- Institute for Aerospace Research, Ottawa (Ontario).**
Applications of the five-hole probe technique for flow field surveys at the Institute for Aerospace Research p 163 N95-19255
- Evaluation of combined wall- and support-interference on wind tunnel models p 122 N95-19278
- Institute for Computer Applications in Science and Engineering, Hampton, VA.**
Algorithms for bilevel optimization [NASA-CR-194980] p 170 N95-16897
- ICASE [NASA-CR-195001] p 170 N95-16898
- Floating shock fitting via Lagrangian adaptive meshes [NASA-CR-194997] p 170 N95-18110
- The stability of two-phase flow over a swept-wing [NASA-CR-194994] p 159 N95-18190
- On the Lighthill relationship and sound generation from isotropic turbulence [NASA-CR-195005] p 159 N95-18191
- Effect of crossflow on Goertler instability in incompressible boundary layers [NASA-CR-195007] p 159 N95-18193
- Instituto de Pesquisas Espaciais, Sao Paulo (Brazil).**
Regenerative cooling for liquid propellant rocket thrust chambers [INPE-5565-TDI/540] p 150 N95-18720

- J**
- Jet Propulsion Lab., California Inst. of Tech., Pasadena, CA.**
Field verification of the wind tunnel coefficients p 109 N95-17291
- Jiaotong Univ., Shanghai (China).**
Simulation investigation on system identification of gas turbine [PB95-104238] p 139 N95-17749
- Johns Hopkins Univ., Columbia, MD.**
The 1993 JANNAF Propulsion Meeting, volume 1 [CPIA-PUBL-602-VOL-1] p 148 N95-16312
- Johnson Controls, Inc., Milwaukee, WI.**
Development of a bipolar lead/acid battery for the more electric aircraft [AD-A284050] p 160 N95-18660

- K**
- Kazan Aviation Inst. (USSR).**
Joint Proceedings on Aeronautics and Astronautics (JPAA) [ISBN-7-80-046602-7] p 104 N95-16249
- Service and physical properties of liquid-jet fuels p 151 N95-16256
- Development of strength analysis methods and design model for aircraft constructions in Kazan Aviation Institute p 127 N95-16264
- Theoretical fundamentals of the aircraft GTE tests p 138 N95-16265
- Generalized method of solving topological optimization problems for electrical airplane equipment systems in computer-aided design p 169 N95-16272
- Development of processes, means, and theoretical principles of thin-walled detail plastic forming at Kazan Aviation Institute p 155 N95-16281
- Krug Life Sciences, Inc., Houston, TX.**
A surgical support system for Space Station Freedom p 149 N95-16776

- L**
- Laboratory for Strength of Materials Components and Structures, Puspiptek (Indonesia).**
Prediction of fatigue crack growth under flight-simulation loading with the modified CORPUS model p 166 N95-19471
- Lockheed Corp., Fort Worth, TX.**
Overview of unsteady transonic wind tunnel test on a semispan straked delta wing oscillating in pitch [AD-A284097] p 117 N95-18380
- Lockheed Sanders, Inc., Nashua, NH.**
New technologies for space avionics [NASA-CR-197574] p 150 N95-18196
- Loral Systems, Inc., Orlando, FL.**
ADST system test report for the rotary wing aircraft airnet aeromodel and weapon model merge with the ATAC 2 baseline [AD-A281580] p 127 N95-16171

- M**
- Marotta Scientific Controls, Inc., Montville, NJ.**
A Lifting Ball Valve for cryogenic fluid applications p 156 N95-16349
- Maryland Univ., College Park, MD.**
Cooperative control theory and integrated flight and propulsion control [NASA-CR-197493] p 142 N95-17404
- Experimental data on the aerodynamic interactions between a helicopter rotor and an airframe p 116 N95-17883
- Massachusetts Inst. of Tech., Cambridge.**
Unsteady flow phenomena in discrete passage diffusers for centrifugal compressors [AD-A281412] p 155 N95-16163
- Workshop on Formal Models for Intelligent Control [AD-A281399] p 169 N95-16864
- Massachusetts Inst. of Tech., Lexington.**
Solid state radar demonstration test results at the FAA Technical Center [AD-A281520] p 154 N95-16097
- McDonnell-Douglas Aerospace, Long Beach, CA.**
Comparison of stochastic and deterministic nonlinear gust analysis methods to meet continuous turbulence criteria p 133 N95-18602
- The crucial role of wall interference, support interference and flow field measurements in the development of advanced aircraft configurations p 162 N95-19252
- McDonnell-Douglas Aerospace, Saint Louis, MO.**
Fiber Optic Control System integration for advanced aircraft. Electro-optic and sensor fabrication, integration, and environmental testing for flight control systems: Laboratory test results [NASA-CR-195408] p 161 N95-18938
- Fiber Optic Control System integration for advanced aircraft. Electro-optic and sensor fabrication, integration, and environmental testing for flight control systems [NASA-CR-191194] p 162 N95-19236
- Transonic wind tunnel boundary interference correction p 147 N95-19271
- McDonnell-Douglas Corp., Long Beach, CA.**
2-D aileron effectiveness study p 110 N95-17851
- McDonnell-Douglas Corp., Saint Louis, MO.**
Aeromechanics technology, volume 1. Task 1: Three-dimensional Euler/Navier-Stokes Aerodynamic Method (TEAM) enhancements [AD-A285713] p 132 N95-18483
- Acoustic fatigue characteristics of advanced materials and structures p 174 N95-19157
- Michigan Univ., Ann Arbor, MI.**
Forced response of mistuned bladed disks p 141 N95-19383
- Mississippi State Univ., Mississippi State, MS.**
Wing design for a civil tiltrotor transport aircraft [NASA-CR-197523] p 130 N95-18090
- Missouri Univ., Rolla, MO.**
Ducted fan acoustic radiation including the effects of nonuniform mean flow and acoustic treatment [NASA-CR-197449] p 172 N95-16401

- N**
- Nangia Associates, Bristol (England).**
Estimating wind tunnel interference due to vectored jet flows p 164 N95-19265
- Nanjing Univ. of Aeronautics and Astronautics, Nanjing, Jiangsu (China).**
Joint Proceedings on Aeronautics and Astronautics (JPAA) [ISBN-7-80-046602-7] p 104 N95-16249
- Investigation of dynamic inflow's influence on rotor control derivatives p 155 N95-16250

- An approach to aerodynamic characteristics of low radar cross-section fuselages p 106 N95-16251
- An improved method of airfoil design p 106 N95-16252
- Wall-signature methods for high speed wind tunnel wall interference corrections p 107 N95-16257
- An investigation of polynomial calibrations methods for wind tunnel balances p 144 N95-16258
- Linear prediction data extrapolation superresolution radar imaging p 155 N95-16268
- Application of GPS/SINS/RA integrated system to aircraft approach landing p 125 N95-16277
- The computer analysis of the prediction of aircraft electrical power supply system reliability p 155 N95-16278
- Naples Univ. (Italy).**
Adaptive wind tunnel walls versus wall interference correction methods in 2D flows at high blockage ratios p 147 N95-19267
- National Academy of Sciences - National Research Council, Washington, DC.**
Assessment of the Space Station program p 149 N95-16352
- National Aeronautical Lab., Bangalore (India).**
Evaluation of the dynamic stability characteristics of the NAL Light Transport Aircraft [NAL-PD-CA-9217] p 142 N95-16392
- National Aeronautics and Space Administration, Washington, DC.**
Revitalizing general aviation [NASA-TM-110113] p 129 N95-16982
- NASA High Performance Computing and Communications program [NASA-TM-4653] p 176 N95-18573
- National Aeronautics and Space Administration. Ames Research Center, Moffett Field, CA.**
A supercritical airfoil experiment p 111 N95-17858
- Low aspect ratio wing experiment p 113 N95-17865
- STOVL CFD model test case p 115 N95-17881
- Parametric study on laminar flow for finite wings at supersonic speeds [NASA-TM-108852] p 116 N95-18101
- VSTOL Systems Research Aircraft (VSRA) Harrier [NASA-TM-110117] p 126 N95-18347
- NASA develops new digital flight control system [NASA-NEWS-RELEASE-94-47] p 144 N95-19029
- An assessment of the adaptive unstructured tetrahedral grid, Euler Flow Solver Code FELISA [NASA-TP-3526] p 119 N95-19041
- 2-D and 3-D oscillating wing aerodynamics for a range of angles of attack including stall [NASA-TM-4632] p 120 N95-19119
- Wall interaction effects for a full-scale helicopter rotor in the NASA Ames 80- by 120-foot wind tunnel p 121 N95-19270
- National Aeronautics and Space Administration. Hugh L. Dryden Flight Research Center, Edwards, CA.**
Development of a low-aspect ratio fin for flight research experiments [NASA-TM-4596] p 108 N95-16858
- Shear buckling analysis of a hat-stiffened panel [NASA-TM-4644] p 158 N95-17490
- National Aeronautics and Space Administration. Hugh L. Dryden Flight Research Facility, Edwards, CA.**
In-flight lift-drag characteristics for a forward-swept wing aircraft and comparisons with contemporary aircraft [NASA-TP-3414] p 117 N95-18565
- Determination of stores pointing error due to wing flexibility under flight load [NASA-TM-4646] p 134 N95-19044
- National Aeronautics and Space Administration. Lyndon B. Johnson Space Center, Houston, TX.**
Virtual environment application with partial gravity simulation p 169 N95-15988
- Documentation and archiving of the Space Shuttle wind tunnel test data base. Volume 1: Background and description [NASA-TM-104806-VOL-1] p 151 N95-19237
- National Aeronautics and Space Administration. Langley Research Center, Hampton, VA.**
A grid generation and flow solution method for the Euler equations on unstructured grids [HTN-95-20003] p 153 A95-63201
- Experimental study at low supersonic speeds of a missile concept having opposing wraparound tails [NASA-TM-4582] p 106 N95-16069
- A study of software standards used in the avionics industry p 137 N95-16456
- Rapid solution of large-scale systems of equations p 169 N95-16458
- Applications of automatic differentiation in computational fluid dynamics p 156 N95-16461
- Matlab as a robust control design tool p 169 N95-16474

- Measurements of unsteady pressure and structural response for an elastic supercritical wing [NASA-TP-3443] p 104 N95-16560
- Applications of automatic differentiation in CFD [NASA-TM-109948] p 157 N95-16828
- Comparison of computational and experimental results for a supercritical airfoil [NASA-TM-4601] p 108 N95-16908
- Modeling of Instrument Landing System (ILS) localizer signal on runway 25L at Los Angeles International Airport [NASA-TM-4588] p 125 N95-17384
- Active load control during rolling maneuvers [NASA-TP-3455] p 129 N95-17397
- Single-engine tail interference model p 115 N95-17879
- Twin engine afterbody model p 115 N95-17880
- Microburst vertical wind estimation from horizontal wind measurements [NASA-TP-3460] p 131 N95-18198
- Special effects of gust loads on military aircraft p 133 N95-18605
- Dynamic Stability Instrumentation System (DSIS). Volume 1: Hardware description [NASA-TM-109160-VOL-1] p 171 N95-18899
- Static investigation of two fluidic thrust-vectoring concepts on a two-dimensional convergent-divergent nozzle [NASA-TM-4574] p 120 N95-19042
- Navier-Stokes, flight, and wind tunnel flow analysis for the F/A-18 aircraft [NASA-TP-3478] p 120 N95-19114
- Impact of dynamic loads on propulsion integration p 174 N95-19148
- FAA/NASA International Symposium on Advanced Structural Integrity Methods for Airframe Durability and Damage Tolerance, part 2 [NASA-CP-3274-PT-2] p 124 N95-19468
- The characterization of widespread fatigue damage in fuselage structure p 166 N95-19472
- Nonlinear analysis of damaged stiffened fuselage shells subjected to combined loads p 137 N95-19499
- National Aeronautics and Space Administration, Lewis Research Center, Cleveland, OH.**
- Sensor fault detection and diagnosis simulation of a helicopter engine in an intelligent control framework [NASA-TM-106784] p 137 N95-15970
- Numerical simulation of supersonic compression corners and hypersonic inlet flows using the RPLUS2D code [NASA-TM-106580] p 105 N95-16038
- Airfoil optimization by the one-shot method p 128 N95-16569
- Static and dynamic friction behavior of candidate high temperature airframe seal materials [NASA-TM-106571] p 152 N95-16905
- A workstation based simulator for teaching compressible aerodynamics [NASA-TM-106799] p 170 N95-16906
- Optimization of adaptive intraply hybrid fiber composites with reliability considerations [NASA-TM-106632] p 157 N95-16911
- Interactive computer graphics applications for compressible aerodynamics [NASA-TM-106802] p 170 N95-17264
- Microgravity isolation system design: A case study [NASA-TM-106804] p 104 N95-17657
- Background noise levels measured in the NASA Lewis 9- by 15-foot low-speed wind tunnel [NASA-TM-106817] p 145 N95-18054
- Numerical mixing calculations of confined reacting jet flows in a cylindrical duct [NASA-TM-106736] p 139 N95-18133
- Microgravity isolation system design: A modern control synthesis framework [NASA-TM-106805] p 105 N95-18197
- Measurement of gust response on a turbine cascade [NASA-TM-106776] p 117 N95-18457
- Microgravity isolation system design: A modern control analysis framework [NASA-TM-106803] p 105 N95-18486
- Collection efficiency and ice accretion calculations for a sphere, a swept MS(1)-317 wing, a swept NACA-0012 wing tip, an axisymmetric inlet, and a Boeing 737-300 [NASA-TM-106831] p 123 N95-18582
- Users guide for NASA Lewis Research Center DC-9 Reduced-Gravity Aircraft Program [NASA-TM-106755] p 146 N95-18586
- Enhanced capabilities and modified users manual for axial-flow compressor conceptual design code CSPAN [NASA-TM-106833] p 119 N95-18933
- Detecting gear tooth fracture in a high contact ratio face gear mesh [NASA-TM-106822] p 162 N95-19125
- Methods for scaling icing test conditions [NASA-TM-106827] p 124 N95-19284
- Ice accretion with varying surface tension [NASA-TM-106826] p 124 N95-19285
- Operating capability and current status of the reactivated NASA Lewis Research Center Hypersonic Tunnel Facility [NASA-TM-106808] p 148 N95-19286
- NASA Lewis Research Center Workshop on Forced Response in Turbomachinery [NASA-CP-10147] p 141 N95-19380
- Steady potential solver for unsteady aerodynamic analyses p 141 N95-19382
- Technology Benefit Estimator (T/BEST): User's manual [NASA-TM-106785] p 167 N95-19501
- National Aeronautics and Space Administration, Marshall Space Flight Center, Huntsville, AL.**
- Tuned mass damper for integrally bladed turbine rotor [NASA-CASE-MFS-28697-1] p 159 N95-18325
- National Aerospace Lab., Amsterdam (Netherlands).**
- Residual-correction type and related computational methods for aerodynamic design. Part 1: Airfoil and wing design p 128 N95-16566
- Residual-correction type and related computational methods for aerodynamic design. Part 2: Multi-point airfoil design p 128 N95-16567
- Two-dimensional 16.5 percent thick supercritical airfoil NLR 7301 p 110 N95-17854
- Low-speed surface pressure and boundary layer measurement data for the NLR 7301 airfoil section with trailing edge flap p 111 N95-17855
- Wind tunnel test on a 65 deg delta wing with a sharp or rounded leading edge: The international vortex flow experiment p 114 N95-17872
- Sectional prediction of 3D effects for separated flow on rotating blades [PB94-201696] p 117 N95-18503
- Results of uniaxial and biaxial tests on riveted fuselage lap joint specimens p 136 N95-19491
- National Aerospace Lab., Bangalore (India).**
- Ageing nuclear power plant management: An aeronautical viewpoint [NAL-PD-SN-9306] p 105 N95-18606
- Solution of full potential equation on an airfoil by multigrid technique [NAL-TM-CSS-9303] p 119 N95-18904
- CFD: Advances and Applications, part 1 [NAL-SP-9322-PT-1] p 165 N95-19444
- Computation of inviscid flows: Full potential method p 165 N95-19447
- Panel methods p 165 N95-19448
- Viscous flow past aerofoils axisymmetric bodies and wings p 123 N95-19457
- Computation of vortex breakdown p 165 N95-19462
- Parabolized Navier-Stokes solution of supersonic/hypersonic flows p 123 N95-19464
- National Defence Research Establishment, Stockholm (Sweden).**
- Military aviation maintenance industry in Western Europe: Concentration and internationalization [PB94-189180] p 104 N95-17451
- Evaluation of an autopilot based multimodelling [PB94-190725] p 142 N95-17454
- National Renewable Energy Lab., Golden, CO.**
- Structural effects of unsteady aerodynamic forces on horizontal-axis wind turbines [DE94-011863] p 157 N95-16939
- Wind turbine blade aerodynamics: The combined experiment [DE94-011866] p 118 N95-18645
- Wind turbine blade aerodynamics: The analysis of field test data [DE94-011867] p 118 N95-18646
- National Research Council of Canada, Ottawa (Ontario).**
- Surface pressure and wake drag measurements on the Boeing A4 airfoil in the IAR 1.5X1.5m Wind Tunnel Facility p 110 N95-17850
- Noise transmission and reduction in turboprop aircraft p 175 N95-19164
- Spectrogram diagnosis of aircraft disasters p 124 N95-19167
- National Technical Univ., Athens (Greece).**
- Single-pass method for the solution of inverse potential and rotational problems. Part 1: 2-D and quasi 3-D theory and application p 107 N95-16563
- Single-pass method for the solution of inverse potential and rotational problems. Part 2: Fully 3-D potential theory and applications p 107 N95-16564
- National Transportation Safety Board, Washington, DC.**
- Aircraft accident report: Stall and loss of control on final approach, Atlantic Coast Airlines, Inc./United Express Flight 6291 Jetstream 4101, N304UE Columbus, OH, 7 January 1994 [PB94-910409] p 123 N95-17646
- Annual review of aircraft accident data: US Air carrier operations, calendar year 1992 (PB95-100319) p 123 N95-17748
- Safety study: Commuter airline safety [PB94-917004] p 124 N95-19132
- Naval Air Development Center, Warminster, PA.**
- Preliminary evaluation of the F/A-18 quantity/multiple envelope expansion [AD-A284119] p 132 N95-18407
- Naval Air Warfare Center, Patuxent River, MD.**
- Flight testing high lateral asymmetries on highly augmented Fighter/Attack aircraft [AD-A284206] p 130 N95-17953
- Comparison of frequency response and perturbation methods to extract linear models from a nonlinear simulation [AD-A284115] p 146 N95-18405
- Tilt Rotor Unmanned Air Vehicle System (TRUS) demonstrator flight test program [AD-A284151] p 132 N95-18415
- Application of photogrammetry of F-14D store separation [AD-A284154] p 132 N95-18417
- The generic simulation executive at Manned Flight Simulator [AD-A283997] p 146 N95-18724
- Helicopter in-flight simulation development and use in test pilot training [AD-A283998] p 146 N95-18725
- Assessing aircraft survivability to high frequency transient threats [AD-A283999] p 134 N95-18726
- Waveform bounding and combination techniques for direct drive testing [AD-A284075] p 161 N95-19035
- E-6A hardness assurance, maintenance and surveillance program [AD-A283994] p 134 N95-19067
- Naval Air Warfare Center, Trenton, NJ.**
- Unmanned aerial vehicle heavy fuel engine test [AD-A284332] p 139 N95-18383
- Naval Air Warfare Center, Warminster, PA.**
- Evaluation of alternate F-14 wing lug coating [AD-A283207] p 129 N95-17631
- Naval Postgraduate School, Monterey, CA.**
- An investigation of the transonic pressure drag coefficient for axis-symmetric bodies [AD-A280990] p 105 N95-15994
- A computational investigation of wake-induced airfoil flutter in incompressible flow and active flutter control [AD-A281534] p 142 N95-16109
- Low rate initial production in Army Aviation systems development [AD-A281871] p 127 N95-16356
- Spread spectrum applications in unmanned aerial vehicles [AD-A281035] p 156 N95-16448
- Mach number, flow angle, and loss measurements downstream of a transonic fan-blade cascade [AD-A280907] p 108 N95-16824
- Numerical optimization of synergetic maneuvers [AD-A283398] p 109 N95-17435
- Wind tunnel performance comparative test results of a circular cylinder and 50 percent ellipse tailboom for circulation control antitorque applications [AD-A283335] p 130 N95-18008
- A platform independent application of Lux illumination prediction algorithms [AD-A283669] p 170 N95-18018
- Course module for AA201: Wing structural design project [AD-A283618] p 133 N95-18616
- Plant and controller optimization by convex methods [AD-A283700] p 133 N95-18621
- Interaction, bursting and control of vortices of a cropped double-delta wing at high angle of attack [AD-A283656] p 119 N95-18669
- Naval Research Lab., Washington, DC.**
- Problems with aging wiring in Naval aircraft p 154 N95-16048
- North Carolina State Univ., Raleigh, NC.**
- Time accurate computation of unsteady inlet flows with a dynamic flow adaptive mesh [AD-A285498] p 157 N95-16736
- Northrop Corp., Pico Rivera, CA.**
- Eddy current for detecting second layer cracks under installed fasteners [AD-A282412] p 158 N95-17507



Office National d'Etudes et de Recherches Aérospatiales, Modane (France).

Calculation of wall effects of flow on a perforated wall with a code of surface singularities p 165 N95-19277

- Office National d'Etudes et de Recherches Aérospatiales, Paris (France).**
 Ellipsoid-cylinder model p 158 N95-17869
 Supersonic vortex flow around a missile body p 114 N95-17870
 Test data on a non-circular body for subsonic, transonic and supersonic Mach numbers p 158 N95-17871
 Delta-wing model p 114 N95-17873
- Office National d'Etudes et de Recherches Aérospatiales, Toulouse (France).**
 Data from the GARTEur (AD) Action Group 02 airfoil CAST 7/DOA1 experiments p 111 N95-17856
 OAT15A airfoil data p 111 N95-17857
- Ohio State Univ., Columbus.**
 Wing-body juncture flows [AD-A281526] p 106 N95-16099
- Old Dominion Univ., Norfolk, VA.**
 Automation of reverse engineering process in aircraft modeling and related optimization problems [NASA-CR-197109] p 129 N95-16899

P

- Pacific Northwest Lab., Richland, WA.**
 An artificial neural network system for diagnosing gas turbine engine fuel faults [DE94-013960] p 138 N95-17371
- Paris VI Univ. (France).**
 Optimal shape design for aerodynamics p 128 N95-16568
- Pennsylvania State Univ., State College, PA.**
 Active minimization of energy density in three-dimensional enclosures [NASA-CR-197213] p 172 N95-16848
- Pennsylvania State Univ., University Park, PA.**
 Anisotropic heat exchangers/stack configurations for thermoacoustic heat engines [AD-A280974] p 168 N95-16506
- Physical Sciences, Inc., Andover, MA.**
 Ultraviolet emissions occurring about hypersonic vehicles in rarefied flows [AD-A281452] p 106 N95-16076
- Pratt and Whitney Aircraft, West Palm Beach, FL.**
 Fatigue in single crystal nickel superalloys [AD-A285727] p 152 N95-18068
- Praxair, Inc., Tonawanda, NY.**
 Airborne rotary separator study [NASA-CR-191045] p 150 N95-18743
- Princeton Univ., NJ.**
 Optimum aerodynamic design via boundary control p 127 N95-16565
 Studies on high pressure and unsteady flame phenomena [AD-A284126] p 152 N95-18410

R

- Research Inst. for Advanced Computer Science, Moffett Field, CA.**
 Mesh quality control for multiply-refined tetrahedral grids [NASA-CR-197595] p 160 N95-18737
- Rocket Research Corp., Redmond, WA.**
 Arcjet thruster research and technology, phase 2 [NASA-CR-182276] p 105 N95-18044
- Rockwell International Corp., Downey, CA.**
 Program test objectives milestone 3 [NASA-CR-197030] p 127 N95-15971
 Strategic avionics technology definition studies. Subtask 3-1A3: Electrical Actuation (ELA) Systems Test Facility [NASA-CR-188360] p 143 N95-18567
 Fatigue loads spectra derivation for the Space Shuttle: Second cycle p 166 N95-19470
- Rome Lab., Griffiss AFB, NY.**
 A VHF/UHF antenna for the Precision Antenna Measurement System (PAMS) [AD-A285673] p 156 N95-16621
- Royal Netherlands Meteorological Inst., De Bilt.**
 Atmospheric effects of high-flying subsonic aircraft: A catalogue of perturbing influences [KNMI-SR-94-03] p 168 N95-18722

S

- Sandia National Labs., Albuquerque, NM.**
 Error propagation equations for estimating the uncertainty in high-speed wind tunnel test results [DE94-014136] p 145 N95-16509
 Evaluation of scanners for C-scan imaging in nondestructive inspection of aircraft [DE94-012473] p 152 N95-19100
- Southwest Research Inst., San Antonio, TX.**
 Aircraft stress sequence development: A complex engineering process made simple p 136 N95-19480

- Stanford Univ., CA.**
 High altitude hypersonic flowfield radiation [AD-A281386] p 106 N95-16160
 Design and flight test of a simplified control system for a transport helicopter p 144 N95-18902
- State Univ. of New York, Farmingdale, NY.**
 Quality optimization of thermally sprayed coatings produced by the JP-5000 (HVOP) gun using mathematical modeling p 152 N95-19008
- State Univ. of New York, Oneonta, NY.**
 A CMC database for use in the next generation launch vehicles (rockets) p 150 N95-18993
- Sundstrand Power Systems, San Diego, CA.**
 Small turbojets: Designs and installations p 138 N95-16323
- Sverdrup Technology, Inc., Brook Park, OH.**
 An analysis code for the Rapid Engineering Estimation of Momentum and Energy Losses (REMEL) [NASA-CR-191178] p 108 N95-16887
- Sydney Univ. (Australia).**
 Six degree of freedom flight dynamic and performance simulation of a remotely-piloted vehicle [AERO-TN-9301] p 131 N95-18097
- Systems and Electronics, Inc., Elk Grove Village, IL.**
 Flight parameters monitoring system for tracking structural integrity of rotary-wing aircraft p 135 N95-19469
- Systems Control Technology, Inc., Arlington, VA.**
 Heliport/vertiport MLS precision approaches [AD-A283505] p 126 N95-18059

T

- Technische Hochschule, Aachen (Germany).**
 Investigation of an NLF(1)-0416 airfoil in compressible subsonic flow p 110 N95-17852
- Technische Hogeschool, Delft (Netherlands).**
 Experiments in the trailing edge flow of an NLR 7702 airfoil p 110 N95-17853
 Experimental investigation of the vortex flow over a 76/60-deg double delta wing p 114 N95-17874
 Fatigue life until small cracks in aircraft structures: Durability and damage tolerance p 135 N95-19478
- Technische Univ., Delft (Netherlands).**
 The utilization of a high speed reflective visualization system in the study of transonic flow over a delta wing p 121 N95-19259
- Technische Univ., Munich (Germany).**
 Velocity measurements with hot-wires in a vortex-dominated flowfield p 121 N95-19261
- Tennessee Technological Univ., Cookeville, TN.**
 Fatigue and residual strength investigation of ARALL(R) -3 and GLARE(R) -2 panels with bonded stringers p 137 N95-19495
- Textron Bell Helicopter, Fort Worth, TX.**
 Aircraft fatigue and crack growth considering loads by structural component p 137 N95-19497
- Toledo Univ., OH.**
 FPCAS2D user's guide, version 1.0 [NASA-CR-195413] p 156 N95-16588
- Tsentralni Aerogidrodinamicheski Inst., Moscow (USSR).**
 The traditional and new methods of accounting for the factors distorting the flow over a model in large transonic wind tunnels p 165 N95-19275

U

- United Technologies Research Center, East Hartford, CT.**
 Unsteady aerodynamic analyses for turbomachinery aeroelastic predictions p 141 N95-19381

V

- Veda, Inc., Dayton, Ohio.**
 Industry review of a crew-centered cockpit design process and toolset [AD-A282966] p 130 N95-17661
- Vigyan Research Associates, Inc., Hampton, VA.**
 Transonic Navier-Stokes calculations about a 65 deg delta wing [NASA-CR-4635] p 108 N95-17273
- Virginia Polytechnic Inst. and State Univ., Blacksburg, VA.**
 Compression strength of composite primary structural components [NASA-CR-197554] p 160 N95-18388
- Von Karman Inst. for Fluid Dynamics, Rhode-Saint-Genese (Belgium).**
 Aerodynamic investigation of the flow field in a 180 deg turn channel with sharp bend p 163 N95-19257

W

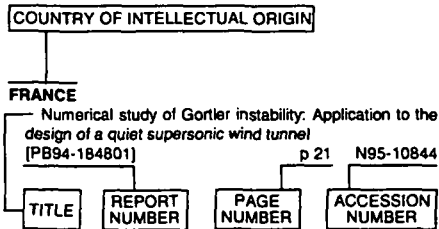
- Wright Lab., Wright-Patterson AFB, OH.**
 An engineering code to analyze hypersonic thermal management systems p 155 N95-16322
 Numerical simulation of transient vortex breakdown above a pitching delta wing [AD-A281075] p 107 N95-16808
 Universal wind tunnel data acquisition and reduction software [AD-A283897] p 171 N95-18365
 Pressure measurements on an F/A-18 twin vertical tail in buffeting flow. Volume 4, part 2: Buffet cross spectral densities [AD-A285555] p 143 N95-18641
 Weapons bay acoustic environment p 173 N95-19146
 High-temperature acoustic test facilities and methods p 174 N95-19149
 Nonlinear dynamic response of aircraft structures to acoustic excitation p 135 N95-19151
 Modeling structurally damaging twin-jet screech p 135 N95-19154
 Thermo-acoustic fatigue design for hypersonic vehicle skin panels p 162 N95-19161
 Determination of solid/porous wall boundary conditions from wind tunnel data for computational fluid dynamics codes p 164 N95-19266

FOREIGN TECHNOLOGY INDEX

AERONAUTICAL ENGINEERING / A Continuing Bibliography (Supplement 316)

April 1995

Typical Foreign Technology Index Listing



Listings in this index are arranged alphabetically by country of intellectual origin. The title of the document is used to provide a brief description of the subject matter. The page number and accession number are included in each entry to assist the user in locating the abstract in the abstract section. If applicable, a report number is also included as an aid in identifying the document.

A

AUSTRALIA

- A PC-based interactive simulation of the F-111C Pavé Tack system and related sensor, avionics and aircraft aspects
[AD-A285500] p 129 N95-16969
- Data acquisition and processing software for the Low Speed Wind Tunnel tests of the Jindivik auxiliary air intake
[AD-A285455] p 108 N95-17178
- Six degree of freedom flight dynamic and performance simulation of a remotely-piloted vehicle
[AERO-TN-9301] p 131 N95-18097

B

BELGIUM

- Aerodynamic investigation of the flow field in a 180 deg turn channel with sharp bend p 163 N95-19257

BRAZIL

- Regenerative cooling for liquid propellant rocket thrust chambers
[INPE-5565-TDI/540] p 150 N95-18720

C

CANADA

- Surface pressure and wake drag measurements on the Boeing A4 airfoil in the IAR 1.5X1.5m Wind Tunnel Facility p 110 N95-17850
- A review of gust load calculation methods at de Havilland p 118 N95-18604
- Noise transmission and reduction in turboprop aircraft p 175 N95-19164
- Spectrogram diagnosis of aircraft distasters p 124 N95-19167

- Applications of the five-hole probe technique for flow field surveys at the Institute for Aerospace Research p 163 N95-19255
- Unsteady flow testing in a passive low-correction wind tunnel p 147 N95-19272
- Evaluation of combined wall- and support-interference on wind tunnel models p 122 N95-19278
- Interference corrections for a centre-line plate mount in a porous-walled transonic wind tunnel p-122 N95-19280

CHINA

- Improved analytical solution for varying specific heat parallel stream mixing
[BTN-94-EIX94481415349] p 103 A95-65339
- Development and application of the double V type flame stabilizer
[BTN-94-EIX94481415355] p 154 A95-65345
- Direct splitting of coefficient matrix for numerical calculation of transonic nozzle flow
[BTN-94-EIX94481415356] p 103 A95-65346
- Aerodynamic design and calculation of flow around the plane cascade of turbine
[BTN-94-EIX94481415357] p 104 A95-65347
- Joint Proceedings on Aeronautics and Astronautics (JPAA) [ISBN-7-80-046602-7] p 104 N95-16249
- Investigation of dynamic inflow's influence on rotor control derivatives p 155 N95-16250
- An approach to aerodynamic characteristics of low radar cross-section fuselages p 106 N95-16251
- An improved method of airfoil design p 106 N95-16252
- Wall-signature methods for high speed wind tunnel wall interference corrections p 107 N95-16257
- An investigation of polynomial calibrations methods for wind tunnel balances p 144 N95-16258
- Linear prediction data extrapolation superresolution radar imaging p 155 N95-16268
- Application of GPS/SINS/RA integrated system to aircraft approach landing p 125 N95-16277
- The computer analysis of the prediction of aircraft electrical power supply system reliability p 155 N95-16278
- Simulation investigation on system identification of gas turbine [PB95-104238] p 139 N95-17749

F

FRANCE

- Optimum Design Methods for Aerodynamics [AGARD-R-803] p 127 N95-16562
- Optimal shape design for aerodynamics p 128 N95-16568
- Review of the EUROPT Project AERO-0026 p 129 N95-16573
- A processing centre for the CNES CE-GPS experimentation p 125 N95-17196
- Experimental and analytical methods for the determination of connected-pipe ramjet and ducted rocket internal performance [AGARD-AR-323] p 149 N95-17278
- Aircraft and sub-system certification by piloted simulation [AGARD-AR-278] p 145 N95-17388
- A selection of experimental test cases for the validation of CFD codes, volume 2 [AGARD-AR-303-VOL-2] p 109 N95-17846
- Data from the GARTEur (AD) Action Group 02 airfoil CAST 7/DOA1 experiments p 111 N95-17856
- OAT15A airfoil data p 111 N95-17857
- Ellipsoid-cylinder model p 158 N95-17869
- Supersonic vortex flow around a missile body p 114 N95-17870
- Test data on a non-circular body for subsonic, transonic and supersonic Mach numbers p 158 N95-17871
- Delta-wing model p 114 N95-17873
- A selection of experimental test cases for the validation of CFD codes. Supplement: Datasets A-E [AGARD-AR-303-SUPPL] p 117 N95-18539

- Aircraft Loads due to Turbulence and their Impact on Design and Certification [AGARD-R-798] p 143 N95-18597
- Gyroscopic and propeller aerodynamic effects on engine mounts dynamic loads in turbulence conditions p 132 N95-18599
- On-line handling of air traffic: Management, guidance and control [AGARD-AG-321] p 126 N95-18927
- Mathematical Models of Gas Turbine Engines and their Components [AGARD-LS-198] p 139 N95-19017
- Impact of Acoustic Loads on Aircraft Structures [AGARD-CP-549] p 173 N95-19142
- Aeroacoustic qualification of HERMES shingles p 173 N95-19145
- Brite-Euram programme: ACOUFAT acoustic fatigue and related damage tolerance of advanced composite and metallic structures p 174 N95-19159
- Wall interference, Support Interference and Flow Field Measurements [AGARD-CP-535] p 162 N95-19251
- Experimental techniques for measuring transonic flow with a three dimensional laser velocimetry system. Application to determining the drag of a fuselage p 163 N95-19258
- Analysis of test section sidewall effects on a two dimensional airfoil: Experimental and numerical investigations p 165 N95-19276
- Calculation of wall effects of flow on a perforated wall with a code of surface singularities p 165 N95-19277
- Interaction of a three strut support on the aerodynamic characteristics of a civil aviation model p 122 N95-19279

G

GERMANY

- Time-optimal turn to a heading: An analytic solution [BTN-94-EIX94511433940] p 142 A95-64606
- Tools for applied engineering optimization p 128 N95-16570
- The global aircraft shape p 128 N95-16571
- Aerodynamic shape optimization p 128 N95-16572
- Safety aspects of spacecraft commanding p 149 N95-17248
- EURECA mission control experience and messages for the future p 149 N95-17252
- Packet utilisation definitions for the ESA XMM mission p 150 N95-17596
- 2-D airfoil tests including side wall boundary layer measurements p 158 N95-17847
- Investigation of an NLF(1)-0416 airfoil in compressible subsonic flow p 110 N95-17852
- DLR-F4 wing body configuration p 130 N95-17863
- DLR-F5: Test wing for CFD and applied aerodynamics p 113 N95-17864
- Wind tunnel investigations of the appearance of shocks in the windward region of bodies with circular cross section at angle of attack p 113 N95-17866
- Three-dimensional boundary layer and flow field data of an inclined prolate spheroid p 158 N95-17867
- Force and pressure data of an ogive-nosed slender body at high angles of attack and different Reynolds numbers p 113 N95-17868
- Wind tunnel test on a 65 deg delta wing with rounded leading edges: The International Vortex Flow Experiment p 114 N95-17875
- Subsonic flow around US-orbiter model FALKE in the DNW p 115 N95-17877
- Pressure distribution measurements on an isolated TPS 441 nacelle p 115 N95-17878
- Treatment of non-linear systems by timeplane-transformed CT methods: The spectral gust method p 143 N95-18600
- Theoretical investigations of shock/boundary layer interactions on a $Ma(\infty) = 8$ waverider [DLR-FB-94-12] p 119 N95-18910
- One-dimensional flow description for the combustion chamber of a scramjet [DLR-FB-94-06] p 139 N95-18911

- Flow field investigation in a free jet - free jet core system for the generation of high intensity molecular beams
[DLR-FB-94-11] p 172 N95-18912
- Helicopter internal noise p 173 N95-19144
- Design and operation of a thermoacoustic test facility p 147 N95-19150
- Acoustic fatigue testing on different materials and skin-stringer elements p 174 N95-19156
- Velocity measurements with hot-wires in a vortex-dominated flowfield p 121 N95-19261
- Wall correction method with measured boundary conditions for low speed wind tunnels p 164 N95-19263
- Development of load spectra for Airbus A330/A340 full scale fatigue tests p 135 N95-19479

GREECE

- Single-pass method for the solution of inverse potential and rotational problems. Part 1: 2-D and quasi 3-D theory and application p 107 N95-16563
- Single-pass method for the solution of inverse potential and rotational problems. Part 2: Fully 3-D potential theory and applications p 107 N95-16564

I

INDIA

- Evaluation of the dynamic stability characteristics of the NAL Light Transport Aircraft
[NAL-PD-CA-9217] p 142 N95-16392
- Ageing nuclear power plant management: An aeronautical viewpoint
[NAL-PD-SN-9306] p 105 N95-18606
- Solution of full potential equation on an airfoil by multigrid technique
[NAL-TM-CSS-9303] p 119 N95-18904
- CFD: Advances and Applications, part 1
[NAL-SP-9322-PT-1] p 165 N95-19444
- Computation of inviscid flows: Full potential method p 165 N95-19447
- Panel methods p 165 N95-19448
- Viscous flow past aerofoils axisymmetric bodies and wings p 123 N95-19457
- Computation of vortex breakdown p 165 N95-19462
- Parabolized Navier-Stokes solution of supersonic/hypersonic flows p 123 N95-19464

INDONESIA

- Prediction of fatigue crack growth under flight-simulation loading with the modified CORPUS model p 166 N95-19471

ITALY

- Impact of noise environment on engine nacelle design p 173 N95-19147
- An overall approach of cockpit noise verification in a military aircraft p 175 N95-19163
- Adaptive wind tunnel walls versus wall interference correction methods in 2D flows at high blockage ratios p 147 N95-19267

N

NETHERLANDS

- On the dynamics of aeroelastic oscillators with one degree of freedom
[BTN-94-EIX94501431527] p 153 A95-64524
- The ICAO CNS/ATM system: New king, new law?
[HTN-95-50218] p 175 A95-64855
- World trends in air transport policies. (Approaching the 21st century)
[HTN-95-50220] p 176 A95-64857
- EC Aviation Scene
[HTN-95-50223] p 176 A95-64860
- Residual-correction type and related computational methods for aerodynamic design. Part 1: Airfoil and wing design p 128 N95-16566
- Residual-correction type and related computational methods for aerodynamic design. Part 2: Multi-point airfoil design p 128 N95-16567
- Experiments in the trailing edge flow of an NLR 7702 airfoil p 110 N95-17853
- Two-dimensional 16.5 percent thick supercritical airfoil NLR 7301 p 110 N95-17854
- Low-speed surface pressure and boundary layer measurement data for the NLR 7301 airfoil section with trailing edge flap p 111 N95-17855
- Wind tunnel test on a 65 deg delta wing with a sharp or rounded leading edge: The international vortex flow experiment p 114 N95-17872
- Experimental investigation of the vortex flow over a 76/60-deg double delta wing p 114 N95-17874
- Sectional prediction of 3D effects for separated flow on rotating blades
[PB94-201696] p 117 N95-18503

Atmospheric effects of high-flying subsonic aircraft: A catalogue of perturbing influences
[KNMI-SR-94-03] p 168 N95-18722

The utilization of a high speed reflective visualization system in the study of transonic flow over a delta wing p 121 N95-19259

Correction of support influences on measurements with sting mounted wind tunnel models p 122 N95-19281

Fatigue life until small cracks in aircraft structures: Durability and damage tolerance p 135 N95-19478

Results of uniaxial and biaxial tests on riveted fuselage lap joint specimens p 136 N95-19491

R

RUSSIA

- Analytical description of and forecast for stress relaxation of aviation materials under the vibration conditions
[BTN-94-EIX94461408751] p 126 A95-63634
- Selection of optimal parameters for a system, controlling the flight height, when information about the state vector is incomplete
[BTN-94-EIX94461408753] p 168 A95-63636
- Gas-turbine engines with increased efficiency of two circuits, due to the use of the utilizing steam-turbine circuit
[BTN-94-EIX94461408755] p 153 A95-63638
- On the particular features of dynamic processes in solids with varying boundary during interaction with intensive heat flows
[BTN-94-EIX94461408756] p 171 A95-63639
- Ultimate characteristics of a rocket engine with a turbo-pump supply system
[BTN-94-EIX94461408757] p 148 A95-63640
- Mathematical modelling concerning the development of a system of similar installations, taking into account their operational intensity (an aircraft-helicopter fleet taken as an example)
[BTN-94-EIX94461408763] p 103 A95-63646
- A stationary flow of a viscous liquid in radial clearances of rotor bearings in the turbocompressor of an internal combustion engine
[BTN-94-EIX94461408765] p 153 A95-63648
- New approach to geometric profiling of the design elements of the passage part in turbo-machines
[BTN-94-EIX94461408769] p 153 A95-63652
- Calculation of geometry of stamps with small allowances for pieces of the aerodynamic profile
[BTN-94-EIX94461408772] p 103 A95-63655
- On a program-information system TDoht
[BTN-94-EIX94461408773] p 175 A95-63656
- Modelling for optimal operations of line milling of aerodynamic surfaces
[BTN-94-EIX94461408774] p 138 A95-63657
- Two projects of V. M. Myasishchev
[HTN-95-50269] p 176 A95-65764
- Service and physical properties of liquid-jet fuels p 151 N95-16256
- Development of strength analysis methods and design model for aircraft constructions in Kazan Aviation Institute p 127 N95-16264
- Theoretical fundamentals of the aircraft GTE tests p 138 N95-16265
- Generalized method of solving topological optimization problems for electrical airplane equipment systems in computer-aided design p 169 N95-16272
- Development of processes, means, and theoretical principles of thin-walled detail plastic forming at Kazan Aviation Institute p 155 N95-16281
- Solution of Navier-Stokes equations using high accuracy monotone schemes p 161 N95-19019
- The mathematical models of flow passage for gas turbine engines and their components p 140 N95-19020
- Simulation of multidisciplinary problems for the thermostress state of cooled high temperature turbines p 140 N95-19021
- Application of multicomponent models to flow passage simulation in multistage turbomachines and whole gas turbine engines p 140 N95-19022
- Simulation of steady and unsteady viscous flows in turbomachinery p 140 N95-19023
- Application of multidisciplinary models to the cooled turbine rotor design p 140 N95-19024
- Verification of multidisciplinary models for turbomachines p 140 N95-19025
- Perspective problems of gas turbine engines simulation p 140 N95-19026
- Optical surface pressure measurements: Accuracy and application field evaluation p 175 N95-19274

S

SPAIN

A study of the effect of store unsteady aerodynamics on gust and turbulence loads p 133 N95-18601

SWEDEN

- Military aviation maintenance industry in Western Europe: Concentration and internationalization
[PB94-189180] p 104 N95-17451
- Evaluation of an autopilot based multimodelling
[PB94-190725] p 142 N95-17454
- Low speed propeller slipstream aerodynamic effects p 116 N95-17882
- Computational simulations for some tests in transonic wind tunnels p 164 N95-19264
- Calculation of low speed wind tunnel wall interference from static pressure pipe measurements p 164 N95-19273

SWITZERLAND

Test bench for rotorcraft hover control
[BTN-94-EIX94511433919] p 169 A95-64585

U

UKRAINE

Engineering methods for the evaluation of transonic flutter characteristics for aerodynamic control surfaces
[BTN-94-EIX94461408589] p 141 A95-63064

Investigation of heat transfer between rotating shafts of transmissions of turbojet engines
[BTN-94-EIX94461408760] p 138 A95-63643

UNITED KINGDOM

- Measurements on a two-dimensional aerofoil with high-lift devices p 109 N95-17848
- Investigation of the flow over a series of 14 percent-thick supercritical aerofoils with significant rear camber p 109 N95-17849
- Measurements of the flow over a low aspect-ratio wing in the Mach number range 0.6 to 0.87 for the purpose of validation of computational methods. Part 1: Wing design, model construction, surface flow. Part 2: Mean flow in the boundary layer and wake, 4 test cases p 112 N95-17860
- Detailed study at supersonic speeds of the flow around delta wings p 112 N95-17861
- Pressure distributions on research wing W4 mounted on an axisymmetric body p 112 N95-17862
- Investigation of the flow development on a highly swept canard/wing research model with segmented leading- and trailing-edge flaps p 114 N95-17876
- Investigation into the aerodynamic characteristics of a combat aircraft research model fitted with a forward swept wing p 116 N95-17884
- Investigation of the influence of pylons and stores on the wing lower surface flow p 116 N95-17885
- The impact of non-linear flight control systems on the prediction of aircraft loads due to turbulence p 143 N95-18598
- Current and future problems in structural acoustic fatigue p 173 N95-19143
- Application of superplastically formed and diffusion bonded structures in high intensity noise environments p 174 N95-19162
- Transonic and supersonic flowfield measurements about axisymmetric afterbodies for validation of advanced CFD codes p 121 N95-19260
- Boundary-flow measurement methods for wall interference assessment and correction: Classification and review p 163 N95-19262
- Estimating wind tunnel interference due to vectored jet flows p 164 N95-19265
- Interference determination for wind tunnels with slotted walls p 147 N95-19269

UNKNOWN

Aircraft accident investigation and airworthiness -- A practical example of the interaction of two disciplines with some reflections on possible legal consequences
[HTN-95-50219] p 176 A95-64856

USSR

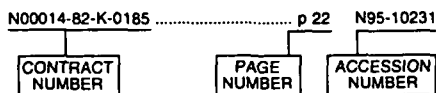
The traditional and new methods of accounting for the factors distorting the flow over a model in large transonic wind tunnels p 165 N95-19275

CONTRACT NUMBER INDEX

AERONAUTICAL ENGINEERING / A *Continuina Bibliography (Supplement 316)*

April 1995

Typical Contract Number Index Listing



Listings in this index are arranged alphanumerically by contract number. Under each contract number the accession numbers denoting documents that have been produced as a result of research done under the contract are shown. The accession number denotes the number by which the citation is identified in the abstract section. Preceding the accession number is the page number on which the citation may be found.

AF PROJ. 1926 p 133 N95-18677
AF PROJ. 2307 p 107 N95-16808
AF PROJ. 2401 p 117 N95-18380
AF PROJ. 2404 p 143 N95-18641
AF PROJ. 2404 p 171 N95-18365
AF PROJ. 2404 p 132 N95-18483
AF PROJ. 3321 p 156 N95-16621
AF-AFOSR-0391-91 p 127 N95-16565
BRITE-EURAM-AERO-0026 p 129 N95-16573
DA PROJ. 1L1-61102-AH-43 p 119 N95-18670
DA PROJ. 1L1-61102-AH-45 p 137 N95-15970
DA PROJ. 1L1-61102-AH-52 p 117 N95-18340
DA PROJ. 1L1-62211-A-47-A p 162 N95-19125
DA PROJ. 1L1-62618-AH-80 p 131 N95-18381
DA PROJ. 1L1-62786-D-283 p 118 N95-18611
DA PROJ. 3E1-62787-A-879 p 117 N95-18340
DAAE07-90-C-R059 p 172 N95-17334
DAAH04-93-C-0015 p 126 N95-17706
DAAH04-93-C-0015 p 106 N95-16076
DAAH04-93-G-0500 p 169 N95-16864
DAAL03-90-G-0031 p 106 N95-16160
DAAL03-90-G-0138 p 155 N95-16163
DAAL03-90-G-0186 p 106 N95-16099
DACA76-89-C-0014 p 126 N95-17706
DE-AC04-94AL-85000 p 145 N95-16509
DE-AC06-76RL-01830 p 152 N95-19100
DE-AC36-83CH-10093 p 138 N95-17371
DE-AC36-83CH-10093 p 157 N95-16939
DE-AC36-83CH-10093 p 118 N95-18645
DE-AC36-83CH-10093 p 118 N95-18646
DTFA01-93-Z-02012 p 154 N95-16097
EPA-68-CO-0003 p 104 N95-17466
F33615-84-C-3627 p 138 N95-18164
F33615-91-C-2142 p 160 N95-18660
F33615-91-C-2189 p 155 N95-16322
F33615-91-C-5660 p 158 N95-17507
F33615-92-C-3400 p 131 N95-18162
F33615-92-C-3400 p 133 N95-18677
F33615-92-C-5936 p 130 N95-17661
F33617-91-C-3004 p 132 N95-18483
F34601-90-C-1336 p 152 N95-19482
F49620-92-J-0189 p 157 N95-16736
F49620-92-J-0227 p 152 N95-18410
F49620-94-C-0042 p 151 N95-16371
NAG1-1184 p 166 N95-19473
NAG1-1311 p 153 N95-19490
NAG1-1557 p 172 N95-16848
NAG1-1571 p 130 N95-18090
NAG1-537 p 160 N95-18388
NAG3-1198 p 137 N95-15970
NAG3-1234 p 156 N95-16588

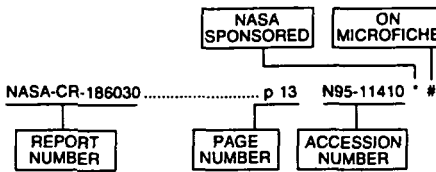
NAG3-178 p 172 N95-16401
NAG3-998 p 142 N95-17404
NAG5-1440 p 150 N95-17493
NAL PROJ. ID-8-117L p 142 N95-16392
NAS1-14101 p 170 N95-16898
NAS1-14472 p 170 N95-16898
NAS1-15810 p 170 N95-16898
NAS1-16394 p 170 N95-16898
NAS1-17070 p 170 N95-16898
NAS1-17130 p 170 N95-16898
NAS1-18107 p 170 N95-16898
NAS1-18450 p 145 N95-16320
NAS1-18585 p 108 N95-17273
NAS1-18605 p 170 N95-16898
NAS1-19299 p 159 N95-18193
NAS1-19317 p 151 N95-16859
NAS1-19480 p 170 N95-16897
NAS1-19480 p 170 N95-16898
NAS1-19480 p 170 N95-18110
NAS1-19480 p 159 N95-18190
NAS1-19480 p 159 N95-18191
NAS1-19480 p 159 N95-18193
NAS1-19480 p 159 N95-18193
NAS1-19656 p 159 N95-18042
NAS1-19708 p 151 N95-16860
NAS2-13571 p 161 N95-18955
NAS2-13571 p 161 N95-18956
NAS2-13721 p 160 N95-18737
NAS2-24631 p 105 N95-18044
NAS2-25266 p 108 N95-16887
NAS2-25560 p 150 N95-18743
NAS2-25685 p 152 N95-16905
NAS2-25796 p 161 N95-18938
NAS2-25796 p 162 N95-19236
NAS2-25796 p 139 N95-18133
NAS2-25796 p 154 N95-16072
NAS2-27186 p 157 N95-16911
NAS2-27186 p 145 N95-18054
NAS2-27186 p 123 N95-18582
NAS2-27186 p 167 N95-19501
NAS2-27186 p 168 N95-18093
NAS8-38776 p 150 N95-18196
NAS9-18873 p 143 N95-18567
NAS9-18880 p 129 N95-16899
NCC1-68 p 157 N95-17418
NCC2-374 p 150 N95-17493
NCC2-374 p 134 N95-19130
NCC2-5061 p 107 N95-16589
NCC2-55 p 164 N95-19266
NCC3-181 p 138 N95-17402
NCC3-365 p 104 N95-17657
NCC3-365 p 105 N95-18197
NCC3-365 p 105 N95-18486
NCC8-47 p 127 N95-15971
N00014-91-C-0001 p 148 N95-16312
N00014-91-C-0124 p 152 N95-18068
N00014-92-J-1976 p 127 N95-16565
N00014-93-1-1127 p 168 N95-16506
N61339-91-D-0001 p 127 N95-16171
PROJ. RHINO p 173 N95-19144
RTOP 314-40-52-01-02 p 109 N95-17291
RTOP 324-01-00 p 154 N95-16072
RTOP 505-59-10-31 p 108 N95-16908
RTOP 505-59-20 p 119 N95-19041
RTOP 505-59-30-01 p 106 N95-16069
RTOP 505-59-50-02 p 159 N95-18042
RTOP 505-59-52 p 120 N95-19119
RTOP 505-59-53 p 161 N95-18955
RTOP 505-59-53 p 161 N95-18956
RTOP 505-59-54-01 p 108 N95-17273
RTOP 505-59-54-02 p 171 N95-18899
RTOP 505-62-0X p 137 N95-15970
RTOP 505-62-10 p 157 N95-16911
RTOP 505-62-30-01 p 120 N95-19042
RTOP 505-62-36 p 162 N95-19125
RTOP 505-62-50 p 161 N95-18938
RTOP 505-62-50 p 162 N95-19236
RTOP 505-62-52 p 170 N95-16906
RTOP 505-62-52 p 170 N95-17264
RTOP 505-62-52 p 138 N95-17402
RTOP 505-63-1A p 152 N95-16905
RTOP 505-63-36-01 p 129 N95-17397
RTOP 505-63-40 p 158 N95-17490
RTOP 505-63-5B p 117 N95-18457

RTOP 505-63-50-13 p 141 N95-19380
RTOP 505-63-50-13 p 167 N95-19501
RTOP 505-64-13-01 p 104 N95-16560
RTOP 505-64-13-01 p 131 N95-18198
RTOP 505-64-13-04 p 125 N95-17384
RTOP 505-66-00 p 108 N95-16858
RTOP 505-68-10 p 123 N95-18582
RTOP 505-68-10 p 124 N95-19284
RTOP 505-68-10 p 124 N95-19285
RTOP 505-68-30-03 p 120 N95-19114
RTOP 505-68-50 p 117 N95-18565
RTOP 505-68-53 p 157 N95-17418
RTOP 505-69-50 p 108 N95-16887
RTOP 505-69-50 p 119 N95-18933
RTOP 505-70-62 p 148 N95-19286
RTOP 505-90-52-01 p 170 N95-16897
RTOP 505-90-52-01 p 170 N95-16898
RTOP 505-90-52-01 p 170 N95-18110
RTOP 505-90-52-01 p 159 N95-18190
RTOP 505-90-52-01 p 159 N95-18191
RTOP 505-90-52-01 p 159 N95-18193
RTOP 506-42-31 p 105 N95-18044
RTOP 510-02-13-01 p 151 N95-16859
RTOP 537-02-21 p 139 N95-18133
RTOP 537-02-23 p 105 N95-16038
RTOP 537-06-20-06 p 151 N95-16860
RTOP 537-07-00 p 116 N95-18101
RTOP 538-02-10-01 p 124 N95-19468
RTOP 538-03-11 p 156 N95-16588
RTOP 538-03-11 p 145 N95-18054
RTOP 694-03-0C p 146 N95-18586
RTOP 963-70-OH p 104 N95-17657
RTOP 963-70-OH p 105 N95-18197
RTOP 963-70-OH p 105 N95-18486
W-31-109-ENG-38 p 157 N95-16828

CONTRACT

REPORT NUMBER INDEX

Typical Report Number Index Listing



Listings in this index are arranged alphanumerically by report number. The page number indicates the page on which the citation is located. The accession number denotes the number by which the citation is identified. An asterisk (*) indicates that the item is a NASA report. A pound sign (#) indicates that the item is available on microfiche.

A-94053 p 120 N95-19119 * #
 A-94146 p 116 N95-18101 * #
 A-94147 p 119 N95-19041 * #

 AD-A279220 p 176 N95-18578 #
 AD-A280907 p 108 N95-16824 #
 AD-A280974 p 168 N95-16506 #
 AD-A280990 p 105 N95-15994 #
 AD-A281035 p 156 N95-16448 #
 AD-A281075 p 107 N95-16808 #
 AD-A281386 p 106 N95-16160 #
 AD-A281399 p 169 N95-16864 #
 AD-A281412 p 155 N95-16163 #
 AD-A281452 p 106 N95-16076 #
 AD-A281520 p 154 N95-16097 #
 AD-A281526 p 106 N95-16099 #
 AD-A281534 p 142 N95-16109 #
 AD-A281580 p 127 N95-16171 #
 AD-A281871 p 127 N95-16356 #
 AD-A281985 p 145 N95-17444 #
 AD-A282412 p 158 N95-17507 #
 AD-A282479 p 125 N95-17373 #
 AD-A282787 p 126 N95-17706 #
 AD-A282966 p 130 N95-17661 #
 AD-A283081 p 172 N95-17334 #
 AD-A283207 p 129 N95-17631 #
 AD-A283335 p 130 N95-18008 #
 AD-A283398 p 109 N95-17435 #
 AD-A283505 p 126 N95-18059 #
 AD-A283618 p 133 N95-18616 #
 AD-A283656 p 119 N95-18669 #
 AD-A283669 p 170 N95-18018 #
 AD-A283688 p 119 N95-18670 #
 AD-A283700 p 133 N95-18621 #
 AD-A283718 p 160 N95-18436 #
 AD-A283828 p 118 N95-18624 #
 AD-A283867 p 119 N95-18674 #
 AD-A283897 p 171 N95-18365 #
 AD-A283925 p 133 N95-18677 #
 AD-A283926 p 131 N95-18162 #
 AD-A283933 p 138 N95-18164 #
 AD-A283981 p 134 N95-18891 #
 AD-A283994 p 134 N95-19067 #
 AD-A283997 p 146 N95-18724 #
 AD-A283998 p 146 N95-18725 #
 AD-A283999 p 134 N95-18726 #
 AD-A284050 p 160 N95-18660 #
 AD-A284057 p 118 N95-18663 #
 AD-A284075 p 161 N95-19035 #
 AD-A284097 p 117 N95-18380 #
 AD-A284099 p 131 N95-18398 #
 AD-A284115 p 146 N95-18405 #
 AD-A284119 p 132 N95-18407 #
 AD-A284126 p 152 N95-18410 #
 AD-A284151 p 132 N95-18415 #

AD-A284154 p 132 N95-18417 #
 AD-A284206 p 130 N95-17953 #
 AD-A284319 p 131 N95-18381 #
 AD-A284332 p 139 N95-18383 #
 AD-A284375 p 117 N95-18340 #
 AD-A284763 p 146 N95-18087 #
 AD-A284765 p 126 N95-18088 #
 AD-A284887 p 120 N95-19110 #
 AD-A284971 p 171 N95-16226 #
 AD-A285190 p 123 N95-16404 #
 AD-A285323 p 151 N95-16371 #
 AD-A285455 p 108 N95-17178 #
 AD-A285498 p 157 N95-16736 #
 AD-A285500 p 129 N95-16969 #
 AD-A285555 p 143 N95-18641 #
 AD-A285673 p 156 N95-16621 #
 AD-A285713 p 132 N95-18483 #
 AD-A285727 p 152 N95-18068 #

 AD-D016423 p 116 N95-18337 #
 AD-D016457 p 151 N95-19073 #
 AD-D016458 p 152 N95-19090 #
 AD-D016475 p 160 N95-18461 #

 ADST/WDL/TR-93-003274 p 127 N95-16171 #

 AEDC-TR-94-5 p 119 N95-18674 #
 AEDC-TR-94-6 p 118 N95-18663 #
 AEDC-TR-94-7 p 134 N95-18891 #

 AERO-TN-9301 p 131 N95-18097 #

 AFIT/CI/CIA-94-013D p 145 N95-17444 #

 AFIT/DS/AA/94-4 p 120 N95-19110 #

 AFOSR-94-0501TR p 152 N95-18410 #
 AFOSR-94-0625TR p 157 N95-16736 #
 AFOSR-94-0640TR p 151 N95-16371 #

 AGARD-AG-321 p 126 N95-18927 #

 AGARD-AR-278 p 145 N95-17388 #
 AGARD-AR-303-SUPPL p 117 N95-18539 #
 AGARD-AR-303-VOL-2 p 109 N95-17846 #
 AGARD-AR-323 p 149 N95-17278 #

 AGARD-CP-535 p 162 N95-19251 #
 AGARD-CP-549 p 173 N95-19142 #

 AGARD-LS-198 p 139 N95-19017 #

 AGARD-R-798 p 143 N95-18597 #
 AGARD-R-803 p 127 N95-16562 #

 AIAA PAPER 94-2112 p 134 N95-19044 * #
 AIAA PAPER 94-2133 p 108 N95-16858 * #
 AIAA PAPER 95-0070 p 170 N95-16906 * #
 AIAA PAPER 95-0119 p 170 N95-17264 * #
 AIAA PAPER 95-0538 p 124 N95-19285 * #
 AIAA PAPER 95-0540 p 124 N95-19284 * #
 AIAA PAPER 95-0720 p 145 N95-18054 * #
 AIAA PAPER 95-0733 p 139 N95-18133 * #
 AIAA PAPER 95-0755 p 123 N95-18582 * #
 AIAA PAPER 95-6146 p 148 N95-19286 * #

 AL/CF-TR-1994-0063 p 130 N95-17661 #

 ANL/MCS/CP-82980 p 157 N95-16828 * #

 ARL-MR-184 p 118 N95-18611 #

 ARL-TR-438 p 119 N95-18670 #
 ARL-TR-489 p 131 N95-18381 #
 ARL-TR-600 p 162 N95-19125 * #
 ARL-TR-637 p 137 N95-15970 * #

 ARO-27480.6-EG-SDI p 106 N95-16160 #
 ARO-27627.3-EG p 155 N95-16163 #
 ARO-28249.2-EG p 106 N95-16099 #
 ARO-31210.2-EG-SDI p 106 N95-16076 #
 ARO-32483.1-MA-CF p 169 N95-16864 #

ASC-TR-94-5026-PHASE-1 p 131 N95-18398 #

 ATC-221 p 154 N95-16097 #

 B-255687 p 176 N95-18578 #

 BRL-IMR-971 p 119 N95-18670 #

 BTN-94-EIX94341340068 p 103 A95-63520 #
 BTN-94-EIX94341340070 p 171 A95-63522 #
 BTN-94-EIX94441380856 p 125 A95-64288 #
 BTN-94-EIX94441380862 p 125 A95-64294 #
 BTN-94-EIX94461408589 p 141 A95-63064 #
 BTN-94-EIX94461408751 p 126 A95-63634 #
 BTN-94-EIX94461408753 p 168 A95-63636 #
 BTN-94-EIX94461408755 p 153 A95-63638 #
 BTN-94-EIX94461408756 p 171 A95-63639 #
 BTN-94-EIX94461408757 p 148 A95-63640 #
 BTN-94-EIX94461408760 p 138 A95-63643 #
 BTN-94-EIX94461408763 p 103 A95-63646 #
 BTN-94-EIX94461408765 p 153 A95-63648 #
 BTN-94-EIX94461408769 p 153 A95-63652 #
 BTN-94-EIX94461408772 p 103 A95-63655 #
 BTN-94-EIX94461408773 p 175 A95-63656 #
 BTN-94-EIX94461408774 p 138 A95-63657 #
 BTN-94-EIX94481415349 p 103 A95-65339 #
 BTN-94-EIX94481415355 p 154 A95-65345 #
 BTN-94-EIX94481415356 p 103 A95-65346 #
 BTN-94-EIX94481415357 p 104 A95-65347 #
 BTN-94-EIX94501431527 p 153 A95-64524 #
 BTN-94-EIX94511309382 p 103 A95-64608 #
 BTN-94-EIX94511309383 p 127 A95-64609 #
 BTN-94-EIX94511309384 p 103 A95-64610 #
 BTN-94-EIX94511433914 p 168 A95-64580 #
 BTN-94-EIX94511433916 p 168 A95-64582 #
 BTN-94-EIX94511433918 p 141 A95-64584 #
 BTN-94-EIX94511433919 p 169 A95-64585 #
 BTN-94-EIX94511433920 p 141 A95-64586 #
 BTN-94-EIX94511433921 p 142 A95-64587 #
 BTN-94-EIX94511433922 p 169 A95-64588 #
 BTN-94-EIX94511433940 p 142 A95-64606 #

 CMU-RI-TR-94-17 p 126 N95-17706 #

 CONF-9204294-1 p 157 N95-16939 #
 CONF-930726-8 p 118 N95-18645 #
 CONF-940113-11 p 118 N95-18646 #
 CONF-9404179-1 p 138 N95-17371 #
 CONF-9406188-1 p 145 N95-16509 #
 CONF-940662-1 p 157 N95-16828 #

 CPIA-PUBL-602-VOL-1 p 148 N95-16312 #

 DE94-011863 p 157 N95-16939 #
 DE94-011866 p 118 N95-18645 #
 DE94-011867 p 118 N95-18646 #
 DE94-012473 p 152 N95-19100 #
 DE94-012470 p 157 N95-16828 #
 DE94-013960 p 138 N95-17371 #
 DE94-014136 p 145 N95-16509 #

 DLR-FB-94-06 p 139 N95-18911 #
 DLR-FB-94-11 p 172 N95-18912 #
 DLR-FB-94-12 p 119 N95-18910 #

 DODA-AR-007-005 p 129 N95-16969 #
 DODA-AR-007-100 p 108 N95-17178 #

 DOT-VNTSC-FAA-94-11 p 160 N95-18436 #
 DOT-VNTSC-FAA-94-12 p 118 N95-18624 #

 DOT/FAA/CT-TN92(41)-1 p 125 N95-17373 #
 DOT/FAA/CT-TN94/29 p 146 N95-18087 #
 DOT/FAA/CT-TN94/6 p 126 N95-18088 #

 DOT/FAA/RD-94-25 p 118 N95-18624 #
 DOT/FAA/RD-94/15 p 160 N95-18436 #
 DOT/FAA/RD-94/23 p 126 N95-18059 #
 DOT/FAA/RD-94/7 p 131 N95-18198 #

 DSTO-TR-0043 p 108 N95-17178 #

 E-8079 p 108 N95-16887 * #

REPORT

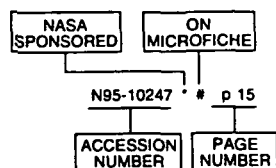
E-8151	p 162	N95-19236 * #	NAS 1.15:104806-VOL-1	p 151	N95-19237 * #	NASA-CR-195007	p 159	N95-18193 * #
E-8725	p 154	N95-16072 * #	NAS 1.15:106571	p 152	N95-16905 * #	NASA-CR-195014	p 159	N95-18042 * #
E-8774	p 152	N95-16905 * #	NAS 1.15:106580	p 105	N95-16038 * #	NASA-CR-195312	p 154	N95-16072 * #
E-8840	p 105	N95-16038 * #	NAS 1.15:106632	p 157	N95-16911 * #	NASA-CR-195390	p 138	N95-17402 * #
E-8933	p 157	N95-16911 * #	NAS 1.15:106736	p 139	N95-18133 * #	NASA-CR-195408	p 161	N95-18938 * #
E-9111	p 141	N95-19380 * #	NAS 1.15:106755	p 146	N95-18586 * #	NASA-CR-195413	p 156	N95-16588 * #
E-9160	p 138	N95-17402 * #	NAS 1.15:106776	p 117	N95-18457 * #	NASA-CR-196543	p 168	N95-18093 * #
E-9175	p 146	N95-18586 * #	NAS 1.15:106784	p 137	N95-15970 * #	NASA-CR-197030	p 127	N95-15971 * #
E-9227	p 117	N95-18457 * #	NAS 1.15:106785	p 167	N95-19501 * #	NASA-CR-197109	p 129	N95-16899 * #
E-9237	p 137	N95-15970 * #	NAS 1.15:106799	p 170	N95-16906 * #	NASA-CR-197213	p 172	N95-16848 * #
E-9239	p 167	N95-19501 * #	NAS 1.15:106802	p 170	N95-17264 * #	NASA-CR-197449	p 172	N95-16401 * #
E-9265	p 161	N95-18938 * #	NAS 1.15:106803	p 105	N95-18486 * #	NASA-CR-197488	p 107	N95-16589 * #
E-9275	p 170	N95-16906 * #	NAS 1.15:106804	p 104	N95-17657 * #	NASA-CR-197493	p 142	N95-17404 * #
E-9279	p 170	N95-17264 * #	NAS 1.15:106805	p 105	N95-18197 * #	NASA-CR-197516	p 134	N95-19130 * #
E-9281	p 105	N95-18486 * #	NAS 1.15:106808	p 148	N95-19286 * #	NASA-CR-197517	p 150	N95-17493 * #
E-9282	p 104	N95-17657 * #	NAS 1.15:106817	p 145	N95-18054 * #	NASA-CR-197523	p 130	N95-18090 * #
E-9283	p 105	N95-18197 * #	NAS 1.15:106822	p 162	N95-19125 * #	NASA-CR-197554	p 160	N95-18388 * #
E-9284	p 148	N95-19286 * #	NAS 1.15:106826	p 124	N95-19285 * #	NASA-CR-197574	p 150	N95-18196 * #
E-9294	p 105	N95-18197 * #	NAS 1.15:106827	p 124	N95-19284 * #	NASA-CR-197595	p 160	N95-18737 * #
E-9299	p 156	N95-16588 * #	NAS 1.15:106831	p 123	N95-18582 * #	NASA-CR-4620	p 151	N95-16859 * #
E-9332	p 105	N95-18044 * #	NAS 1.15:106833	p 119	N95-18933 * #	NASA-CR-4635	p 108	N95-17273 * #
E-9349	p 139	N95-18133 * #	NAS 1.15:106833	p 116	N95-18101 * #	NASA-CR-4642-VOL-1	p 161	N95-18955 * #
E-9356	p 145	N95-18054 * #	NAS 1.15:108852	p 171	N95-18899 * #	NASA-CR-4642-VOL-2	p 161	N95-18956 * #
E-9366	p 162	N95-19125 * #	NAS 1.15:109160-VOL-1	p 157	N95-16828 * #	NASA-NEWS-RELEASE-94-47	p 144	N95-19029 * #
E-9375	p 124	N95-19285 * #	NAS 1.15:109948	p 120	N95-19042 * #	NASA-TM-104806-VOL-1	p 151	N95-19237 * #
E-9376	p 124	N95-19284 * #	NAS 1.15:4574	p 106	N95-16069 * #	NASA-TM-106571	p 152	N95-16905 * #
E-9381	p 123	N95-18582 * #	NAS 1.15:4582	p 125	N95-17384 * #	NASA-TM-106580	p 105	N95-16038 * #
E-9387	p 150	N95-18743 * #	NAS 1.15:4588	p 108	N95-16858 * #	NASA-TM-106632	p 157	N95-16911 * #
E-9394	p 119	N95-18933 * #	NAS 1.15:4596	p 108	N95-16908 * #	NASA-TM-106736	p 139	N95-18133 * #
EPA/600/R-94/127	p 104	N95-17466	NAS 1.15:4601	p 120	N95-19119 * #	NASA-TM-106755	p 146	N95-18586 * #
ERL-0656-RR	p 129	N95-16969 #	NAS 1.15:4632	p 158	N95-17490 * #	NASA-TM-106776	p 117	N95-18457 * #
FOA-C-10358-1.3	p 104	N95-17451	NAS 1.15:4644	p 134	N95-19044 * #	NASA-TM-106784	p 137	N95-15970 * #
FOA-C-20957-2.1	p 142	N95-17454	NAS 1.15:4653	p 176	N95-18573 * #	NASA-TM-106785	p 167	N95-19501 * #
GAO/NSIAD-94-71	p 176	N95-18578 #	NAS 1.26:182276	p 105	N95-18044 * #	NASA-TM-106799	p 170	N95-16906 * #
H-1913	p 117	N95-18565 * #	NAS 1.26:186031	p 143	N95-18567 * #	NASA-TM-106802	p 170	N95-17264 * #
H-1993	p 108	N95-16858 * #	NAS 1.26:188360	p 108	N95-16887 * #	NASA-TM-106803	p 105	N95-18486 * #
H-2019	p 158	N95-17490 * #	NAS 1.26:191045	p 162	N95-19236 * #	NASA-TM-106804	p 104	N95-17657 * #
H-2022	p 134	N95-19044 * #	NAS 1.26:191178	p 170	N95-16897 * #	NASA-TM-106805	p 105	N95-18197 * #
H-2027	p 157	N95-17418 * #	NAS 1.26:191194	p 159	N95-18190 * #	NASA-TM-106808	p 148	N95-19286 * #
H-2030-VOL-1	p 161	N95-18955 * #	NAS 1.26:194980	p 170	N95-18110 * #	NASA-TM-106817	p 145	N95-18054 * #
H-2030-VOL-2	p 161	N95-18956 * #	NAS 1.26:194997	p 170	N95-16898 * #	NASA-TM-106822	p 162	N95-19125 * #
HTN-95-20003	p 153	A95-63201 *	NAS 1.26:195001	p 151	N95-16860 * #	NASA-TM-106826	p 124	N95-19285 * #
HTN-95-50218	p 175	A95-64855	NAS 1.26:195004	p 159	N95-18191 * #	NASA-TM-106827	p 124	N95-19284 * #
HTN-95-50219	p 176	A95-64856	NAS 1.26:195007	p 159	N95-18193 * #	NASA-TM-106831	p 123	N95-18582 * #
HTN-95-50220	p 176	A95-64857	NAS 1.26:195014	p 159	N95-18042 * #	NASA-TM-106833	p 119	N95-18933 * #
HTN-95-50223	p 176	A95-64860	NAS 1.26:195312	p 154	N95-16072 * #	NASA-TM-108852	p 116	N95-18101 * #
HTN-95-50269	p 176	A95-65764	NAS 1.26:195390	p 138	N95-17402 * #	NASA-TM-109160-VOL-1	p 171	N95-18899 * #
ICASE-94-77	p 170	N95-16897 * #	NAS 1.26:195408	p 161	N95-18938 * #	NASA-TM-109948	p 157	N95-16828 * #
ICASE-94-86	p 159	N95-18190 * #	NAS 1.26:195413	p 156	N95-16588 * #	NASA-TM-110113	p 129	N95-16982 * #
ICASE-94-89	p 170	N95-18110 * #	NAS 1.26:196543	p 168	N95-18093 * #	NASA-TM-110117	p 126	N95-18347 * #
ICASE-94-92	p 159	N95-18191 * #	NAS 1.26:197030	p 127	N95-15971 * #	NASA-TM-4574	p 120	N95-19042 * #
ICASE-94-94	p 159	N95-18193 * #	NAS 1.26:197109	p 129	N95-16899 * #	NASA-TM-4582	p 106	N95-16069 * #
INPE-5565-TDI/540	p 150	N95-18720 #	NAS 1.26:197213	p 172	N95-16848 * #	NASA-TM-4588	p 125	N95-17384 * #
INT-PATENT-CLASS-F16F-7/10	p 159	N95-18325 *	NAS 1.26:197449	p 172	N95-16401 * #	NASA-TM-4596	p 108	N95-16858 * #
ISBN-7-80-046602-7	p 104	N95-16249 #	NAS 1.26:197488	p 107	N95-16589 * #	NASA-TM-4601	p 108	N95-16908 * #
ISBN-90-369-2054-X	p 168	N95-18722	NAS 1.26:197493	p 142	N95-17404 * #	NASA-TM-4632	p 120	N95-19119 * #
ISBN-92-835-0755-X	p 149	N95-17278 #	NAS 1.26:197516	p 134	N95-19130 * #	NASA-TM-4644	p 158	N95-17490 * #
ISBN-92-835-0756-8	p 162	N95-19251 #	NAS 1.26:197517	p 150	N95-17493 * #	NASA-TM-4646	p 134	N95-19044 * #
ISBN-92-835-0757-6	p 145	N95-17388 #	NAS 1.26:197523	p 130	N95-18090 * #	NASA-TM-4653	p 176	N95-18573 * #
ISBN-92-835-0758-4	p 126	N95-18927 #	NAS 1.26:197554	p 160	N95-18388 * #	NASA-TP-3414	p 117	N95-18565 * #
ISBN-92-836-0001-0	p 173	N95-19142 #	NAS 1.26:197574	p 150	N95-18196 * #	NASA-TP-3443	p 104	N95-16560 * #
ISBN-92-836-0002-9	p 143	N95-18597 #	NAS 1.26:197595	p 160	N95-18737 * #	NASA-TP-3455	p 129	N95-17397 * #
ISBN-92-836-1003-2	p 109	N95-17846 #	NAS 1.26:4620	p 151	N95-16859 * #	NASA-TP-3460	p 131	N95-18198 * #
ISBN-92-836-1007-5	p 127	N95-16562 #	NAS 1.26:4635	p 108	N95-17273 * #	NASA-TP-3478	p 120	N95-19114 * #
ISBN-92-836-1008-3	p 139	N95-19017 #	NAS 1.26:4642-VOL-1	p 161	N95-18955 * #	NASA-TP-3526	p 119	N95-19041 * #
ISTIC-TR-93123	p 139	N95-17749	NAS 1.26:4642-VOL-2	p 161	N95-18956 * #	NASA-TP-3526	p 119	N95-19041 * #
KNMI-SR-94-03	p 168	N95-18722	NAS 1.55:10147	p 141	N95-19380 * #	NAVY-CASE-74885	p 160	N95-18461 #
L-17053	p 129	N95-17397 * #	NAS 1.55:3274-PT-2	p 117	N95-18565 * #	NAWCAD-SAB0	p 132	N95-18407
L-17073	p 104	N95-16560 * #	NAS 1.60:3414	p 104	N95-16560 * #	NAWCADTRN-PE-261	p 139	N95-18383
L-17330	p 108	N95-16908 * #	NAS 1.60:3455	p 129	N95-17397 * #	NAWCADWAR-93082-60	p 129	N95-17631 #
L-17334	p 125	N95-17384 * #	NAS 1.60:3460	p 131	N95-18198 * #	NLR-TP-92409-U	p 117	N95-18503
L-17336	p 120	N95-19114 * #	NAS 1.60:3478	p 120	N95-19114 * #	NONP-AGARD-SUPPL-VT-95-3838	p 117	N95-18539
L-17337	p 106	N95-16069 #	NAS 1.60:3526	p 119	N95-19041 * #	0	p 117	N95-18539
L-17350	p 120	N95-19042 * #	NASA-ASR-268	p 129	N95-16982 *	NONP-NASA-VT-95-35013	p 129	N95-16982 *
L-17376	p 131	N95-18198 * #	NASA-CASE-MFS-28697-1	p 159	N95-18325 *	NONP-NASA-VT-95-37002	p 126	N95-18347 *
L-17432-PT-2	p 124	N95-19468 * #	NASA-CP-10147	p 141	N95-19380 * #	NREL/TP-441-7078	p 157	N95-16939 #
NAL-PD-CA-9217	p 142	N95-16392 #	NASA-CP-3274-PT-2	p 124	N95-19468 #	NREL/TP-441-7107	p 118	N95-18645 #
NAL-PD-SN-9306	p 105	N95-18606 #	NASA-CR-182276	p 105	N95-18044 * #	NREL/TP-441-7108	p 118	N95-18646 #
NAL-SP-9322-PT-1	p 165	N95-19444 #	NASA-CR-186031	p 157	N95-17418 * #	NTSB/AAR-94/07	p 123	N95-17646 #
NAL-TM-CSS-9303	p 119	N95-18904 #	NASA-CR-188360	p 143	N95-18567 * #	NTSB/ARC-94/02	p 123	N95-17748 #
			NASA-CR-191045	p 150	N95-18743 * #	NTSB/SS-94/02	p 124	N95-19132 #
			NASA-CR-191178	p 108	N95-16887 * #	ODURF-124303	p 129	N95-16899 * #
			NASA-CR-191194	p 162	N95-19236 * #			
			NASA-CR-194980	p 170	N95-16897 * #			
			NASA-CR-194994	p 159	N95-18190 * #			
			NASA-CR-194997	p 170	N95-18110 * #			
			NASA-CR-195001	p 170	N95-16898 * #			
			NASA-CR-195004	p 151	N95-16860 * #			
			NASA-CR-195005	p 159	N95-18191 * #			

REPORT NUMBER INDEX

PB94-189180	p 104	N95-17451
PB94-190725	p 142	N95-17454
PB94-193323	p 104	N95-17466
PB94-194883	p 123	N95-17476 #
PB94-201696	p 117	N95-18503
PB94-910409	p 123	N95-17646 #
PB94-917004	p 124	N95-19132 #
PB95-100319	p 123	N95-17748 #
PB95-104238	p 139	N95-17749
PNL-SA-22914	p 138	N95-17371 #
PSI-1177/TR-1305	p 106	N95-16076
REPT-63193-94U/P60099	p 130	N95-17661 #
REPT-91-R-1475	p 105	N95-18044 * #
REPT-92RR-28	p 126	N95-18059 #
RIACS-TR-94-19	p 160	N95-18737 * #
RL-TR-94-85	p 156	N95-16621 #
S-786-VOL-1	p 151	N95-19237 * #
SAND-93-0208C	p 145	N95-16509 #
SAND-94-0945	p 152	N95-19100 #
SSD94D0298	p 143	N95-18567 * #
SSD94D0335	p 127	N95-15971 * #
TR-2-FSRC-93	p 171	N95-18564 #
UCLA ENG-93-43	p 150	N95-17493 * #
US-PATENT-APPL-SN-020940	p 116	N95-18337
US-PATENT-APPL-SN-134443	p 159	N95-18325 *
US-PATENT-APPL-SN-279037	p 160	N95-18461 #
US-PATENT-APPL-SN-329621	p 152	N95-19090
US-PATENT-APPL-SN-666104	p 151	N95-19073
US-PATENT-CLASS-149-19.9	p 152	N95-19090
US-PATENT-CLASS-188-379	p 159	N95-18325 *
US-PATENT-CLASS-244-130	p 116	N95-18337
US-PATENT-CLASS-244-3.22	p 151	N95-19073
US-PATENT-CLASS-416-144	p 159	N95-18325 *
US-PATENT-CLASS-74-573R	p 159	N95-18325 *
US-PATENT-CLASS-74-574	p 159	N95-18325 *
US-PATENT-5,303,882	p 116	N95-18337
US-PATENT-5,320,304	p 151	N95-19073
US-PATENT-5,320,692	p 152	N95-19090
US-PATENT-5,373,922	p 159	N95-18325 *
USAARL-94-29	p 172	N95-17334 #
USAARL-94-37	p 171	N95-16226 #
USAARL-94-42	p 123	N95-16404 #
USAATCOM-TR-94-A-011	p 120	N95-19119 * #
WL-TM-94-3132-VOL-4-PT-2	p 143	N95-18641 #
WL-TR-91-7020	p 138	N95-18164 #
WL-TR-93-3010-VOL-1	p 132	N95-18483 #
WL-TR-93-3048	p 107	N95-16808 #
WL-TR-94-2025	p 160	N95-18660
WL-TR-94-3017	p 117	N95-18380
WL-TR-94-3063	p 171	N95-18365 #
WL-TR-94-4006	p 158	N95-17507
WL-TR-94-4083-VOL-1	p 133	N95-18677
WL-TR-94-4084-VOL-2	p 131	N95-18162 #

ACCESSION NUMBER INDEX

Typical Accession Number Index Listing



Listings in this index are arranged alphanumerically by accession number. The page number indicates the page on which the citation is located. The accession number denotes the number by which the citation is identified. An asterisk (*) indicates that the item is a NASA report. A pound sign (#) indicates that the item is available on microfiche.

A95-63064	p 141	N95-16226	# p 171	N95-17874	# p 114	N95-18660	p 160
A95-63201	p 153	N95-16249	# p 104	N95-17875	* # p 114	N95-18663	p 118
A95-63520	p 103	N95-16250	# p 155	N95-17876	# p 114	N95-18669	p 119
A95-63522	p 171	N95-16251	# p 106	N95-17877	# p 115	N95-18670	p 119
A95-63634	p 126	N95-16252	# p 106	N95-17878	* # p 115	N95-18674	p 119
A95-63636	p 168	N95-16256	# p 151	N95-17879	# p 115	N95-18677	p 133
A95-63638	p 153	N95-16257	# p 107	N95-17880	* # p 115	N95-18720	# p 150
A95-63639	p 171	N95-16258	# p 144	N95-17881	* # p 115	N95-18722	p 168
A95-63640	p 148	N95-16264	# p 127	N95-17882	# p 116	N95-18724	p 146
A95-63643	p 138	N95-16265	# p 138	N95-17883	# p 116	N95-18725	p 146
A95-63646	p 103	N95-16268	# p 155	N95-17884	# p 116	N95-18726	p 134
A95-63648	p 153	N95-16272	# p 169	N95-17885	# p 116	N95-18737	* # p 160
A95-63652	p 153	N95-16277	# p 125	N95-17886	# p 116	N95-18743	* # p 150
A95-63655	p 103	N95-16278	# p 155	N95-17887	* # p 108	N95-18891	* # p 134
A95-63656	p 175	N95-16281	# p 155	N95-17889	* # p 129	N95-18899	* # p 171
A95-63657	p 138	N95-16312	# p 148	N95-17890	* # p 129	N95-18901	p 161
A95-64288	p 125	N95-16316	# p 148	N95-17891	* # p 129	N95-18902	p 144
A95-64294	p 125	N95-16317	# p 138	N95-17892	* # p 129	N95-18903	p 146
A95-64524	p 153	N95-16318	# p 144	N95-17893	* # p 129	N95-18904	# p 119
A95-64580	p 168	N95-16319	# p 144	N95-17894	* # p 129	N95-18910	# p 119
A95-64582	p 168	N95-16320	* # p 145	N95-17897	* # p 138	N95-18911	# p 139
A95-64584	p 141	N95-16321	# p 148	N95-17902	* # p 138	N95-18912	# p 172
A95-64585	p 169	N95-16322	# p 155	N95-17903	* # p 142	N95-18927	# p 126
A95-64586	p 141	N95-16323	# p 138	N95-17904	* # p 157	N95-18933	* # p 119
A95-64587	p 142	N95-16333	# p 149	N95-17938	* # p 125	N95-18938	* # p 161
A95-64588	p 169	N95-16334	# p 156	N95-17987	* # p 145	N95-18955	* # p 161
A95-64606	p 142	N95-16349	# p 156	N95-17988	* # p 129	N95-18956	* # p 161
A95-64608	p 103	N95-16352	# p 149	N95-17989	* # p 129	N95-18993	* # p 150
A95-64609	p 127	N95-16356	# p 127	N95-17997	* # p 138	N95-19008	# p 152
A95-64610	p 103	N95-16371	# p 151	N95-17999	* # p 138	N95-19017	# p 139
A95-64855	p 175	N95-16392	# p 142	N95-17999	* # p 138	N95-19019	# p 161
A95-64856	p 176	N95-16401	# p 172	N95-17999	* # p 138	N95-19020	# p 140
A95-64857	p 176	N95-16404	# p 123	N95-17999	* # p 138	N95-19021	# p 140
A95-64860	p 176	N95-16448	# p 156	N95-17999	* # p 138	N95-19022	# p 140
A95-65339	p 103	N95-16458	* # p 137	N95-17999	* # p 138	N95-19023	# p 140
A95-65345	p 154	N95-16458	* # p 169	N95-17999	* # p 138	N95-19024	# p 140
A95-65346	p 103	N95-16461	* # p 156	N95-17999	* # p 138	N95-19025	# p 140
A95-65347	p 104	N95-16474	# p 169	N95-17999	* # p 138	N95-19026	# p 140
A95-65764	p 176	N95-16506	# p 168	N95-17999	* # p 138	N95-19029	* # p 144
		N95-16509	# p 145	N95-17999	* # p 138	N95-19035	p 161
N95-15970	* # p 137	N95-16560	# p 104	N95-17999	* # p 138	N95-19041	* # p 119
N95-15971	# p 127	N95-16562	# p 127	N95-17999	* # p 138	N95-19042	# p 120
N95-15988	* # p 169	N95-16563	# p 107	N95-17999	* # p 138	N95-19044	* # p 134
N95-15994	# p 105	N95-16564	# p 107	N95-17999	* # p 138	N95-19067	p 134
N95-16038	* # p 105	N95-16565	# p 127	N95-17999	* # p 138	N95-19073	p 151
N95-16048	* # p 154	N95-16566	# p 128	N95-17999	* # p 138	N95-19090	p 152
N95-16069	* # p 106	N95-16567	# p 128	N95-17999	* # p 138	N95-19100	# p 152
N95-16072	* # p 154	N95-16568	# p 128	N95-17999	* # p 138	N95-19110	# p 120
N95-16076	p 106	N95-16569	* # p 128	N95-17999	* # p 138	N95-19114	* # p 120
N95-16097	p 154	N95-16570	# p 128	N95-17999	* # p 138	N95-19119	* # p 120
N95-16099	p 106	N95-16571	# p 128	N95-17999	* # p 138	N95-19125	* # p 162
N95-16109	p 142	N95-16572	# p 128	N95-17999	* # p 138	N95-19130	* # p 134
N95-16160	# p 106	N95-16573	# p 129	N95-17999	* # p 138	N95-19132	# p 124
N95-16163	# p 155	N95-16588	# p 156	N95-17999	* # p 138	N95-19142	# p 173
N95-16171	# p 127	N95-16589	* # p 107	N95-17999	* # p 138	N95-19143	# p 173
		N95-16621	# p 156	N95-17999	* # p 138	N95-19144	# p 173
				N95-17858	* # p 111	N95-19145	# p 173
				N95-17859	* # p 111	N95-19146	# p 173
				N95-17860	* # p 111	N95-19147	# p 173
				N95-17861	* # p 111	N95-19148	# p 174
				N95-17862	* # p 111	N95-19149	# p 174
				N95-17863	* # p 111	N95-19150	# p 147
				N95-17864	* # p 111	N95-19151	# p 135
				N95-17865	* # p 111	N95-19154	# p 135
				N95-17866	* # p 111	N95-19156	# p 174
				N95-17867	* # p 111	N95-19157	# p 174
				N95-17868	* # p 111	N95-19159	# p 174
				N95-17869	* # p 111	N95-19161	# p 162
				N95-17870	* # p 111	N95-19162	# p 174
				N95-17871	* # p 111	N95-19163	# p 175
				N95-17872	* # p 111	N95-19164	# p 175
				N95-17873	* # p 111	N95-19167	# p 124
						N95-19236	* # p 162
						N95-19237	* # p 151
						N95-19251	# p 162
						N95-19252	# p 162
						N95-19255	# p 163
						N95-19257	# p 163
						N95-19258	# p 163
						N95-19259	# p 121
						N95-19260	# p 121
						N95-19261	# p 121
						N95-19262	# p 163

ACCESSION

N95-19263

N95-19263 # p 164
N95-19264 # p 164
N95-19265 # p 164
N95-19266 * # p 164
N95-19267 # p 147
N95-19268 * # p 121
N95-19269 # p 147
N95-19270 * # p 121
N95-19271 # p 147
N95-19272 # p 147
N95-19273 # p 164
N95-19274 # p 175
N95-19275 # p 165
N95-19276 # p 165
N95-19277 # p 165
N95-19278 # p 122
N95-19279 # p 122
N95-19280 # p 122
N95-19281 # p 122
N95-19282 # p 122
N95-19284 * # p 124
N95-19285 * # p 124
N95-19286 * # p 148
N95-19380 * # p 141
N95-19381 * # p 141
N95-19382 * # p 141
N95-19383 * # p 141
N95-19444 # p 165
N95-19447 # p 165
N95-19448 # p 165
N95-19457 # p 123
N95-19462 # p 165
N95-19464 # p 123
N95-19468 * # p 124
N95-19469 * # p 135
N95-19470 * # p 166
N95-19471 * # p 166
N95-19472 * # p 166
N95-19473 * # p 166
N95-19477 * # p 166
N95-19478 * # p 135
N95-19479 * # p 135
N95-19480 * # p 136
N95-19482 * # p 152
N95-19483 * # p 167
N95-19485 * # p 136
N95-19486 * # p 136
N95-19488 * # p 136
N95-19490 * # p 153
N95-19491 * # p 136
N95-19495 * # p 137
N95-19496 * # p 167
N95-19497 * # p 137
N95-19499 * # p 137
N95-19501 * # p 167

AVAILABILITY OF CITED PUBLICATIONS

OPEN LITERATURE ENTRIES (A95-60000 Series)

Inquiries and requests should be addressed to NASA Center for AeroSpace Information, 800 Elkridge Landing Road, Linthicum Heights, MD 21090-2934. Orders are also taken by telephone, (301) 621-0390, e-mail, help@sti.nasa.gov, and fax, (301) 621-0134. Please refer to the accession number when request-ing publications.

STAR ENTRIES (N95-10000 Series)

One or more sources from which a document announced in *STAR* is available to the public is ordinarily given on the last line of the citation. The most commonly indicated sources and their acronyms or abbreviations are listed below, and their addresses are listed on page APP-3. If the publication is available from a source other than those listed, the publisher and his address will be displayed on the availability line or in combination with the corporate source line.

Avail: CASI. Sold by the NASA Center for AeroSpace Information. Prices for hard copy (HC) and microfiche (MF) are indicated by a price code following the letters HC or MF in the *STAR* citation. Current values for the price codes are given in the tables on page APP-5.

NOTE ON ORDERING DOCUMENTS: When ordering publications from NASA CASI, use the N accession number or other report number. It is also advisable to cite the title and other bibliographic identification.

Avail: SOD (or GPO). Sold by the Superintendent of Documents, U.S. Government Printing Office, in hard copy.

Avail: BLL (formerly NLL): British Library Lending Division, Boston Spa, Wetherby, Yorkshire, England. Photocopies available from this organization at the price shown. (If none is given, inquiry should be addressed to the BLL.)

Avail: DOE Depository Libraries. Organizations in U.S. cities and abroad that maintain collections of Department of Energy reports, usually in microfiche form, are listed in *Energy Research Abstracts*. Services available from the DOE and its depositories are described in a booklet, *DOE Technical Information Center - Its Functions and Services* (TID-4660), which may be obtained without charge from the DOE Technical Information Center.

Avail: ESDU. Pricing information on specific data, computer programs, and details on Engineering Sciences Data Unit (ESDU) topic categories can be obtained from ESDU International Ltd. Requesters in North America should use the Virginia address while all other requesters should use the London address, both of which are on page APP-3.

Avail: Fachinformationszentrum Karlsruhe. Gesellschaft für wissenschaftlich-technische Information mbH 76344 Eggenstein-Leopoldshafen, Germany.

Avail: HMSO. Publications of Her Majesty's Stationery Office are sold in the U.S. by Pendragon House, Inc. (PHI), Redwood City, CA. The U.S. price (including a service and mailing charge) is given, or a conversion table may be obtained from PHI.

Avail: Issuing Activity, or Corporate Author, or no indication of availability. Inquiries as to the availability of these documents should be addressed to the organization shown in the citation as the corporate author of the document.

Avail: NASA Public Document Rooms. Documents so indicated may be examined at or purchased from the National Aeronautics and Space Administration (JBD-4), Public Documents Room (Room 1H23), Washington, DC 20546-0001, or public document rooms located at NASA installations, and the NASA Pasadena Office at the Jet Propulsion Laboratory.

Avail: NTIS. Sold by the National Technical Information Service. Initially distributed microfiche under the NTIS SRIM (Selected Research in Microfiche) are available. For information concerning this service, consult the NTIS Subscription Section, Springfield, VA 22161.

Avail: Univ. Microfilms. Documents so indicated are dissertations selected from *Dissertation Abstracts* and are sold by University Microfilms as xerographic copy (HC) and microfilm. All requests should cite the author and the Order Number as they appear in the citation.

Avail: US Patent and Trademark Office. Sold by Commissioner of Patents and Trademarks, U.S. Patent and Trademark Office, at the standard price of \$1.50 each, postage free.

Avail: (US Sales Only). These foreign documents are available to users within the United States from the National Technical Information Service (NTIS). They are available to users outside the United States through the International Nuclear Information Service (INIS) representative in their country, or by applying directly to the issuing organization.

Avail: USGS. Originals of many reports from the U.S. Geological Survey, which may contain color illustrations, or otherwise may not have the quality of illustrations preserved in the microfiche or facsimile reproduction, may be examined by the public at the libraries of the USGS field offices whose addresses are listed on page APP-3. The libraries may be queried concerning the availability of specific documents and the possible utilization of local copying services, such as color reproduction.

FEDERAL DEPOSITORY LIBRARY PROGRAM

In order to provide the general public with greater access to U.S. Government publications, Congress established the Federal Depository Library Program under the Government Printing Office (GPO), with 53 regional depositories responsible for permanent retention of material, inter-library loan, and reference services. At least one copy of nearly every NASA and NASA-sponsored publication, either in printed or microfiche format, is received and retained by the 53 regional depositories. A list of the regional GPO libraries, arranged alphabetically by state, appears on the inside back cover of this issue. These libraries are *not* sales outlets. A local library can contact a regional depository to help locate specific reports, or direct contact may be made by an individual.

PUBLIC COLLECTION OF NASA DOCUMENTS

An extensive collection of NASA and NASA-sponsored publications is maintained by the British Library Lending Division, Boston Spa, Wetherby, Yorkshire, England for public access. The British Library Lending Division also has available many of the non-NASA publications cited in *STAR*. European requesters may purchase facsimile copy or microfiche of NASA and NASA-sponsored documents, those identified by both the symbols # and * from ESA — Information Retrieval Service European Space Agency, 8-10 rue Mario-Nikis, 75738 CEDEX 15, France.

STANDING ORDER SUBSCRIPTIONS

NASA SP-7037 supplements and annual index are available from the NASA Center for Aerospace Information (CASI) on standing order subscription. Standing order subscriptions do not terminate at the end of a year, as do regular subscriptions, but continue indefinitely unless specifically terminated by the subscriber.

ADDRESSES OF ORGANIZATIONS

British Library Lending Division
Boston Spa, Wetherby, Yorkshire
England

Commissioner of Patents and Trademarks
U.S. Patent and Trademark Office
Washington, DC 20231

Department of Energy
Technical Information Center
P.O. Box 62
Oak Ridge, TN 37830

European Space Agency-
Information Retrieval Service ESRIN
Via Galileo Galilei
00044 Frascati (Rome) Italy

Engineering Sciences Data Unit International
P.O. Box 1633
Manassas, VA 22110

Engineering Sciences Data Unit
International, Ltd.
251-259 Regent Street
London, W1R 7AD, England

Fachinformationszentrum Karlsruhe
Gesellschaft für wissenschaftlich-technische
Information mbH
76344 Eggenstein-Leopoldshafen, Germany

Her Majesty's Stationery Office
P.O. Box 569, S.E. 1
London, England

NASA Center for Aerospace Information
800 Elkridge Landing Road
Linthicum Heights, MD 21090-2934

National Aeronautics and Space Administration
Scientific and Technical Information Office
(JTT)
Washington, DC 20546-0001

National Technical Information Service
5285 Port Royal Road
Springfield, VA 22161

Pendragon House, Inc.
899 Broadway Avenue
Redwood City, CA 94063

Superintendent of Documents
U.S. Government Printing Office
Washington, DC 20402

University Microfilms
A Xerox Company
300 North Zeeb Road
Ann Arbor, MI 48106

University Microfilms, Ltd.
Tylers Green
London, England

U.S. Geological Survey Library National Center
MS 950
12201 Sunrise Valley Drive
Reston, VA 22092

U.S. Geological Survey Library
2255 North Gemini Drive
Flagstaff, AZ 86001

U.S. Geological Survey
345 Middlefield Road
Menlo Park, CA 94025

U.S. Geological Survey Library
Box 25046
Denver Federal Center, MS914
Denver, CO 80225

Page Intentionally Left Blank

NASA CASI PRICE CODE TABLE

(Effective January 1, 1995)

CASI PRICE CODE	NORTH AMERICAN PRICE	FOREIGN PRICE
A01	\$ 6.00	\$ 12.00
A02	9.00	18.00
A03	17.50	35.00
A04-A05	19.50	39.00
A06-A09	27.00	54.00
A10-A13	36.50	73.00
A14-A17	44.50	89.00
A18-A21	52.00	104.00
A22-A25	61.00	122.00
A99	Call For Price	Call For Price

IMPORTANT NOTICE

For users not registered at the NASA CASI, prepayment is required. Additionally, a shipping and handling fee of \$1.00 per document for delivery within the United States and \$9.00 per document for delivery outside the United States is charged.

For users registered at the NASA CASI, document orders may be invoiced at the end of the month, charged against a deposit account, or paid by check or credit card. NASA CASI accepts American Express, Diners' Club, MasterCard, and VISA credit cards. There are no shipping and handling charges. To register at the NASA CASI, please request a registration form through the NASA Access Help Desk at the address or numbers below.

NASA Center for AeroSpace Information
800 Elkridge Landing Road
Linthicum Heights, MD 21090-2934
Telephone: (301) 621-0390
E-mail: help@sti.nasa.gov
Fax: (301) 621-0134

REPORT DOCUMENT PAGE

1. Report No. NASA SP-7037 (316)	2. Government Accession No.	3. Recipient's Catalog No.	
4. Title and Subtitle Aeronautical Engineering A Continuing Bibliography (Supplement 316)		5. Report Date April 1995	
		6. Performing Organization Code JTT	
7. Author(s)		8. Performing Organization Report No.	
		10. Work Unit No.	
9. Performing Organization Name and Address NASA Scientific and Technical Information Office		11. Contract or Grant No.	
		13. Type of Report and Period Covered Special Publication	
12. Sponsoring Agency Name and Address National Aeronautics and Space Administration Washington, DC 20546-0001		14. Sponsoring Agency Code	
		15. Supplementary Notes	
16. Abstract This report lists 413 reports, articles and other documents recently announced in the NASA STI Database.			
17. Key Words (Suggested by Author(s)) Aeronautical Engineering Aeronautics Bibliographies		18. Distribution Statement Unclassified - Unlimited Subject Category - 01	
19. Security Classif. (of this report) Unclassified	20. Security Classif. (of this page) Unclassified	21. No. of Pages 152	22. Price A08/HC

FEDERAL REGIONAL DEPOSITORY LIBRARIES

ALABAMA

AUBURN UNIV. AT MONTGOMERY LIBRARY
Documents Dept.
7300 University Dr.
Montgomery, AL 36117-3596
(205) 244-3650 Fax: (205) 244-0678

UNIV. OF ALABAMA

Amelia Gayle Gorgas Library
Govt. Documents
P.O. Box 870266
Tuscaloosa, AL 35487-0266
(205) 348-6046 Fax: (205) 348-0760

ARIZONA

DEPT. OF LIBRARY, ARCHIVES, AND PUBLIC RECORDS
Research Division
Third Floor, State Capitol
1700 West Washington
Phoenix, AZ 85007
(602) 542-3701 Fax: (602) 542-4400

ARKANSAS

ARKANSAS STATE LIBRARY
State Library Service Section
Documents Service Section
One Capitol Mall
Little Rock, AR 72201-1014
(501) 682-2053 Fax: (501) 682-1529

CALIFORNIA

CALIFORNIA STATE LIBRARY
Govt. Publications Section
P.O. Box 942837 - 914 Capitol Mall
Sacramento, CA 94337-0091
(916) 654-0069 Fax: (916) 654-0241

COLORADO

UNIV. OF COLORADO - BOULDER
Libraries - Govt. Publications
Campus Box 184
Boulder, CO 80309-0184
(303) 492-8834 Fax: (303) 492-1881

DENVER PUBLIC LIBRARY

Govt. Publications Dept. BSG
1357 Broadway
Denver, CO 80203-2165
(303) 640-8846 Fax: (303) 640-8817

CONNECTICUT

CONNECTICUT STATE LIBRARY
231 Capitol Avenue
Hartford, CT 06106
(203) 566-4971 Fax: (203) 566-3322

FLORIDA

UNIV. OF FLORIDA LIBRARIES
Documents Dept.
240 Library West
Gainesville, FL 32611-2048
(904) 392-0366 Fax: (904) 392-7251

GEORGIA

UNIV. OF GEORGIA LIBRARIES
Govt. Documents Dept.
Jackson Street
Athens, GA 30602-1645
(706) 542-8949 Fax: (706) 542-4144

HAWAII

UNIV. OF HAWAII
Hamilton Library
Govt. Documents Collection
2550 The Mall
Honolulu, HI 96822
(808) 948-8230 Fax: (808) 956-5968

IDAHO

UNIV. OF IDAHO LIBRARY
Documents Section
Rayburn Street
Moscow, ID 83844-2353
(208) 885-6344 Fax: (208) 885-6817

ILLINOIS

ILLINOIS STATE LIBRARY
Federal Documents Dept.
300 South Second Street
Springfield, IL 62701-1796
(217) 782-7596 Fax: (217) 782-6437

INDIANA

INDIANA STATE LIBRARY
Serials/Documents Section
140 North Senate Avenue
Indianapolis, IN 46204-2296
(317) 232-3679 Fax: (317) 232-3728

IOWA

UNIV. OF IOWA LIBRARIES
Govt. Publications
Washington & Madison Streets
Iowa City, IA 52242-1166
(319) 335-5926 Fax: (319) 335-5900

KANSAS

UNIV. OF KANSAS
Govt. Documents & Maps Library
6001 Malott Hall
Lawrence, KS 66045-2800
(913) 864-4660 Fax: (913) 864-3855

KENTUCKY

UNIV. OF KENTUCKY
King Library South
Govt. Publications/Maps Dept.
Patterson Drive
Lexington, KY 40506-0039
(606) 257-3139 Fax: (606) 257-3139

LOUISIANA

LOUISIANA STATE UNIV.
Middleton Library
Govt. Documents Dept.
Baton Rouge, LA 70803-3312
(504) 388-2570 Fax: (504) 388-6992

LOUISIANA TECHNICAL UNIV.

Prescott Memorial Library
Govt. Documents Dept.
Ruston, LA 71272-0046
(318) 257-4962 Fax: (318) 257-2447

MAINE

UNIV. OF MAINE
Raymond H. Fogler Library
Govt. Documents Dept.
Orono, ME 04469-5729
(207) 581-1673 Fax: (207) 581-1653

MARYLAND

UNIV. OF MARYLAND - COLLEGE PARK
McKeldin Library
Govt. Documents/Maps Unit
College Park, MD 20742
(301) 405-9165 Fax: (301) 314-9416

MASSACHUSETTS

BOSTON PUBLIC LIBRARY
Govt. Documents
666 Boylston Street
Boston, MA 02117-0286
(617) 536-5400, ext. 226
Fax: (617) 536-7758

MICHIGAN

DETROIT PUBLIC LIBRARY
5201 Woodward Avenue
Detroit, MI 48202-4093
(313) 833-1025 Fax: (313) 833-0156

LIBRARY OF MICHIGAN

Govt. Documents Unit
P.O. Box 30007
717 West Allegan Street
Lansing, MI 48909
(517) 373-1300 Fax: (517) 373-3381

MINNESOTA

UNIV. OF MINNESOTA
Govt. Publications
409 Wilson Library
309 19th Avenue South
Minneapolis, MN 55455
(612) 624-5073 Fax: (612) 626-9355

MISSISSIPPI

UNIV. OF MISSISSIPPI
J.D. Williams Library
106 Old Gym Bldg.
University, MS 38677
(601) 232-5857 Fax: (601) 232-7465

MISSOURI

UNIV. OF MISSOURI - COLUMBIA
106B Ellis Library
Govt. Documents Sect.
Columbia, MO 65201-5149
(314) 882-6733 Fax: (314) 882-8044

MONTANA

UNIV. OF MONTANA
Mansfield Library
Documents Division
Missoula, MT 59812-1195
(406) 243-6700 Fax: (406) 243-2060

NEBRASKA

UNIV. OF NEBRASKA - LINCOLN
D.L. Love Memorial Library
Lincoln, NE 68588-0410
(402) 472-2562 Fax: (402) 472-5131

NEVADA

THE UNIV. OF NEVADA LIBRARIES
Business and Govt. Information Center
Reno, NV 89557-0044
(702) 784-6579 Fax: (702) 784-1751

NEW JERSEY

NEWARK PUBLIC LIBRARY
Science Div. - Public Access
P.O. Box 630
Five Washington Street
Newark, NJ 07101-7812
(201) 733-7782 Fax: (201) 733-5648

NEW MEXICO

UNIV. OF NEW MEXICO
General Library
Govt. Information Dept.
Albuquerque, NM 87131-1466
(505) 277-5441 Fax: (505) 277-6019

NEW MEXICO STATE LIBRARY

325 Don Gaspar Avenue
Santa Fe, NM 87503
(505) 827-3824 Fax: (505) 827-3888

NEW YORK

NEW YORK STATE LIBRARY
Cultural Education Center
Documents/Gift & Exchange Section
Empire State Plaza
Albany, NY 12230-0001
(518) 474-5355 Fax: (518) 474-5786

NORTH CAROLINA

UNIV. OF NORTH CAROLINA - CHAPEL HILL
Walter Royal Davis Library
CB 3912, Reference Dept.
Chapel Hill, NC 27514-8890
(919) 962-1151 Fax: (919) 962-4451

NORTH DAKOTA

NORTH DAKOTA STATE UNIV. LIB.
Documents
P.O. Box 5599
Fargo, ND 58105-5599
(701) 237-8886 Fax: (701) 237-7138

UNIV. OF NORTH DAKOTA

Chester Fritz Library
University Station
P.O. Box 9000 - Centennial and University Avenue
Grand Forks, ND 58202-9000
(701) 777-4632 Fax: (701) 777-3319

OHIO

STATE LIBRARY OF OHIO
Documents Dept.
65 South Front Street
Columbus, OH 43215-4163
(614) 644-7051 Fax: (614) 752-9178

OKLAHOMA

OKLAHOMA DEPT. OF LIBRARIES
U.S. Govt. Information Division
200 Northeast 18th Street
Oklahoma City, OK 73105-3298
(405) 521-2502, ext. 253
Fax: (405) 525-7804

OKLAHOMA STATE UNIV.

Edmon Low Library
Stillwater, OK 74078-0375
(405) 744-6546 Fax: (405) 744-5183

OREGON

PORTLAND STATE UNIV.
Branford P. Millar Library
934 Southwest Harrison
Portland, OR 97207-1151
(503) 725-4123 Fax: (503) 725-4524

PENNSYLVANIA

STATE LIBRARY OF PENN.
Govt. Publications Section
116 Walnut & Commonwealth Ave.
Harrisburg, PA 17105-1601
(717) 787-3752 Fax: (717) 783-2070

SOUTH CAROLINA

CLEMSON UNIV.
Robert Muldrow Cooper Library
Public Documents Unit
P.O. Box 343001
Clemson, SC 29634-3001
(803) 656-5174 Fax: (803) 656-3025

UNIV. OF SOUTH CAROLINA

Thomas Cooper Library
Green and Sumter Streets
Columbia, SC 29208
(803) 777-4841 Fax: (803) 777-9503

TENNESSEE

UNIV. OF MEMPHIS LIBRARIES
Govt. Publications Dept.
Memphis, TN 38152-0001
(901) 678-2206 Fax: (901) 678-2511

TEXAS

TEXAS STATE LIBRARY
United States Documents
P.O. Box 12927 - 1201 Brazos
Austin, TX 78701-0001
(512) 463-5455 Fax: (512) 463-5436

TEXAS TECH. UNIV. LIBRARIES

Documents Dept.
Lubbock, TX 79409-0002
(806) 742-2282 Fax: (806) 742-1920

UTAH

UTAH STATE UNIV.
Merrill Library Documents Dept.
Logan, UT 84322-3000
(801) 797-2678 Fax: (801) 797-2677

VIRGINIA

UNIV. OF VIRGINIA
Alderman Library
Govt. Documents
University Ave. & McCormick Rd.
Charlottesville, VA 22903-2498
(804) 824-3133 Fax: (804) 924-4337

WASHINGTON

WASHINGTON STATE LIBRARY
Govt. Publications
P.O. Box 42478
16th and Water Streets
Olympia, WA 98504-2478
(206) 753-4027 Fax: (206) 586-7575

WEST VIRGINIA

WEST VIRGINIA UNIV. LIBRARY
Govt. Documents Section
P.O. Box 6069 - 1549 University Ave.
Morgantown, WV 26506-6069
(304) 293-3051 Fax: (304) 293-6638

WISCONSIN

ST. HIST. SOC. OF WISCONSIN LIBRARY
Govt. Publication Section
816 State Street
Madison, WI 53706
(608) 264-6525 Fax: (608) 264-6520

MILWAUKEE PUBLIC LIBRARY

Documents Division
814 West Wisconsin Avenue
Milwaukee, WI 53233
(414) 286-3073 Fax: (414) 286-8074

National Aeronautics and
Space Administration
Code JTT
Washington, DC 20546-0001